UNIVERSITY OF HULL

Thesis submitted for the Degree of Doctor of Philosophy

Sex-related responses of blue mussels to the plasticiser DEHP under climate change scenarios

Luana Fiorella Mincarelli

BSc, MSc (Hons)

January 2023

Declaration of Authorship

I hereby declare that this thesis and work herein are my own. All methodologies were approved by the University of Hull Ethics Committee and all procedures were performed in accordance with the unlicensed animal ethics approval reference no. #U080/FEC_2021_11/FEC_2021_10 from the University of Hull. The thesis received revision and contribution from my supervisors Katharina Wollenberg Valero and Alexander Turner. Data chapters received contributions from advisors and collaborators:

Chapter 2

Published in **Mincarelli, L. F.,** Rotchell, J. M., Chapman, E. C., Turner, A. P., & Wollenberg Valero, K. C. (2021). Consequences of combined exposure to thermal stress and the plasticiser DEHP in Mytilus spp. differ by sex. *Marine Pollution Bulletin*, *170*, 112624.

LFM was responsible for Conceptualization, Methodology, Software, Validation, Formal analysis, Investigation, Data curation, Writing – original draft, Visualization. **JR** was responsible for Conceptualization, Methodology, Resources, Writing – review & editing. **EC** was responsible for Methodology, Resources, Writing – review & editing. **AP** was responsible for Software, Formal analysis, Resources, Data curation, Writing – review & editing, Supervision, Funding acquisition**. KWV** was responsible for Conceptualization, Methodology, Software, Formal analysis, Resources, Data curation, Writing – original draft, Visualization, Supervision, Project administration, Funding acquisition.

Chapter 3

LFM was responsible for Conceptualization, Methodology, Software, Validation, Formal analysis, Investigation, Data curation, Writing – original draft, Visualization. **JR** was responsible for Conceptualization, Methodology, Resources. **EC** was responsible for Methodology and Resources. **AP** was responsible for Software, Formal analysis, Resources, Data curation, Writing – review & editing, Supervision, Funding acquisition. **KWV** was responsible for Conceptualization, Methodology, Software, Formal analysis, Resources, Data curation, Writing – original draft, Visualization, Supervision, Project administration, Funding acquisition.

Chapter 4

Published in **Mincarelli, L. F.,** Chapman, E. C., Rotchell, J. M., Turner, A. P., & Wollenberg Valero, K. C. (2022). Sex and gametogenesis stage are strong drivers of gene expression in Mytilus edulis exposed to environmentally relevant plasticiser levels and pH 7.7. *Environmental Science and Pollution Research*, 1-13.

LFM was responsible for Conceptualization, Methodology, Software, Validation, Formal analysis, Investigation, Data curation, Writing – original draft, Visualization. **EC** was responsible for Methodology, Resources, Writing – review & editing. **JR** was responsible for Conceptualization, Methodology, Resources, Writing – review & editing. **AP** was responsible for Software, Formal analysis, Resources, Data curation, Writing – review & editing, Supervision, Funding acquisition. **KWV** was responsible for Conceptualization, Methodology, Software, Formal analysis, Resources, Data curation, Writing – original draft, Visualization, Supervision, Project administration, Funding acquisition.

Chapter 5

LFM was responsible for Conceptualization, Methodology, Software, Validation, Formal analysis, Investigation, Data curation, Writing – original draft, Visualization. George Anderson (**GA**) was responsible for Formal analysis and Investigation. **EC** and **JR** were responsible for Resources. **AP** was responsible for Software, Formal analysis, Resources, Data curation, Writing – review & editing, Supervision, Funding acquisition. **KWV** was responsible for Conceptualization, Methodology, Software, Formal analysis, Resources, Data curation, Writing – original draft, Visualization, Supervision, Project administration, Funding acquisition.

Chapter 6

LFM was responsible for Conceptualization, Methodology, Software, Validation, Formal analysis, Investigation, Data curation, Writing – original draft, Visualization. **EC** and **JR** were responsible for Resources. **AP** was responsible for Software, Formal analysis, Resources, Data curation, Writing – review & editing, Supervision, Funding acquisition. **KWV** was responsible for Conceptualization, Methodology, Software, Formal analysis, Resources, Data curation, Writing – original draft, Visualization, Supervision, Project administration, Funding acquisition.

Acknowledgement

Firstly, I would like to thank my supervisors Dr. Katharina Wollenberg Valero and Dr. Alexander Turner for their guidance throughout this Ph.D. and all the help during these years.
I would also like to deeply thank Prof. Jeanette Rotchell and Dr. Emma Chapman for their assistance and helpfulness working in the lab and during the experiments.

Thanks to Adam Bates, Lauric Feugère, Maggy Harley, Sonia Jennings, Paula Schirrmacher, Victoria Scott, Victor Swetez and Rose Terschak for their time helping in sample collection.

I would like to especially thank Andrew Jones and Alan MacKenzie from Cromarty Mussels Ltd. (Cromarty, Scotland) for the access to their mussel population.

A massive thanks to Helga Bartels-Hardege, Jörg Hardege, the members of the MolStressH2O cluster, the ChemEcoHull group, the mezzanine Hardy-340, the Spiderverse and the VIPER team for all the valuable and interesting discussions.

I would like to thank my new labmates and colleagues from IZS for being supportive and understanding if some days I had to work on this thesis.

Thanks to my family, my friends e tutti quelli che mi seguono da casa for the encouragement and support.

I am not good with words, but I hope you know how much these years together have meant to me.

"Tu prova ad avere un mondo nel cuore e non riesci ad esprimerlo con le parole"

Table of Content

List of Figures

List of Tables

List of Abbreviations

$2^{-\Delta CT}$	2 delta Ct
$2^{-\Delta\Delta CT}$	2 delta delta Ct
5-HT	5-hydroxytryptamine (monoamine serotonin)
α-CA	carbonic anhydrase, α-type family
AICc	Akaike information criterion
AICcWT	Akaike weights
AR4	fourth Assessment Reports from the IPCC (2007)
AR5	fifth Assessment Reports from the IPCC (2014)
AR6	sixth Assessment Reports from the IPCC (2021)
As	arsenic
ATP	adenosine triphosphate
BBP	benzyl butyl phthalate
bp	base pairs
BP	biological process
BPA	bisphenol A
BUSCO	Benchmarking Universal Single-Copy Orthologs
CA2	carbonic anhydrase 2, gene coding for
CAII	carbonic anhydrase 2, enzyme
$CaCO_3$	calcium carbonate
CAs	carbonic anhydrases (family of proteins)
cat	catalase, gene coding for
CAT	catalase, enzyme
CC	cellular component
cDNA	complementary DNA
CH_4	methane
cm	centimetre
CO_2	carbon dioxide
$CO_3^{=}$	carbonic ions
Cq	quantification cycle (qPCR)
Cr	chromium
Ct	cycle threshold

Cu	copper
CumWT	cumulative Akaike weights
Cu/Zn-SOD	copper/zinc superoxide dismutase
ΔAICc	second order Akaike information criterion
ΔCt	delta Ct
ΔΔCt	delta delta Ct
DBP	dibutyl phthalate
DEHP	di-2-ethylhexyl phthalate
DEP	diethyl phthalate
DiBP	di-isobutyl phthalate
DIC	dissolved inorganic carbon
DIDP	diisodecyl phthalate
DIOP	diisooctyl phthalate
DMEP	dimethyl glycol phthalate
DMP	dimethyl phthalate
DMSO	dimethyl sulfoxide
DNA	deoxyribonucleic acid
DnBP	dibutyl phthalate
DnOP	di-n-octyl phthalate
DPP	dipentyl phthalate
DSBs	double-strand breaks
E2	17β-estradiol
EB	estradiol benzoate
EC	enzyme commission number
EC50	half maximal effective concentration
ECPI	European Union commission regulation
EDCs	endocrine disruptive chemicals
EDTA	ethylenediaminetetraacetic acid
EE2	17α-ethinylestradiol
ER	estrogen receptor
ER1	estrogen related receptor, gene coding for
ER2	estrogen receptor, gene coding for
EREs	estrogen responsive elements
ERR	estrogen related receptor

EtOH	ethanol
Fe	iron
Fe-SOD	iron superoxide dismutase
FLU	fluoranthene
GABA	gamma-aminobutyric acid
GC	guanine-cytosine content
GHG	greenhouse gases
GO	gene ontology
GoI	gene of interest
GPx	glutathione peroxidase
GR	glutathione reductase
GS	glutamine synthetase, gene coding for
GSH	glutathione
GSSG	glutathione disulfide
GST	glutathione S-transferases
H^+	protons
H_2CO_3	carbonic acid
H_2O	water
H_2O_2	hydrogen peroxide
HAB	harmful algal bloom
HCO_3^-	bicarbonate
Hg	mercury
HSC70	heat shock protein 70, constitutive form, protein
HSPs	heat shock proteins (family of proteins)
HPS70, *hsp70*	heat shock protein 70, gene coding for
HSP70	heat shock protein 70
HSP90	heat shock protein 90, gene coding for
HSP90	heat shock protein 90
KCl	potassium chloride
kDa	kilodalton
IPCC	Intergovernmental Panel on Climate Change
KW-H	Kruskal-Wallis H test
LL	log likelihood
M	molar

Mb	million bases
MeER1	*M. edulis* estrogen related receptor, gene coding for
MeER2	*M. edulis* estrogen receptor, gene coding for
Me15	*M. edulis* sense primer for *mfp-1*
Me16	*M. edulis* antisense primer for *mfp-1*
MEP	monoethyl phthalate
MF	metabolic function
mfp-1	*Mytilus* foot protein 1, gene coding for
MgER1	*M. galloprovincialis* estrogen related receptor, gene coding for
MgER2	*M. galloprovincialis* estrogen receptor, gene coding for
MIQE	minimum information for publication of quantitative real-time PCR experiments
Mn	manganese
µg	micrograms
µg/mL	micrograms per millilitres
µm	micrometre
μm^2	squared micrometre
mg/L	milligrams per litre
mL	millilitres
Mn-SOD	manganese superoxide dismutase
MXR	multi xenobiotic resistance
NBD	nucleotide binding domain
ND	non detectable
N_2O	nitrous oxide
O_2	oxygen
O_2^-	superoxide anion
ORFs	open reading frames
p	*p* value
P	phosphorus
PAH	polycyclic aromatic hydrocarbon
Pb	lead
PBDEs	polybrominated diphenyl ethers
PBS	phosphate-buffered saline
PCB	polychlorinated biphenyls

PCR	polymerase chain reaction
ppb	parts per billion
ppm	parts per million
PSTs	paralytic shellfish toxins
psu	practical salinity unit
PVC	polyvinyl chloride
RFU	relative fluorescence units
RG	reference gene
RNA	ribonucleic acid
RNA-seq	RNA sequencing
ROS	reactive oxygen species
RT	reverse transcriptase
qPCR	quantitative PCR
SBD	substrate binding domain
SEM	standard error of the mean
SMI	sexual maturity index
sod, *SOD*	superoxide dismutase, gene coding for
SOD	superoxide dismutase, enzyme
SRH	Scheirer-Ray-Hare test
SSPs	shared socio-economic pathways
T	temperature, testosterone
Tm	melting temperature
TMM	trimmed mean of M values
TPM	transcript per million
UV	ultraviolets
V	volts
Vtg	vitellogenin, gene conding for
VTG	vitellogenin, protein
WHO	World Health Organisation
Zn	zinc

Scope of the thesis

Climate change and plastic pollution are both pressing environmental issues. Little is known, however, about the combined effect of climate change conditions (such as global warming and ocean acidification) and plastic contaminants (such as the additive di-2-ethylhexyl phthalate DEHP), and whether this effect differs by sex. In fact, sex and gametogenesis status of individuals can influence a vast array of biological responses of several species, including the commercially important blue mussel *Mytilus* spp.

This thesis investigates the consequences of DEHP exposure at environmentally relevant concentrations, alone or in combination with end-of-the-century simulated climate change conditions. A general effect of DEHP on mussel reproductive traits was observed, which confirmed the endocrine disruptive nature of this plasticiser. Specifically, fertility outcomes and estrogen receptor-related pathways were affected by the exposure, especially in female individuals. Overall, when combined with increased temperature or lowered pH, DEHP affected histological, molecular, transcriptomic, metabolic and behavioural systems at various degrees. Furthermore, as it was previously noted for other endocrine disruptive chemicals, the additive DEHP seemed to display a non-monotonic dose-response curve, provoking a stronger effect at low concentrations than at higher levels. Climate change stressors were also noticed to elicit a response in exposed individuals, especially increased temperature on spawning events and lowered pH on valve behaviours. Finally, when analysing the gene expression outcomes, sex and gametogenesis stage were considered useful predictive factors for interpreting the molecular datasets.

Chapter 1

Introduction and Literature Review

1.1 Mussels as bioindicator species

Bioindicators are useful sentinel species for the estimation of ecosystem quality, as they can evaluate contaminant presence and monitor environmental pollution in their habitats (Broeg and Lehtonen, 2006; Li et al., 2019a; Nigro et al., 2006; Rainbow and Phillips, 1993). More specifically, responses of bioindicators provide an accurate image of the ecosystem health at biomolecular, biochemical or community levels (Adams and Greeley, 2000; Burger, 2006). Essential characteristics of a valuable bioindicator can be summed as follows (Burger and Gochfeld, 2001; Gerhardt, 2002):

- Easy taxonomy.
- Large distribution and representativeness of the area.
- Sedentary status.
- Clear positions in the trophic web and definite feeding strategy.
- Sufficient long life and medium-long generation time.
- Cost-effective.
- Easiness to collect, handle and culture.
- Testable under natural and laboratory conditions.
- Unambiguous responses that can be measured and attributed to a cause.
- Reactiveness to anthropogenic action on the environment.
- Social relevance.

For these reasons, molluscs such as mussels are considered non-controversial biomonitors and key species for their habitats, as they are capable of high bioaccumulation and bioconcentration of toxicants (Markert et al., 2003). They are also common species for ecotoxicological experimental exposures to pollutants such as metals or anthropogenic chemicals (Burger, 2006; Pruell et al., 1986).

Mytilus is a complex and cosmopolitan genus of mussels (Koehn, 1991). In the temperate regions of the Northern Hemisphere, the most predominant *Mytilus* species are *Mytilus edulis* (Linnaeus, 1758), *Mytilus galloprovincialis* (Lamarck, 1819) and *Mytilus trossulus* (Gould, 1850). They often interbreed throughout their distribution area, due to incomplete reproductive isolation (Simon et al., 2019; Toro et al., 2002). Genomic overlaps and natural selection are the major drivers of hybrid zones in terms of their presence and

structure (Hilbish et al., 2002; Simon et al., 2019). In Great Britain, hybrids between *M. edulis* and *M. galloprovincialis* are found distributed in Scotland (Dias et al., 2009a; Dias et al., 2009b), southwest (Hilbish et al., 2002; Secor et al., 2001) and northeast England (**Chapter 2**, Mincarelli et al., 2021) at different proportions between the two main genotypes. Hybrids between *M. edulis* and *M. trossulus* are less frequent in nature, mostly due to the asynchronous reproductive cycles of the two species (Toro et al., 2002). Nonetheless, there are reports of their presence in Scotland (Dias et al., 2009a; Dias et al., 2009b).

1.2 Plastic pollution

Due to its characteristic of cheapness and durability, plastic has been considered in the past decades as a primary commodity for the manufacture of several everyday products (Andrady, 2011; Thompson et al., 2009). World plastic production reached almost 370 million tonnes in 2019 (including thermoplastics, polyurethanes, thermosets, elastomers, adhesives, coating, sealants and polypropylene fibres), and Europe is the third-largest producer of plastics in the world (PlasticsEurope, 2020). Present-day marine plastic waste is often associated with aquaculture and fishing practices, or improper disposal (Galgani et al., 2015; Schmaltz et al., 2020). Due to their resilient nature, plastic products can endure in different environments and through time (Thompson et al., 2009). Moreover, plastic can act as a carrier of additional chemicals, such as toxic plastic additives, contaminants or pathogens that the matrix has absorbed from the environment (Katsumiti et al., 2021; von Hellfeld et al., 2022; Rodrigues et al., 2022).

In the Northern Hemisphere, densities of plastic items from micro (<5 mm diameter) to macroparticles (>20 mm) are detected even in remote areas such as polar regions and the deep sea, where they are coupled with longer time for complete degradation (Barnes et al., 2009). The resulting environmental contamination of terrestrial (de Souza Machado et al., 2018) and aquatic organisms is widely recognised, affecting marine trophic levels from zooplankton (Heindler et al., 2017) to cetaceans (De Stephanis et al., 2013). In humans, plastic traces were recently found in faeces (Schwabl et al., 2019), lungs (Jenner et al., 2022) and in the placenta of pregnant women (Ragusa et al., 2021). In aquatic environments, small plastic parts or micro fractions may at ease be taken up and filtered by filter-feeding organisms (Browne, 2008) and be transferred via the food chain to higher

trophic levels such as crabs (Farrell and Nelson, 2013). Plastic traces are found in mussels from various sources, such as coastal waters, farms and supermarkets (Birnstiel et al., 2019; Li et al., 2018; Rochman et al., 2015). Fibres are detected as well in organs such as mantle and foot or fused with the byssus, suggesting an uptake and accumulation of plastics by adherence and not only by ingestion (Kolandhasamy et al., 2018; Li et al., 2019b). Exposure of bivalves to plastic particles has repercussions on their general health, from physical tissue abrasion (Hariharan et al., 2021; Masiá et al., 2021; Vasanthi et al., 2021) or reproductive disruption (Choi et al., 2022; Sussarellu et al., 2016) to metabolic, immune and genotoxic response (Bringer et al., 2022; Capolupo et al., 2021; Chelomin et al., 2022; Choi et al., 2021; Détrée and Gallardo-Escárate, 2018).

1.3 Endocrine disruptors and di-2-ethyl hexyl phthalate (DEHP)

Endocrine disrupting chemicals (EDCs) are exogenous substances or mixtures with effects on the general health of an organism or population (Rotchell and Ostrander, 2003; Soto et al., 2004). EDCs usually disrupt the production or the function of hormones and receptors or behave on the receptors with agonist or antagonist effects by hormone-mimicking (Goksøyr, 2007). Generally, endocrine disruptive substances can be of both natural and anthropogenic nature. Examples include estrogens, phytoestrogens, plasticisers, pesticides or herbicides (Aarab et al., 2006; Bila et al., 2007; Canesi et al., 2004). In the past, they were widely used in the industrial and agriculture sectors, while nowadays the use of most EDCs is restricted and limited to the pharmaceutical industry (Ciocan et al., 2010b; Porte et al., 2006). Despite the controlled use, EDCs can still enter the aquatic environment via effluent from industry or urban areas, where they can persist, accumulate and magnify in biological matrices due to their lipophilic nature (Arukwe et al., 1997; Langston et al., 2005; Matthiessen, 2003). Furthermore, numerous endocrine disrupting additives are still commonly used also to provide distinguishing characteristics to plastic products (Hermabessiere et al., 2017). Among plastic additives, phthalates have been widely used as emollients and plasticisers in polyvinyl chloride (PVC) products (Erythropel et al., 2014; Net et al., 2015; Parkerton and Konkel, 2000), with annual worldwide use of 8.4 million tonnes (ECPI, 2020). Phthalates could represent up to 50% of the total weight of certain plastic products (Earls et al., 2003; Van Wezel et al., 2000) and are typically found in the environment affecting habitats and organisms (**Table 1.2**;

Supplementary Tables 1.1 – 1.3; Lithner et al., 2011; Oehlmann et al., 2008). These additives leach from the plastic matrix as they are not chemically bonded to it, resulting in a consequent ubiquitous presence in the environment (Engler, 2012; Erythropel et al., 2014; Wittassek et al., 2011). For example, phthalate presence at various concentrations was detected in dust samples from Chinese houses and dormitories (Xu and Li, 2020). In aqueous environments, the migration of plastic chemical additives from everyday products was highlighted by Zimmerman et al. (2021), who identified in the sampled water several leachates able to cause oxidative response, antiandrogenic and estrogenic effects.

For humans, skin route and inhalation are possible ways of phthalate absorption, but the food chain remains the most probable, in particular for phthalates with a long molecular chain such as di-2-ethylhexyl phthalate (DEHP, **Fig. 1.1**, Schettler et al., 2006; Wittassek et al., 2011). Despite the restricted use in the European Union, especially in toys and childcare articles (EU Regulation 2018/2005) and the evidence of its toxicity in aquatic (Carnevali et al., 2010; Kim et al., 2002; Lu et al., 2013b; Zanotelli et al., 2010; **Table 1.3** and **1.4**) and terrestrial (Kalo et al., 2015; Mu et al., 2015) species, DEHP represents 40% of the global plastic softener market (ECPI, 2020). Natural production of DEHP by red algae (e.g., *Bangia atropurpurea*) was reported by Chen (2004) but the levels related to natural sources are considered negligible compared to the massive anthropogenic production (Net et al., 2015). Traces of DEHP have also been detected in the past in cosmetics and personal care products, such as nail polishes, sanitary pads, fragrances and baby lotions (Koniecki et al., 2011; Park et al., 2019). Even though phthalates were not classified as highly persistent compounds in many environments (Staples et al., 1997), DEHP levels were commonly measured in freshwater (Fatoki and Vernon, 1990) and marine systems (Hermabessiere et al., 2017, **Table 1.2**). Environmental persistence values for DEHP are approximately 1 day for atmospheric half-life, and 0.35 – 3.5 days for surface water and sediment half-life in aerobic conditions (Peterson and Staples, 2003). Nonetheless, DEHP was quantified at variable concentrations in marine environments up to 0.6 µg/L in coastal Mediterranean waters (Sánchez-Avila et al., 2012) and 71.6 µg/L in Tunisian marine waters (Jebara et al., 2021), with presence in open remote environments up to 0.005 µg/L in Arctic waters (Xie et al., 2007).

DEHP effects on *Mytilus* spp. range from alterations in antioxidant and peroxisomal enzyme activities at high levels of 100 - 500 µg/L (Cancio et al., 1998; Orbea et al., 2002) to hormetic effects on the expression of estrogen receptor-like (Mincarelli et al., 2021,

Chapter 2) and stress-related genes (Xu et al., 2021a) when environmentally relevant concentrations are dosed (**Table 1.4**). The hormetic effect is defined as a non-monotonic dose-response action of some endocrine-active chemicals such as DEHP. It can provoke a stronger effect at low concentrations and inhibition at higher levels (Conolly and Lutz, 2004; Do et al., 2012; Li et al., 2007, **Fig. 1.2**). The non-linear dose responses of EDCs such as DEHP is one of the main challenges for regulatory agencies in the course of risk assessment. In fact, a linear extrapolation of the compound toxicity from high-dosed experiments is not valid in most cases, as the occupancy of receptor-mediated pathways can saturate already at low doses. Furthermore, xenoestrogens such as EDCs modulate a physiologically active system, which in most cases already acts above the threshold (Welshons et al., 2003, **Fig. 1.2**).

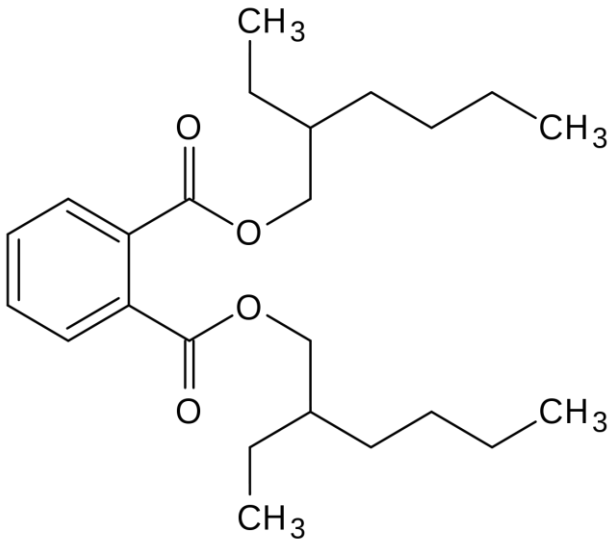

Fig. 1.1 DEHP structure. Chemical formula $C_{24}H_{38}O_4$. CAS Registry Number 117-81-7

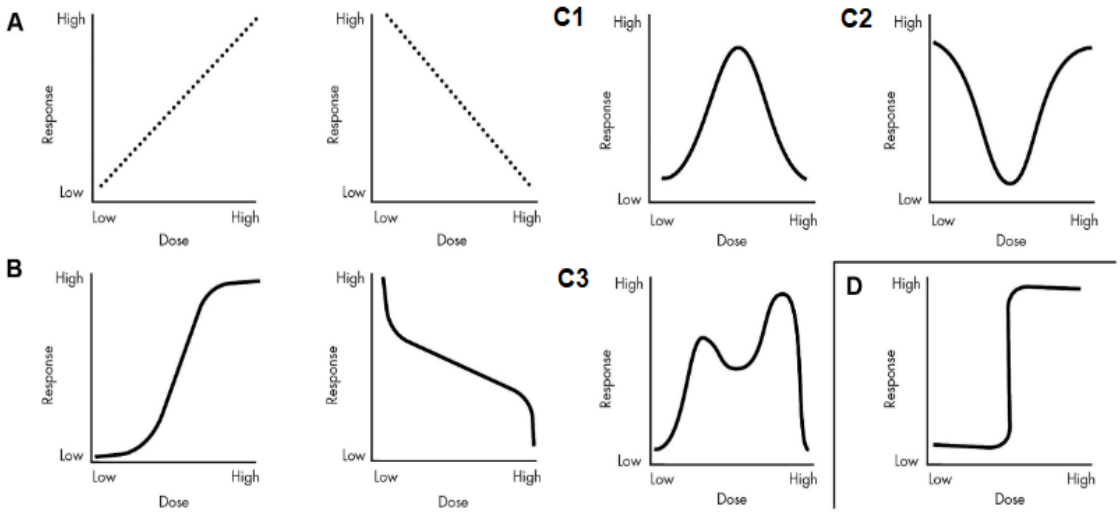

Fig. 1.2 Examples of dose-response curves from Vandenberg et al. (2012). **A)** Linear response. The predictions of the effects at variable concentrations are accurate as there is either a positive or an inverse linear association between dose and response. **B)** monotonic, non-linear response. In this case the slope changes in value but not in sign. The prediction of the effect at moderate doses cannot be extrapolated by the very low or very high doses. **C)** Non-monotonic dose-response curves (NMDRCs), including an inverted U-shaped curve (C1), a U-shaped curve (C2) and a multiphasic curve (C3). In this case, the sign of the slope can change one or more times and knowing one or more data points does not allow for projections or calculations about the effect of variable doses. **D)** Binary response. High doses have the same effect passing a threshold, while below the threshold low doses have no effect

1.4 Climate change and multiple stressors

Anthropogenic activities such as deforestation and the burning of fossil fuels have been causing an increase in levels of atmospheric greenhouse gases (GHG) such as methane (CH_4), nitrous oxide (N_2O) and carbon dioxide (CO_2) since the Industrial Revolution. It has been reported that CO_2 levels increased from ~280 parts per million (ppm) in the pre-industrial era to ~410 ppm today (IPCC, 2021). In 2014, the fifth assessment report (AR5) from the Intergovernmental Panel on Climate Change (IPCC) communicated a linear increase of CO_2 emissions in the past decades and a consequent rise of average temperatures around the globe, with the ocean temperature increasing on average a little more than 0.1°C per decade in the last 30 years (Lima and Wethey, 2012, **Fig. 1.3**). Additionally, around 30% of the CO_2 produced by anthropogenic activities is reported being absorbed by the ocean (IPCC, 2014). CO_2 that enters the ocean system reacts with

H_2O to form carbonic acid (H_2CO_3), which dissociates in protons (H^+) and bicarbonate (HCO_3^-). The latter dissociates in carbonate ($CO_3^=$) and protons (Dickson et al., 2007; Gattuso et al., 2010). Thus, the additional CO_2 added to the water system shifts the carbonate balance between CO_2, HCO_3^- and $CO_3^=$, increasing the free protons and therefore decreasing the oceanic pH. The increase in atmospheric CO_2 levels has already led to a reduction of 0.1 pH units in surface oceanic layers with respect to pre-industrial levels (IPCC 2021, **Fig. 1.4**).

The sixth report (AR6) from the IPCC assessed the climate responses for the end of the century under five different scenarios (shared socio-economic pathways SSPs), calculated by considering climate mitigation, air pollution and socio-economic assumptions. SSPs vary accordingly to GHG emission projections for the middle and the end of the century, as follows:

I. Very low SSP (1 - 1.9) and low SSP (1 - 2.6), where the emissions of CO_2 decline to zero around or after the middle of the century.
II. Intermediate SSP (2 - 4.5) where CO_2 emissions remain around the current level until the year 2050.
III. High (SSP 3 - 7) and very high (SSP 5 - 8.5) scenarios, where CO_2 emissions double from current levels by 2100 and 2050, respectively.

The projected conditions of global warming and ocean acidification are also leading to additional processes such as enhanced ocean stratification, increased vertical density gradients, changes in oceanic currents, modification in the seawater chemistry and alteration of nutrient input, primary production, tropospheric ozone and oxygen concentration (Bijma, 2013; Kwiatkowski et al., 2020; Noyes et al., 2009). Interestingly, a recent study reported that *M. edulis* adults exposed to moderate environmental acidification are metabolically more tolerant to this stressor compared to increased temperature exposures (Matoo et al., 2021). Similarly, in Gazeau et al. (2014), Wang et al. (2015) and Newcomb et al. (2019), future thermal conditions were hypothesised to be a major threat to *M. galloprovincialis*, *M. coruscus* and *M. trossulus* rather than ocean acidification. This could be related to the fact that species inhabiting coastal areas are already adapted to natural pH fluctuations of the intertidal zone (Pansch et al., 2014).

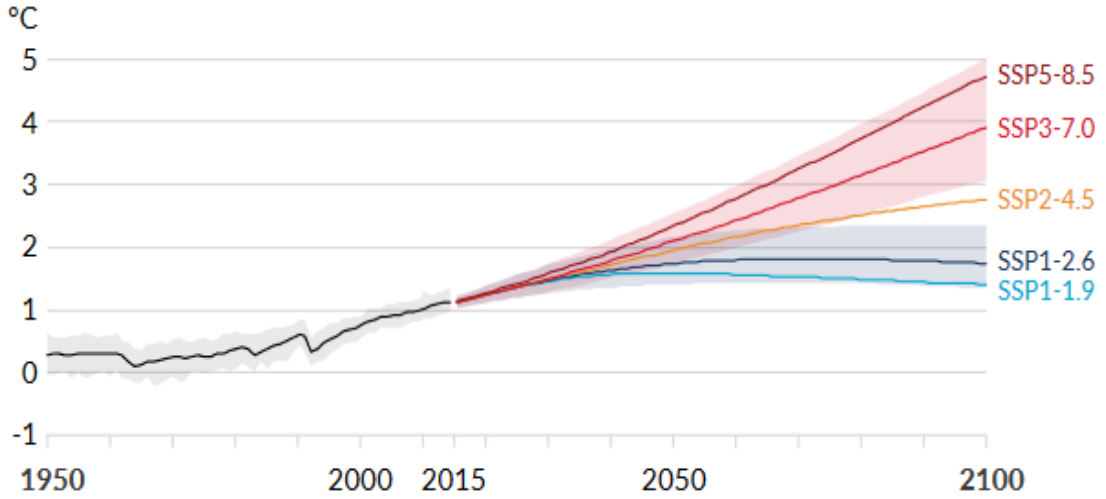

Fig. 1.3 Current and projected values for global surface temperature under five different simulated scenarios (shared socio-economic pathways, SSP 1 - 8.5), where shades represent very likely ranges for SSPs 1 - 2.6 and SSP 3 - 7. Data were obtained by combining model simulations (CMIP6) and observational constraints based on past warming simulations and updated assessments of equilibrium climate sensitivity. From Climate Change 2021: The Physical Science Basis. Contribution of Working Group I to the Sixth Assessment Report of the Intergovernmental Panel on Climate Change (IPCC, 2021)

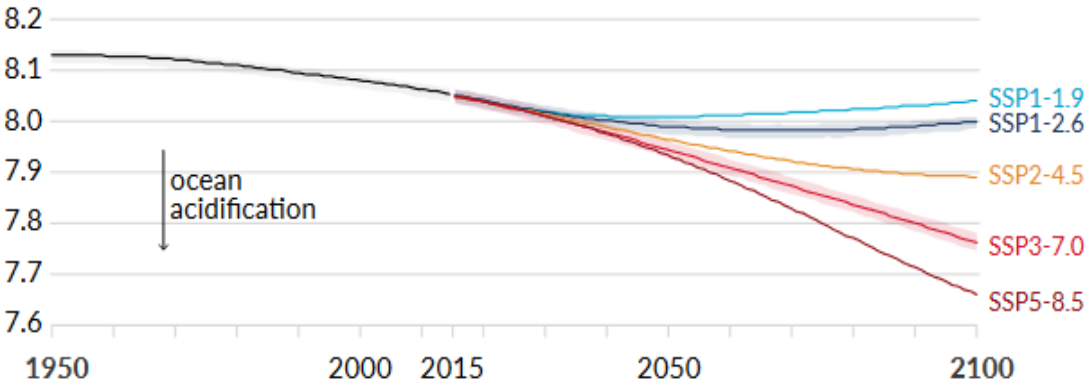

Fig. 1.4 Current and projected values for oceanic surface pH based on model simulations (CMIP6) under five different simulated scenarios (Shared socio-economic pathways, SSP 1 - 8.5), with shades representing very likely ranges for SSPs 1 - 2.6 and SSP 3 - 7. From Climate Change 2021: The Physical Science Basis. Contribution of Working Group I to the Sixth Assessment Report of the Intergovernmental Panel on Climate Change (IPCC, 2021)

In addition, pollutants frequently alter their toxicity in such environmental-changing conditions, and chemicals often impact the adaptation ability of organisms to environmental fluctuations (Bijma et al., 2013; Han et al., 2014; Kibria et al., 2021;

Landis et al., 2014; Nikinmaa, 2013; Noyes et al., 2009; Patra et al., 2007; Schiedek et al., 2007). Contaminants and environmental factors can act synergistically and weaken the defence systems and regulation mechanisms as well (Bodin et al., 2004, **Table 1.5**). In this climate-changing era, it becomes clear that it is extremely important to investigate the repercussions of exposure to certain chemicals when global warming and ocean acidification conditions are considered.

1.5 Sex- and season- associated alterations in *Mytilus* spp.

The reproductive cycle of molluscs is dissimilar between males and females, in terms of timing for reaching ripe and resting stages (Mladineo et al., 2007; Sunila, 1981), number of gametes released at different time points of the spawning season (Anantharaman and Craft, 2012), and estrogen and androgen content (Smolarz et al., 2018). Sex may affect both contaminant uptake and elimination, and biomarker levels and activities (Blanco-Rayón et al., 2020; Burger, 2007; Damiens et al., 2004; Jiang et al., 2021; Matozzo and Marin, 2010; McClellan-Green et al., 2007; Wilhelm Filho et al., 2001) and natural differences in basal antioxidant levels between males and females could favour one sex over the other when coping with stressful environments (Gismondi et al., 2012; Grilo et al., 2018; Sroda and Cossu-Leguille, 2011). Sex-specific differences were noted in exposure studies, such as *M. galloprovincialis* exposed to tetrabromobisphenol A (TBBPA) or 17β-estradiol (E2, Ciocan et al., 2010a; Ji et al., 2016) or *D. polymorpha* exposed to benzo(a)pyrene (Riva et al., 2011). With regard to plastic exposure experiments, the literature about sex-specific differences in aquatic organisms is still scarce, but it seems that exposure to environmentally relevant levels of polystyrene microplastic for two months has sex-specific endocrine disruptive ability in fish *Oryzias melastigma* sexes. In fact, females displayed downregulation of genes involved in the hypothalamus-pituitary-gonadal axis and steroidogenesis, with consequent decreased E2 and testosterone levels in plasma, with opposite results in males (Wang et al., 2019).

Furthermore, as for many aquatic species, the basal levels of cellular biomarkers in mussels vary naturally through the seasons, which also influence the gametogenesis cycle. As examples for *M. edulis*, seasonal changes within sexes were observed for clock-associated genes involved with endogenous biological rhythms (Chapman et al., 2017) and innate immune functionalities were noted to be temperature- and season- sensitive

(Wu and Sokolova, 2021). The environmental changes associated with seasons play also a decisive role in antioxidant activities, which display low values in winter, due to the reallocation of energies for reproduction (Angilletta and Sears, 2000; Power and Sheehan, 1996), with a consequent increase in reactive oxygen species (ROS) production due to the increase in the intracellular respiration (Béguel et al., 2013). Conversely, antioxidant levels are usually found high in spring and summer (Agnaou et al., 2014; Dellali et al., 2001; Elazzaoui et al., 2019), often associated with increased metabolic rate (Orbea et al., 1999; Viarengo et al., 1991). In exposure experiments, season-related responses were also noticed on the hazard quotient of cadmium in *M. galloprovincialis* exposed to combinations of low pH and high temperature in different seasons (Nardi et al., 2017, 2018).

Abiotic factors such as temperature and contaminant presence can also have contrasting effects when the exposed organisms are in a particular stage of their reproductive cycle. The different sensitivity of aquatic species to xenobiotic exposure during the reproductive phases has been investigated over the years (Ciocan et al., 2010a; Cubero-Leon et al., 2010; González-Fernández et al., 2016; Louis et al., 2021; McCahon and Pascoe, 1988). For example, in *M. galloprovincialis*, gonadal bioaccumulation of elements such as manganese (Mn), zinc (Zn), arsenic (As) or phosphorus (P) was noted to be sex- and maturation- driven (Kapranov et al., 2021). Additionally, the gonadal initial development period seemed to be the most sensitive stage to endocrine disruption for mussels (Ciocan et al., 2010a). Considering this, assessing sex and gametogenesis stage could be a valuable asset in contextualising molecular datasets and interpreting toxicology results, especially the ones involving sex-related or reproduction-depended genes.

1.6 Biological responses investigated in this thesis

This thesis investigated the biological responses of blue mussels, an economically relevant species, when exposed to the endocrine disrupting additive DEHP under different environmental scenarios. The experimental conditions were chosen considering the current state of marine environmental plastic pollution and the expected average climate change conditions for the year 2100. Moreover, the choice of combined exposure was rationalised considering that exposure experiments involving multiple stressors

frequently present a complex array of responses that differ from the ones observed from the exposure to the single stress sources (Nowicki and Kashian, 2018).

In this thesis, **Chapters 2** and **3** investigate the effect of different concentrations of the endocrine disruptor DEHP in combination with a global warming scenario. **Chapter 2** considers the gonadal alterations at the histological and molecular levels, investigating gametogenesis-, stress- and reprotoxicity- related biological responses (**Table 1.1**). Using RNA-sequencing analysis, **Chapter 3** focuses on the overall gene expression in male gonads. **Chapter 4** and **5** analyse mussel responses to DEHP under an ocean acidification scenario. Similar to **Chapter 2**, **Chapter 4** analyses mussel responses from histological and molecular datasets (**Table 1.1**), while **Chapter 5** analyses behaviours and metabolic changes. For the final **Chapter 6**, the effect of DEHP on female reproductive capacity and fertility is examined. The biological responses investigated in this thesis are described in detail in the following paragraphs.

Table 1.1 Molecular biomarkers of general stress, reproductive toxicity and pH homeostasis with correspondent genes and GenBank accession numbers investigated in this thesis. Biomarkers are defined as any measurement at molecular, biochemical, cellular or physiological levels that reflect any interaction between a biological system and a potential hazard (WHO, 2001)

BIOMARKER	GENE	GENBANK ACCESS NO.	SIZE	REFERENCE AUTHOR
Superoxide dismutase	*sod*	**AJ581746**	765 bp	Molecular cloning of the Cu/Zn superoxide dismutase in the blue mussel *Mytilus edulis*, Manduzio et al., unpublished
Catalase	*cat*	**AY580271**	813 bp, partial code	Peterson et al., (2004)
Estrogen related receptor	*MeER1*	**AB257132**	2036 bp	Puinean et al., (2006)
Estrogen receptor	*MeER2*	**AB257133**	1744 bp	Puinean et al., (2006)
Heat shock protein 70	*hsp70*	**AF172607**	570 bp, partial code	Differential expression of MXR related genes in blue mussel (*Mytilus edulis*), Luedeking et al., unpublished
Carbonic anhydrase	*CA2*	**LK934681.1**	1531 bp, partial code	Pratt et al., (2015)

1.6.1 Gametogenesis stage and histological changes

The reproductive cycle of British mussels has been extensively examined in the past decades (Chapman et al., 2017; Lowe et al., 1982; Secor et al., 2001; Seed, 1969). The dependency of mollusc gametogenesis on geographic distribution (Virgin and Barbeau, 2017), endocrine disruptor presence (Siah et al., 2003), environmental conditions (Fearman and Moltschaniwskyj, 2010; Numata and Udaka, 2010; Subramaniam et al., 2021; Tessmar-Raible et al., 2011), nutrient availability and energy reserves (Fearman et al., 2009; Hilbish and Zimmerman, 1988; Kang et al., 2006; Newell et al., 1982: Roden and Burnell, 1984) is likewise well-known. Considering the sensitivity of *Mytilus* spp. reproductive stages to external stimuli, it is worth noting that their gametogenesis cycle cannot be universalised, as it differs between regions or through different years in terms of development time or number and duration of the spawning events (Ciocan et al., 2010a; Duinker et al., 2021; Lowe, 1982; Secor et al., 2001; Seed, 1969).

Variations of temperature can also influence the reproductive cycle in molluscs (Fabioux et al., 2005; Zapata-Restrepo et al., 2019), similar to other species such as gastropods (Sternberg et al., 2010) and fish (Anguis and Cañavate, 2005). Together with other environmental stress cues, temperature could induce attenuated seasonality in bivalve gametogenesis cycle and increased or advanced spawning activity (Bayne 1976; Petes et al., 2008; Philippart et al., 2003; Sreedevi et al., 2014), especially if the gametes are mature (Seed, 1976). In male molluscs, thermal stress was previously reported to affect *M. galloprovincialis* sperm quality (Boni et al., 2016) and *Crassostrea virginica* testicular functions (Nash and Rahman, 2019).

Regarding the acidification effect on mollusc gametogenesis, there is still scarce knowledge about the effect of low pH conditions on the reproductive cycle, especially considering that coastal species could be highly tolerant to local pH variability due to tides, currents or the proximity to river and estuary ecosystems. Recently, Zhao and colleagues (2019) found that 40-day exposure to 7.7 pH decreased the percentage of *M. senhousia* spawning gonads, suggesting susceptibility to prolonged acidified conditions in the final gametogenesis stages. Reed et al. (2021) also observed unaltered responses in terms of size-frequency of oocytes in the benthic bivalves *Astarte crenata* and *Bathyarca glacialis* under the combination of acidification and warming, suggesting some sort of resiliency of Arctic mollusc gametogenesis to climate-changing conditions. However, the authors still doubted a successful fertilisation or viable development of eggs in natural

conditions. In fact, some associated factors such as food availability could still be compromised in future climate scenarios, also considering that an abnormal gametogenesis cycle could not provide the time necessary for energy storage during the resting period, causing consequences such as impairment of the offspring quality or alteration in the reproductive capacity (Fearman et al., 2009).

Considering the effect of EDCs, exposure to these xenoestrogens can cause a wide set of histological reactions in molluscs. Exposure to E2 was observed to induce alteration in oocyte diameter and vitellin protein content in *Crassostrea gigas* (Li et al., 1998) and increase the gamete release by serotonin in scallops *Patinopecten yessoensis* and *P. magellanicus* (Osada et al., 1992, 1998). However, little is still known about the effect of plasticisers on gametogenesis traits of mussels.

1.6.2 Antioxidant system

Changes in antioxidant levels are biomarkers of contamination and stress for a wide variety of marine organisms, including mussels (Regoli et al., 2004; Regoli and Principato, 1995). In fact, the incomplete reduction of oxygen (O_2) during the respiration process is a source of ROS production, which are potent oxidants (Morel and Barouki, 1999). In normal conditions, the adverse effects of radical species are blocked by a wide range of cellular scavengers and antioxidant enzymes (**Fig. 1.5**, Halliwell and Gutteridge, 2015; Regoli and Giuliani, 2014). Imbalanced redox homeostasis causes oxidative stress in the cell and it can occur after a ROS overproduction or antioxidant defence perturbation, leading to DNA damage, lipid peroxidation and enzyme inhibition (Winston and Di Giulio, 1991). This can be the effect of exogenous stress such as contaminant and xenobiotic presence, hyperoxia or UV irradiation (Morel and Barouki, 1999).

Superoxide dismutase (SOD), catalase (CAT) and glutathione peroxidase (GPx) are considered first-line defence antioxidants (Ighodaro and Akinloye, 2018). SOD (EC 1.15.1.1) enhances the dismutation of two molecules of the reactive superoxide anion (O_2^-) into oxygen and hydrogen peroxide (H_2O_2), whereas CAT and GPx decompose the H_2O_2. H_2O_2 is known to be toxic if accumulated at high levels, while at low amounts is involved in some cellular functions such as cell proliferation or apoptosis (Ighodaro and Akinloye, 2018). SOD is a metalloenzyme that requires a metal as cofactor such as iron (Fe), zinc (Zn), copper (Cu) or manganese (Mn) for its activity. Fe-SOD is distributed in

prokaryotes and chloroplasts, Mn-SOD is found in eukaryotic mitochondria and in prokaryotes, and Cu/Zn-SOD is commonly observed in the cytosol of eukaryotes, peroxisomes and chloroplasts (Gill and Tuteja, 2010; Ighodaro and Akinloye, 2018; Karuppanapandian et al., 2011). CAT (EC 1.11.1.6) is a 240 kilodalton (kDa) tetrameric protein with four similar subunits, each weighing 60 kDa containing one ferriprotoporphyrin. It is usually found in the peroxisomes and uses iron or manganese as cofactor, reducing hydrogen peroxide (H_2O_2) to water and oxygen. At low concentrations, CAT modules the detoxification of phenols and alcohols in conjunction with the H_2O_2 reduction (Regoli and Giuliani, 2014).

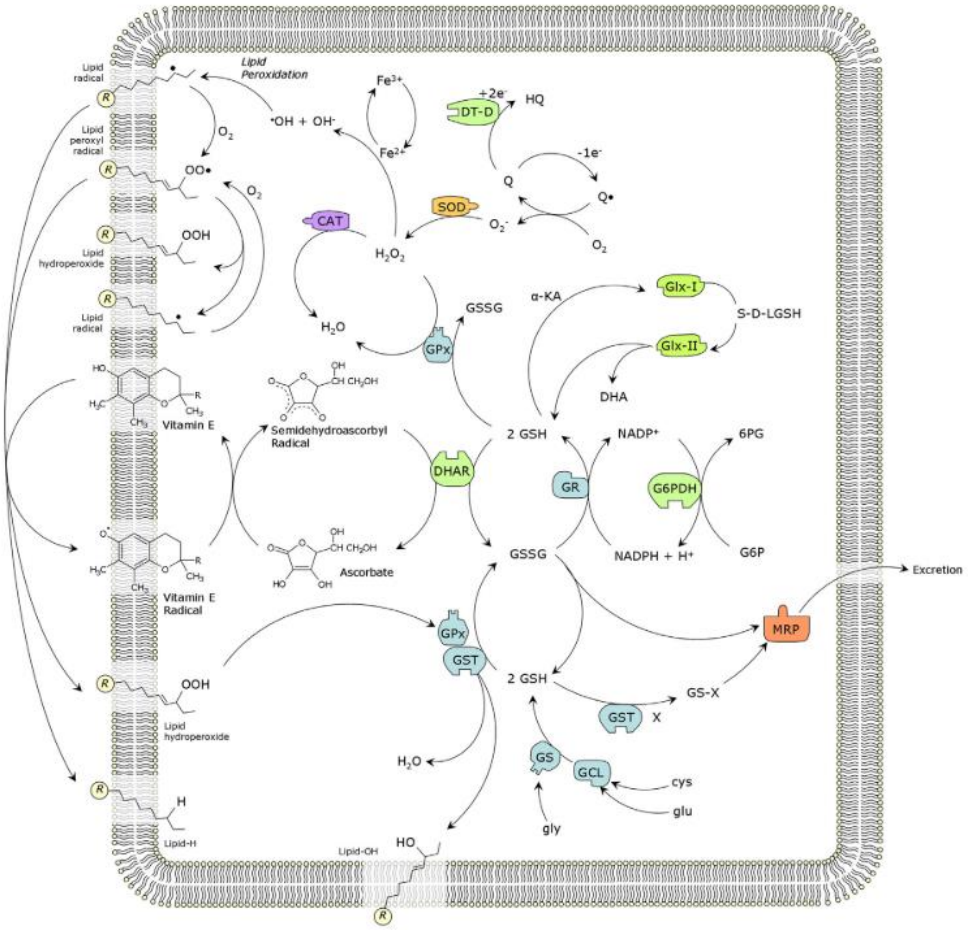

Fig. 1.5 Cellular antioxidant defences and pathways in marine organisms from Regoli and Giuliani (2014)

1.6.3 Heat shock protein 70

Heat shock proteins (HSPs) are molecular chaperones involved in cellular protection against stressors such as heat, UV light and xenobiotic exposure (Sanders, 1993). HSPs

are usually synthesised during normal conditions, highly conserved between bacteria and eukaryotes and essential for cell functionality (Wu, 1995). They are found in several cell compartments such as cytosol, mitochondria or endoplasmic reticulum (Tutar and Tutar, 2010). HSPs' primary function is the prevention of protein aggregation, achieved by the interaction of several HSP isoforms and regulatory cofactors that ensure the correct spatial arrangement and folding of cellular proteins (Franzellitti and Fabbri, 2005; Kabani et al., 2002; Shorter and Lindquist, 2008, **Fig. 1.6**).

The HSP isoform 70 (70 kDa) is a highly conserved and versatile member of the HSP family that conserves 50% of its sequence between *E. coli* and humans (Schlesinger, 1990). HSP70 is linked with protein metabolism under stress conditions, membrane translocation, regulatory processes and misfolded protein sequestration (Feder and Hofmann, 1999; Fink, 1999; Franzellitti and Fabbri, 2005; Hartl, 1996). For these reasons, it is used as a biomarker of stress response to environmental perturbation (Encomio and Chu, 2005; Lewis et al., 1999) or xenobiotic exposure (Del Rey, 2011; Franzellitti and Fabbri, 2005; Geraci et al., 2004; Koagouw et al., 2021a, b; Liu et al., 2014). HSP70 consists of a calmodulin-binding site connected to a C-terminal substrate-binding domain (SBD, ~25 kDa) and an N-terminal nucleotide-binding and highly conserved domain (NBD, ~45 kDa) containing an ATP binding site (Mayer, 2010; Schlesinger, 1990). The NBD has a horse-shoe structure and it is divided into four sub-domains (IA, IB, IIA, IIB), while the SBD is divided into a β-sheet base and an α-helical lid (Kumar and Mapa, 2018; Tutar and Tutar, 2010).

In several organisms including mussels, HSP70 is present in a constitutive (HSC70) and an inducible (HSP70) form (Franzellitti and Fabbri, 2005; Tutar and Tutar, 2010). The constitutive form HSC70 was previously described solely as a molecular chaperon in unstressed conditions. In fact, several *in vitro* experiments reported HSC70 not to be stress-dependent in frog kidney epithelial cell lines (Ali et al., 1996) or trout hepatocytes (Boone and Vijayan, 2002). However, recent studies observed that prolonged or chronic stressors can induce its expression in some animals such as fish exposed to salinity and temperature alterations (Deane and Woo, 2004, 2005). Exposure time and different heavy metal exposures were as well noted to alter both the constitutive and inducible forms of sea urchin *Paracentrotus lividus* HSP70 (Geraci et al., 2004). Similarly, *M. galloprovincialis* exposed for one week to thermal stress and heavy metals (mercury Hg^{2+} or chromium Cr^{6+}) exhibited distinct temporal-related expressions of the two forms in the

digestive glands, constituted by an HSP70 short-term induction and higher levels of HSC70 after prolonged exposure (Franzellitti and Fabbri, 2005).

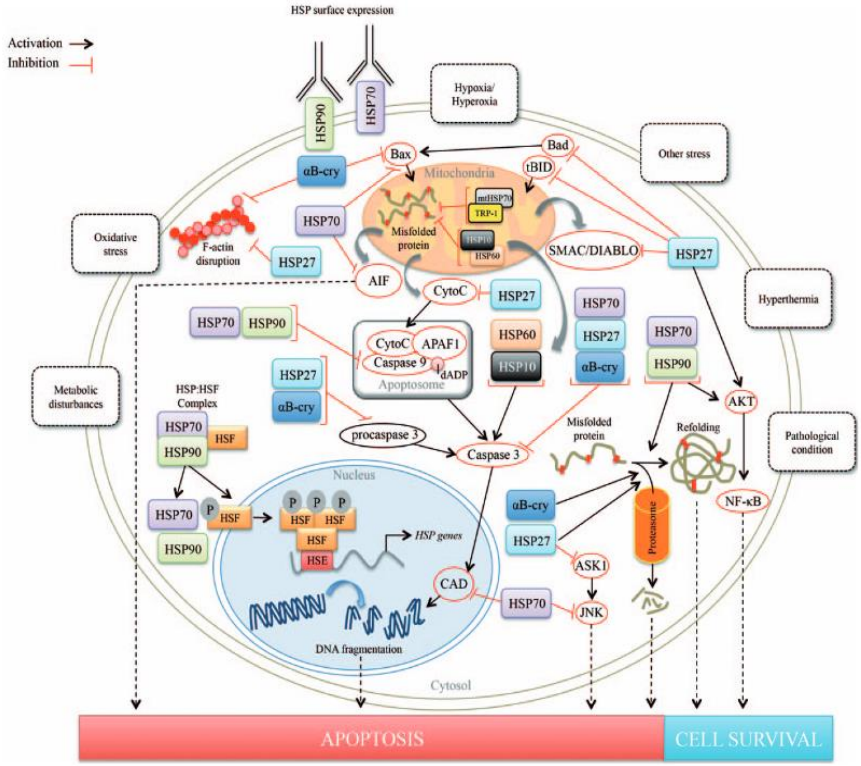

Fig. 1.6 Overview of the mammal's major HSP cellular pathways activated by heat, metabolic state, hypoxia and hyperoxia, oxidative stress and pathologies from Fittipaldi et al., (2013)

1.6.4 Carbonic anhydrase 2

Carbonic anhydrase enzymes (CAs, EC 4.2.1.1) are a group of zinc metalloenzymes present in both prokaryotes and eukaryotes that control the intra- and extracellular pH homeostasis, catalysing the reversible hydration from carbonic dioxide to bicarbonate $CO_2 + H_2O \leftrightarrows HCO_3^- + H^+$ (Richier et al., 2011). They are found in animals, photosynthesising organisms and in some non-photosynthetic bacteria (Lindskog, 1997). CA isoforms are involved in controlling calcium reserves, ionic transportation, electrolyte balance, biocalcification, carboxylation or decarboxylation reactions (Bertucci et al., 2013; Henry and Swenson, 2000; Lionetto et al., 2006; Sharker et al., 2021; Voigt et al., 2021; Zoccola et al., 2016, **Fig. 1.7**). Additionally, some CA isoforms are involved in gluconeogenesis and ureagenesis in mammals and photosynthesis in photosynthetic organisms (Badger and Price, 1994; Davis et al., 2010).

The biomineralization-related α CA family catalyses carboxylation and decarboxylation (Sharker et al., 2021). The α type is a family majorly found in the animal kingdom that includes different vertebrate isozymes, classified accordingly to their localisation in the cell: cytosolic (which includes CAII form), membrane-bound, transmembrane, mitochondrial and extracellular (Cardoso et al., 2019; Picaud et al., 2009). They present an amino-terminal region, a central antiparallel and twisted β-sheet that surrounds the Zn^{2+} ion with short helices on the molecule surface. The zinc ion is located at the bottom of a cone-shaped cavity of the CA active site and interacts with three conserved residues of histidine (Lindskog, 1997). So far, there are 16 known isoforms from the α family in mammals and numerous novel isozymes in other vertebrates, with distinct biophysical properties and localisation in the cells (Esbaugh and Tufts, 2006; Hassan et al., 2012). CAII is one of the most studied forms of the α family, as it is well-distributed in animal tissues and expressed in almost all cells with a high hydration turnover rate for CO_2 (Lindskog, 1997; Sterling et al., 2001). In mammals, it was observed that I, II and III isoforms shared a high similarity of the secondary structures and CAII is involved in nasal CO_2 chemosensitivity, bone resorption, urine acidification and gas exchange and it could be a target in the drug treatment of glaucoma, obesity or cancer (Hassan et al., 2012; Lindskog, 1997). In molluscs such as oysters and mussels, it appears that many members of the αCA family evolved from different lineage pressures and species-specific gene duplication events, which occurred before the divergence between protostome and deuterostome (Cardoso et al., 2019).

A drop in pH is known to induce down-regulation of carbonic anhydrase gene transcription in several calcifying species (Zebral et al., 2019), including coccolithophores (Richier et al., 2011), corals (Zoccola et al., 2016) and molluscs (Dickinson et al., 2012; Ren et al., 2014). A related consequence is the loss of shell structural integrity, due to alteration in the capacity to deposit the aragonite and calcite (calcium carbonate forms, Fitzer et al, 2014). This makes CA a useful biomarker for pH-induced responses. Additionally, the measurement of CA activity is a useful tool for assessing organism sensitivity to chemical pollutant toxicity (Lionetto et al., 1998). Metalloid elements are known to induce alteration in CAs for molluscs and crustaceans (Lionetto et al., 2006; Skaggs and Henry, 2002). This could be related to the metal-binding affinities of CAs and to the effective osmo-, iono- regulatory and acid-base disruption ability of certain metals with respect to other chemicals (Bianchini, 2005;

Bianchini and Carvalho De Castilho, 1999; Lionetto et al., 1998; Skaggs and Henry, 2002).

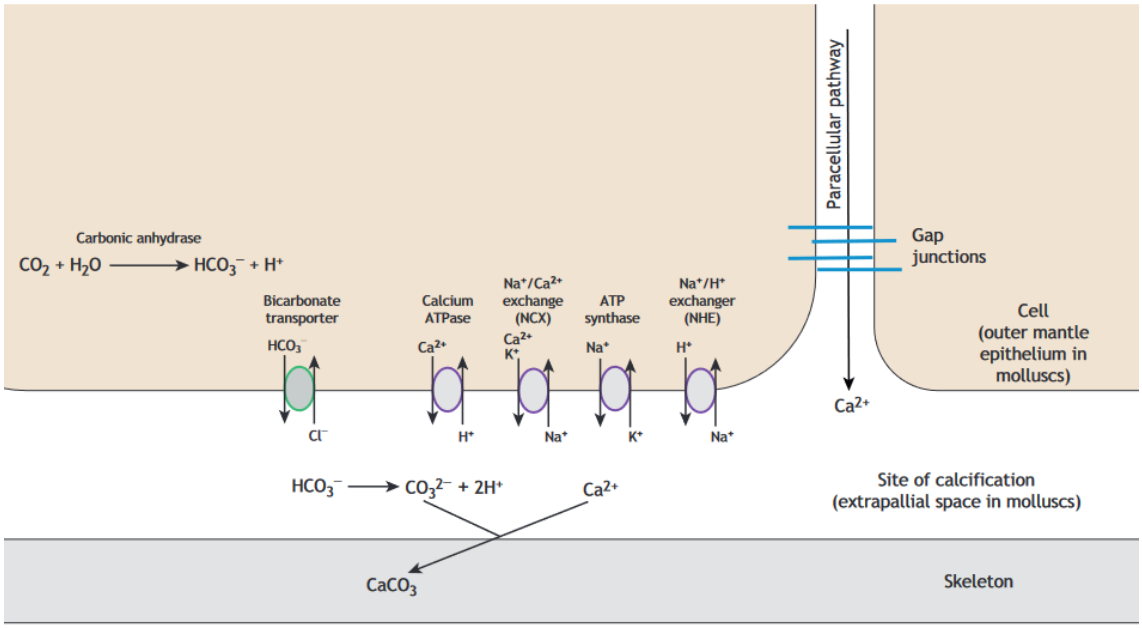

Fig. 1.7 Molecular mechanisms of ion transporters for biomineralisation and calcification in marine invertebrates from Clark, (2020). Calcium ions enter the calcification site via calcium ATPase and Na^+/Ca^{2+} exchangers. To regulate the balance between internal pH and water, carbonic anhydrase produces the by-products bicarbonate ions, which are secreted in the extra pallial space and form calcium carbonate with calcium ions

1.6.5 Estrogen receptor-like genes

In most invertebrates, the functions and regulation of endogenous sex steroid hormones remain partially understood or unclear in many cases with a consequent lack of knowledge about their biomarkers (Puinean and Rotchell, 2006). The presence of sex steroids and their related receptor has been studied in several projects involving invertebrate species (Bannister et al., 2007; Kajiwara et al., 2006; Köhler et al., 2007; Ni et al., 2013; Reis-Henriques et al., 1990; Stefano et al., 2003), highlighting the possibility for molluscs to share an archaic estrogen-related signalling mechanism with vertebrates (Eick and Thornton, 2011; Thornton et al., 2003). It is worth noting that the presence of putative endogenous sex steroids (e.g., progesterone, androstenedione, testosterone, 5α-dihydrotestosterone, 17β-estradiol, estrone, androsterone or 3α-androstanediol) in molluscs and their role in the reproductive system has been investigated for over three decades and testosterone, estradiol and estrone were as well detected in mussel tissues

(Lafont and Mathieu, 2007; Reis-Henriques et al., 1990; Stefano et al., 2003; Zhu et al., 2003). Some studies still doubt that the presence of steroid hormones in mussels is due to an endogenous origin but related to the animals' filtration and concentration of hormones released from other organisms in the water environment (Scott, 2012, 2013). However, tissue-specificity and alterations of the receptors involved in the endocrine pathway were found after exposure to synthetic estrogens in several publications. As an example, estrogen receptor (ER) gene expression was confirmed to occur in the female oocytes and follicles but not in the vesicular tubular clusters of *M. galloprovincialis* (Agnese et al., 2019; Nagasawa et al., 2015). Furthermore, diverse levels of steroids such as progesterone or E2 were found in the two sexes (Reis-Henriques and Coimbra 1990) or in different seasons of the year (Kaloyianni et al. 2005).

In vertebrates, estrogen receptors (ERs) are a group of nuclear receptors belonging to a superfamily of steroid hormones that mediate the signalling involved in the estrogen pathway, including the interaction with agonist and antagonist disruptors. They are the first regulators within a complex web of signals which regulate reproduction and behaviours of vertebrates (Keay and Thornton, 2009). ER consists of an N-terminal domain that modulates the transcription, a conserved C-terminal domain that interacts with the DNA helix and a ligand-binding domain (Klinge, 2001). When estrogen crosses the cell membrane, it binds the estrogen receptor that dimerises in order to bind target estrogen-responsive elements (EREs) located in the promoters of target genes and induces specific gene transcriptions (Rotchell and Ostrander, 2003). ERs can also regulate the target gene expression without binding EREs, for example via protein-protein interaction or non-genomic mediation by membrane-associated ERs and signal cascade pathways (Björnström and Sjöberg, 2005). ER in mammals is encoded by two subtypes α and β and it is activated in response to the binding to the ligand, changing its conformation in addition to the dissociation of proteins such as HSPs. Similarly, in fish, receptors for androgen and estrogen are located in a nucleus complex with different HSPs that act as stabilisers of the dissociation of the receptors during inactivity periods (Rotchell and Oestander, 2003).

Estrogen-related receptors (ERRs) are orphan nuclear receptors that share a similar structure and sequence with ERs, being however not activated by estrogens and binding their own response elements (Nagasawa et al., 2015). In humans, some ERR isoforms were proposed to be prognostic breast tumour markers and it appears that an *in vitro* protein-protein interaction is present between ERR type α and ER type α. Like many

nuclear receptors, ERR presents a DNA-binding domain and a C-terminal ligand-binding domain. Binding to ligands results in conformational change and cofactor recruitment that modify the chromatin and cause expression of the target genes (Horard and Vanacker, 2003). In invertebrates, the ERRs are not very well understood.

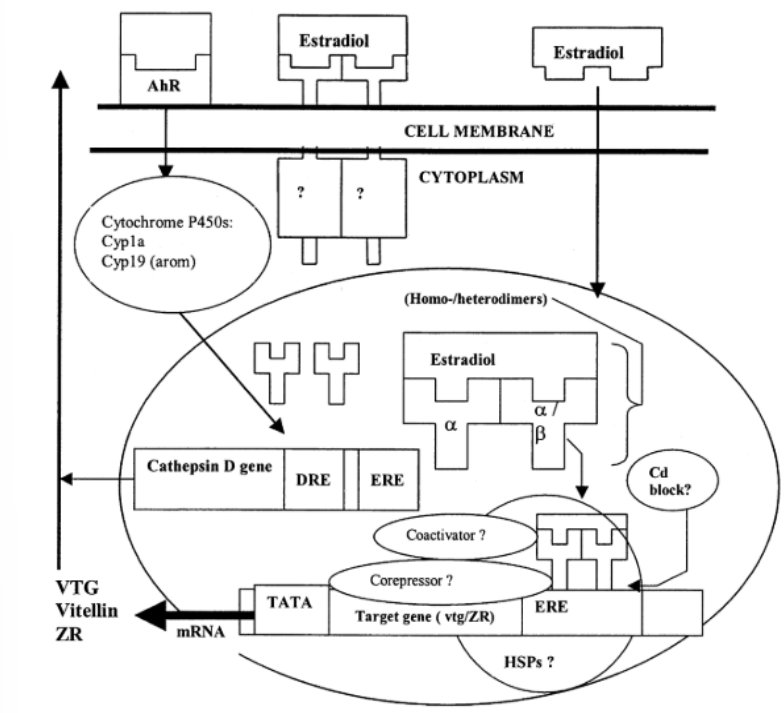

Fig. 1.8 ER hypothetical activation process in invertebrates from Rotchell and Ostrader (2003), after the estradiol cross of the membrane and the bind within the nucleus and the subsequent bind of the estrogen-responsive elements (ERE) and the possible involvement of coactivators and corepressors

Regarding *Mytilus* spp., the pattern of expression of estrogen receptor-like genes seems to follow the natural reproductive cycle of mussel gonads. A recent study by Agnese et al. (2019) observed the *M. galloprovincialis* estrogen-related receptor *MgER1* highest levels in full-grown oocytes, while estrogen receptor *MgER2* had the highest level during the vitellogenesis stage, when follicles are ripe. This highlights the possibility of a different involvement of the two receptors in the gametogenesis, considering that *ER1* is activated via a feedback mechanism by downstream factors (Horard and Vanacker, 2003; Nagasawa et al., 2015) and *ER2* is responsive to estrogen-like factors (**Fig. 1.8**). Bivalves are as well sensitive to endocrine disruptive compounds (Puinean et al., 2006) and xenobiotics may interfere in the signalling cascades involved in the endocrine pathways and induce abnormalities in invertebrates (Aarab et al., 2006; Janer and Porte, 2007).

1.6.6 Respiration and valve behaviours

For freshwater and marine mussels, behavioural analysis is a non-lethal technique that usually observes the movement of valves and feet and quantifies the filtration of water through the mantle (Chmist et al., 2019; Curley et al., 2021; Marshall and McQuaid, 2020; Naddafi and Rudstam, 2013; Nicastro et al., 2007; Rovero et al., 1999; Shen and Nugegoda, 2022). Valve activity can reflect the behavioural reactions of the animal to external factors is a well-established analysis for assessing the bivalve stress status (Shen and Nugegoda, 2022). Valve gaping activities are known to follow circadian and circalunar rhythms (García-March et al., 2008) but can display unique defence mechanisms when exposed to different concentrations of contaminants or mechanical stressors such as conspecific alarm cues, predator infochemicals, or predator presence (Dzierżyńska-Białończyk et al., 2019; Tran et al., 2003). Chemical cues from predators cause behavioural reactions of prey such as bivalves (Nicastro et al., 2007; Rovero et al., 1999) and observed mussel responses to risk cues include increasing aggregation, attachment strength, decreasing the clearance and feeding rate or burial behaviours (Hutchison et al., 2016; Naddafi et al., 2007; Naddafi and Rudstam, 2013). Investing energy in closing the shells is a first-line defence and an effective anti-predator behaviour, as the chances of survival increase if the valves remain shut and predators cannot breach the valve gap (Kobak and Kakareko, 2011; Robson et al., 2010).

Behavioural changes would usually require at least an additional metabolic estimator for monitoring the physiological status (Rovero et al., 1999) and respirometry assays are often used in combination with animal behaviours (Anacleto et al., 2014; Curley et al., 2021; Greenshield et al., 2021). Respiration rate is a useful tool for measuring physiological state of mussels, considering that environmental stressors can force mussels to alter the filtration rate, switch to catabolic process and increase oxygen consumption and ammonium excretion rate (Ganser et al., 2015; Spooner and Vaughn, 2008). In control conditions, it was evaluated that blue mussels *M. edulis* of 5.65 cm length had a filtration rate of 2800 - 4800 mL of water per hour (Winter, 1973). In mussels such as *Dreissena polymorpha,* it also appears that the clearance rate of cyanobacteria and diatoms is impacted differently during predation risk than the clearance of cryptophytes and chrysophytes microalgae (Naddafi et al., 2007), suggesting that filtration mechanisms are affected by different stressors.

Table 1.2 DEHP concentrations found in natural environments. Levels for other phthalates can be found in the **Supplementary Table 1.1**

COMPOUND	TOXICITY	SITE	CONCENTRATION	REFERENCES
DEHP di (2- ethylhexyl) phthalate $C_{24}H_{38}O_4$ CAS Number 117-81-7	Reproductive toxicity	Rivers in the Manchester area (UK)	0.4 to 1.9 µg/L	Fatoki and Vernon, 1990
		Seawater from Tees Bay (UK)	0.98 to 2.2 µg/L	Law et al., 1991
		Klang River estuary (Australia)	3.10 to 64.3 µg/L	Tan, 1995
		Rivers, lakes and channels, sewage effluents, sewage sludges (Germany)	0.33 to 97.8 µg/L (surface water) 1.74 to 182 µg/L (sewage effluents) 27.9 to 154 mg/kg dw (sewage sludge) 0.21 to 8.44 mg/kg (sediment)	Fromme et al., 2002
		Surface seawater (Netherlands)	0.9 to 5 µg/L	Vethaak et al., 2005
		Seawater and sediment from False Creek Harbour (Canada)	0.275 µg/L in seawater 2.1 µg/g dw in sediment	Mackintosh et al., 2006
		Freshwater, sediment (Netherlands)	Medial levels 0.33 µg/L (freshwater) 67.4 µg/kg (sediments)	Peijnenburg and Struijs, 2006
		Rainwater depositions from Paris urban area (France)	0.423 µg/L	Teil et al., 2006
		Seawater from Bay of Biscay (Spain)	$(64 \pm 4) \times 10^{-3}$ µg/L	Prieto et al., 2007
		Seawater and atmosphere in the North Sea	0.00052 to 0.0053 µg/L in seawater (dissolved) 0.00016 to 0.0058 µg/L in the total suspended matter 0.22 to 0.36 ng/m in atmosphere vapour	Xie et al., 2007

			0.95 to 1.1 in the particle (air)	
		Arctic	448 x 10^{-6} µg/L	Xie et al., 2007
		Atlantic coastal marine sediments (Spain)	0.19 to 2.6 µg/g[1] in sediments	Antizar-Ladislao, 2009
		Barkley Sound (Canada)	0.01 to 0.95 µg/L	Keil et al., 2011
		Puget Sound (USA)	0.06 to 0.64 µg/L	Keil et al., 2011
		Coastal seawater, Mediterranean Sea (Spain)	0.03 to 0.62 µg/L	Sánchez-Avila et al., 2012
		Seawater, Pelagos Sanctuary (Italy)	0.05 to 0.172 µg/g in the Ligurian Sea 0.05 to 0.084 µg/g in the Sardinian Sea	Fossi et al., 2012
		Marseille Bay (French)	0.0158 to 0.9238 µg/L	Paluselli et al., 2018
		Bohai Sea and Yellow Sea (China)	0.0616 to 4.352 µg/L	Zhang et al., 2018b
		Coastal waters (South Korea)	0.03–0.30 µg/L	Heo et al., 2020
		Cochin estuary (India)	ND – 3.861 µg/L	Ramzi et al., 2020
		House dust	23.5 to 2838.5 µg/g	Xu and Li, 2020
		Microplastics and wastewater in the wastewater treatment plant (Iran)	Averages between 17.49 and 83.3 µg/g for microplastics Averages between 8.13 and 30.8 µg/L for wastewater	Takdastan et al., 2021
		Marine water (Tunisia)	Average 71.7 µg/L	Jebara et al., 2021

Table 1.3 Selected exposure experiments with aquatic species exposed to DEHP concentrations. Levels for other phthalates can be found in the **Supplementary Table 1.2**

COMPOUND	LEVEL	TIME	SPECIES	REFERENCES
DEHP	0, 500, 1000, and 5000 µg/L	1 – 90 dph	*O. latipes* (Japanese medaka, embryo-larval stage)	Metcalfe et al., 2001
	1, 5 and 10 µg/L	1 - 3 months	*O. latipes* (Japanese medaka) (Embryo-larval stage)	Kim et al., 2002
	400, 800, and 1500 mg/kg	4 weeks	*Salmo salar* (Atlantic salmon early stages)	Norman et al., 2007
	0.1-10 µg/L	91 days	*Poecilia reticulata* (guppy fish)	Zanotelli et al., 2010
	0.5, 50 and 5000 mg/kg	10 days	*Danio rerio* (males)	Uren-Webster et al., 2010
	0.02, 0.2, 2, 20, 40 µg/L	21 days	*D. rerio* (Adult females)	Carnevali et al., 2010
	0.05, 0.1, 1, 10 and 100 nM	4 days	*D. rerio* (Primary hepatocyte cultures)	Maradonna et al., 2013
	0.4 mg/L and 4.0 mg/L	0, 12, 36, 60, 96 hours	*Venerupis philippinarum* (clam)	Lu et al., 2013b
	0.1 and 0.5 mg/L	6 months	*O. melastigma* (From hatching to adulthood)	Ye et al., 2014
	1, 10, and 100µg/L	30 days	*Carassius auratus* (fish)	Golshan et al., 2015
	up to 2 mg/L	96 h	*Brachionus calyciflorus* (rotifer)	Cruciani et al., 2016
	up to 5120 µg /L (adults) Up to 1.95 µg /L (nauplii)	48 hours	*Parvocalanus crassirostris* (calanoid)	Heindler et al., 2017
	10 µM, 100 µM and 500 µM	2.5 days of incubation at room temperature	*Caenorhabditis elegans* (germline)	Cuenca et al., 2020
	10, 1, and 0.1 mg/L	72 hours	*C. elegans*	Li et al., 2021b
DEHP, DMP (dimethyl phthalate) and **DBP**	100 µg/L and 500 µg/L	24 hours	*Crassostrea virginica* (oyster)	Wofford et al., 1981

(dibutyl phthalate)				
	100 µg/L and 500 µg/L	24 hours	*Penaeus aztecus* (Brown shrimp)	Wofford et al., 1981

Table 1.4 Selected exposure experiments with mussels exposed to DEHP. Levels for other phthalates or endocrine disruptive chemicals can be found in the **Supplementary Table 1.3**

PHTHALATE	LEVEL	TIME	SPECIES	REFERENCES
Plasticiser **DEHP**	100 µL injected through the adductor muscle 100 µg/L for water exposure	Injection through the adductor muscle for 7 days or Water exposure for 21 days	*M. galloprovincialis*	Cancio et al., 1998
	500 µg/L every day	21 days	*M. galloprovincialis*	Orbea, et al, 2002
	100 µL injected through the adductor muscle 100 µg/L for water exposure	Injection through the adductor muscle for 7 days or Water exposure for 21 days	*M. galloprovincialis*	Marigómez and Baybay-Villacorta, 2003
Plasticisers **DEHP** and **DIDP**	5 µg/L and 50 µg/L	28 days + 14 days of depuration	*M. edulis*	Brown and Thompson, 1982

Table 1.5 Selected experiments with bivalve molluscs exposed to multiple stressors

COMPOUND	STRESS CONDITIONS	TIME	SPECIES	REFERENCES
Heavy metal **Cadmium**	50 mg/L in combination with thermal stress (12, 20 and 28ºC)	45 days	*C. virginica*	Cherkasov et al., 2007
Heavy metal **Mercury**	45µg/L in combination with thermal stress	72h or 14 days	*P. viridis*	Verlecar et al., 2007
Heavy metals **Cadmium, Lead, Copper**	30mg/L at at two pH levels (7.7 and 6.2)	35 days	*M. edulis*	Han et al., 2014
Heavy metal **Cadmium**	50 µg/L in combination with +8 ℃ thermal stress	24 hours	*M. galloprovincialis*	Izagirre et al., 2014
Polycyclic aromatic hydrocarbon **Fluoranthene**	30 µg/L in combination with nano- and micro-plastic particles (mix of 2 and 6 µm for a final concentration of 32 µg/L)	7 days exposure + 7 days depuration	*Mytilus* spp.	Paul-Pont et al., 2016
Heavy metal **Arsenic**	4 mg/L under - 0.5 pH reduction	28 days	*Crassostrea angulata* and *C.gigas*	Moreira et al., 2016
Pharmaceutical **Diclofenac**	0.00, 0.05 and 0.50 µg/L under pH −0.4 units and pH −0.7 units	7, 14 and 21 days	*M. galloprovincialis* and *R. philippinarum*	Munari et al., 2018
Paralytic shellfish toxins (PSTs) mix	*Gymnodinium catenatum* diet for 5 days and non-toxic diet for 10 days in combination with +5 ℃ elevated temperature and -0.4 units pH	5 days + 10 days	*M. galloprovincialis*	Braga et al., 2018
Pharmaceutical **Carbamazepine**	6.3 µg/L in combination with 0.05- 50 mg/L nano- and micro- plastic particles	96 hours	*M. galloprovincialis*	Brandts et al., 2018
Heavy metal **Cadmium**	20 µg/L in combination with +5 ℃ elevated temperature and -0.6 units pH	28 days	*M. galloprovincialis*	Nardi et al., 2017, 2018
Polycyclic aromatic hydrocarbon **Phenanthrene**	100 µg/L in combination with pH changes (6.5, 7.0 and 8.2)	24 and 96 h	*Crassostrea gasar*	Lima et al., 2019
Antibacterial Pharmaceutical drugs **Triclosan Diclofenac**	1 µg/L in combination with 30 (control), 25 and 35 psu salinity	28 days	*M. galloprovincialis*	Freitas et al., 2019

Heavy metal **Copper**	25 µg/L at three pH levels (8.1, 7.8 and 7.6)	14 and 28 days	*C. gigas*	Cao et al., 2019
Heavy metal **Mercury**	10 µg L and 25 µg L red fluorescent PE microbeads (144 ± 27 particles per mL)	96 h	*R. philippinarum*	Sıkdokur et al., 2020
Pharmaceutical drug **Diclofenac**	0.05 and 0.5 µg/L under −0.4 units and pH −0.7 units	14 and 21 days	*M. galloprovincialis*	Munari et al., 2020
Heavy metal **Cadmium**	10 µg/L and + 5 ℃	7 days	*D. polymorpha*	Louis et al., 2021
Food **Caffeine**	0.05 and 0.5 µg/L under pH −0.4 units and pH −0.7 units	14 and 21 days	*M. galloprovincialis*	Munari et al., 2020
Plastic additive Antibacterial **Triclosan**	1 µg/L After 30 days of acclimation at climate change conditions to +3 ℃ elevated temperature and -0.4 units pH	7 days	*Ruditapes philippinarum* and *R. decussatus*	Costa et al., 2020
Irregular polystyrene microplastics	6.4, 160, 4000, 100,000 p/mL at either 14, 23 or 27 ℃	14 days	*D. polymorpha*	Weber et al., 2020
Pharmaceutical drug **Carbamazepine**	3.00 µg/L in combination with 7.1 pH	28 days	*Scrobicularia plana*	Freitas et al., 2020
Polystyrene Microspheres	2 mm, 0, 10, 104 and 106 particles/L under two pH levels (7.7 and 8.1)	14 days + 7-day recovery	*M. coruscus*	Wang et al., 2020
Plastic additive **DEHP**	0.5 and 50 µg/L in combination with +3 ℃ elevated temperature	7 days	*Mytilus* spp.	Mincarelli et al., 2021
Plastic additive **DEHP**	0.5 and 50 µg/L in combination with -0.4 units pH	7 days	*M. edulis*	Mincarelli et al., 2022
Illicit drug **Cocaine**	0.5, 5.0, and 50 µg/L in combination with different pH values (8.3, 8.0, 7.5, 7.0, 6.5, and 6.0)	96 h	*P. perna*	da Silva Souza et al., 2021
Pharmaceutical drug **Carbamazepine**	1 µg/L under 7.6 pH	28 days + 10 days of depuration	*M. galloprovincialis*	Mezzelani et al., 2021
Zinc oxide nanoparticles	(0, 10, 100 µg/L and warming (+5 ℃)	21 days	*M. edulis*	Wu and Sokolova, 2021
Pharmaceutical drug **Carbamazepine Cetirizine**	CBZ, 1 µg/L + CTZ, 0.6 µg/L under +4 ℃ thermal stress	28 days	*R. philippinarum*	Almeida et al., 2021
Personal care	4 mg/L in combination with			

product additive **Sodium lauryl sulfate**	30 (control), 25 and 35 psu salinity	28 days	*M. galloprovincialis*	Freitas et al., 2021
Pharmaceutical drug **Carbamazepine Cetirizine**	CBZ, 1 µg/L + CTZ, 0.6 µg/L and salinity changes (15, 25 and 35 psu)	28 days	*R. philippinarum*	Almeida et al., 2022a
Pharmaceutical drug **Carbamazepine Cetirizine**	CBZ, 1 µg/L + CTZ, 0.6 µg/L and pH changes (8.0 and 7.6)	28 days	*R. philippinarum*	Almeida et al., 2022b

1.7 Thesis aim and hypothesis

The present project aims to investigate the relationship between single and combined short-term responses of blue mussels to contaminants and environmental factors (i.e., DEHP exposure, increased temperature and low pH). This work is relevant for understanding the effect of plastic additives on sentinel species, alone or against the climate-changing backdrop of global warming and ocean acidification.

This thesis hypothesises that:

- The endocrine disruptive chemical DEHP will have an effect on reproductive traits of mussels.
- The combined effect of climate change conditions with plasticiser exposure will be able to stimulate a stronger effect in comparison with the responses to the single stressors.

Assuming that future climate conditions (i.e., global warming and ocean acidification) will increase the leakage of dangerous additives from plastic items into the environment, marine species will be exposed to significant concentrations of these toxic compounds. Considering this, the combination of altered climate conditions and DEHP presence could possibly result in more pronounced consequences in terms of general stress responses and variations in the reproduction cycle. Direct exposure to endocrine disruptors such as DEHP could lead to alterations of males and females' endocrine systems, such as the expression of reproductive pathway-related genes (i.e., *MeER1*, *MeER2*), possibly at different stages of the gametogenesis cycle. In addition, the altered climate conditions will induce an additional imbalance in the cellular system involved in the stress response, intended as the expression of genes involved in the antioxidant pathway, general stress or pH homeostasis (*sod*, *cat*, *hsp70*, *CA2*), metabolic alterations (i.e., respiration and valve

behaviours) and histological abnormalities, such as spawning events out of the spawning season.

Chapter 2

The effects of thermal stress and DEHP exposure on histological and molecular outcomes

2.1 Introduction

This chapter aims to investigate the effect of plastic pollution in the context of global warming on sentinel species. Specifically, blue mussels *Mytilus* spp. were exposed to DEHP and increased temperature, separately and in combination through a factorial design. Two temperatures and two concentrations of DEHP were chosen following the IPCC scenarios for the end of the century and the current phthalate levels found in marine environments. Biomarkers for cellular stress and alterations of the reproductive cycle were investigated and the changes in the gametogenesis status of male and female mussels were observed as a biomarker of reproductive alterations. Genes coding for the heat shock protein 70 and the antioxidant enzymes superoxide dismutase and catalase (*hsp70, sod* and *cat*) were studied as representatives of the mussel cellular response to stress. Genes *sod* and *cat* were chosen as they can counteract the damaging effect of oxyradicals (Regoli and Giuliani, 2014), while *hsp70* is linked not only to changes in temperature, but also with protein metabolism under stress conditions, such as environmental perturbation and xenobiotic exposure (Encomio and Chu 2005; Franzellitti and Fabbri, 2005; Koagouw et al. 2021a, b; Lewis et al. 1999). Genes for estrogen-related receptor (*MeER1*) and estrogen receptor (*MeER2*) were chosen as reprotoxicity parameters because of their possible involvement in estrogen signalling and the reproductive cycle in *Mytilus* species (Ciocan et al., 2011; Nagasawa et al., 2015). Their expression is also reported to be different during the reproductive stages of mussel gonadal maturation and exposure to estrogens (Agnese et al., 2019; Ciocan et al., 2010b).

From the second half of the 20th century, greenhouse gases (GHG) and aerosols have been considered the most-likely major climate drivers (responsible for >50% of the global change) of the tropospheric warming and the increase of their levels is unequivocally caused by human activities (IPCC, 2021). Increasing GHG levels contribute to the forcing imbalance between the radiation from the Sun and the energy lost to space as reflected sunlight and thermal emissions from Earth. This positive net radiation has been causing an over-accumulation of energies that transmuted into heat, which is only partly reduced by the increased loss of energy to space in response to surface warming (Hansen and Sato,

2004; Hughes, 2000; IPCC, 2021; Mitchell et al., 1989; Solomon, 2009). In the period 2011 - 2019, CO_2 atmospheric levels reached 410 ppm, while other GHGs such as CH_4 and N_2O reached 1866 ppb and 332 ppb, respectively. These concentrations were reported with high confidence to be the highest in at least 2 million years for CO_2 and 800,000 years for CH_4 and N_2O. Between 2001 and 2020, the global surface temperature increase by anthropogenic cause was estimated to be almost 1 degree (0.84 - 1.10 °C) higher than the temperature in the 1850 - 1900 time period, which represents the earliest complete observations for the estimation of the global surface temperature (IPCC, 2021). Likewise, the ocean temperature has been increasing on average by a little more than 0.1 °C per decade in the last 30 years (Lima and Wethey, 2012). According to the different emission scenarios (SSPs), the most recent report from IPCC (AR6, 2021) assessed the current and projected values for global surface temperature (**Fig. 1.3** and **2.1**).

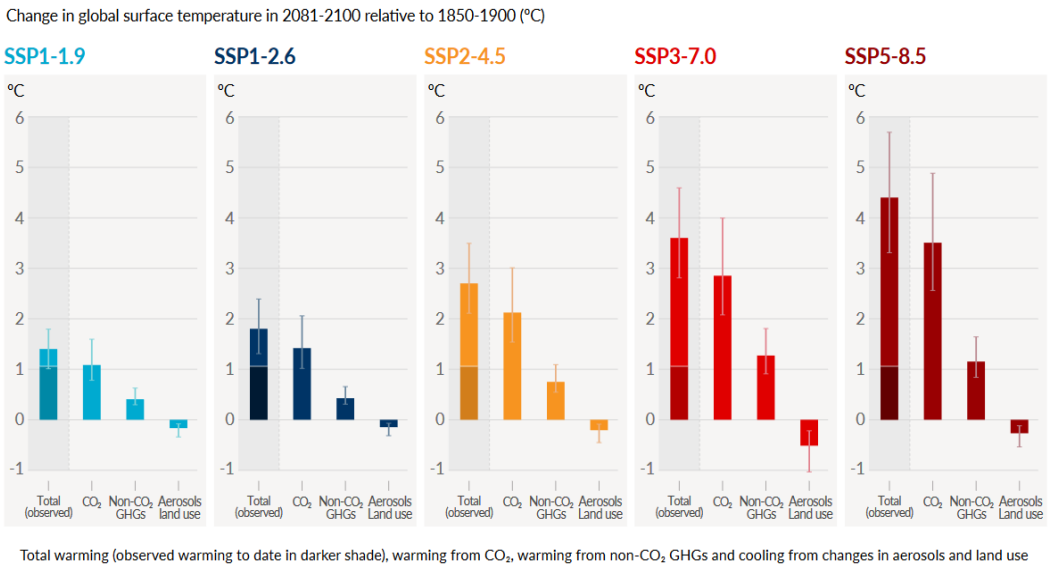

Fig. 2.1 Contributions to the increase of global surface temperature according to the different SSPs and projected emissions. From Climate Change 2021: The Physical Science Basis. Contribution of Working Group I to the Sixth Assessment Report of the Intergovernmental Panel on Climate Change (IPCC, 2021)

The number of publications on the effect of temperature on plastic products has grown exponentially in the past decades, whether taking fragments (Bertucci and Bellas, 2021; Weber et al., 2020) or additives (Ho et al., 1999; Rose et al., 2012; Wu et al., 2022) into observation. Considering *Mytilus* spp. experiments, the exposure to plastic additives alone can have negative effects on lipid homeostasis (Balbi et al., 2017), shell formation (Balbi et al., 2016), antioxidant and peroxisomal enzyme activities (Cancio et al., 1998;

Orbea et al., 2002; Xu et al., 2021a), lysosomal enlargement and membrane stability (Marigómez and Baybay-Villacorta, 2003) at levels of 1 –500 μg/L.

Temperature is one of the factors that promote migrations of chemicals from the plastic matrix into the environment (Teuten et al., 2009). Increasing temperature and relative humidity enhanced the degradation of polylactic acid plastic films of high molecular weight (Ho et al., 1999) and can accelerate the leaching of DEHP from medical PVC infusion equipment both in dynamic systems and after static contact in lipid infusates (Rose et al., 2012). Zimmermann et al. (2021) recorded the leaching process from eight common polymer types with everyday use and available from the market (high-density and low-density polyethylene; polystyrene; polypropylene; polyethylene terephthalate; polyvinyl chloride; polyurethane; and polylactic acid) into a water environment at 40 °C. After 10 days, between 1 and 88% of additives migrated into the water medium, some of them related to oxidative, anti-androgen and estrogen effects. Leachates from plastic items are known to induce alteration in general stress parameters of *M. galloprovincialis* (Capolupo et al., 2021) and affect the early stages of bivalve molluscs, such as in the development of the commercial clam *Meretrix meretrix* D-veliger larvae (Ke et al., 2019) or in the survival and morphology of *Perna perna* embryos (Gandara e Silva et al., 2016). In this chapter, the responses of blue mussels *Mytilus* spp. to DEHP exposure and increased temperature were investigated, separately and in combination, through a factorial design. The following outcomes were analysed: histological changes at the level of gonadal maturation and gene expression of genes involved in the stress response (*sod, cat* and *hsp70*) and biomarkers of reprotoxicity (*MeER1* and *MeER2*). The following hypotheses were tested: I) the endocrine disruptive additive DEHP will have an effect on reproductive features (i.e., histological changes of the gonads and expression of biomarkers of reprotoxicity) and II) the combined effect of high temperature and DEHP exposure will have a stronger effect in comparison with the responses to the single stressors.

2.2 Materials and Methods: Experimental design

Adult blue mussels (n = 180) were collected at low tide from the intertidal zone at Filey Bay, North Yorkshire, UK (54° 13´ longitude; 0° 16´ latitude, T_{water} = 11 °C; pH = 8.07, **Fig. 2.2**), in November 2018 and transported to the aquarium facilities of the University

of Hull. Mussels were not cleaned from sand and mud nor scrubbed from seaweed and barnacles to avoid additional physical stress. Mussel lengths were measured to be 5.4 cm ± 0.6 cm (length mean ± standard deviation). Mussels were randomly divided into the treatment tanks, independently from their different size, to keep the experiment unbiased and as possible comparable to the natural conditions of a mussel population. This condition was chosen also considering that animals from the same locality are usually found to be at the same sexual maturation state independently by their size (Seed, 1969). Mussels were randomly divided into six different 4-litre continuously aerated glass tanks for each treatment (5 mussels for each tank at a density of 1 mussel per 0.8 litre) and kept for acclimation for 12 days in artificial saltwater (Premium REEF-Salt, Tropical Marine Centre©, Chorleywood, UK) at laboratory conditions. These were a salinity of 35‰ and a pH of 8.1 units, a photoperiod of light: dark = 10h:14h and water temperature of 11°C (temperature control treatments CTRL) and 14°C (high temperature treatments HIGH T). The control temperature was chosen in line with the average temperature of Filey Bay recorded in the days preceding the collection. The acclimation of 12 days was chosen as the optimal period for temperate marine bivalves in laboratory-based experiments to ensure the reach of a new physiological steady state after an environmental shift (8-12 days, Khlebovich, 2017; Thompson et al., 2012; Wu and Sokolova, 2021). A total increase of 3°C for the high-temperature treatment (T = 14°C, HIGH T) was chosen considering the SSP 3 - 7 mean temperature range of the global warming scenarios projected for the end of the century, assuming the CO_2 emissions remain high and double from current levels by 2100 (IPCC, 2021). Animals in Filey are subjected to similar temperatures during spring-summer months, but 14°C in wintertime is still considered an out-of-the-season alarming thermal event.

Fig. 2.2 Filey Brigg, Filey Bay, North Yorkshire, UK (54° 13´ longitude; 0° 16´ latitude), the collection site adjacent to the Holderness marine conservation zone

Mussels were not fed during the exposure, as the interpretation and comparison of laboratory findings in short-term exposure experiments is often biased and modulated by administered food type and feeding regime (Kloukinioti et al., 2020). Artificial saltwater was prepared the day before each water change, in order to allow the water to adjust to the temperature-controlled rooms. In the high temperature treatment, temperature was progressively raised by 1°C during the first three days of acclimation by adjusting ambient air temperature in a climate-controlled room, in order to avoid an immediate temperature-induced shock. After the acclimation period, mussels from normal and higher temperature treatments were exposed for seven days to two different concentrations of DEHP (0.5 and 50 µg/L). Water was changed every second day and DEHP was dosed right after (i.e., days 1, 3 and 5). Temperatures were kept at 11 °C or 14 °C, respectively, which yielded a total of six treatments (**Fig. 2.3 - 2.7**). Salinity remained constant at 35 ± 1 psu over the course of the experiment in all conditions. Temperature, pH and salinity were measured daily (**Table 2.1**) with a digital thermometer (model ama-digit ad 15 th, Amarell Thermometer, Kreuzwertheim, Germany), an Accumet® portable pH-metre (Thermo Fisher Scientific, Loughborough, UK) and a digital seawater refractometer (Hanna Instruments, Woonsocket, USA).

DEHP (≥ 99.5% purity) was obtained by Sigma Aldrich®, Gillingham (UK). Due to its low solubility in water, DEHP was dissolved in ethanol, in order to prepare a stock solution of 1 mg/mL. Ethanol was chosen as a suitable solvent already used in experimental exposure to DEHP (Carnevali et al., 2010; Heindler et al., 2017; Lu et al.,

2013b; Maradonna et al., 2013). DEHP was dosed every other day and the two DEHP concentrations of 0.5 µg/L and 50 µg/L were chosen from the literature, aligned to the DEHP levels detected in natural environments, where the minimum and maximum average levels for marine environments were found to be 0.145 µg/L (Sánchez-Avila et al., 2012) and 71.7 µg/L (Jebara et al., 2021). After seven days of exposure, mussels were sampled (Unlicensed animal ethics approval reference no #U080/FEC_2021_11, University of Hull) and tissues from gonads were collected for molecular and histological analyses. For the molecular analysis, *ca.* 1.0 cm^2 of gonad tissue was dissected and immersed in 1 mL RNAlater® Stabilisation Solution (Thermo Fisher Scientific, Loughborough, UK) and stored at -80 °C until the analysis. Approximately the same quantity of tissues was stored in 1 mL neutral-buffered 10% formalin solution (Sigma Aldrich, Gillingham, UK) at room temperature for histological analysis.

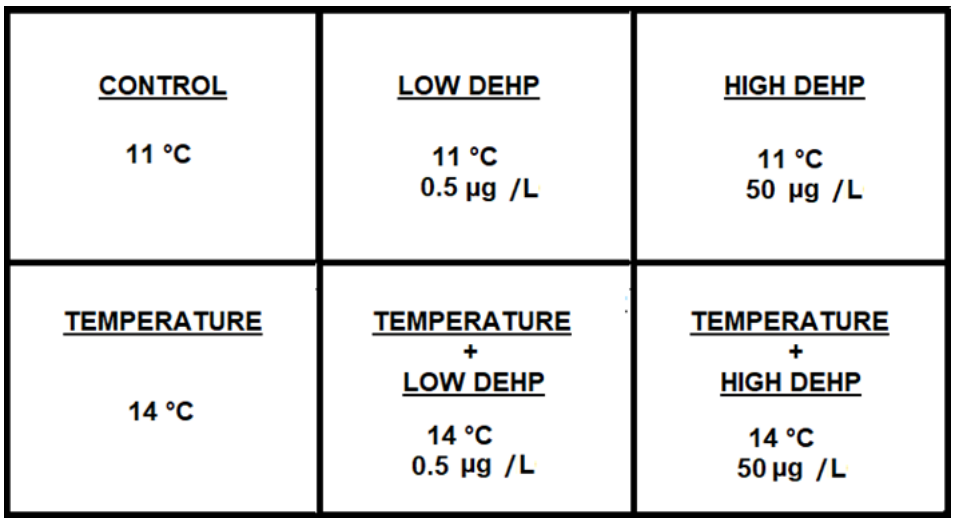

Fig. 2.3 Experimental design for the 7-day exposure with the chosen parameters for temperature (11 and 14°C) and DEHP (nominal concentrations 0, 0.5 and 50 µg/L)

Fig. 2.4 Picture from exposure room 1 (control temperature room) - experimental tanks with mussels at 11℃, covered in non-PVC cling film

Fig. 2.5 Picture from exposure room 2 (high temperature room) - experimental tanks with mussels at 14℃, covered in non-PVC cling film

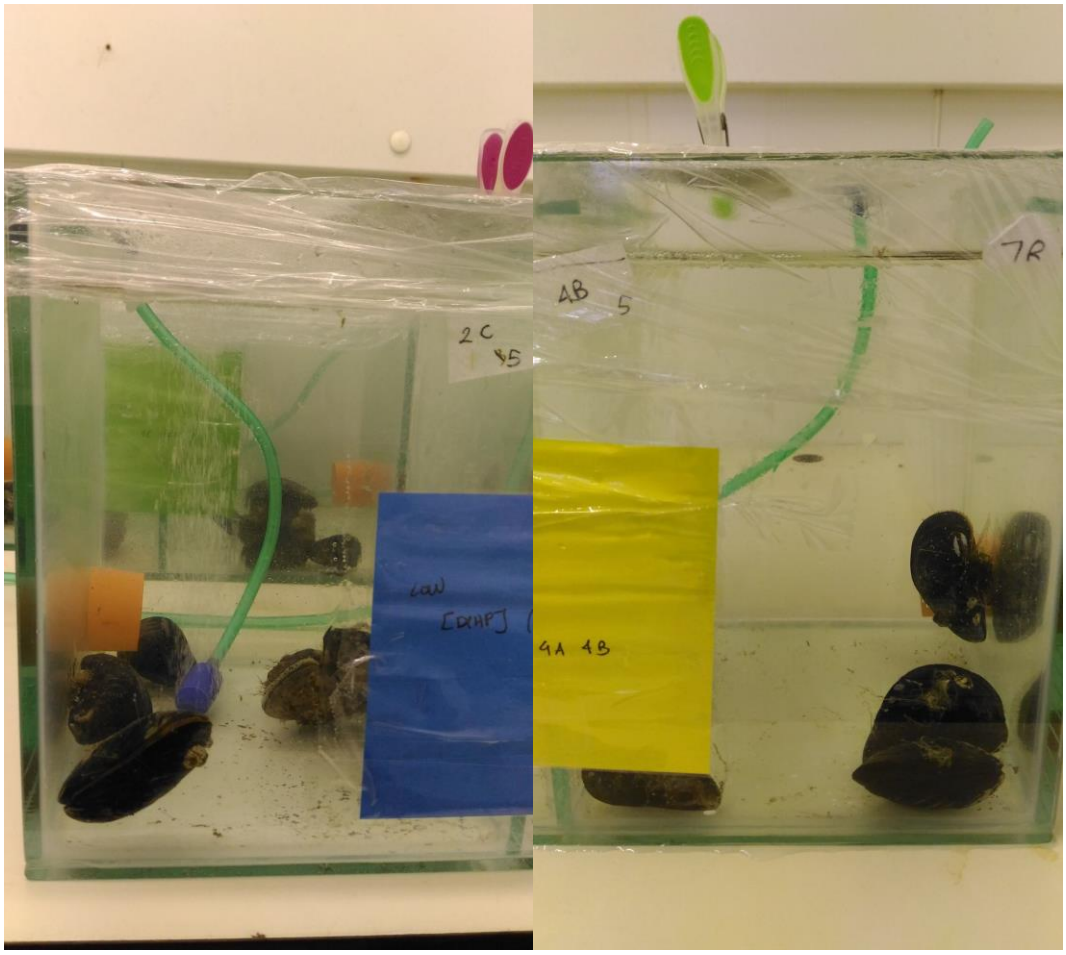

Fig. 2.6 and 2.7 Details of mussels (5 individuals for 4 litres) in the exposure tanks, covered in non-PVC cling film

Table 2.1 Experimental treatments, and measurements of temperature, pH, and salinity values. All parameters are expressed as mean ± standard deviation

Name of treatment	Description	Temperature (°C)	pH (Units)
CTRL	Control temperature, no DEHP	11.16 ± 0.22	8.16 ± 0.09
LOW DEHP	Low DEHP concentration	11.22 ± 0.23	8.09 ± 0.07
HIGH DEHP	High DEHP concentration	11.31 ± 0.23	8.06 ± 0.07
HIGH T	Future temperature, no DEHP	13.92 ± 0.48	8.19 ± 0.09
LOW DEHP HIGH T	Future temperature and low DEHP concentration	13.95 ± 0.55	8.16 ± 0.09
HIGH DEHP HIGH T	Future temperature and high DEHP concentration	14.06 ± 0.55	8.06 ± 0.10

2.3 Materials and Methods: Wax infiltration and H/E staining

Samples fixed in 10% buffered formalin (Sigma-Aldrich, Gillingham, UK) were initially washed with 0.01 M phosphate-buffered saline (PBS, Sigma Aldrich, Irvine, UK) for 15

minutes. After that, samples were dehydrated with increasing ethanol (EtOH, Fisher Scientific, Loughborough, UK) concentrations as follows: 70% for 15 min, 90% for 15 min, 100% for 15 min, a second 100% EtOH step for 15 min step and a final 100% step for 30 min. Finally, samples were cleared with Histoclear II (National Diagnostics, Atlanta, USA) for an initial 20 min and again left overnight, to allow the removal of alcohol from the tissues. The day after, the samples were embedded in paraffin wax (VWR, Poole, UK) in an EG 1160 Paraffin Wax Embedding Centre (Leica Microsystems, Milton Keynes, UK). The wax was left to infiltrate the tissues at high temperature (~65°C) in a first step for 30 min and a second step for 45 min. In the final step, tissues were allowed to set on the chilled surface (~ -5°C) on PrintMate™ Slotted Cassettes (Fisher Scientific, Loughborough, UK). Tissue sections (10 µm) of wax-embedded gonads were cut on a Shandon Finesse® Manual Rotary Microtome 325 (Thermo Fisher Scientific, Loughborough, UK) and placed briefly in a heated warm bath (~50°C) to warm the wax before positioning the sample on a SuperFrost™ Ground 90° Microscope Slide (Fisher Scientific, Loughborough, UK). The slides were dried overnight and the next day they were briefly passed through a Bunsen burner flame to melt the wax. Slides were placed in Histoclear II for 10 min and rehydrated following the steps: 3 min in EtOH 100%, 3 min in EtOH 95%, 3 min in EtOH 75%, 3 min in EtOH 45% and 3 min in EtOH 25%. In order to stain the basophil structures, samples were placed in the red stainer Mayer's haematoxylin solution (Sigma-Aldrich, Schnelldorf, Germany) for 5 min and then rinsed in running tap water for 10 min. Tap water was used as the contained minerals cause the pH to be basic enough to change the colour contrast to purple/blue. Samples were then dehydrated following the steps: 2 min in EtOH 25%, 2 min in EtOH 45%, 2 min in EtOH 75%, 2 min in EtOH 95% and counterstained with the pink acidic dye eosin Y alcoholic solution (Sigma-Aldrich, Schnelldorf, Germany) for 1 min, which allowed to counterstain acidophilic structures such as the cytoplasm in pink. Slides were then washed in 95% and 100% ethanol and finally cleared in Histoclear II for 5 min. Samples were left overnight to dry and then mounted with non-aqueous DPX (Sigma-Aldrich, Gillingham, UK) and borosilicate glass rectangular coverslips (Fisher Scientific, Loughborough, UK). Prior to microscopic analysis, microscope slides were coded, in order to conduct a blind observation. Males and females were identified under a light microscope, and the following stages were assessed, as described by Seed (1969):

I. Resting or spent gonad: no evident presence of sexuality (**Fig. 2.8 A**). This includes virgin juveniles with immature reproductive systems and spawned animals in a spent state.

II. Development stage 1: small follicles in males (**Fig. 2.8 B**), and irregular follicles and small oocytes in females (**Fig. 2.9 A**). The sex of very early stages is often difficult to recognise, as the connective tissue appears as a dense matrix with islands of germinal tissue.

III. Development stage 3: larger follicles half occupied by early gametogenesis stages and mature and ripe gametes (**Fig. 2.8 C** and **2.9 B**). The stored food in the connective tissue participates in the increase of the gonadal mass.

IV. Development stage 5: mature stage (**Fig. 2.8 D** and **2.9 C**). The transition from morphological to physiological ripeness could last for weeks or a few months, and in this stage, females exhibit a few small oocytes, with compacted and polygonal-shaped ova. In males, there are distended follicles with ripe spermatozoa.

V. Spawning stage 3: follicles display empty spaces, with some ripe spermatozoa (**Fig. 2.8 E**) or mature rounded eggs still present (**Fig. 2.9 D**). Very few early stages are observable and the mantle is not fully covered by the reproductive tissues.

VI. Spawning stage 1: this stage is characterised by the presence of residual spermatozoa and ova in the follicles (**Fig. 2.8 F**). They might undergo cytolysis by ameboid phagocytes whose nuclei usually are darkly stained with haematoxylin.

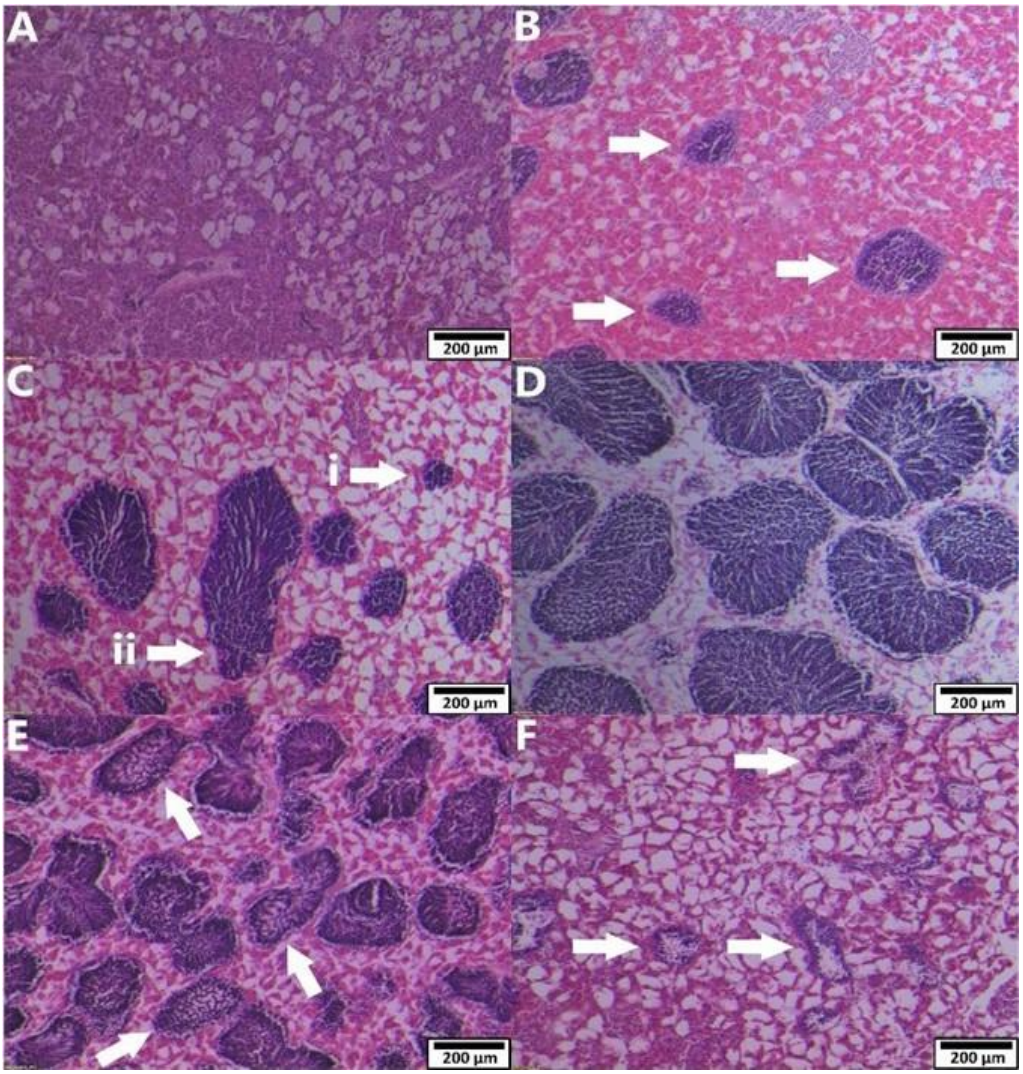

Fig. 2.8 Gametogenesis stages of 10 µm gonadal tissue sections stained with haematoxylin and eosin of males. Resting stage (undetermined sex, A, at 10× magnification), follicles at development 1 (B, 10×), development 3 with different follicle sizes (i and ii, C, 10×), mature stage (D, 10×), empty follicles at spawning 3 (E, 10×) and spawning 1 (F, 10×). Scale bars represent 200 µm. Images were modified for brightness and contrast

Each stage was categorised by a maturity factor (MF):

I. MF = 1 for resting or spent gonad.

II. MF = 2, developing gonads (stage 1 and 3).

III. MF = 3, mature gonads.

IV. MF = 4, spawning gonads (stage 1 and 3).

Then, the sexual maturity index (SMI) was calculated according to the equation established by Siah et al., (2003): $SMI = \Sigma$ *(proportion of each stage * maturity factor)*.

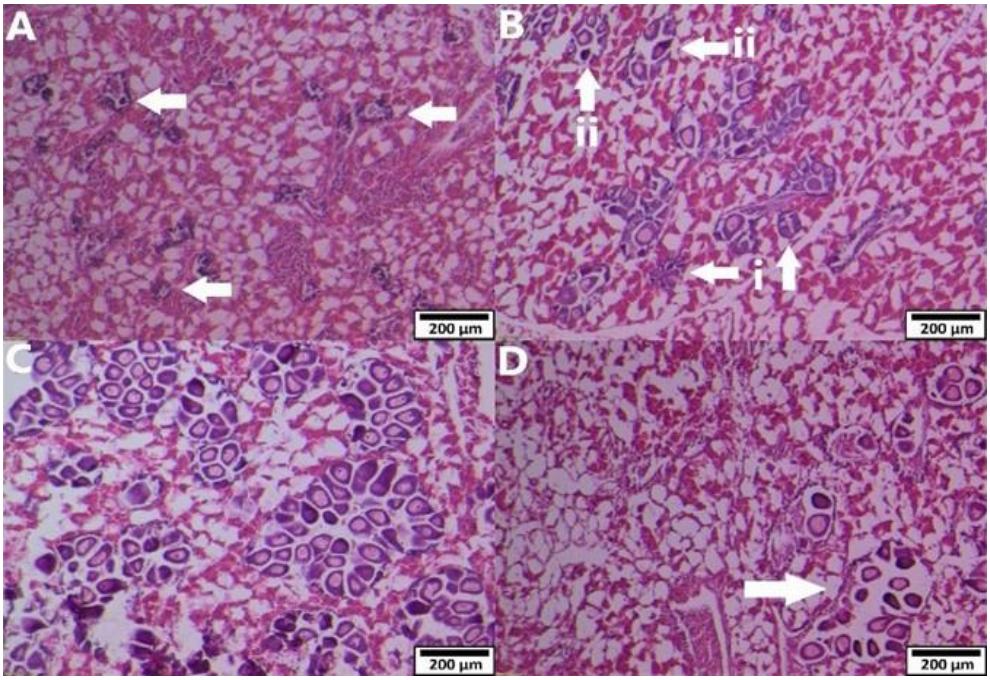

Fig. 2.9 Gametogenesis stages of 10 µm gonadal tissue sections stained with haematoxylin and eosin of females. Irregular follicles and small oocytes in development 1 (A, 10×), early (i) and mature (ii) gametes in development 3 (B, 10×), mature stage (C, 10×) and empty follicles in spawning 3 (D, 10×). Scale bars represent 200 µm. Images were modified for brightness and contrast

2.4 Materials and Methods: Total RNA isolation

Gonad tissues were preserved in RNAlater® Stabilisation Solution (Thermo Fisher Scientific, Loughborough, UK) and stored at -80°C until molecular analysis. Random samples (*approx.* 10 mg of gonad tissue, n = 96) were selected and blindly coded for the analysis. In detail, 8 female gonads and 8 male gonads for each treatment were processed for the total RNA extraction. Before every RNA extraction, all the equipment and work surfaces were cleaned with RNAse Away (Fisher Scientific, Loughborough, UK), to eliminate RNase and DNA contamination. The High Pure RNA Isolation Kit (Roche Applied Science, Burgess Hill, UK) was used for the purification of the intact total RNA from tissue samples, with an additional DNase I digestion step, in order to remove contaminating DNA. Approximately 10 mg of gonadal tissue was weighed on an analytical table scale PS-100 (Fisherbrand, Loughborough, UK) and homogenised in 400 µL of Lysis Binding Buffer (4.5 M guanidine-HCl, 100 mM sodium phosphate pH 6.6 at 25°C) using a rotor-stator homogeniser (IKA, Staufen, Germany) in a nuclease-free 2 mL

microcentrifuge tube (Fisher Scientific, Loughborough, UK). The homogenisation step is considered essential for an efficient disruption of the cell walls and plasma membranes for the release of the sample RNA. Moreover, the homogenisation step reduces the viscosity of the lysates produced by the disruption and shears the high-molecular weight cellular components, such as genomic DNA. All the steps (unless stated otherwise in the manufacturer's protocol) were conducted on ice. The lysate was centrifuged for 2 minutes at 13.000 x g in a centrifuge 5424 (Eppendorf®, Hamburg, Germany) which eventually formed a pellet of insoluble cell debris. After the centrifugation, the supernatant was transferred into a clean nuclease-free 1.5 mL "Crystal Clear" microcentrifuge tube and half of its volumes of EtOH 100% (Fisher Scientific, Loughboroug, UK) was added and mixed well. The mix was then transferred into a High Pure filter tube (polypropylene tubes with two layers of glass fibre fleece, Roche Applied Science, Burgess Hill, UK) combined with a collection tube. Then, the tubes were centrifuged for 30 seconds at 13,000 × g in a standard tabletop microcentrifuge miniSpin plus (Eppendorf®, Hamburg, Germany). After inspection of the dryness of the glass fleece, the flow-through liquid was discarded. In the event of the glass fleece still appearing wet, another centrifuge step (30 seconds at 13,000 × g) was added. Then, a solution made of 10 µL DNase I working solution (0.18 kU) and 90 µL DNase incubation buffer (1 M NaCl, 20 mM Tris-HCl, 10 mM $MnCl_2$, pH 7.0) was added to the upper reservoir of each tube and incubated for 15 min at room temperature (+15 to +25°C) in order to remove residual genomic DNA. 500 µL of wash buffer I (5 M guanidine-HCl, 20 mM Tris-HCl, pH 6.6, final concentration after the addition of absolute EtOH) was then added to remove inhibitors and the samples were centrifuged 15 s at 8,000 × g. The flow-through liquid was discarded, and 500 µL of wash buffer II (20 mM NaCl, 2 mM Tris-HCl, pH 7.5, final concentration after the addition of absolute EtOH) was added for a final purification from residual impurities followed by another centrifugation step at 8,000 × g for 15 s. The final washing step consisted of the addition of 300 µL of wash buffer II and a centrifugation at 13,000 x g for 2 min. Finally, 50 µL of elution buffer (sterile nuclease-free double distilled water PCR grade, Roche Applied Science, Burgess Hill, UK) was added and the assembly tubes were centrifuged for 1 min at 8,000 × g two times. Samples were then stored at -80 °C.

2.5 Materials and Methods: RNA quantification and integrity

The total RNA in the samples was quantified with a Qubit 1.0 Fluorometer (Life Technologies, Paisley, UK) and Quant-iT™ Qubit RNA BR assay kit and Qubit assay tubes (Life Technologies, Paisley, UK). The working solution was made with 200 μL Qubit RNA buffer and 1 μL Qubit RNA reagent (concentration 200X in DMSO) for each assay. Two standard solutions were used for calibration from 190 μL of the working solution mixed with i) 10 μL of Qubit RNA Standard no. 1 (0 ng/μL in TE buffer) and ii) 10 μL of Qubit RNA Standard no. 2 (10 ng/μL in TE Buffer) to a final volume of 200 μL. For the sample assay, 199 μL of the working solution was mixed with 1 μL RNA and incubated at room temperature for 2 min. For each batch of assays on different days or times of the same day, new standard curves were calibrated, as fluorometer assays are affected by environmental factors such as room temperature and humidity. Only RNA concentrations higher than 20 ng/μL were accepted for the consecutive analysis (**Fig. 2.10**).

The integrity and size distribution of the total RNA were then checked by denaturing agarose gel electrophoresis and GelRed™ Nucleic Acid Gel Stain staining (10,000X in DMSO, Cambridge Bioscience, Cambridge, UK). The 1% agarose gel was prepared by mixing agarose powder (Fisher Scientific, Loughborough, UK) and 1x TBE (0.089 M Tris, 0.089 M boric acid and 0.002 M EDTA, Fisher Scientific, Loughborough, UK) and heated in the microwave at 450 watts until the dissolution of the agarose powder. After cooling, GelRed™ was added and the mixture was then transferred to a gel tray and left to set for approximately 1-1.5 hours. 5 μL of RNA samples were then loaded with 1 μL 6X DNA Loading Dye (2.5% Ficoll-400, 10 mM EDTA, 3.3 mM Tris-HCl (pH 8.0 25°C), 0.02% Dye 1 and 0.0008% Dye 2, New England Biolabs, Knowl Piece, UK) and separated by electrophoresis for *ca.* one hour at 70 v and viewed using a UV transilluminator (Gel Doc™ EZ System, BioRad, Watford, UK). Particular attention was made to degradation in the low-molecular range. Furthermore, the characteristic bands for mollusc's 28S and 18S RNA fractions were taken into consideration, as in electrophoresis the 28S ribosomal RNA migrates differently than mammal cells, breaking into two fractions during the agarose run and appearing less bright than the 18S band (**Fig. 2.10**, Barcia et al., 1997).

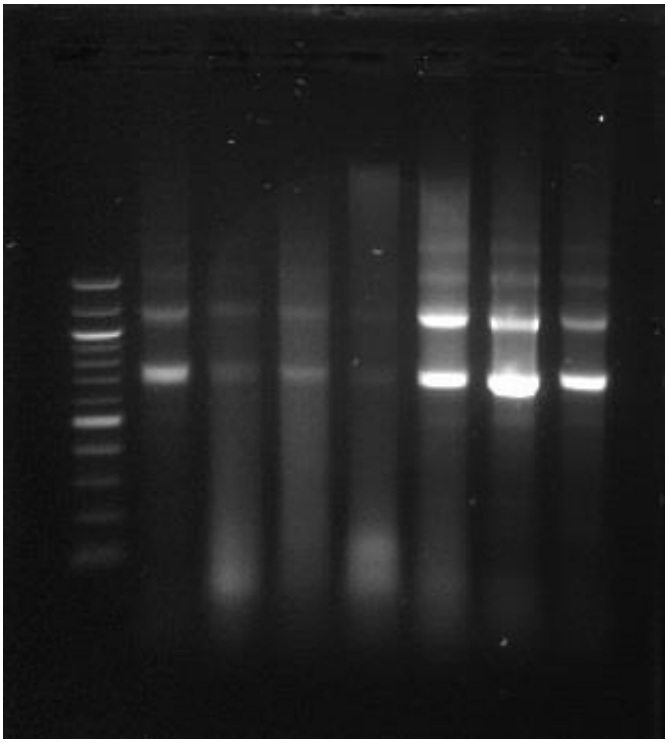

Fig. 2.10 RNA samples in 1% agarose-TBE gel stained with GelRed™. From left to right: 100 bp DNA ladder, RNA samples at 45.3 ng/µL, 24 ng/µL (below quality standard of integrity (smeared appearance in the low molecular weight) - not accepted), 16 ng/µL (below quantity standard of 20 ng/ µL - not accepted), 13 ng/µL (below quantity and quality standards - not accepted), 98.1 ng/µL, 348 ng/µL, 82.1 ng/µL

2.6 Materials and Methods: cDNA synthesis

Complementary DNA (cDNA) was synthesised from the RNA samples using the SuperScript™ II Reverse Transcriptase, with reduced RNase H activity and thermal stability, used for synthesising first-strand high-yield cDNA at high temperature and specificity. To standardise the samples as recommended by Bustin et al. (2009), the same RNA concentration (228 ng) was used for all cDNA synthesis. Specifically, 228 ng of total RNA was added to 1 µL of random primers and 1 µL of dNTP Mix (PrimerDesign Ltd, Camberley, UK) and sterile PCR-grade water. The mixture was heated at 65°C for 5 min in a Techne TC-4000 Thermal Cycler (Bibby Scientific, Stone, UK) and quickly chilled on ice. Then, 4 µL of 5X First-Strand Buffer, 2 µL of 0.1 M DTT and 1 µL of water were added and incubated at 25°C for 2 min. Finally, 200 units of SuperScript™ II RT were added. The mixture was then incubated at 25°C for 10 min, 42°C for 50 min and at 70°C for 15 min. cDNA was stored at -20°C until further analysis.

2.7 Materials and Methods: PCR species identification

As they often hybridise without any phenotypic differences between hybrids, *Mytilus* species were identified by PCR of the non-repetitive region *Mytilus* foot protein 1 *mfp-1* in a final volume of 25 µL, using the sense primer *Me15* 5'-CCAGTATACAAACCTGTGAAGA-3' and anti-sense primer *Me16* 5'-TGTTGTCTTAATAGGTTTGTAAGA-3' from Inoue et al. (1995). Protocols for primer concentration and thermal conditions from Bignell et al. (2008), Brooks and Farmen (2013), Inoue et al. (1995) and Lynch et al. (2014) were tested to find the optimal one. Finally, thermal conditions from Bignell et al. (2008) were slightly modified according to the Taq polymerase guidelines. Primer concentration of 300 nM for each primer was used in combination with 12.5 µL of PCRBIO Taq Mix Red (containing 6mM $MgCl_2$, 2mM dNTPs, PCR BioSystems, London, UK), 1.25 µL of cDNA and the following thermal conditions: pre-heating to 95°C for 5 min, followed by 40 cycles of: 1 min at 95°C, 1 min at 60.5°C and 1 min at 72°C followed by a final extension step of 10 min at 72°C. PCR and agarose gel techniques were chosen as a routine method for species identification, as *Me15* and *Me16* are genetic markers located in the nuclear gene and encode for the polyphenolic adhesive foot protein involved in the byssus thread formation. *M. edulis* individuals show an amplified fragment size of 180 bp, while *M. galloprovincialis* have 126 bp smaller sizes of *mfp-1*. PCR products were separated by electrophoresis in a 2% TBE-agarose gel stained with GelRed™ and the band sizes were assessed by comparison to the 100bp DNA ladder (New England Biolabs Ltd, Knowl Piece, UK).

2.8 Materials and Methods: Primer optimisation via PCR and qPCR amplifications

Primers for reference genes (18S ribosomal RNA *Me18S*, 28S ribosomal RNA *Me28S* and elongation factor-1 alpha *EF1α*) and genes of interest (superoxide dismutase *sod*, catalase *cat*, heat shock protein 70 *hsp70*, estrogen related receptor *MeER1* and estrogen receptor *MeER2*) were chosen accordingly to the current literature and state of the art. Specifically, primers for *cat*, *sod* and *hsp70* were chosen as representatives of the stress response, specifically the antioxidant enzyme (*sod* and *cat*) and cellular protection (*hsp70*) pathways. *MeER1* and *MeER2* were chosen because of their possible involvement

in estrogen signalling and the reproductive cycle. *Me18S*, *Me28S* and *EF1α* were chosen as they represent suitable reference genes during mussel gametogenesis and exogenous estrogen exposures, contrary to other common reference genes such as *β-actin* (Cubero-Leon et al., 2012; Jarque et al., 2014).

Three or four sets of primers (i.e., forward and reverse) for each gene were chosen from the literature or designed online using Primer3 (http://primer3.ut.ee/) from published sequences (**Table 2.2**) for the optimisation step, in order to increase the likelihood to find any absence of secondary product formations and acceptable efficiencies between 90 and 110% during the qPCR analysis (**Fig. 2.11 - 2.20** and **Table 2.3**). The lyophilised primers (Integrated DNA Technology, Leuven, Belgium) were resuspended in molecular grade water to a final concentration of 100 µM, aliquoted and stored at -20 ℃ until the analysis. For each set, primer specificity was firstly assessed by Polymerase Chain Reaction (PCR) amplification and 2% agarose-TBE gel electrophoresis. PCR products were prepared using the Q5 High-Fidelity Polymerase (NewEngland BioLabs, Knowl Piece, UK) and PCR reactions were performed on a Techne TC-4000 Thermal Cycler (Bibby Scientific, Stone, UK). Specifically, 0.5 - 1 µL of template cDNA was mixed with 5 µL of 5x Q5 Reaction Buffer, 10 mM of dNTPs, 0.25 - 1.25 µL of forward and reverse primers, 0.25 µL of Q5 high-fidelity DNA Polymerase and PCR grade water. Specificity of the primer sets was performed at different thermal cycling programs run as follows: pre-heating to 94℃ for 2 min, followed by 35 cycles of: 30 sec at 94°C, 30 sec at 55-62°C and 30 sec at 72°C followed by a final extension step of 2 min at 72°C. Then, 10 µL PCR products were loaded with 2 µL of 6X gel DNA Loading Dye (New England Biolabs Ltd, Knowl Piece, UK) in a 2% agarose-TBE gel and run at 80V. Band sizes were assessed by comparison to the 100bp DNA ladder, loaded into the gel for reference.

Table 2.2 List of primers tested via PCR and 2% agarose gel, with associated reference gene (RF), gene of interest (GoI), GenBank access number, melting temperature (Tm), guanine-cytosine content (% GC) (5'-3') sequences for forward (F) and reverse (R) primers. Primer sets in grey are the ones chosen for the final qPCR analysis

Reference Gene/ Gene of Interest	GenBank Access. No.	Primer name	(5'-3') sequence	Tm (°C)	% GC	Reference
GoI: *Superoxide Dismutase*	**AJ581746**	*SOD_F1* *SOD_R1*	TTTCTCGCAGTTTACGGTCA AACTCGTGAACGTGGAAACC	54.2 55.5	45.0 50.0	Barrick et al., (2018)
		SOD_F2 *SOD_R2*	TCTCGCAGTTTACGGTCACT GTGGAAACCGTGTTCTCCTG	56.0 55.9	50.0 55.0	Designed online
		SOD_F3 *SOD_R3*	TCTCGCAGTTTACGGTCACT CTGAAAGCGACTGTTCCTGT	56.0 55.1	50.0 50.0	Designed online
GoI: *Catalase*	**AY580271**	*CAT_F1* *CAT_R1*	TGGGATCTGGTGGGAAATAA ATCAGGAGTTCCACGGTCAG	53.3 56.5	45.0 55.0	Barrick et al., (2018)
		CAT_F2 *CAT_R2*	ACTTCGACCAGAGACAACCC GCCTGTCCATCCTTGTTGAC	56.7 56.1	55.0 55.0	Designed online
		CAT_F3 *CAT_R3*	CACCAGGTGTCCTTCCTGTT CTTCCGAGATGGCGTTGTAT	57.1 54.8	55.0 50.0	Lacroix et al., (2014)
GoI: *Heat Shock Protein 70*	**AF172607**	*HSP70_ F1* *HSP70_ R1*	GGGTGGTGGAACTTTTGATG CTCTTTGCCCTTTCACAAGC	54.1 54.5	50.0 50.0	Barrick et al., (2018)
		HSP70_ F2 *HSP70_ R2*	ACAAGAGCCAGGTTTGAGGA CAGCAGCCTTGTCTAGTTTGG	56.3 56.0	50.0 52.4	Designed online
		HSP70_ F3 *HSP70_ R3*	ACAAGAGCCAGGTTTGAGGA GTTTGGCATCACGTAGAGCT	56.3 55.2	50.0 50.0	Designed online
		HSP_F4 *HSP_R4*	GGGTGGTGAAGACTTTGACA TGCCCTTTCACAAGCAGTTC	54.9 56.0	50.0 50.0	Designed online
GoI: *Estrogen related receptor*	**AB257132**	*MeER1_ F1* *MeER1_ R1*	TTACGAGAAGGTGTGCGTTT TTTTTCACCATAGGAAGGATA TGT	54.5 52.0	45.0 33.3	Puinean et al., (2006)

		MeER1_F2 *MeER1_R2*	ATACTCTTGCCCTGCCAACT CGGTCTAAACGCACACCTTC	56.4 56.1	50.0 55.0	Designed online
		MeER1_F3 *MeER1_R3*	CCAGATCTTCAGGGTGACGA CTTGTTTGGCCCAGCTGATT	56.2 56.2	55.0 50.0	Designed online
GoI: *Estrogen Receptor*	**AB257133**	*MeER2_F1* *MeER2_R1*	GGAACACAAAGAAAAGAAAGGAAG ACAAATGTGTTCTGGATGGTG	52.7 53.4	37.5 42.9	Puinean et al., (2006)
		MeER2_F2 *MeER2_R2*	CAGGTCTGCAGTGATAACGC TGCAGGCCTGACAACTTTTC	56.0 56.0	55.0 50.0	Designed online
		MeER2_F3 *MeER2_R3*	CAGGTCTGCAGTGATAACGC AGGTCCCTGAATACTGCGTT	56.0 56.0	55.0 50.0	Designed online
RG: *18s ribosomal RNA*	**L33448**	*18S_f1* *18S_r1*	CATTAGTCAAGAACGAAAGTCAGAG GCCTGCCGAGTCATTGAAG	53.6 56.4	40.0 57.9	Cubero-Leon et al., (2012)
		18S_f2 *18S_r2*	GTGCTCTTGACTGAGTGTCTCG CGAGGTCCTATTCCATTATTCC	57.4 52.5	54.5 45.5	Ciocan et al., (2011)
		18S_f3 *18S_r3*	CGTTCTTAGTTGGTGGAGCG CTCTAAGAAGTTGCGCCGAC	55.9 55.9	55.0 55.0	Designed online
	AY527062.1	*18S_f4* *18S_r4*	CGCGTTTATTAGATCAAAACCAG AGTTTACAGACGGGATAGTTGAA	55.1 55.8	52.6 45.4	Designed online
		18S_f5 *18S_r5*	CCGGCGACGTATCTTTCAA AGGCATATCACGTACCATCGAA	52.4 53.5	39.1 39.1	Hüning et al., (2013)
RG: *28s ribosomal RNA*	**Z29550**	*28S_f1* *28S_r1*	AGCCACTGCTTGCAGTTCTC ACTCGCGCACATGTTAGACTC	58.1 57.3	55.0 52.4	Ciocan et al., (2011)
		28S_f3 *28S_r3*	CCTTGGAGTCGGGTTGTTTG ACTCGTGCCGGTATTTAGCT	56.3 56.2	55.0 50.0	Designed online

	AF339512	*28S_f2* *28S_r2*	CTGGCCTTCACTTTCATTGTGCC GACCCGTCTTGAAACACGGACCA	59.0 61.4	52.2 56.5	Zanette et al., (2013)
RG: *Elongation Factor 1-α*	**AY580270**	*Ef1_F1* *Ef1_R1*	CACCACGAGTCTCTCCCAGA GCTGTCACCACAGACCATTCC	58.2 58.2	60.0 57.1	Ciocan et al., (2011)
		Ef1_F2 *Ef1_R2*	GCCTGGGTTTTGGACAAACT ATAGGGCGTGTTCTCTGGTC	56.1 56.6	50.0 55.0	Designed online
	AF063420	*Ef1_F3* *Ef1_R3*	ACCCAAGGGAGCCAAAAGTT TGTCAACGATACCAGCATCC	57.2 54.8	50.0 50.0	Lacroix et al., (2014)

For each set of reference genes and genes of interest, primer efficiency was assessed by qPCR reactions in accordance with the MIQE guidelines (Bustin et al. 2009) on a CFX96 Real-Time PCR Detection System (Bio-Rad, Hemel Hempstead, UK) using 0.2 mL 8-tube PCR strips and Optical Flat 8-cap strips (BioRad, Watford, UK). At the end of each qPCR reaction, an amplification plot was generated showing the Cq value for each qPCR product. The Cq is a value showing the cycle number at which the fluorescent signal from the sample is detected from the background and it is considered acceptable when it occurs before the 40th cycle (Bustin et al., 2009). The reactions were performed using 10 µL of PrecisionPlus qPCR Master Mix premixed with SYBR Green (PrimerDesign, Eastleigh, UK), 7.5 µL molecular-grade water, 1 µL of each primer, and 0.5 µL cDNA at different dilutions. Primer specificity was tested at final concentrations of 100, 300 and 500 nM for each set, through any absence of secondary product formations by the melt peaks at the conclusion of the reactions (**Fig. 2.12 - 2.19**). Cq values, amplification plots and melt curve peaks were generated by the BioRad CFX Manager software (V1.6.541.1028). Primer efficiency was tested over a range of cDNA dilutions (10X or 5X). The standard curve was built in Microsoft Office 365 Excel from Cq values against log cDNA dilutions, displaying lines of best fit, slope and R^2 value. The R^2 value represents the pipetting accuracy and should therefore be as close to 1 as possible. The efficiency slope was produced by at least a minimum of 4 acceptable dilution points to % efficiency (Efficiency = $-1+10^{(-1/\text{slope})}$). The slope value was input in the qPCR Standard Curve Slope to Efficiency Calculator website (http://www.genomics.agilent.com/biocalculators/calcSlopeEfficiency.jsp?_requestid=851955) and only slopes between -3.1 and -3.6 with resulting efficiencies between 90 and

110% were accepted (**Table 2.3** and **Fig. 2.12 - 2.19**, Taylor et al., 2010). qPCR products were ultimately checked using 2% agarose-TBE gel (80V) stained with GelRed™ Nucleic Acid Gel Stain (**Fig. 2.20**).

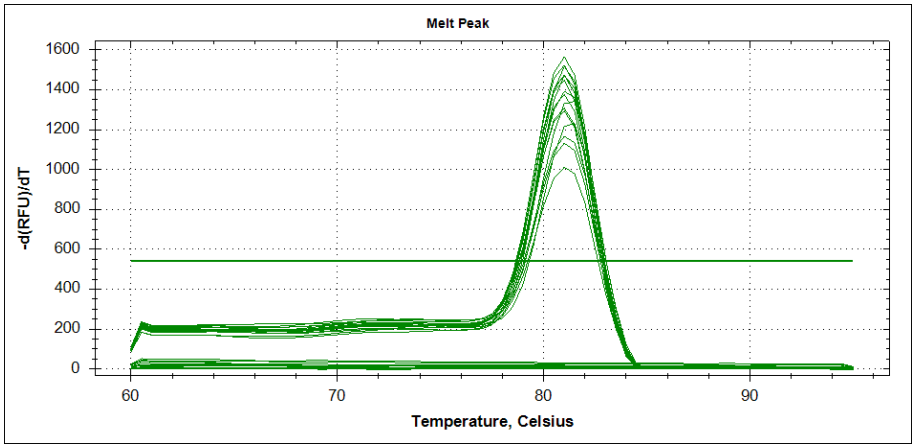

Fig. 2.11 Example of a melt peak at the end of qPCR cycles for *sod* primers for sets 1, 2 and 3 at the same melting temperatures with different sample dilutions during the optimisation steps

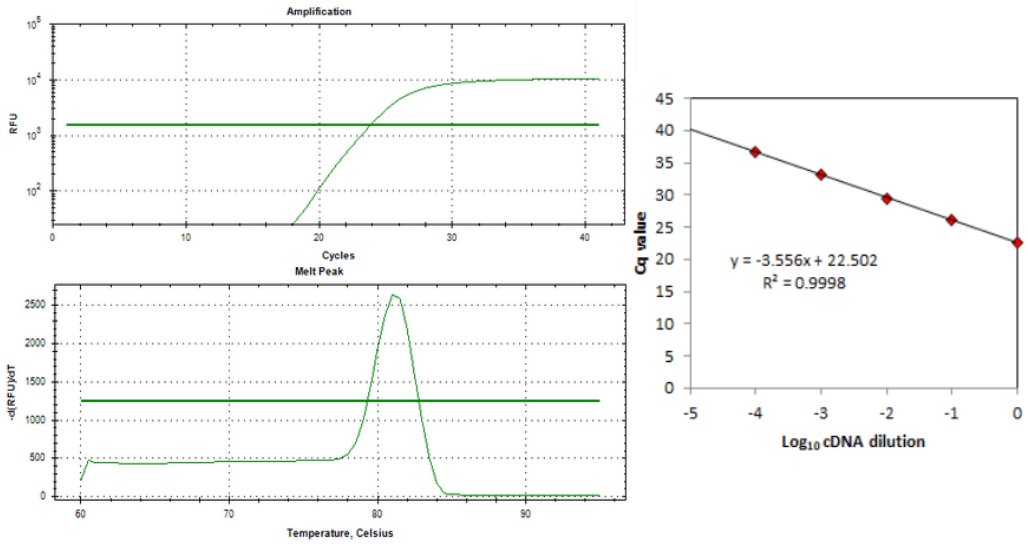

Fig. 2.12 Optimisation for *sod* primer set no. 2 at 100 nm. Amplification plots (log scale, in Relative Fluorescence Units), melt temperature peak plot and standard curve plot (10X dilutions) with R^2 values displayed

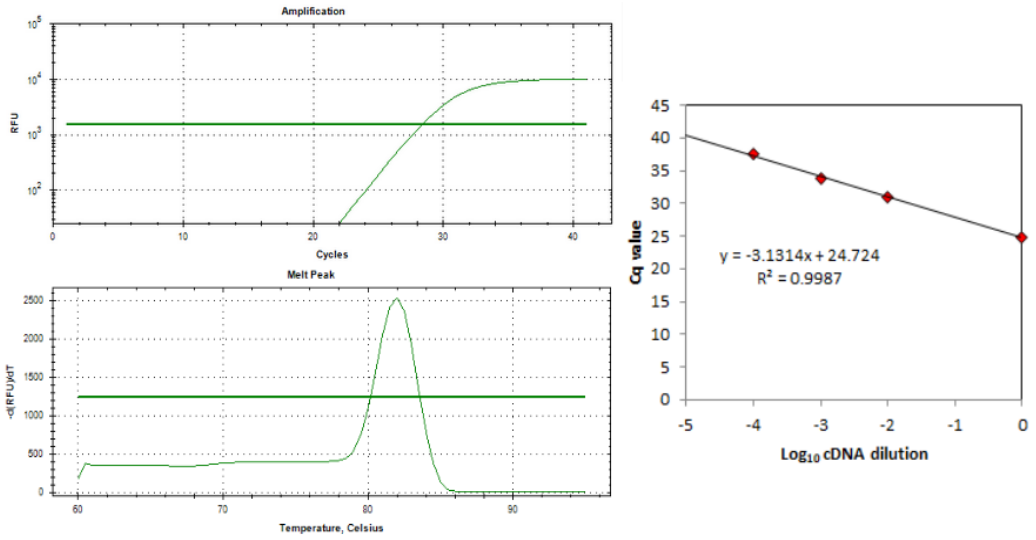

Fig. 2.13 Optimisation for *cat* primer set no. 3 at 100 nm. Amplification plots (log scale, in Relative Fluorescence Units), melt temperature peak plot and standard curve plot (10X dilutions) with R^2 values displayed

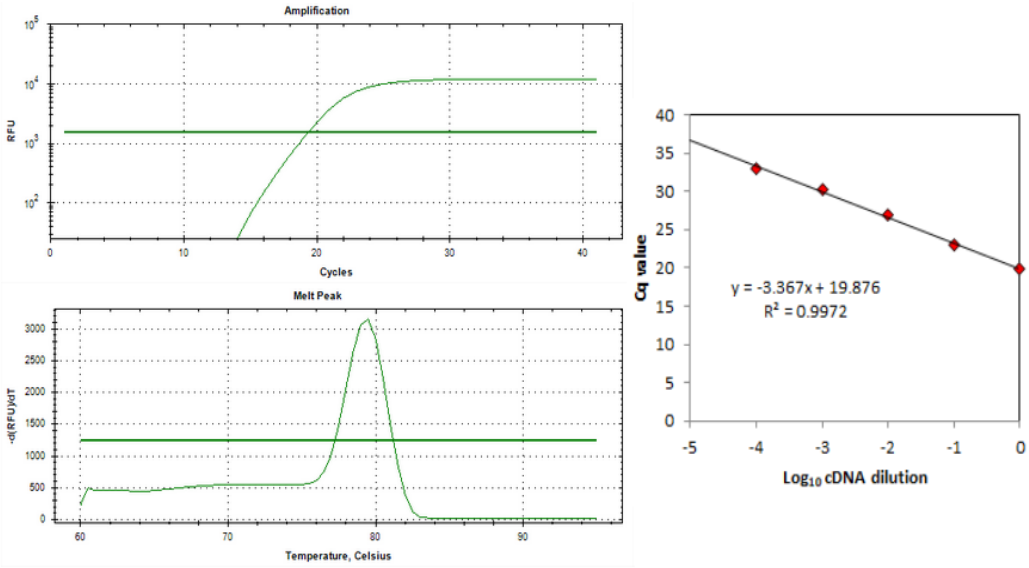

Fig. 2.14 Optimisation for *hsp70* primer set no. 4 at 100 nm. Amplification plots (log scale, in Relative Fluorescence Units), melt temperature peak plot and standard curve plot (10X dilutions) with R^2 values displayed

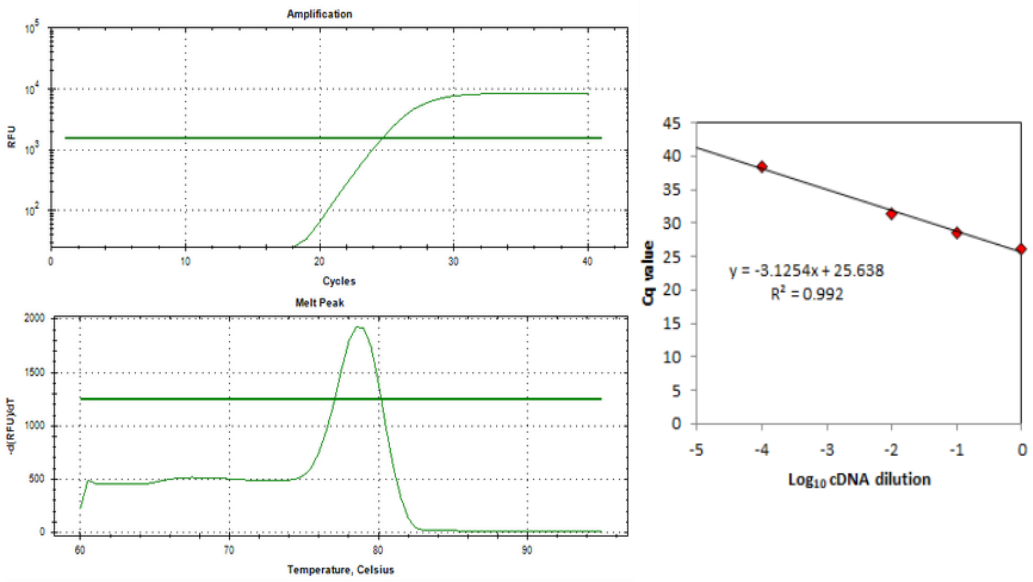

Fig. 2.15 Optimisation for *MeER1* primer set no. 3 at 100 nm. Amplification plots (log scale, in Relative Fluorescence Units), melt temperature peak plot and standard curve plot (10X dilutions) with R^2 values displayed

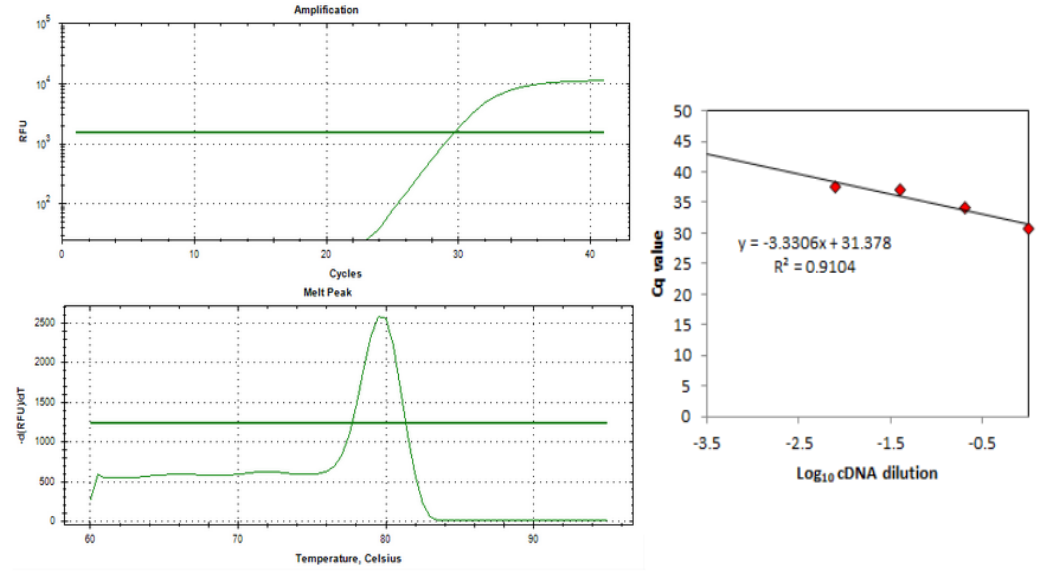

Fig. 2.16 Optimisation for *MeER2* primer set no. 1 at 100 nm. Amplification plots (log scale, in Relative Fluorescence Units), melt temperature peak plot and standard curve plot (5X dilutions) with R^2 values displayed

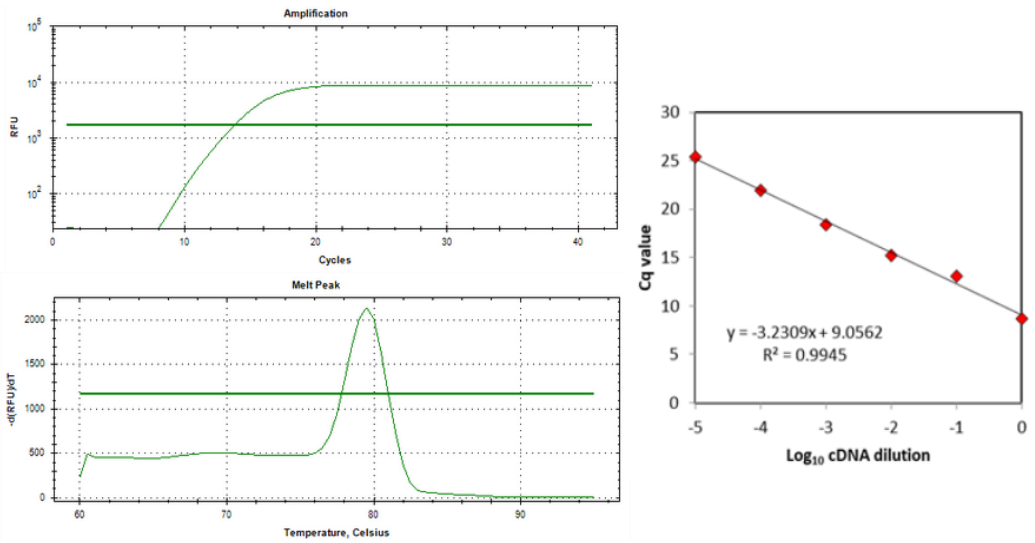

Fig. 2.17 Optimisation for *Me18s* primer set no. 2 at 50 nm. Amplification plots (log scale, in Relative Fluorescence Units), melt temperature peak plot and standard curve plot (10X dilutions) with R^2 values displayed

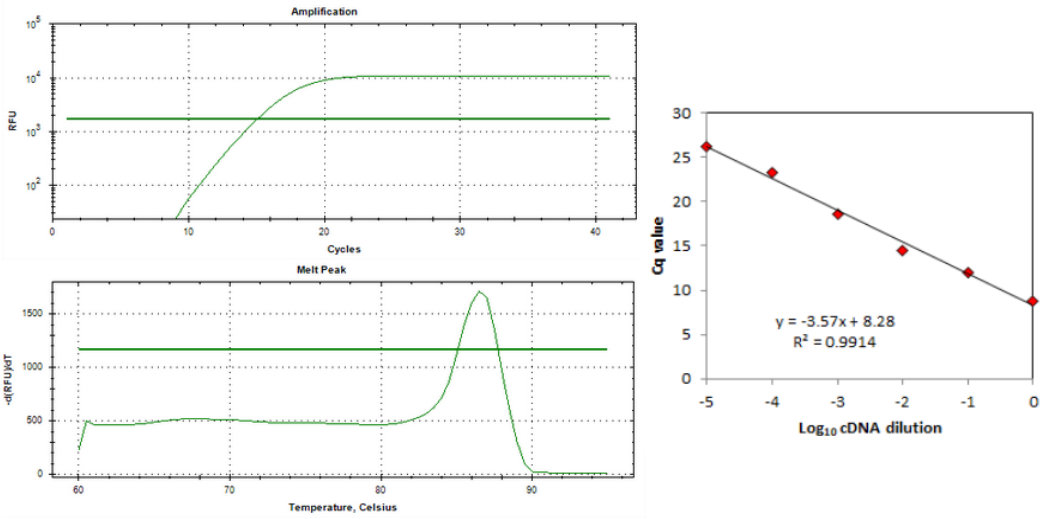

Fig. 2.18 Optimisation for *Me28s* primer set no. 1 at 100 nm. Amplification plots (log scale, in Relative Fluorescence Units), melt temperature peak plot and standard curve plot (10X dilutions) with R^2 values displayed

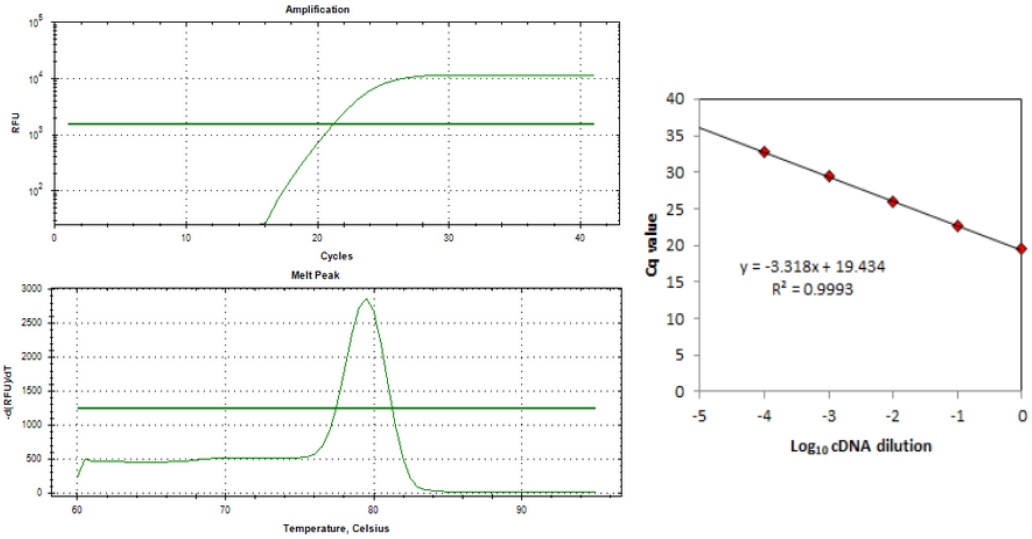

Fig. 2.19 Optimisation for *EF1α* primer set no. 1 at 100 nm. Amplification plots (log scale, in Relative Fluorescence Units), melt temperature peak plot and standard curve plot (10X dilutions) with R^2 values displayed

Final primer sequences were: *elongation factor-1 alpha (EF1α)* set no. 1 (GenBank accession no. **AY580270**), *18S ribosomal RNA (Me18S)* set no. 2 (GenBank accession no. **L33448**) and *28S ribosomal RNA (Me28S)* set no. 1 (GenBank accession no. **Z29550**) from Ciocan et al. (2011); *catalase (cat)* set no. 3 (GenBank accession no. **AY580271**) from Lacroix et al. (2014)*; estrogen receptor 2 (MeER2)* set no. 1 (GenBank accession no. **AB257133**) from Puinean et al. (2006). Additionally, new primers were designed using Primer3 (http://primer3.ut.ee/) from published sequences (*superoxide dismutase (sod)* set no. 2 (GenBank accession no. **AJ581746**)*; heat shock protein 70 (hsp70)* set no. 4 (GenBank accession no. **AF172607**)*; estrogen receptor 1 (MeER1)* set no. 3 (GenBank accession no. **AB257132**). For each chosen set, primers' specie identification was additionally confirmed by identification using BLAST searches (blastn) to compare the gene sequences against the NCBI nucleotide collection (*nr/nt*) database optimised for highly similar sequences (*megablast*). Primer details are provided in **Table 2.2** for the optimisation steps and **Table 2.3** and **Fig. 2.12 - 2.20** for the final chosen sets.

In order to determine the most suitable combination of reference genes for data normalisation, the stability of *Me18S*, *Me28S*, and *EF1α* was tested over 25% of the total samples (n = 30) using Kruskal-Wallis test (Rstudio 3.6.2) and RefFinder software (https://www.heartcure.com.au/reffinder/). Kruskal-Wallis test revealed no significant effects among treatments for the three reference genes (*Me18S* KW-H= 4.96, p = 0.42; *Me28S* KW-H = 5.46, p = 0.36; *EF1α* KW-H = 4.45, p = 0.49) and the combination of

Me18S and *Me28S* genes was the recommended most stable one for this dataset by the RefFinder software. Consequently, *Me18S* and *Me28S* genes were chosen for normalisation of the final dataset using the $2^{-\Delta Ct}$ and $2^{-\Delta\Delta Ct}$ methods (Schmittgen and Livak, 2008). Final primer concentrations are given in **Table 2.3**. Sample dilutions (1:10) were used in the final reactions for *Me18S* and *EF1α.* Thermal cycling was as follows: 95°C for 2 min, 40 cycles of 95°C for 10 sec, 60°C for 1 min and 72° C for 1 min. Template-negative reactions were included alongside samples. Eventually, qPCR duplicate reactions were performed for 8 female and 8 male cDNA samples for each treatment using Hard-Shell® Low-Profile Thin-Wall 96-Well Skirted PCR plates and Microseal® 'B' adhesive seals (BioRad, Watford, UK) in duplicates to standardise fluorescence reflection across the samples. For each sample, the GOI Cts were normalised with the RG Cts, calculating the ΔCt value as *ΔCt = Ct (Gene of Interest) - geometric mean Ct (Reference Genes)*. Additionally, for each treatment condition, the *ΔCt* values were normalised with the *ΔCt* values of the control condition, calculating the *ΔΔCt* value as *ΔΔCt = ΔCt (Treatment) - ΔCt (Control).* Then, $2^{-\Delta Ct}$ and $2^{-\Delta\Delta Ct}$ values were calculated (Livak and Schmittgen, 2001; Schmittgen and Livak, 2008). Calculations were performed in Microsoft 365 Excel.

Table 2.3 Final primers used for qPCR amplification of reference genes and genes of interest

Gene name	GenBank accession no.	Primer	Sequence (5'-3')	Amplicon length (bp)	Amplif. efficiency %	R^2	Final conc. (nM)
sod	**AJ581746**	For Rev	TCTCGCAGTTTACGGTCACT GTGGAAACCGTGTTCTCCTG	208	91.1	0.999	100
cat	**AY580271**	For Rev	CACCAGGTGTCCTTCCTGTT CTTCCGAGATGGCGTTGTAT	235	108.6	0.999	100
hsp 70	**AF172607**	For Rev	GGGTGGTGAAGACTTTGACA TGCCCTTTCACAAGCAGTTC	127	98.2	0.997	100
Me ER1	**AB257132**	For Rev	CCAGATCTTCAGGGTGACGA CTTGTTTGGCCCAGCTGATT	94	108.9	0.992	100
Me ER2	**AB257133**	For Rev	GGAACACAAAGAAAAGAAAG GAAG ACAAATGTGTTCTGGATGGTG	232	99.6	0.910	100
EF1α	**AY580270**	For Rev	CACCACGAGTCTCTCCCAGA GCTGTCACCACAGACCATTCC	105	100.2	0.999	100
Me 18S	**L33448**	For Rev	GTGCTCTTGACTGAGTGTCTCG CGAGGTCCTATTCCATTATTCC	116	103.9	0.995	50
Me 28S	**Z29550**	For Rev	AGCCACTGCTTGCAGTTCTC ACTCGCGCACATGTTAGACTC	143	90.6	0.991	100

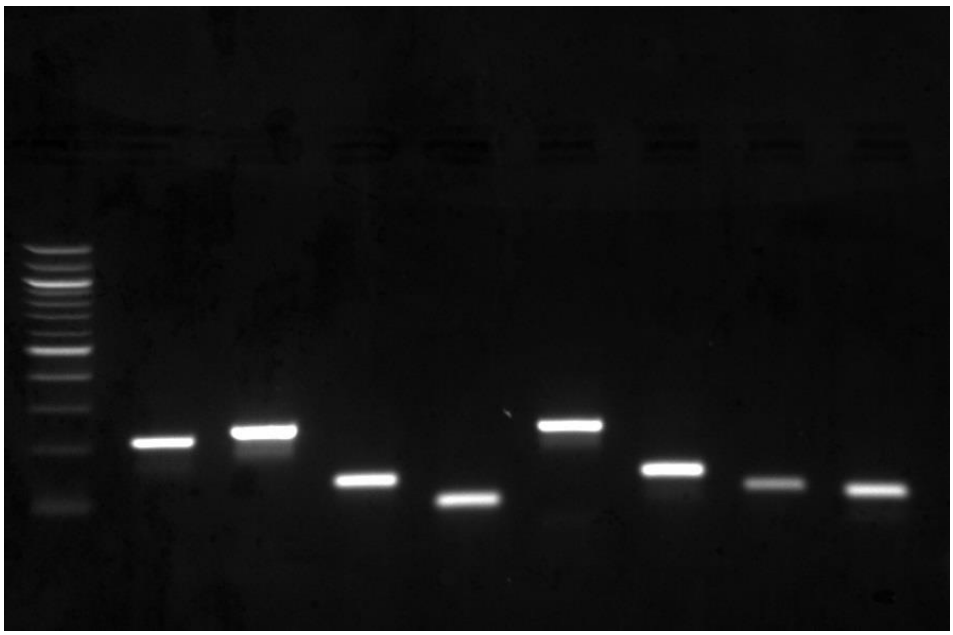

Fig. 2.20 Agarose gel 2% (2%, GelRed, run at 80V) after a qPCR run, showing the final chosen primer sets. From left to right: 100bp DNA ladder, *sod* (208 bp), *cat* (235 bp), *hsp70* (127 bp), *MeER1* (94 bp), *MeER2* (232 bp), *Me28S* (143 bp), *Me18S* (116 bp), *EF1α* (105 bp)

2.9 Materials and Methods: Statistical analysis

Ordinal logistic regression was used to predict the ordinal dependent variables "Gametogenesis stage", assuming "DEHP", "Temperature" and "Sex" as independent variables. The dependent variable "Gametogenesis stage" was measured at the ordinal level (i.e., a 3-point scale ranging from "development" to "mature" to "spawning"). Independent variables "DEHP", "Temperature" and "Sex" were considered categorical variables. Ordinal logistic regression was applied considering males and females as two conditions of the variable "Sex", having previously verified that the model including both sexes (males and females, n = 154) was a better fit to the data than two separate models for males (n = 82) and females (n = 72), respectively. Model uncertainty was assessed by comparing ΔAICc values and Akaike weights in which the lowest values for ΔAICc indicate second best to last parsimonious models of the set (**Table 2.4**). Model selection was carried out in Rstudio with the *AICcmodavg* package (Mazerolle, 2013) in R 3.6.2 (CRAN). Models with ΔAIC > 10 were omitted from considerations since they have considerably less support compared to the best-fitting model (Burnham and Anderson, 2002). Ordinal logistic regression was carried out using the *polr* function (*MASS* package, Venables and Ripley, 2002), calculating the *p* value by comparing the *t*-value against the

standard normal distribution (**Table 2.5**). The proportional odds assumption (test of Parallel Lines) was tested using the *ordinal* package (Christensen, 2019).

Permutation multivariate analysis of variance (PERMANOVA, Anderson, 2014) with Bray-Curtis distance and 9999 permutations was used in Rstudio (*vegan* package, Oksanen et al., 2013) to test the effects of the exposure conditions on the $2^{-\Delta\Delta Ct}$ values of the stress-related mRNA expression (*sod*, *cat* and *hsp70*) and estrogen receptor-like mRNA expression (*MeER1* and *MeER2*) introducing "Sex" (males or females) and "Stages" (developing, mature, spawning) to underline sex-driven differences between the treatments. Pairwise multilevel comparison with Benjamini & Hochberg *p*-adjustment was used to compare different groups. Statistical significance was set to $p < 0.05$. All graphs were created using MATLAB R2021a. A focus on the $2^{-\Delta\Delta Ct}$ values analysed for each sex separately is available in the **Supplementary Appendix to Chapter 2 (S2.1** and **S2.3)**.

Regarding the effect of different treatments on the mRNA expressions of each gene, the non-parametric Scheirer-Ray-Hare (*rcompanion* package, Mangiafico, 2017) test was additionally used on the $2^{-\Delta Ct}$ values, after verifying non-normal distribution (Shapiro-Wilk test) and homogeneity of variances (Levene's test). Dunn's multiple comparison test with Benjamini & Hochberg *p*-adjustment was used for comparisons between groups (Benjamini and Hochberg, 1995). Possible outliers were identified by Grubb's test (Grubbs, 1969) and outlier values beyond the significance level of $\alpha = 0.05$ were rejected (Burns et al., 2005). A focus on the $2^{-\Delta Ct}$ values in each sex analysed for each gene separately is available in the **Supplementary Appendix to Chapter 2 (S2.2** and **S2.4).**

2.10 Results and Discussion: Histology to determine sex and gametogenesis stages

For the histology analysis, control individuals exhibited gametogenesis stages in line with values previously reported from the Filey Beach area during wintertime (Chapman et al., 2017; Seed, 1969), with some individuals having spawning gonads alongside a higher percentage of still-developing mussels. The most parsimonious ordered logistic regression model (TEMP*SEX) showed that there was a significant difference between sexes (p SEX = 0.046, t value = -1.99) and the difference in temperature had a significant effect on the transition from development to spawning stage alone (p TEMP = 0.005, t

value = 2.84) on in combination with the sex variable (*p* TEMP*SEX = 0.007, t value = -2.69 **Table 2.5**). This does not come as an unexpected result, as increased temperature is commonly used in fertility experiments to accelerate the formation of mature gametes in bivalve gonadal follicles and induce spawning within just a few hours (Gazeau et al., 2010; Rayssac et al., 2010), as well as a regulator for broodstock conditioning in intensive bivalve cultures (Fearman and Moltschaniwskyj, 2010; Utting and Millican, 1997).

The normal gametogenesis cycle of North Yorkshire mussels starts in late autumn with declining temperatures, until maturation and spawning in spring and summer (Bayne, 1976). However, high temperature and other environmental stress cues are shown to induce attenuated seasonality in bivalve gametogenesis cycle and increased or advanced spawning activity instead of only one peak per season (Bayne, 1976; Petes et al., 2008; Philippart et al., 2003; Sreedevi et al., 2014). Here, control male groups displayed percentages of developing and spawning stages in line with the natural cycle of *M. edulis* during the winter season (**Fig. 2.8, 2.9** and **2.21**). A similar trend is noticeable in the treatments exposed to DEHP (LOW DEHP and HIGH DEHP) at control temperature. On the contrary, all the high-temperature treatments (HIGH T, LOW DEHP HIGH T and HIGH DEHP HIGH T) exhibited higher percentages of spawning gonads, with a consequent increase of the SMIs (**Fig. 2.21**). An accelerated gametogenesis cycle might not provide the time necessary to store energy (e.g., glycogen) during resting periods, causing deleterious consequences in offspring quality and impairment of reproductive capacity (Fearman et al., 2009). For example, in the Mediterranean mussel *M. galloprovincialis,* chronic exposure to thermal stress had noticeable effects on males in terms of sperm concentration, motility and morphology (Boni et al., 2016), questioning the fertilisation ability of males in a global warming condition.

Males and females presented an inverted SMI trend in the high temperature treatments, showing advanced state in males, but a delay in females. In fact, female mussels displayed similar gametogenesis stages and SMIs for all the treatments (**Fig. 2.8, 2.9** and **2.21**). Females can naturally present a slight asynchrony with males with no repercussions on reproductive success (Azpeitia et al., 2017). This could also be related to the scheme of classification of the different stages of the gonadal cycle, for which female sex often appear to be slightly behind males. However, it is also possible that the production of spermatozoa is faster than the ova, due to the large yolk reserves of the latter (Seed, 1969). Nonetheless, if periods of thermal stress accelerate only the male cycle, this asynchrony would get further pronounced. Both an increase in the release of gametes through

continuous spawning, and a reduction of fertilisation events through increased asynchrony in gametogenesis are possible outcomes. Both mechanisms, however, could alter the temporal pattern of juvenile densities, which might impact coastal population dynamics of mussels. Considering as well that mussels in their mature state appear to be more sensitive to exposure to stressors (Ciocan et al., 2010a), it is a hypothesis that future global warming conditions may increase the sensitivity of mussels to pollutants while accelerating their reproductive cycle. Nevertheless, this experiment reinforced the belief that variation of temperature influences the reproductive system and gametogenesis cycle of mussels, as already seen in oysters (Fabioux et al., 2005; Zapata-Restrepo et al., 2019).

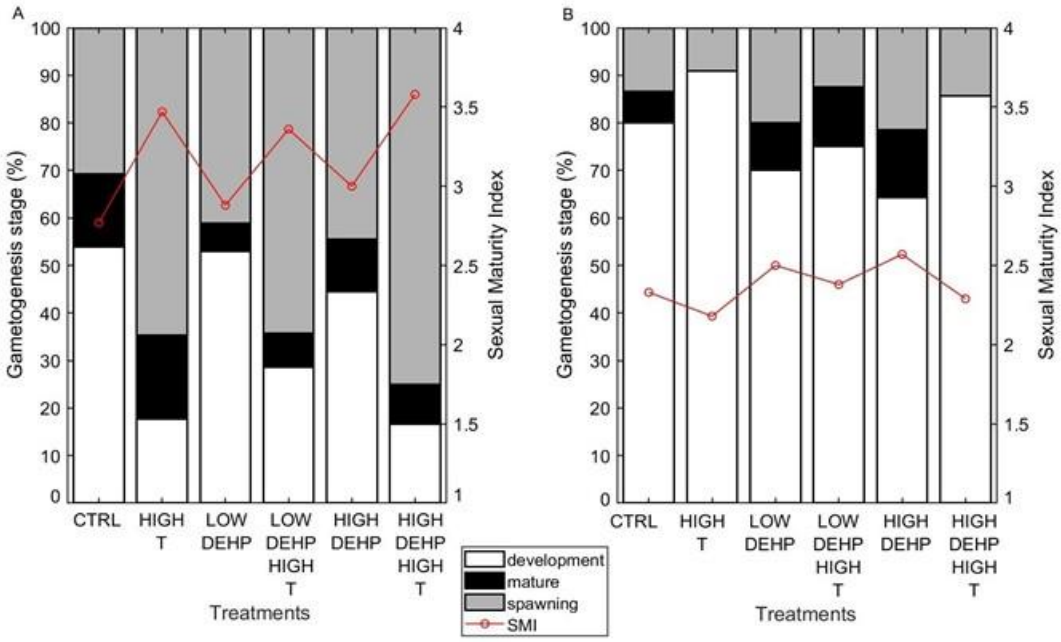

Fig. 2.21 Effects of temperature and DEHP on gametogenesis stages. Percentage of each stage and sexual maturity index (SMI) of males (A, left) and females (B, right) in CTRL (n = 13 (A), 15 (B)), HIGH T (n = 17 (A), 11 (B)), LOW DEHP (n = 17 (A), 10 (B)), LOW DEHP HIGH T(n = 14 (A), 8 (B)), HIGH DEHP (n = 9 (A), 14 (B)) and HIGH DEHP HIGH T (n = 12 (A), 14 (B))

Conversely to other studies that reported an effect of common contaminants such as antifoulants (Iyapparaj et al., 2013), insecticides (Bacchetta and Mantecca, 2009), metals (Zorita et al., 2006), tar mixture (Alonso et al., 2019), synthetic estrogens (Canesi et al., 2007a) on mussel gametogenesis, DEHP treatments did not significantly affect either males or females in this exposure. Plastic exposure was recently observed to skew the ratio of females oysters in a first-year population (Sorini et al., 2021) but to the best of

our knowledge, no published material reported an effect of DEHP exposure on gonadal maturation and spawning.

Table 2.4 Model classification, number of estimated parameters (K) for each model, Akaike Information Criterion (AICc), delta AIC (ΔAIC), Akaike weights (AICcWT), cumulative Akaike weights (CumWT), log-likelihood of each model (LL) for the three independent variables (+) temperature (TEMP), DEHP concentration (DEHP) and sex (SEX) and their interactions (*) on gametogenesis stages

model	K	AICc	Δ AIC	AICcWT	Cum WT	LL
TEMP*SEX	5	251.13	0.00	0.82	0.82	-120.50
TEMP+SEX	4	256.71	5.58	0.05	0.87	-124.31
SEX	3	257.04	5.91	0.04	0.91	-125.50
TEMP+DEHP+SEX	5	357.79	6.66	0.03	0.94	-123.83
TEMP*DEHP*SEX	9	258.02	6.89	0.03	0.97	-119.81
DEHP+SEX	4	258.09	6.96	0.03	0.99	-125.00
DEHP*SEX	5	260.04	8.94	0.01	1	-124.97

Table 2.5 Results of ordinal logistic regression for the best model of treatments (TEMP*SEX). Estimated value, standard error, *t*-value and *p* for the independent variables temperature (TEMP, 11 and 14 °C), and sex (SEX, males and females) and their interactions

Variable	Value	Std. Error	*t*-value	*p*
TEMP	1.27	0.45	2.84	0.005
SEX	-0.93	0.47	-1.99	0.046
TEMP: SEX	-2.01	0.75	-2.69	0.007

2.11 Results and Discussion: PCR species identification

As already mentioned, *Mytilus* species and putative hybrids are challenging to identify without histological or genetic analysis, considering the hybridisation between species

and environmental pressure that could affect the somatic characteristics of the shells, especially in wave-exposed habitats (Kijewski et al., 2011). In the present study, cDNA samples were identified as a blue mussel complex, due to the natural admixture and genomic overlaps between *Mytilus* spp. species that commonly occur in the Northern Hemisphere caused by incomplete reproductive isolation (Simon et al., 2020). Samples were identified as mostly pure *M. edulis* (91.7%), with a minor percentage (8.3%) of hybrids between *M. edulis* and *M. galloprovincialis* (amplified double band of 180 bp/126bp, **Fig. 2.22**).

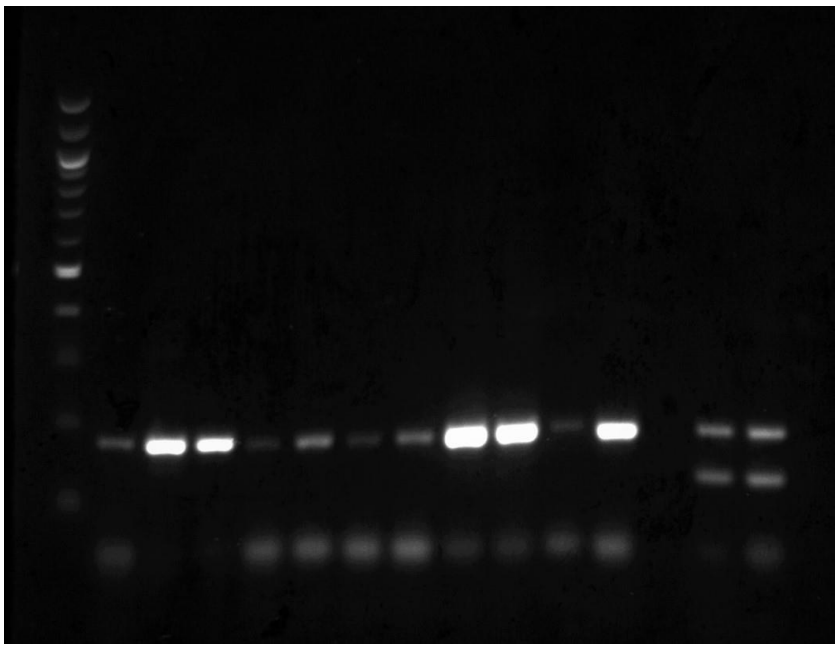

Fig. 2.22 Agarose gel (2%, GelRed™, run at 80V) for PCR species identification showing from left to right: NeB DNA ladder, 100 bp; 180 bp fingerprints of the *mfp-1* region (*M. edulis*), and two hybrid samples showing a double band of 180 bp (*M. edulis*) and 126 bp (*M. galloprovincialis*). No pure *M. galloprovincialis* or other *Mytilus* species were found

To the best of our knowledge, this could also well be the first study that reports a small percentage of mussel hybrids on the northeastern coast of England. Hybrids and pure specimens were considered as a homogeneous group and referred to as *Mytilus* spp., as no differences in amplicon sizes (similar melting temperatures during qPCR reactions) were observed between genotypes following Lacroix et al., (2014). Recently, Boutet et al. (2021) hypothesised that the proportion and distribution of hybrids in a population are subjected to the environmental status of the origin site, as the highest number of *M. galloprovincialis* in their published experiment was detected coming from a polluted area.

2.12 Results and Discussion: influence of sex and gametogenesis status on the stress-related response

When adding sex (SEX) and gametogenesis status (STAGE) as predictors of the stress-related response alongside temperature (TEMP) and DEHP exposure (DEHP), an overall difference between sexes is noticeable (p SEX < 0.001, F = 9.64), as well as an effect of all the factors together (TEMP*DEHP*SEX*STAGE p = 0.03, F = 2.88) and, similarly to the histological results, we observed a small effect of TEMP*SEX, although being not significant at the molecular level (p = 0.06, F = 2.97, **Fig. 2.23** and **Fig. 2.24**).

The general cellular stress response is influenced by environmental parameters, such as temperature, salinity, food availability and light exposure (Khessiba et al., 2005; Leiniö and Lehtonen, 2005; Sroda and Cossu-Leguille, 2011; Wilhelm Filho et al., 2001), with observed effects documented also in molluscs (Heise et al., 2003; Wang et al., 2018). Interestingly, the environmental history of the organism plays an important role in adaptation to stressors (Buckley et al., 2001). For example, gastropod populations from the same *Xeropicta derbentina* species but from different habitats were found to exhibit distinct strategies to cope with thermal stress (Troschinski et al., 2014). Native clams *Ruditapes decussatus* presented stronger responses to thermal stress compared to the alien-invasive *Ruditapes philippinarum*, in terms of activities of antioxidant enzymes and HSP70/HSC70, probably due to their less energy-demanding strategy as a response to high temperature (Anacleto et al., 2014). Furthermore, a *M. galloprovincialis* population coming from a chronically polluted environment showed attenuated effects when exposed to gradual warming at laboratory conditions over the different seasons, while a healthy population was noted to present alterations not correlated to the usual seasonal changes (Marigómez et al., 2017).

Similarly, sex and sexual stage are known to influence physiological and morphological traits differently, including the stress response, and lead to a disparate uptake and effects of contaminants (Blanco-Rayón et al., 2020; Burger, 2007; Jarque et al., 2014; Louis et al., 2021). Sex-associated differences in energy allocation and metabolic status could also influence the vulnerability of either sex to thermal stress, which could alter the composition or abundance of populations (Bedulina et al., 2017). In *M. edulis*, differences between sexes were already noted in regard to gonadal seasonal expression of clock-associated genes in response to environmental cues (Chapman et al., 2017; Chapman et

al., 2020), and polar mantle metabolite concentrations after spawning (Hines et al., 2007). When considering other tissues, sex dissimilarities in protein profiles of the zebra mussel *D. polymorpha* gills were noticed after exposure to different concentrations of the polycyclic aromatic hydrocarbon (PAH) benzo(α)pyrene (Riva et al., 2011).

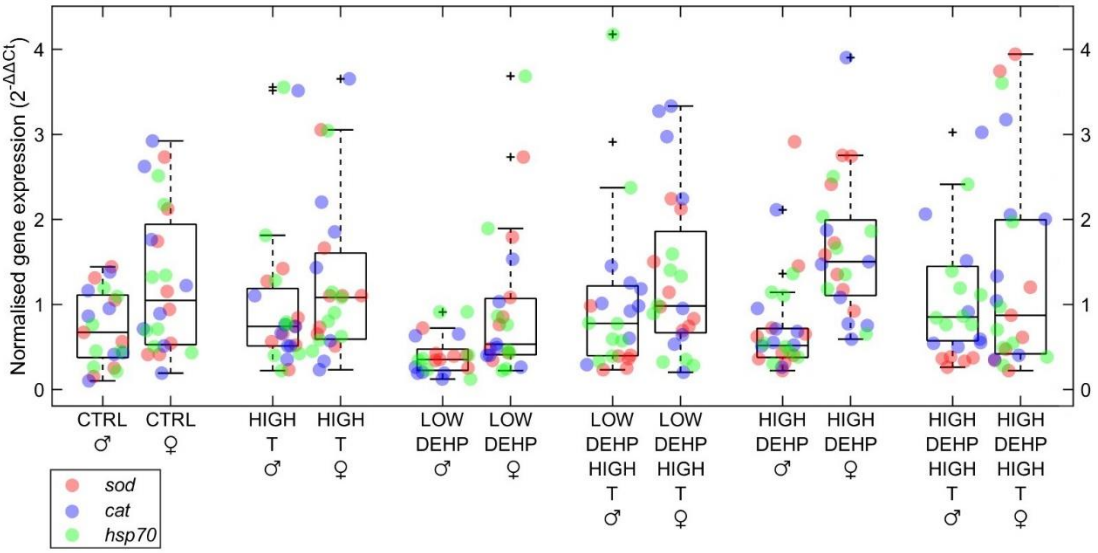

Fig. 2.23 Boxplots showing stress-related (*sod, cat, hsp70)* gene expression in males and females, n = 6 to 8. Excluded outliers are not shown, while the furthest accepted values are identified by black crosses. Different gene expressions are displayed in red (*sod*), blue (*cat*) and green (*hsp70*). Abbreviations are control (CTRL), high temperature (HIGH T), low DEHP concentration (LOW DEHP), low DEHP at high temperature (LOW DEHP HIGH T), high DEHP concentration (HIGH DEHP) and high DEHP at high temperature (HIGH DEHP HIGH T). PERMANOVA error probabilities are SEX $p < 0.001$, TEMP*SEX $p = 0.06$ and TEMP*DEHP*SEX*STAGE $p < 0.05$

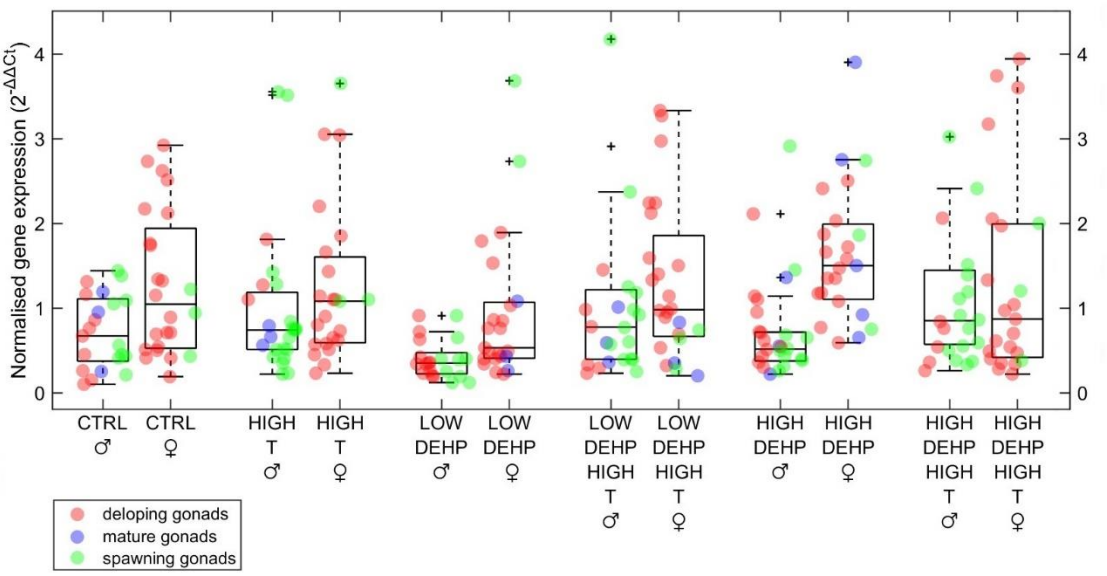

Fig. 2.24 Boxplots showing stress-related (*sod, cat, hsp70)* gene expression in males and females, n = 6 to 8. 8 considering sex and gametogenesis stage (developing. mature, spawning) of the gonads. Excluded outliers are not shown, while the furthest accepted values are identified by black crosses. Different gene expressions are displayed in in red (developing gonads), blue (mature gonads) and green (spawning gonads). Abbreviations are control (CTRL), high temperature (HIGH T), low DEHP concentration (LOW DEHP), low DEHP at high temperature (LOW DEHP HIGH T), high DEHP concentration (HIGH DEHP) and high DEHP at high temperature (HIGH DEHP HIGH T). PERMANOVA error probabilities are SEX $p < 0.001$, TEMP*SEX $p = 0.06$ and TEMP*DEHP*SEX*STAGE $p < 0.05$

Here, females showed higher stress-related gene expression than males in all treatments (**Fig. 2.23** and **Fig. 2.24**) but the statistical analysis on females only and on each of their gene separately found no particular influence by temperature and DEHP treatments (**Supplementary Fig. 2.1** and **Supplementary Fig 2.5 – 2.7**). On the other hand, males were noticed significantly affected by the exposure to thermal stress (**Supplementary Fig. 2.1**), especially regarding the antioxidant *cat* individual gene expression (**Supplementary Fig. 2.3**). The different stress response between sexes to the treatments (and in particular to the DEHP exposure) was also underlined by the pairwise multilevel comparison, which reported significant differences in both LOW DEHP and HIGH DEHP treatments (**Table 2.6**). Overall, these results show a higher sensitivity of males under environmental stressors, which in turn could suggest a more resilient status of females under prolonged stress conditions. In support of this, it is common in the animal kingdom that females have stronger immunocompetence defences, possibly related to sex-related

steroid hormone synthesis and presence (Kelly et al., 2018). A focus on the stress response in each sex and each gene analysed separately is available in the **Supplementary Appendix to Chapter 2 (S2.1** and **S2.2)**.

Table 2.6 Pairwise multilevel comparisons of the stress response (*sod, cat, hsp70*) between males and females in the same treatments

Treatment males	Treatment females	*p*
CTRL	CTRL	0.138
HIGH T	HIGH T	0.131
LOW DEHP	*LOW DEHP*	*0.046*
LOW DEHP HIGH T	LOW DEHP HIGH T	0.108
HIGH DEHP	*HIGH DEHP*	*0.001*
HIGH DEHP HIGH T	HIGH DEHP HIGH T	0.454

2.13 Results and Discussion: influence of sex and gametogenesis status on the estrogen receptor-like response

When adding sex (SEX), and gametogenesis status (STAGE) as predictors alongside temperature (TEMP) and DEHP exposure (DEHP) for estrogen receptor-related gene expression, the PERMANOVA analysis showed an effect of DEHP on the estrogen receptor-related responses (*p* DEHP = 0.03, F = 3.01) and a slight difference between sexes (*p* SEX = 0.06, F = 2.94, **Fig. 2.25 and 2.26**). Males were again observed to be highly affected by the thermal stress (**Supplementary Fig. 2.8**), especially on the individual gene expression of *MeER2* (**Supplementary Fig. 2.10**). On the other hand, a significant effect of DEHP was noted on estrogen receptor-like responses of females (**Supplementary Fig. 2.8**), particularly on *MeER1* expression (**Supplementary Fig. 2.11**). A focus on the estrogen receptor-related response in each sex and each gene analysed separately is available in the **Supplementary Appendix to Chapter 2 (S2.3** and **S2.4)**.

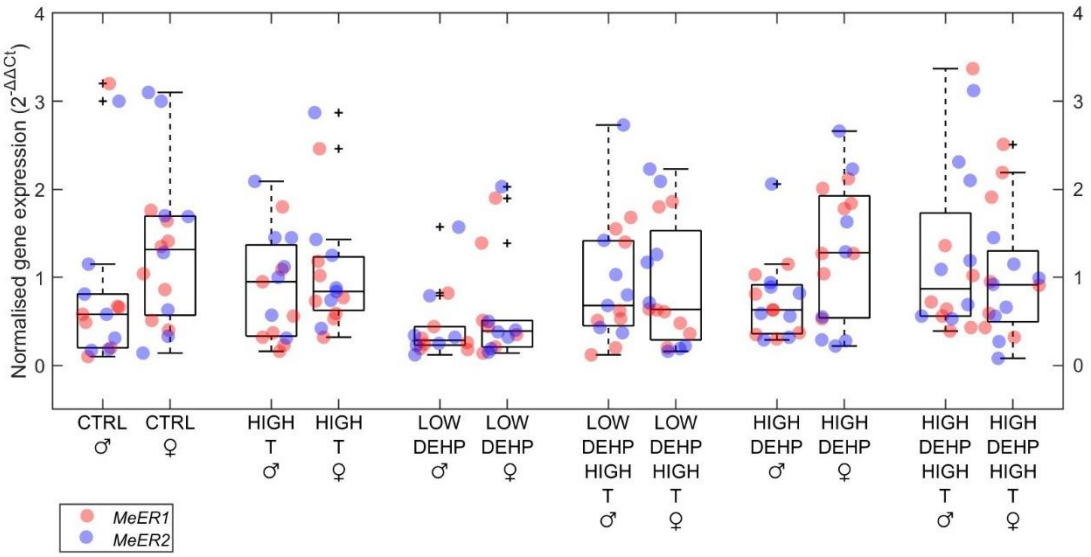

Fig. 2.25 Boxplots showing estrogen receptor-like (*MeER1, MeER2*) gene expression in males and females, n = 6 to. Excluded outliers are not shown, while the furthest accepted values are identified by black crosses. Means and standard deviations for each gametogenesis stage are displayed in red (*MeER1*) and blue (*MeER2*). Abbreviations are control (CTRL), high temperature (HIGH T), low DEHP concentration (LOW DEHP), low DEHP at high temperature (LOW DEHP HIGH T), high DEHP concentration (HIGH DEHP) and high DEHP at high temperature (HIGH DEHP HIGH T). PERMANOVA error probabilities are DEHP $p < 0.05$ and SEX $p = 0.06$

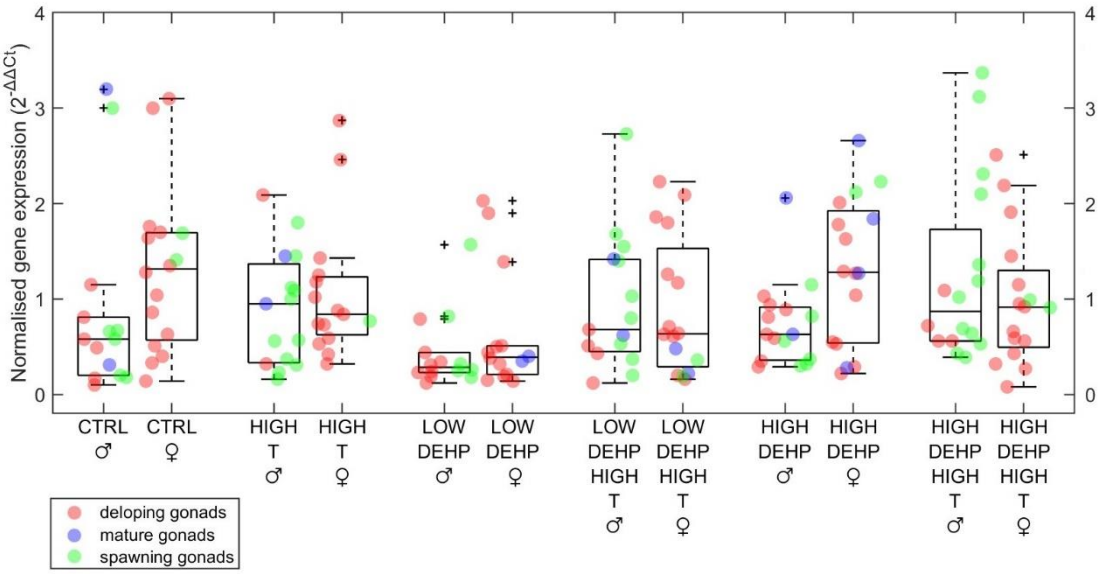

Fig. 2.26 Boxplots showing estrogen receptor-like (*MeER1, MeER2*) gene expression in males and females, n = 6 to 8 considering the gametogenesis stage (developing, mature, spawning) of the gonads. Excluded outliers are not shown, while the furthest accepted values are identified by black crosses. Means and standard deviations for each gametogenesis stage are displayed in red (developing gonads), blue (mature gonads) and green (spawning gonads). Abbreviations are control (CTRL), high temperature (HIGH T), low DEHP concentration (LOW DEHP), low DEHP at high temperature (LOW DEHP HIGH T), high DEHP concentration (HIGH DEHP) and high DEHP at high temperature (HIGH DEHP HIGH T). PERMANOVA error probabilities are DEHP $p < 0.05$ and SEX $p = 0.06$

Estrogen receptor ER and estrogen-related receptor ERR were recently found expressed in ovaries and testes of *M edulis* and *M. galloprovincialis* by Nagasawa et al. (2015) suggesting their involvement in reproduction (Croll and Wang, 2007). Both transcripts were detected in the gonads, but also *ER1* was identified distributed in gills and digestive glands and *ER2* in the ovary and pedal ganglion (Cocci et al., 2017; Nagasawa et al., 2015). Their expression was also recently found to differ between maturation stages during the ovarian cycle of *M. galloprovincialis* (Agnese et al., 2019), but the exact nature of their involvement in the estrogen signalling and the reproductive cycle, alongside their function and regulation in *Mytilus* spp., is still unknown.

Here, the LOW DEHP treatment caused a decrease in gene expression, which however was not mirrored by the HIGH DEHP treatment (**Fig 2.25** and **2.26**), even though the expression in the HIGH DEHP treatment was significantly different between sexes and higher in females (**Table 2.7**). Interestingly, a wide variation in estrogen receptor-like

expression was noted in mature males from the CTRL treatment. This could be related to the high variability in these genes in mature gonads that was already observed for mature animals from the same area in different years (Ciocan et al., 2010b). Some plastic additives have the ability to interfere with the vertebrate immune and endocrine systems following transcriptional and non-transcriptional pathways (Burgos-Aceves et al., 2021 a, b; Combarnous, 2017; Ghisari and Bonefeld-Jorgensen, 2009; Nowak et al., 2019). As part of the transcriptional ways, EDCs such as bisphenol-A (BPA) and polychlorinated biphenyls (PCBs) activate the signalling pathway by binding the hormone receptors (Bruno et al., 2019; Boas et al., 2012). Considering the non-transcriptional pathways, there are several ways of action of EDCs such as phthalate and polybrominated diphenyl ethers (Combarnous and Nguyen, 2019), including interference with the synthesis and degradation of hormones and hormone-binding proteins (Boas et a., 2012; Ptak and Gregoraszczuk, 2012; Qiu et al., 2013; Rebuli et al., 2014; Schöpel et al., 2018; Sheikh et al., 2016). In invertebrates, high concentrations of BPA were observed to upregulate estrogen-receptor levels in the New Zealand mud snail *Potamopyrgus antipodarum* (Stange et al., 2012) and estrogen-related receptor in *Marisa cornuarietis* (Bannister 2013) after a chronic exposure. However, there is still uncertainty on the exact purpose and way of action of these two receptors in mussels, with a consequent lack of knowledge about their disruption mechanisms.

Table 2.7 Pairwise multilevel comparisons of the estrogen receptor-like response (*MeER1*, *MeER2*) between males and females in the same treatments

Treatment males	Treatment females	*p*
CTRL	CTRL	0.056
HIGH T	HIGH T	0.543
LOW DEHP	LOW DEHP	0.525
LOW DEHP HIGH T	LOW DEHP HIGH T	0.618
HIGH DEHP	*HIGH DEHP*	*0.020*
HIGH DEHP HIGH T	HIGH DEHP HIGH T	0.438

2.14 Conclusions

In conclusion, a sex-dependent response is observable after the exposure to high temperature (+3°C) and two environmentally relevant concentrations of the plasticiser DEHP (0.5 µg/L and 50 µg/L), highlighting, as other studies (Banni et al., 2011; Chapman et al., 2017; Dos Reis et al., 2023; Koagouw and Ciocan, 2018; Liu et al., 2017; Matozzo and Marin, 2010), the importance for sex identification in bivalve experiments. Significant dissimilarities between males and females were in fact found when considering histological changes of the gonads (more advanced in males) and the stress response (higher in females). Furthermore, the two sexes were noted to be differently affected by the exposure to either one of the two stressors. Male mussels were observed to be more sensitive to thermal stress, demonstrated by advanced gametogenesis and by the alteration of the stress response (particularly the antioxidant *cat*) and the estrogen receptor-related system (especially *MeER2*). Conversely, females were influenced by the presence of the plastic additive, which affected the estrogen receptor-related response and in particular *MeER1*, a gene putatively involved in the endocrine pathway. In both sexes, reproduction-related outcomes seemed to be overall affected by the experimental conditions of increased temperature and DEHP exposure, demonstrated by the significant effect of DEHP on the reprotoxicity biomarkers *MeER1* and *MeER2*, and of temperature on the gonadal maturation. Considering this, further studies are needed to better understand the consequences of environmental stress on reproductive pathways in aquatic species, as the effects of external stressors such as plastic additive exposure or increased water temperature are still not fully comprehended.

Chapter 3

The effects of thermal stress, DEHP exposure and their combination on M. edulis gene expression

3.1 Introduction

This chapter aims to investigate the effect of plastic pollution in the context of global warming, analysing data generated by RNA-seq analysis of gonadal samples from *M. edulis* males. Specifically, RNA was extracted from male blue mussels *M. edulis* exposed to DEHP and increased temperature, separately and in combination (i.e., HIGH T, LOW DEHP, LOW DEHP HIGH T, as described in **Chapter 2**). This design was chosen because, as seen in **Chapter 2**, male mussels responded most to treatments of high temperature and low DEHP concentration.

In the special report of 2018, the scientific committee of the United Nations from the IPCC expressed its concern regarding the rising global temperature if no policies for reducing CO_2 emissions are promptly undertaken (IPCC, 2018). The warming climate has already caused an increase in the sea level, due to land ice loss and thermal expansion, with stronger projections in Arctic regions (i.e., polar amplification, Sampaio and Rosa, 2020). The average sea level has rapidly increased by 0.20 m between 1901 and 2018 and the annual average ice level of the Arctic Sea was observed to have reached its lowest in the decade 2011-2020 since 1850. Other consequences of global warming are heat waves and heavy precipitation, which have become more frequent and intense since 1950. Anthropogenic sources are considered also the likely main cause of "compound extreme events", defined as the combination of multiple drivers or hazards that can contribute to societal and environmental risks (IPCC, 2021). According to the SSP projections for the end of the century (described in detail in **Chapter 1.4**), temperatures will rise without reasonable doubt in the Northern Hemisphere, especially in the Arctic Ocean and North Pacific, reaching +2°C for the SSP 1 - 2.6 scenario and +5°C for the SSP 5 - 8.5 scenario (Kwiatkowski et al., 2020). These changing environmental conditions could enhance degradation, release, transport and biotransformation of a wide set of hydrophobic and hydrophilic pollutants such as persistent organic pollutants or pesticides. Temperature changes could furthermore increase the toxicity of heavy metals, carbamates, flame

retardants, fungicides, or oil compounds, causing them to partition into more bioactive and toxic metabolites and to eventually accumulate in organisms intended for human consumption such as shellfish (Kibria et al., 2021; Noyes et al., 2009). This could either happen as a direct consequence of global warming, which will increase the processes of hydrolysis, leaching and volatilisation (Bloomfield et al., 2006; Lamon et al., 2009), or indirectly via additional phenomena associated with increasing temperature such as sea level rise (Kallenborn et al., 2012) or ice melts (Ma et al., 2011; Todd et al., 2012).

Due to their resilient properties, plastic items are ubiquitously present in the Northern Hemisphere, where they endure through time even in remote areas such as the deep-sea (Barnes et al., 2009; Thompson et al., 2009). In aquatic environments, plastic fragments may at ease be absorbed by filter-feeding organisms such as bivalves (Browne, 2008) and provoke reproductive, immune and genotoxic consequences (Detree et al., 2017; Sussarellu et al., 2016). Plastic fragments are considered a long-term source of toxic additives such as phthalates, which may leach from the plastic surface into the environment (Engler, 2012). As an example, concentrations of the endocrine disruptive additive DEHP up to 83.3 μg/g were recently found in microplastic fragments during wastewater treatment processes (Takdastan et al., 2021). As already remarked, its toxic effects on the endocrine system at levels as low as 0.02 μg/L were reported in several aquatic species such as fish and crustaceans (Carnevali et al., 2010; Heindler et al., 2017; Ye et al., 2014).

Even though mussels are commonly used for scientific purposes in several fields, we are yet to fully comprehend their specialised and unique biology that differs from model animals whose genome is completely mapped (Armengaud et al., 2014). As an example, it was recently discovered that *M. galloprovincialis* is the first species in the animal kingdom possessing a pan-genomic architecture with 25% of genes subject to presence/absence variation, most of them possibly involved in stress response and survival systems (Gerdol et al., 2020). As biomonitors with high tolerance and potential for adaptation to stressors, invertebrates such as *Mytilus* should be considered potential key species for *de novo* discovery (Leoni et al., 2017). However, specific methodologies and protocol adaptations are usually required for these non-model organisms (Armengaud et al., 2014). In fact, *Mytilus* lineage-specific duplications after the divergence of the Mytilida order generated the large gene repertoire recently discovered in Gerdol et al. (2020). The same authors published a reference *M. galloprovincialis* digestive gland transcriptome using Illumina-based sequencing and *de novo* assembly (Gerdol et al.,

(2014). Later, Moreira et al. (2015) compared RNA-seq assembled reads from different *M. galloprovincialis* tissues, observing that only 55% of transcripts were present concurrently in haemocytes, mantle, muscle and gills, with mantle and muscle tissues sharing a high percentage (77%) of transcripts. In ecotoxicology experiments, RNA sequencing methods were recently used for analysing the transcriptomic responses to the polycyclic aromatic hydrocarbon benzo(a)pyrene in embryos of the green mussel *Perna viridis* (Jiang et al., 2016). Similarly, Philipp et al. (2012) sequenced a transcriptome from several tissues of Baltic Sea *M. edulis* exposed to stress sources such as lowered pH or dextran sodium sulfate (DSS) chemical.

Transcriptomics aims to catalogue and quantify the expression of transcripts, provide information about the transcriptional activity and structure of genes, and characterise splicing and post-transcriptional modifications (Mathew et al., 2015; Wang et al., 2009b). RNA-seq is a precise and refined approach for accurate transcriptome profiling, measurement and mapping of not only transcript levels, but also the related isoforms of mRNA, as well as non-coding RNA and small RNAs (Marguerat and Bähler, 2010; Wang et al., 2009b). It is considered the first sequencing-based method able to detect low-expressed genes and therefore survey the entire transcriptome in a high-rate resolution (Denoeud et al., 2008; Wang et al., 2009b). The first advantage of using RNA-seq technology is that it reconstructs overlapping reads into transcripts by using the redundancy of sequencing reads (Lu et al., 2013). Secondly, RNA-seq can uncover splicing patterns, which gives information about how exons are connected in the mature transcripts. Moreover, RNA-seq covers a large range of expression levels, which can be mapped to unique genomic regions (Lu et al., 2013a; Wang et al., 2009b). However, there is no assembly method universally suitable for the evaluation of all RNA-seq data sets, depending on species, protocols and parameter settings (Escudero, 2021; Hölzer and Marz, 2019). In the case of no reference genome being completely sequenced or available (as for non-model organisms), the *Trinity* assembly pipeline is a unified and sensitive approach for the *de novo* reconstruction of transcriptomes that can efficiently recover and reconstruct high-quality transcript fractions, including spliced isoforms and duplicated gene transcripts, resolving ~99% of the initial sequencing errors (Grabherr et al., 2011b). In general, *Trinity* pools together sets of unique sequences that overlap, then creates an independent De Bruijn graph for each group and assembles isoforms within the group (Martin and Wang, 2011). It also generates statistics for assessing the quality of the assembly, wraps external tools and conducts downstream analysis (Freedman et al.,

2020). *Trinity* was developed by the Broad Institute and Hebrew University of Jerusalem and it combines the use of three different software: Inchworm, Chrysalis and Butterfly, which are applied in sequence in order to process the large number of reads. The software workflow follows the steps (Grabherr et al., 2011a, **Fig. 3.1**):

I. *Inchworm*: assembles the reads into a k-mer (a fixed-length sequence of *k* nucleotides) graph consisting of unique sequences, then generates full-length transcripts for the most frequent isoforms and reports the unique portions of alternatively spliced transcripts.

II. *Chrysalis*: clusters minimally overlapping *Inchworm* contigs together, partitioning de Bujin graphs for each of them. Each cluster reflects the complexity of the transcripts from each gene.

III. *Butterfly*: reconciles and processes in parallel the single de Bruijn graphs from *Chrysalis* and reconstructs distinct full-length transcripts that are plausible.

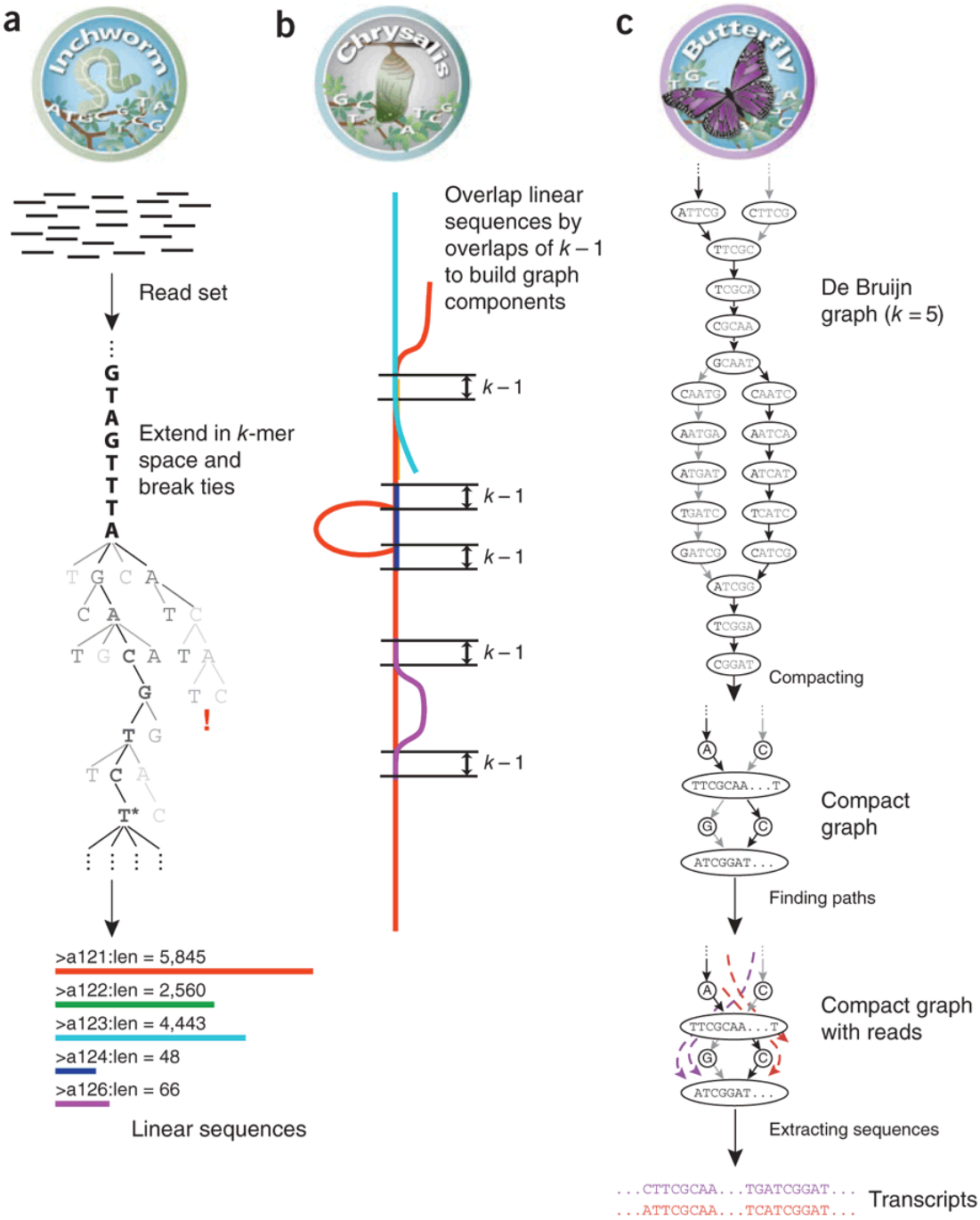

Fig. 3.1 Trinity overview, comprising the workflow for software *Inchworm*, *Chrysalis* and *Butterfly*. From Grabherr et al. (2011a)

In this chapter, an RNA-seq dataset was generated and analysed from gonadal tissues from males exposed to either a +3°C condition (TEMP), 0.5 µg DEHP /L (DEHP) or the combination of the two (COMB). In **Chapter 2**, male mussels were observed to be sensitive to thermal stress, demonstrated by an increase in both the expression of estrogen receptor- and stress response- related genes. A small effect of DEHP was also noted on

male stress response (**Supplementary Fig. 2.1**). It is hypothesised that these outcomes will find confirmation in the furthered RNA-seq analysis, and several genes involved in the stress response and reprotoxicity will be found significantly upregulated.

3.2 Materials and Methods: Experimental design

Adult blue mussels (length mean ± standard deviation = 5.4 cm ± 0.6 cm) were collected at low tide from the intertidal zone at Filey Bay, North Yorkshire, UK (54° 13´ longitude; 0° 16´ latitude) in November 2018 and transported to the aquarium facilities of the University of Hull for 12 days of acclimation in artificial saltwater (Premium REEF-Salt, Tropical Marine Centre, Chorleywood, UK) under laboratory conditions. Details of the exposure experimental design were provided in **Chapter 2.2**: Experimental design, as the individuals treated for this experiment were part of the same population exposed to the experiment described in **Chapter 2.**

3.3 Materials and Methods: Illumina library preparation

Approximately 1.0 cm^2 of left gonadal tissue from 3 male samples for the treatments HIGH T, LOW DEHP and LOW DEHP HIGH T (*approx.* 10 mg of gonad tissue, n = 9 in total) was immersed in 1 mL neutral-buffered 10% formalin solution (Sigma Aldrich, Gillingham, U.K.) at room temperature for histological observations. The same gonadal amount was dissected and preserved in 1 mL RNAlater® stabilisation solution for gene expression analysis (Thermo Fisher Scientific, Loughborough, U.K.) and stored at -80°C. Male samples were chosen considering that stress and estrogen-related responses were more affected by high temperature and low DEHP exposures, as previously observed by qPCR analysis on genes superoxide dismutase (*sod*), catalase (*cat*), heat shock protein 70 (*hsp70*), estrogen-related receptor (*MeER1*) and estrogen receptor (*MeER2*) on the same sample population in Mincarelli et al., (2021) and described in **Chapter 2**.

Samples for the RNA-seq analysis were randomly chosen from the exposed population (**Chapter 2**) and coded as TEMP_08, TEMP_13, TEMP_18 for the samples belonging to the HIGH T treatment, DEHP_12, DEHP_13_DEHP_17 for the samples belonging to the LOW DEHP treatment and COMB_07, COMB_10, COMB_26 for the samples belonging to the LOW DEHP HIGH T treatment. Gonadal samples for histological observation were

fixed in 10% buffered formalin (Sigma-Aldrich, Gillingham, UK) and washed with 0.01 M PBS (Sigma Aldrich, Irvine, UK), dehydrated with increasing ethanol (Fisher Scientific, Loughborough, UK) concentrations (70%, 90%, 100%), and cleared with Histoclear II (National Diagnostics, Atlanta, USA). The day after, the samples were embedded in paraffin wax (VWR, Poole, UK) in an EG 1160 Paraffin Wax Embedding Centre (Leica Microsystems, Milton Keynes, UK) and tissue sections (10 µm) of wax-embedded gonads were cut on a Shandon Finesse® Manual Rotary Microtome 325 (Thermo Fisher Scientific, Loughborough, UK). Slides were stained with Mayer's haematoxylin solution (Sigma-Aldrich, Schnelldorf, Germany) and eosin Y alcoholic solution (Sigma-Aldrich, Schnelldorf, Germany). Prior to microscopic analysis, microscope slides were coded, in order to conduct a blind observation. Sex and gametogenesis stage were assessed based on Seed (1969). A detailed protocol was provided in **Chapter 2.3:** Wax infiltration and H/E staining.

Gonadal samples for molecular analysis (*approx.* 10 mg of gonad tissue, n = 9) were selected and blindly coded for the analysis. Gonad tissues were preserved in RNAlater® Stabilisation Solution (Thermo Fisher Scientific, Loughborough, UK) and stored at -80°C for total RNA extraction. The High Pure RNA Isolation Kit (Roche Applied Science, Burgess Hill, UK) was used for the purification of the intact total RNA from approximately 10 mg of gonadal tissue, with an additional Dnase I digestion step, in order to remove contaminating DNA. After the extraction samples were then stored at -80 °C. A detailed protocol was provided in **Chapter 2.4**: total RNA isolation.

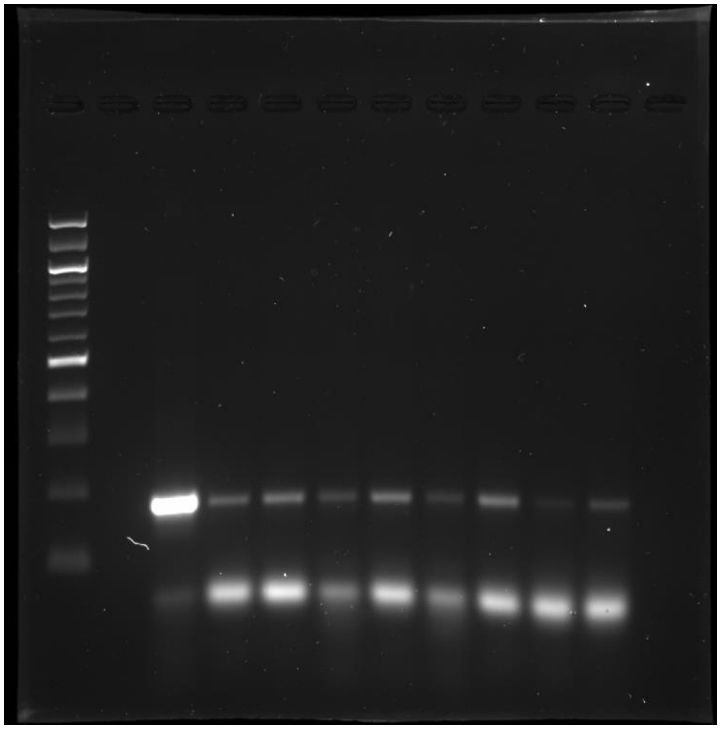

Fig. 3.2 Agarose gel (2%, GelRed™, run at 80V) showing from left to right: 100 bp NeB DNA ladder and 180 bp fingerprints of the *mfp-1* region (*M. edulis*) for the 9 male samples

Mytilus species were identified through PCR of the non-repetitive region *Mytilus* foot protein 1 *mfp-1* in a final volume of 25 µL, using the sense primer *Me15* 5'-CCAGTATACAAACCTGTGAAGA-3' and anti-sense primer *Me16* 5'-TGTTGTCTTAATAGGTTTGTAAGA-3' from Inoue et al. (1995). Thermal conditions from Bignell et al. (2008) were slightly modified according to the Taq polymerase guidelines. Primer concentration of 300 nM for each primer was used in combination with 12.5 µL of PCRBIO Taq Mix Red (containing 6mM $MgCl_2$, 2mM dnNTPs, PCR BioSystems, London, UK), 1.25 µL of cDNA and the following thermal conditions: pre-heating to 95°C for 5 min, followed by 40 cycles of: 1 min at 95°C, 1 min at 60.5°C and 1 min at 72°C followed by a final extension step of 10 min at 72°C. PCR products were separated by electrophoresis in a 2% TBE-agarose gel stained with GelRed™ and the band sizes were assessed by comparison to the 100bp DNA ladder (**Fig. 3.2**). Detailed protocol was provided in **Chapter 2.7**: PCR species identification.

RNA concentrations were quantified using a Qubit 1.0 Fluorometer (Life Technologies, UK) and the integrity was checked by 1% agarose gel electrophoresis (**Fig. 3.3** and **3.4**). As already described in **Chapter 2.5:** RNA quantification and integrity**,** the characteristic bands for mollusc 28S and 18S RNA fractions were taken into consideration (Barcia et

al., 1997). Samples were then shipped to Novogene Company Ltd. (Cambridgeshire, UK) for sequencing. On site, following the total RNA quality control pipeline, samples were then tested for purity (Nanodrop), degradation or contamination (agarose gel electrophoresis) and integrity (Agilent 2100 Bioanalyzer).

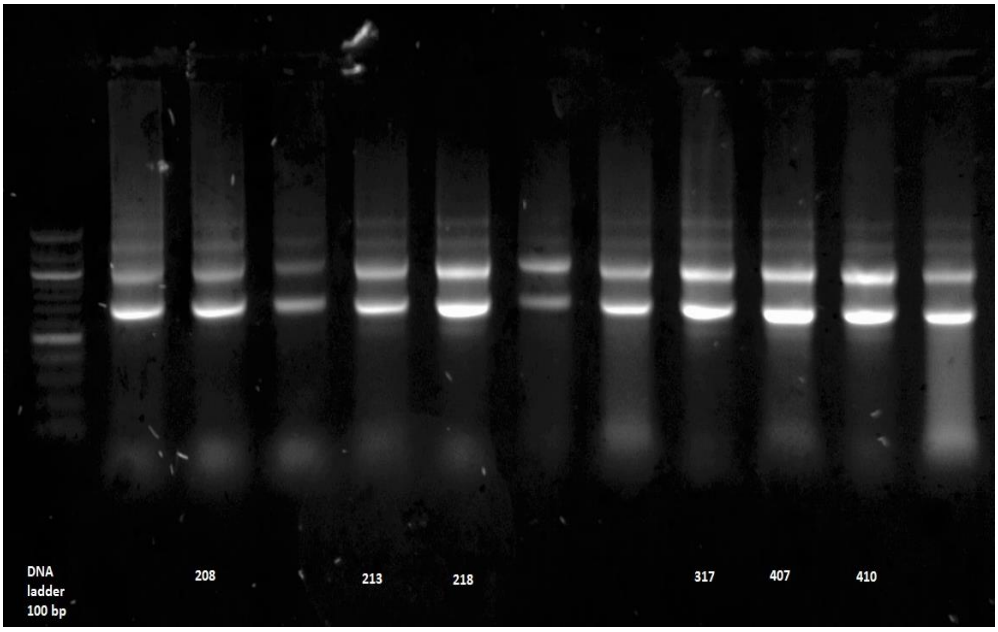

Fig. 3.3 Chosen RNA samples run in 1% agarose-TBE gel stained with GelRed™. From left to right: 100 bp DNA ladder, RNA samples no. **208**) TEMP_08 170 ng/µL; **213**) TEMP_13 184 ng/µL; **218**) TEMP_18 290 ng/µL; **317**) DEHP_17 379 ng/µL; **407**) COMB_07 440 ng/µL; **410**) COMB_10 315 ng/µL. Sample code refers to the exposure treatment (2 for HIGH T, 3 for LOW DEHP, 4 for HIGH TEMP LOW DEHP) and the name of the individual (i.e., sample 213 belongs to the 13th individual from the HIGH TEMP treatment)

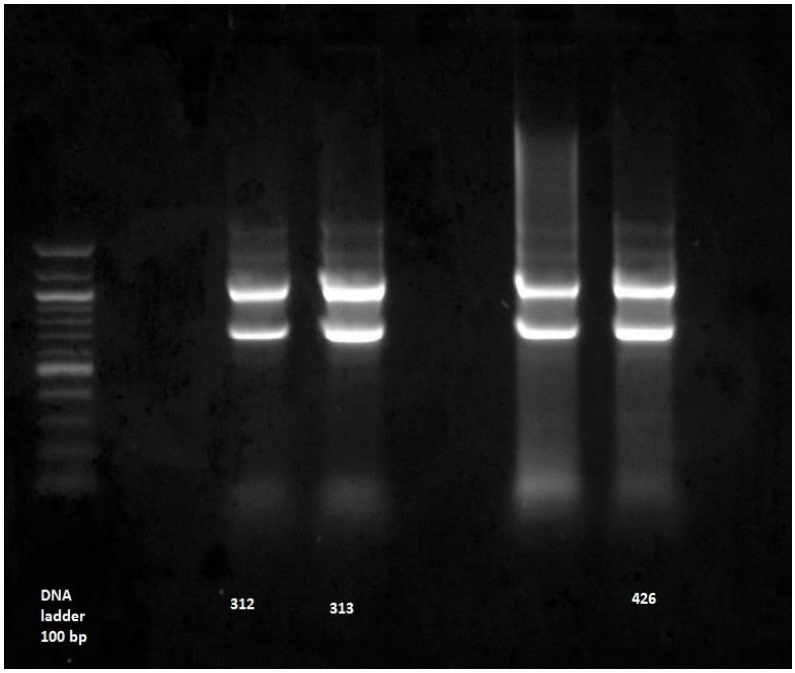

Fig. 3.4 Chosen RNA samples run in 1% agarose-TBE gel stained with GelRed™. From left to right: 100 bp DNA ladder, RNA samples no. **312**) DEHP_12 208 ng/µL; **313**) DEHP_13 395 ng/µL; **426**) COMB_26 367 ng/µL. Sample code refers to the exposure treatment (2 for HIGH TEMP, 3 for LOW DEHP, 4 for HIGH TEMP LOW DEHP) and the name of the individual (i.e., sample 426 belongs to the 26th individual from the HIGH TEMP LOW DEHP treatment)

After the quality control procedure, the mRNA was then enriched using oligo(dT) beads. The mRNA was fragmented randomly in fragmentation buffer, followed by cDNA synthesis using random hexamers and Reverse Transcriptase. After first-strand synthesis, the complete cDNA was then synthesised using Illumina second-strand synthesis buffer, dNTPs, RnaseH and *E. coli* Polymerase I to generate the second strand by nick-translation. The cDNA sequencing library was finally built after purification, terminal repair, A-tailing, ligation of sequencing adapters, size selection and PCR enrichment. TruSeqTM RNA and DNA- sample prep kits were used. Library quality control was carried out using a Qubit 2.0 fluorometer (Life Technologies), an Agilent 2100 Bioanalyzer and quantitative PCR (**Fig. 3.5**).

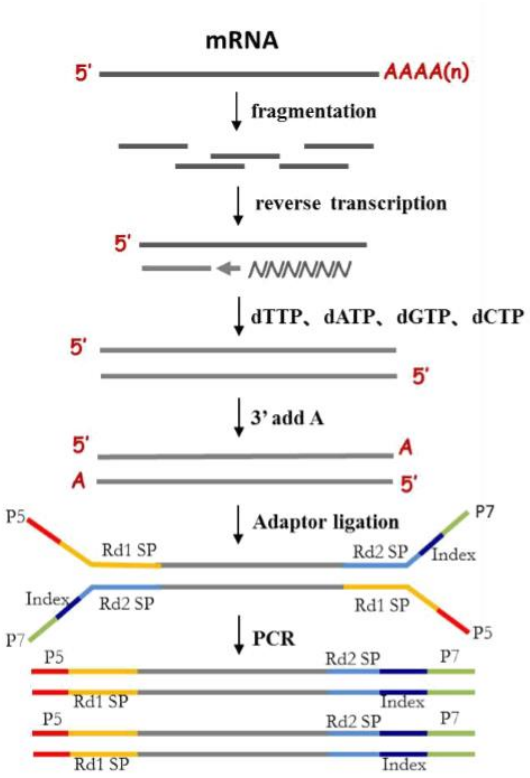

Fig. 3.5 Graphical description for the Novogene mRNA enrichment, cDNA synthesis and sequencing library preparation. From Novogene Ltd. (2020)

The original raw data from the Illumina run were then transformed into sequenced reads (called raw data or raw reads) by *CASAVA* base recognition (base calling). Raw data were then stored in FASTQ (.fq) format files, which contained sequences of reads and corresponding base quality information (**Table 3.1**).

Table 3.1 Example of a FASTQ (fq) format file identification. From Novogene Ltd. (2020)

HWI-ST1276	Instrument – unique identifier of the sequencer
71	Run number – run number on instrument
C1162ACXX	FlowCell ID – ID of flowcell
1	LaneNumber – positive integer
1101	TileNumber – positive integer
1208	X – x coordinate of the spot. Integer which can be negative
2458	Y – y coordinate of the spot. Integer which can be negative
1	ReadNumber – 1 for single reads; 1 or 2 for paired end
N	Whether it is filtered – NB: Y if the read is filtered out, not in the delivered fastq file, N otherwise

0	Control number – 0 when none of the control bits are on, otherwiseit is an even number
CGATGT	Illumina index sequences

The Illumina paired-end technology generated two .fq-format files for each sample (e.g., COMB_10_1.fq and COMB_10_2.fq for the sample COMB_10), each containing one direction of the read. The FASTQ Sequence Reads (raw reads) were then downloaded into University of Hull's Viper High-Performance Computer student database. An in-house *de novo* transcriptome assembly from the Illumina paired-end FASTQ files was then carried out using the University of Hull's Viper High-Performance Computer and the *Trinity* pipeline.

3.4 Materials and Methods: *FastQC* quality control

As recommended by Freedman et al. (2021), before any analysis, quality control on the raw reads was carried out using *FastQC* module (v 0.11.9). *FastQC* is considered a fundamental tool that is able to provide quality control checks, which are essential to ensure that the raw sequences coming from high-throughput sequencers are not biased and of good quality for the subsequent pipeline analysis. Most sequencers already generate quality control within their reports as part of their analysis pipeline, but these are mostly focused on problems generated by the sequencer itself, but *FastQC* is used to check both sequencer- and library- related quality. The quality control job was submitted to the HPC Viper as a SLURM submission batch script that can be referred to in the **Supplementary Appendix to Chapter 3 (S3.1).** The output files generated as HTML file reports presented the following modules (from https://www.bioinformatics.babraham.ac.uk/projects/fastqc/):

- *Basic statistics* (**Chapter 3.4.1**).
- *Per base sequence quality* (**Chapter 3.4.2**).
- *Per tile sequence quality* (**Chapter 3.4.3**).
- *Per sequence quality score* (**Chapter 3.4.4**).
- *Per base sequence content* (**Chapter 3.4.5**).
- *Per sequence GC content* (**Chapter 3.4.6**).
- *Per base N content* (**Chapter 3.4.7**).

- *Sequence length distribution* (**Chapter 3.4.8**).
- *Duplicate sequences* (**Chapter 3.4.9**).
- *Overrepresented sequences* (**Chapter 3.4.10**).
- *Adapter content* (**Chapter 3.4.11**).

3.4.1 Basic statistics

Basic statistics presented an overview of the main characteristics of each file as shown in **Fig. 3.6** as an example for sample COMB_07.fq:

Measure	Value
Filename	COMB_07_1.fq.gz
File type	Conventional base calls
Encoding	Sanger / Illumina 1.9
Total Sequences	25792440
Sequences flagged as poor quality	0
Sequence length	150
%GC	37

Fig. 3.6 Example of a basic statistics report for the file COMB 07.fq (treatment LOW DEHP HIGH TEMP sample no. 7)

The resulting total number of sequences, poor quality sequence, sequence length and %GC for each sample are shown in **Table 3.2.**

Table 3.2 Basic Statistics from *FastQC* Report on the raw data before trimming (Conventional base calls and Sanger / Illumina 1.9)

Treatment	Filename	Total Sequences	Sequences flagged as poor quality	Sequence length	%GC
Future average temperature, no DEHP	TEMP_08	26474425	0	150	36
	TEMP_13	28575793	0	150	36
	TEMP_18	26186404	0	150	37
Low temperature and low DEHP concentration	DEHP_12	26404546	0	150	36
	DEHP_13	25253601	0	150	37
	DEHP_17	24060842	0	150	37

Future average temperature and low DEHP concentration	COMB_07	25792440	0	150	37
	COMB_10	25878970	0	150	37
	COMB_26	30190045	0	150	37

3.4.2 Per base sequence quality

The *Per base sequence quality* shows an overview of the quality range across the bases, with the quality score on the y-axis. The mean read quality is shown as a blue line. Very good calls are shown in the green range, while calls of reasonable and poor quality are shown in orange and red, respectively. Here, all submitted files for this experiment reported a satisfactory *Per base sequence quality* score, as shown in the example **Fig. 3.7.**

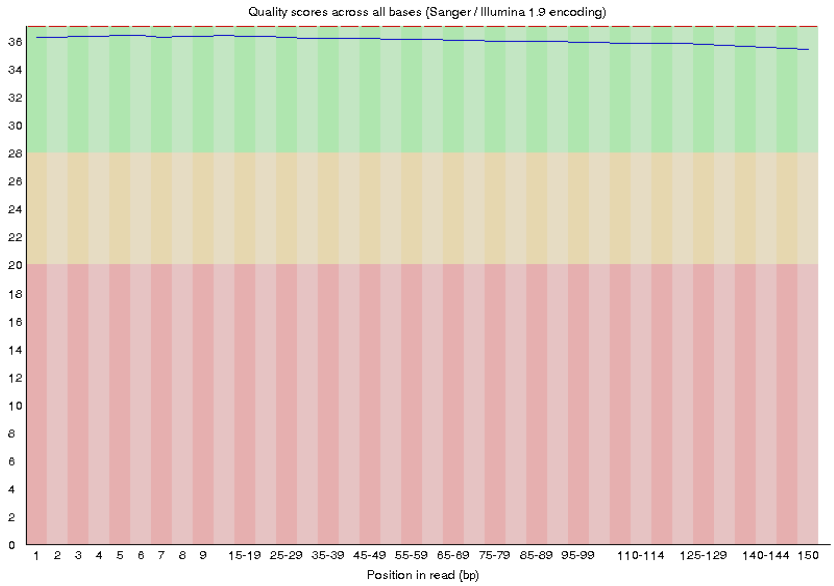

Fig. 3.7 Example of a per base sequence quality report for the file DEHP_12.fq (treatment LOW DEHP sample no. 12) with the mean quality (blue line) in the range of very good quality (in green)

3.4.3 Per tile sequence quality

This report appears when Illumina libraries are used. It shows the quality score for each tile across all the bases, in order to see if there is a quality loss in some parts of the flow cell. The colours are in a cold-to-hot scale, where cold colours represent above-the-average quality positions and hot colours represent below-quality tiles. In our case, for each sample, the module raised a yellow warning for one of the two .fq-format files containing a direction of the read, possibly related to a loss of quality of the sequencer flow cell (**Fig. 3.8**).

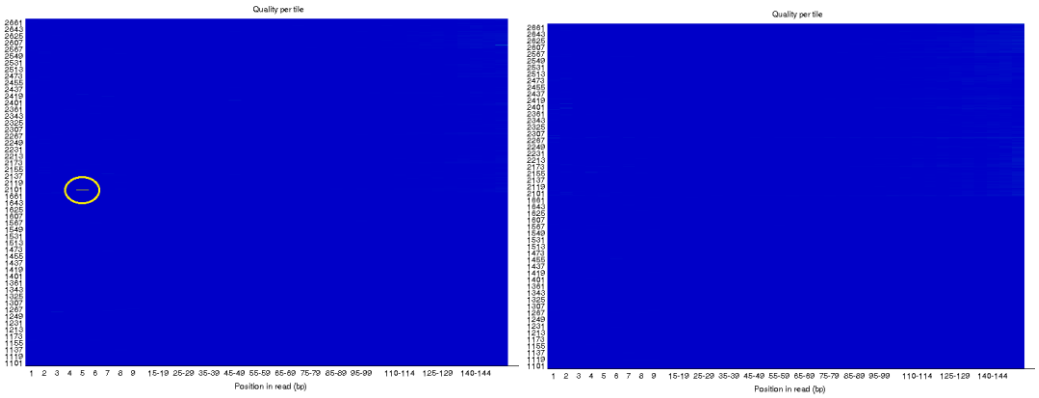

Fig. 3.8 Examples of a per tile sequence quality report for the files DEHP_12_1.fq (LOW DEHP no. 12) with a warning (flagged in yellow in the graph) and DEHP_12_2.fq without warnings

3.4.4 Per sequence quality score

Per sequence quality score is meant to report universally low-quality values of the subset of sequences. Generally, the quality score plot should not present bumps in the lower quality range. Here, all submitted files presented satisfactory *Per sequence quality scores* (**Fig. 3.9**).

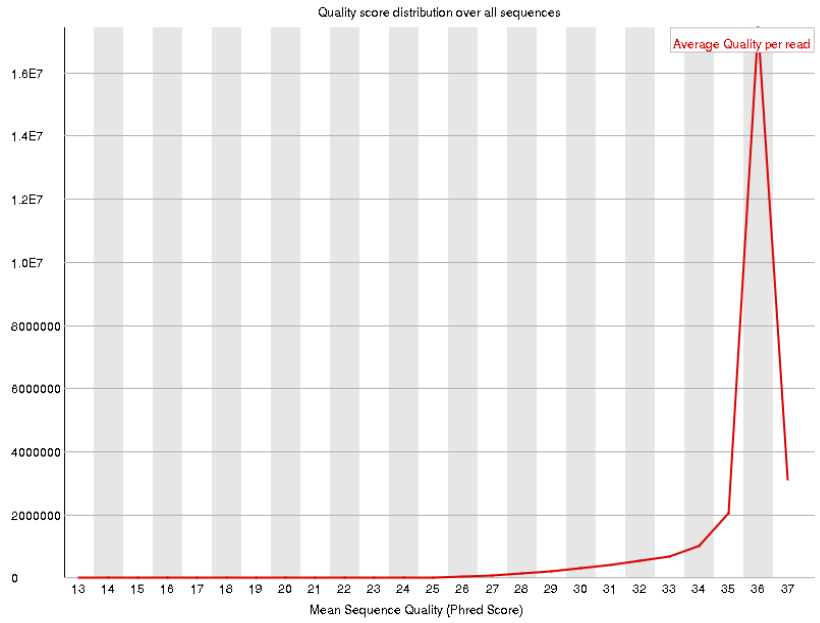

Fig. 3.9 Examples of a per sequence quality score report for the files TEMP_18.fq (HIGH T no. 18)

3.4.5 Per base sequence content

Per base sequence content shows the proportion of each base position. Usually, a random library should show little or no imbalance between the different bases as in theory, the G content should be equal to the C content, and for all As there should be an equal amount

of Ts. Some types of libraries, however, will produce intrinsic biases at the start of the read, often associated with using random hexamers or transposases. *Per base sequence content* raises a warning if there is a difference greater than 10% between A, T, G, and C and a failure is issued if this difference is greater than 20% in any position. Flags are raised in case of i) overrepresented sequences such as adapter dimers or rRNA; ii) biased fragmentation around the first 12bp of each run due to the use of random hexamers; ii) biased composition libraries (for example, library treated with sodium bisulphite will have their cytosines converted to thymines); iv) aggressive trimming. It is reported that nearly all RNA-seq libraries will fail this module, due to the fact that the first 10-12 bases are the results of random hexamer priming used during the library preparation. Similarly, our results showed red flags for all submitted files, as shown in the example in **Fig. 3.10**.

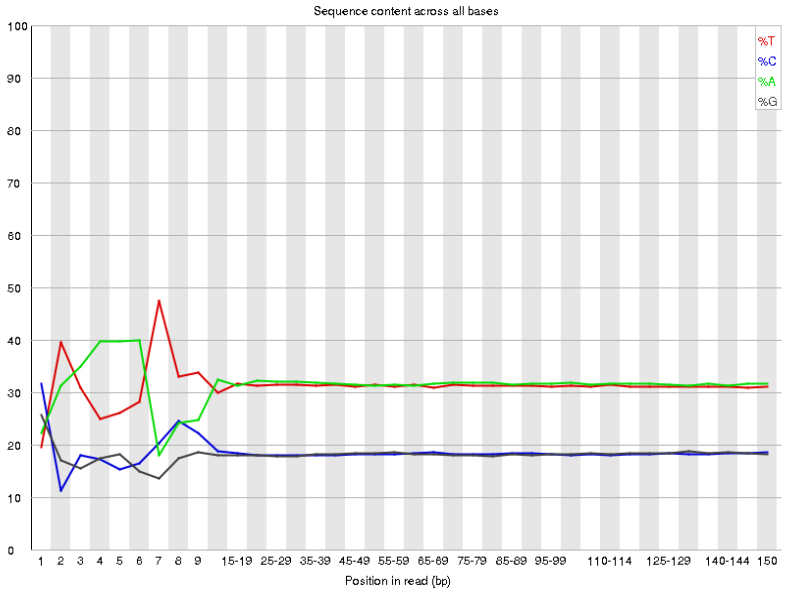

Fig. 3.10 Example of a per base sequence content (red flagged) for the files TEMP_8.fq (HIGH TEMP no. 8). Reports for all submitted samples (i.e., TEMP_08, TEMP_13, TEMP_18, DEHP_12, DEHP_13_DEHP_17, COMB_07, COMB_10, COMB_26) showed red flags for the first 11 reads

3.4.6 Per sequence GC content

This module measures the GC content of each sequence and compares it to a normal distribution. In a normal-distributed library, the central peak shows the overall GC content. A non-normal shape could be related to a contaminated or biased library. In our case, a yellow warning was raised for all submitted samples, as the sum of deviations from the normal distribution was more than 15% of the total reads (**Fig. 3.11)**.

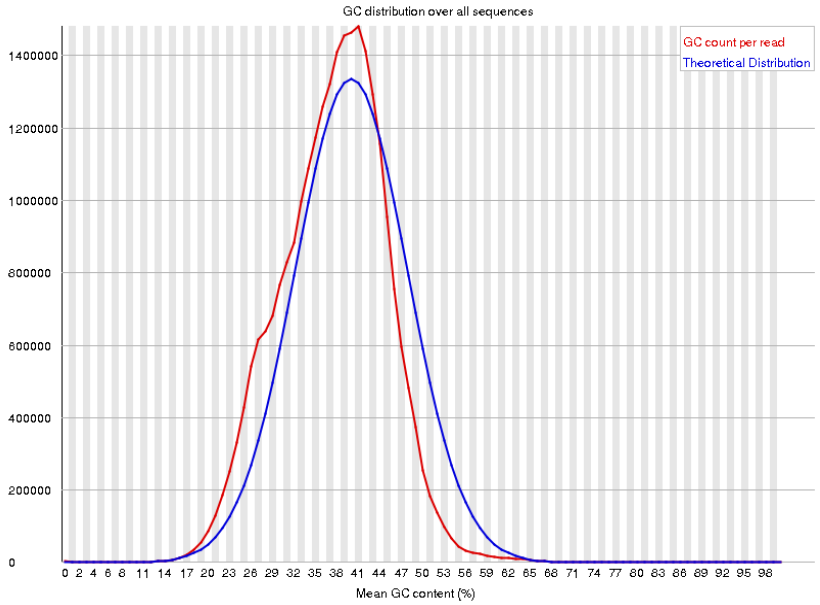

Fig. 3.11 Example of a per sequence GC content (yellow flagged) for the files TEMP_18.fq (HIGH TEMP no. 18). Reports for all submitted samples (i.e., TEMP_08, TEMP_13, TEMP_18, DEHP_12, DEHP_13_DEHP_17, COMB_07, COMB_10, COMB_26) showed yellow flags

3.4.7 Per base N content

This module measures the N content percentage that the sequencer had used as substitutes when unable to make a confident base call. Here, all submitted files met the satisfactory requirements (**Fig. 3.12**).

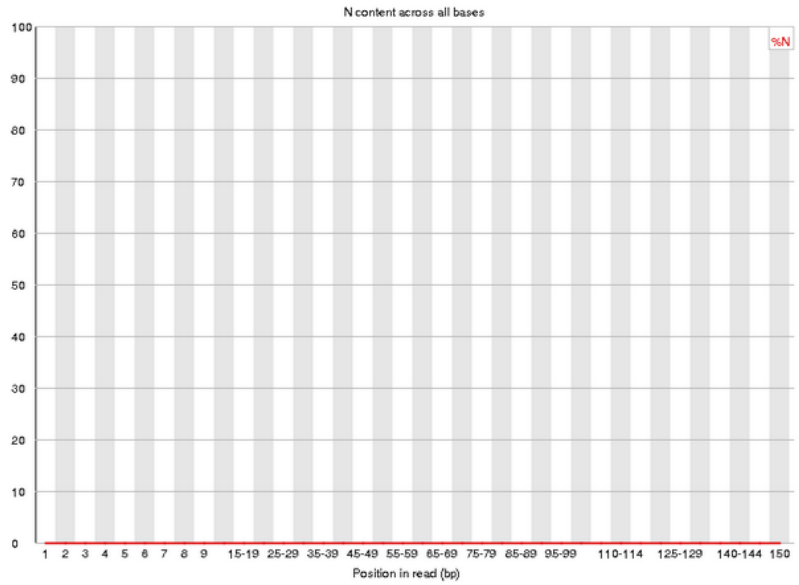

Fig. 3.12 Example of a per base N content report for the file DEHP_17.fq (LOW DEHP no. 17)

3.4.8 Sequence length distribution

This module highlights the distribution of fragmented sequences of varying lengths generated by the sequencer. In most cases, the graph plots the distribution with a single peak at one size, as shown in **Fig. 3.13**. Here, all submitted files presented satisfactory *Sequence length distribution* results.

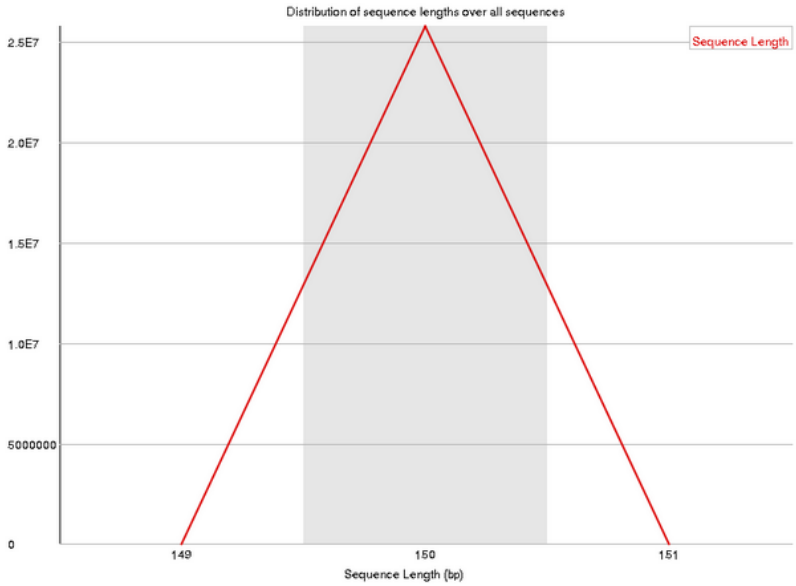

Fig. 3.13 Example of a sequence length distribution report for the file COMB_7.fq (LOW DEHP HIGH T no. 7)

3.4.9 Sequence duplication levels

This module plots the degree of duplication for each sequence. Low duplication levels could mean a high level of library coverage for the target sequence, while high duplication levels could be related to the use of an enrichment bias. Library duplicates are usually divided into technical duplicates (made from PCR artifacts) or biological replicates, such as different copies of the same sequence. In the graph, the blue line shows the full sequence set and how the duplications are distributed, while the red line plots the de-duplicated sequences.

In our dataset, all submitted files reported red flags for this module (**Fig. 3.14**), presenting spikes of the blue plot at the right end of the graph. However, it is quite normal that flags are raised for RNA-seq outcomes, because usually these libraries are made of significantly different sequence levels. Therefore, highly expressed transcripts are often

over-sequenced and possibly create duplicates but the warning does not need to be fixed (**Fig. 3.14**).

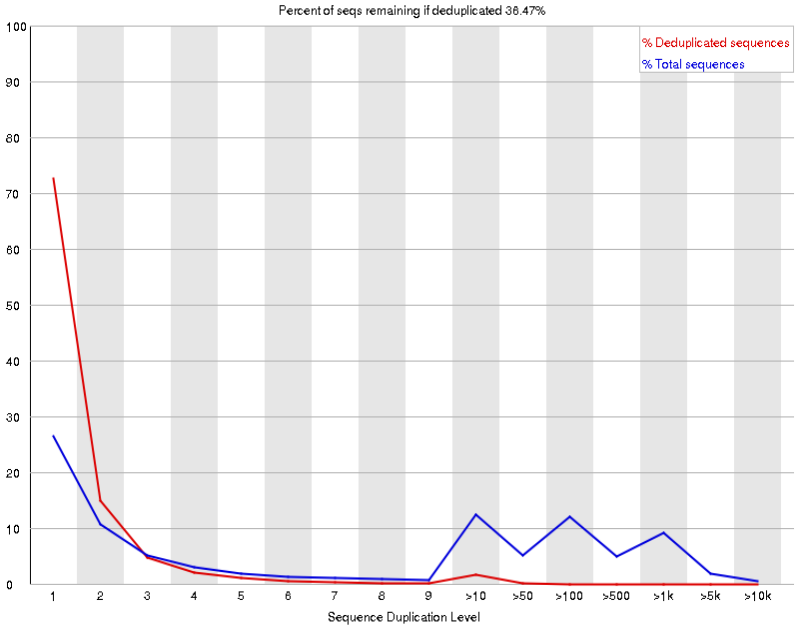

Fig. 3.14 Example of a duplicate sequences report (red flagged) for the file TEMP_18.fq (HIGH T no. 18). Reports for all submitted files showed red flags

3.4.10 Overrepresented sequences

The module flags overrepresented sequences if they are highly biologically significant (more than 0.1% of the total). In our case, three yellow flags were raised for files DEHP_13, DEHP_17 and TEMP_08 (**Fig. 3.15**). A *Blast* search was carried out to recognise the overrepresented sequences found with this module, revealing the first sequence belonging to *M. edulis meb55a* mitochondrial gene, while it was inconclusive for the second sequence. They were not removed, as natural overrepresentation could occur for RNA-seq data.

Sequence	Count	Percentage	Possible Source
CTCCCATCAAAATCGTATAAAAGCCTAAAACCTTCAATTAAGATAAAGCT	29459	0.11665267064289168	No Hit

Sequence	Count	Percentage	Possible Source
CAGAAATGTTGATGCTGATTGTTATTCTTGTGTGTTGTGATCGTGCCTTA	47484	0.19734970205947072	No Hit

Fig. 3.15 Overrepresented sequences report flagged for files DEHP_13.fq and TEMP_08.fq (first sequence), and DEHP_17.fq (second sequence)

3.4.11 Adapter content

Adapters are known sequences of artificial oligonucleotides that are added during the library preparation to ensure a correct clustering during the sequencing (**Fig. 3.5**). This module searches for read-through adapter sequences, helping to decide if adapter trimming is needed or not. The graph will plot the cumulative percentage count of adapter sequences for each position. All submitted files presented satisfactory outcomes (**Fig. 3.16, Table 3.3**).

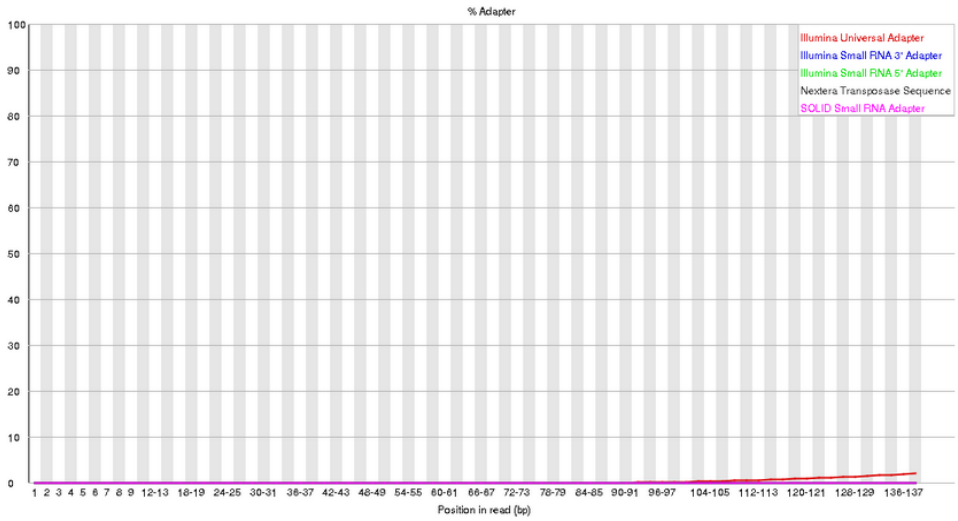

Fig. 3.16 Example of adapter content report for COMB_10.fq (LOW DEHP HIGH TEMP no. 10)

Table 3.3 RNA-seq adapter sequences used in this experiment (oligonucleotide sequences of adapters from TruSeqTM RNA and DNA sample prep kits)

P5 Adaptor Sequence	P5-AATGATACGGCGACCACCGAGA (5'-3') P5'-TTACTATGCCGCTGGTGGCTCT (3'-5')
P7 Adaptor Sequence	CGTATGCCGTCTTCTGCTTG-P7' (5'-3') GCATACGGCAGAAGACGAAC-P7 (3'-5')

3.5 Materials and Methods: Read trimming

Trimming is a method for removing low-quality bases from a read and it could improve the general quality of the assembly. On the other hand, the filtering process discards the entire read, leading to a loss of data. Standard filtering could i) remove sequences with a median score of < 20 or < 25; ii) remove sequences with a high N score (high number of unknown nucleotide proportion); iii) remove small reads (<25 bp).

Data trimming was carried through the *Trimmomatic* module (v 0.38), which is a module used to trim, filter or crop Illumina sequences and remove adapters. *Trimmomatic* allows one to choose between i) LEADING, which cuts bases off the start of the read if below a certain chosen point; ii) TRAILING, which cuts bases off the end of the read if below a certain chosen point; iii) MINLEN, which drops the read if below a certain chosen length value; iv) AVQUAL, which drops the read if average quality is below a certain chosen point; v) HEADCROP, which cuts the specified chosen number of bases from the start of the read. Furthermore, ILLUMINACLIP command cuts adapters and other illumina-specific sequences from the read. A focus on the *Trimmomatic* code command is available in the **Supplementary Appendix to Chapter 3 (S3.2)**. The resulting outputs `Paired_sample` and `Unpaired_sample` were generated from the two fq-format files of each sample. `Paired_sample` refers to reads that have passed the quality control in both `sample_1.fq` and `sample_2.fq`. `Unpaired_sample` refers to reads that have not passed the quality control in both files. After the trimming and filtering steps, the quality control was repeated on the trimmed `Paired_sample` files.

3.6 Materials and Methods: *Trinity de novo* assembly

All *Trinity* steps were carried out in Viper in a singularity container image (v 3.5.3), that can operate like a lightweight virtual machine (Freedman et al., 2020). A focus on the *Trinity* code command is available in the **Supplementary Appendix to Chapter 3 (S3.3)**. The quality of the assembly was checked by the *TrinityStats.pl* script, used to generate N50 statistics and count the number of *Trinity* contigs:

```
$TRINITY_HOME/util/TrinityStats.pl
/home/userID/Trinity.output.fastafile
```

The N50 statistics gives a measure of the completeness and continuity of the genome by assessing the distribution of contig (i.e., a contiguous set of overlapping segments of DNA that together represent a consensus region) lengths (Gregory, 2005). In detail, if all the longest contigs in a set were arranged to cover 50% of the assembly with their length, the contig N50 is defined as the length of the shortest contig of the set (Miller et al., 2010).

3.7 Materials and Methods: Transcriptome assembly evaluation

After completion of the transcriptome assembly, it is a good practice to assess its quality by some general modules. The modules used in this experiment were:

- *Bowtie* to assess the read content (**Chapter 3.7.1**).
- *BUSCO* to explore the read completeness (**Chapter 3.7.2**).
- *Trinity* to compute the ExN50-length statistics (**Chapter 3.7.3**).

3.7.1 Assessing the read content of the transcriptome assembly

This module used the function *bowtie* to align short and fragmented reads to the transcriptome assembly and then counted the number of pairs and single alignments. The assembled transcripts do not always have properly represented paired-end reads, because of fragmentation of transcripts and in the case of a short transcript, only one read of a pair might align. Typically, 70-80% of the RNA-seq reads are represented by the assembly and found mapped as proper pairs. The unassembled ones remaining are usually related to low-expressed transcripts or low-quality reads. From https://github.com/trinityrnaseq/trinityrnaseq/wiki/RNA-Seq-Read-Representation-by-Trinity-Assembly. Details of the used code are available in the **Supplementary Appendix to Chapter 3 (3.4).**

3.7.2 Explore completeness with BUSCO

Benchmarking Universal Single-Copy Orthologs (*BUSCO*) is a software based on evolutionary-informed expectations of the gene content of near-universal single-copy orthologs across higher taxonomic groupings (Simão et al., 2015). In Viper, a miniconda environment (*environment1*) was first built and then the *BUSCO* command was launched, as shown in **Supplementary Appendix to Chapter 3 (S3.5)**.

3.7.3 Trinity transcriptome ExN50 statistics

This module computed the ExN50-length statistics, defined as the percentages of the nucleotides in the transcriptome assembly that are found in contigs of N50-length. Before carrying on the transcript analysis on the gene expression and length, the transcript abundance estimation was performed, using *salmon* as a fast alignment-free method, which examined k-mer abundances and in the assemblies

(https://github.com/trinityrnaseq/trinityrnaseq/wiki/Trinity-Transcript-Quantification).
The following matrices were generated:

- `Trinity.isoform.counts.matrix` : the estimated RNA-seq fragment counts (raw reads).
- `Trinity.isoform.TPM.not_cross_norm`: a matrix of TPM (transcript per million) expression values (not cross-sample normalized).
- `Trinity.isoform.TMM.EXPR.matrix` : a matrix of TMM-normalized (trimmed mean of M values) expression values.

This also provided the abundance estimation at the transcript level of the RNA-seq fragment counts deriving from each transcript and a normalised expression by the transcript length. Code details are available in **Supplementary Appendix to Chapter 3 (S3.6)**.

3.8 Materials and Methods: Identification and filtering of non-target data

A standard nucleotide-type *BlastN* search for transcripts' species and taxon ID was performed using the *megablast* algorithm (highly similar sequences) against the *nt* (nucleotide) database (**Supplementary Appendix to Chapter 3, S3.7**).
The assembly was further analysed with *Blobtools* (**Fig. 3.17**) by parsing the *BlastN* output hitfile against the sorted bowtie.bam file and the *Trinity* assembly output datafile. For each entry of the hit file, the taxonomy identification was also generated.

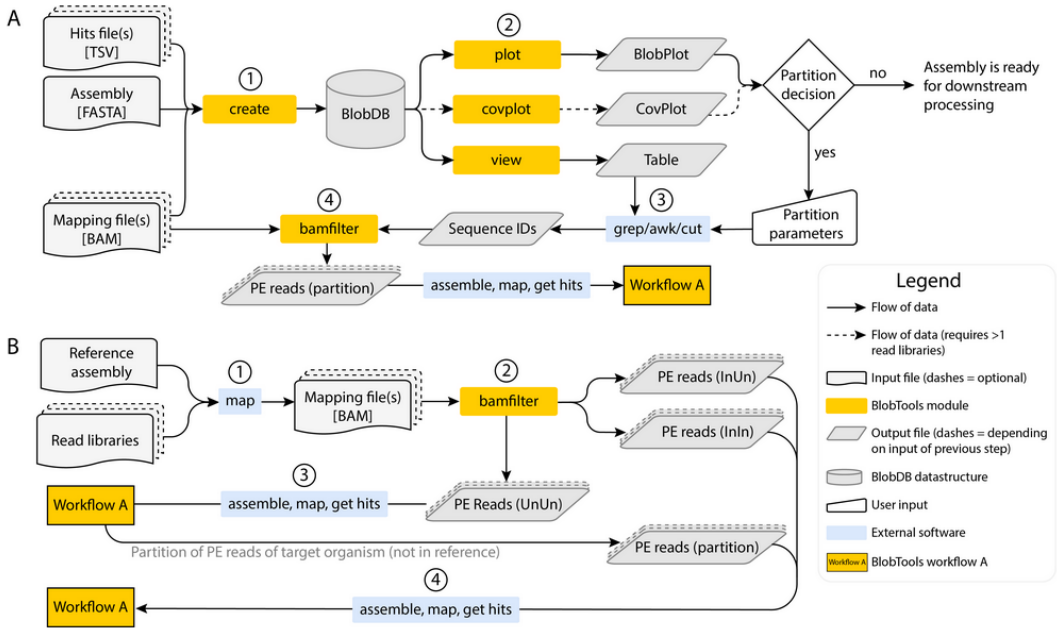

Fig. 3.17 BlobTools pipeline for taxonomic analysis. Workflow A is used for *de novo* genome assembly targets when no reference genome is available while Workflow B is used for genome re-sequencing with a reference genome. In this study Workflow A was used. From https://blobtools.readme.io/docs

3.9 Materials and Methods: Differential expression using *DESeq2*

Deseq2 is an accurate tool part of the *Bioconductor* package I that can easily be used in the *Trinity* package to identify RNAseq-based differentially expressed transcripts. Beforehand, low-expressed genes were removed by taking out the rows where only a few reads were counted (< 10), to increase robustness of the analysis and improve visualisation across treatments. Then, the *DESeq2* analysis was launched inside the *Trinity* singularity container, using as input the matrix files `Trinity.isoform.counts.matrix` and `Trinity.isoform.TMM.EXPR.matrix` created beforehand and described in **Chapter 3.7.3**.

The *DeSeq2* analysis performed three pairwise comparisons (DEHP vs TEMP, DEHP vs COMB, COMB vs TEMP). Transcripts differentially expressed at significance of <= 0.001 were also extracted from all treatments and three reports containing the transcript upregulation in each experimental condition were generated. Details on the used script are available in **Supplementary Appendix to Chapter 3 (S3.8).**

3.10 Materials and Methods: Assembly annotation

The assembly annotation was then carried out on the upregulated entries. The following modules were used for post-transcriptome analysis:

- *TransDecoder* to extract and identify coding sequences (**Chapter 3.10.1**).
- *Trinotate* to annotate the transcripts (using modules *SQlite* and *Blast+*, **Chapter 3.10.2 – 3.10.5**).

3.10.1 TransDecoder

TransDecoder (v. 5.5.0) was used to extract coding regions within the transcript sequences generated by *Trinity* assembly, identifying likely coding sequences. Firstly, the long open reading frames (ORFs) were extracted and the ones at least 100 amino acids long were identified in Viper using a miniconda environment (*environment1*) using *TransDecoder.LongOrfs* command:

```
TransDecoder.LongOrfs -t home/userID/Trinity.output.fastafile
```

Then, ORFs with homology to known proteins were identified using *Blast* searches using *TransDecoder.Predict* command:

```
TransDecoder.Predict -t /home/userID/Trinity.output.fastafile
```

3.10.2 Preparing the Trinotate annotation report

Trinotate (v. 3.2.2) functionally annotated the transcripts. For a correct usage of the *Trinotate* module, several tools needed to be present and installed into Viper, along with the required software:

- *Trinity* (v. 2.13.1, **Chapter 3.6**).
- *TransDecoder* (v. 5.5.0) to predict coding regions in transcripts (**Chapter 3.10.1**).
- *SQlite* (v. 3.39.0) a *Trinotate* boilerplate sqlite database for database integration that comes pre-populated with Swissprot records and Pfam domains.
- *NCBI Blast+* database for homology search: searches for *Trinity* transcripts (*blastx.outfmt6*) and *Transdecoder* predicted proteins (*blastp.outfmt6*), as described in **Chapter 3.10.3.**

The following required databases were installed as well:

- Uniprot

- SwissProt

And the following files were used:

- `Trinity.output.fastafile`, final file produced by *Trinity* containing all the assembled transcript (see **Chapter 3.6**: *Trinity de novo* assembly).
- `Trinity.output.fastafile.transdecoder.pep`, the most likely longest ORFs generated (see previous **Chapter 3.10.1**) containing the transcript protein sequences corresponding to the predicted coding regions.

3.10.3 Sequence homology searches

The module *Blast+* evaluated the quality of the assembly, examining the number of assembled transcripts that appeared completely or nearly full-length. Usually, with model organisms, this module aligns the assembled transcripts to the reference ones, in order to examine the length coverage. For non-model organisms with no reference genome, different solutions are available. If there is a present annotation of high quality of a closely related species, the module might compare it to the assembled transcript (https://github.com/trinityrnaseq/trinityrnaseq/wiki/Counting-Full-Length-Trinity-Transcripts). Otherwise, a general analysis is performed to align the assembled transcript to known protein databases, such as SwissProt, which was downloaded in Viper**.** The cutoff e-value was set at 25 to conclude that genes in the analysed species were equivalent to a known gene. Additionally, a scan for sequence homologies with the command *blastp* in *Transdecoder*-predicted protein sequences was run to maximise the sensitivity for functionally significant ORFs. The used script is available in the **Supplementary Appendix to Chapter 3 (S3.9).**

3.10.4 Loading the generated results into a Trinotate SQLite Database

The SQlite database was populated by adding the following:

- Transcript sequence (from *Trinity de novo* assembly, **Chapter 3.6**).
- Protein sequences (from *TransDecoder* definition, **Chapter 3.10.1**).
- Blast homologies (*blastx.outfmt6* and *blastp.outfmt6,* **Chapter 3.10.3**).
- Pfam domain (database for protein families, **Supplementary Appendix to Chapter 3, S3.9**).

3.10.5 Output annotation report

The report annotation file was generated with:

```
./Trinotate-Trinotate-v3.2.2/Trinotate ./sqlite/Trinotate.sqlite report
> trinotate_annotation_report.xls
```

And transcript names were imported:

```
./Trinotate-Trinotate-
v3.2.2/util/annotation_importer/import_transcript_names.pl
./sqlite/Trinotate.sqlite trinotate_annotation_report.xls
```

3.11 Materials and Methods: Gene Ontology enrichment using GOseq

For all the transcripts in each treatment that were identified as upregulated in **Chapter 3.9,** the Gene Ontology (GO) assignments for each gene feature were extracted and the Bioconductor packaI(R) *Goseq* was used to perform functional enrichment tests (**Supplementary Appendix to Chapter 3, S3.11**). The resulting GO matrix was visualised in *Revigo* with *Simrel* semantic similarity measure and Uniprot database research (http://revigo.irb.hr/). The GO term IDs for all the experimental treatments were plotted together in a scatter plot (**Fig. 3.28, 3.29** and **3.30**) for enriched transcripts. Additionally, scatter plots and tree maps were chosen to visualise the results for each individual treatment (**Supplementary Fig. 3.1 – 3.18**). For enriched features, scatterplot used the overrepresented *p* value given by the GoSeq and displayed the entries by semantic similarities (with similar categories shown close together). Treemaps displayed the GO terms from the cluster representatives into groups based on their interaction (Supek et al., 2011). The Gene Ontology analysis usually divides each GO category into three hierarchies of the biological domain: Biological Process (BP), Cellular Component (CC) and Molecular Function (MF). Biological Process represents the main biological activities, which comprehend multiple molecular pathways. Cellular Component is an anatomical description of the cellular structures and compartments where the categories belong. Molecular Function describes the activities of the GO category at the molecular level (e.g., transcription, catalysis). Category definitions were then examined on http://geneontology.org/.

3.12 Results and Discussion: Quality control on trimmed data

The Illumina paired-end technology generated two fq-format files for each sample (e.g. COMB_10_1.fq and COMB_10_2.fq for the sample COMB_10), each containing one direction of the read. After cutting the first 11 specified bases from the start of the read, most likely associated with random hexamer priming, the quality control was repeated on the `Paired_samples` using *FastQC* in Viper. Trimming and filtering resolved the flags for *Per tile sequence quality* (**Chapter 3.4.3**) and *Per base sequence content* (**Chapter 3.4.5**). The flags that remained unresolved after the trimming were for the modules *Per sequence GC content* (**Chapter 3.4.6**), *Sequence duplication levels* (**Chapter 3.4.9**) and *Overrepresented sequences* (**Chapter 3.4.10**). As reported by McManes et al., (2014), setting a high-base quality threshold could lead to excessive trimming and filtering and a consequent negatively impacted assembly, thus no additional filtering or trimming was performed (**Fig. 3.18**).

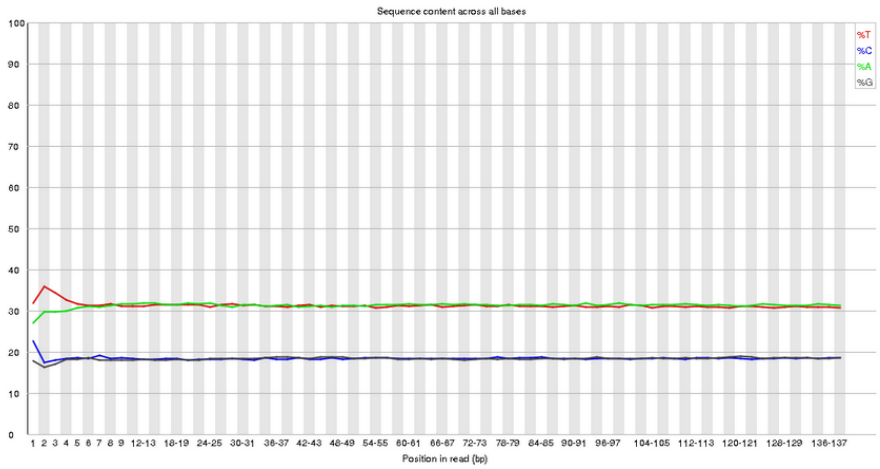

Fig. 3.18 Example for *per base sequence content* after base trimming

3.13 Results and Discussion: *Trinity de novo* assembly

Transcripts from *Trinity* analysis were grouped in clusters with shared sequence content. An example of the Fasta entry formatting is:

```
TRINITY_DN283248_c0_g1_i1 len=371 path=[0:0-370]
GTTTATTTCAGATTTGAAAAAATATTGTAAGACCCACAATTTCGACTAAAATTATCTGCT
TGTATGATATATAATGAATTGCTTTGAACAATACGAGTATGAAGAATGTTCAAGCAGGTA
TATATTGTCCACTTAAACGTTCATAAAAACAGACATTACATTTAACTAACCACTGGTTAT
ATTTTACGAACACATTGCAACGTCATTCAAAATCAACATCAAAACTTACAGGTCATGGAG
AACTATAACTAATTTTAAAATAATAATACTGACGCTTTTTAACATTTCATATTTGGTAAC
ATATACGGAATTAGTTTATTTCATGCAACATATAGGTTGAGTATTGCAATCATTATCTGT
TGTTTTCAATT
```

The example above `TRINITY_DN283248_c0_g1_i1 len=371 path=[0:0-370]` indicates the cluster TRINITY_DN283248_c0, gene 1 (g1) and isoform 1 (i1) with length (len) 371 bp. The path information indicates the path for the de Bruijn graph to construct that transcript by traversing nodes.

The N50 statistics was also generated and the number of *Trinity* contigs was counted (**Chapter 3.6**). For the counts of transcripts, the *TrinityStats.pl* gave the following N50 results: 430015 total *Trinity* genes and 785867 total *Trinity* transcripts with a percent GC of 33.25%. The total assembled bases were 579369677, with a median contig length of 403 bases and average contig of 737.24 bases. The count for contig N was as follows: 4882 bases (N10), 3171 bases (N20), 2256 bases (N30), 1635 bases (N40) and 1172 bases (N50). The stats based on only the longest isoform per gene reported a total assembled bases count of 240581164, with median contig length of 332 bases and average contig of 559.47 bases. Count for contig N was as follows: 4099 bases (N10), 2420 bases (N20), 1569 bases (N30), 1022 bases (N40) and 696 bases (N50). These results were in line with similar statistics obtained from RNA-seq analysis in other bivalves (Moreira et al., 2012, 2015).

3.14 Results and Discussion: Transcriptome assembly evaluation

3.14.1 Assessing the read content of the transcriptome assembly

A typical *Trinity* transcriptome assembly will have the vast majority of all reads mapping back to the assembly, and ~70-80% of the fragments found mapped as proper pairs (yielding concordant alignments 1 or more times to the reconstructed transcriptome). In this case, 100% of the total reads (238817066 reads) were paired. Of these, 20850471 reads (8.73%) were aligned concordantly 0 times (of these, 3.21% were aligned discordantly 1 time), 13758203 (5.76%) aligned concordantly exactly 1 time, and 85.51% (204208329 reads) aligned concordantly more than one time. 20181567 pairs were aligned 0 times concordantly or discordantly and of those that made up the pairs, 14255128 reads (35.32%) were aligned 0 times, 1856388 reads (4.60%) were aligned exactly 1 time and 60.08% were aligned more than one time. Ultimately a 97.02% overall alignment rate was reached, a satisfactory result.

3.14.2 Explore completeness with BUSCO

BUSCO analysis (https://busco.ezlab.org/) provided quantitative measures for the assessment of genome assembly, gene set and transcriptome completeness, as some genes are found in a genome only in single copy (Simão et al., 2015). In our case, BUSCO analysis calculated a value of 99.2% completeness from a final number of 255 searched groups. This value was determined for the assembled transcriptome (C), made of 11.4% of complete and single-copy genes (n = 29 BUSCOs) and 97.8% complete and duplicated (n = 224 BUSCOs) genes, with 0.8% fragmented (n = 2) and 0.0% missing (M), with "fragmented" representing the percentage of genes only partially recovered and "missing" representing the not recovered ones (Simão et al., 2015).

3.14.3 Trinity transcriptome ExN50 statistics

The *salmon* software was used for each of the sample files to estimate transcript expression values (i.e., the percentages of the nucleotides in the transcriptome assembly that are found in contigs of N50-length). Different outputs were generated for each replicate and between them, the `quant.sf` file reported the transcript identifier (`name`), the number of RNA-seq fragments predicted to derive from the specific transcript (`NumReads`), and the normalized expression values of that transcript (Transcripts per million, `TPM`, **Table 3.4**).

Table 3.4 Example of the first 10 entries for the example file TEMP_13

Name	Length	Effective Length	TPM	Num Reads
TRINITY_DN346232_c0_g1_i1	301	78.5	0.00	0.00
TRINITY_DN346292_c0_g1_i1	249	43.2	0.00	0.00
TRINITY_DN346287_c0_g1_i1	332	105.2	0.33	2.00
TRINITY_DN346218_c0_g1_i1	208	25.5	0.00	0.00
TRINITY_DN346271_c0_g1_i1	206	24.9	1.38	2.00
TRINITY_DN346224_c0_g1_i1	252	44.8	0.00	0.00
TRINITY_DN346290_c0_g1_i1	240	38.9	0.00	0.00
TRINITY_DN346244_c0_g1_i1	452	221.7	0.15	2.00
TRINITY_DN346227_c0_g1_i1	325	98.9	0.17	1.00

Given the estimated expressions for each transcript, the values were pulled in one matrix for the estimated counts `Trinity.isoform.counts.matrix` for all treatments (**Table 3.5**).

Table 3.5 Example of the first 10 entries for the `Trinity.isoform.counts.matrix`

	COMB_07	**COMB_10**	**COMB_26**	**DEHP_12**	**DEHP_13**	**DEHP_17**	**TEMP_08**	**TEMP_13**	**TEMP_18**
TRINITY_DN132347_c0_g1_i1	0.0	0.0	0.0	1.0	1.0	0.0	0.0	1.0	0.0
TRINITY_DN5289_c3_g1_i1	4.8	0.0	0.0	9.8	0.0	0.0	0.0	0.0	0.0
TRINITY_DN100861_c0_g1_i3	0.0	0.0	17.8	0.0	0.0	0.0	0.0	0.0	8.0
TRINITY_DN194097_c0_g1_i1	2.0	0.0	0.0	0.0	0.0	0.0	0.0	0.0	0.0
TRINITY_DN112049_c0_g1_i4	0.0	13.5	0.0	0.0	1.6	0.0	1.9	7.3	0.0
TRINITY_DN125251_c1_g1_i1	0.0	0.0	0.0	1.0	0.0	0.0	0.0	0.0	8.0
TRINITY_DN29077_c1_g1_i2	0.0	0.0	3.4	1.0	1.0	1.0	3.3	0.0	4.0
TRINITY_DN207333_c0_g1_i1	0.0	0.0	0.0	0.0	1.0	0.0	0.0	0.0	2.0
TRINITY_DN334941_c0_g1_i1	0.0	4.0	0.0	0.0	0.0	0.0	1.0	0.0	0.0
TRINITY_DN27016_c6_g1_i1	1.0	1.0	0.0	3.0	11.0	4.0	0.0	7.4	0.0

The expression matrix was further normalised using TMM normalisation by linearly scaling the expression values of the investigated entries to generate the `Trinity.isoform.TMM.EXPR.matrix` (**Table 3.6**).

Table 3.6 Example of the first 10 entries for the `Trinity.isoform.TMM.EXPR.matrix`

	COMB_07	**COMB_10**	**COMB_26**	**DEHP_12**	**DEHP_13**	**DEHP_17**	**TEMP_08**	**TEMP_13**	**TEMP_18**
TRINITY_DN132347_c0_g1_i1	0.0	0.0	0.0	0.4	0.4	0.0	0.0	0.4	0.0
TRINITY_DN5289_c3_g1_i1	0.7	0.0	0.0	1.4	0.0	0.0	0.0	0.0	0.0
TRINITY_DN100861_c0_g1_i3	0.0	0.0	1.6	0.0	0.0	0.0	0.0	0.0	0.8
TRINITY_DN194097_c0_g1_i1	0.2	0.0	0.0	0.0	0.0	0.0	0.0	0.0	0.0
TRINITY_DN112049_c0_g1_i4	0.0	0.9	0.0	0.0	0.1	0.0	0.1	0.4	0.0
TRINITY_DN125251_c1_g1_i1	0.0	0.0	0.0	0.2	0.0	0.0	0.0	0.0	2.0
TRINITY_DN29077_c1_g1_i2	0.0	0.0	0.3	0.1	0.1	0.1	0.3	0.0	0.3
TRINITY_DN207333_c0_g1_i1	0.0	0.0	0.0	0.0	0.3	0.0	0.0	0.0	0.6
TRINITY_DN334941_c0_g1_i1	0.0	0.5	0.0	0.0	0.0	0.0	0.1	0.0	0.0
TRINITY_DN27016_c6_g1_i1	0.3	0.3	0.0	0.9	3.4	1.3	0.0	2.0	0.0

3.15 Results and Discussion: Identification and filtering of non-target data

Blobtools is a useful module to identify and isolate reads from a target genus (in our case, *Mytilus*) from other sources that could have contributed to the assembled transcriptome (for example, parasites or symbionts naturally living in association with the analysed species, Kumar and Blaxter, 2012). *Blobtools* identifies different taxa by their GC proportions, which for example have ranges from 44 - 58% in mammals and 16 - 75% in bacteria (Lightfield et al., 2011; Romiguier et al., 2010). Here, the initial taxonomic assessment of the assembly via *blobtools* and *BlastN* reported 87.61% of unmapped

versus 12.4% of mapped assembly (**Fig. 3.19** and **3.20**). These values were related to the nature of the transcripts from non-model organisms that do not yet correspond to discovered and registered genomic sequences.

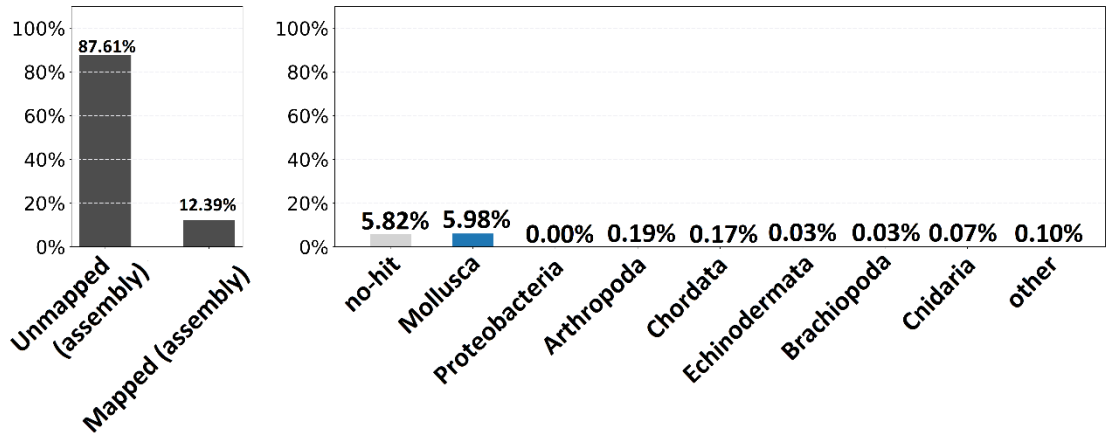

Fig. 3.19 Percentages of unmapped and mapped assembly entries with taxa characterisation

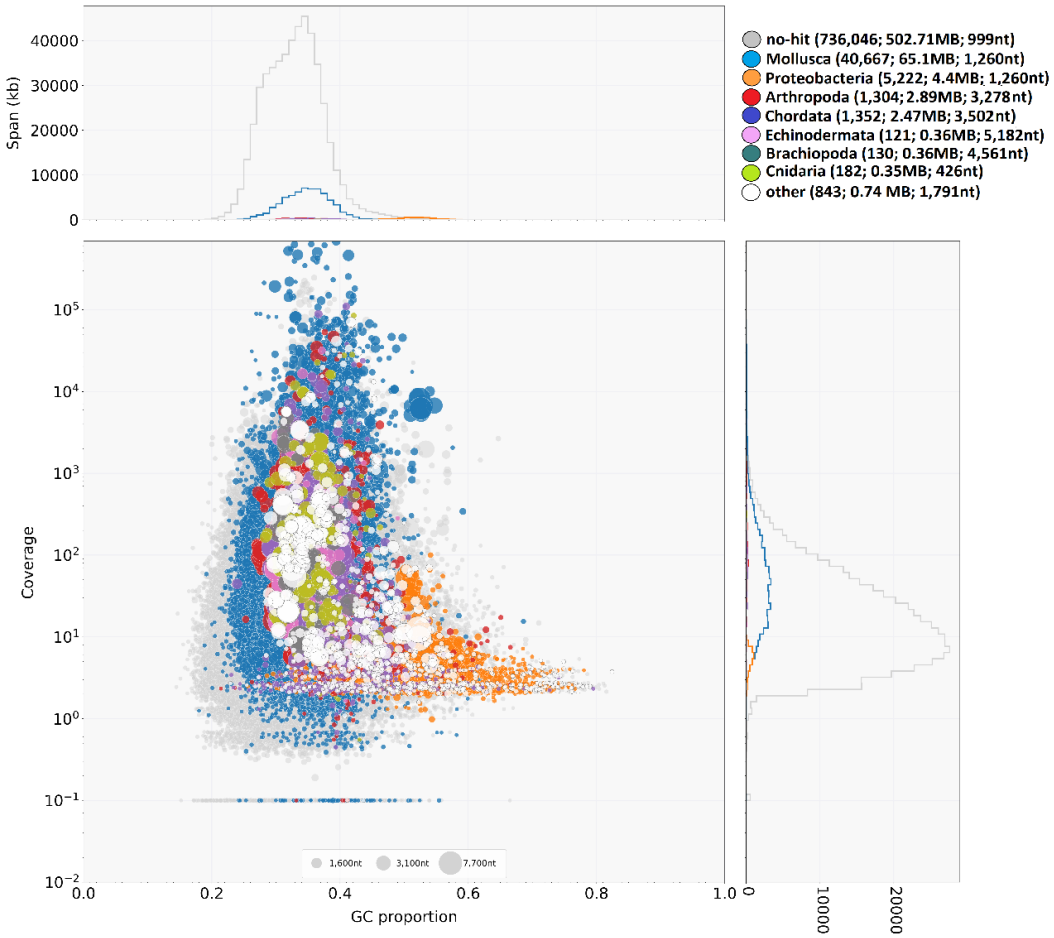

Fig. 3.20 kB span, coverage and GC proportion of the assembly taxa characterisation

Of the mapped entries, 65.1 Mb belonged to the Mollusca phylum (5.98%), followed by Proteobacteria (4.4 Mb), Arthropoda (2.89 Mb), Chordata (2.47 Mb), Echinodermata (0.36 Mb), Brachiopoda (0.36 Mb), Cnidaria (0.35 Mb) and others (0.74 Mb).

The output file was therefore filtered with the *grep* function to isolate only Mollusca entries and the sister phylum of Brachiopods and Annelids and *blobtools* functions were run again. In fact, Mollusca, Brachiopoda and Annelida are part of the Lophotrochozoa taxon, and are hypothesised to have articulated halkieriids as stem ancestors (Conway Morris and Peel, 1995). The final taxonomic assessment filtered out the additional species (**Fig. 3.21** and **3.22**). The filtered matrix was then used for downstream analysis.

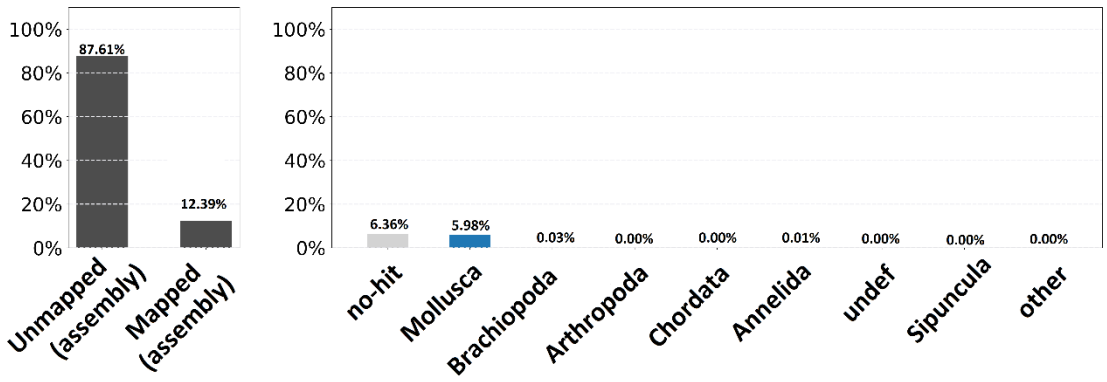

Fig. 3.21 Percentages of unmapped and mapped assembly entries with taxa characterisation in the filtered dataset

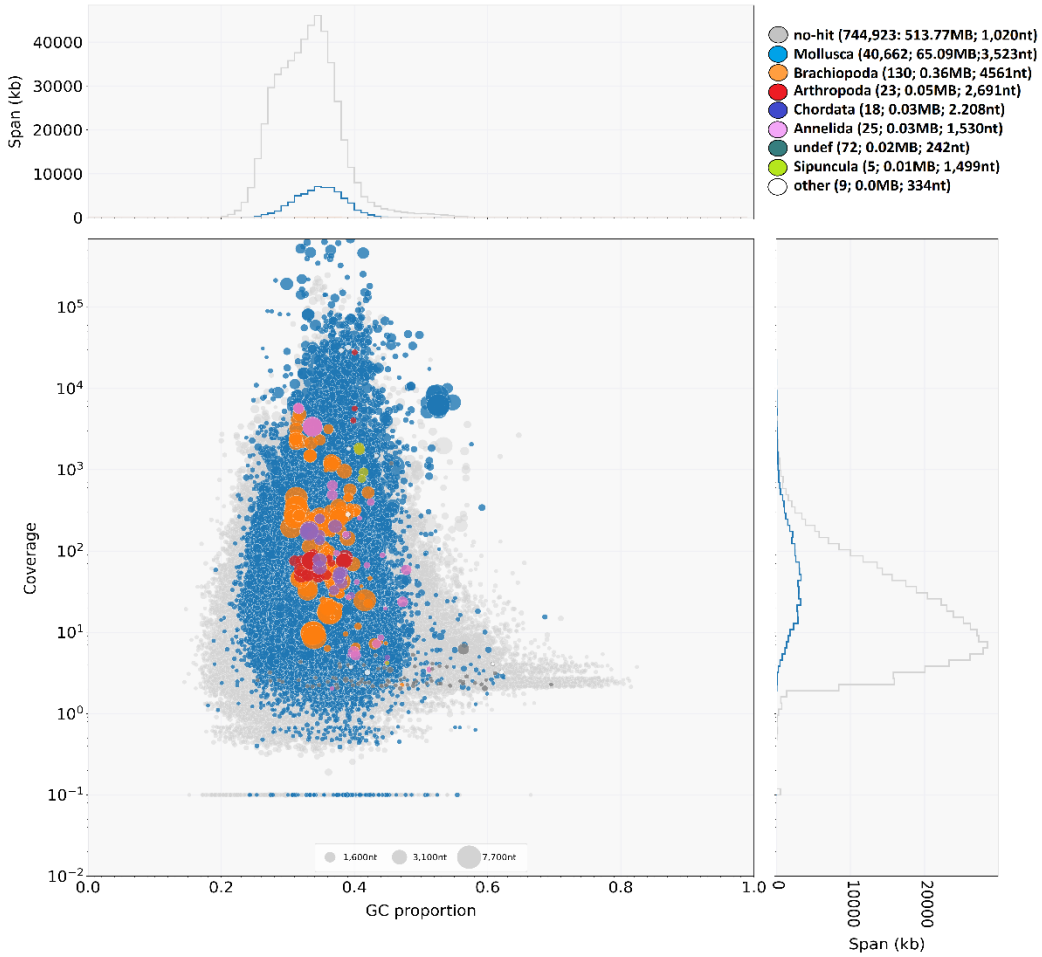

Fig. 3.22 kB span, coverage and GC proportion of the assembly taxa characterisation in the filtered dataset

3.16 Results and Discussion: Annotation report and differential expression using *DESeq2*

The *DeSeq2* analysis generated the output folder *DESeq2_trans* directory containing a DE analysis matrix for each pairwise sample comparison (i.e., DEHP vs TEMP, DEHP vs COMB, COMB vs TEMP), which included log2FC and *p* adjusted value associated with each *Trinity* transcript. As an example, in **Table 3.7** there are reported the first 10 entries for the DESeq2 result matrix `COMB_vs_DEHP`.

Table 3.7 First 10 entries for the *DESeq2* result matrix COMB_vs_DEHP, displaying the transcript IDs, baseMean (the average values of the normalised count divided by size factors), log2FC (measurement of the change of transcript's expression), *p* value and adjusted *p* value

	sampleA	sampleB	Base Mean	log2FC	pvalue	padj
TRINITY_DN1544_c1_g1_i1	COMB	DEHP	173.5	-3.4	$3.4e^{-19}$	$5.6e^{-15}$
TRINITY_DN4117_c0_g1_i9	COMB	DEHP	169.9	-5.1	$3.5e^{-18}$	$2.9e^{-14}$
TRINITY_DN5254_c0_g1_i4	COMB	DEHP	122.1	3.8	$8.3e^{-16}$	$1.8e^{-12}$
TRINITY_DN1824_c0_g1_i10	COMB	DEHP	157.2	10.8	$6.1e^{-16}$	$2.5e^{-12}$
TRINITY_DN4774_c0_g1_i17	COMB	DEHP	161.4	10.8	$8.1e^{-16}$	$2.2e^{-19}$
TRINITY_DN3442_c0_g1_i11	COMB	DEHP	129.5	10.5	$4.2e^{-14}$	$1.2e^{-10}$
TRINITY_DN1094_c0_g1_i18	COMB	DEHP	212.3	-11.3	$5.1e^{-11}$	$1.2e^{-10}$
TRINITY_DN2364_c0_g1_i10	COMB	DEHP	850.6	-4.4	$6.7e^{-14}$	$1.4e^{-10}$
TRINITY_DN3411_c0_g1_i1	COMB	DEHP	125.0	10.4	$1.0e^{-13}$	$1.8e^{-10}$
TRINITY_DN958_c0_g1_i23	COMB	DEHP	212.1	11.2	$2.1e^{-13}$	$3.4e^{-10}$

DeSeq2 also generated three reports showing upregulated transcripts in each experimental comparison. These results were combined with the annotations from *BlastX, Blastp, BlastN* from the *Trinotate* report. Shown below is an example table from the first 20 entries of the *Trinity* gene and transcript IDs followed by annotation from *BlastN* search (*nt* database), *BlastX* and *BlastP* top hits from genome-sequenced organisms. Significant comparisons, base means for each treatment (average of the normalized count values, divided by size factors, taken over all samples), log2FC (effect size estimate in logarithmic scale to base 2) and the *p* value were added from the *DeSeq2* analysis (**Table 3.8**). As expected, entries were found particularly conserved between the *BlastN* entries for Mollusca and the top hits from model organisms. Missing results for BlastX/BlastP protein entries (for example TRINITY_DN339_c1_g1 in **Table 3.8**) originated from absent hits from model organism databases.

Table 3.8 First 20 entries for the upregulated *DESeq2* result matrix for all treatments. Gene ID, transcript ID, *BlastN* top hits, *BlastX/BlastP* top hits from model organisms, significant comparisons, basemeans, log2 fold change (log2 FC) and *p*-adjusted values between treatments are shown

#Gene ID	#Transcript ID	BlastN Nucleotide sequence top hits	BlastX/BlastP protein top hits (from model organisms)	Comparison	Base Means	log2 FC	*p* adj value
TRINITY_DN12801_c0_g1	TRINITY_DN12801_c0_g1_i5	*Limnoperna fortunei* genome assembly, chromosome: 9	Mediator of RNA polymerase II transcription subunit 1 (*Homo sapiens*)	COMB_vs_TEMP	COMB: 0 TEMP: 130.9	-9.5	$5.07e^{-7}$
TRINITY_DN12785_c1_g1	TRINITY_DN12785_c1_g1_i3	*Mytilus coruscus* CYP3A-like isoform 2 mRNA, complete cds	Cytochrome P450 3A41 (*Ovis aries*)	DEHP_vs_TEMP	DEHP: 36.4 TEMP:0	7.8	$1.39e^{-5}$
TRINITY_DN12741_c0_g1	TRINITY_DN12741_c0_g1_i1	PREDICTED: *Ostrea edulis* arginine kinase-like (LOC125677116), mRNA	Arginine kinase (*Liolophura japonica*)	DEHP_vs_TEMP	DEHP: 51529.3 TEMP:10250.2	2.3	0.0003
TRINITY_DN12741_c0_g1	TRINITY_DN12741_c0_g1_i13	PREDICTED: *Ostrea edulis* arginine kinase-like (LOC125677116), mRNA	Arginine kinase *(Liolophura japonica*)	COMB_vs_TEMP DEHP_vs_TEMP	COMB: 867.5 TEMP: 114.7 DEHP: 1126.1 TEMP:111.2	2.9 3.3	$7.88e^{-10}$ $1.57e^{-27}$
TRINITY_DN12781_c0_g1	TRINITY_DN12781_c0_g1_i10	PREDICTED: *Ostrea edulis* dnaJ homolog subfamily C member 13-like (LOC125682299), transcript variant X3, mRNA	DnaJ homolog subfamily C member 13 (*Homo sapiens*)	COMB_vs_DEHP	COMB: 56.7 DEHP: 0	8.3	0.0006
TRINITY_DN348_c8_g1	TRINITY_DN348_c8_g1_i8	*Patella vulgata* genome assembly, chromosome: 6	Lipoyl synthase, mitochondrial (*Bos taurus*)	DEHP_vs_TEMP	DEHP: 141.3 TEMP: 0	9.7	$2.03e^{-2}$

TRINITY_DN339_c1_g1	TRINITY_DN339_c1_g1_i10	*Limnoperna fortunei* ii genome assembly, chromosome: 14		COMB_vs_TEMP	COMB: 0 TEMP: 43.4	-7.9	$1.35e^{-5}$
TRINITY_DN339_c1_g1	TRINITY_DN339_c1_g1_i2	*Limnoperna fortunei* i genome assembly, chromosome: 14		DEHP_vs_TEMP	DEHP: 0 TEMP: 62.8	-8.4	$4.06e^{-7}$
TRINITY_DN328_c0_g1	TRINITY_DN328_c0_g1_i13	PREDICTED :*Patellea vulgata* replication factor C subunit 5-like (LOC126823407), mRNA	Replication factor C subunit 5 (*Homo sapiens*)	COMB_vs_DEHP	COMB: 0 DEHP: 263.2	-10.6	$4.06e^{-8}$
TRINITY_DN318_c2_g1	TRINITY_DN318_c2_g1_i13	PREDICTED: *Ostrea edulis* mothers against decapentaplegic homolog 3-like (LOC125662011), transcript variant X2, mRNA	Mothers against decapentaplegic homolog 3 (*Rattus norvegicus*)	COMB_vs_DEHP	COMB: 195.9 DEHP: 0	10.1	$1.63e^{-5}$
TRINITY_DN20005_c0_g1	TRINITY_DN20005_c0_g1_i23	*Mytilus galloprovincialis* glutathione S-transferase kappa mRNA, complete cds	Glutathione S-transferase kappa 1 (*Rattus norvegicus*)	DEHP_vs_TEMP	DEHP: 0 TEMP: 24.0	-7.0	0.0004
TRINITY_DN19938_c0_g1	TRINITY_DN19938_c0_g1_i19	PREDICTED: *Haliotis rufescens* atrial natriuretic peptide receptor 1-like (LOC124145742), mRNA	Atrial natriuretic peptide receptor 1 (*Mus musculus*)	DEHP_vs_TEMP	DEHP: 0 TEMP: 28.6	-7.3	0.0001
TRINITY_DN19938_c0_g1	TRINITY_DN19938_c0_g1_i5	PREDICTED: *Haliotis rufescens* atrial natriuretic peptide receptor 1-like (LOC124145742), mRNA	Atrial natriuretic peptide receptor 1 (*Mus musculus*)	DEHP_vs_TEMP	DEHP: 0 TEMP: 22.1	-6.9	0.0003

TRINITY_DN13493_c0_g1	TRINITY_DN13493_c0_g1_i20	*Mytilus galloprovincialis* hsp70-1 gene for heat shock protein 70, clone lambdaMg70_II_4		DEHP_vs_TEMP	DEHP: 0 TEMP: 47.3	-8.0	$4.69e^{-5}$
TRINITY_DN3973_c0_g1	TRINITY_DN3973_c0_g1_i9	PREDICTED :*Patella vulgata* ADP-ribosylation factor-like protein 1 (LOC126824784), mRNA	ADP-ribosylation factor-like protein 1 (*Caenorhabditis elegans*)	DEHP_vs_TEMP	DEHP: 86.6 TEMP: 0	9.0	0.0003
TRINITY_DN3929_c0_g1	TRINITY_DN3929_c0_g1_i12	*Limnoperna fortunei* genome assembly, chromosome: 15		COMB_vs_DEHP	COMB: 0 DEHP: 38.0	-7.7	$9.41e^{-6}$
TRINITY_DN3977_c1_g1	TRINITY_DN3977_c1_g1_i4	*Mytilus edulis* eg gene for endo-1,4-beta-D-glucanase, exons 1-3	RING finger protein 150 (*Homo sapiens*)	COMB_vs_DEHP	COMB: 0 DEHP: 101.7	-9.2	$1.74e^{-5}$
TRINITY_DN8493_c0_g1	TRINITY_DN8493_c0_g1_i5	PREDICTED: *Crassostrea gigas* cilia- and flagella-associated protein 251 (LOC105334009), mRNA	Cilia- and flagella-associated protein 251 (*Homo sapiens*)	COMB_vs_TEMP	COMB: 0 TEMP: 105.4	-9.2	$1.37e^{-7}$
TRINITY_DN8471_c0_g1	TRINITY_DN8471_c0_g1_i3	*Limnoperna fortunei* genome assembly, chromosome: 11	Telomerase-binding protein EST1A (*Mus musculus*)	DEHP_vs_TEMP	DEHP: 131.1 TEMP: 0	9.6	$4.42e^{-6}$
TRINITY_DN8434_c1_g1	TRINITY_DN8434_c1_g1_i4	*Limnoperna fortunei* genome assembly, chromosome: 10	Homeodomain-interacting protein kinase 2 (*Homo sapiens*)	COMB_vs_TEMP	COMB: 1166.0 TEMP: 0	12.7	$1.87e^{-14}$
TRINITY_DN10910_c0_g1	TRINITY_DN10910_c0_g1_i11	PREDICTED: *Pecten maximus* nucleolar protein 4-like (LOC117325233), transcript variant X4, mRNA	Nucleolar protein 4 (*Mus musculus*)	COMB_vs_DEHP COMB_vs_TEMP	COMB: 0 DEHP: 77.1 COMB: 0 TEMP: 50.6	-8.8 -8.1	$7.04e^{-8}$ $1.48e^{-5}$

TRINITY_DN10910_c0_g1	TRINITY_DN10910_c0_g1_i8	PREDICTED: *Pecten maximus* nucleolar protein 4-like (LOC117325233), transcript variant X4, mRNA	Nucleolar protein 4 (*Mus musculus*)	COMB_vs_DEHP DEHP_vs_TEMP	COMB: 49.8 DEHP: 0 DEHP: 0 TEMP: 54.8	8.1 -8.2	$4.15e^{-6}$ $1.26e^{-5}$
TRINITY_DN69899_c0_g1	TRINITY_DN69899_c0_g1_i1	PREDICTED: *Ostrea edulis* transformation/transcription domain-associated protein-like (LOC125661219), mRNA	Transformation/transcription domain-associated protein (*Mus musculus*)	DEHP_vs_TEMP	DEHP: 19.2 TEMP: 0	6.9	0.0004
TRINITY_DN5053_c0_g1	TRINITY_DN5053_c0_g1_i15	*Lottia gigantea* hypothetical protein mRNA	Probable N-acetylgalactosaminyltransferase 9 (*Caenorhabditis elegans*)	COMB_vs_DEHP	COMB: 89.9 DEHP: 0	9.0	$1.49e^{-8}$
TRINITY_DN5025_c10_g1	TRINITY_DN5025_c10_g1_i12	PREDICTED: *Ostrea edulis* protein FAM135A-like (LOC125671383), transcript variant X6, mRNA	Protein FAM135A (*Mus musculus*)	COMB_vs_DEHP	COMB: 74.9 DEHP: 0	8.7	$1.52e^{-6}$
TRINITY_DN5025_c10_g1	TRINITY_DN5025_c10_g1_i17	PREDICTED: *Ostrea edulis* protein FAM135A-like (LOC125671383), transcript variant X6, mRNA	Protein FAM135A (*Mus musculus*)	COMB_vs_DEHP	COMB: 0 DEHP: 70.1	-8.7	$1.13e^{-6}$
TRINITY_DN5023_c5_g1	TRINITY_DN5023_c5_g1_i1	*Mytilus galloprovincialis* hsc71 gene for heat shock cognate 71, exons 1-6		COMB_vs_DEHP	COMB: 0 DEHP: 49.0	-8.2	$4.85e^{-5}$
TRINITY_DN5219_c0_g1	TRINITY_DN5219_c0_g1_i3	*Mytilus coruscus* beta-alanine transaminase-1 mRNA, complete cds	Alanine aminotransferase 2 (*Homo sapiens*)	DEHP_vs_TEMP	DEHP: 0 TEMP: 145.9	-9.6	$1.78e^{-5}$

TRINITY_DN5204_c0_g1	TRINITY_DN5204_c0_g1_i9	PREDICTED: *Ostrea edulis* serine/threonine-protein kinase NLK-like (LOC125677980), transcript variant X1, mRNA	Serine/threonine-protein kinase NLK (*Homo sapiens*)	COMB_vs_DEHP	COMB: 30.3 DEHP: 0	7.4	0.0002

Consequently, MA and Volcano plots were generated for each pairwise comparison as follows, where the red points correspond to false discovery rate (FDR) corrected *p* values ≤ 0.05 (**Fig. 3.23 - 3.25**).

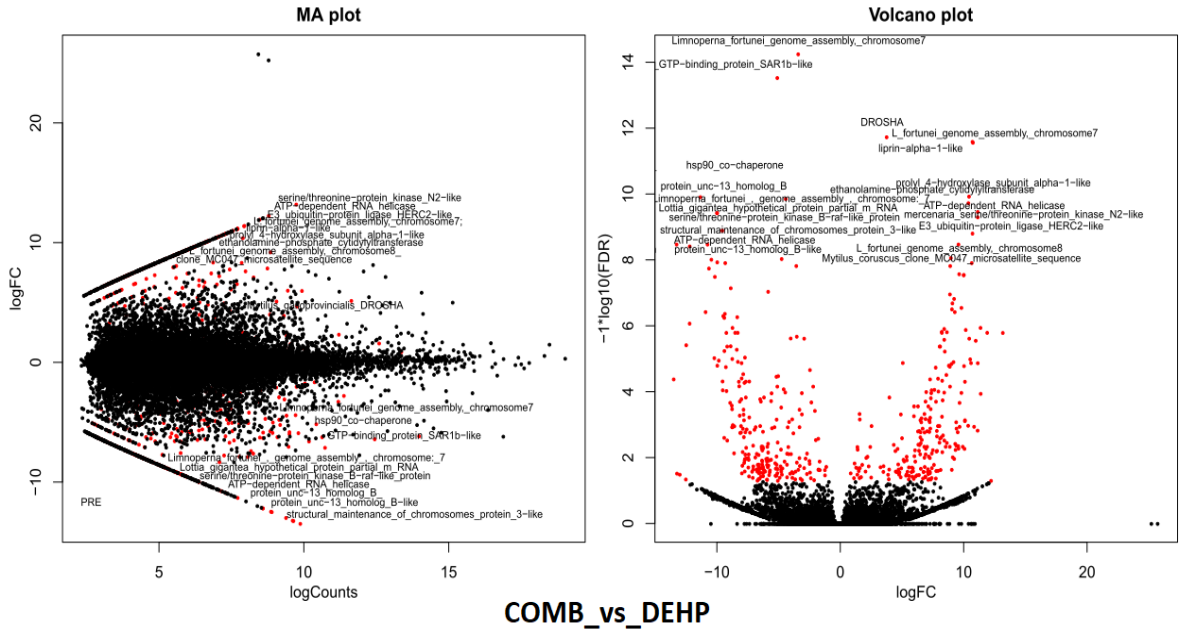

Fig. 3.23 MA and volcano plot for the pairwise comparison of COMB against DEHP for the filtered assembly, with annotations and features found differentially expressed at FDR <0.05 in red. In the Volcano plot, upregulated transcripts for DEHP are shown on the left arm of the "V", compared to upregulated COMB transcripts that are on the right arm of the "V"

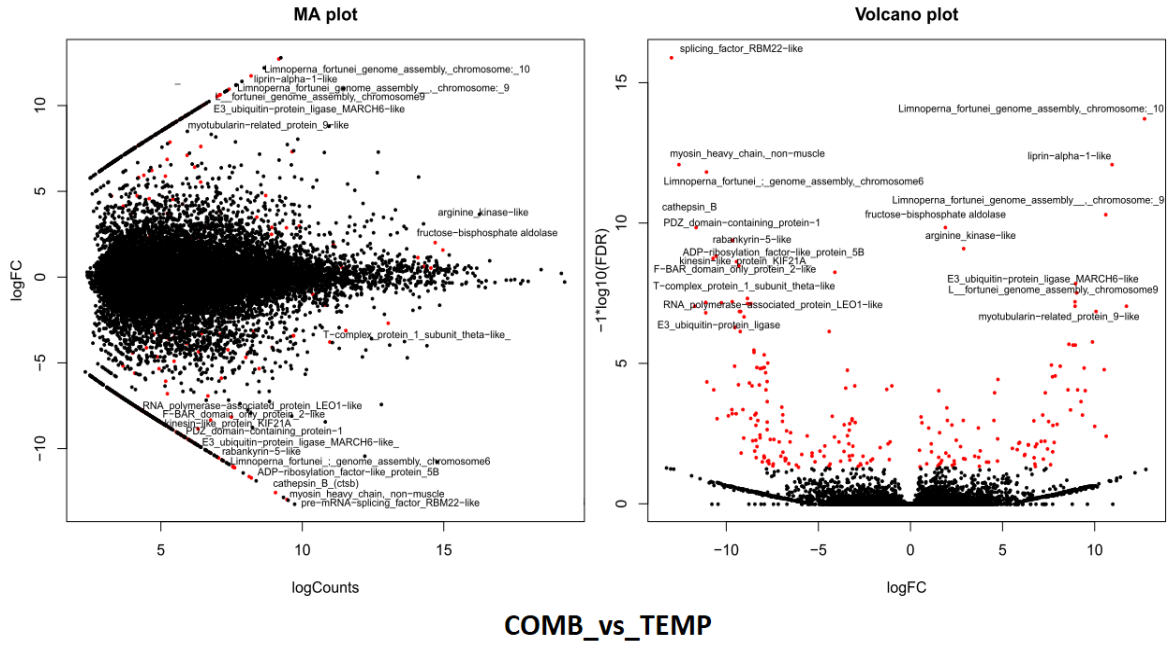

Fig. 3.24 MA and volcano plot for the pairwise comparison of COMB against TEMP for the filtered assembly, with annotations and features found differentially expressed at FDR <0.05 in red. In the Volcano plot, upregulated transcripts for TEMP are shown on the left arm of the "V", compared to upregulated COMB transcripts that are on the right arm of the "V"

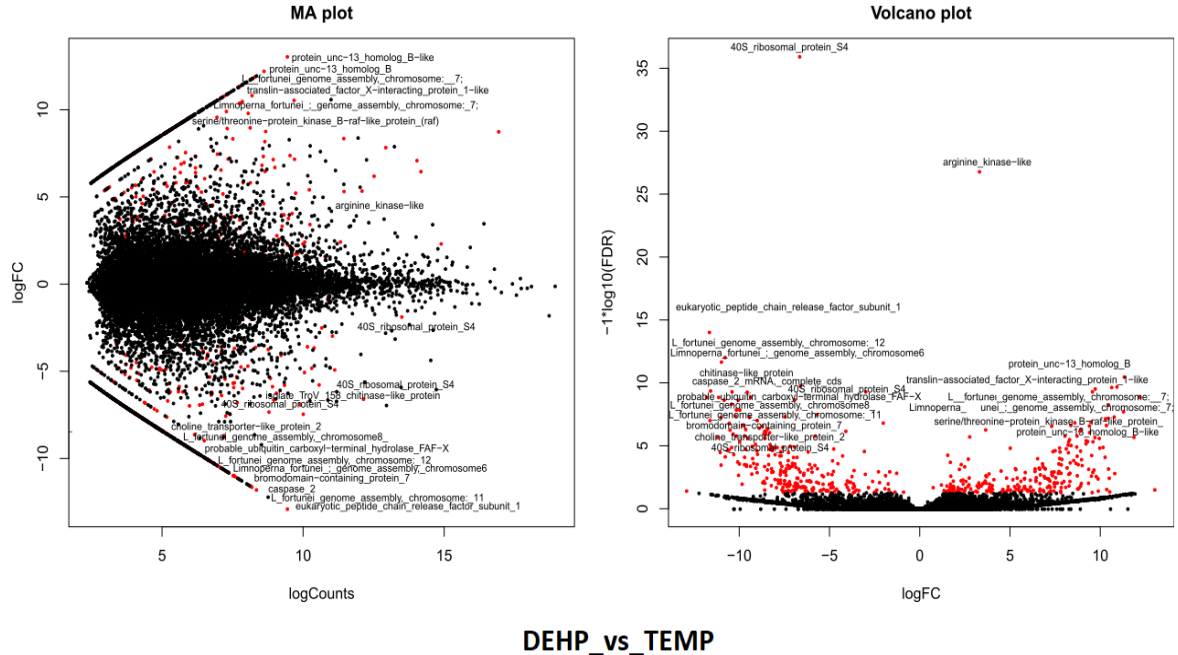

Fig. 3.25 MA and volcano plot for the pairwise comparison of TEMP against DEHP for the filtered assembly, with annotations and features found differentially expressed at FDR <0.05 in red. In the Volcano plot, upregulated transcripts for TEMP are shown on the left arm of the "V", compared to upregulated DEHP transcripts that are on the right arm of the "V"

The *De2Seq* analysis also generated a Pearson correlation for pairwise sample comparison (**Fig. 3.26**) and a clustered heatmap (**Fig. 3.27**) from a threshold *p* value of $1e^{-3}$ and 2^2 fold differentially expression (**Supplementary Appendix to Chapter 3, S3.8**).

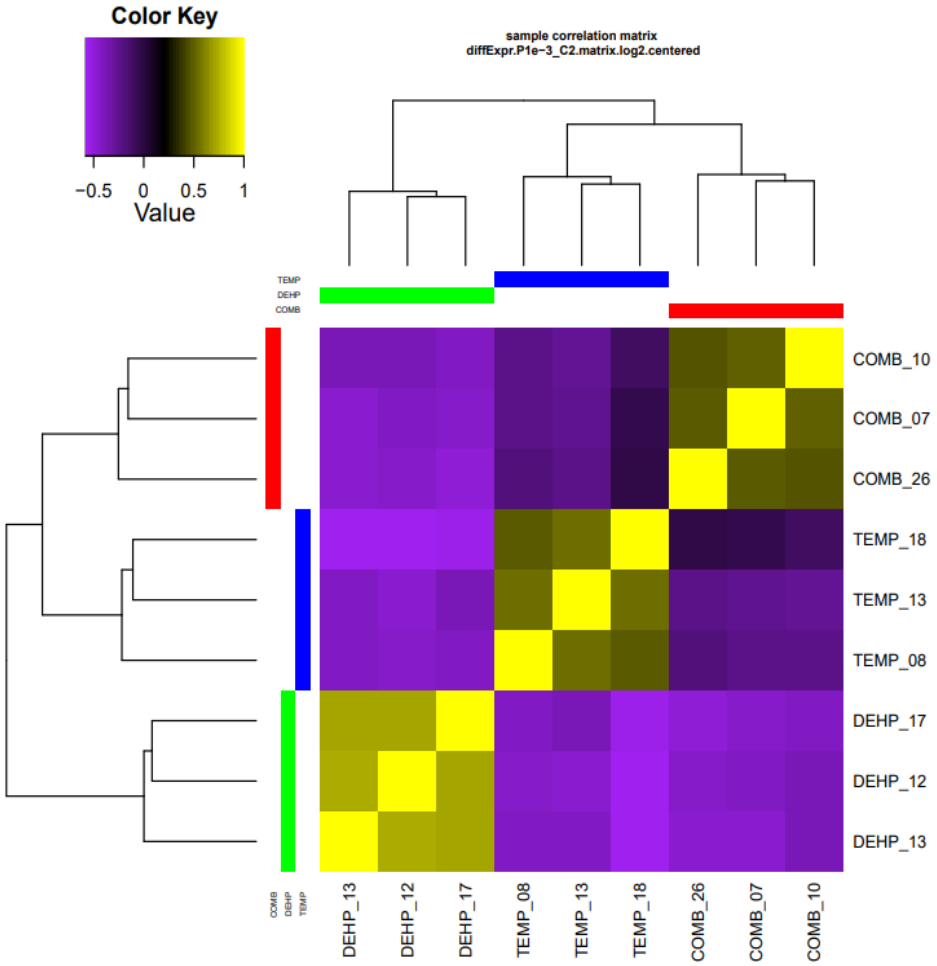

Fig. 3.26 Pearson correlation between individuals for pairwise sample comparison

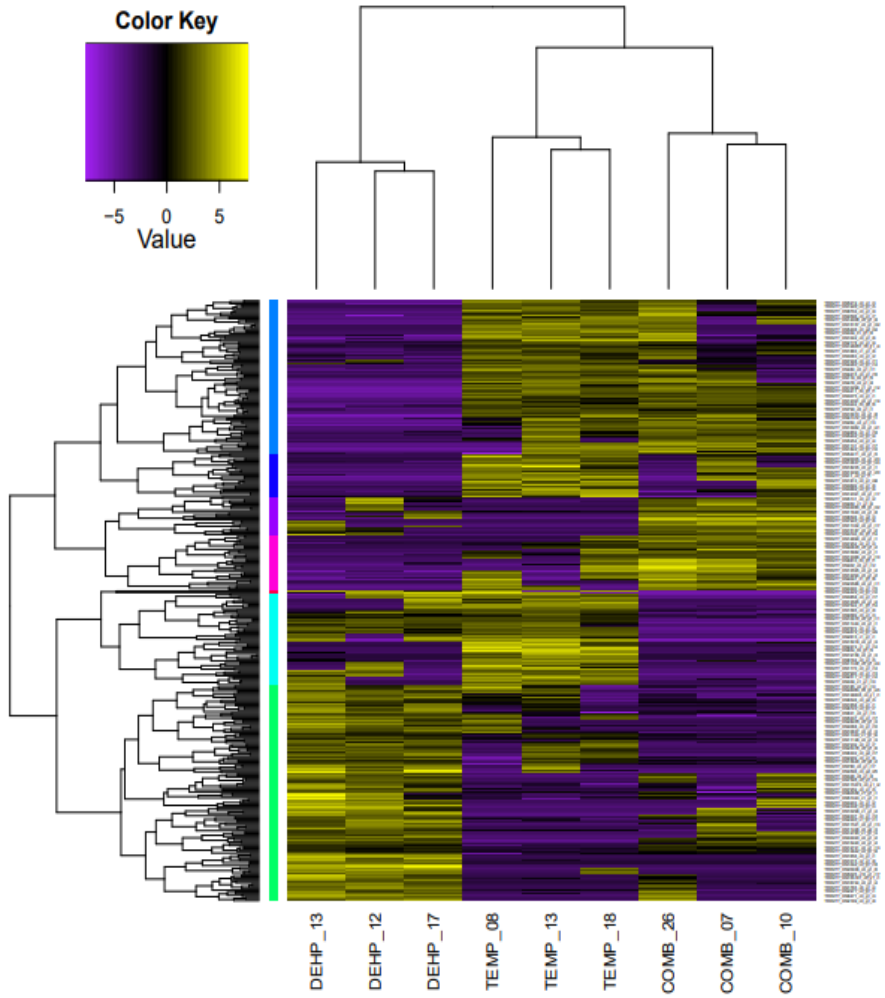

Fig. 3.27 Heatmap with upregulated expression in yellow and downregulated expression in purple. Expression values are plotted in $\log_2$ space and mean-centered (mean expression value for each feature is subtracted from each of its expression values in that row)

A general upregulation of gene expression (in yellow) is visible for the TEMP treatment (**Fig. 3.27**), which also shared a higher similarity to the COMB samples with respect to the DEHP treatment (**Fig. 3.26**). The resulting DE matrix counted 405 transcripts significantly expressed, of which 172 between COMB against DEHP (of which 84 upregulated for COMB and 88 upregulated for DEHP, **Table 3.9)**, 90 significantly expressed between COMB against TEMP (of which 31 upregulated for COMB and 59 upregulated for TEMP, **Table 3.10**), and 198 between DEHP against TEMP (79 upregulated for DEHP and 119 upregulated for TEMP, **Table 3.11**). When available in the literature, the characteristics of the associated mollusc proteins were annotated. Otherwise, the functions of these transcripts were checked in https://www.uniprot.org/

from the database of the main model organisms. Shown in the tables are the first 10 most upregulated transcripts for treatment in each pairwise comparison (**Table 3.9 - 3.11**). Considering the TEMP treatment, the following example transcripts resulted upregulated in comparison with the other two treatments (DEHP or COMB **Table 3.10** and **3.11**):

- Pre-mRNA-splicing factor RBM22 (*RBM22*): it monitors the first part of the splicing of pre-mRNA in humans and it is reported to be translocated into the nucleus during heat stress in yeast cells (Janowicz et al., 2011).
- Non-muscle myosin (*zip*): it is involved in cellularisation, morphogenesis and cytokinesis in *Drosophila melanogaster* (Sechi et al., 2014).
- Cathepsin B (*Ctsb*): it was identified in *M. galloprovincialis,* by Romero et al., (2022) with a presence in all analysed tissues (mantle, foot, muscle, gills, gland, haemocytes and gonads), possibly involved in the development of early stages and immune response to virus infection.
- PDZ domain-containing protein-1 (*PDZD1*): it arranges membrane proteins in the correct spatial position in humans (Ferreira et al., 2018).
- Rabankyrin-5 (*Ankfy1*): in mice, it is involved in the transport and localisation of endosomes and lysosomes (Schnatwinkel et al., 2004).
- ADP-ribosylation factor-like protein 5B (*ARL5B*): it is involved in the development of male reproductive germ cells (Schürmann et al., 2002).
- Kinesin-like protein KIF21A (*Kif21a*): it is a microtubule-binding protein that in mice possibly controls motor activity (Marszalek et al., 1999).
- F-BAR domain only protein 2 (*FCHO2*): it is a protein that in humans serves as a co-factor in the early steps of clathrin-mediated endocytosis (Henne et al., 2010).
- T-complex protein 1 subunit theta (*CCT8*): it is a chaperon that plays a role in assembling the protein folding in humans (Freund et al., 2014).
- 40S ribosomal protein S4 (*Rps4*): commonly used as a reference gene in *M. galloprovincialis* gills, digestive glands and mantle (Salatiello et al., 2022).
- Eukaryotic peptide chain release factor subunit 1 (*ETF1*): it is involved in terminating the synthesis of peptides after the termination codon signal in humans (Frolova et al., 1994).
- Chitinase (*CHI3L2*): this is a biomineralization protein, and the associated TroV_158 contig was identified in the mantle transcript of *Mytilus* spp. by Malachowicz and Wenne (2019).

- Caspase 2 (*CASP12*): this is a protein involved in the apoptotic process. In *M. galloprovincialis*, the sequence for caspase-2 was identified by Romero et al., (2011), and it seems to be regulated by external stressors such as UV treatment, but not by the exposure to pathogens or environmental pollutants such as polychlorinated biphenyls, phenanthrene and benzopyrene.
- Ubiquitin carboxyl-terminal hydrolase FAF-X (*Usp9x*): it might regulate and prevent protein degradation (Zhang et al., 2018a).

Considering the DEHP treatment, the following example transcripts resulted upregulated in comparison with the other two treatments (TEMP or COMB **Table 3.9** and **3.11**):

- GTP-binding protein Sar1b (*SAR1B*): in humans, it transports and delivers lipoproteins from the endoplasmic reticulum to the Golgi apparatus (thereby involved in the maintenance of lipid homeostasis, Wang et al., 2021).
- Unc-13 homolog B (*UNC13B, unc-13)*: in humans, it monitors the second messenger pathway for vesicle maturation. In nematode *C. elegans*, it is also possibly involved in the release of neurotransmitters from neurons (Maruyama and Brenner, 1991).
- hsp90 co-chaperone Cdc37 (*CDC37*): this is a chaperone that generally assists HSP90 in several activities, such as signalling pathways and in the cell cycle progression (Stepanova et al., 1996).
- Serine/threonine-protein kinase B-raf (*Braf*): this is a protein involved in fertility and progression of oocyte maturation in nematodes (Schouest et al., 2009).
- Structural maintenance of chromosomes protein 3 (*smc-3*): in nematodes, it is involved in DNA repair and chromosome cohesion during meiosis (Baudrimont et al., 2011).
- Translin-associated factor X-interacting protein 1 (*Tsnaxip1*): in mice, it has a possible role in spermatogenesis (Bray et al., 2002).
- Tuberin (*TSC2*): it controls the cell cycle progression, as a loss of it shortens the G1 phase (Liang and Slingerland, 2003).

For COMB treatment, the following example transcripts were upregulated in comparison to the other two treatments (DEHP or TEMP, **Table 3.9** and **3.10**):

- DROSHA (*DROSHA*): it is a double-stranded RNA-specific ribonuclease III generally involved in the processing of miRNA transcripts (pri-miRNAs) in the nucleus (Denli et al., 2004).
- Liprin-alpha-1 (*PPFIA1*, *syd-2*): in humans, it is allegedly involved in the regulation of receptor-like tyrosine phosphatases type 2A (Serra-Pagès, 1995). On the contrary, in *C. elegans*, liprin-alpha does not seem to bind these receptors, but it is involved in the regulation of synaptic functions and neuronal region structure (Wang and Wang, 2009).
- Prolyl 4-hydroxylase subunit alpha-1 (*P4HA1*): it is involved in the synthesis of components of collagen synthesis in organisms such as humans or nematodes (Annunen, 1997; Friedman et al., 2000).
- Ethanolamine-phosphate cytidylyltransferase (*PCYT2*): it is an enzyme involved in stabilising membrane-anchored protein, apoptosis, cell division and fusion (Nakashima et al., 1997).
- ATP-dependent RNA helicase (*DHX9*): it is involved in post transcriptional gene expression and possibly in pre-mRNA splicing. In mussel *M. galloprovincialis*, it was recently sequenced by Gerdol and Venier (2015) with a putative function of double-stranded DNA sensing in the cytoplasm. This was found upregulated also in DEHP-treated samples (**Table 3.9**).
- Serine/threonine-protein kinase N2 (*PKN2*): in humans, it is possibly involved in the regulation of cell cycle progression, actin cytoskeleton assembly, cell migration, cell adhesion and transcription activation signalling processes (Guen et al., 2016).
- E3 ubiquitin-protein ligase HERC2 (*HERC2*): in humans, it is involved in the response to DNA damage (Osorio et al., 2016).
- Arginine kinase (*mcsB*): a transferase that generally synthetise phospho-arginine by catalysing the chemical reaction from ATP γ-phosphate group to L-arginine (Lopez-Zavala et a., 2016). This was found upregulated also in DEHP-treated samples (**Table 3.11**).
- Myotubularin-related protein 9 (*Mtmr9*): in mice, it regulates myotubularin-related phosphatases, and it seems to be involved also in the apoptotic process (Mochizuki and Majerus, 2003).

- THY domain-containing protein-1 (*Ppp2r2b*): In *M. galloprovincialis* it is a protein that contains a beta actin-binding motif that was isolated in the myostracum, which is a part of the shell where soft tissues are attached (Gao et al., 2015).
- Ryanodine receptor (*RYR3*): it is involved (in humans) in muscle contraction by controlling the release of Ca^{2+} into the cytoplasm from the sarcoplasmic reticulum (Schwarzmann et al., 2002).

Table 3.9 List of the most 10 significant upregulated COMB and DEHP transcripts in the COMB_vs_DEHP comparison (also observable in **Fig. 3.23**). In grey are shown the transcripts with aspecific or hypothetical mollusc equivalents in the *BlastN* database, followed by the corresponding *BlastX* and *BlastP* top hits from the model organism database

COMB	**DEHP**
Mytilus galloprovincialis DROSHA mRNA, complete cds	*Limnoperna fortunei* genome assembly, chromosome: 7
Limnoperna fortunei genome assembly, chromosome: 7 transmembrane channel-like protein 5 (*Homo sapiens*)	PREDICTED:*Patella vulgata* GTP-binding protein SAR1b-like (LOC126810142), transcript variant X1, mRNA
PREDICTED:*Patella vulgata* liprin-alpha-1-like (LOC126825605), transcript variant X3, mRNA	PREDICTED: *Crassostrea gigas* protein unc-13 homolog B (LOC105330539), transcript variant X17, mRNA
PREDICTED: *Crassostrea virginica* prolyl 4-hydroxylase subunit alpha-1-like (LOC111127387), mRNA	PREDICTED: *Crassostrea gigas* hsp90 co-chaperone Cdc37 (LOC105317959), transcript variant X2, mRNA
PREDICTED: *Octopus sinensis* ethanolamine-phosphate cytidylyltransferase (LOC115210933), transcript variant X1, mRNA	*Limnoperna fortunei* genome assembly, chromosome: 7 integrator complex subunit 1 (*Mus musculus*)
Mytilus galloprovincialis ATP-dependent RNA helicase DDX41 mRNA, complete cds	*Lottia gigantea* hypothetical protein partial mRNA Tripeptidyl-peptidase 2 (*Homo sapiens*)
PREDICTED: *Mercenaria mercenaria* serine/threonine-protein kinase N2-like (LOC123556614), transcript variant X3, mRNA	*Pinctada imbricata* serine/threonine-protein kinase B-raf-like protein (raf) mRNA, complete cds

PREDICTED: *Crassostrea virginica* E3 ubiquitin-protein ligase HERC2-like (LOC111127369), transcript variant X3, mRNA	PREDICTED: *Crassostrea virginica* structural maintenance of chromosomes protein 3-like (LOC111134732), mRNA
Limnoperna fortunei genome assembly, chromosome: 8 Anoctamin-1 (*Mus musculus*)	*Mytilus galloprovincialis* ATP-dependent RNA helicase DDX41 mRNA, complete cds
Mytilus coruscus clone MC047 microsatellite sequence endoplasmic reticulum-Golgi intermediate compartment protein 3 (*Danio rerio)*	PREDICTED: *Mizuhopecten yessoensis* protein unc-13 homolog B-like (LOC110456312), transcript variant X13, mRNA

Table 3.10 List of the most 10 significant upregulated COMB and TEMP transcripts in the COMB_vs_TEMP comparison (also observable in **Fig. 3.24**). In grey are shown the transcripts with aspecific or hypothetical mollusc equivalents in the *BlastN* database, followed by the corresponding *BlastX* and *BlastP* top hits from the model organism database

COMB	**TEMP**
Limnoperna fortunei genome assembly, chromosome: 10 Homeodomain-interacting protein kinase 2 (*Homo sapiens*)	PREDICTED:*Patella vulgata* pre-mRNA-splicing factor RBM22-like (LOC126810789), mRNA
PREDICTED:*Patella vulgata* liprin-alpha-1-like (LOC126825605), transcript variant X3, mRNA	PREDICTED: *Crassostrea gigas* myosin heavy chain, non-muscle (LOC105332339), transcript variant X12, mRNA
Limnoperna fortunei genome assembly, chromosome: 9 pericentrin (*Homo sapiens*)	*Limnoperna fortunei* genome assembly, chromosome: 6 Sorting nexin-2 (*Homo sapiens*)
PREDICTED: *Ostrea edulis* arginine kinase-like (LOC125677116), mRNA	*Mytilus galloprovincialis* cathepsin B (ctsb) mRNA, complete cds
PREDICTED: *Crassostrea virginica* E3 ubiquitin-protein ligase MARCH6-like (LOC111134723), mRNA	*Mytilus coruscus* PDZ domain-containing protein-1 mRNA, complete cds
Limnoperna fortunei genome assembly, chromosome: 9 dynein-1-beta heavy chain (*Chlamydomonas reinhardtii)*	PREDICTED: *Mizuhopecten yessoensis* rabankyrin-5-like (LOC110460738), transcript variant X2, mRNA

PREDICTED: *Pecten maximus* myotubularin-related protein 9-like (LOC117316531), mRNA	PREDICTED: *Mizuhopecten yessoensis* ADP-ribosylation factor-like protein 5B (LOC110459636), mRNA
Limnoperna fortunei genome assembly, chromosome: 8	PREDICTED: *Gigantopelta aegis* kinesin-like protein KIF21A (LOC121381972), transcript variant X3, mRNA
Mytilus galloprovincialis THY domain-containing protein-1 mRNA, partial cds	PREDICTED: *Mercenaria mercenaria* F-BAR domain only protein 2-like (LOC123525878), mRNA
PREDICTED: *Ostrea edulis* ryanodine receptor-like (LOC125648892), transcript variant X9, mRNA	PREDICTED: *Mercenaria mercenaria* T-complex protein 1 subunit theta-like (LOC123551855), transcript variant X2, mRNA

Table 3.11 List of the most 10 significant upregulated DEHP and TEMP transcripts in the DEHP_vs_TEMP comparison (also observable in **Fig. 3.25**). In grey are shown the transcripts with aspecific or hypothetical mollusc equivalents in the *BlastN* database, followed by the corresponding *BlastX* and *BlastP* top hits from the model organism database

DEHP	**TEMP**
PREDICTED: *Ostrea edulis* arginine kinase-like (LOC125677116), mRNA	*Mytilus edulis* 40S ribosomal protein S4 mRNA, partial cds
PREDICTED: *Crassostrea gigas* protein unc-13 homolog B (LOC105330539), transcript variant X17, mRNA	PREDICTED: *Crassostrea gigas* eukaryotic peptide chain release factor subunit 1 (LOC105325000), mRNA
Limnoperna fortunei genome assembly, chromosome: 7 Telomere attrition and p53 response 1 protein (*Xenopus tropicalis*)	*Limnoperna fortunei* genome assembly, chromosome: 12 SPRY domain-containing SOCS box protein 1 (*Bos taurus)*
PREDICTED: *Crassostrea virginica* translin-associated factor X-interacting protein 1-like (LOC111138192), mRNA	*Limnoperna fortunei* genome assembly, chromosome: 6) Sorting nexin-2 (*Homo sapiens*)
Limnoperna fortunei genome assembly, chromosome: 7 DnaJ homolog subfamily B member 12 (*Homo sapiens*)	*Mytilus trossulus* isolate TroV_158 chitinase-like protein mRNA, complete cds

Pinctada imbricata serine/threonine-protein kinase B-raf-like protein (raf) mRNA, complete cds	*Mytilus galloprovincialis* caspase 2 mRNA, complete cds
REDICTED: *Mizuhopecten yessoensis* protein unc-13 homolog B-like (LOC110456312), transcript variant X13, mRNA	*Mytilus edulis* 40S ribosomal protein S4 mRNA, partial cds
Limnoperna fortunei genome assembly, chromosome: 8 Dynein axonemal heavy chain 5 (Homo sapiens)	PREDICTED: *Ostrea edulis* probable ubiquitin carboxyl-terminal hydrolase FAF-X (LOC125659115), transcript variant X3, mRNA
Lottia gigantea hypothetical protein partial mRNA Cilia- and flagella-associated protein 65 (*Gallus gallus*)	*Limnoperna fortunei* genome assembly, chromosome: 8 Anoctamin-1 (*Mus musculus*)
PREDICTED:*Lingula anatina* tuberin (LOC106155018), mRNA	*Limnoperna fortunei* genome assembly, chromosome: 11

Furthermore, several transcripts were recognised by the *BlastN* search as belonging aspecifically to *Limnoperna fortunei* genome assembly or hypothetical mollusc proteins (in grey in **Table 3.9 – 3.11**). This is due to the lack of a complete genome mapping of non-model organisms such as mussels. In this case, the *BlastX* and *BlastP* top hits from the model organism database were taken into consideration.

Specifically, for TEMP treatment, the following example transcripts were analysed from model organisms:

- TRINITY_DN14995_c0_g1_i12 (*Limnoperna fortunei* genome assembly, chromosome: 6): Sorting nexin-2 (*Snx2*), involved in intracellular trafficking (Van Weering et al., 2012).
- TRINITY_DN5174_c0_g1_i11 (*Limnoperna fortunei* genome assembly, chromosome: 12): SPRY domain-containing SOCS box protein 1 (*SPSB1*), which binds E3 ubiquitin-protein ligase complex and monitor the ubiquitination and degradation of target proteins (Nishiya et al., 2011).
- TRINITY_DN5409_c0_g1_i7 (*Limnoperna fortunei* genome assembly, chromosome: 8): Anoctamin-1 (*Ano1*): it is a chloride channel activated by calcium, involved in muscle contraction, intestinal mucus secretion, vomeronasal sensory neurons, non-histaminergic response and radial glial cell extension (Benedetto et al., 2019; Hong et al., 2019; Paulino et al., 2017).
- TRINITY_DN1026_c0_g1_i1 (*Limnoperna fortunei* genome assembly,

chromosome: 11): no results

For the DEHP treatment:

- TRINITY_DN1544_c1_g1_i1 (*Limnoperna fortunei* genome assembly, chromosome: 7): no results
- TRINITY_DN8301_c0_g1_i42 (*Limnoperna fortunei* genome assembly, chromosome: 7): integrator complex subunit 1 (*INTS7*), a part of a complex that monitors the transcriptions of small nuclear RNAs, U1 and U2 (Cotta-Ramusino et al., 2011).
- TRINITY_DN2375_c7_g1_i3 (*Lottia gigantea* hypothetical protein partial mRNA): Tripeptidyl-peptidase 2 (*TPP2*), which monitors the intracellular amino acid homeostasis (Lu et al., 2014).
- TRINITY_DN4891_c0_g1_i15 (*Limnoperna fortunei* genome assembly, chromosome: 7): Telomere attrition and p53 response 1 protein (*TAPR1*), which protects the cell against telomerase shortening and apoptosis (Santos et al., 2021).
- TRINITY_DN8645_c1_g1_i10 (*Limnoperna fortunei* genome assembly, chromosome: 7): DnaJ homolog subfamily B member 12 (*DNAJB12*), co-chaperon with HSPA8/Hsc70, involved in protein folding, aggregation and trafficking (Grove et al., 2011; Yamamoto et al., 2010).
- TRINITY_DN63_c1_g1_i6 (*Limnoperna fortunei* genome assembly, chromosome: 8): Dynein axonemal heavy chain 5 (*Dnah5*), which generates respiratory ciliary proteins (Dougherty et al., 2016).
- TRINITY_DN2788_c0_g1_i15 (*Lottia gigantea* hypothetical protein partial mRNA): Cilia- and flagella-associated protein 65 (*CFAP65*), which monitors the formation of flagella and sperm motility (Liu et al., 2021).

And for COMB treatment:

- TRINITY_DN1824_c0_g1_i10 (*Limnoperna fortunei* genome assembly, chromosome: 7): transmembrane channel-like protein 5 (*TMC1*), in humans and mice it is an ion channel allegedly involved in cochlear hair cells (Kurima et al., 2002).
- TRINITY_DN5409_c0_g1_i7 (*Limnoperna fortunei* genome assembly, chromosome: 8): Anoctamin-1 (*Ano1*).

- TRINITY_DN10102_c0_g1_i23 (*M. coruscus* clone MC047 microsatellite sequence): endoplasmic reticulum-Golgi intermediate compartment protein 3 (*ERGIC1*), possibly involved in the endoplasmic reticulum - Golgi transport (Breuza et al., 2004).
- TRINITY_DN8434_c1_g1_i4 (*Limnoperna fortunei* genome assembly, chromosome: 10): Homeodomain-interacting protein kinase 2 (*HIPK2*), it is a serine/threonine-protein kinase that is involved in transcription regulation, apoptosis and cell cycle (Liebl et al., 2021).
- TRINITY_DN1901_c0_g1_i16 (*Limnoperna fortunei* genome assembly, chromosome: 9): pericentrin (*PCNT*), which organises microtubules in mitosis and meiosis (Flory et al., 2000).
- TRINITY_DN11332_c0_g1_i17 (*Limnoperna fortunei* genome assembly, chromosome: 9): dynein-1-beta heavy chain, flagellar inner arm I1 complex (*DHC10*), which monitors cilia and flagella formation (Perrone et al., 2000).
- TRINITY_DN33020_c0_g1_i32 (*Limnoperna fortunei* genome assembly, chromosome: 8): no results

3.17 Results and Discussion: Gene Ontology enrichment using *GOseq*

The DE_results (**Chapter 3.9**) for upregulated transcripts in each treatment were used to generate GO assignments for each gene feature. Specifically, a matrix of enriched (over-represented) and depleted (under-represented) transcripts among the set of significantly upregulated genes for each treatment was generated. The resulting Gene Ontology matrix was visualised in *Revigo* with *Simrel* semantic similarity measure and Uniprot database research (http://revigo.irb.hr/). The GO term IDs for all the experimental treatments were plotted together in a scatter plot (**Fig. 3.28 - 3.30**) for enriched transcripts. Additionally, scatter plots and treemaps were chosen to visualize the results for each individual treatment (**Supplementary Fig. 3.1 – 3.18**).

For the TEMP treatment, 58 GO categories were found significantly over-represented (enriched). Of these, 31 categories for Biological Process were found and grouped based on their interactions (**Fig. 3.28, Supplementary Fig. 3.1** and **3.2**):

- Dephosphorylation: involved in the removal of phosphoric residues (ester or anhydride) from molecules.

- Cell differentiation and post-embryonic animal morphogenesis: processes involved in characterisation of unspecialised cells by structures and functional features during the development to the mature state.
- Homeostatic process: process involved in the maintenance of stable internal physical and chemical conditions.
- Cellular nitrogen compound biosynthetic process and peptide metabolic process: comprehend all the reactions involved in the synthesis of nitrogenous compounds, both organic and inorganic and pathways that comprehend peptides.
- Positive regulation of nucleobase-containing compound metabolic process, regulation of macroautophagy, negative regulation of phosphate metabolic process, negative regulation of cell population proliferation, negative regulation of phosphorus metabolic process, regulation of reproductive process, positive regulation of reproductive process and positive regulation of chromosome organisation: involved in chemical reactions, processes and pathways that comprehend nucleobase-containing compounds (such as DNA, RNA), phosphorus compounds, phosphate compounds and also include cell proliferation, macroautophagy, reproduction.
- Organelle fusion, membrane organisation, plasma membrane organisation and membrane fusion: involved in the assembly/disassembly and arrangement of plasma membrane constituents, including organelle generation and membrane fusion.
- Protein localisation to membrane, protein targeting, endocytosis, cellular localisation, cellular macromolecule localisation, protein localisation to plasma membrane and establishment of protein localisation to organelle: involved in transportation and maintenance of proteins and macromolecules in a specific membrane location or particular cell regions, such as organelles.

For the DEHP treatment, 41 GO categories were found significantly over-represented (enriched). Of these, 10 categories for Biological Process were found and grouped based on their interactions (**Fig. 3.28, Supplementary Fig. 3.7** and **3.8**):

- Cellular component disassembly.
- Cell cycle G2/M phase transition and mitotic cell cycle process.

- Response to stimulus, which comprehends the detection of a stimulus and the corresponding resulting state/activity change (e.g., movement, secretion, gene expression).
- Localisation.
- Anion transmembrane transport.
- Positive regulation of transferase activity, negative regulation of DNA metabolic process, regulation of transferase activity: involved in the donor-acceptor transfer of a group (e.g., methyl, glycosyl, acyl, phosphorus-containing groups) and down-regulation of DNA metabolic process.

For COMB treatment, 27 GO terms were found significantly overrepresented. Of these, 15 categories for Biological Process were found and grouped based on their interactions in one group (**Fig. 3.28, Supplementary Fig. 3.13** and **3.14**):

- Negative regulation of protein catabolic process, regulation of catabolic process, negative regulation of catabolic process, regulation of transforming growth factor beta receptor signalling pathway, transmembrane receptor protein serine/threonine kinase signalling pathway, negative regulation of proteolysis, negative regulation of proteolysis involved in protein catabolic process, smoothened signalling pathway, regulation of transmembrane receptor protein serine/threonine kinase signalling pathway: involved in the regulation of signalling pathway and protein catabolic process, with or without the hydrolysis of peptide bonds.

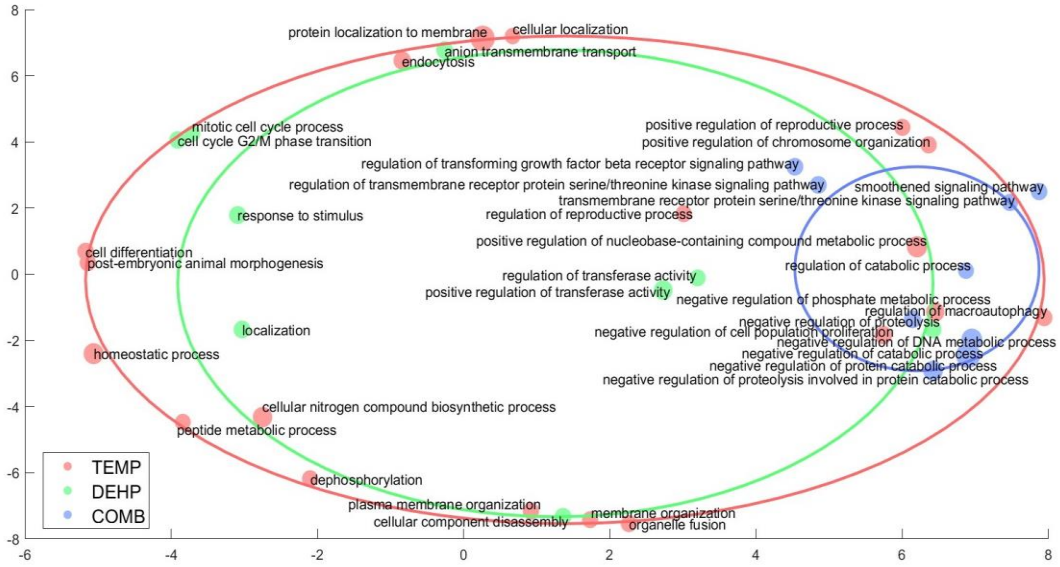

Fig. 3.28 Enriched Biological Process for TEMP (red), DEHP (green) and COMB (blue) with 95 % confidence ellipse. Data points are plotted by semantic similarities. Different sizes of the data points represent their over-represented *p* value

For Cellular Component, 13 TEMP GO categories were found and grouped as follows (**Fig. 3.29, Supplementary Fig. 3.3** and **3.4**):

- Endoplasmic reticulum and endosome.
- Cell projection: the prolongation or a process that extends from a cell (e.g., flagellum or axon).
- Dendrite and cell projection membrane.
- Site of polarised growth: defined as the part of a cell involved in non-isotropic growth.
- Cell body: defined as the cell bearing surface projections (e.g., axons, dendrites, cilia, or flagella), including the nucleus and excluding all cell projections.
- Plasma membrane region.
- Membrane parts.

For Cellular Component, 3 DEHP GO categories were found and grouped as follows (**Fig. 3.29, Supplementary Fig. 3.9** and **3.10**):

- Secretory granule.
- Presynapse and hippocampal mossy fibre to CA3 synapse.

For Cellular Component, 5 COMB GO categories were found and grouped as follows (**Fig. 3.29, Supplementary Fig. 3.15** and **3.16**):

- Endoplasmatic reticulum membrane, nuclear membrane, perinuclear region of cytoplasm.
- Endoplasmic reticulum part.

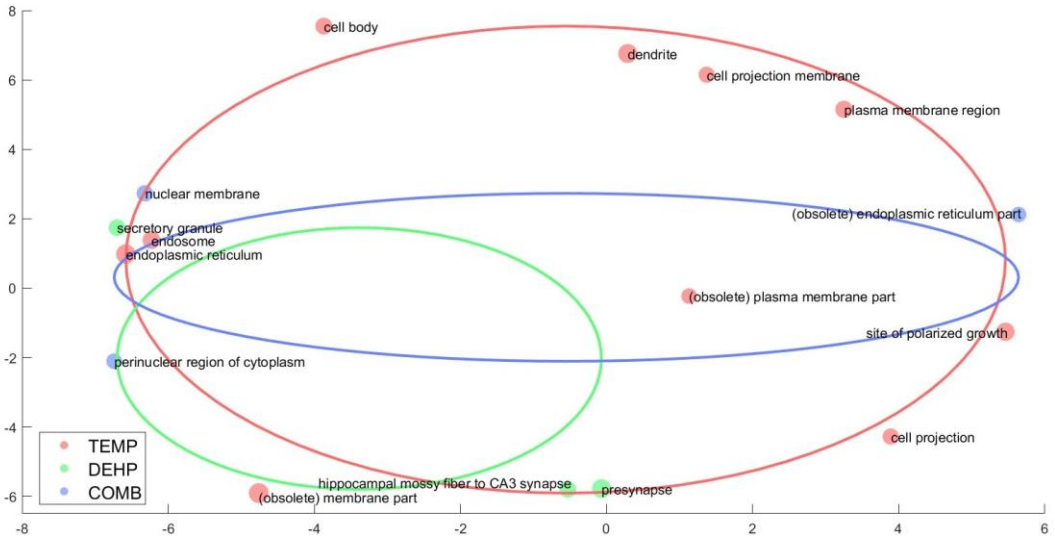

Fig. 3.29 Enriched Cellular Component for TEMP (red), DEHP (green) and COMB (blue) with 95 % confidence ellipse. Datapoints are plotted by semantic similarities. Different sizes of the data points represent their over-represented *p* value

For Metabolic Function, 11 TEMP GO categories were found and grouped as follows (**Fig. 3.30, Supplementary Fig. 3.5** and **3.6**):

- Transcription regulatory region nucleic acid binding.
- Structural constituent of ribosome.
- Phosphatidylinositol-4,5-bisphosphate binding.
- Protein domain specific binding, histone binding and signalling receptor binding.
- Enzyme regulatory activity.
- Protein-containing complex binding.

For Metabolic Function, 26 DEHP GO categories were found and grouped as follows (**Fig. 3.30, Supplementary Fig. 3.11** and **3.12**):

- Catalytic activity.
- Hydrolase activity: involved in the hydrolysis of several bonds (e.g., C-O, C-N, C-C).

- Ribonucleoside triphosphate phosphatase activity and hydrolase activity acting on acid anhydrides: involved in NTPase activity and subcellular movements.
- Purine ribonucleotide binding, small molecule binding, ion binding, anion binding, carbohydrate derivative binding, organic cyclic compound binding, nucleoside phosphate binding, heterocyclic compound binding.
- Xenobiotic transport activity: it enables the directed movement across a membrane of a xenobiotic.

For Metabolic Function, 2 GO categories for COMB were found and grouped as follows (**Fig. 3.30, Supplementary Fig. 3.17** and **3.18**):

- Protein dimerization activity and protein homodimeric activity: the formation and binding of dimers and homodimers (two non-covalently associated identical or non-identical proteins).

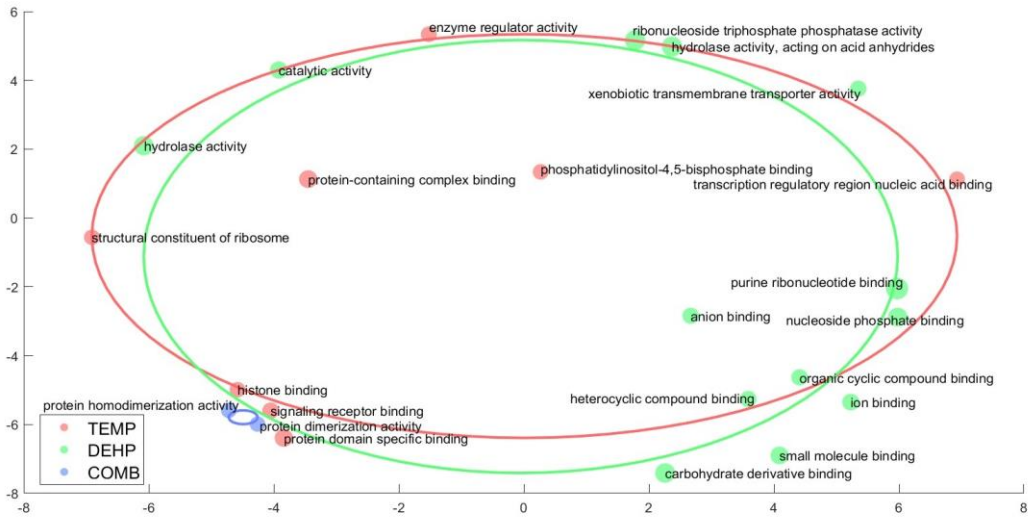

Fig. 3.30 Enriched Molecular Function for TEMP (red), DEHP (green) and COMB (blue) with 95 % confidence ellipse. Data Points are plotted by semantic similarities. Different sizes of the data points represent their over-represented *p* value

Overall, the TEMP samples showed the most varying GO features for the assembly (especially for Biological Process), due to the higher number of enriched categories observed with respect to the other two treatments DEHP and COMB. Several pathways seemed to be influenced by TEMP treatment, most of them associated with protein arrangement, transport, maintenance and regulation (e.g., *PDZD1*, *CCT8*, *Usp9x*, putative *SPSB1*) and metabolic processes. Metabolic process is one of the most dominant BP GO

categories in mussels and includes for example DNA transcription or protein degradation (Venier et al., 2009). Muscle and motor activity (e.g., *Kif21a*, putative *Ano1*) were also found here being enriched. Similarly, Moreira et al. (2015) underlined the similarity of *M. galloprovincialis* gonads to the muscle, finding in fact GO categories related to muscle activity and contraction in both examined tissues. This could also be related to gonadal contractions during the spawning event, suggesting an additional effect of DEHP on reproductive success, considering as well that liver, kidney and testis are critical target organs for DEHP toxicity (Sanco, 2002). Other influenced systems in TEMP were homeostatic processes, cell differentiation and development of early stages (e.g., *zip*, *Ctsb*), with some proteins also involved with reproduction (e.g., *ARL5B*), apoptosis (e.g., *CASP12*), biomineralisation (e.g., *CHI3L2*) or associated with stress response (e.g., *RBM22*, *Ctsb*).

Regarding DEHP samples, the most populated GO hierarchy was the Molecular Function one (26 GO categories in contrast to 11 in TEMP and 2 in COMB). We can as well conclude that the most relevant pathways affected by the exposure to the plasticiser were the response to stimuli, cell cycle and reproduction. As remarked by Venier et al. (2009), the GO class "response to stimulus" includes genes involved in the stress response, for example HSPs, metallothioneins, ferritin, cytochrome P450 or GST. Here, alongside the upregulated pathways associated with xenobiotic transport (MF), the response to stimuli (BP) was represented by two chaperones to HSP (e.g., *CDC37* and putative *INTS7*). Transcripts associated with the HSP pathway and immune system were also found upregulated in *P. viridis* embryos exposed to the contaminant benzo(a)pyrene (Jiang et al., 2016). The DEHP-treated cell cycle seemed to be affected as well, for example with proteins *smc-3* and *TSC2*. It is also interesting to notice that reproduction-related proteins involved in fertility (e.g., *Braf*), spermiogenesis (e.g., *Tsnaxip1*) and sperm motility (e.g., putative *CFAP65*) resulted significantly enriched.

With respect to the single treatments TEMP and DEHP, COMB samples presented a higher number of BP related to signalling, possibly activated by the combination of the stressors. As with TEMP, the protein regulation process seemed to be most represented in the GO terms, as well as motor activity (e.g., *RYR3*, putative *Ano1*) and apoptosis (e.g., *Mtmr9*, *PCYT2*, putative *HIPK2*), remarking the complex mollusc apoptotic pathways as already observed by Philipp et al. (2012). Similar to the DEHP treatment, *PKN2* and putatives *PCNT* and *HIPK2* were associated with cell cycle progression. Response to

DNA damage (e.g., *HERC2*) was also noted enriched, as well as processes associated with pre-mRNA, miRNA and post-transcription (e.g., *DROSHA* and *DHX9*).

In *M. galloprovincialis*, when considering other tissues such as haemocytes and gills, Moreira et al. (2015) noted a high number of GO annotations related to the immune system and the response to infections. These outcomes were not noticed in this experiment, where transcripts for the immune biological processes were found in fact under-represented in DEHP and COMB treatments (**Supplementary Table 3.1 - 3.3**). This is probably related to the nature of the investigated gonadal tissues, more involved in processes such as the reproduction cycle instead of the immune defences.

It can be concluded that, as shown in **Chapter 2,** male mussels are affected by temperature and DEHP stressors in various forms. As remarked, increased temperature affected the stress response, but also the metabolic processes, the motor activity, and mostly protein-associated functions. Likewise, DEHP elicited a general response to external stimuli, but the effect on the reproductive traits was prevailing, more pronounced than the one seen in the candidate gene qPCR results of the previous Chapter. The combined effect of the two conditions (COMB) supported the hypothesis that a combination of the two stressors could be deleterious for marine organisms, considering the significant presence of apoptosis-, post-transcriptional and DNA damage- related processes.

3.18 Conclusions

This chapter analysed the data generated by RNA-seq analysis of gonadal samples from *M. edulis* males exposed to the plastic additive DEHP (0.5 µg/L), increased temperature (+3°C) and the combination of the two. This experiment generated a transcriptome dataset that provided additional information on the transcript activity and characteristics in *M. edulis*, a non-model organism. Firstly, *Trinity* was chosen as an assembly method for the *de novo* transcript reconstruction. The assembly was filtered to exclude transcripts belonging to other species (e.g., parasites and symbionts of mussels). Several different transcripts were observed to be upregulated in one group compared to the others. Specifically, in the TEMP treatment, features for stress response, cell differentiation, motor activity, early development, homeostasis, apoptosis, biomineralization and protein maintenance were found significantly expressed and over-represented. In the DEHP treatment, features for reproductive traits, cell cycle and response to stimuli were

significantly expressed and over-represented. For the combination of the two stressors, DNA damage response, post-transcriptional gene expression and cell cycle (also upregulated in the DEHP treatment), apoptosis and muscle activity (also upregulated in the TEMP treatment) were found upregulated and over-represented.

Overall, RNA-seq technology and *Trinity* assembly pipeline proved to be useful approaches for transcriptome profiling of non-model organisms that lack complete referenced genomic sequences. This experiment contributed to the growing literature regarding the mapping and characterisation of molluscs' genome, to better comprehend the unique biology that identifies the sentinel species *M. edulis*. Furthermore, this study offered a rare perspective to analyse transcriptomic data of aquatic organisms exposed to external stressors, eventually revealing the majority and the complexity of biological pathways most likely to be affected in future climate scenarios of global warming and plastic pollution.

Chapter 4

The effects of low pH and DEHP exposure on histological and molecular outcomes

4.1 Introduction

This chapter aims to investigate the multi-factor responses of blue mussels *M. edulis* under an ocean acidification scenario combined with DEHP exposure. Similar to **Chapter 2**, sex-based and reproductive differences were taken into consideration. Investigations were conducted at two pH conditions (8.1 and 7.7) and three different concentrations of DEHP (0, 0.5 and 50 μg/L), following the IPCC scenarios projected for the end of the century and the current phthalate concentrations found in marine environments. The changes in the gametogenesis status of male and female mussels were investigated as a biomarker of reproductive alterations. Genes for superoxide dismutase (*sod*) and catalase (*cat*) were chosen as part of the antioxidant enzyme system due to their roles in reducing superoxide anion O_2^-, a reactive oxygen species (ROS, Regoli and Giuliani, 2014). Heat shock protein 70 (*hsp70*) was selected as a biomarker of stress responsive to environmental perturbation (Encomio and Chu, 2005; Lewis et al., 1999) and xenobiotic exposure (Franzellitti and Fabbri, 2005; Koagouw et al., 2021a, b). Genes coding for carbonic anhydrase 2 (*CA2*), estrogen-related receptor (ERR, *MeER1*), and estrogen receptor (ER, *MeER2*) were chosen as they are associated with biomineralization, pH homeostasis and reproductive cycle, whose expression can be affected by estrogenic compounds (Balbi et al., 2016; Ciocan et al., 2010a, 2011; Nagasawa et al., 2015).

As the seawater pH is equal to the -log of the proton concentration ($[H^+]$), the acidification process is mainly defined by the amount of CO_2 absorbed by the ocean environment and its consequent dissociation in seawater (Bindoff et al., 2019; Feely et al., 2009; Orr et al., 2005). Furthermore, the oceanic pH is strongly influenced by environmental conditions such as changes in temperature and pressure, gas exchange, water layer mixing, biological production, organic matter, mineral and carbon cycles (Lauvset et al., 2020). Ocean acidification, intended as the global decrease in oceanic pH, is virtually certain to be caused by the aquatic uptake of CO_2 emissions originating from anthropogenic activities such as land use, cement production or fossil fuel burning (IPCC, 2021, Lauvset et al.,

2020). It is quantified that the ocean environment has absorbed approximately 30% of the carbon emission since the pre-industrial era (Khatiwala et al., 2009, 2013; Gruber et al., 2019), with oceanic areas showing uneven distributions of the absorbed CO_2. For instance, higher values of absorption are reported in the North Atlantic basin and in the near-surface layers (Sabine et al., 2004). Over the last 40 years, oceanic pH has been declining by 0.003-0.026 units per decade and has decreased by approximately 0.1 units since the Industrial Revolution with a consequent increase in water acidity (IPCC, 2014). Paleo-evidence indicates a long-term increase in oceanic surface pH over the past 50 million years and the current records of low values are with high confidence unusual and unprecedented (IPCC, 2021, Lauvset et al., 2020).

As already anticipated in **Chapter 1.4,** under very low (SSP 1 - 1.9) and low (SSP 1 - 2.6) emission scenarios, ocean surface pH values will decrease around the year 2070 and then increase slightly to the end of the century. Nonetheless, for the other scenarios, the pH values are projected to decrease monotonically until 2100. The SSP 3 - 7 (high emission scenario) and SSP 5 - 8.5 (very high emission scenario), predict a reduction in pH of around 0.3 (SSP 3 - 7) and 0.44 (SSP 5 - 8.5) for ocean layers at a depth of a few hundred metres, with stronger values projected for high-latitude oceans (Kwiatkowski et al., 2020; Terhaar et al., 2020, **Fig. 1.4** and **4.1**). The model confidence for oceanic pH future projections is high for all the scenarios for surface values, high latitude and upwelling zones. Uncertainty is attributed to the simulations for oceanic deep layers, as they are affected by water circulation and currents (Cheng et al., 2013; Feely et al., 2018; Franco et al., 2018; Hauri et al., 2013; Kwiatkowski et al., 2020; Negrete-García et al., 2019).

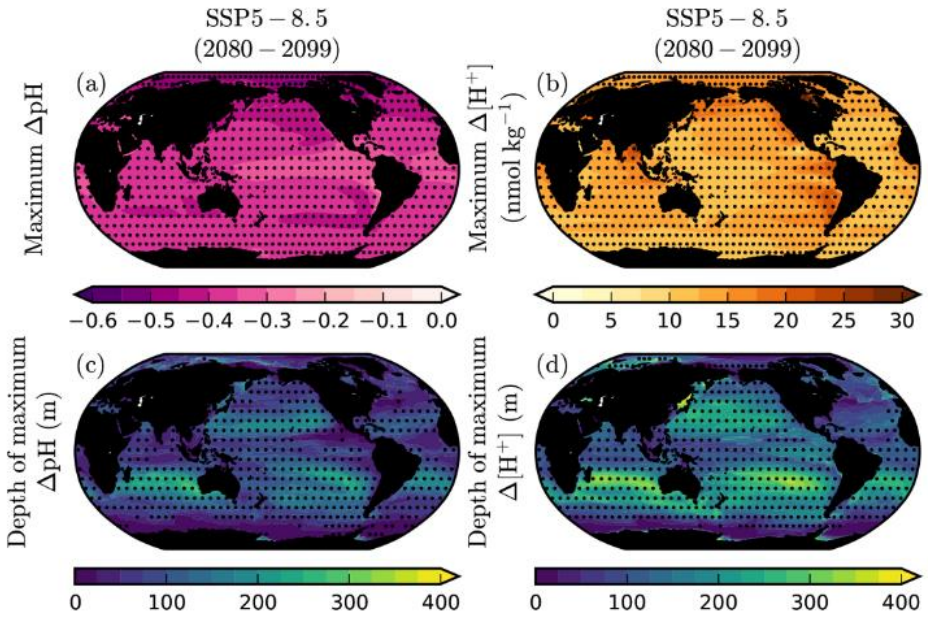

Fig. 4.1 Maximum pH and $[H^+]$ changes under the projected scenarios SSP 5 - 8. From Kwiatkowski et al. (2020)

For surface water, dissolved inorganic carbon (DIC) percentages are typically constituted by 90% of bicarbonate ions, about 9% as carbonate ions and the remaining 1% as dissolved $CO_{2(aq)}$ and H_2CO_3 (Feely et al., 2009). As the oceanic pH and the concentration of carbonate ions are declining, the level of calcium carbonate saturation decreases accordingly (Orr et al., 2005). Besides the well-studied outcomes and possible economic repercussions of decreased oceanic pH on calcifying organisms such as mussels (Callaway et al., 2012; Hofmann et al., 2010; Kroeker et al., 2011; Mangi et al., 2018), short-to-medium term pH drop can also have a range of other negative consequences on aquatic species. In fact, marine biota is differently and interactively affected by the changes in the carbon cycle constituents, such as absorbed CO_2, proton concentration and bicarbonate, carbonate, calcite and aragonite levels (Hurd et al., 2018; Kroeker et al., 2010; Orr et al., 2005). The reduction in the saturation of the shell- and skeleton-constituent $CaCO_3$ is already noticeable in marine invertebrates such as cnidarians, bryozoans, molluscs and echinoderms, regardless of the different calcification strategies (Kroeker et al., 2010; Kwiatkowski et al., 2016; Maas et al., 2018; Orr et al., 2005). In addition, the high variability of coastal organisms to ocean acidification is well-known, with distinct effects on the species inhabiting the areas potentially related to biochemical adaptivity and phenotypic plasticity (Lardies et al., 2014; Stillman and Paganini, 2015; Vargas et al., 2017). Recently, it was observed that 10-week acidification exposure did

not impact the ability of *M. edulis* and *M. trossulus* mussels to repair drill holes in their valves but affected the inorganic content and the force required to dislodge the repaired shells (George and Carrington, 2022).

Pollutants frequently alter their toxicity in climate-changing conditions, and chemicals often impact the adaptation ability of organisms to environmental fluctuations (Landis et al., 2014; Nikinmaa, 2013; Noyes et al., 2009; Schiedek et al., 2007). Exposure to climate change scenarios could also enhance the bivalve uptake of several toxic compounds and modulate the related enzyme activity (Belivermiş et al., 2020; Braga et al., 2018; Britto et al., 2020; Coppola et al., 2018; Ivanina et al., 2013; Mubiana and Blust, 2007). For example, very low pH (6.5 - 6.2) is known to enhance the accumulation of heavy metals such as copper, zinc, lead, arsenic, nickel, chromium and mercury in clams *R. philippinarum* (Han et al., 2014). In addition, various biological responses under low pH were observed in bivalves such as *Crassostrea* spp. co-exposed to heavy metals arsenic (Moreira et al., 2016), copper (Cao et al., 2019) or the polycyclic aromatic hydrocarbon phenanthrene (Lima et al., 2019) and *Mytilus* spp. co-exposed to pharmaceutical products (Mezzelani et al., 2021; Munari et al., 2018, 2020) or illicit drugs (da Silva Souza et al., 2021). Likewise, the actions of plasticisers on mussels could be exacerbated by the concomitant changes in ocean chemistry with respect to CO_2-induced ocean acidification, but the existing knowledge about the combination of plastic pollutants and climate change conditions on marine invertebrates is still incomplete.

The picture is further complicated by additional factors such as sex and reproductive status. In *Mytilus* spp. basal conditions, levels of cellular biomarkers for biological mechanisms vary naturally through the seasons and can be biologically distinct between males and females (Chapman et al., 2017, 2020). Moreover, carbonic anhydrase (CA) activity was found at different levels during the life cycle of *M. edulis*, being maximal at the end of the developing stages (Medaković, 2000). As already demonstrated in **Chapter 2**, their identification can be advantageous in analysing exposure experiment results (Ekelund Ugge et al., 2020; Koagouw and Ciocan, 2020; Louis et al., 2021; Mincarelli et al., 2021). In this scenario, this chapter's experiment focuses on the effect on sentinel species of toxic plastic additives in the context of ocean acidification, taking the sex and gametogenesis status of organisms into consideration. The following hypothesis were tested: I) the endocrine disruptive additive DEHP will have an effect on reproductive features (i.e., histological changes of the gonads and expression of biomakers of reprotoxicity), II) the combined effect of low pH and DEHP exposure will have a stronger

effect in comparison with the responses to the single stressors and III) responses of mussels to pH variations will be subjected to the climate history of the habitat they were harvested from.

4.2 Materials and Methods: Experimental design

Adult blue mussels (n = 180; length mean ± standard deviation = 4.9 cm ± 0.5 cm) were collected from the suspended ropes farm of Cromarty Mussels, Ltd. in Cromarty Firth, Scotland, U.K. (57.40.741 N 4.06.062 W, **Fig. 4.2 - 4.6**) in January 2020 and transported to the aquarium facilities of the University of Hull. Mussels were not cleaned from sand and mud nor scrubbed from seaweed and barnacles, to avoid additional physical stress. Thirty mussels for each of the six treatments were randomly divided into six 4-L continuously aerated glass tanks, for a total number of 5 mussels for each replicate tank at a density of 1 mussel per 0.8 L. They were kept for acclimation for 12 days in artificial saltwater (Premium REEF-Salt, Tropical Marine Centre, Chorleywood, UK) in a climate-controlled room at photoperiod 10:14 light: dark, salinity of 35 psu, pH of 8.1 units and temperature of 9 °C, in line with the natural environmental conditions in Cromarty Firth at the time of collection. The number of 30 individuals was chosen for each exposure treatment to ensure an adequate number of animals for each sex. After the acclimation period, mussels were exposed for seven days to two different pH levels (8.1 and 7.7) and three concentrations of DEHP (0, 0.5 and 50 µg/L), for a final yield of six experimental treatments (CTRL, LOW pH, LOW DEHP, LOW DEHP LOW pH, HIGH DEHP, HIGH DEHP LOW pH, **Fig. 4.7 - 4.11**). For the pH exposure, a total decrease of 0.4 units for the 7.7 low pH treatment was chosen considering the SSP 3 - 7 projected ranges for ocean acidification conditions for the year 2100, assuming the CO_2 emissions remain high and double from current levels by the end of the century (IPCC, 2021). Exposures of 0.5 and 50 µg DEHP/L were chosen from the literature, considering the levels found in coastal waters (Jebara et al., 2021; Sánchez-Avila et al., 2012). The seven-day DEHP exposure was chosen accounting for the non-persistency of DEHP in the environment (Staples et al., 1997), with a half-life of approximately 0.35–3.5 days for surface water and sediments in aerobic conditions (Peterson and Staples, 2003). Mussels were not fed during the exposure and artificial saltwater was prepared the day before each water change, to allow the water temperature to adjust to the controlled room. Water was changed every second

day and DEHP was dosed right after (i.e., days 1, 3 and 5) from a stock solution of 1 mg/mL DEHP (≥ 99.5% purity, Sigma Aldrich®, Gillingham, U.K.) in ethanol. The 7.7 pH values were adjusted by mixing seawater with small amounts of CO_2-saturated water (Nardi et al., 2017; Schulz et al., 2013). Temperature, pH and salinity were measured daily (**Table 4.1**) with a digital thermometer (Amarell Thermometer, Kreuzwertheim, Germany), a pH-metre (Jenway, Bibby Scientific Limited, Stone, UK) and a digital seawater refractometer (Hanna Instruments, Woonsocket, USA). Alkalinity was measured twice a week with a HI 84531 mini titrator (Hanna Instruments, Woonsocket, USA). After seven days of exposure, tissues from gonads were collected for molecular and histological analyses (Unlicensed animal ethics approval; reference no #U080/FEC_2021_11, University of Hull). Approximately 1.0 cm^2 of left gonad tissue was immersed in 1 mL neutral-buffered 10% formalin solution (Sigma Aldrich, Gillingham, U.K.) at room temperature for histological observations. The same gonadal amount was dissected and preserved in 1 mL RNAlater® stabilisation solution for gene expression analysis (Thermo Fisher Scientific, Loughborough, U.K.) and stored at -80 °C.

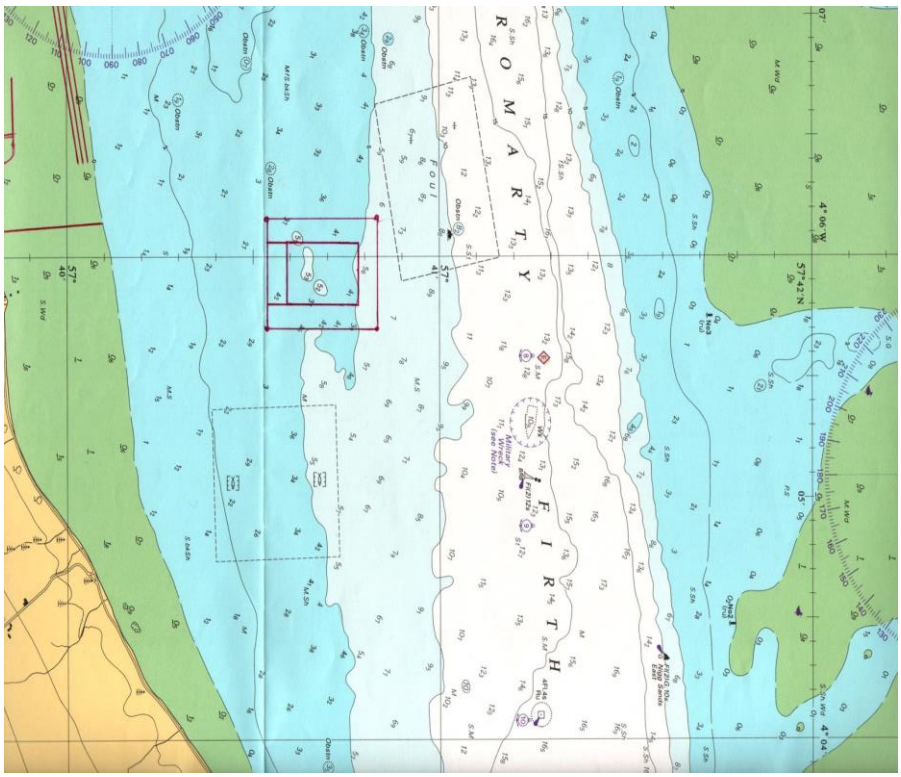

Fig. 4.2 Cromarty Firth, Scotland, U.K. (57.40.741 N 4.06.062 W), the collection site (in red)

Fig. 4.3 and 4.4 Details of the suspended ropes

Fig. 4.5 and 4.6 Details of the *M. edulis* blue mussel populations from the suspended ropes

CONTROL 8.1 pH	**LOW DEHP** 8.1 pH + 0.5 µgr/L	**HIGH DEHP** 8.1 pH + 50 µgr/L
LOW pH 7.7 pH	**LOW pH** + **LOW DEHP** 7.7 pH + 0.5 µgr/L	**LOW pH** + **HIGH DEHP** 7.7 pH + 50 µgr/L

Fig. 4.7 Experimental design for the 7-day exposure with the chosen parameters for pH (8.1 and 7.7 units) and DEHP (0, 0.5 and 50 µg/L)

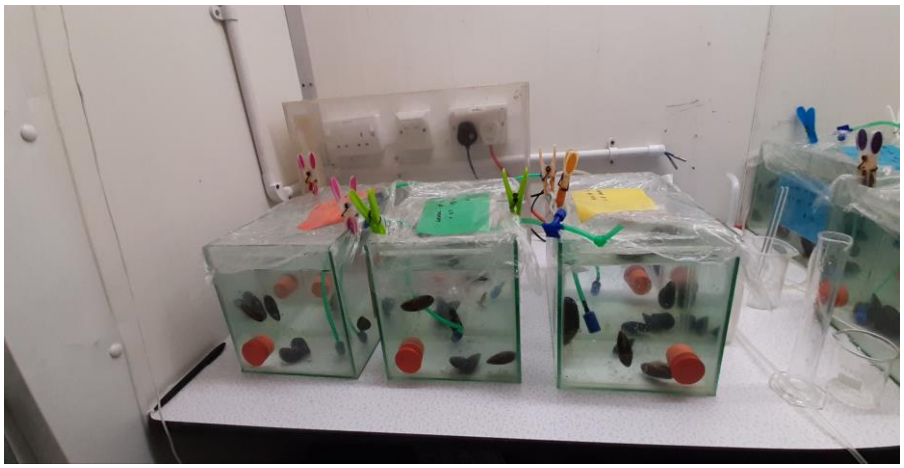

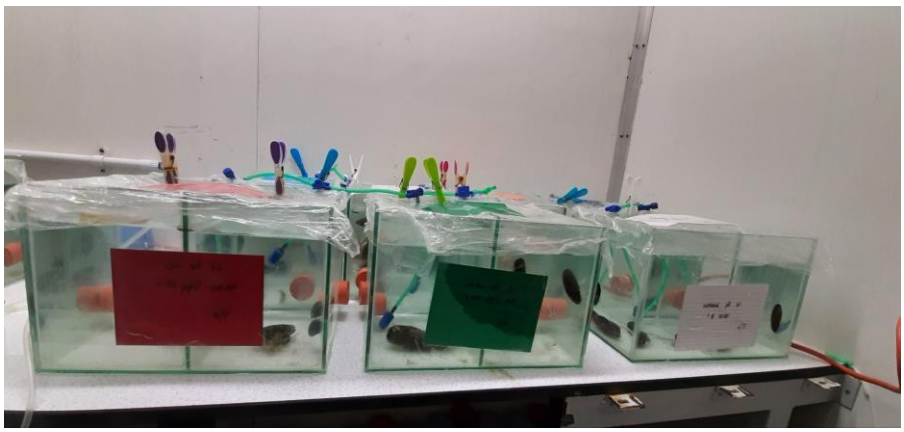

Fig. 4.8 and 4.9 Pictures from the exposure room - *M. edulis* blue mussels at 9°C in the exposure tanks, covered in non-PVC cling film

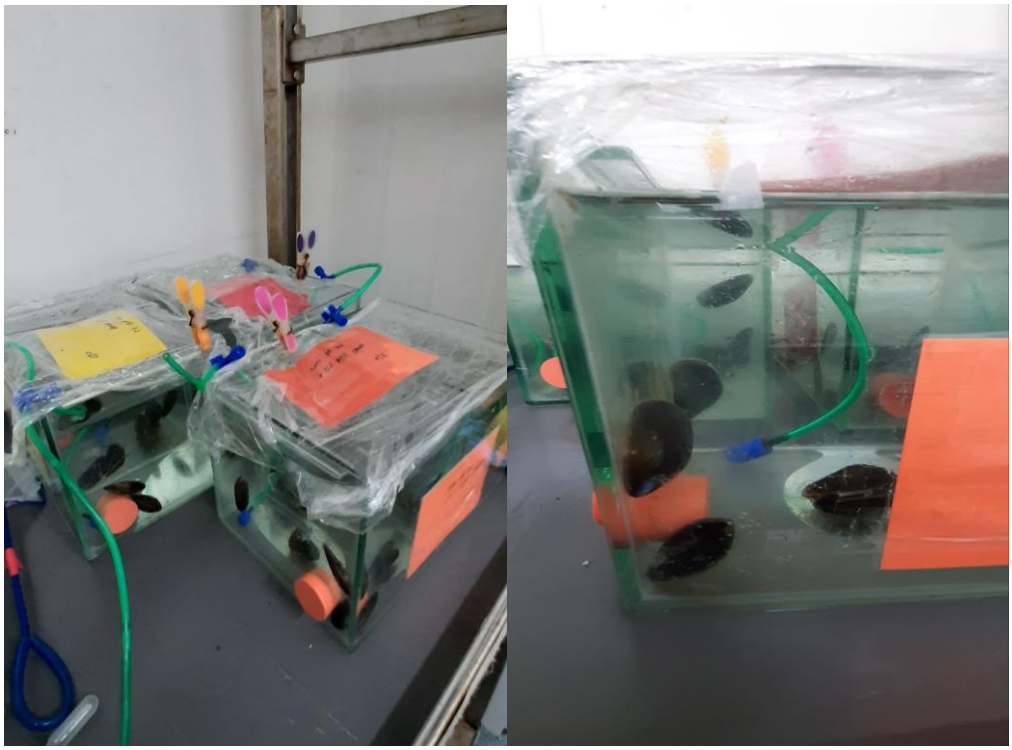

Fig. 4.10 and 4.11 Details of mussels (5 individuals for 4 litres) in the exposure tanks, covered in non-PVC cling film

Table 4.1 Experimental treatments and measurement of temperature, pH and alkalinity values at 35 ± 1 psu salinity. All parameters are expressed as mean ± standard deviation

Name of treatment	Description	Temperature (°C)	pH (Units)	Alkalinity (mg/L)
CTRL	Control pH, no DEHP	9.03 ± 0.34	8.06 ± 0.06	141.92 ± 9.35
LOW DEHP	Low DEHP concentration	8.76 ± 0.32	8.12 ± 0.09	136.63 ± 7.64
HIGH DEHP	High DEHP concentration	8.72 ± 0.44	8.12 ± 0.11	147.68 ± 13.59
LOW pH	Future pH, no DEHP	8.74 ± 0.36	7.72 ± 0.08	134.95 ± 9.21
LOW DEHP LOW pH	Future pH and low DEHP concentration	8.75 ± 0.34	7.74 ± 0.06	134.65 ± 14.83
HIGH DEHP LOW pH	Future pH and high DEHP concentration	8.65 ± 0.53	7.74 ± 0.06	128.48 ± 15.93

4.3 Materials and Methods: Wax infiltration and H/E staining

Samples fixed in 10% buffered formalin (Sigma-Aldrich, Gillingham, UK) were washed with 0.01 M PBS (Sigma Aldrich, Irvine, UK), dehydrated with increasing ethanol (Fisher Scientific, Loughboroug, UK) concentrations (70%, 90%, 100%) and cleared with Histoclear II (National Diagnostics, Atlanta, USA). The day after, the samples were embedded in paraffin wax (VWR, Poole, UK) in an EG 1160 Paraffin Wax Embedding Centre (Leica Microsystems, Milton Keynes, UK) and tissue sections (10 µm) of wax-embedded gonads were cut on a Shandon Finesse® Manual Rotary Microtome 325 (Thermo Fisher Scientific, Loughborough, UK). Slides were stained with Mayer's haematoxylin solution (Sigma-Aldrich, Schnelldorf, Germany) and eosin Y alcoholic solution (Sigma-Aldrich, Schnelldorf, Germany). Prior to microscopic analysis, microscope slides were coded, in order to conduct a blind observation. Males and females were identified, and the following stages were blindly assessed, following the stage descriptions reported by Seed (1969) and each stage was categorised by a maturity factor (MF):

I. Resting or spent gonad (MF = 1): no evident presence of sexuality. This includes virgin juveniles with immature reproductive systems and spawned animals in a spent state.
II. Development, stage 1 and 3 (MF = 2): small follicles in males and irregular oocytes in females that progressively mature and occupy half of the follicles (**Fig. 4.12 A** and **B**).
III. Development stage 5 (MF = 3): mature stage. Distended follicles in males and compacted and polygonal-shape ova in females with a few small oocytes still present (**Fig. 4.12 C** and **D**).
IV. Spawning stage 3 and 1 (MF = 4): follicles display empty spaces, with ripe spermatozoa and mature rounded eggs or residuals of the gametes undergoing cytolysis (**Fig. 4.12 E** and **F**).

Then, the sexual maturity index (SMI) was calculated according to the equation established by Siah et al. (2003): $SMI = \Sigma$ *(proportion of each stage * maturity factor)*. A detailed protocol is provided in **Chapter 2.3**: Wax infiltration and H/E staining.

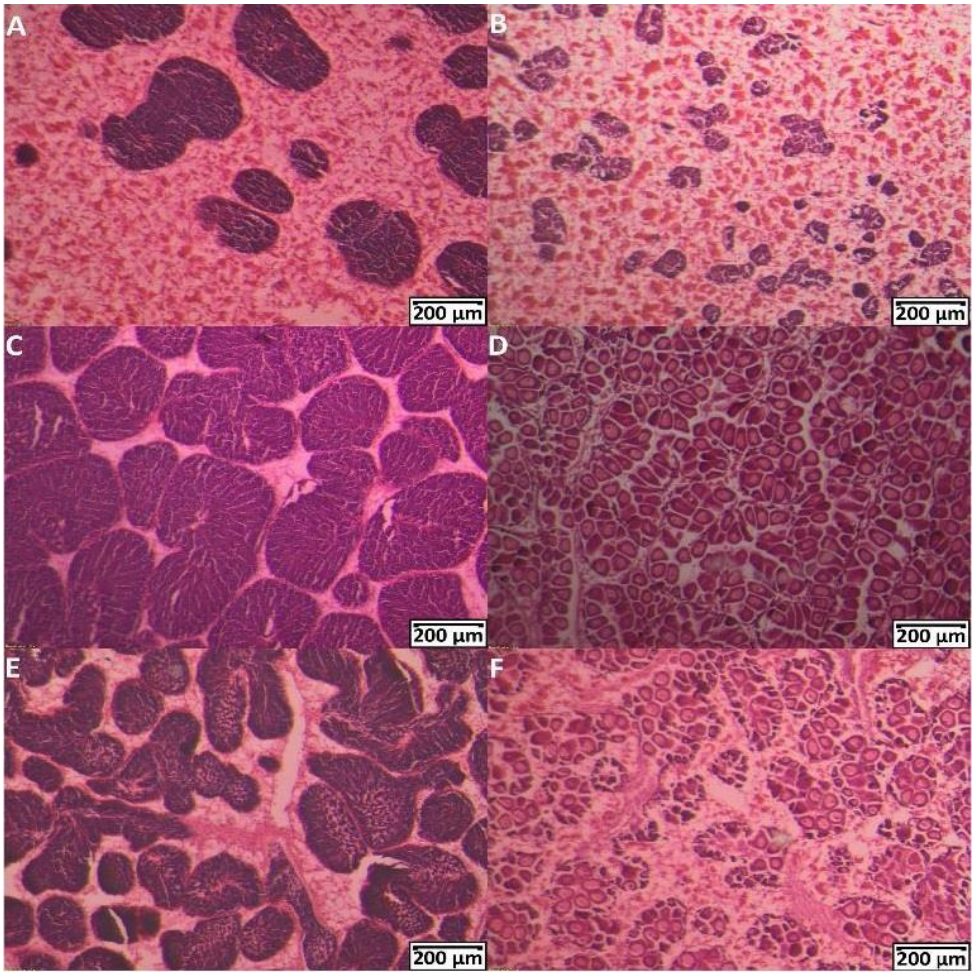

Fig. 4.12 Gametogenesis stages of 10 µm gonadal tissue sections stained with haematoxylin and eosin in males and females. Developing status in males (A) and females (B), mature gonads in males (C) and females (D), spawning stage in males (E) and females (F). Scale bars represent 200 µm. Images were modified for brightness and contrast

4.4 Materials and Methods: total RNA isolation

Gonad tissues were preserved in RNAlater® Stabilisation Solution (Thermo Fisher Scientific, Loughborough, UK) and stored at -80°C until molecular analysis. Random samples (*approx.* 10 mg of gonad tissue, n = 96) were selected and blindly coded for the analysis. In detail, 8 female gonads and 8 male gonads for each treatment were processed for total RNA extraction. The High Pure RNA Isolation Kit (Roche Applied Science, Burgess Hill, UK) was used for the purification of the intact total RNA from approximately 10 mg of gonadal tissue, with an additional DNase I digestion step, in order to remove contaminating DNA. After the extraction, samples were then stored at -80℃. A detailed protocol was provided in **Chapter 2.4**: total RNA isolation.

4.5 Materials and Methods: RNA quantification and integrity

The total RNA in the samples was quantified with a Qubit 1.0 Fluorometer, Quant-iT™ Qubit RNA BR assay kit and Qubit assay tubes (Life Technologies, Paisley, UK). The integrity and size distribution of the total RNA were then checked by denaturing agarose gel electrophoresis and GelRed™ Nucleic Acid Gel Stain staining (10,000X in DMSO, Cambridge Bioscience, Cambridge, UK). A detailed protocol was provided in **Chapter 2.5**: RNA quantification and integrity.

4.6 Materials and Methods: cDNA synthesis

Complementary DNA (cDNA) was synthesised from the RNA samples using the SuperScript™ II Reverse Transcriptase. To standardise the samples as recommended by Bustin et al. (2009), the same RNA concentration (500 ng) was used for all cDNA synthesis and sample were stored at -20℃. Detailed protocol was provided in **Chapter 2.6**: cDNA synthesis.

4.7 Materials and Methods: PCR species identification

Mytilus species were identified by PCR of the non-repetitive region *Mytilus* foot protein 1 *mfp-1* in a final volume of 25 µL, using the sense primer *Me15* 5'-CCAGTATACAAACCTGTGAAGA-3' and anti-sense primer *Me16* 5'-TGTTGTCTTAATAGGTTTGTAAGA-3' from Inoue et al. (1995). Thermal conditions from Bignell et al. (2008) were slightly modified according to the Taq polymerase guidelines. Primer concentrations of 300 nM for each primer were used in combination with 12.5 µL of PCRBIO Taq Mix Red (containing 6mM $MgCl_2$, 2mM dnNTPs, PCR BioSystems, London, UK), 1.25 µL of cDNA and the following thermal conditions: pre-heating to 95°C for 5 min, followed by 40 cycles of: 1 min at 95°C, 1 min at 60.5°C and 1 min at 72°C followed by a final extension step of 10 min at 72°C. PCR products were separated by electrophoresis in a 2% TBE-agarose gel stained with GelRed™ and the band sizes were assessed by comparison to the 100bp DNA ladder (New England Biolabs

Ltd, Knowl Piece, UK). A detailed protocol was provided in **Chapter 2.7**: PCR species identification.

4.8 Materials and Methods: Primer optimisations via PCR and qPCR amplifications

Primers for reference genes (18S ribosomal RNA *Me18S*, 28S ribosomal RNA *Me28S* and elongation factor-1 alpha *EF1α*) and genes of interest (superoxide dismutase *sod*, catalase *cat*, heat shock protein 70 *hsp70*, carbonic anhydrase *CA2*, estrogen receptor 1 *MeER1* and estrogen receptor 2 *MeER2*) were chosen accordingly to the current literature and state of the art. Details for the primer choice were provided in **Chapter 2.8:** Primer optimisations via PCR and qPCR amplifications. Additionally, primer sets for *CA2* were added in this pH-exposure experiment as the carbonic anhydrase is involved in cellular pH homeostasis. *Me18S*, *Me28S* and *EF1α* were chosen as they represent suitable reference genes during mussel gametogenesis and exogenous estrogen exposures, contrary to other common reference genes such as β-*actin* (Cubero-Leon et al., 2012; Jarque et al., 2014). Two or three sets of primers (i.e., forward and reverse) for each gene were chosen from the literature or designed online using Primer3 (http://primer3.ut.ee/) from published sequences (**Table 4.2**), for increasing the possibility of optimisation to find absence of secondary product formations and acceptable efficiencies (**Fig. 4.13 - 4.21** and **Table 4.3**). The lyophilised primers (Integrated DNA Technology, Leuven, Belgium) were resuspended in molecular grade water to a final concentration of 100 µM, aliquoted and stored at -20 °C until the analysis. For each set, primer specificity was assessed by Polymerase Chain Reaction (PCR) amplifications and 2% agarose-TBE gel electrophoresis. PCR products were prepared using the PCRBIO Taq Mix Red (PCR BioSystems, London, UK) and PCR reactions were performed on a Techne TC-4000 Thermal Cycler (Bibby Scientific, Stone, UK). Specifically, 0.5 - 1 µL of template cDNA was mixed with 12.5 µL of PCRBIO Taq Mix Red (containing 6mM $MgCl_2$, 2mM dnNTPs) and 0.25 - 1.25 µL of forward and reverse primers and PCR grade water. Specificity of the primer sets was performed at different thermal cycling programs run as follows: pre-heating to 94°C for 2 min, followed by 35 cycles of: 30 sec at 94°C, 30 sec at 55-62°C and 30 sec at 72°C followed by a final extension step of 2 min at 72°C. 10 µL PCR products were then loaded with 2 µL of 6X gel DNA Loading Dye (New England

Biolabs Ltd, Knowl Piece, UK) in a 2% agarose-TBE gel and run at 80V. Band sizes were assessed by comparison to the 100bp DNA ladder, loaded onto each gel for reference.

Table 4.2 List of primers tested via PCR and 2% agarose gel, with associated reference gene (RG), gene of interest (GoI), GenBank access number and 5'-3' sequences for forward and reverse primers, melting temperature (Tm ℃) and guanine cytosine content (%). Primer sets in grey are the ones chosen for the final qPCR analysis

Reference Gene/ Gene of Interest	**GenBank Access. No.**	**Primer name**	**(5'-3') sequence**	**Tm (℃)**	**GC (%)**	**Reference**
GoI: *Superoxide Dismutase*	**AJ581746**	*SOD_1F*	TCTCGCAGTTTACGGTCACT	56.0	50.0	Mincarelli et al., (2021)
		SOD_1R	GTGGAAACCGTGTTCTCCTG	55.9	55.0	
		SOD_2F	TTTCTCGCAGTTTACGGTCA	54.2	45.0	Barrick et al., (2018)
		SOD_2R	AACTCGTGAACGTGGAAACC	55.5	50.0	
		SOD_3F	TCTCGCAGTTTACGGTCACT	56.0	50.0	Designed online
		SOD_3R	CTGAAAGCGACTGTTCCTGT	55.1	50.0	
GoI: *Catalase*	**AY580271**	*CAT_1F*	CACCAGGTGTCCTTCCTGTT	57.1	55.0	Lacroix et al., (2014)
		CAT_1R	CTTCCGAGATGGCGTTGTAT	54.8	50.0	
		CAT_2F	ACTTCGACCAGAGACAACCC	56.7	55.0	Designed online
		CAT_2R	GCCTGTCCATCCTTGTTGAC	56.1	55.0	
		CAT_3F	TGGGATCTGGTGGGAAATAA	53.3	45.0	Barrick et al., (2018)
		CAT_3R	ATCAGGAGTTCCACGGTCAG	56.5	55.0	
GoI: *Heat Shock Protein 70*	**AF172607**	*HSP_1F*	GGGTGGTGAAGACTTTGACA	54.9	50.0	Mincarelli et al., (2021)
		HSP_1R	TGCCCTTTCACAAGCAGTTC	56.0	50.0	
		HSP70_ 2F	GGGTGGTGGAACTTTTGATG	54.1	50.0	Barrick et al., (2018)
		HSP70_ 2R	CTCTTTGCCCTTTCACAAGC	54.5	50.0	
		HSP70_ 3F	ACAAGAGCCAGGTTTGAGG A	56.3	50.0	Designed online
		*HSP70_*	CAGCAGCCTTGTCTAGTTTG	56.0	52.4	

		3R	G			
GoI: *Carbonic Anhydrase 2*	**LK934681.1**	*CA_F1* *CA_R1*	ACCAGATGGTCTTGCAGTTT TCATCTCTGACTGCTGCTAATG	54.5 54.5	45.0 45.5	Balbi et al., (2016)
		CA_F2 *CA_R2*	AGCAGTCAGAGATGAAGGCA AACTATAGGCCACCCGTTCC	56.0 56.7	50.0 55.0	Designed online
GoI: *Estrogen related receptor*	**AB257132**	*MeER1_F1* *MeER1_R1*	CCAGATCTTCAGGGTGACGA CTTGTTTGGCCCAGCTGATT	56.2 56.2	55.0 50.0	Mincarelli et al., (2021)
		MeER1_F2 *MeER1_R2*	ATACTCTTGCCCTGCCAACT CGGTCTAAACGCACACCTTC	56.4 56.1	50.0 55.0	Designed online
		MeER1_F3 *MeER1_R3*	TTACGAGAAGGTGTGCGTTT TTTTTCACCATAGGAAGGATATGT	54.5 52.0	45.0 33.3	Puinean et al., (2006)
GoI: *Estrogen Receptor*	**AB257133**	*MeER2_F1* *MeER2_R1*	GGAACACAAAGAAAAGAAAGGAAG ACAAATGTGTTCTGGATGGTG	52.7 53.4	37.5 42.9	Puinean et al., (2006)
		MeER2_F2 *MeER2_R2*	CAGGTCTGCAGTGATAACGC TGCAGGCCTGACAACTTTTC	56.0 56.0	55.0 50.0	Designed online
		MeER2_F3 *MeER2_R3*	CAGGTCTGCAGTGATAACGC AGGTCCCTGAATACTGCGTT	56.0 56.0	55.0 50.0	Designed online
RG: *Elongation Factor 1-α*	**AY580270**	*Ef1_1F* *Ef1_1R*	CACCACGAGTCTCTCCCAGA GCTGTCACCACAGACCATTCC	58.2 58.3	60.0 57.2	Ciocan et al., (2011)
	AF063420	*Ef1_2F* *Ef1_2R*	ACCCAAGGGAGCCAAAAGTT TGTCAACGATACCAGCATCC	57.2 54.8	50.0 50.0	Lacroix et al., (2014)
RG: *18s ribosomal*	**L33448**	*18S_F1*	GTGCTCTTGACTGAGTGTCTCG	57.4	54.5	Ciocan et al., (2011)

RNA		*18S_R1*	CGAGGTCCTATTCCATTATTCC	52.5	45.5	
		18S_F2 *18S_R2*	CATTAGTCAAGAACGAAAGTCAGAG GCCTGCCGAGTCATTGAAG	53.6 56.4	40.0 57.9	Cubero-Leon et al., (2012)
RG: *28s ribosomal RNA*	**Z29550**	*28S_F1* *28S_R1*	AGCCACTGCTTGCAGTTCTC ACTCGCGCACATGTTAGACTC	58.1 57.3	55.0 52.4	Ciocan et al., (2011)
	AF339512	*28S_2F* *28S_2R*	CTGGCCTTCACTTTCATTGTGCC GACCCGTCTTGAAACACGGACCA	59.0 61.4	52.2 56.5	Zanette et al., (2013)

For each set of reference genes and genes of interest, primer efficiency was assessed by qPCR reactions in accordance with the MIQE guidelines (Bustin et al. 2009). qPCR reactions were performed on a CFX96 Real Time PCR Detection System (Bio- Rad, Hemel Hempstead, U.K.) using 10 µL of qPCRBIO SyGreen Mix Lo-ROX (PCRBioSystem, London, U.K.), 7.5 µL molecular-grade water, 1 µL of each primer, and 0.5 µL cDNA at different dilutions. Primer sets were first tested at final concentrations of 100, 300 and 500 nM. For each primer set, the efficiency slope was produced by at least a minimum of 4 acceptable dilution points to % efficiency (Efficiency = $-1+10^{(-1/\text{slope})}$). and only slopes between -3.1 and -3.6 with resulting efficiencies between 90 and 110% were accepted (**Table 4.3** and **Fig. 4.13 - 4.21**, Taylor et al., 2010). qPCR products were checked using 2% agarose - TBE gel (80V) stained with GelRed™ Nucleic Acid Gel Stain. A detailed protocol was provided in **Chapter 2.8** Primer optimisation via PCR and qPCR amplification.

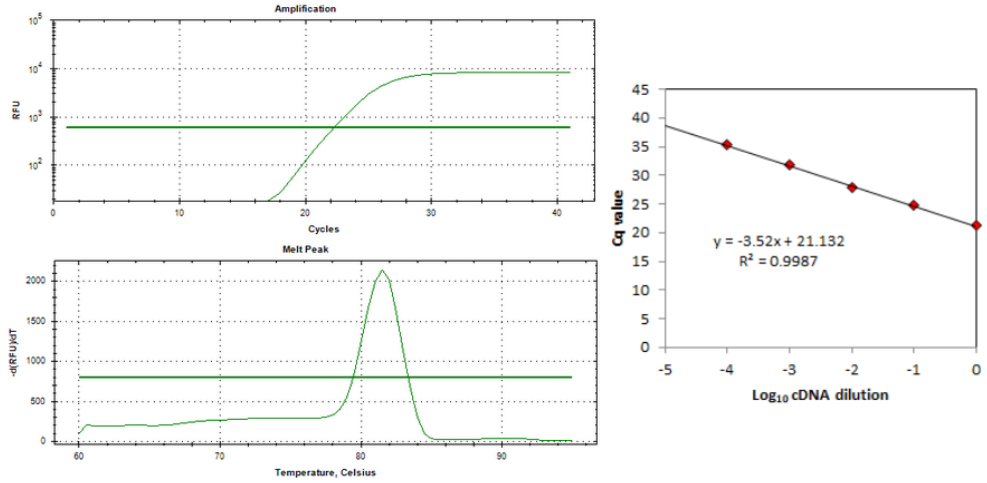

Fig. 4.13 Optimisation for *sod* primer set no. 1 at 200 nm. Amplification plots (log scale, in Relative Fluorescence Units), melt temperature peak plot and standard curve plot (10X dilutions) with R^2 values displayed

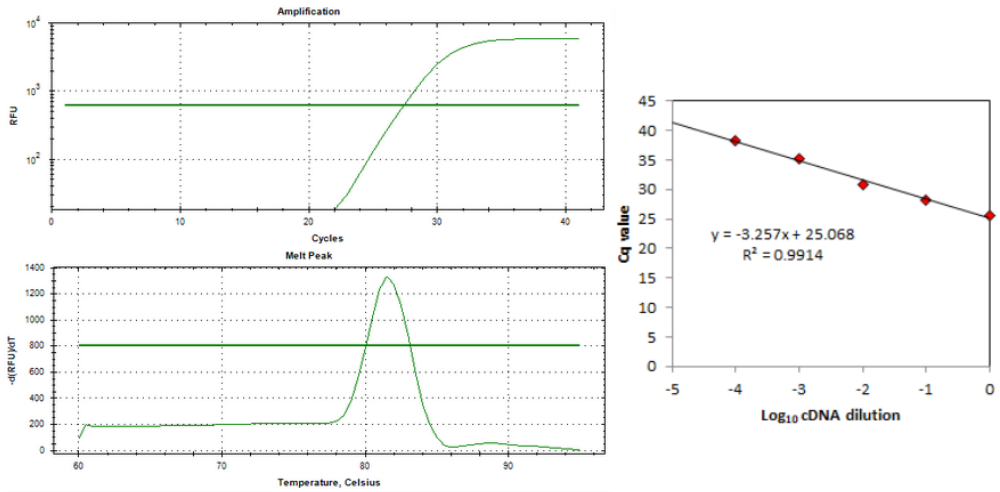

Fig. 4.14 Optimisation for *cat* primer set no. 2 at 200 nm. Amplification plots (log scale, in Relative Fluorescence Units), melt temperature peak plot and standard curve plot (10X dilutions) with R^2 values displayed

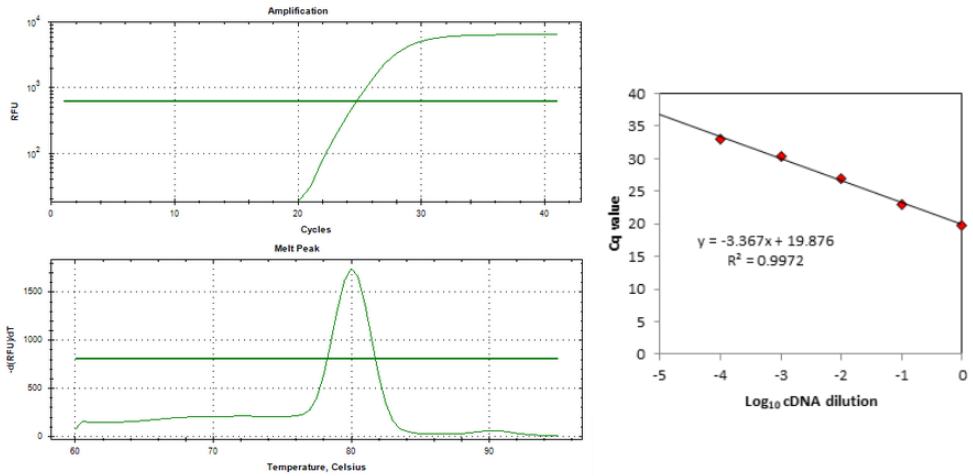

Fig. 4.15 Optimisation for *hsp70* primer set no. 1 at 500 nm. Amplification plots (log scale, in Relative Fluorescence Units), melt temperature peak plot and standard curve plot (10X dilutions) with R^2 values displayed

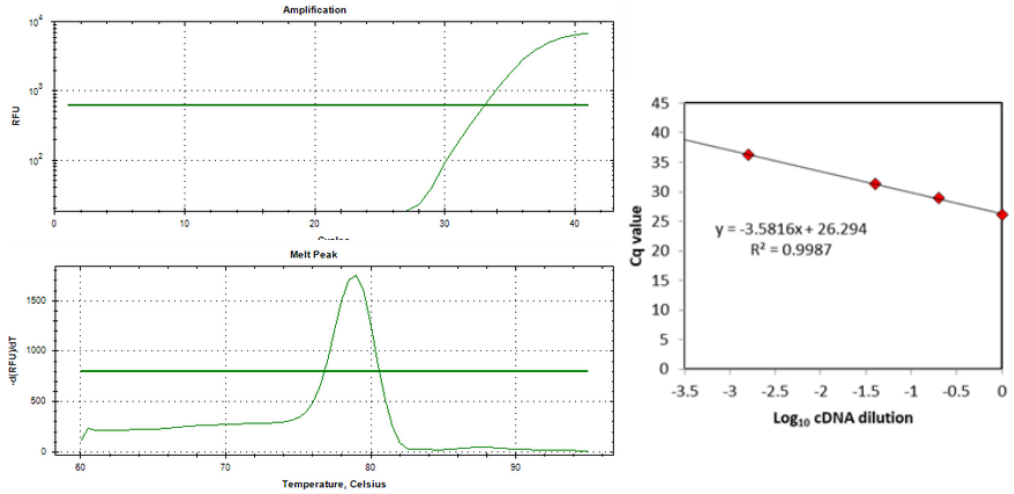

Fig. 4.16 Optimisation for *CA2* primer set no. 1 at 200 nm. Amplification plots (log scale, in Relative Fluorescence Units), melt temperature peak plot and standard curve plot (5X dilutions) with R^2 values displayed

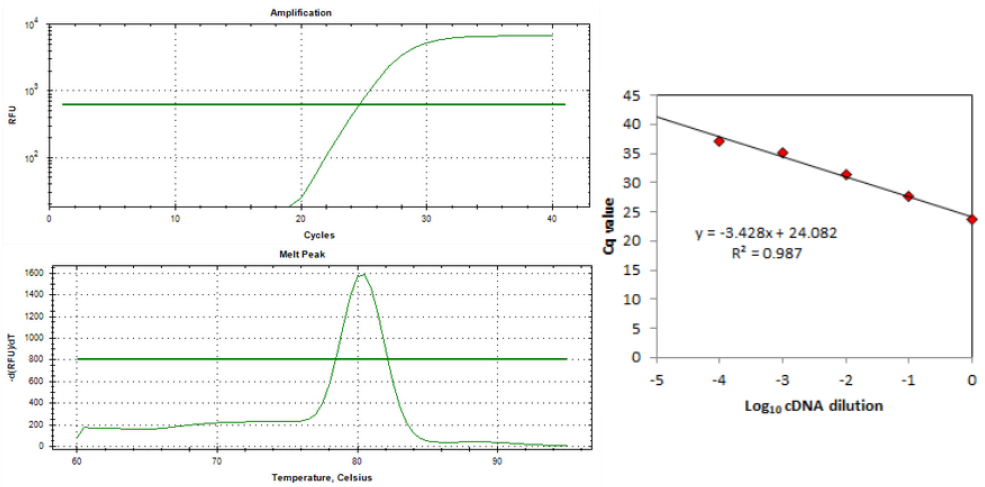

Fig. 4.17 Optimisation for *MeER1* primer set no. 1 at 500 nm. Amplification plots (log scale, in Relative Fluorescence Units), melt temperature peak plot and standard curve plot (10X dilutions) with R^2 values displayed

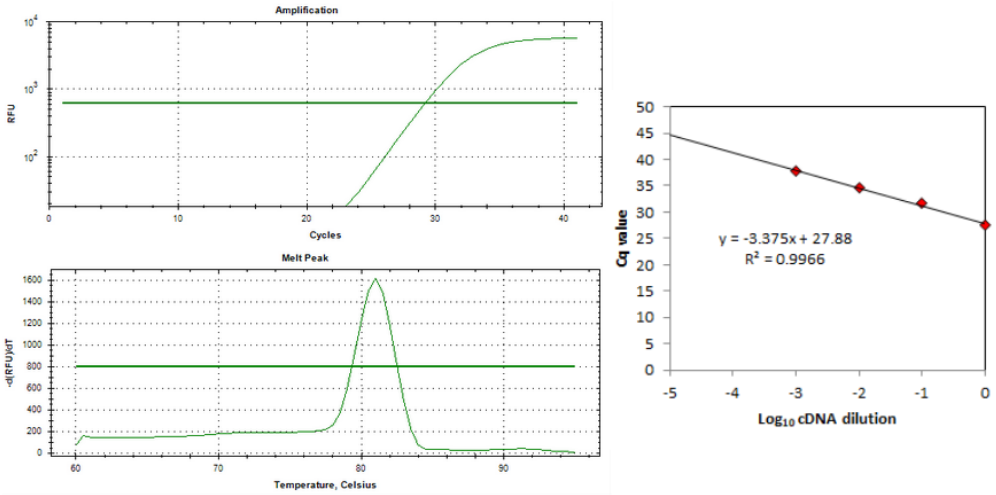

Fig. 4.18 Optimisation for *MeER2* primer set no. 1 at 300 nm. Amplification plots (log scale, in Relative Fluorescence Units), melt temperature peak plot and standard curve plot (10X dilutions) with R^2 values displayed

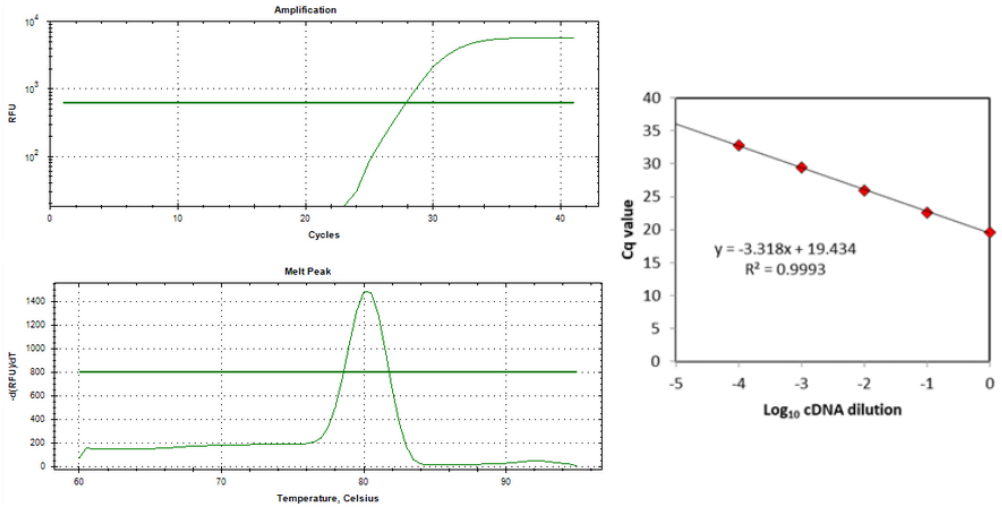

Fig. 4.19 Optimisation for *EF1* primer set no. 1 at 300 nm. Amplification plots (log scale, in Relative Fluorescence Units), melt temperature peak plot and standard curve plot (10X dilutions) with R^2 values displayed

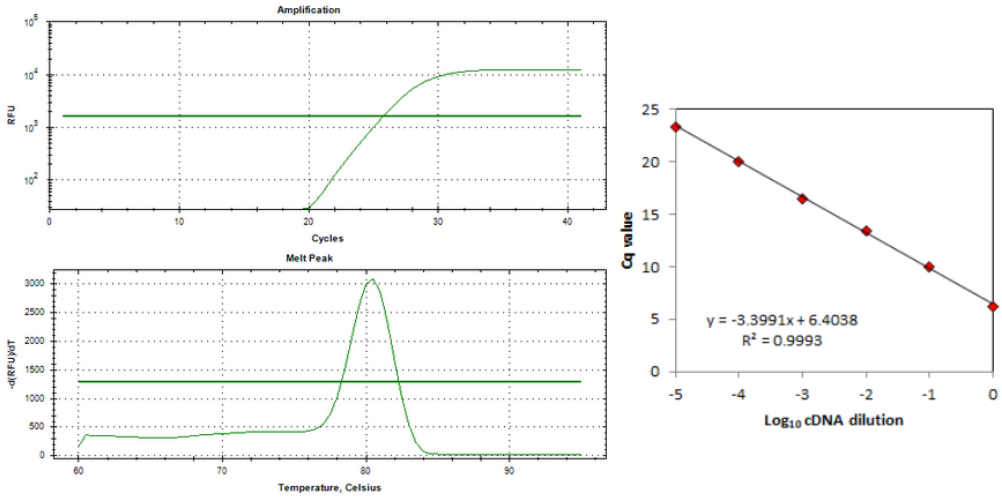

Fig. 4.20 Optimisation for *Me18S* primer set no. 1 at 300 nm. Amplification plots (log scale, in Relative Fluorescence Units), melt temperature peak plot and standard curve plot (10X dilutions) with R^2 values displayed

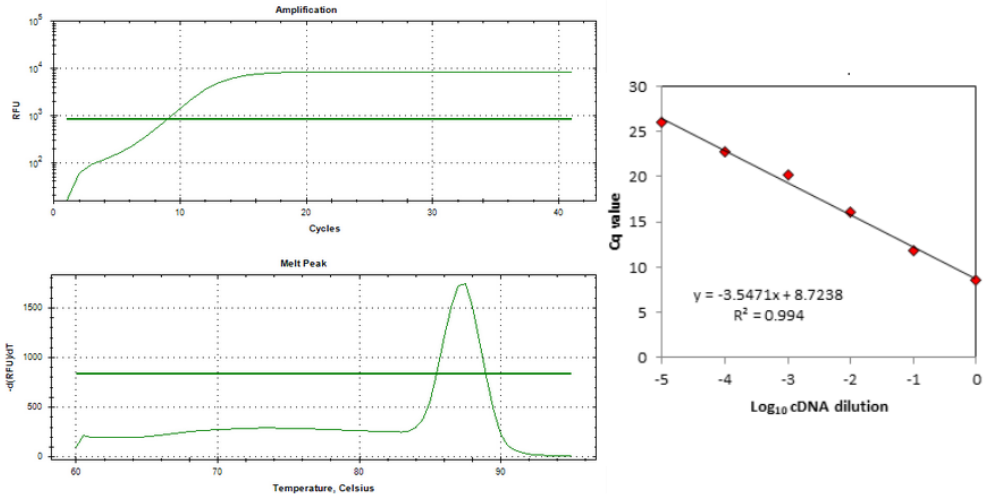

Fig. 4.21 Optimisation for *Me28S* primer set no. 1 at 300 nm. Amplification plots (log scale, in Relative Fluorescence Units), melt temperature peak plot and standard curve plot (10X dilutions) with R^2 values displayed

Final primer sequences for qPCR were: *elongation factor-1 alpha (EF1α,* GenBank accession no. **AF063420**), *18SrRNA (Me18S,* **L33448**) and *28SrRNA (Me28S,* **Z29550**) from Ciocan et al. (2011); s*uperoxide dismutase (sod*, **AJ581746**), *heat shock protein 70 (hsp70*, **AF172607**) and *estrogen receptor 1 (MeER1*, **AB257132**) from Mincarelli et al. (2021); *carbonic anhydrase 2 (CA2*, **LK934681.1**) from Balbi et al. (2016) and *estrogen receptor 2 (MeER2,* **AB257133**) from Puinean et al. (2006). Additionally, new primers were designed using Primer3 (http://primer3.ut.ee/) from the published sequence for *catalase (cat,* **AY580271**). Only primer efficiencies between 90 and 110% were accepted, in accordance with the MIQE guidelines (Bustin et al., 2009). For each chosen set, primers specificity was additionally confirmed by identification using BLAST searches (blastn) to compare the gene sequences against the NCBI nucleotide collection (*nr/nt*) database optimised for highly similar sequences (*megablast*). Primer details are provided in **Table 4.2** for the optimisation steps and **Table 4.3** and **Fig. 4.13 - 4.22** for the final chosen sets.

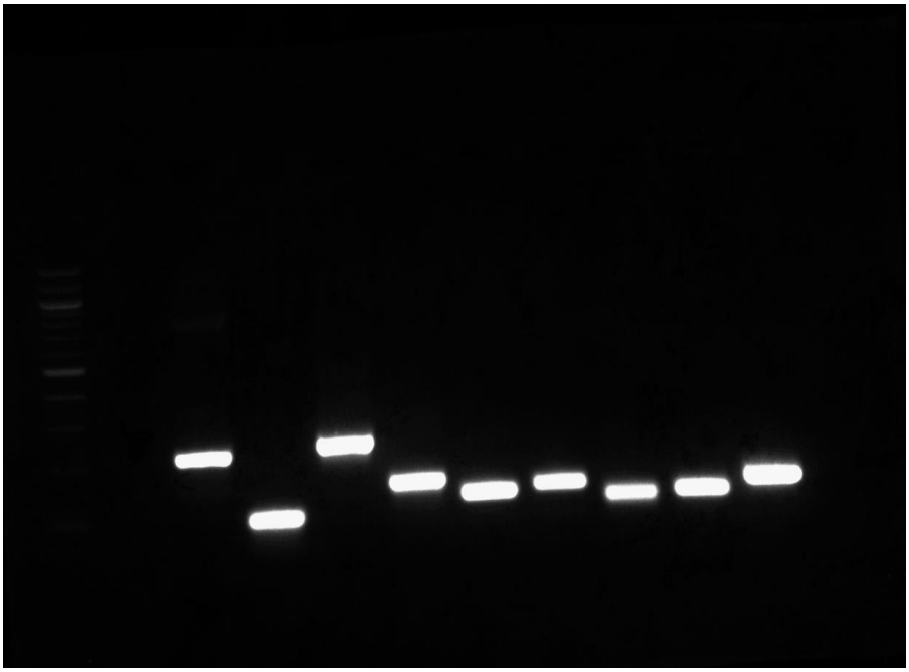

Fig. 4.22 Agarose gel 2% (2%, GelRed, run at 80V) after a qPCR run, showing the final sets chosen. From left to right: 100 bp NeB DNA ladder, *sod* (208 bp), *MeER1* (94 bp), *MeER2* (232 bp), *Me28S* (143 bp), *Me18S* (116 bp), *cat* (126 bp), *CA2* (102 bp), *EF1α* (105 bp), *hsp70* (127 bp)

EF1α and *Me28S* genes were furthermore chosen for normalisation of the final dataset, being considered the most stable combination by RefFinder (https://www.heartcure.com.au/reffinder/) software and Kruskal-Wallis test (Rstudio 3.6.2) over 25% of the total samples (n = 30). Kruskal-Wallis test revealed no significant effects among treatments for the three reference genes (*Me18S* KW-H =2.19, p = 0.82; *Me28S* KW-H = 3.05, p = 0.69; *EF1α* KW-H = 7.70, p = 0.17) and the combination of *EF1α* and *Me28S* genes was the recommended most stable one by RefFinder software. Consequently, the final dataset was normalised using the $2^{-\Delta Ct}$ and $2^{-\Delta\Delta Ct}$ methods (Schmittgen and Livak, 2008). Calculation details for $2^{-\Delta Ct}$ and $2^{-\Delta\Delta Ct}$ methods are provided in **Chapter 2.8:** Primer optimisation via PCR and qPCR amplifications. Final primer concentrations are given in **Table 4.3**. Sample dilutions were used in the final reactions as follows: *cat* and *CA2* (1:10), *hsp70* (1:100), *EF1α* (1:1000) and *Me18S* (1:10000). Thermal cycling was as follows: 95°C for 2 min, 40 cycles of 95°C for 5 sec, 60°C for 30 sec and 72° C for 1 min. Template-negative reactions were included alongside samples. Primer specificity and absence of secondary product formations were demonstrated by the melt peaks at the conclusion of the reactions. Eventually, qPCR duplicate reactions were performed for 8 female and 8 male cDNA samples for each

treatment using Hard-Shell® Low-Profile Thin-Wall 96-Well Skirted PCR plates and Microseal® 'B' adhesive seals (BioRad, Watford, UK) for standardising fluorescence reflection across the samples.

Table 4.3 Final primers used for qPCR amplification of reference genes and genes of interest

Gene name	GenBank accession no.	Primer	Sequence (5'-3')	Amplicon length (Bp)	Amplif. efficiency %	R^2	Final conc. (nM)
sod	**AJ581746**	For Rev	TCTCGCAGTTTACGGTCACT GTGGAAACCGTGTTCTCCTG	208	92.3	0.999	200
cat	**AY580271**	For Rev	ACTTCGACCAGAGACAACCC GCCTGTCCATCCTTGTTGAC	126	102.8	0.991	200
CA2	**LK934681.1**	For Rev	ACCAGATGGTCTTGCAGTTT TCATCTCTGACTGCTGCTAATG	102	90.2	0.999	200
hsp70	**AF172607**	For Rev	GGGTGGTGAAGACTTTGACA TGCCCTTTCACAAGCAGTTC	127	98.2	0.997	500
Me ER1	**AB257132**	For Rev	CCAGATCTTCAGGGTGACGA CTTGTTTGGCCCAGCTGATT	94	95.8	0.987	500
Me ER2	**AB257133**	For Rev	GGAACACAAAGAAAAGAAAGGAAG ACAAATGTGTTCTGGATGGTG	232	97.8	0.997	300
Me 28S	**Z29550**	For Rev	AGCCACTGCTTGCAGTTCTC ACTCGCGCACATGTTAGACTC	143	91.4	0.994	300
EF1	**AF063420**	For Rev	CACCACGAGTCTCTCCCAGA GCTGTCACCACAGACCATTCC	105	100.2	0.999	300
Me 18S	**L33448**	For Rev	GTGCTCTTGACTGAGTGTCTCG CGAGGTCCTATTCCATTATTCC	116	96.9	0.999	300

4.9 Materials and Methods: Statistical analysis

The histology dataset was analysed with general ordered logit with partial proportional odds model, to predict the dependent variable "Gametogenesis stage" assuming "DEHP", "pH" and "Sex" as independent variables, after verifying the rejection of the proportional odds assumption (test of Parallel Lines, *ordinal* package, Christensen, 2019). Model uncertainty was assessed by comparing ΔAICc values and Akaike weights. Model selection was carried out in RStudio with the *AICcmodavg* package (Mazerolle, 2020) in R 4.0.3 (CRAN). The model was estimated using the *vglm* function (*VGAM* package, Yee et al., 2015), calculating the *p* error probability by comparing the z-value against the standard normal distribution.

Permutation multivariate analysis of variance (PERMANOVA, Anderson, 2014) with Bray-Curtis distance and 9999 permutations was used in Rstudio (*vegan* package, Oksanen et al., 2013) to test the effects of the exposure conditions on the $2^{-\Delta\Delta Ct}$ values of the stress-related mRNA expression (*sod*, *cat* and *hsp70*), biomineralization and homeostasis (*CA2*) and estrogen receptor-like mRNA expression (*MeER1* and *MeER2*) introducing "Sex" (males or females) and "Stages" (developing, mature, spawning) to underline sex-driven differences between the treatments. Pairwise multilevel comparison with Benjamini & Hochberg *p*-adjustment was used to compare different groups. Statistical significance was set to $p < 0.05$. All graphs were created using MATLAB R2021a. A focus on the $2^{-\Delta\Delta Ct}$ values analysed for each sex separately is available in the **Supplementary Appendix to Chapter 4 (S4.1** and **S4.4)**.

Regarding the effect of the exposure treatments on the mRNA expressions of each gene, the non-parametric Scheirer-Ray-Hare (*rcompanion* package, Mangiafico, 2017) test was additionally used on the $2^{-\Delta Ct}$ values, after verifying non-normal distribution (Shapiro-Wilk test) and homogeneity of variances (Levene's test). Dunn's multiple comparison test with Benjamini & Hochberg *p*-adjustment was used for comparisons between groups (Benjamini and Hochberg, 1995). Possible outliers were identified by Grubb's test (Grubbs, 1969) and outlier values beyond the significance level of $\alpha = 0.05$ were rejected (Burns et al., 2005). A focus on the $2^{-\Delta Ct}$ values in each sex analysed for each gene separately is available in the **Supplementary Appendix to Chapter 4 (S4.2 – S4.4)**.

4.10 Results and Discussion: Histology results to determine sex and gametogenesis stages

The most parsimonious model (using only "Sex" as predictor variable) showed a predictably significant difference between males and females in the transition from developing to the more advanced states (mature and spawning stages, $p = 0.01$), with male SMI being overall higher than that of females (**Fig. 4.23**, **Table 4.4** and **4.5**). In line with winter observations, males and females were found to be in later stages of the gametogenesis cycle, with the majority of females late developing or mature and the majority of males ripening or spawning. Overall, there was *ca.* a difference of one point between sexual maturity indices, in line with previous late-winter observations in North England and Scotland (Dias et al., 2009b; Seed, 1969). Such an asynchrony between sexes

in ripeness proportions was already shown in *M. barbatus* (Mladineo et al., 2007), as well as different timing of spawning events for *M. galloprovincialis*, which nonetheless should not preclude successful fertilisation (Azpeitia et al., 2017; Seed, 1969).

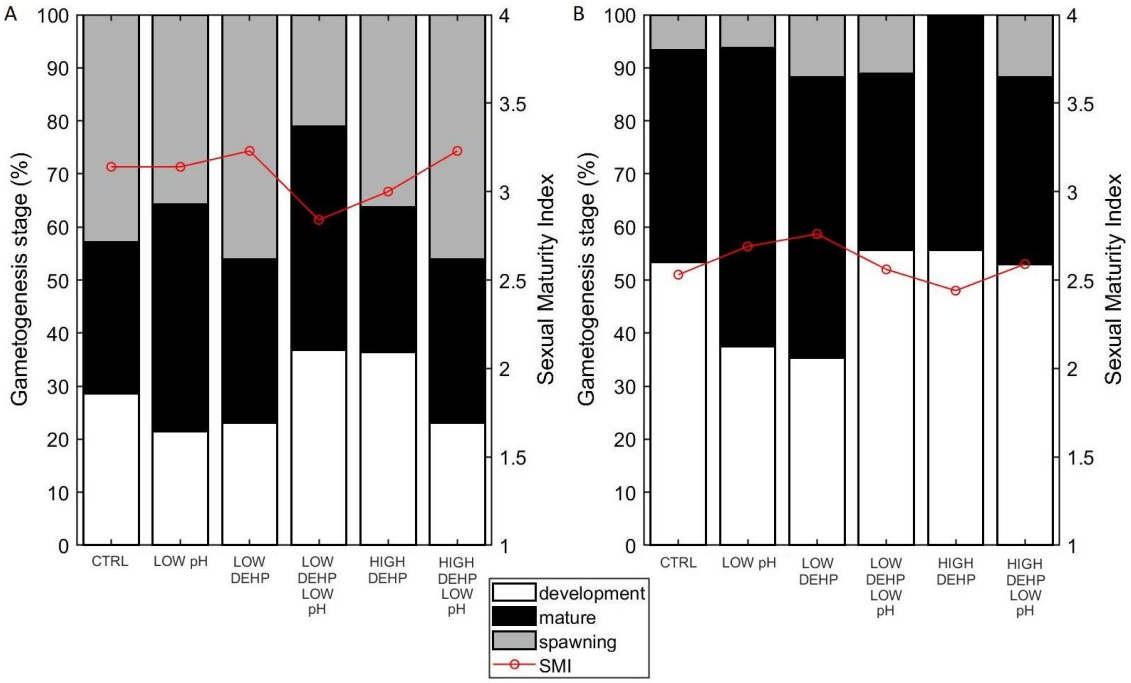

Fig. 4.23 Effects of pH and DEHP on gametogenesis stages. Percentage of each stage and sexual maturity index (SMI) of males (A, left) and females (B, right) in CTRL (n = 14 (A), 15 (B)), LOW pH (n = 14 (A), 16 (B)), LOW DEHP (n = 13 (A), 17 (B)), LOW DEHP LOW pH (n = 19 (A), 9 (B)), HIGH DEHP (n = 18 (A), 11 (B)) and HIGH DEHP LOW pH (n = 17 (A), 13 (B))

The effect of the predictors "pH" and "DEHP" was also tested, confirming no significant effect for either of them ($p > 0.05$). By itself, DEHP was observed not to induce any modification in the gametogenesis cycle, as we have previously found in blue mussels from Filey, North Yorkshire (Mincarelli et al., 2021). Similarly, no alterations of the gametogenesis cycle seemed to be present after seven days of exposure to low pH in either sex. This could mean that the maturation induction might be more responsive to alkaline pH, as shown for sea snails' oocytes (Aquino De Souza et al., 2009; Gould et al., 2001). On the other hand, mussels inhabit naturally pH-variable coastal environments and could be tolerant to local pH fluctuations, possibly resulting in no immediate repercussions for the reproductive cycle. However, according to other spawning-induction experiments (Xu et al., 2016; Zhao et al., 2019), exposure to 7.7 pH for 40 days decreased the percentage of bivalves *M. senhousia* and *R. philippinarum* spawning gonads, suggesting that a higher

susceptibility to prolonged acidified conditions in the final gametogenesis stages is possible.

Table 4.4 Model classification, number of estimated parameters (K) for each model, Akaike Information Criterion (AICc), delta AIC (ΔAIC), Akaike weights (AICcWT), cumulative Akaike weights (CumWT), log-likelihood of each model (LL) for the three independent variables (+) pH (pH), DEHP concentration (DEHP) and sex (SEX) and their interactions (*) on gametogenesis stages

model	K	AICc	Δ AIC	AICcWT	Cum WT	LL
SEX	4	358.08	0.00	0.82	0.82	-174.92
SEX+pH	6	361.75	3.66	0.13	0.95	-174.62
SEX*pH	8	364.84	6.76	0.028	0.98	-173.98
SEX+DEHP	8	365.79	7.72	0.017	1.00	-174.46
SEX+DEHP+pH	10	369.67	11.60	0.0025	1.00	-174.17

Table 4.5 Results of general ordered logit with partial proportional odds for the best model of treatments (SEX). Estimated value, standard error, *z*-value and *p* for the independent variables "Sex" (SEX, males and females), in the transition from developing to the more advanced stages (mature and spawning)

Variable	Estimate	Std. Error	z value	*p* value
SEX	0.80	0.32	2.49	0.013

4.11 Results and Discussion: PCR species identification

Molecular species identification confirmed that the sampled population from the suspended ropes farm of Cromarty Mussels, Ltd. in Cromarty Firth, Scotland, U.K. (57.40.741 N 4.06.062 W) consisted of *M. edulis* (amplified segments at 180 bp) and neither hybrids with *M. galloprovincialis* (amplified segments at 126 bp) nor other *Mytilus* species were present (**Fig. 4.24**).

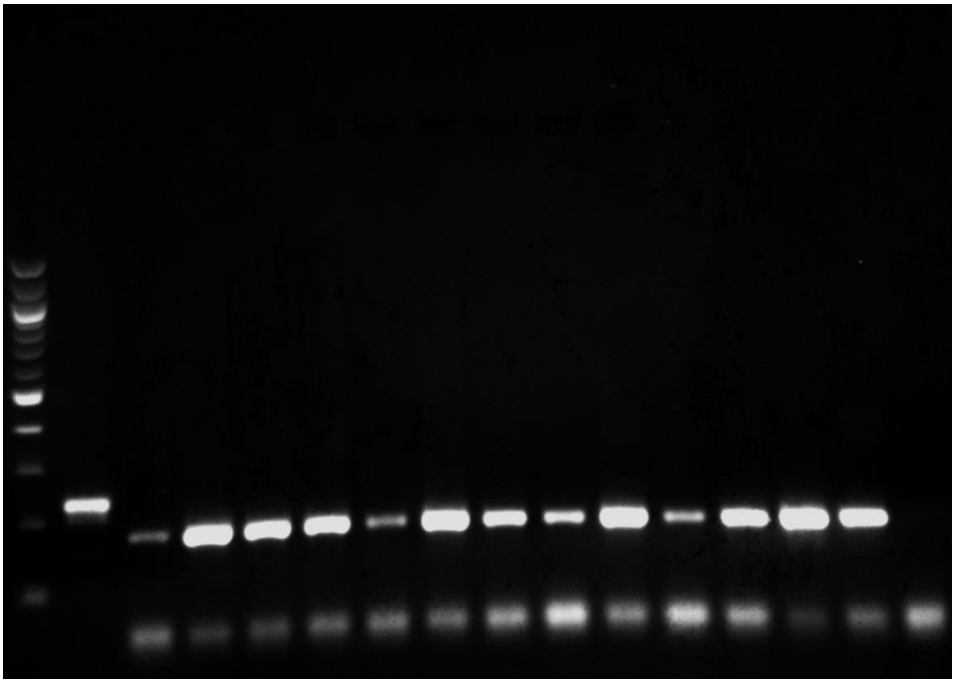

Fig. 4.24 Example of an agarose gel run (2%, GelRed™, run at 80V) for PCR species identification showing from left to right: NeB DNA ladder, 100 bp; 235 bp positive control; 180 bp fingerprints of the *mfp-1* region (*M. edulis*); negative control (water)

4.12 Results and Discussion: Influence of sex and gametogenesis status on the stress-related response

When using pH, DEHP, sex (SEX), and gametogenesis stage (STAGE) as predictors for stress-related gene expression in PERMANOVA analysis, we observed significant differences between sexes (*p* SEX = 0.001, F = 6.97, **Fig. 4.25, Fig. 4.26** and **Table 4.6**) and an effect of DEHP exposure in interaction with gametogenesis stage (*p* DEHP*STAGE = 0.005, F = 2.79, **Fig. 4.25** and **Fig. 4.26**). Overall, stress-related gene expression was higher in females than in males (as already noticed in **Chapter 2**). In males, the response was higher in mature gonads than in developing ones exposed to the high DEHP treatments. In females, an opposite trend was observed in the groups co-exposed to the two stressors, with a downregulation in the LOW DEHP LOW pH group and an upregulation in the HIGH DEHP LOW pH treatment following the progression of gonadal maturation. Ji et al. (2016) noted that male *M. galloprovincialis* displayed a higher concentration of proteins associated with defence mechanisms and energy metabolism, possibly indicating an enhanced ability of males to react to stress with respect to females. In our study, females were equipped with the ability for higher expression of stress-related genes. Similar to our findings, dissimilar levels between sexes

of stress-related heat shock proteins were previously noticed in crustaceans *Pachygrapsus marmoratus* and *Daphnia magna* with higher levels in females (Madeira et al. 2012; Mikulski et al. 2011), reinforcing the belief of a different adaptive control of the HSP system in females that could possibly allow them to be more resilient to stressed conditions than males (Gismondi et al. 2012). Additionally, Yu et al. (2021) observed that the expression of HSP90 isoforms was significantly higher in gonads of the scallop *Chlamys farreri* compared to non-reproductive tissues, suggesting an involvement of these proteins in the gametogenesis process. Moreover, levels and activities of oxidative stress biomarkers are known to vary during the annual reproductive cycle of bivalves (Blanco-Rayón et al., 2020; Jarque et al., 2014; Wilhelm Filho et al., 2001). Therefore, the gametogenesis state could have contributed to the basal antioxidant levels and their reaction to contaminants, as reported in González-Fernández and colleagues (2016), where activities of CAT and glutathione peroxidase (GPx) were noticed to be affected by the chemical fluoranthene only during the gonadal resting period. It was also recently published that the DNA methylation (also involved in the gene regulation of several biological processes) in the gonads of scallops *Patinopecten yessoensis* fluctuates during the gametogenesis cycle and peaks during the mature stage for females and developing for males (Li et al., 2019b).

A slight but non-significant trend was observed for the combination of pH, DEHP and stage (*p* pH*DEHP*STAGE = 0.09, F = 1.76, **Fig. 4.25** and **Fig. 4.26**) and DEHP, sex and stage (*p* DEHP*SEX*STAGE = 0.09, F = 1.82, **Fig. 4.25** and **Fig. 4.26**). Other studies before ours investigated the altered effect on marine invertebrates of high-CO_2 exposure conditions in combination with xenobiotics such as heavy metals (Cao et al., 2019; Han et al., 2014; Ivanina et al., 2013) or pharmaceuticals (Freitas et al., 2016; Munari et al., 2019) at different exposure durations. Our findings seem to contribute to the hypothesis that when environmentally relevant stressors are used in combination, a different magnitude of responses is noticed on some of the biomarkers analysed.

The mild results in the stress response to the low pH exposure seem to be in line with the hypothesis that organisms from habitats characterised by fluctuating conditions could be less sensitive and more tolerant to stressors. In detail, Cromarty Firth is fed at the western end by the River Conon which collects rain and snowmelt from the mountains in Sutherland and mussels harvested there could be more tolerant to the alteration of parameters such as water pH, temperature or salinity. Additionally, areas influenced by river contribution or freshwater inputs can be characterised by changes in the biological

activities also due to organic matter and nutrient supply (Cai et al. 2011; Pérez et al. 2016; Vargas et al. 2016) and mussels are also reported to be able to cope with decreased surface water pH if the food supply is sufficient (Thomsen et al., 2013; Thomsen and Melzner, 2010). It is already known that the magnitude of responses to environmental changes varies accordingly to life history (Parisi et al., 2021) and animals are more sensitive to small changes if they are adapted to a limited range of environmental variations (Kleypas, 2019; Sokolova et al., 2011). In support of this theory, considering other invertebrates, early stages of *Strongylocentrotus purpuratus* purple sea urchins from naturally low and variable pH habitats showed adaptive calcification strategies and the absence of a generalised stress response when exposed to high pCO_2 (Evans et al., 2013). Similarly, *Saccostrea glomerata* oysters farmed in estuaries characterised by different pH regimes (pH 7.5 – 8.2) showed resilience to ocean acidification conditions by altering the biomineralization pathways (Fitzer et al., 2019). In laboratory conditions, the pre-exposure of *Panopea generosa* clams to moderate (~3000 μatm) or severe (~5000 μatm) pCO_2 conditions during the post-larval period resulted in the enhancement of gene ability to adapt and cope with subsequent hypercapnic stress (Gurr et al., 2022).

Regan et al., (2021) recently found that the high tolerance of bivalves to external stressors lays in their evolutionary history, which is shaped mostly by their expansion into niches exposed to environmental stressors and specific pathogens. In fact, being sessile and filter feeders mean for bivalves a quick adaptation to stressors (such as air exposure, temperature, pH, salinity variations) and robust tolerance to water chemicals and pathogens (Burge et al. 2016). Climate history is known to also affect genome variability and population structure, while the genetic expansion could improve the plasticity of bivalve phenotypes to changing habitats (Li et al., 2021a). However, other alterations from ocean acidification in the medium-long term on vital responses of marine molluscs such as the immune system (Beesley et al., 2008; Bibby et al., 2008), calcification (Ries et al., 2009; Rodolfo-Metalpa et al., 2011) and other metabolic processes such as respiration or feeding (Fernández-Reiriz et al., 2011; Navarro et al., 2013) cannot be ruled out, as the reaction to stress is an integrated response involving molecular, cellular and physiological systems within the organisms (Sokolova et al., 2011). A focus on the stress response in each sex and each gene analysed separately is available in the **Supplementary Appendix to Chapter 4 (S4.1** and **S4.2)**.

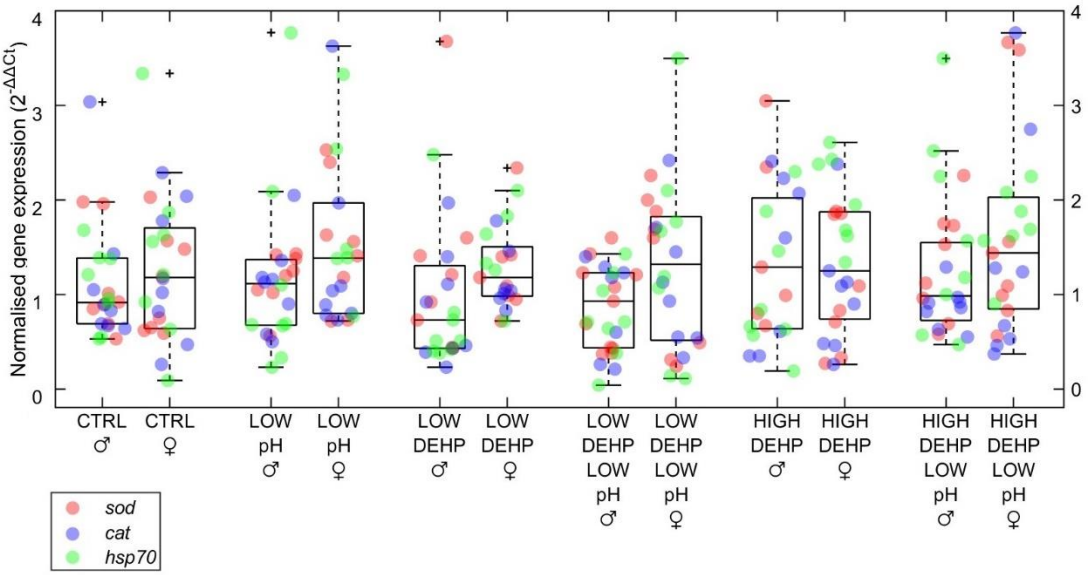

Fig. 4.25 Boxplots showing stress-related (*sod, cat, hsp70)* gene expression in males and females, n = 6 to 8. Excluded outliers are not shown, while the furthest accepted values are identified by black crosses. Different gene expressions are displayed in red (*sod*), blue (*cat*) and green (*hsp70*). Abbreviations are control (CTRL), low pH (LOW pH), low DEHP concentration (LOW DEHP), low DEHP at low pH (LOW DEHP LOW pH), high DEHP concentration (HIGH DEHP) and high DEHP at low pH (HIGH DEHP LOW pH). Significant factors in PERMANOVA are SEX $p < 0.01$, DEHP*STAGE $p < 0.01$, pH*DEHP*STAGE $p = 0.09$ and DEHP*SEX*STAGE $p = 0.09$

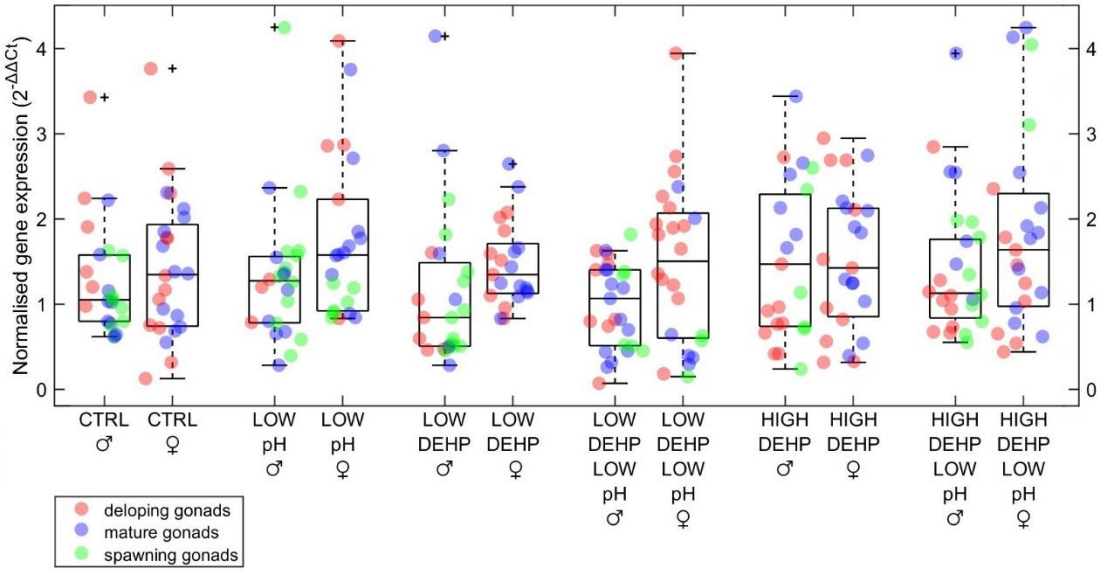

Fig. 4.26 Boxplots showing stress-related (*sod, cat, hsp70)* gene expression in males and females, n = 6 to 8 considering sex and gametogenesis stage (developing. mature, spawning) of the gonads. Excluded outliers are not shown, while the furthest accepted values are identified by black crosses. Different gene expressions are displayed in in red (developing gonads), blue (mature gonads) and green (spawning gonads). Abbreviations are control (CTRL), low pH (LOW pH), low DEHP concentration (LOW DEHP), low DEHP at low pH (LOW DEHP LOW pH), high DEHP concentration (HIGH DEHP) and high DEHP at low pH (HIGH DEHP LOW pH). Significant factors in PERMANOVA are SEX $p < 0.01$, DEHP*STAGE $p < 0.01$, pH*DEHP*STAGE $p = 0.09$ and DEHP*SEX*STAGE $p = 0.09$

Table 4.6 Pairwise multilevel comparisons of the stress response (*sod*, *cat*, *hsp70*) between males and females in the same treatments

Treatment males	Treatment females	*p*
CTRL	CTRL	0.77
LOW pH	LOW pH	0.12
LOW DEHP	*LOW DEHP*	*0.05*
LOW DEHP LOW pH	LOW DEHP LOW pH	0.37
HIGH DEHP	HIGH DEHP	0.09
HIGH DEHP LOW pH	HIGH DEHP LOW pH	0.29

4.13 Results and Discussion: Influence of sex and gametogenesis status on *CA2* gene expression

When adding sex and gametogenesis status as predictors of the stress-related response alongside pH and DEHP, we found a significant sex-driven difference in basal expression for *CA2*, independent of treatments, with a higher expression level of *CA2* in males with respect to females (p SEX < 0.001 **Fig. 4.27** and **Fig. 4.28, Table 4.7**) and possibly associated with metabolic profiles, hormonal state, or fitness strategies (Ji et al., 2013; Mikulski et al., 2011; Wong et al., 2014). The interaction term of sex and gametogenesis status also resulted significant (p SEX*STAGE = 0.02 **Fig. 4.27** and **Fig. 4.28**). With the exception of the LOW DEHP LOW pH treatment, males and females in the groups exposed to 7.7 pH (LOW pH and HIGH DEHP LOW pH) statistically differ in their *CA2* expression (**Table 4.7**). Interestingly, in Wang et al. (2017), expression of the *CAII-1* gene in *C. gigas* exposed to low pH was downregulated only in male gonads, in contrast with a significant upregulation in other non-reproductive tissue samples. Despite the fact that *CA2* in our experiment was upregulated in male gonads, not downregulated, together these findings suggest again a tissue-specific regulation of this metalloenzyme and a potential link to the reproductive system status which could explain the differences we observed between sexes.

Expression of *CA2* was also slightly modulated by low pH (p pH = 0.06), with a general downregulation of the enzyme in both sexes in the 7.7 pH treated groups. This contrasted with Wäge et al., (2016), where a short exposure to low pH induced an upregulation of *CA* in polychaete worms *Platynereis dumerilii*. Carbonic anhydrases (CAs) are known to control the intra- and extracellular pH homeostasis, catalysing the reversible carbonic hydration from CO_2 in HCO_3^- (Richier et al., 2011). Their expression could be influenced by the surrounding environment, such as water pH values (Li et al., 2016) or physical conditions such as tides (Connor and Gracey, 2011). For example, organisms from hydrothermal vents are equipped with high CA activities with respect to species inhabiting surface zones (Kleypas, 2019). In agreement with our results, a pH drop is known to induce down-regulation of this enzyme and loss of shell structural integrity in several calcifying species including molluscs (Fitzer et al, 2014; Zebral et al., 2019). This might be caused by a compensatory strategy in response to the alteration of the acid-base balance in the body fluid from hypercapnic conditions. Ventura et al., (2016) suggested a shift in the main carbon source from an HCO_3^- to a CO_2 -based use of the DIC to explain

the reduction in CA activity of the non-calcifying photosynthetic sea anemones *Anemonia viridis* short-term exposed to high pCO_2. Downregulation of CA in clam *Panopea globosa* larvae was explained as a feedback response to its decreased activity at low pH (López-Landavery et al., 2021), probably caused by enzyme denaturation or lowered efficiency (Sun et al., 2016). Interestingly, Beniash and colleagues (2010), found a marginal change in expression of *CA* in *C. virginica* oysters (p = 0.06 - 0.07) exposed to hypercapnic conditions, with an upregulated trend in mantle and the opposite tendency in gills, proposing a CA tissue-specific regulation.

DEHP chemical exposure did not induce consequences on *CA2*, as opposed to other compounds such as metalloid elements in molluscs and crustaceans (Lionetto et al., 2006; Skaggs and Henry, 2002). This could be related to the metal-binding affinities of CAs and to the more effective osmo-, ionoregulatory and acid-base disruption ability of certain metals with respect to other chemicals (Bianchini et al., 2005; Bianchini and Carvalho De Castilho, 1999; Lionetto et al., 1998; Skaggs and Henry, 2002), also considering that metals such as Zn are co-factors of carbonic anhydrases. However, Balbi and colleagues, (2016) found an effect on carbonic anhydrases in *M. galloprovincialis* larvae exposed for a short term (24 – 48 h post fertilisation) to the estrogenic chemical BPA (1-10 mg/L), used as an additive in polycarbonate plastic production. This could suggest a greater effect of chemicals in the vulnerable first phases of the bivalve larval development, when the biomineralization process is still at early stages and thus more sensitive. A focus on the stress response in each gene analysed separately is available in the **Supplementary Appendix to Chapter 4 (S4.3)**.

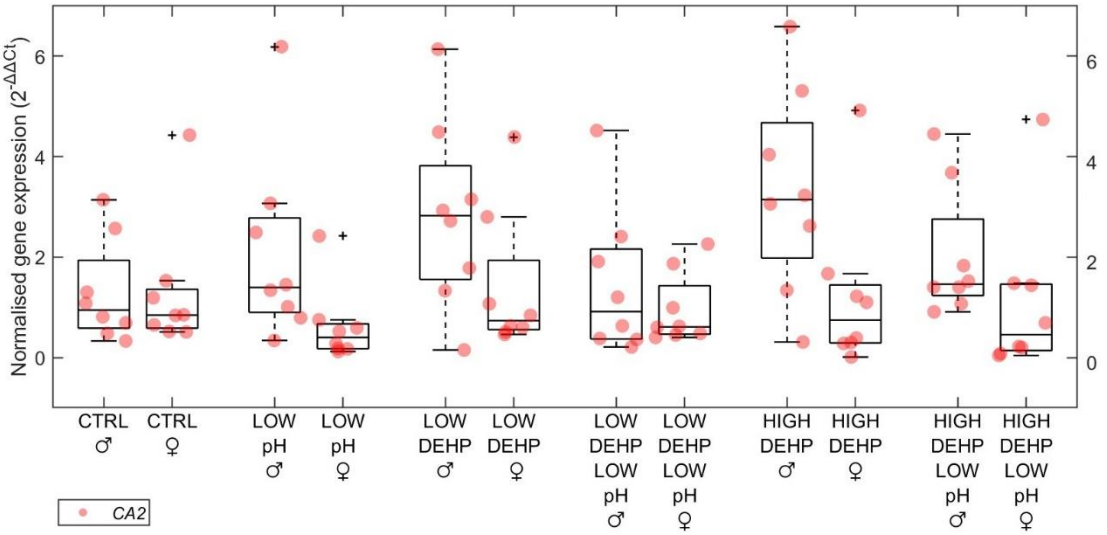

Fig. 4.27 Boxplots showing *CA2* gene expression in males and females, n = 8 The furthest accepted values are identified by black crosses. Abbreviations are control (CTRL), low pH (LOW pH), low DEHP concentration (LOW DEHP), low DEHP at low pH (LOW DEHP LOW pH), high DEHP concentration (HIGH DEHP) and high DEHP at low pH (HIGH DEHP LOW pH). PERMANOVA error probabilities are SEX $p <$ **0.001,** SEX*STAGE $p = 0.02$ and pH $p = 0.06$

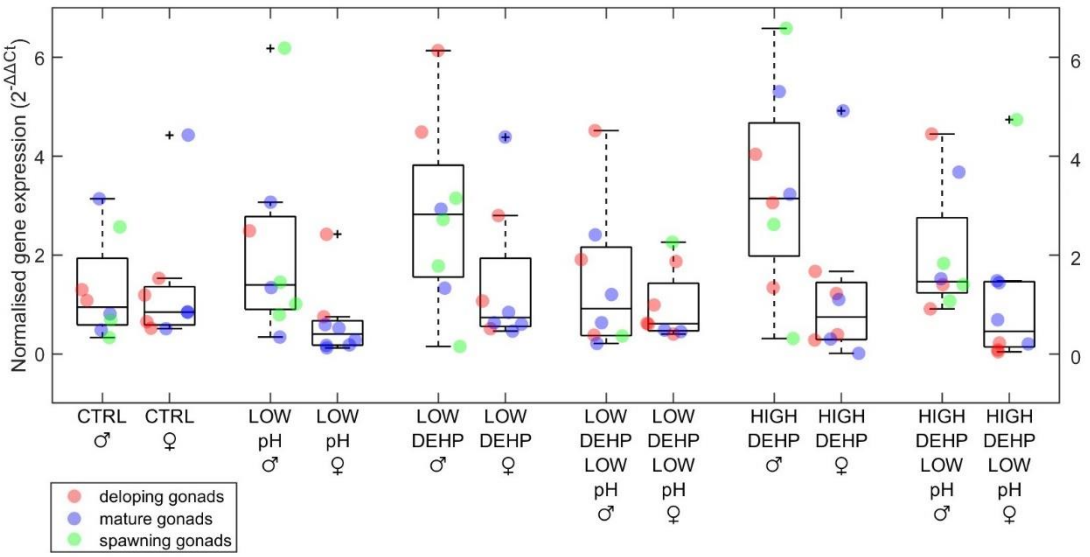

Fig. 4.28 Boxplots showing *CA2* gene expression in males and females, n = 8 considering sex and gametogenesis stage (developing. mature, spawning) of the gonads. Different gene expressions are displayed in red (developing gonads), blue (mature gonads) and green (spawning gonads). Abbreviations are control (CTRL), low pH (LOW pH), low DEHP concentration (LOW DEHP), low DEHP at low pH (LOW DEHP LOW pH), high DEHP concentration (HIGH DEHP) and high DEHP at low pH (HIGH DEHP LOW pH). PERMANOVA error probabilities are SEX $p < 0.001$ (***), SEX*STAGE $p = 0.02$ (**) and pH $p = 0.06$

Table 4.7 Pairwise multilevel comparisons of the *CA2* response between males and females in the same treatments

Treatment males	Treatment females	*p*
CTRL	CTRL	0.98
LOW pH	*LOW pH*	*0.02*
LOW DEHP	LOW DEHP	0.18
LOW DEHP LOW pH	LOW DEHP LOW pH	0.65
HIGH DEHP	*HIGH DEHP*	*0.04*
HIGH DEHP LOW pH	*HIGH DEHP LOW pH*	*0.04*

4.14 Results and Discussion: Influence of sex and gametogenesis status on the estrogen receptor-related response

Regarding reprotoxicity biomarkers, as already noted with respect to the gametogenesis status, a drop to 7.7 pH did not induce any consequences on *MeER1* and *MeER2* (**Fig. 4.29** and **Fig. 4.30, Table 4.8**). Contrasting responses of the reproductive cycle to low water pH in invertebrates was already reported, from unaffected (Byrne et al., 2010) to reduced fertilisation success (Havenhand et al., 2008) in invertebrates such as *C. gigas* and *Heliocidaris erythrogramma* sea urchin.

Interestingly, DEHP did not elicit a response on estrogen receptor-like gene expression in either sex. This contrasts with the previous findings of our team in Mincarelli et al. (2021) and in **Chapter 2**, where a one-week exposure to DEHP significantly affected the estrogen receptor-like pathway, especially in developing females' *MeER1*. Some factors which may account for these differences between the two experiments are that mussels originated from two different populations (North Yorkshire in contrast to Cromarty Firth), years (2018 and 2020) and seasons (early in contrast to late winter), and the related gonadal reproductive status. Natural variation in the estrogen receptor-like physiological conditions could be based on annual and seasonal contexts, as already noted for *M. edulis MeER2* expression (Ciocan et al., 2010b). Similarly, variable expression of estrogen receptor-like genes was found during *M. galloprovincialis* ovarian cycle (Agnese et al., 2019) and throughout larval development (Balbi et al., 2016). On the other hand, in Puinean et al., (2006), the unchanged expression of blue mussel's *MeER1* and *MeER2* after exposure to estradiol was explained by either a regulatory mechanism of estradiol transformation or the receptor independence to estrogen in molluscs. In this case, the initial hypothesis that the action of certain stressors such as low pH and DEHP additive could be more robust when organisms are in a particular stage of the gametogenesis cycle did not find confirmation in this experiment, as the PERMANOVA analysis that considered the effect of the gametogenesis showed no particular influence on the gene expression of estrogen receptor-like response. A focus on the stress response in each sex analysed separately is available in the **Supplementary Appendix to Chapter 4**.

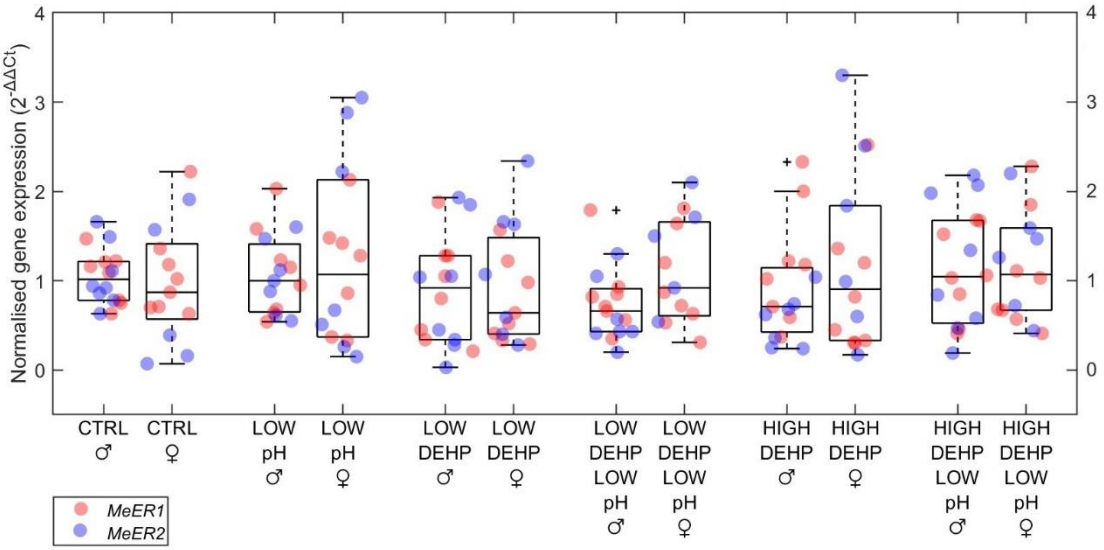

Fig. 4.29 Boxplots showing estrogen receptor- like (*MeER1*, *MeER2*) gene expression in males and females, n = 5 to 8. Excluded outliers are not shown, while the furthest accepted values are identified by black crosses. Means and standard deviations for each gametogenesis stage are displayed in red (*MeER1*) and blue (*MeER2*) and green (spawning gonads). Abbreviations are control (CTRL), low pH (LOW pH), low DEHP concentration (LOW DEHP), low DEHP at low pH (LOW DEHP LOW pH), high DEHP concentration (HIGH DEHP) and high DEHP at low pH (HIGH DEHP LOW pH). No significant PERMANOVA differences were found

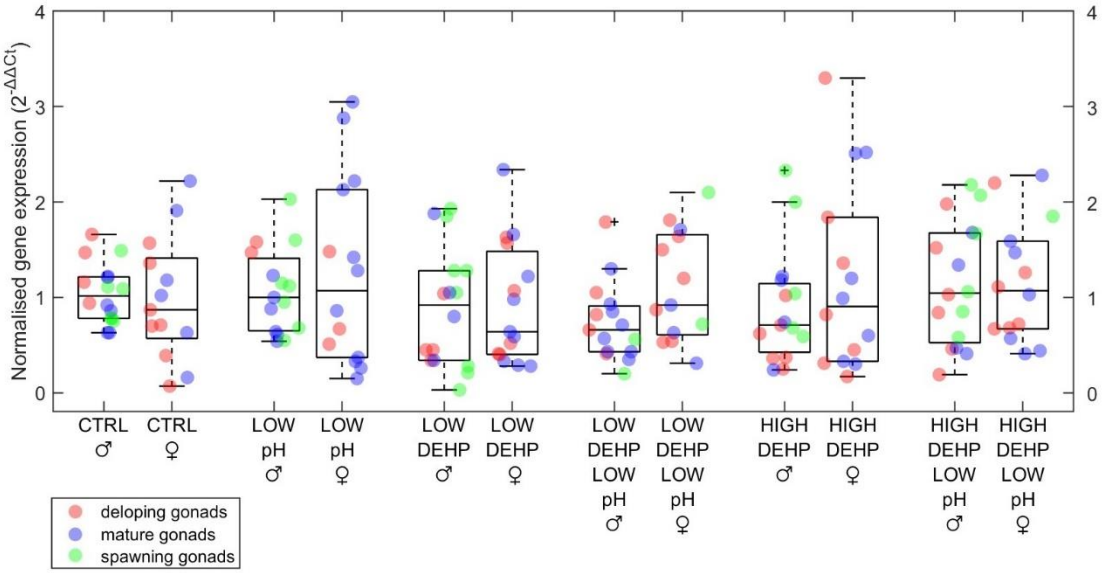

Fig. 4.30 Boxplots showing estrogen receptor- like (*MeER1*, *MeER2*) gene expression in males and females, n = 5 to 8, considering sex and the gametogenesis stage (developing. mature, spawning) of the gonads. Excluded outliers are not shown, while the furthest accepted values are identified by black crosses. Different gene expressions are displayed in red (developing gonads), blue (mature gonads) and green (spawning gonads). Abbreviations are control (CTRL), low pH (LOW pH), low DEHP concentration (LOW DEHP), low DEHP at low pH (LOW DEHP LOW pH), high DEHP concentration (HIGH DEHP) and high DEHP at low pH (HIGH DEHP LOW pH). No significant PERMANOVA differences were found

Table 4.8 Pairwise multilevel comparisons of the estrogen receptor-like response (*MeER1*, *MeER2*) between males and females in the same treatments

Treatment males	Treatment females	*p*
CTRL	CTRL	0.41
LOW pH	LOW pH	0.54
LOW DEHP	LOW DEHP	0.66
LOW DEHP LOW pH	*LOW DEHP LOW pH*	*0.05*
HIGH DEHP	HIGH DEHP	0.16
HIGH DEHP LOW pH	HIGH DEHP LOW pH	0.71

4.15 Conclusions

In conclusion, we found mainly sex- and gametogenesis- based responses to lowered pH and DEHP exposure, in terms of expression of genes involved in the antioxidant system, general stress response, biomineralization/pH homeostasis and reproduction. As shown before, sex differences were observed for genes involved in the basal cellular mechanisms, underlying the possibility of a better adaption of either sex in future climate conditions. Interestingly, the maturation state of the gonads and the gametogenesis cycle seem to influence the gene expression of various genes involved in the stress response and pH homeostasis (*sod*, *cat*, *hsp70, CA2*) but did not seem to affect the estrogen receptor-like system (*MeER1, MeER2*). However, further investigations are needed for a better understanding of this pattern of response, as our study provided a small set of observations for each gametogenesis state. Likewise, the consequences of ocean acidification in marine mussels inhabiting naturally pH-variable coastal environments and therefore tolerant to local pH fluctuations should be deeply investigated through a wider set of endpoints involved in the pH response other than CAs. Nevertheless, this experiment contributes to the understanding of histological and molecular endpoints in mussels exposed to combinations of multiple stressors, which is necessary for a scenario of plastic-polluted and climate-changing conditions.

Chapter 5

The effects of low pH and DEHP exposure on valve behaviour and metabolic rate

5.1 Introduction

This chapter aims to investigate the effect on *M. edulis* respiration and valve behaviours of lowered pH alone and in combination with two concentrations of DEHP at environmentally relevant levels. Mussels were first exposed for one week to either a control pH (pH 8.1) or low pH (pH 7.7; -0.4 units) condition. After the pH exposure, oxygen consumption and valve behaviours were tested in a series of respirometer and behavioural tests. The results for day one were then compared (control against low pH), in order to analyse the effect of the seven-day exposure to low pH alone. The day after, the same mussels were exposed to either a low (0.5 µg/L), or high dose (50 µg/L) of di-2-ethylhexyl phthalate (DEHP) and the respirometer and behavioural assays were immediately repeated. Outcomes from day two were plotted against day one results to analyse the effect of the single-dose exposure to various levels of DEHP on mussels pre-exposed to either control or low pH.

As already highlighted in **Chapter 4**, pH is known to fluctuate in coastal areas (Yu et al., 2011) and in zones like intertidal rock pools where photosynthesis and tides control the CO_2 levels and consequently the pH (Pörtner et al., 2008). It is well-known that global oceanic pH has unprecedentedly decreased over the past four decades as a consequence of taking CO_2 up from anthropogenic emissions, with a 30% increase in water acidity since the beginning of the Industrial era (IPCC, 2021). Under all most likely projected scenarios from the IPCC (SSPs, **Chapter 1.4**), surface pH is predicted to decrease by 2100. These conditions are hypothesised to a larger extent in high-latitude oceans, especially the Arctic Sea, which will also be undersaturated in calcite and aragonite by 2100 (Feely et al., 2009, **Fig. 1.4** and **Fig. 5.1**). This may also exacerbate naturally occurring pH fluctuations in coastal and near-shore habitats, to which intertidal species are adapted (Baumann and Smith 2018; Wolfe et al. 2020).

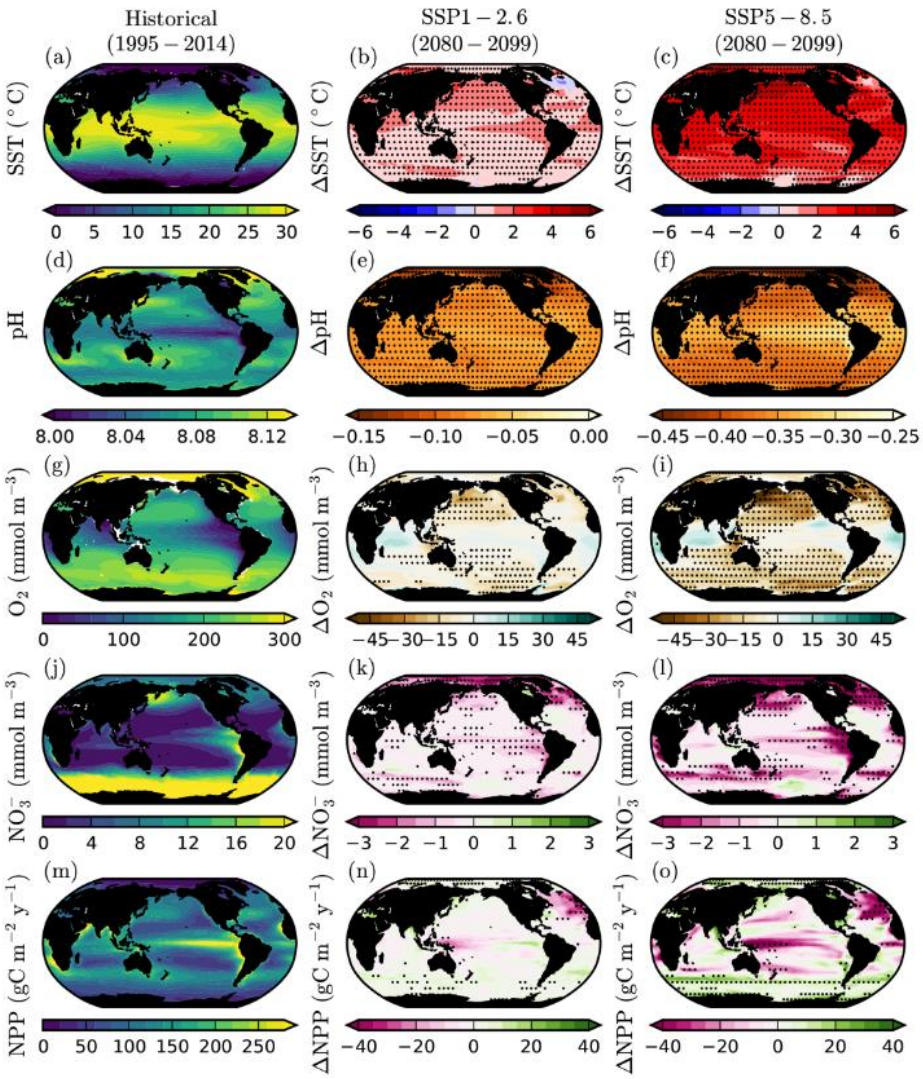

Fig. 5.1 Historical climatologies (1995 - 2014), SSP 1 - 2.6 and SSP 5 - 8.5 projections for 2080 - 2099 for **a-c)** sea surface temperature, **d-f)** surface oceanic pH, sub-surface (100-600 m), **g-i)** dissolved oxygen concentration, **j-l)** euphotic-zone (0-100 m) NO_3^- and **m-o)** depth-integrated net primary production from Kwiatkowski et al. (2020)

In plankton communities, future acidification conditions could lead to considerable consequences at the levels of pelagic ecosystems and biogeochemical cycling (Riebesell et al., 2013, 2018). For example, phytoplankton can often grow more rapidly in acidified conditions, as the carbon availability increases with CO_2 levels and this could result in optimal conditions for the growth and bloom of harmful algae such as the genus *Alexandrium* (Lian et al., 2022), increasing the toxic forms of paralytic neurotoxins associated with harmful algal blooms (HAB, Roggatz et al., 2019). Various consequences on aquaculture species are hypothesised according to different climate change scenarios

(Fuentes-Santos et al., 2021). In bivalves, some studies reported an unlikely adaptivity of mussels to future water pH conditions (Guo et al., 2021). A decrease in pH can alter immune and anti-predator responses (Bibby et al., 2008; Jahnsen-Guzmán et al., 2022), affect calcification and energy metabolism-related gene expression (Hüning et al., 2013), and impact growth performances in larvae (Gazeau et al., 2010). On the other hand, contrasting effects of low pH exposure on mussels were noticed on byssus thread properties (Dickey et al., 2018; O'Donnell et al., 2013; Zhao et al., 2017) and valve behaviours (Clements et al., 2020; Lassoued et al., 2019, 2021), probably due to local adaptation (Kong et al., 2019), environmental history (Clements et al., 2020), post-spawning status (Clements et al., 2018) or eutrophication and food availability (Jakubowska and Normant, 2015; Lassoued et al., 2019).

Increased stratification and weakened water circulation will also influence the metabolic physiology of aquatic organisms, increasing the oxygen consumption rate via the respiration process (Breitburg et al., 2018; Thyrring et al., 2015). During the respiration mechanism, aerobic organisms convert organic matter to carbon dioxide, producing the by-product CO_2 while consuming oxygen and releasing energy. Without sufficient ventilation, the accumulation of inorganic carbon derived from respiration will contribute to ocean acidification as well (Fennel and Testa, 2019; Lowe et al., 2019; Wallace et al., 2014). Conversely, pH could affect respiration rate and the associated metabolic processes in marine organisms at individual and population levels. As an example, CO_2 could limit the oxygen affinity of proteins involved in *Dosidicus gigas* squid respiration (Seibel, 2013), decreasing hypoxia tolerance in sculpins *Clinocottus analis* (Hancock and Place, 2016), and silversides *Menidia menidia* and *M. beryllina*, thus increasing their mortality rate (Miller et al., 2016). On the other hand, when exposed to hypercapnic conditions (7.6 pH) for five days, sea limpet *Patella vulgata* showed no changes in metabolism defined as O_2 uptake or feeding rate (Marchant et al., 2010).

Oxygen consumption is a common estimator for the basal metabolic rate in invertebrates (Greenshield et al., 2021; López-Landavery et al., 2021) and valve behaviour observations are as well used as a biomonitoring analysis in response to pollutant exposure (Liao et al., 2009). Due to their feeding and respiratory behaviours, mussels can pump large water volumes and thus filtrate and accumulate contaminants, toxins, bacteria and viruses, as their gills have both a respiratory and a feeding role (Gosling, 2021). As remarked by Zeng et al. (2015), pollutants found in marine environments can increase eutrophication and lead to an increase in respiration rate, as seen after the Deep Water

Horizon oil spill disaster (Bælum et al., 2012), eventually being a major driver for ocean acidification. Pollutants such as heavy metals or polyaromatic hydrocarbons are known to affect and lower the respiration rate (Halldórsson et al. 2005; Jorge et al., 2007), but sulphide, microplastics or nanoparticles were noticed to increase the respiration rate as consequence of physiological stress (Lee et al., 1996; Van Cauwenberg et al., 2015; Saggese et al., 2016). External chemical administration could also affect the avoidance behaviours and consequently increase the predation risk, as demonstrated by the reduction in burying ability of polychaete worms *Nereis diversicolor* and bivalve molluscs *Scrobicularia plana* and *Macomona liliana* exposed to copper (Bonnard et al., 2009; Roper and Hickey, 1994) and slowed valve closure in *Argopecten ventricosus* scallops or *M. galloprovincialis* exposed to heavy metals (Shen and Nugegoda, 2022; Sobrino-Figueroa and Cáceres-Martínez, 2009). Considering this, this chapter's experiment explores the consequences on behavioural and metabolic traits of blue mussels (i.e., respiration and valve movement) after a single-dose exposure to the plastic additive DEHP alone and in combination with an ocean acidification scenario, with the hypothesis that low pH will affect mussel respirations, while the valve behaviours will be responsive to the injection of either concentration of DEHP.

5.2 Materials and Methods: Experimental design

Adult blue mussels (n = 72; mean length 5.5 cm ± 0.45 cm) were collected from Cromarty Mussels, Ltd. (Cromarty Firth) in January 2021 for behavioural and physiological analysis (**Fig. 5.2**). Details about the collection site were provided in **Chapter 4.2:** Experimental design. Mussels were transported to the aquarium facilities of the University of Hull, and subsequently randomly divided into two 30-litre continuously aerated glass tanks and left to acclimate for 12 days in artificial saltwater. Mussels were not cleaned from sand or mud nor scrubbed from seaweed or barnacles, to avoid additional physical stress. Measured parameters for the control and low pH treatments are shown in **Table 5.1.** Water was partially (approx. 15-20 litre) changed every second day. The pH was constantly monitored with a pHControl system (JBL ProFlora pH Control) connected to a CO_2 cylinder for the LOW pH treatment (**Fig. 5.3**). Mussels were not fed during the experiment. Temperature and salinity were measured daily with a digital thermometer (Amarell Thermometer, Kreuzwertheim, Germany) and a digital seawater

refractometer (Hanna Instruments, Woonsocket, USA). Alkalinity was measured twice a week with a HI 84531 mini titrator (Hanna Instruments, Woonsocket, USA).

Table 5.1 Experimental treatments and measurement of temperature, pH and alkalinity values at 35 ± 1 psu salinity. All parameters are expressed as mean ± standard deviation

Name of treatment	Description	Temperature (°C)	pH (Units)	Alkalinity (mg/L)
CTRL	Control pH conditions	8.62 ± 0.28	8.86 ± 0.03	104.23 ± 6.03
LOW pH	Future pH conditions	8.68 ± 0.28	7.69 ± 0.03	121.30 ± 7.89

Fig. 5.2 Cromarty Firth, Scotland, U.K. (57.40.741 N 4.06.062 W), the collection site. Details of the suspended ropes on the water surface

Fig. 5.3 Pictures from the exposure tank - *M. edulis* blue mussels at 7.7 pH

For the respirometer and behavioural assays, the 2 exposed groups were tested on day 1 (CTRL pH and LOW pH, n = 35 - 36). The following day (day 2), the same groups were exposed to a single dose of either 0.5 µg/L or 50 µg/L of DEHP for a total yield of 4 treatments groups: CTRL pH LOW DEHP, CTRL pH HIGH DEHP, LOW pH LOW DEHP, LOW pH HIGH DEHP each with n = 17 - 18. A graphic summary of the experimental design for day 1 and 2 assays and the respective exposures is available in **Fig. 5.4**. Each mussel was tested once per day and at the same time over the two days, in order to minimise animal stress and the possible effects of circadian rhythm on valve movements (Englund and Heino, 1994; García-March et al., 2008; Ortmann and Grieshaber, 2003).

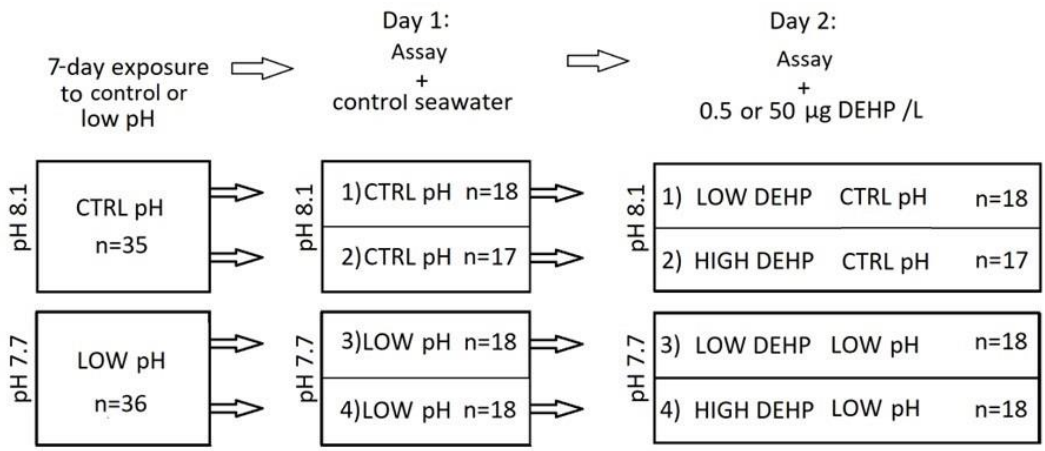

Fig. 5.4 Summary of mussel treatment groups after the 7-day exposure to either control or low pH on day 1 (CTRL pH and LOW pH, n = 35 – 36 divided into two groups for each pH-treatment) and after a single dose of either 0.5 or 50 µg/L of DEHP (LOW DEHP, HIGH DEHP, LOW DEHP LOW pH, HIGH DEHP LOW pH, n = 17 - 18) on day 2

5.3 Materials and Methods: Oxygen meter settings

Oxygen consumption was measured with a USB-powered fibre optic meter *FireStingO_2* with fibre optical oxygen sensor. The compact USB-powered fibre-optic meter *FireStingO_2* is a multi-functional oxygen meter used for oxygen measurements in water that utilises a measuring principle based on red light excitation and detection in the near-infrared using luminescent oxygen indicators (REDFLASH technology) with integrated atmospheric pressure and humidity sensors. Sensor spots carrying an optical isolation on the sensing surface were then placed in contact with the aqueous samples (**Fig. 5.5**). Every optical sensor was calibrated by selecting a 1-point in water/humid air option, where the 0% calibration value was given by the sensor code and the second point was taken from seawater saturated air (100% RH) obtained by bubbling pure oxygen into a closed 200-mL jar filled with seawater for no less than 10 minutes, as recommended by the manufacturer for precise measurement around 100% calibration.

5.4 Materials and Methods: Respirometer assay

Animal respiration is used to estimate the overall energy metabolism (Lannig et al., 2010). For this assay, closed respirometry assays were conducted under unlicensed animal ethics approval University of Hull # FEC_2021_11 as follows:

I. Mussels were individually placed into 200-mL jars and acclimated for 5 minutes.
II. After acclimation, 10 µL of either control seawater (on day 1) or DEHP (0.5 or 50 µg/L on day 2) were injected in the proximity of the gills.
III. After lid closure, the valve behaviour was recorded on video and oxygen consumption was measured with the USB-powered fiber optic meter *FireStingO_2* for a 5-minute assay.

As an estimator for the basal metabolic rate, oxygen consumption (mg/L) was recorded by the respirometer every 30 seconds to yield a total of 10 data points over the 5-minute assay for each individual. The 5-minute interval was chosen considering the filtration rate of 46 - 80 mL/min (230 - 400 mL in 5 minutes) for *M. edulis* individuals of 5.65 cm in length (Winter, 1973). The partial oxygen consumption Δmg/L for each time point *t* was calculated as follows: *oxygen concentration (mg/L) at time point t - oxygen concentration (mg/L) at time point t-1*. Before the experiment, 15 blank tests were conducted in the same 200-mL jars, in order to assess the background microbial water consumption from the experimental water tanks and a final average value of 0.067 was subtracted from the final oxygen concentration from all individuals during the respirometer tests.

Fig. 5.5 Details of the respirometer assay (before the lid closure) with the sensor spot highlighted by the red circle

5.5 Materials and Methods: Valve behavioural assay

During the same 5-minute interval of the respirometer assay, behaviours of the valves were recorded on video. Behavioural changes are usually recorded at the same time as

physiological assays, as respiration is closely related to activity and movements of the valves (Widdows, 1985). Videos were then coded and behaviours were scored blindly in order to remove possible observer bias. The following valve behaviours were assessed for the same data points as the respirometer test over the 5-minute assay (10 data points of 30 seconds each):

- Valve status: valves were either closed (**Fig. 5.6**) or open (**Fig. 5.7**).
- Valve changes: number of changes between opening and closure or *vice versa* (none, one, more than one).
- Valve openings: number of only opening events (from closed to open, measure as none, one, more than one).

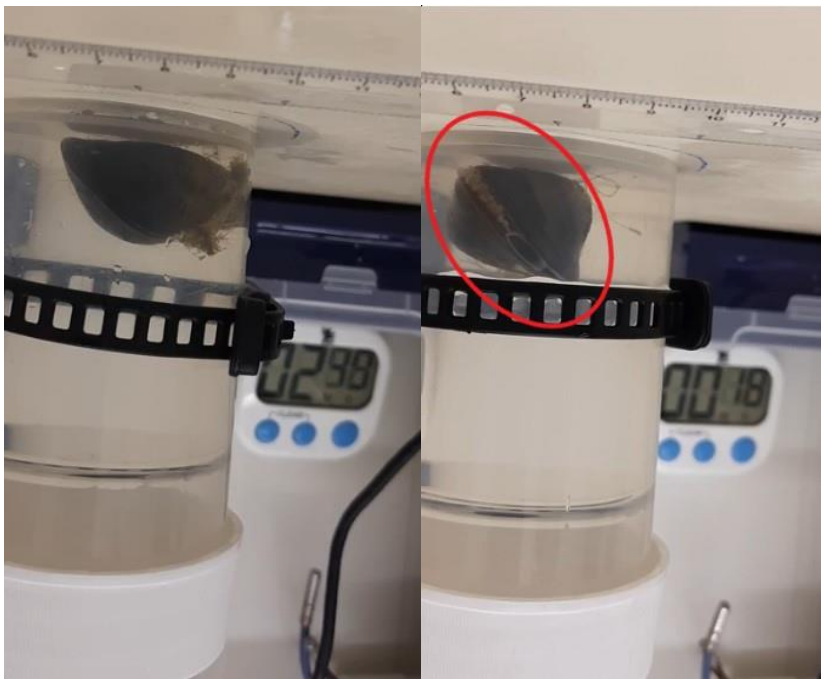

Fig. 5.6 and 5.7 Frames from the recorded videos showing the respirometer assays for mussels with closed (left) and open (right) valves (highlighted in red) and the recorded time

5.6 Materials and Methods: Statistical analysis

For the analysis of respiration and valve behaviours, the data was divided as follows (**Fig. 5.4**):

I. "Day 1" for testing the effect of
   - low pH

   against

- control pH

II. "Day 2" for testing

- low DEHP (0.5 µg/L) in combination with either 8.1 or 7.7 pH

and

- high DEHP (0.5 µg/L) in combination with either 8.1 or 7.7 pH

For the respirometry assay, no significant relationship was found between mussel length and oxygen consumption (Pearson's correlation $p > 0.05$).

For each dataset, the partial oxygen consumption measurements over the 30-second data points were analysed by ANOVA for Randomised Block Design after data normalisation (*bestNormalize* package, Peterson, 2021), to determine the impact of treatments while correcting for time points as a blocking factor. For valve behaviours, one-way PERMANOVA (Anderson, 2014) using Jaccard dissimilarity matrix and 9999 permutations (*vegan* package, Oksanen, 2018) were applied to the valve status (either "closed" or "open"), valve changes (number of changes between open and closed valves and vice versa) and valve openings (number of valve opening events) to test the effect of pH (day 1) and DEHP (day 2) exposures. All graphs were created using MATLAB R2021a.

5.7 Results and Discussion: Respirometer assay

No differences were found in the partial oxygen consumption over the ten 30-second time points between mussels at control pH against low pH for day one ($p > 0.05$, **Fig. 5.8**). On the other hand, considering the DEHP exposure on day two, the low DEHP exposure influenced the respiration of mussels at low pH ($p = 0.03$, F value = 4.94, **Fig. 5.9 C**), while high DEHP dose significantly affected mussels at control pH ($p < 0.001$, F value = 13.53, **Fig. 5.9 B**). Adding "time points" as a blocking factor resulted in a $p = 0.04$ (F value = 4.31) of the factor time on mussels at low pH and high DEHP (**Fig. 5.9 D**) on day two. It was already observed that respiration and oxyregulation capacities are affected by high temperature in molluscs such as *M. galloprovincialis* (Barbariol and Razouls, 2000), *Pecten maximus* (Artigaud et al., 2014) or *Cyclonaias* spp. (Haney et al., 2020), which eventually impacted the energetic metabolism. Decreased oceanic pH might affect respiratory performances of marine invertebrates as well, alongside other biological

consequences (Pörtner, 2008). In fact, in order to buffer the internal fluid acidosis in hypercapnic conditions, calcifying organisms are also known to use the $CaCO_3$ from the shell to increase the HCO_3^- in the haemolymph or manipulate the excretion of H^+ ions in the Na^+-H^+ exchangers and reduce the oxygen consumption rate (Byrne and Dietz, 1997; Hannan et al., 2016; Michaelidis et al., 2005; Pörtner, 2008) with in most cases long-term repercussions on growth or reproductive functions, along with metabolic suppression (Pörtner et al., 2004). Reduced shell length and mass development in *M. edulis* was noted by Thomsen and Melzner (2010) under increasing hypercapnic conditions (from control pH 8.0 to pH values of 7.7, 7.4 and 7.1), who suggested increased cellular energy demand and nitrogen loss as synergistic cause for the absence of growth. Melzner et al. (2011) hypothesised that in response to strong pCO_2 and under food limitation, the metabolic energy in *M. edulis* is reallocated to vital biological process such as the maintenance of somatic mass, at the expense of processes such as shell growth and conservation.

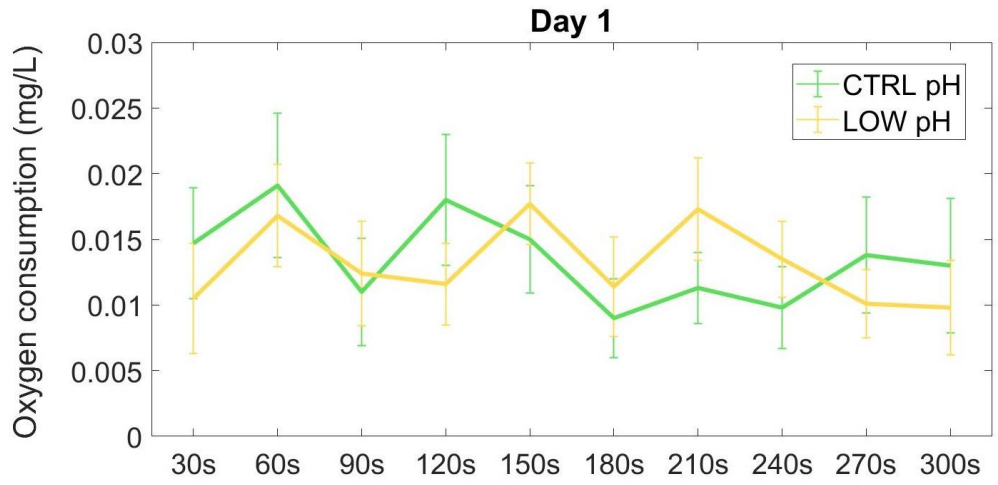

Fig. 5.8 Low pH effect on oxygen consumption throughout the 30 seconds time on day 1, n = 35 - 36. Abbreviations are pH 8.1 (CTRL pH, in green) and pH 7.7 (LOW pH, in yellow). Datapoints are expressed as mean ± standard error of the mean (SEM). No ANOVA significant effect was observed

The results from the respirometer assay seem to indicate that the low pH short-term exposure for one week did not affect *M. edulis* respiration. Conversely, decreased respiration was observed for *R. decussatus* after 87 days of exposure to –0.4 and –0.7 pH units (Fernández-Reiriz et al., 2011), suggesting that an effect of water acidification on mussel responses for a long period is possible. Saavedra et al. (2018) noticed a reduction of oxygen consumption for intertidal mussel *Perumytilus purpuratus* exposed to 750 (7.6

pH) and 1200 (7.5 pH) µatm pCO_2 levels, but not at 380 µatm (7.8 pH) and the same species from another region showed no significant difference when exposed to the same conditions. This might suggest again, as shown in **Chapter 4**, that the adaptive strategies to coastal habitat fluctuations could lead to organisms being more tolerant and resilient to environmental stressors. There are no available data on the fluctuations of water pH in Cromarty Firth in the literature and due to restricted access to the area, operators were unable to frequently register the pH fluctuations. However, it is known that the area is fed at the western end by the River Conon, which collects rain and snowmelt from the mountains in Sutherland, so mussels harvested there could be more tolerant to the alteration of parameters such as water pH, temperature or salinity.

The oxygen consumption of various bivalves could also be affected by external chemical exposure, for example metals and hydrocarbons (Jorge et al., 2007). As an example, when exposed to xenobiotics such as metals, mussels decreased the oxygen consumption as a result of decreased ventilation, impaired cellular respiration or inhibited gas exchange and transport (Spicer and Weber, 1991). Recently, in Tallec et al. (2022), juvenile oysters were gradually exposed to leachates from tires (0, 1, 10, and 100 µg tire / mL) for 40.5 hours for each concentration, in order to analyse the ability to modify the organism responses to the increasing doses. From 1 µg tire / mL, leachates reduced oyster clearance and respiration in a significant way, confirming that the xenobiotic exposure affected the gills. Many studies that investigated the actions and effects of chemicals in a low pH environment reported altered cue perception of the compound due to changes in the protonation state of cues and/or receptors, as shown for fish at lowered pH in Porteus et al. (2018) and Velez et al. (2019).

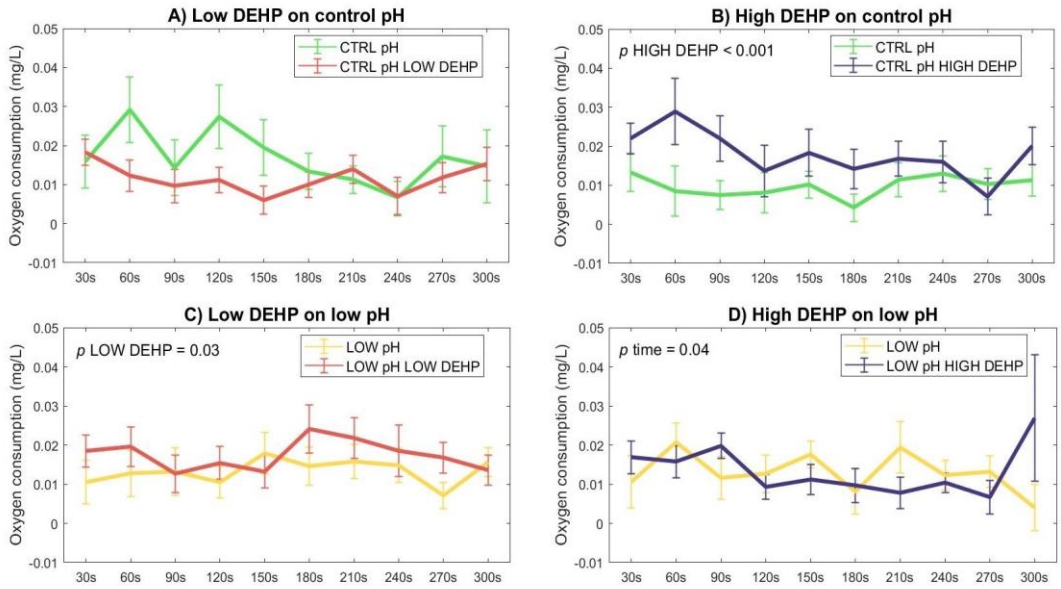

Fig. 5.9 DEHP effect on the mg/L water oxygen concentration (consumed oxygen estimation) throughout the 30-second time points on day 2. Abbreviations are pH 8.1 (CTRL pH, in green), pH 7.7 (LOW pH, in yellow), low DEHP dose at pH 8.1 (CTRL pH LOW DEHP, in red), high DEHP at pH 8.1 (CTRL pH HIGH DEHP, in blue), low DEHP at pH 7.7 (LOW pH LOW DEHP, in red), high DEHP at pH 7.7 (LOW pH HIGH DEHP, in blue), n = 17 - 18. Datapoints are expressed as mean ± standard error of the mean (SEM). ANOVA significant *p* values are annotated on the graphs

The seven-day DEHP exposure was chosen accounting for the non-persistency of DEHP in the environment (Staples et al., 1997), with a half-life of approximately 0.35–3.5 days for surface water and sediments in aerobic conditions (Peterson and Staples, 2003). Here, for mussels pre-exposed to low pH for a week, the single low DEHP dose (0.5 µg/L) resulted in a significant increased oxygen consumption especially in the last 3 minutes (**Fig. 5.9 C**), but this was not reflected in the high DEHP dose (50 µg/L) assay, where the oxygen consumptions of treatments LOW pH and LOW pH HIGH DEHP were similar (**Fig. 5.9 D**). The difference in the reaction to DEHP at the two concentrations in lowered pH could once again suggest a hormetic effect of this chemical. In fact, the effect here of only the low dose of DEHP on respiration could in part be explained by the non-linear effect of some endocrine disrupting chemicals on bivalves (Xu et al., 2021) and already noted in **Chapter 2.** This outcome is most likely to be related to receptor actions, or the presence of antagonists, regulators, and co-activators (Conolly and Lutz, 2014: Li, 2007; Vandenberg et al., 2012).

However, in this experiment, the high DEHP dose was found to be significantly effective in increasing the oxygen consumption of mussels at control pH, especially in the first 180 seconds after the injection (**Fig. 5.9 B**), but no significance was shown for the low dose at the same pH (**Fig. 5.9 A**). A hypothesis reported by Neuberger-Cywiak (2005) suggested that animals could protect themselves from pollutant exposure by either evading the area or excreting the toxicant. The latter necessitates energetic processes that would require an increase in the oxygen supplied. Even though not significant, a lowered oxygen consumption is observable in the CTRL pH LOW DEHP mussels with respect to the CTRL pH group, especially in the first 180 seconds (**Fig. 5.9 A**), highlighting an inverted trend of the two concentrations on mussel oxygen consumption.

5.8 Results and Discussion: Valve behavioural assay

Mussel gills are usually protruded in the outside environment following the shell margin, richly supplied with haemolymph and with a large area exposed to the water flow for gas exchange when the valves are open (Gosling, 2021). In this experiment, modal valve status (predominantly open, closed or equally split) was significantly affected by low pH exposure (p = 0.04, F = 4.55), with valves being more open in the 7.7 pH condition than in control pH (**Fig. 5.10 A**). Interestingly, as already remarked in the previous Result and Discussion section in **Chapter 5.8,** it was not mirrored by an increase in respiration in this treatment **(Fig. 5.8**). This could suggest that valve opening could be an adaptive strategy of mussels to circumvent the metabolic distress of high-CO_2 water, increasing the time spent with valves open for maintaining a balanced respiration rate similar to control conditions. Acidic pH is known to affect the valve behaviours of bivalves, for example an increased valve activity in the bivalve *Arctica islandica* was observed in Bamber and Westerlund (2016), even though the response was recorded only after a drop of 1.9 pH units. Moreover, in Hasler et al., (2017) specie-specific valve status alterations were noticed in freshwater mussels when exposed to high pCO_2. In fact, Unionidae *Lampsilis cardium* and *L. siliquoidea* valves were noted to remain open for long periods during the entire exposure, in contrast to the closed valves of giant floater *Pyganodon grandis.* Spending time with open valves could be a coping behaviour for mediating the acid/base disturbance (Hannan et al., 2016) and preventing respiratory acidosis and accumulation of anaerobic end products, which can be harmful (Hasler et a., 2017).

Avoidance behaviours in a low pH environment, such as burrowing in the sediment, were also noticed for the bivalve *Mya arenaria* and attributed to the activation of gamma-aminobutyric acid (GABA) -like receptors in response to increasing pCO_2 (Clements et al., 2017). Another hypothesis from Salánki, (1963) suggested that acidic conditions could cause anaesthesia in the posterior adductor muscle, and its consequent inability to contract and close the shells.

No significant effects were observed for the low DEHP dose on control or low pH and for the high DEHP dose on control or low pH ($p > 0.05$, **Fig. 5.10 B, C, D, E**). A trend in valves being more often closed was noted for the low DEHP-treated mussels at CTRL pH (**Fig. 5.10 B**) and high DEHP-treated mussels at low pH (**Fig. 5.10 E**), both however not statistically significant. Valve closure is a common avoidance and escape response to unfavourable conditions for marine molluscs and it could also contribute to the tolerance to stress (Ivanina and Sokolova, 2015). It could be possible that different concentrations of the plasticiser DEHP are sensed as a stimulus by the animals at different pH, which leads to shell movements and closure as a defence reaction (Dzierżyńska-Białończyk et a., 2019; Nagai et al., 2006). Neuberger-Cywiak et al. (2005) reported that exposure to pollutants might force mussels to reduce feeding and to close valves in order to reduce the contaminant uptake and a resulting decrease in respiration. In fact, even though not significant, a decreased oxygen consumption was noticed at control pH in the first 180 seconds after the low DEHP dose (**Fig. 5.9 A**).

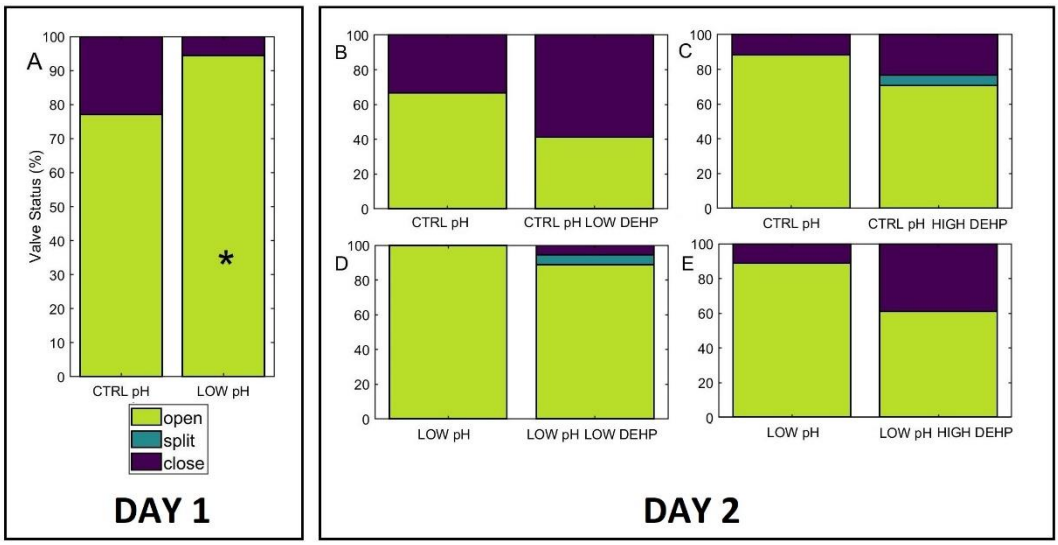

Fig. 5.10 Percentages of individuals with open (green) or closed (purple) valves (modal values). "Split" (blue) values indicate mussels that have spent an equal time in open and closed states exposed to **A**) low pH (day 1) and **B, C, D, E**) each two DEHP concentrations at the two pH regimes (day two), n = 35 - 36 (**A**); n = 17 - 18 (**B, C, D, E**). Abbreviations are pH 8.1 (CTRL pH), pH 7.7 (LOW pH), low DEHP at pH 8.1 (CTRL pH LOW DEHP), high DEHP at pH 8.1 (CTRL pH HIGH DEHP), low DEHP at pH 7.7 (LOW pH LOW DEHP), high DEHP at pH 7.7 (LOW pH HIGH DEHP). Significant effect of pH (p = 0.04) is denoted by *

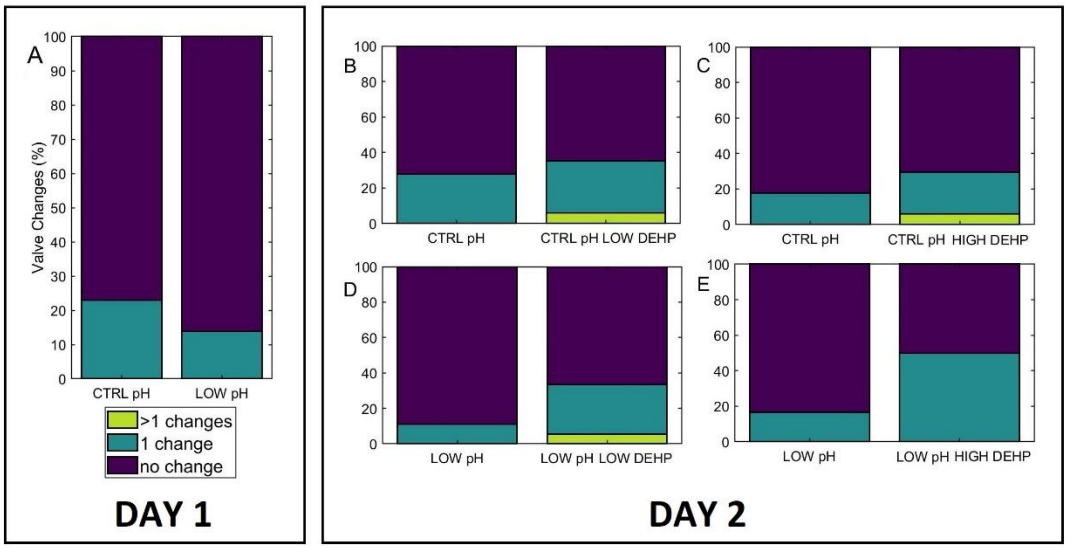

Fig. 5.11 Percentages of individuals with more than one change from open to closed valves or *vice versa* (green), one change (blue) or no changes from the initial status (purple) exposed to **A**) low pH and **B, C, D, E**) two DEHP concentrations at the two pH regimes, n = 35 - 36 (**A**); n = 17 - 18 (**B, C, D, E**). Abbreviations are pH 8.1 (CTRL pH), pH 7.7 (LOW pH), low DEHP at pH 8.1 (CTRL pH LOW DEHP), high DEHP at pH 8.1 (CTRL pH HIGH DEHP), low DEHP at pH 7.7 (LOW pH LOW DEHP), high DEHP at pH 7.7 (LOW pH HIGH DEHP). A small effect of high DEHP on low pH (p = 0.07) was observed

Even though we noted an increase of oxygen consumption in the treatments where the DEHP injection was significant, no particular effects on valve activity were observed, except for a small but non-significant effect of high DEHP on low pH treated mussels. In fact, high DEHP exposure resulted in an increased valve changes and opening events at low pH (p = 0.07 **Fig. 5.11 E** and **5.12 E**). When considering valve changes (number of changes between open and close and *vice versa*) and opening events in the other treatments, no significant impact of either pH or DEHP was otherwise found (p > 0.05, **Fig. 5.11** and **5.12**).

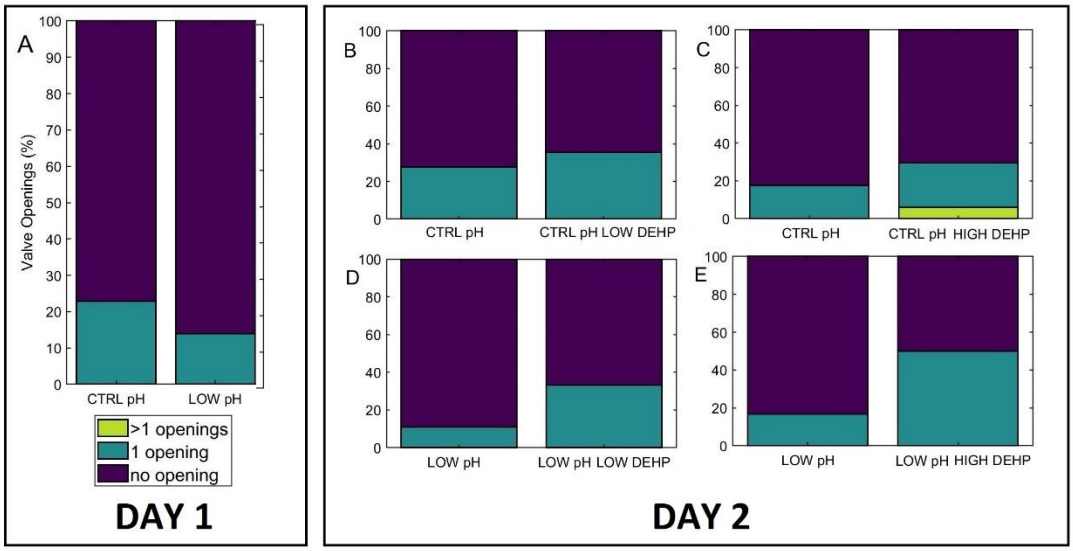

Fig. 5.12 Percentages of individuals with more than opening events (from closed to open, measure as none (purple), one (blue), more than one(green)). exposed to A) low pH and B, C, D, E) two DEHP concentrations at the two pH regimes, n = 35 - 36 (**A**); n = 17 - 18 (**B, C, D, E**). Abbreviations are pH 8.1 (CTRL pH), pH 7.7 (LOW pH), low DEHP at pH 8.1 (CTRL pH LOW DEHP), high DEHP at pH 8.1 (CTRL pH HIGH DEHP), low DEHP at pH 7.7 (LOW pH LOW DEHP), high DEHP at pH 7.7 (LOW pH HIGH DEHP). A small effect of high DEHP on low pH (p = 0.07) was observed

5.9 Conclusions

Mussels exposed to decreased pH (7.7 units) for one week and subsequently exposed to a single dose of either low (0.5 μg/L) or high (50 μg/L) concentration of the plasticiser DEHP presented varying responses regarding the metabolic system (i.e., oxygen consumption) and the behavioural system (i.e., the valve activity) observed in the same 5-min interval. The pH manipulation for a week led to an increase of mussels with predominantly open valves, which however was not mirrored by alterations in the oxygen consumption. This is possibly related to an adaptive strategy to maintain the same metabolism as the control conditions by increasing the time of valves spent open. The same mussels were then exposed to one of the two DEHP levels and tested in the time immediately after the injection. The high DEHP dose was able to increase the respiration of mussels at control pH (8.1), but this effect was not noticed for the low DEHP concentration at the same pH condition. On the contrary, the low DEHP had an effect on mussels at low pH (7.7), not mirrored in the high DEHP treatment under the same lowered

pH condition (which in turn presented increased valve activity). The discrepancy in the effect of either dose at different pH could be attributable to a series of hypotheses, including altered cue perception at lowered pH, adaptive strategies or hormetic effect of EDCs. The non-monotonic hormesis of EDCs such as DEHP will be discussed in **Chapter 6.** This experiment underlines again the unique endocrine disruptor pathways, whose way of action could be altered in an end-of-the-century acidified scenario.

Chapter 6

The effects of DEHP exposure on fertility and reproductive outcomes

6.1 Introduction

This chapter aims to analyse the effect of a short-term exposure to two environmentally relevant concentrations of the endocrine disruptive chemical DEHP on the number and size of eggs spawned during a synchronised reproductive event. Over the past years, the effect of plastic contamination on molluscs has been investigated for particles of all sizes (Bringer et al., 2022; Franzellitti et al., 2019b; Haegerbaeumer et al., 2019), and experiments involving mussel exposure are also well-represented (Avio et al., 2015; Bråte et al., 2018; Cappello et al., 2021; Gonçalves et al., 2022; Green et al., 2019; Khalid et al., 2021; Paul-Pont et al., 2016; Pittura et al., 2018; Vasanthi et al., 2021). As an example, styrene particles at concentrations of 0.01 - 1000 µg/L impaired the normal embryo development of *M. galloprovincialis* after a 48h exposure (Wathsala et al., 2018). Genotoxic effects of polystyrene microspheres at a concentration of 10^6 particles /L were observed in digestive glands and gills of *M. trossulus* after 5 days of exposure (Chelomin et al., 2022). Furthermore, endocrine disruptor plasticiser BPA was noted to affect the full development of *M. galloprovincialis* larvae when the fertilised eggs were exposed to concentrations of 0.01 - 1000 µg/L (Balbi et al., 2016; Fabbri et al., 2014).

Plastic additives are often known to induce disruptive effects on organisms, especially targeting the endocrine system. Effects of ECDs are diverse, from altered fertility and fecundity to masculinization and feminisation of females and males, respectively (Jobling et al., 2004). In vertebrates, there are documented effects of DEHP on the reproductive cycle. In fish, DEHP exposures (0.1 and 0.5 mg/L) for 6 months from hatching to adulthood of the marine medaka *O. melastigma* affected reproduction, accelerating spawning and decreasing egg production in females (Ye et al., 2014). DEHP exposures at 3.9 - 39 µg/L were also noticed to increase the vitellogenin levels in primary hepatocyte cultures of zebrafish sexes (Maradonna et al., 2013). In humans, it was measured that the daily intake of DEHP is in the range of 0.004 − 70 µg/kg/day (Das et al., 2014), with detectable levels found in blood, breast milk, umbilical cord and urine (Net et al., 2015).

These are relevant results, considering that it was recently reported that plasticisers such as phthalates appear to shorten gestational duration and sperm quality (Wormuth et al., 2006) and promote adipogenic activity and ultimately favour obesity (Völker et al., 2022) in mammals.

Documented effects of DEHP on aquatic species include reproductive dysfunction and endocrine disorders in crustaceans (Heindler et al., 2017), reptiles (De Solla et al., 1998) and fish (Carnevali et al., 2010; Ye et al., 2014). However, the exact effect of DEHP and other EDCs on molluscs is still not entirely established. This is due to the limited number of studies available on the characteristic irregular dose-response disruptive actions of these chemicals (**Chapter 1. 3,** Vandenberg et al., 2012). In fact, as other EDCs investigated in the literature, DEHP is observed to be more active and promote stronger responses at low doses (that usually are the levels found in nature) rather than high levels. This scenario is further complicated by the still not fully uncovered endocrine physiology of several invertebrate species. In this chapter, we investigate the effect of this plastic contaminant on reproductive outcomes, hypothesising an effect in lowering the number and the size of eggs spawned by mature females during the fertilisation event.

6.2 Materials and Methods: Experimental design

Adult blue mussels (n = 90; length mean ± standard deviation = 5.7 cm ± 0.6 cm) were collected from the suspended ropes farm of Cromarty Mussels, Ltd. in Cromarty Firth, Scotland, U.K. (57.40.741 N 4.06.062 W **Fig. 4.2 - 4.6**) in April 2021 and transported to the aquarium facilities of the University of Hull. Mussels were not cleaned from sand and mud nor scrubbed from seaweed and barnacles, to avoid additional physical stress. A detailed description of the collection site is available in **Chapter 4.1:** Experimental design. Spring months were chosen as this is the period with the highest likelihood to find ripe gonads in mature to spawning stages. Thirty mussels for each of the three treatments were randomly divided into six 4-L continuously aerated glass tanks, for a total number of 5 mussels for each replicate tank at a density of 1 mussel per 0.8 L. Prior to the exposure, mussels were kept at laboratory conditions for 19 days in artificial saltwater (Premium REEF-Salt, Tropical Marine Centre©, Chorleywood, U.K.) in a final number of 18 continuously aerated glass tanks and fed with PhytoGreen-M phytoplankton (Brightwell Aquatics, Fort Payne, USA). The longer maintenance period (with respect to

the other exposure experiments described in **Chapters 2**, **4**, and **5**) was chosen in order to achieve ripeness of the gonads, which was confirmed by histology analysis of test mussels during the course of the acclimation. Mussels were kept in a climate-controlled room, where the temperature was progressively raised by a total of 2°C over the first week in order to avoid an immediate temperature-induced shock and to facilitate the maturation of gonads, as it was observed in Mincarelli et al. (2021) and in **Chapter 2**, where an increase in temperature was noted to accelerate the gametogenesis cycle, especially in males.

After the acclimation period, mussels were exposed for seven days to three concentrations of DEHP (0, 0.5 and 50 µg/L), for a final yield of three experimental treatments (CTRL, LOW DEHP, HIGH DEHP, **Fig. 6.1 - 6.3**). Exposures of 0.5 and 50 µg DEHP/L were chosen from the literature, in accordance with the levels found in coastal waters (Jebara et al., 2021; Sánchez-Avila et al., 2012). The seven-day DEHP exposure was chosen accounting for the non-persistency of DEHP in the environment (Peterson and Staples, 2003; Staples et al., 1997). Mussels were not fed during the exposure and artificial saltwater was prepared the day before each water change, to allow the water temperature to adjust to the controlled room conditions. Water was partially (approx. 2-3 litre) changed every second day and DEHP was dosed right after (i.e., days 1, 3 and 5) from a stock solution of 1 mg/mL DEHP (≥ 99.5% purity, Sigma Aldrich®, Gillingham, U.K.) in ethanol. Temperature, pH and salinity were measured daily (**Table 6.1**) with a digital thermometer (Amarell Thermometer, Kreuzwertheim, Germany), a pH-metre (Jenway, Bibby Scientific Limited, Stone, UK) and a digital seawater refractometer (Hanna Instruments, Woonsocket, USA). After seven days of exposure, animals were stimulated to spawn using potassium chloride (KCl) 0.5 M injected in the valve cavity (Unlicensed animal ethics approval; reference no #U080/FEC_2021_10, University of Hull). Eggs were collected from the tanks with a single-use pipette and mussel gonads were dissected. Approximately 1.0 cm^2 of left gonad tissue was cut and immersed in 1 mL neutral-buffered 10% formalin solution (Sigma Aldrich, Gillingham, U.K.) at room temperature for histological observations.

Table 6.1 Experimental treatments, and measurements of temperature, pH, and salinity values. All parameters are expressed as mean ± standard deviation

Name of treatment	Description	Temperature (°C)	pH (Units)
CTRL	Control temperature, no DEHP	12.76 ± 0.39	7.85 ± 0.14
LOW DEHP	Low DEHP concentration	12.61 ± 0.32	7.77 ± 0.16
HIGH DEHP	High DEHP concentration	12.71 ± 0.34	7.83 ± 0.14

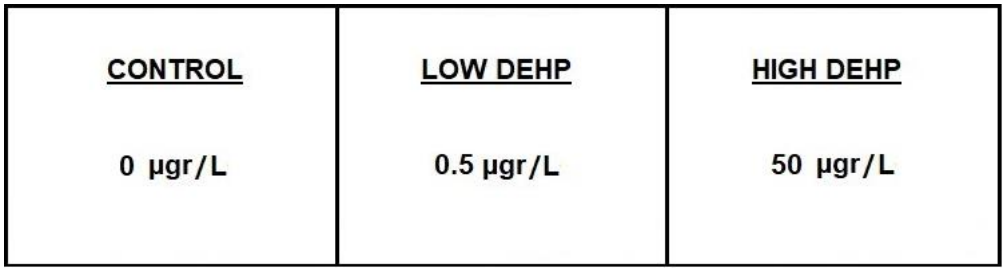

Fig. 6.1 Experimental design for the 7-day exposure with the chosen parameters for DEHP (0, 0.5 and 50 µg/L)

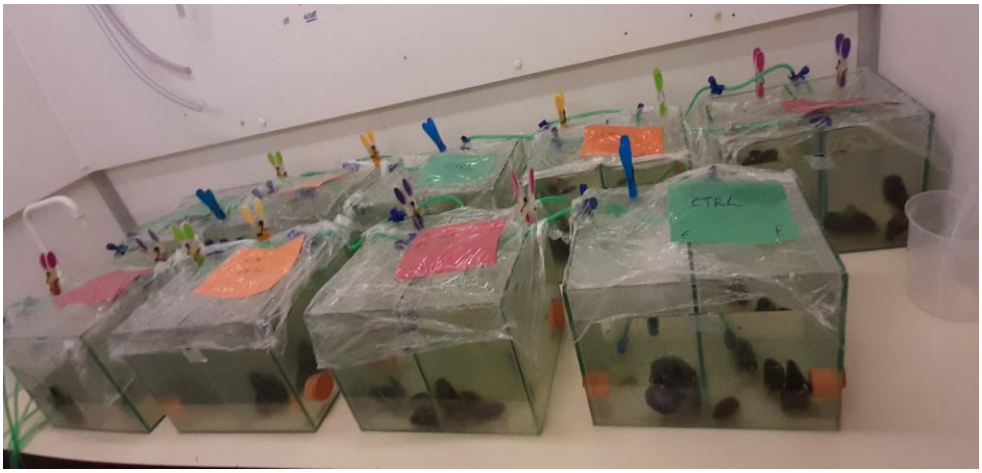

Fig. 6.2 Pictures from the exposure room - *M. edulis* blue mussels at 12°C in the exposure tanks, covered in non-PVC cling film

Fig. 6.3 Details of mussels (5 individuals for 4 litres) in the exposure tanks, covered in non-PVC cling film

6.3 Materials and Methods: Spawning induction

During the fertilisation event, eggs are released as an intermittent pink cloud, while sperm is released in a thin, steady stream through the exhaling syphon cloud (Helm et al., 2004). Before the spawning assay, the following different spawning inductors were tested on test mussels, in order to determine the optimal method:

- Thermal shock (Fitzpatrick et al., 2012; Sreedevi et al., 2014).
- Air exposure shock (Gago and Luís, 2011).
- Serotonin 10^{-3} M (dissolved in water or injected in the valve cavity, from Ram et al., 1993 and Fong et al., 1998).
- Potassium chloride (KCl) 0.5 M (dissolved in water or injected in the valve cavity, from Resgalla, 2016).

Other spawning induction methods such as *ad libitum* algae feeding (Smith and Strehlow, 1983), the addition of H_2O_2 (Morse et al., 1977), high frequency-low amplitude vibrations (Newell and Thomson, 1984) or exposure to ultraviolet (UV)- irradiated sea water (Moss et al., 1995) were considered but not included in this experiment as per the impracticability of these methods.

Monoamine serotonin, also known as 5-hydroxytryptamine (5-HT), is a neurotransmitter involved in bivalve reproduction traits such as spawning, oocyte maturation and sperm motility (Canesi et al., 2022). It also regulates the storage of the branched polysaccharide glycogen that is stored in the adipogranular (in small amounts) and vesicular connective (in large quantity) cells as the main energy reserve for gametogenesis (Berthelin et al.

2000). Serotonin is also involved in the reinitiation of ovarian cell meiosis (Deguchi and Osanai, 1995) and regulates other systems such as immune, cardiovascular, muscular and respiration (Canesi et al., 2022). In mammals, it acts as a peripheral hormone as well. The serotonergic system was observed to potentially be a target for endocrine disrupting chemicals such as BPA (Balbi et al., 2016), diclofenac (Balbi et al., 2018), carbamazepine and propranolol (Franzellitti et al., 2019a), thus we decided to use another spawning inductor for this experiment, to avoid a possible agonist/antagonist effect between the endocrine disruptive chemical activity of DEHP and the external addition of serotonin.

Fig. 6.4 and 6.5 Details of mussels during the 2-hour exposure to air (left) and details of a female mussel spawning eggs (in pink, picture on the right)

The KCl method from (Resgalla, 2016) was finally chosen, and carried out as follows: mussels were injected with 2 mL of 0.5 M KCl in the valve cavity and left for 2 hours outside water. Then, they were randomly divided into 5 tanks for each treatment (n = 6 in a final volume of 2 L), considering that preliminary tests showed that mussels were more likely to spawn when placed with conspecifics and not in individual jars. Mussels were then let to spawn overnight in water (**Fig. 6.4** and **6.5**). KCl injection is provided to be an easy spawning inductor in many invertebrates, including sea urchins (Lotterhos and Levitan, 2010) and mussels, with literature reports dating back to 1950 (Iwata, 1951). KCl was also observed in the past to activate *Ruditapes* spp. oocytes that were previously

arrested in the first meiotic metaphase (Abdelmajid et al., 1993) and induce larval metamorphosis in mussel *M. galloprovincialis* (Yang et al., 2008).

6.4 Materials and Methods: Wax infiltration and H/E staining

Samples were fixed in 10% buffered formalin (Sigma-Aldrich, Gillingham, UK) and then washed with 0.01 M PBS (Sigma Aldrich, Irvine, UK), dehydrated with increasing ethanol (Fisher Scientific, Loughborough, UK) concentrations (70%, 90%, 100%) and cleared with Histoclear II (National Diagnostics, Atlanta, USA). The day after, the samples were embedded in paraffin wax (VWR, Poole, UK) in an EG 1160 Paraffin Wax Embedding Centre (Leica Microsystems, Milton Keynes, UK) and tissue sections (10 µm) of wax-embedded gonads were cut on a Shandon Finesse® Manual Rotary Microtome 325 (Thermo Fisher Scientific, Loughborough, UK). Slides were stained with Mayer's haematoxylin solution (Sigma-Aldrich, Schnelldorf, Germany) and eosin Y alcoholic solution (Sigma-Aldrich, Schnelldorf, Germany). Prior to microscopic analysis, microscope slides were coded, in order to conduct a blind observation. Males and females were identified, and the following stages were blindly assessed, following the stage descriptions reported by Seed (1969) and each stage was categorised by a maturity factor (MF):

I. Spent/resting gonad (MF = 1, **Fig. 6.12** and **6.13**).
II. Development, stages 1 and 3 (MF = 2).
III. Development stage 5 (mature/ripe gonads, MF = 3, **Fig. 6.6** and **6.9**).
IV. Spawning stages 3 and 1 (MF = 4, **Fig. 6.7, 6.8, 6.10** and **6.11**).

Then, the sexual maturity index (SMI) was calculated according to the equation established by Siah et al. (2003): $SMI = \Sigma$ *(proportion of each stage* * *maturity factor)*. A more detailed protocol is provided in **Chapter 2.3** Wax infiltration and H/E staining.

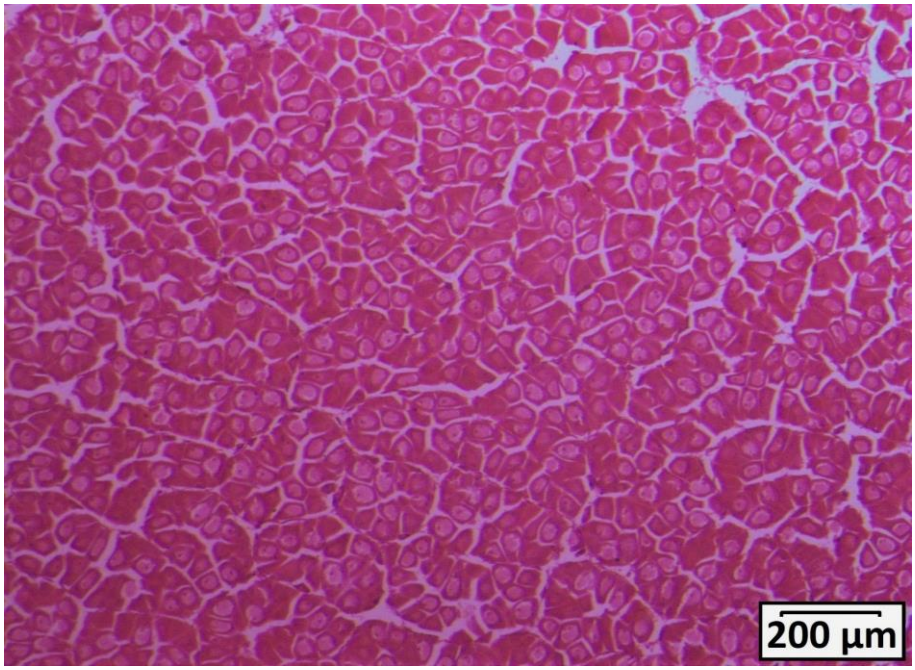

Fig. 6.6 Female mature gonad, with compacted and polygonal-shape ova and a few small oocytes

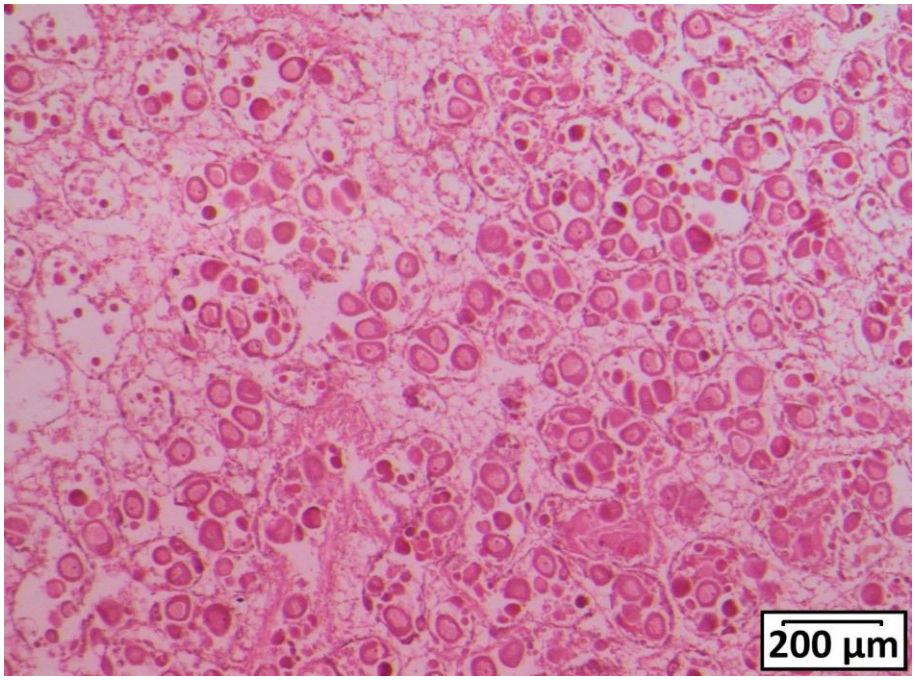

Fig. 6.7 Female spawning stage 3 gonad with follicles displaying empty spaces and mature rounded eggs

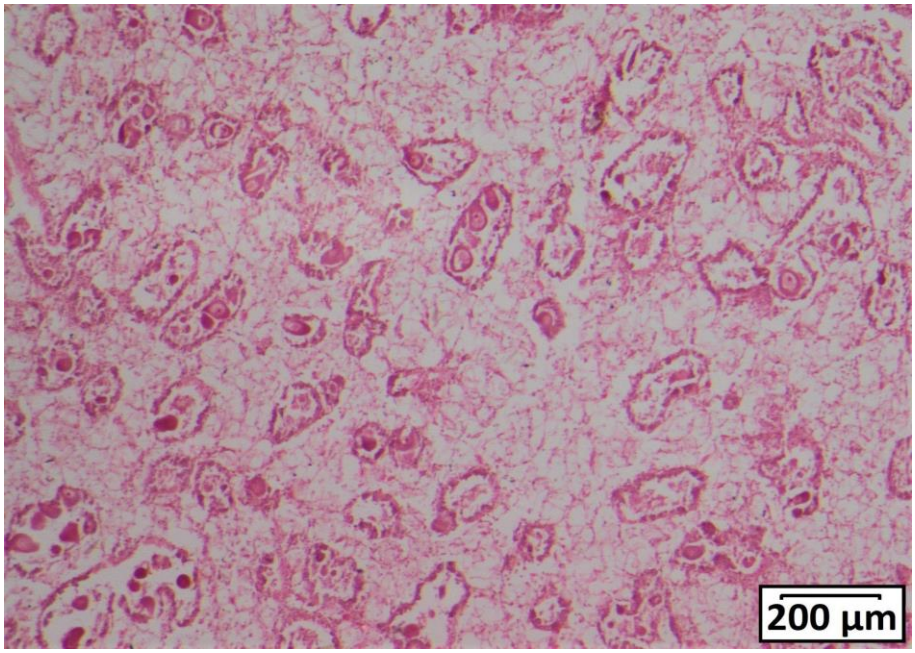

Fig. 6.8 Female spawning stage 1 gonad with some residual ova

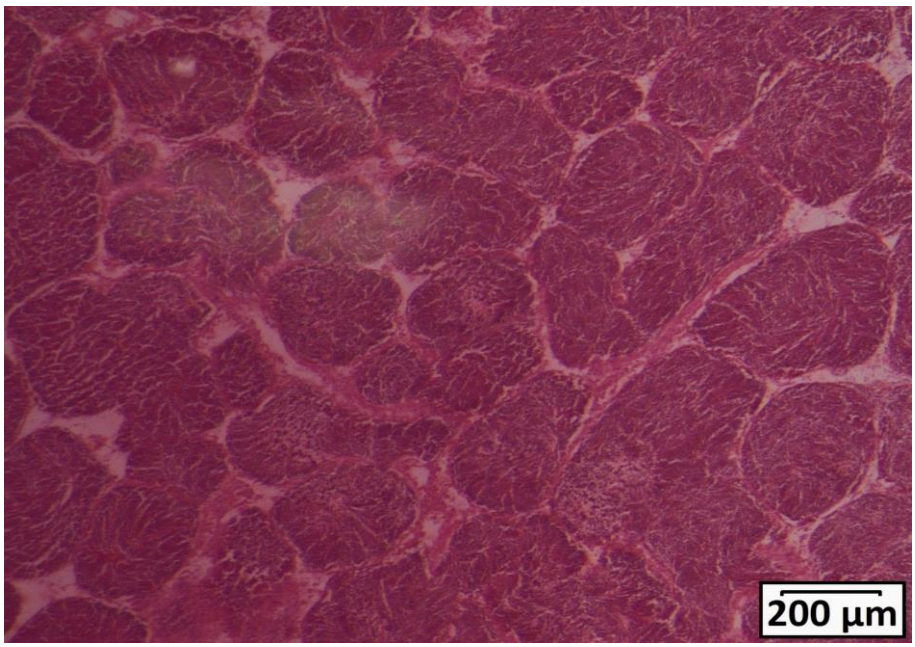

Fig. 6.9 Distended follicles in male mature gonad

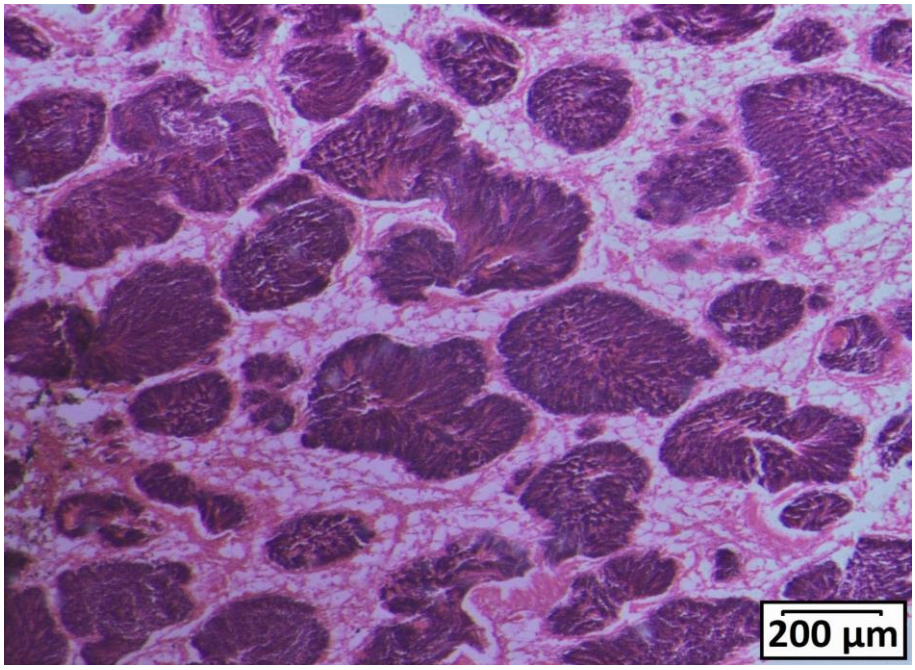

Fig. 6.10 Male spawning stage 3 gonad

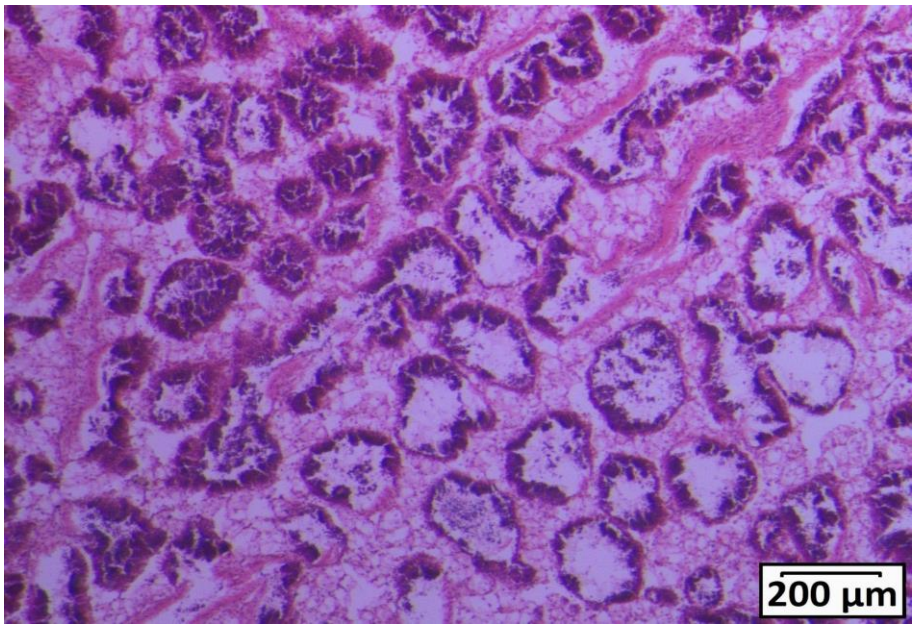

Fig. 6.11 Male spawning stage 1 gonad

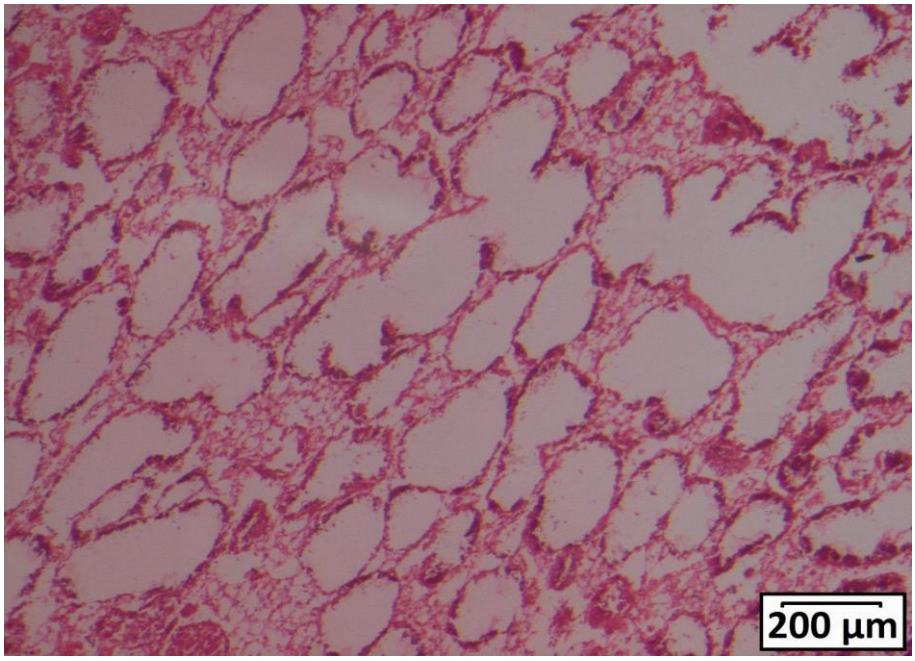

Fig. 6.12 Empty follicles

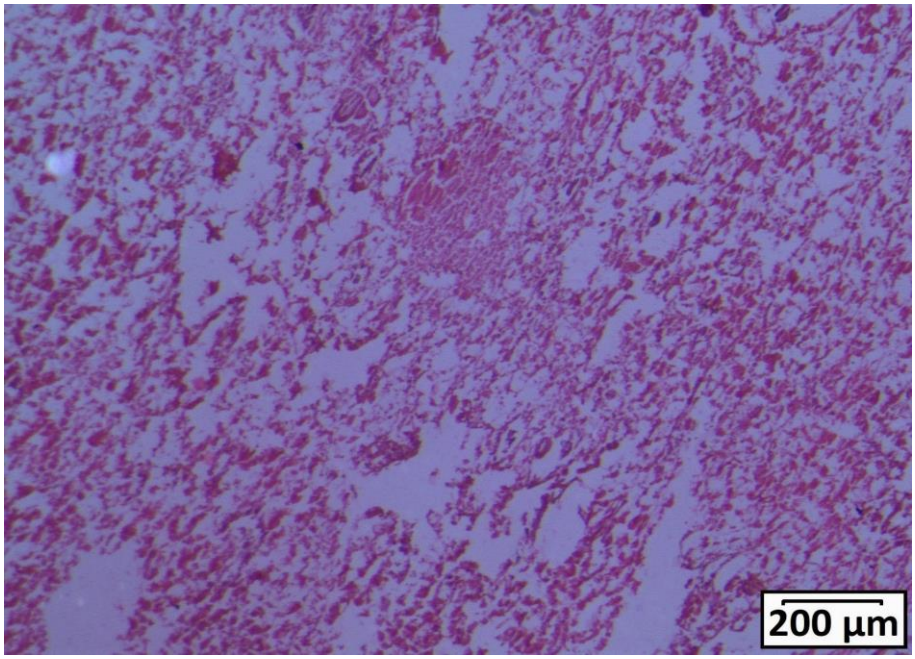

Fig. 6.13 Spawned gonad in a spent state with no evident presence of follicles or gametes. Spent gonads are described usually as thin and transparent or thick and opaque according to the feeding status

6.5 Materials and Methods: Egg counting and size measurement

Mussels were left to spawn overnight, and the morning after water samples containing eggs were transferred into 2 mL tubes and fixed with formalin 10%. 8 aliquots of 10 µL

each were immediately observed under a ZEISS Zen light microscope with retro illumination and Axiocam camera (**Fig. 6.14**). Pictures of each aliquot were taken and later analysed with the image software ImageJ. The software ImageJ was used to count the number of eggs (*cell_counter* plugin) for each aliquot and to measure the area of one egg per aliquot. (**Fig. 6.15** and **Fig. 6.16**). Egg diameter was also calculated from the area using the formula *diameter (D) = (√ area (A) / Π) x 2* (**Fig. 6.16**).

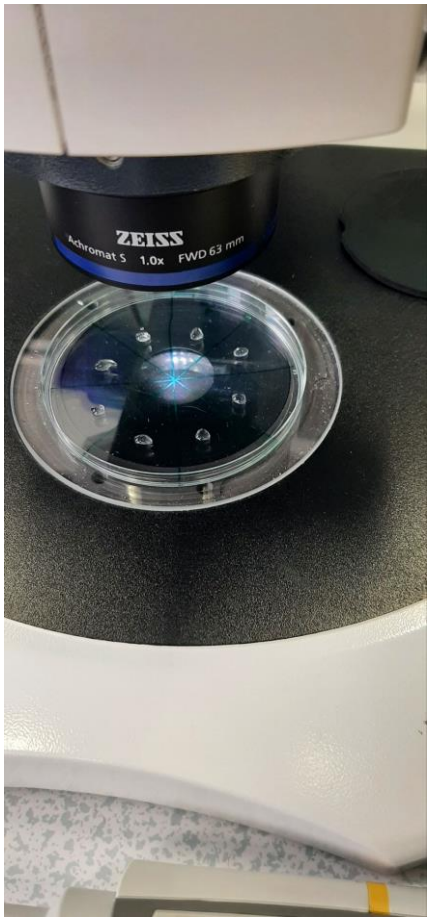

Fig. 6.14 Details of the aliquots under the microscope

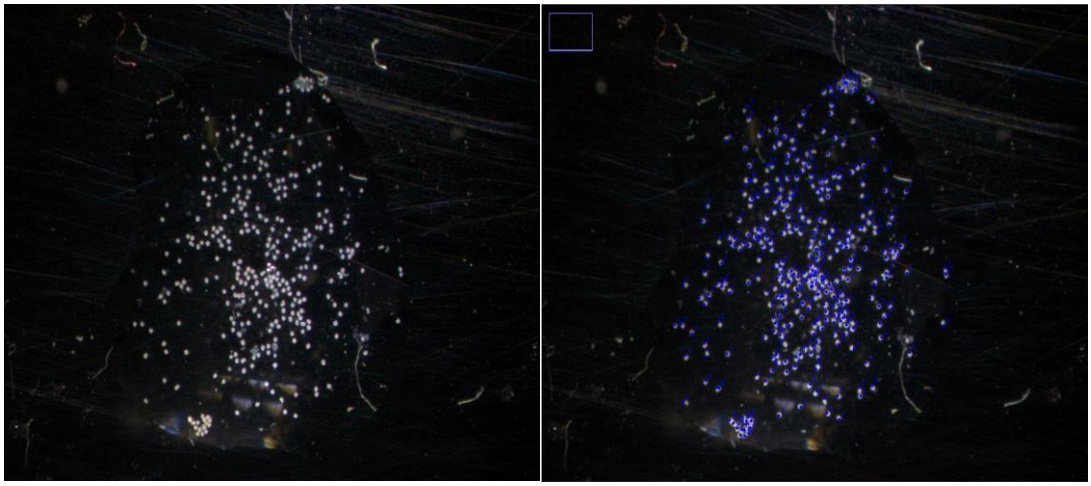

Fig. 6.15 Details of the aliquots under the microscope, before (left) and after (right, in blue) the *cell_counter* plugin from ImageJ software

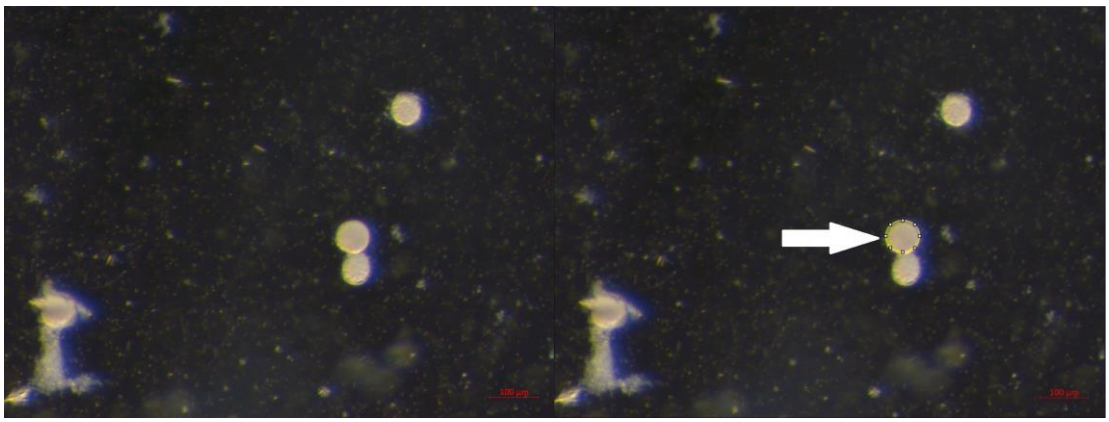

Fig. 6.16 Details of the aliquots under the microscope, before (left) and after (right, in yellow) the size measurement from ImageJ software

6.6 Materials and Methods: Statistical analysis

Ordinal logistic regression was used to predict the ordinal dependent variables "Gametogenesis stage", assuming "DEHP" and "SEX" as independent variables. The dependent variable "gametogenesis stage" was measured at the ordinal level (i.e., a 4-point scale ranging from "development" to "mature" to "spawning" to "spent"). Independent variables "DEHP" and "SEX" were considered categorical variables. Model uncertainty was assessed by comparing ΔAICc values and Akaike weights in which the lowest values for ΔAICc indicate second best to last parsimonious models of the set (**Table 6.2**). Model selection was carried out in Rstudio with the *AICcmodavg* package (Mazerolle, 2013) in R 3.6.2 (CRAN). Models with ΔAIC > 10 were omitted from

considerations since they have considerably less support compared to the best-fitting model (Burnham and Anderson, 2002). Ordinal logistic regression was carried out using the *polr* function (*MASS* package, Venables and Ripley, 2002), calculating the *p* value by comparing the *t*-value against the standard normal distribution (**Table 6.3**). The proportional odds assumption (test of Parallel Lines) was tested using the *ordinal* package (Christensen, 2019).

Since the sex of mussels could not be determined through external morphology but only by histology, we investigated whether the number of eggs observed was correlated with the number of females in the tank post-histology. A significant correlation between the number of spawned eggs and the number of females in the tanks was found by Pearson's test ($p < 0.001$, $t = 3.63$). Therefore, the number of eggs was counted for each of the eight aliquots and then divided by the number of females present in the tank before undertaking the statistical analysis. One female in the HIGH DEHP treatment was taken out from the calculation, as displaying gonads in early developing state, thus unlikely to spawn when induced. Additional calculations were carried out adding resting/spent gonads (i.e., undetermined sex) to the statistical analysis, considering them as possible fully spawned and spent females.

The relative number of eggs and the average egg size were then analysed via non-parametric Kruskal-Wallis (number of eggs) and ANOVA (egg area and diameter), after verifying normality (Shapiro-Wilk's test) and homogeneity (Levene's test) of the dataset. Tukey's multiple comparison test was used for comparisons between ANOVA groups.

6.7 Results and Discussion: Histology to determine sex and gametogenesis status

The most parsimonious ordered logistic regression model (with SEX as the only predictor variable) showed that there was a significant difference between sexes (p SEX = 0.01, t-value = -2.54) and in their SMIs. When analysing the effect of DEHP as well, there was no effect of the plasticiser on the transition between stages ($p > 0.05$, **Fig. 6.17**, **Table 6.3**). The effect of the predictor "DEHP" was also tested, confirming no significant effect ($p > 0.05$).

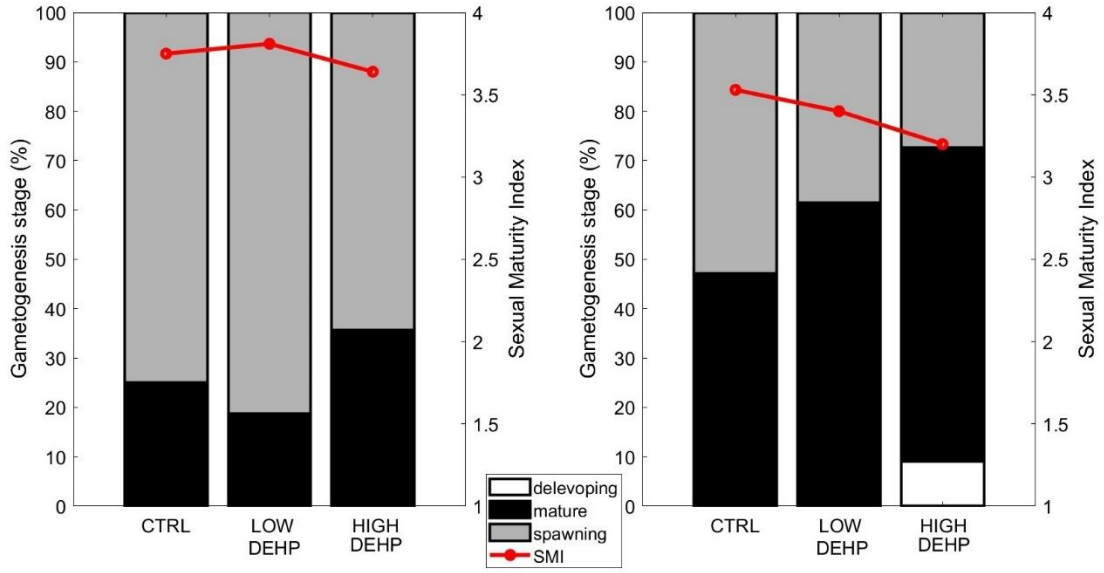

Fig. 6.17 Effects of DEHP treatments on gametogenesis stages. Percentage of each stage and sexual maturity index (SMI) of males (A) and females (B) in CTRL (n = 13 (males), 15 (females)) LOW DEHP (n = 17 (males), 10 (females)), HIGH DEHP (n = 9 (males), 14 (females)) and the associated SMIs

Table 6.2 Model classification, number of estimated parameters (K) for each model, Akaike Information Criterion (AICc), delta AIC (ΔAIC), Akaike weights (AICcWT), cumulative Akaike weights (CumWT), log-likelihood of each model (LL) for the two independent variables (+) sex (SEX) and DEHP concentration (DEHP) and their interactions (*) on gametogenesis stages

model	**K**	**AICc**	**Δ AIC**	**AICcWT**	**Cum WT**	**LL**
SEX+DEHP	4	118.15	0.00	0.47	0.47	-54.99
SEX	3	118.82	0.67	0.67	0.80	-56.36
SEX*DEHP	5	119.89	1.74	0.20	0.99	-54.82
DEHP	3	126.92	8.78	0.01	1.0	-60.41

Table 6.3 Results of ordinal logistic regression for the best model of treatments (SEX). Estimated value, standard error, *t*-value and *p* value for the independent variables sex and DEHP concentration (DEHP)

Variable	Value	Std. Error	*t*-value	*p* value
SEX	-1.56	0.50	-3.14	0.002
DEHP	-0.50	0.31	-1.62	0.104

Exogenous factors such as temperature, food availability, nutrient quality, salinity, circadian rhythm or tides could control certain aspects of the reproductive cycle, such as duration and periodicity of the gametogenesis and larval stages (Dixon et al. 2006; Kautsky 1982; Suárez et al. 2005; Tyler et al. 2007). Endogenous factors and species-specific characteristics such as animal hormone levels or individual responses to environmental conditions might also affect and regulate gametogenesis or spawning (Zardi et al., 2007). Moreover, gametes in the water represent a chemical stimulus to ripe mussels, in order to induce spawning and increase the success of the fertilisation (Gosling, 2021). As shown in Mincarelli et al. (2021, 2022), as well as **Chapter 2** and **4**, DEHP in environmentally relevant concentrations does not seem to induce any alteration of the gametogenesis stage in males or females. Likewise, here, even though a small decrease in the SMI for females was noted with the exposure to increasing concentrations of DEHP (**Fig. 6.17**), it was not significant. This does not preclude additional dysfunctions from the endocrine disruptor DEHP on reproductive traits, as already shown for fish (Ye et al., 2014, Carnevali et al., 2010) or crustaceans (Forget-Leray et al., 2005; Heindler et a., 2017) at various concentrations from 0.02 to 500 ug/L.

6.8 Results and Discussion: Effects of DEHP on egg count and size

Similar to the sexual maturity index, Kruskal-Wallis test did highlight a lowered but slightly not significant effect of DEHP on the number of spawned eggs by females (p = 0.10, KW chi-squared = 4.52 **Fig. 6.18**). This could be related to the fact that the gametes were already present in the gonads at the time of the exposure and just needed to grow to maturation, hence there was only very little effect on the number spawned. However, it is important to highlight that when adding possible fully spawned and spent females to

the statistical analysis (i.e., undetermined sex of resting/spent gonads), the effect of DEHP in lowering the number of counted eggs got further pronounced, displaying a significant difference between the treated individuals with respect to the control.

LOW and HIGH DEHP treatments showed the lowest average egg count in the 10 microliter aliquots (57.1 ± 9.0 SEM eggs/female for LOW DEHP and 54.0 ± 8.9 SEM egg/female for HIGH DEHP), lower when compared to the control spawned eggs (77.0 ± 11.8 SEM eggs/female). Usually, *M. edulis* females emit *ca* 10^6 - 10^9 eggs per female, depending on body size (Honkoop & van der Meer, 1998; Sprung et al., 1983; Thompson 1979). In this experiment, female body sizes were coherent between treatments (5.6 ± 0.7 cm in CTRL; 5.7 ± 0.5 cm in LOW DEHP; 5.9 ± 0.6 cm in HIGH DEHP), with no significant difference between groups (one-way ANOVA $p > 0.05$). It is therefore unlikely that differing relative egg counts have resulted from different body sizes. When considering mature and spawning females, DEHP treatments had the lowest number of eggs per individual (albeit not significantly different from the control condition), and eggs were significantly smaller in the low DEHP condition. When adding spent gonads (n = 1 for CTRL, n = 1 for LOW DEHP, n = 4 for HIGH DEHP) to the total number of females, the effect of DEHP was observed to intensify. In fact, adjusting the spawned eggs by the additional resting gonads resulted in mean ± standard error of the mean SEM of 74.9 ± 12.1 eggs/female in CTRL, 50.0 ± 7.7 eggs/female for LOW DEHP and 29.3 ± 4.2 egg/female for HIGH DEHP. In this case, Kruskal-Wallis test uncovered a significant effect of DEHP in lowering the egg count ($p = 0.01$, KW-H= 9.05, **Fig. 6.19**).

In line with these results, when exposed for a year to concentrations 10-100 ng/L of tributyltin (TBT), adult periwinkle *Littorina littorea* showed decreased egg production, but with marginal effect after a short-term exposure of 9 days (Matthiessen et al., 1995). The exposure to the antiandrogenic compound flutamide over an exposure of 21 days resulted in a decrease in eggs spawned per female due to a delay in the maturation of eggs in fathead minnow *Pimephales promelas* (Jensen et al., 2004). Significant reductions of eggs spawned for females were also noted in *Danio rerio* long-term exposed to concentrations >1.67 ng/L and 1500 µg/L of 17α-ethinylestradiol (EE2) and BPA, respectively. The effects were often associated with increased vitellogenin plasma levels and gonadal alterations, while exposure to the same compounds for a shorter time of 0 – 3 days post-fertilisation provoked no effect on spawned eggs (Segner et al., 2003). A similar reduction in female fecundity was found for *D. rerio* exposed to nonylphenol (100 µg/L) or EE2 (10 µg/L) for two months (Hill and Janz, 2003). These effects could be

caused by interference with mitosis, cell cycle progression, protein metabolism and/or the final maturation of oocytes (Santos et al., 2007). The results from the literature might suggest a possible effect of EDCs on the number of spawned egg if the females are exposed for a prolonged period, even though a 7-day exposure was noted here to already induce a slight decrease in the DEHP-treated groups.

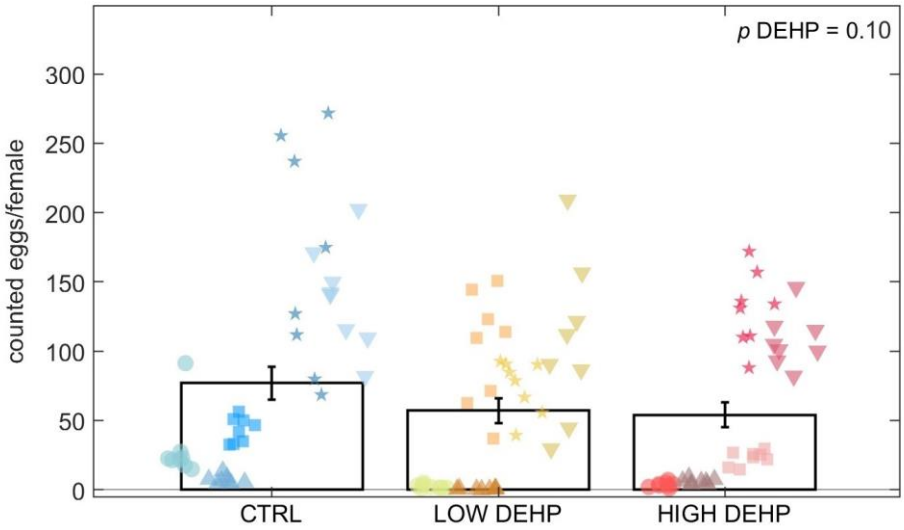

Fig. 6.18 Total eggs for females counted in 10 microliters (8 replicate aliquots counted in 5 tanks for each treatment). Data are expressed as the mean ± standard error of the mean (SEM). Abbreviations are control (CTRL), low DEHP (LOW DEHP) and high DEHP (HIGH DEHP). Different shapes represent different replicate tanks. ANOVA *p* value are annotated and differences between groups are indicated by bars and * over the histograms

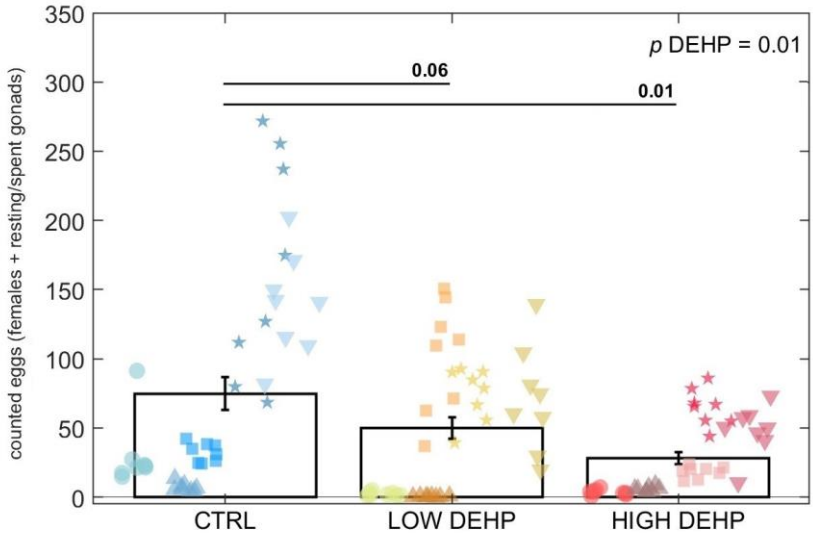

Fig. 6.19 Counted eggs adjusted by mature and spawning females in 10 microliters (8 replicate aliquots counted in 5 tanks for each treatment). Data are expressed as the mean ± standard error of the mean. Abbreviations are control (CTRL), low DEHP (LOW DEHP) and high DEHP (HIGH DEHP). Different shapes represent different replicate tanks. Kruskal-Wallis *p* value is annotated in the top right corner

For the egg area measurement (squared micrometre), ANOVA found an effect of DEHP on the egg area ($p < 0.001$, F value = 7.63, **Fig. 6.20** and **6.21**). Tukey's test highlighted a significant difference between the control eggs and those exposed to a low concentration of DEHP ($p = 0.004$) and between low and high DEHP treatment groups ($p < 0.001$). This seems to confirm the non-monotonic dose-response effect of endocrine disruptive chemicals such as DEHP. In fact, the LOW DEHP exposure had a significant effect in lowering the size of the eggs, with the smallest cells observable in the tanks exposed to the low concentration of DEHP (area = 2853 ± 67 SEM μm^2; diameter = 60.1 ± 0.7 SEM µm), while the high concentration treatments were of similar size to the control condition tanks. Specifically, average values for HIGH DEHP groups were 3377 ± 100 SEM μm^2 for the egg area and 65.3 ± 1.0 SEM µm for the egg diameter, while in CTRL condition the average area was 3200 ± 101 SEM μm^2 and diameter = 63.5 ± 1.0 SEM µm. In the literature, the egg diameter of *Mytilus* eggs is reported being around 70 µm (Honkoop & van der Meer, 1998) and more specifically, fertilised eggs are usually 60 - 65 µm in diameter (Gosling, 2021), and low DEHP treated eggs were just at that threshold which may indicate lower fertilisation rates.

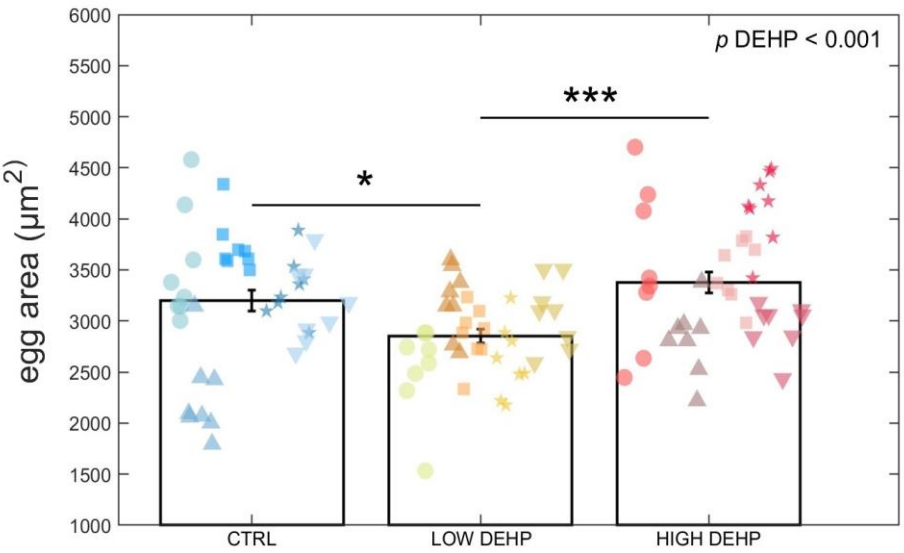

Fig. 6.20 Egg area (squared micrometre) for each treatment (8 replicate aliquots measured in 5 tanks for each treatment). Data are expressed as the mean ± standard error of the mean (SEM). Abbreviations are control (CTRL), low DEHP (LOW DEHP) and high DEHP (HIGH DEHP). Different shapes represent different replicate tanks. ANOVA *p* value are annotated and differences between groups are indicated by bars and * over the histograms

As mentioned in **Chapter 1**, chemicals such as plasticisers or synthetic drugs are defined as selective modulators of the endocrine system. This means that they often cause nonlinear responses and either interfere with the synthesis and/or metabolism of hormones and their receptors (Amaral Mendes, 2002; Markey et al., 2002). In some cases, the resulting dose responses follow a biphasic curve characterised by stimulation at low doses and inhibition at higher doses (Agathokleous, 2018). In fact, it is well known that some pollutants present dose responses that show not only linear, power, or exponential distributions, but also U-shape, inverted U-shape, J-shape, and inverted J-shape (Agathokleous, 2018). Inverted U-shape dose-response curves were for example observed for cadmium exposure on the activity of SOD and CAT in the earthworm *Eisenia fetida*, while higher doses provoked inhibition of these antioxidant enzymes, possibly related to the activation of pathways of adaptation (Zhang et al., 2009). Several studies reported that low-concentration exposure to xenobiotics such as heavy metals could elicit an adaptive mechanism characterised by increasing energy storage, which is overcompensated by excessive energy consumption at higher doses, to balance the energy metabolism and maintain homeostasis (Agathokleous et al., 2018; Calabrese, 2001; Costantini and Borremans, 2019; Kim et al., 2018). It is interesting to notice that when

increasing the exposure concentrations, DEHP elicited two different response curves: a linear one for the number of eggs spawned and a biphasic one for the egg sizes. Similarly, after 14 days at environmentally relevant exposures of 12 and 36 µg/L of DEHP, a U-shaped response was noted in *M. galloprovincialis* for antioxidant gene expression, while an inverted U-shaped response was noticed for their enzyme activities at the same exposure concentrations (Xu et al. 2021). Considering the number of spawned eggs, it is important to note as well a slight trend towards a lower proportion of spawning female gonads with high DEHP concentration, which could also have affected egg number.

Considering reproductive outcomes, in De Nicola et al., (2007), sperm and embryos of sea urchins *P. lividus* and *Sphaerechinus granularis* exposure to vegetal- and chemical-based tannins resulted in a general initial increase of fertilisation rate at concentrations of 0.1 - 0.3 mg/L and a shift to toxicity at higher concentration doses. These types of hormetic effects are also induced by natural and environmental factors such as temperature, ground-level ozone, magnetic field and radiation (Agathokleous and Calabrese, 2020).

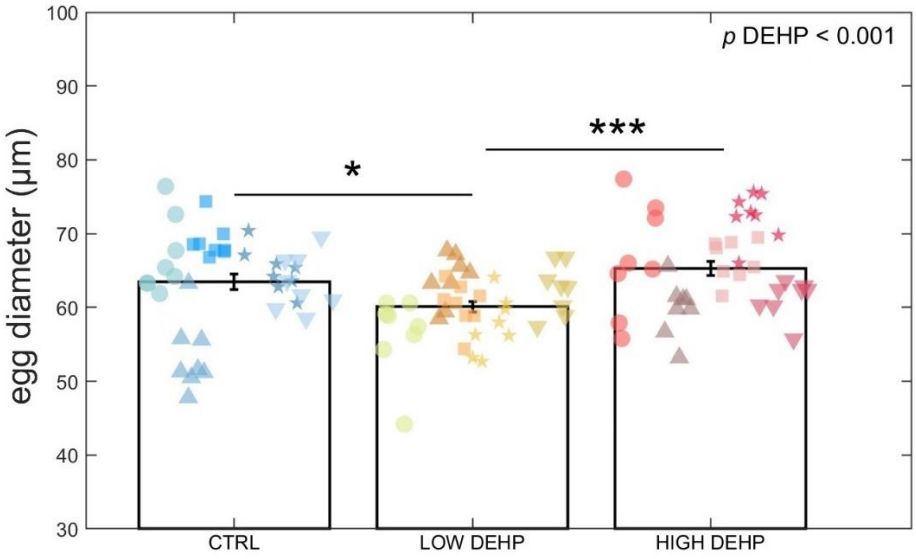

Fig. 6.21 Egg diameter (micrometre) for each treatment (8 replicate aliquots measured in 5 tanks for each treatment). Data are expressed as the mean ± standard error of the mean (SEM). Abbreviations are control (CTRL), low DEHP (LOW DEHP) and high DEHP (HIGH DEHP). Different shapes represent different replicate tanks. ANOVA *p* value are annotated and differences between groups are indicated by bars and * over the histograms

The “low dose concept” describes the lowest dose at which biological change and/or damage is observable. In particular, the endocrine system is very sensitive to very low hormone concentrations (Vandenberg, 2012) and biphasic dose responses are often observed at the µg/L magnitude scale, considered low concentrations for most pollutants (Chapman, 2002). Recently, the hormetic effect of DEHP on mussels was extensively examined in *M. galloprovincialis* by Xu et al. (2021a). After 14 days at environmentally relevant exposures of 12 and 36 µg/L, a U-shaped response was noted for antioxidant GST and CAT gene expression, while an inverted U-shaped response was noticed for their enzyme activities.

In bivalves, gonads consist of branching tubules united to form ducts (that eventually lead into a short gonoduct), with gametes situated in the epithelial lining that are subsequently shed into the water through the exhaling mantle opening (Gosling, 2021). In females, primary oogonia follow repeated mitosis to secondary oogonia (5 – 7 µm diameter), which as primary oocytes undergo meiosis until it is arrested at prophase I (as the remaining part of meiosis is completed at fertilisation). Then, vitellogenesis takes place, when oocytes accumulate nutritive substances such as lipid globules, vitellogenin (egg yolk vitellin precursor) and cortical granules (Pipe et al., 1987). Contrary to our results, in Li et al. (1998), the exposure to the estrogenic compound E2 of the Pacific oyster *C. gigas* for 40 days increased the diameter and the vitellin content in the oocytes, suggesting that the chemical E2 is involved in the vitellogenesis in female oysters. This could suggest that DEHP in mussels might negatively affect the same pathway, affect the oocyte reserves and eventually, the size of the spawned eggs. Furthermore, it was recently found that DEHP exposure was able to affect nematode embryogenesis and alter chromosome morphological structures (Cuenca et al., 2020). Considering this, it is possible that in this experiment the low DEHP exposure for one week had affected female oocytes by disrupting the meiotic process and/or the accumulation of nutritive deposits during the vitellogenesis, eventually impacting the egg size.

6.9 Conclusions

In conclusion, a clear non-monotonic dose-response is observable for the plastic additive DEHP during the synchronised reproductive event, especially on the size of the eggs spawned. Females exposed to a low concentration of DEHP (0.5 ug/L) for seven days

spawned fewer and smaller eggs compared to the control groups and to the higher concentration (50 ug/L, with regard to the measured egg area). Regarding the egg count, no significant effect was noticed, even though the number of spawned eggs decrease in the DEHP-treated groups, with the effect further pronounced when considering spawned gonads. As already observed, a linear toxicity response is not observable for endocrine disruptiing chemicals such as DEHP, highlighting the importance for ecotoxicological studies to address the effect of EDCs at low concentrations, which are the most prominent levels found in natural environments. In fact, as this chapter and many other studies before have underlined, DEHP and other endocrine disruptors (used in herbicides, fungicides, insecticides, UV screens, lubricants and paints) could stimulate stronger effects and affect organisms at low environmental concentrations. Thus, policies regulating the use and disposition of these chemicals, along with the setting of new safe environmental levels, should be developed.

Chapter 7

General Discussion and Conclusions

Sex-related responses of blue mussels to the plasticiser DEHP under climate change scenario

7.1 The effect of DEHP on *Mytilus* spp.

Among molluscs, Bivalvia is the second-largest class in the phylum. It includes about 900 living species, characterised by lateral compression of the body and bilateral symmetry by two shell valves (Gosling, 2021). About 80% of the Bivalvia molluscs populate marine environments, with the genus *Mytilus* inhabiting rocky shores from high intertidal to shallow subtidal regions (Gosling, 2021). *Mytilus* spp. started to disperse into the Atlantic Ocean from the Pacific about 3.5 million years ago during the Pliocene epoch after the opening of the Bering Strait (Vermeij 1991). For years, *Mytilus* spp. have been commonly used in biomonitoring programs worldwide (Gorbi et al., 2008; Laouati et al., 2021; Markert et al., 2003; Marigómez et al., 2013b; O'Connor 1998) especially after ecological disasters such as oil spills (Marigómez et al., 2013a; Moreira et al., 2004; Ortiz-Zarragoitia et al., 2011; Viarengo et al., 2007). Mussels are also used as distinctive indicators of health and food safety because of their position in the food chain and their close relationship with the human diet (Chiesa et al., 2018; Van Cauwenberghe and Janssen 2014). In fact, the global harvest of the blue mussel *M. edulis* for human consumption is reported to have reached more than 200,000 tonnes in 2018 (FAO, 2018). Plastic pollution is a pressing environmental issue. Yet, its effect on the biological responses of *Mytilus* spp. is not fully understood. In this thesis, two environmentally relevant concentrations of the endocrine disruptive plasticiser DEHP were chosen as exposure levels. Overall, the low DEHP exposure (0.5 µg/L) had a stronger impact on mussels in contrast to the high DEHP level (50 µg/L) exposure. Specifically, in **Chapter 2** significant effects from the low concentration of DEHP on the estrogen receptor-related response were noted (represented by the genes estrogen-related receptor *MeER1* and estrogen receptor *MeER2*), and especially on the expression of *MeER1* in developing female gonads (**Supplementary Appendix to Chapter 2**). Likewise, in **Chapter 6**, a similar non-monotonic dose-response curve was observed. The LOW DEHP dose of 0.5 µg/L significantly lowered the size (i.e., area and diameter) of spawned eggs in mature

females. The effect of the low DEHP exposure was also investigated in **Chapter 3**, from data generated from RNA sequencing of male gonadal tissues. Overall, features for stimuli response, cell cycle and DNA repair were found significantly upregulated, with several transcripts related to fertility, spermiogenesis and sperm motility. From these results, it is unambiguous that DEHP has a direct effect on many aspects of the reproductive cycle of mussels in both sexes, from fertility outcomes to expression of genes of the endocrine or reproductive pathway, especially at low concentrations that are commonly and widely found in nature. Thus, after the European Union, other countries should reconsider the use of this chemical in plastic production, to avoid the commercialisation and the consequent release of disruptive plastic additives in the environment.

7.2 The effect of DEHP in combination with high temperature

Global warming and its direct human origin were already highlighted in the Fourth (AR4) and Fifth (AR5) Assessment Reports from the IPCC in 2007 and 2014. It is well-known that temperature is a pivotal parameter for ecological responses of marine species (Kwiatkowski et al., 2020; Thomas et al., 2018). In mollusc biology, alteration in temperature and thermal tolerance influences various traits, such as survival (Beukema et al., 2009; Denny et al., 2011; Jones et al., 2009; Said and Nassar, 2022; Verdelhos et al., 2015), respiration (Barbariol and Razouls 2000; Jansen et al., 2007), reproduction (Borcherding, 1991; Fearman and Moltschaniwskyj, 2010; Thomas and Bacher, 2018), immune responses (Rahman et al., 2019), energetic processes (Georgoulis et al., 2021; Louis et al., 2020; Pernet et al., 2007), population abundance (Thyrring et al., 2017) and larval growth and recruitment (Lazo and Pita, 2012; Philippart et al., 2003; Talmage and Gobler, 2011). Future temperature conditions may as well be optimal for growing toxic microorganisms such as pathogens (Anestis et al., 2010; Encomio and Chu, 2005; Hernández-Cabanyero et al., 2020; Rosenberg and Ben-Haim, 2002) or expanding the limit of distribution of harmful algal bloom (HAB, Glibert, 2020; Gobler, 2020; Visser et al., 2016), with inevitable consequences on health and food safety, tourism and local economy (Bindoff et al., 2019).

Frequently, a seasonal presence of several contaminants such as pharmaceutical and personal care products is noted in water bodies due to temperature variations (Archana et

al., 2017; Comber et al., 2020; Yang et al., 2017). Recently, phthalate ester levels were found to display a seasonality in Korean and Chinese coastal water, often influenced by weather, seasons, river contiguity and proximity to residential or industrial areas (Heo et al., 2020; Sun et al., 2021). Furthermore, temperature was noticed to alter the toxicity of certain chemicals, as the increasing temperature can affect the ventilation rate of organisms due to increasing metabolic rate and decreasing oxygen solubility (Schiedek et al., 2007). In aquatic species, bioaccumulation of certain pollutants such as metals is also well-known to be regulated by abiotic factors such as water temperature (Baines and Fisher, 2008; Mubiana and Blust, 2007; Richards and Chaloupka, 2009). In this thesis, the consequences of DEHP exposure (either low 0.5 μg/L or high 50 μg/L concentration) in combination with a +3°C increased temperature scenario were studied.

An increase in temperature accelerates metabolic rate, mitochondrial respiration and production of ROS, raising the energy demand with a consequent oxygen deficit (Abele, 2002; Heise et al., 2003; Lushchak, 2011). The related damage in mitochondrial membrane and the increased reduction of oxygen in O_2^- may eventually lead to cellular damage and death when not counterbalanced by the antioxidant system (Sokolova et al., 2011). A moderate thermal increase can stimulate essential antioxidant defences such as catalase (CAT), a key enzymatic catalyst for reduction of the ROS hydrogen peroxide (H_2O_2) to water (Halliwell and Gutteridge, 2015; Regoli and Giuliani, 2014). Rising CAT levels by increasing temperature have already been demonstrated in different phyla, including molluscs (Abele et al., 1998; Hu et al., 2015; Rahman et al., 2019; Verlecar et al., 2007). Interestingly, in **Supplementary Appendix to Chapter 2**, high temperature did not only have a significant effect on *cat* expression in males but seemed to accentuate the toxic effect of DEHP as well on this enzyme. A significant effect was found for both stressors combined, especially for the low DEHP concentration treatment (LOW DEHP HIGH T). When combined, the two stressors provoked a wide array of responses also in RNA-seq analysis (**Chapter 3**). In fact, the combination of the two stressors (by +3°C increased temperature and low DEHP exposure at 0.5 μg/L) resulted in a significant upregulation of transcripts related to fertility, muscle activity, DNA damage response and apoptosis, indicating that environmentally relevant concentrations of DEHP combined with average predicted increases in temperature over a seven-day timeframe have negative consequences for mussels at various biological levels.

7.3 The effect of DEHP in combination with low pH

The anticipated decrease in oceanic pH will primarily be caused by the water absorption of CO_2 and marginally by other conditions such as regional variability in physical, biological and chemical parameters (Hurd et al., 2018). The predicted pH drop of 0.4 units by 2100 for the high-emission scenario (SSP 3 - 7) would represent a 2.5 time increase in hydrogen ion presence with respect to pre-industrial values (Feely et al., 2009). Oceanic pH is also projected to decrease greatly at high latitudes and in the Arctic Sea, considering that the melting of ice due to global warming conditions causes an expansion of the air-sea gas exchange surface and enhances the CO_2 flux by the dilution of dissolved inorganic carbon with freshwater (Kwiatkowski et al., 2020; Terhaar et al., 2020; Yamamoto-Kawai et al., 2009). Moreover, the surface pH seasonal amplitude is projected to decrease at low- and mid- latitudes with high certainty by -10 ± 5 % (Kwiatkowski et al., 2020).

Ocean acidification could eventually lead to important consequences such as physiological alterations and changes at molecular, sensory or metabolic levels in fish (Feugére et al., 2021; Munday et al., 2009; Nilsson et al., 2012), worms (Langenbuch et al., 2006) snails (Watson et al., 2003) or crustaceans (Roggatz et al., 2016; Schirrmacher et al., 2021) and at the ecosystem levels as well (Kroeker et al., 2010), even if some of these species could better tolerate this acidification due to their high mobility, metabolism or control of the ion exchange (Gutowska et al. 2008; Kroeker et al., 2010; Melzner et al. 2009). Moreover, elevated CO_2 is known to increase the H^+ concentrations in the extracellular space and body fluids and disrupt acid - base regulation and balance (Feely et al., 2018; Kroeker et al., 2010) especially in early stages (Durland et al., 2021; Kroeker et al., 2010; Tseng et al., 2013), which can result in delayed development or altered growth. In bivalves, a decrease in pH can alter immune and anti-predator responses (Bibby et al., 2008; Jahnsen-Guzmán et al., 2022), affect calcification and energy metabolism gene expressions (Hüning et al., 2013), and impact growth performances in larvae and adults during gonadal development (Gazeau et al., 2010; Zhao et al., 2019). There were also reports of low-pH impairment of bioenergetic processes (Shang et al., 2022) or fertilisation success (Munari et al., 2022).

The scenario of increased atmospheric CO_2 levels coincides nowadays with increased plastic pollution of aquatic environments. In this work, the two concentrations of DEHP caused a complex array of responses in combination with different pH (as noted in **Chapter 5)** on the oxygen consumption, a proxy for mussel metabolism. In fact, it seemed

that low DEHP increased the respiration of mussels at low pH (7.7), while high DEHP had an effect in mussels at control pH (8.1), along with a small effect on the valve movements at low pH. In **Chapter 4,** a small effect from only pH was also noticed on the biomineralisation-related gene carbonic anhydrase (*CA2*), but in general, mild consequences of the lowered pH conditions are observable across these experiments. This is possible due to the high adaptability of coastal organisms to fluctuating pH conditions, as described by Thomsen et al. (2017), who observed the high evolutionary fitness adaptation of mussel cohorts pre-adapted to high pCO_2, in contrast to non-adapted ones.

7.4 The influence of sex and gametogenesis status

This thesis, along with other studies, demonstrated how the effect of exogenous stressors could be affected by sex and gametogenesis stage and highlighted the different responses between males and females. In detail, in **Chapters 2** and **4**, significant molecular outcomes were found differentially expressed between sexes, especially in the stress response and for the biomineralisation gene *CA2* (analysed in **Chapter 4**). When exposed to increased temperature, male mussels were observed to be more sensitive to thermal stress, demonstrated by advanced gametogenesis, and an increase in both the expression of reprotoxicity- as well as antioxidant- related genes (particularly *MeER2* and *cat,* **Supplementary Appendix to Chapter 2**). A slight difference between males and females was also noted on the estrogen receptor-related pathway, and females were found more affected by the plasticiser, especially regarding the expression of *MeER1* gene (**Supplementary Appendix to Chapter 2**). When considering the low pH exposure, no effect of the stressors was noticed on either sex when exposed to DEHP and lowered pH, possibly due to the different origin of the population or the more advanced maturation state of the gonads. On the other hand, the gametogenesis stage of the two sexes influenced significantly the stress response (*sod, cat, hsp70*) in **Chapter 4**, alone or in combination with the plasticiser**.**

It is well known that common biomarkers of stress such as antioxidant and peroxisomal enzymes undergo seasonal variation during the mussel annual cycle (Bocchetti and Regoli, 2006; Jarque et al., 2014). As an example, in *Mytilus* spp., a reduction of SOD and CAT was noticed during the winter months (Viarengo et al., 1991) and HSP70 presented variable levels between autumn and summer (Hamer et al., 2004; Roberts et al.,

1997). This could be related to external conditions such as water temperature or food availability, but also to the annual reproductive cycle. The expression of the estrogen receptors shows seasonal variations as well, with low values in winter (Raingeard et al., 2013) and increased levels in spring (Zhu et al., 2022), with differences through the years possibly associated to environmental cues and nutrient supply (Ciocan et al., 2010b). In the literature, there are many examples of altered responses of different maturation stages of mussels when exposed to external chemicals (e.g., synthetic estrogens or polycyclic aromatic hydrocarbons), with a significant effect on the activity of antioxidants such as CAT and GPx or on the expression of genes such as *MeER2* and *VTG* (Ciocan et al., 2010a; Cubero-Leon et al., 2010; González-Fernández et al., 2016), with no or little effect on mature stages. This finding emphasises, along with other studies (Banni et al., 2011; Chapman et al., 2017; Koagouw and Ciocan, 2019; Liu et al., 2017; Matozzo and Marin, 2010), the relevance of the identification of sex and maturation state of the investigated individuals when analysing molecular datasets.

7.5 Relevance and contribution to the field

Plastic pollution and changes in oceanic pH are both pressing environmental issues. Following the high (SSP 3 - 7) and very high (SSP 5 - 8.5) scenarios predicted by the IPCC (2021), the CO_2 emissions will double from current levels by 2100 and 2050, respectively, with a consequent increase in global temperature of 3 - 5 °C and a decrease in oceanic pH of 0.3 - 0.5 units. The actions of these conditions are already having effects on oceanic life from algal populations to benthic organisms (Harvey et al., 2013). The induced responses are often species-specific (Gu et al., 2019; Lefevre, 2016) and include shifts in population distributions, alterations in dispersal patterns and decreasing densities of sensitive species (Bijma et al., 2013; Doney et al., 2012). The biological effects of climate change stress on aquatic species were investigated in the past decades in combination with pharmaceuticals (Cardoso et al., 2019; Koagouw and Ciocan, 2018; Mezzelani et al., 2021; Munari et al., 2018, 2020), heavy metals (Cherkasov et al., 2007; Coppola et al., 2018; Izagirre et al., 2014; Verlecar et al., 2007), illicit drugs (da Silva Souza et al., 2021), polycyclic aromatic hydrocarbon (Kamel et al., 2012), endocrine disruptive chemicals (Wang and Zhang, 2013), pesticides and herbicides (Baag et al.,

2021; Greco et al., 2011), alongside the contributory papers derived from this thesis and further unpublished results herein (Mincarelli et al., 2021; Mincarelli et al., 2022).

This thesis underlined the biological responses that mussels express when exposed to environmentally relevant concentrations of the endocrine disruptor DEHP, alone and in combination with climate change conditions, with particular attention to the sex-related outcomes. As already documented for other endocrine disruptive chemicals, a linear dose-response curve is improbable for DEHP, due to a possible over-saturation of endocrine receptors. In the case of bivalves, it might be also possible that the shell movements in response to different levels of contaminants could modify the xenobiotic uptake and absorption, with a consequent altered effect on biological traits.

The initial hypothesis of this thesis that the endocrine disruptive chemical DEHP will influence the reproductive traits of mussels was found validated. In fact, the reproductive network seems to be the pathway most affected by the plasticiser, but other systems (i.e., antioxidant complex, homeostasis, respiration, behaviours) were shown to be sensitive to DEHP, alone or in combination with end-of-the-century environmental conditions (i.e., high temperature in **Chapter 2** and **3** and low pH in **Chapter 4** and **5**). However, the initial hypothesis that the combined effect of climate change conditions and DEHP exposure would be able to stimulate a stronger stress reaction in comparison with the responses to the single stressors found no uniform confirmation. In fact, these Chapters showed different magnitudes of the stress response mainly on the base of sex and the gametogenesis state in which the individuals were at the time of sampling. However, the results from the RNA-seq (**Chapter 3**) showed DNA damage-related processes that took place in male gonads exposed to the combined conditions of increased temperature and low DEHP concentration, suggesting an intensification of the damage that was not otherwise observed when analysing the effect of the single stressors. Regarding the hypothesised histological abnormalities from the exposure to the altered climate conditions, we found a sex-associated pattern of response, with an effect of simulated global warming in only male gonads (i.e., acceleration of gonadal maturation, **Chapter 2**), while female eggs were affected by the DEHP exposure at low concentration (i.e., smaller eggs, possibly associated with altered meiosis and/or vitellogenesis, **Chapter 6**). Considering that also male spermiogenesis and sperm motility were affected by the LOW DEHP treatment (**Chapter 3**), it could be hypothesised that the small female egg size is related to altered or failed fertilisation. These results are relevant to the field of ecotoxicology, as they might assist in understanding the effect of plastic additives on

sentinel species, alone or against the climate-changing backdrop of global warming and ocean acidification.

7.6 Limitation to the research

This thesis provided new insights into the research on plastic additive effects on marine invertebrates in future climate-changing scenarios. However, some limitations out of our control need to be addressed. First, chemical analysis on water and/or tissues to measure the presence and/or the accumulation of DEHP were not performed, due to the lack of access to lab facilities during the COVID-19 pandemic and reduced funds intended for additional research. Secondly, the potential contamination of samples through plastic consumables and equipment was unavoidable. Nonetheless, thanks to the use of internal group controls to which the DEHP-treated mussels were compared, this thesis provided strong data about the effect of this plasticiser on histological, molecular, transcriptomic, metabolic and behavioural systems of marine mussels and whether these responses differ by sex.

7.7 Future work

This thesis aimed to investigate the relationship between single and combined short-term responses of blue mussels to contaminants and environmental factors (i.e., DEHP exposure, increased temperature and low pH). Assuming that the future climate conditions (i.e., global warming and ocean acidification) will increase the leakage of dangerous additives from plastic items into the environment, marine species will be exposed to ubiquitous concentrations of these toxic compounds, possibly leading to more pronounced responses in terms of general biological (i.e., stress, homeostasis, metabolism, behaviours) responses and variations in the reproduction cycle. This thesis firstly assessed the *Mytilus* spp. responses to two environmentally relevant levels of DEHP in combination with either one of the climate stressors. However, there is still a knowledge gap in discovering the exact way of action and response curves of the plasticiser DEHP, and whether lower concentrations or prolonged exposures than the ones used in this experiment are dangerous to marine life. It is important to note that even though DEHP is restricted in the European Union, it is still used worldwide as a plastic

additive and low levels are commonly found in natural environments. Additionally, these experiments assessed the background effect of the single climate-changing scenarios on marine mussels. Considering the projected high-emission conditions for 2100 will include the combination of global warming and ocean acidification conditions, future projects should definitely include both these experimental designs together.

Supplementary Appendix to Chapter 1

Supplementary Table 1.1 Phthalate concentrations found in natural environments

COMPOUND	TOXICITY	SITE	CONCENTRATION	REFERENCES
DMP Dimethyl phthalate $C_{10}H_{10}O_4$ CAS Number 131-11-3	Not a hazardous substance	Seawater from Tees Bay (UK)	<1 x 10^{-3} µg/L	Law et al., 1991
		Seawater and atmosphere in the North Sea	0.02 to 0.68 ng/L in seawater (dissolved) 0.01 to 0.07 ng/L in the total suspended matter 0.16 to 0.54 ng/m^2 in atmosphere vapour ND in the particle (air)	Xie et al., 2005
		Surface seawater (Netherlands)	0.004 to 0.49 µg/L	Vethaak et al., 2005
		Seawater and sediment from False Creek Harbour (Canada)	0.0035 µg/L in seawater	Mackintosh et al., 2006
		Rainwater depositions from Paris urban area (France)	0.116 µg/L	Teil et al., 2006
		Seawater from Bay of Biscay (Spain)	(7.5 $\pm$ 0.4) x 10^{-3} µg/L	Prieto et al., 2007
		Arctic	40 x 10^{-6} µg/L	Xie et al., 2007
		Caspian Sea (Iran)	0.49 µg/L	Hadjmohammadi et al., 2011
		Coastal seawater, Mediterranean Sea (Spain)	0.003 to 0.14 µg/L	Sánchez-Avila et al., 2012
		Marseille Bay (France)	0.0008 to 0,0011 µg/L	Paluselli et al., 2018
		Bohai Sea and Yellow Sea (China)	0.00153 to 0.00654 µg/L	Zhang et al., 2018
		Coastal waters (South Korea)	0.02–0.10 µg/L	Heo et al., 2020
		Cochin estuary (India)	ND - 1.945 µg/L	Ramzi et al., 2020

DEP Diethyl phthalate $C_{12}H_{14}O_4$ CAS Number 84-66-2	Not a hazardous substance	Rivers in the Manchester area (UK)	0.1 to 0.6 µg/L	Fatoki and Vernon, 1990
		Seawater from Tees Bay, (UK)	0.025 to 0.5 µg/L	Law et al., 1991
		Seawater and atmosphere in the North Sea	0.03 to 0.71 ng/L in seawater (dissolved) ND to 0.068 ng/L in the total suspended matter 0.64 to 1.6 ng/m in atmosphere vapour ND to 0.18 in the particle (air)	Xie et al., 2005
		Surface seawater (Netherlands)	0.007 to 2.3 µg/L	Vethaak et al., 2005
		Rainwater depositions from Paris urban area (France)	0.333 µg/L	Teil et al., 2006
		Seawater from Bay of Biscay (Spain)	$(33 \pm 3) \times 10^{-3}$ µg/L	Prieto et al., 2007
		Arctic	138×10^{-6} µg/L	Xie et al., 2007
		Caspian Sea (Iran)	0.52 µg/L	Hadjmohammadi et al., 2011
		Coastal seawater, Mediterranean Sea (Spain)	0.024 to 0.48 µg/L	Sánchez-Avila et al., 2012
		Marseille Bay (France)	0.0033 to 0.50 µg/L	Paluselli et al., 2018
		Bohai Sea and Yellow Sea (China)	0.00176 to 0.00873 µg/L	Zhang et al., 2018
		Coastal waters (South Korea)	0.02–0.15 µg/L	Heo et al., 2020
		Cochin estuary (India)	ND - 3.193µg/L	Ramzi et al., 2020
		Marine water (Tunisia)	Average 12.6 µg/L	Jebara et al., 2021
DPP Dipentyl phthalate $C_{18}H_{26}O_4$ CAS Number 131-18-0	Reproductive toxicity	Bohai Sea and Yellow Sea (China)	ND to 0.00107 µg/L	Zhang et al., 2018

DBP or DnBP Dibutyl phthalate $C_{16}H_{22}O_4$ CAS Number 84-74-2	Reproductive toxicity Acute aquatic toxicity	Rivers in the Manchester area (UK)	6.0 to 33.5 µg/L	Fatoki and Vernon, 1990
		Seawater from Tees Bay, UK	0.47 to 0.55 µg/L	Law et al., 1991
		Lakes in Tianjin City (China)	0.00925 to 0.02394 µg/mL (subsurface water) 10.89 to 89.78 ng/mL (water surface microlayer)	Huang et al., 1999
		Rivers, lakes and channels, sewage effluents and sludges (Germany)	0.12 to 9.80 µg/L (surface water) 0.06 to 2.08 mg/kg(sediment)	Fromme et al., 2002
		Seawater and atmosphere in the North Sea	0.45 to 6.6 ng/L in seawater (dissolved) 0.01 to 0.04 ng/L in the total suspended matter 0.17 to 0.53 ng/m^2 in atmosphere vapour 0.10 to 1.2 in the particle (air)	Xie et al., 2005
		Surface seawater (Netherlands)	<0.066 to 3.1 µg/L	Vethaak et al., 2005
		Freshwater, sediment (Netherlands)	Medial levels 0.21 µg/L (freshwater) 25.3 µg/kg (sediments)	Peijnenburg and Struijs, 2006
		Rainwater depositions from Paris urban area (France)	0.592 µg/L	Teil et al., 2006
		Seawater from Bay of Biscay (Spain)	$(83 \pm 7) \times 10^{-3}$ µg/L	Prieto et al., 2007
		Arctic	51×10^{-6} µg/L	Xie et al., 2007
		Barkley Sound (Canada)	0.18 to 3.0 µg/L	Keil et al., 2011
		Marseille Bay (France)	0.012 to 0.596 µg/L	Paluselli et al., 2018
		Bohai Sea and Yellow Sea (China)	0.266 to 1.584 µg/L	Zhang et al., 2018

		Coastal waters (South Korea)	0.04 – 0.36 µg/L	Heo et al., 2020
		Cochin estuary (India)	ND - 20.368 µg/L	Ramzi et al., 2020
		House dust	17.6–666.8 µg/g	Xu and Li, 2020
		Marine water (Tunisia)	Average 17.2 µg/L	Jebara et al., 2021
DiBP Diisobutyl phthalate $C_{16}H_{22}O_4$ CAS Number 84-69-5	Reproductive toxicity Acute aquatic toxicity Chronic aquatic toxicity	Seawater from Tees Bay (UK)	0.66 to 1.1 µg/L	Law et al., 1991
		Seawater and sediment from False Creek Harbour (Canada)	4.0 ng/g dw in sediment	Mackintosh et al., 2006
		Arctic	22 x 10^{-6} µg/L	Xie et al., 2007
		Marseille Bay (France)	0.0275 to 0,3834 µg/L	Paluselli et al., 2018
		Bohai Sea and Yellow Sea (China)	0.0955 to 0.767 µg/L	Zhang et al., 2018
		House dust	9.6–242.3 µg/g	Xu and Li, 2020
		Marine water (Tunisia)	Average 75.4 µg/L	Jebara et al., 2021
DnOP Di-n-octyl phthalate $C_{24}H_{38}O_4$ CAS Number 117-84-0	Chronic aquatic toxicity	Surface seawater (Netherlands)	0.002 to 0.078 µg/L	Vethaak et al., 2005
		Rainwater depositions from Paris urban area (France)	0.010 µg/L	Teil et al., 2006
		Seawater from Bay of Biscay (Spain)	(3.6 $\pm$ 0.4) x 10^{-3} µg/L	Prieto et al., 2007
		Cochin estuary (India)	ND - 0.838 µg/L	Ramzi et al., 2020
DIOP Diisooctyl phthalate $C_{24}H_{38}O_4$ CAS Number 27554-26-3	Low toxicity via the oral and dermal routes (Toxnet)	Rivers in the Manchester area (UK)	0.8 to 3.0 µg/L	Fatoki and Vernon, 1990
BBP Benzyl butyl	Reproductive toxicity	Seawater and atmosphere in the North Sea	0.01 to 0.26 ng/L in seawater (dissolved) ND to 0.03 ng/L in the	Xie et al., 2005

phthalate $C_{19}H_{20}O_4$ CAS Number 85-68-7	Acute aquatic toxicity Chronic aquatic toxicity		total suspended matter 0.01 to 0.05 ng/m in atmosphere vapour 0 to 0.06 in the particle (air)	
		Surface seawater (Netherlands)	0.001 to 1.8 µg/L	Vethaak et al., 2005
		Rainwater depositions from Paris urban area (France)	0.081 µg/L	Teil et al., 2006
		Seawater from Bay of Biscay (Spain)	$(8 \pm 1) \times 10^{-3}$ µg/L	Prieto et al., 2007
		Arctic	8×10^{-6} µg/L	Xie et al., 2007
		Coastal seawater, Mediterranean Sea (Spain)	0.001 to 0.10 µg/L	Sánchez-Avila et al., 2012
		Marseille Bay (France)	0.0026 to 0,061 µg/L	Paluselli et al., 2018
		Bohai Sea and Yellow Sea (China)	ND to 0.00362 µg/L	Zhang et al., 2018
		Cochin estuary (India)	ND to 10.634 µg/L	Ramzi et al., 2020
DMEP Dimethylglycol phthalate		Bohai Sea and Yellow Sea (China)	ND to 0.223 µg/L	Zhang et al., 2018
MEP Monoethyl phthalate $C_{10}H_{10}O_4$ CAS Number 2306-33-4	Moderate skin, respiratory and eye irritation (Toronto Research Chemical)	Seawater, marine sediments from False Creek (Canada)	4.41 to 38.83 ng/L in seawater 0.45 to 3.63 ng/g dw in sediments	Blair et al., 2009
MBzP Monobenzyl phthalate $C_{15}H_{12}O_4$ CAS Number 2528-16-7	Eye irritation	Seawater, marine sediments, from False Creek (Canada)	ND to 6.05 ng/L in seawater 0.19 to 3.02 ng/g dw in sediments	Blair et al., 2009

Supplementary Table 1.2 Selected exposure experiments with aquatic species exposed to phthalate concentrations

COMPOUND	[ ]	TIME	SPECIES	REFERENCES
DAP	50 µg/L	21 days	*Gadus morhua* (Atlantic cod)	Baršiene et al., 2006
	50 µg/L	21 days	*Scophthalmus maximus* (turbot)	Baršiene et al., 2006
	50 µg/L	21 days	*Hyas araneus* (Arctic spider crab)	Minier et al., 2008
	50 µg/L every two days	3 months	*Haliotis diversicolor supertexta* (marine gastropod mollusc)	Zhou et al., 2010
DBP	0, 2.59, 5.18, 6.90, And 10.35 mg/L	24 hours	*Daphnia magna*	Huang et al., 1999
	up to 2 mg/L	96 h	*B. calyciflorus* (rotifer)	Cruciani et al., 2016
DiNP	0.42, 4.2 and 42 µg/L	21 days	*Danio rerio* (females)	Godoi et al., 2021
DnBP	125, 250, 500 and 1000 µg/L everyday	7 days	*Melanotaenia fluviatilis* (female adult Murray rainbowfish)	Bhatia et al., 2013
BBP	up to 2 mg/L	96 h	*B. calyciflorus* (rotifer)	Cruciani et al., 2016

Supplementary Table 1.3 Selected exposure experiments with mussels exposed to phthalate or endocrine disruptive chemicals

PHTHALATE	[ ]	TIME	SPECIES	REFERENCES
BPA Bisphenol A (Plastic additive)	1 and 10 µg/L	24 and 48 hours	*M. galloprovincialis* (trochophore and D-veligers)	Balbi et al., 2016
BPA Bisphenol A (Plastic additive)	22.83 ng/L –228.3 µg/L	3 and 24 hours	*M. galloprovincialis* (digestive gland primary cell cultures)	Balbi et al., 2017
	4, 12, 36, 108, and 324 µg/L	14 days	*M. galloprovincialis*	Xu et al., 2021
DAP	50 µg/L	21 days	*M. edulis*	Baršiene et al., 2006; Sundt et al., 2006
	50 µg/L	21 days	*M. edulis*	Aarab et al., 2006; Sundt et al., 2006
	50 µg/L	21 days	*M. edulis*	Burlando et al., 2006
	50 µg/L	One month	*M. edulis*	Jonsson et al., 2006; Sundt et al., 2006
	50 µg/L	21 days	*M. edulis*	Cajaraville and Ortiz-Zarragoitia, 2006; Ortiz-Zarragoitia and Cajaraville, 2006; Sundt et al., 2006
KHP	250, 500, 750 and 1000 mg/kg of mussel	21 days	*M. galloprovincialis*	Sif et al., 2016
DBP	20 nCi into the medium (phytoplankton)	0.5, 1, 1.5, 2 hours	*P. viridis*	Wang and Zhang, 2013

Supplementary Appendix to Chapter 2

S2.1 Stress-related response: male and female gene expression

Considering the overall expression (i.e., *sod*, *cat*, or *hsp70* gene expression) of stress-related genes in males, PERMANOVA analysis underlined a significant effect of temperature on increased mRNA expressions of *sod*, *cat* and *hsp70* (*p* TEMP = 0.014, F = 4.72, **Supplementary Fig. 2.1 left**). Regarding females, no significant effect of DEHP and temperature was noticeable on these stress response markers (**Supplementary Fig. 2.1 right**). A non-significant but marginal effect was noted on the male stress response when exposed to only DEHP additive (*p* DEHP = 0.060, F = 2.35, **Supplementary Fig. 2.1 left**), while examples of significant results about the activity of these enzymes were found in bivalve molluscs from urban and polluted areas (El Jourmi et al., 2015; Nasci et al., 2002; Vlahogianni et al., 2007) or when exposed to heavy metals (Boudjema et al., 2014), synthetic estrogens (Canesi et al., 2007a) or antibacterials (Canesi et al., 2007b).

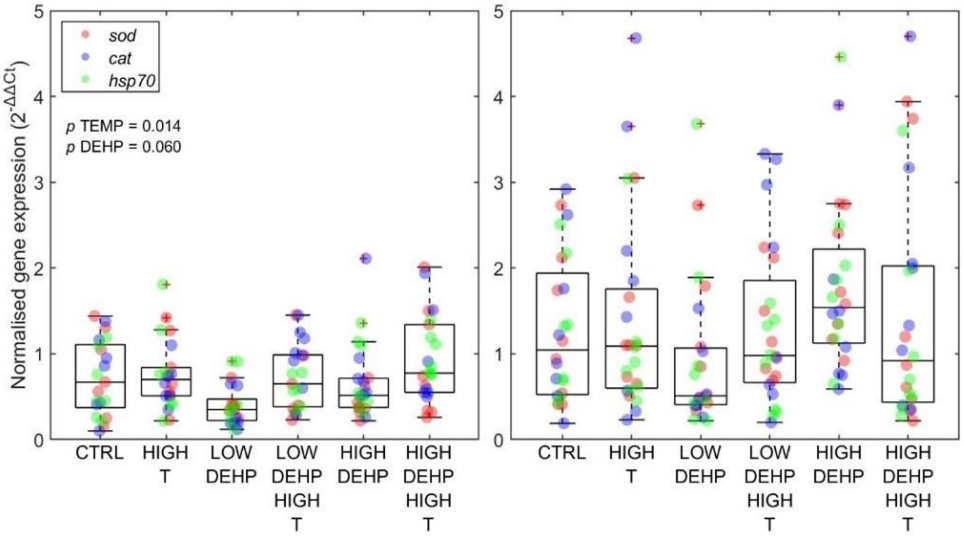

Supplementary Fig. 2.1 left) Stress-related (*sod*, *cat*, *hsp70*) gene expression in males, n = 6 to 8 **right)** Stress-related (*sod*, *cat*, *hsp70)* gene expression in females, n = 7 to 8. Abbreviations are control (CTRL), high temperature (HIGH T), low DEHP concentration (LOW DEHP), low DEHP at high temperature (LOW DEHP HIGH T), high DEHP concentration (HIGH DEHP) and high DEHP at high temperature (HIGH DEHP HIGH T). PERMANOVA error probabilities are annotated

S2.2 Stress-related response: individual gene expression

Regarding the individual gene expression in male mussels, *cat* mRNA expression was significantly increased by temperature (SRH *p* TEMP = 0.041, H = 4.17) and by the combined effect of temperature and DEHP (SRH *p* TEMP*DEHP = 0.040, H = 6.46 **Supplementary Fig. 2.3**). It is worth noting that while *cat* expression was influenced by environmental stressors, temperature and DEHP exposure had no effect on the expression of the related antioxidant *sod* ($p > 0.05$, **Supplementary Fig. 2.2**). Antioxidant enzymes can be inhibited by cellular products, such as singlet oxygen, ozone hydroxyl and peroxyl radicals (Escobar et al., 1996). Differences in the activities of CAT and SOD were already observed in previous experiments involving bivalves on different days of exposure to heavy metals and endocrine disruptors (Gonzalez-Rey and Bebianno, 2013; Orbea et al., 2002; Zhang et al., 2010), showing in some cases even an inverted trend (Monteiro et al., 2019). Similarly, in *D. polymorpha* and *Unio tumidus*, various tissues and time-specific enzymatic responses of SOD were noted after exposure to microcystin-LR or cyanobacterial crude extract, with not always a clear dose-response pattern (Burmester et al., 2012). Manduzio et al., (2003) found three available isoforms of the Cu/Zn SOD in *M. edulis*, with only one of them (SOD-3 130 kDa) inducible by a 7-day exposure to 25 μg/L of copper pollution. The presence of a presumed weak Mn- isozyme was also hypothesised, with a considered negligible activity in mussels with respect to the Cu/Zn form (Livingstone et a., 1992). These results underline the lack of knowledge about inhibition patterns, structure and transient activity of the antioxidant system in mussels exposed to multiple or prolonged stressors.

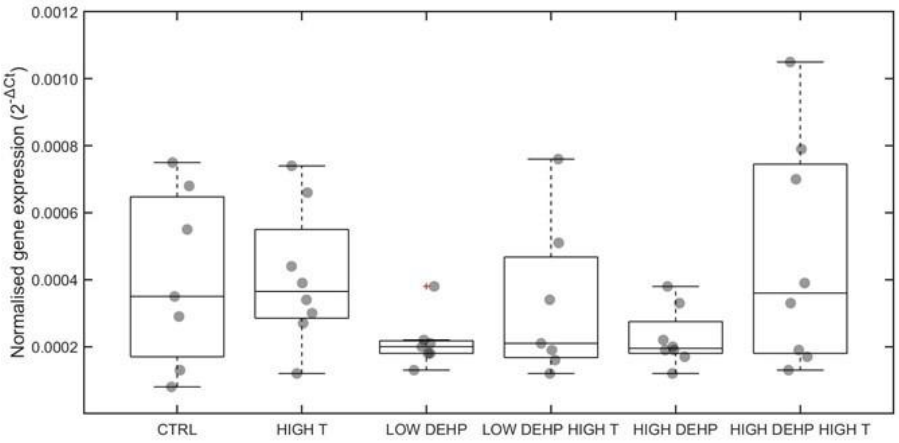

Supplementary Fig. 2.2 *sod* mRNA expression in males, n = 7 to 8. Abbreviations are control (CTRL), high temperature (HIGH T), low DEHP concentration (LOW DEHP), low DEHP at high temperature (LOW DEHP HIGH T), high DEHP concentration (HIGH DEHP) and high DEHP at high temperature (HIGH DEHP HIGH T). No significant differences were found

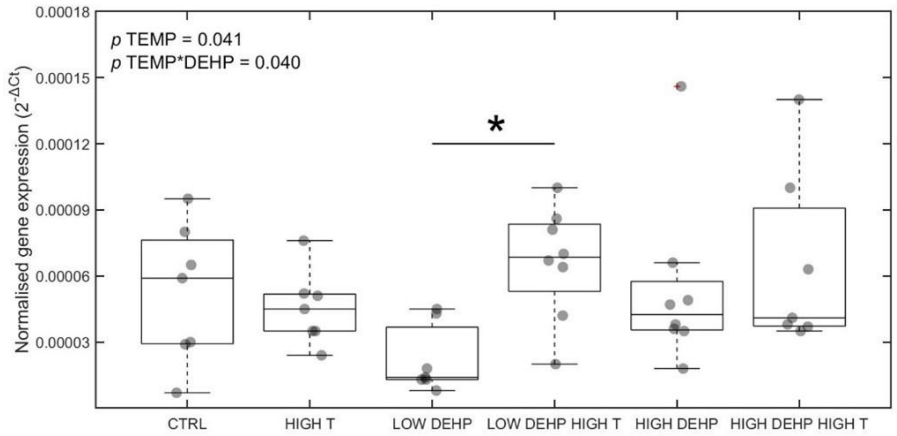

Supplementary Fig. 2.3 *cat* mRNA expression in males, n = 7 to 8. Abbreviations are control (CTRL), high temperature (HIGH T), low DEHP concentration (LOW DEHP), low DEHP at high temperature (LOW DEHP HIGH T), high DEHP concentration (HIGH DEHP) and high DEHP at high temperature (HIGH DEHP HIGH T). Significant differences between groups and relative error probabilities are denoted by bars above the boxplots

Regarding *hsp70* expression in males, it was marginally (but not significantly) modulated by DEHP exposure (SRH *p* DEHP = 0.079, H = 5.06) and a slight but also non-significant effect of temperature was observed (SRH *p* TEMP = 0.102, H = 2.68**, Supplementary Fig. 2.4**). HSP70s play a crucial role in repairing partially denatured proteins and in the cellular protection from stress-induced damage, protein folding and translocation (Feder and Hofmann, 1999; Fink, 1999) and they can be induced by both physical and chemical stressors (Sanders, 1993). The slight but not significant increase of *hsp70* expression to a

higher temperature in males could be explained by an attenuated heat-shock response under laboratory acclimation (Roberts et al., 1997), or the recent thermal history of the organism (Buckley et al., 2001). Due to the high-energy cost required for the HSP synthesis, a heat shock response that is mitigated over periods of persistent stress, might allow the allocation of energy reserves to other fitness-relevant processes (Tomanek and Somero, 1999; Troschinski et al., 2014). On the other hand, total HSP70 in *M. californicanus* increased in mussels exposed to higher thermal and desiccation stress, along with an earlier spawning activity (Petes et al., 2008). Another hypothesis for the mild HSP70 response is that, as remarked by Franzellitti and Fabbri (2005), the partial sequence for *M. edulis hsp70* used in this work could encode for a constitutive HSP70 isoform that is more associated with prolonged stress exposure instead of short-term responses.

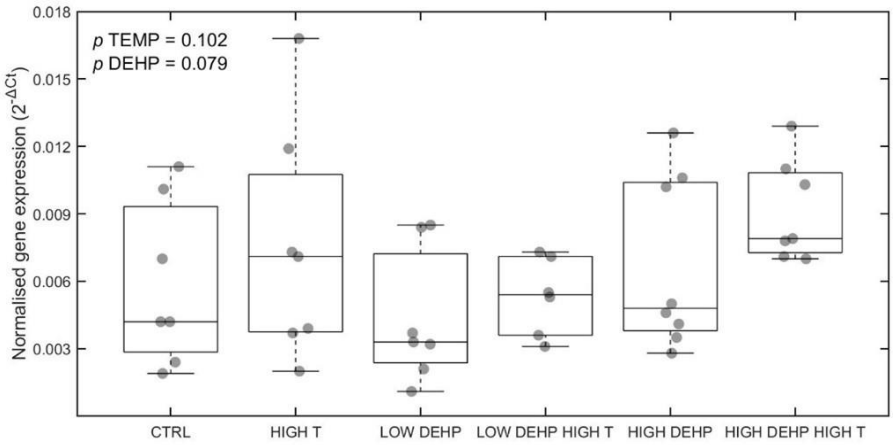

Supplementary Fig. 2.4 *hsp70* mRNA expression in males, n = 6 to 8. Abbreviations are control (CTRL), high temperature (HIGH T), low DEHP concentration (LOW DEHP), low DEHP at high temperature (LOW DEHP HIGH T), high DEHP concentration (HIGH DEHP) and high DEHP at high temperature (HIGH DEHP HIGH T). Scheirer-Ray-Hare test error probabilities are annotated

In contrast to males, females did not show any significant differences in the expression of *sod, cat, hsp70* from either the temperature or the DEHP exposure (SRH $p > 0.05$, **Supplementary Fig. 2.5, 2.6, 2.7**).

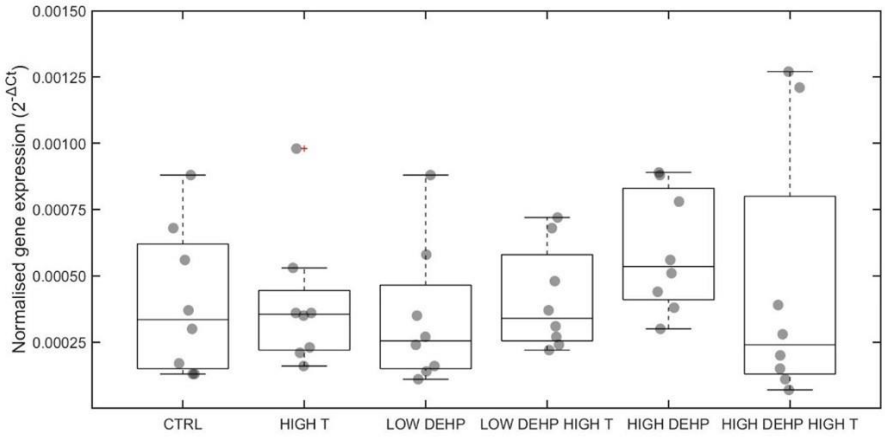

Supplementary Fig. 2.5 *sod* mRNA expression in females, n = 8. Abbreviations are control (CTRL), high temperature (HIGH T), low DEHP concentration (LOW DEHP), low DEHP at high temperature (LOW DEHP HIGH T), high DEHP concentration (HIGH DEHP) and high DEHP at high temperature (HIGH DEHP HIGH T). No significant differences were found

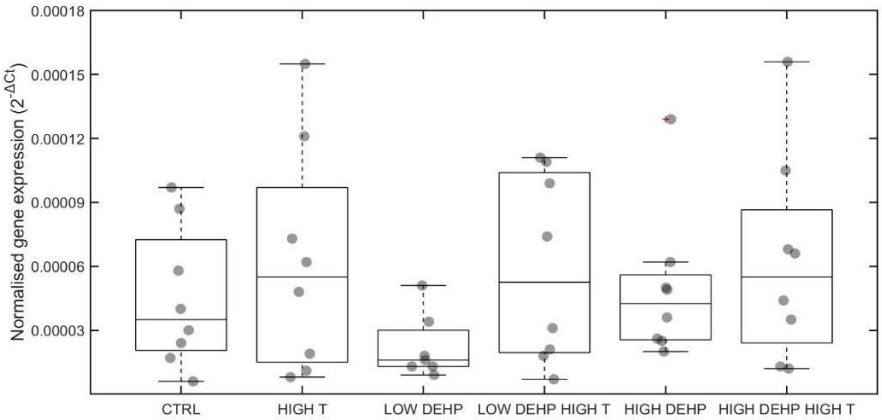

Supplementary Fig. 2.6 *cat* mRNA expression in females, n = 7 to 8. Abbreviations are control (CTRL), high temperature (HIGH T), low DEHP concentration (LOW DEHP), low DEHP at high temperature (LOW DEHP HIGH T), high DEHP concentration (HIGH DEHP) and high DEHP at high temperature (HIGH DEHP HIGH T). No significant differences were found

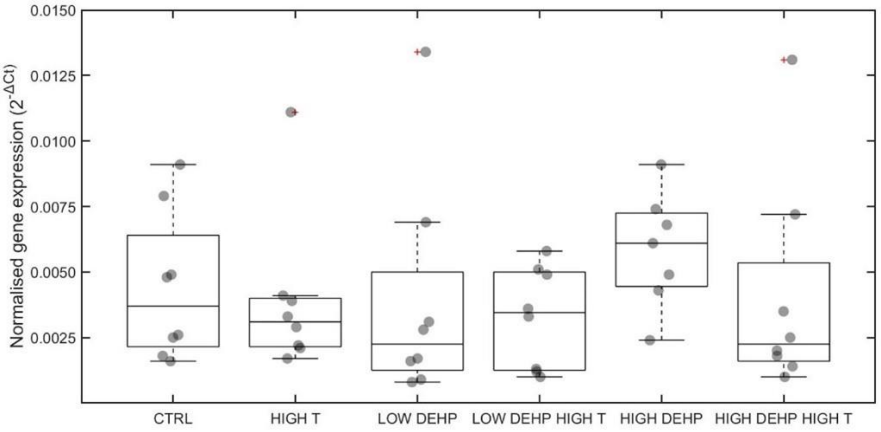

Supplementary Fig. 2.7 *hsp70* mRNA expression in females, n = 7 to 8. Abbreviations are control (CTRL), high temperature (HIGH T), low DEHP concentration (LOW DEHP), low DEHP at high temperature (LOW DEHP HIGH T), high DEHP concentration (HIGH DEHP) and high DEHP at high temperature (HIGH DEHP HIGH T). No significant differences were found

S2.3 Estrogen receptor-like response: male and female gene expression

High temperature increased the expression of *MeER1* and *MeER2* in males (*p* TEMP = 0.005, F = 5.93, **Supplementary Fig. 2.8 left**). In females, low and high DEHP treatments had opposite effects on gene expression (*p* DEHP = 0.049, F = 0.11, **Supplementary Fig. 2.8 right**).

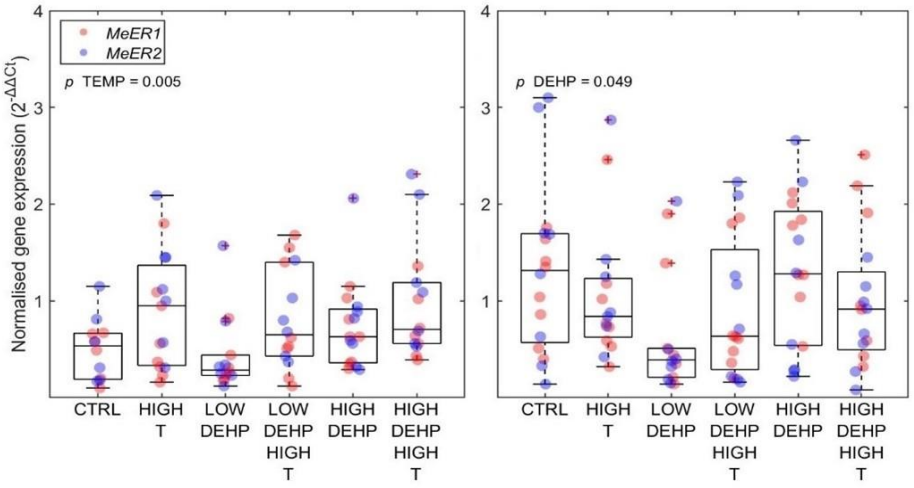

Supplementary Fig. 2.8 left) Estrogen receptor-like (MeER1, MeER2) gene expression in males, n = 6 to 8 **right)** Estrogen receptor-like (MeER1, MeER2) expression in females, n = 7 to 8. Abbreviations are control (CTRL), high temperature (HIGH T), low DEHP concentration (LOW DEHP), low DEHP at high temperature (LOW DEHP HIGH T), high DEHP concentration (HIGH DEHP) and high DEHP at high temperature (HIGH DEHP HIGH T). PERMANOVA error probabilities are annotated

S2.4 Estrogen receptor-like response: individual estrogen receptor-like responses

Considering the individual gene response, no effect on the expression of males' *MeER1* was noted ($p > 0.05$, **Supplementary Fig. 2.9**). Surprisingly, our study highlighted a temperature effect on *MeER2* expression in males treatments (SRH p TEMP = 0.011, H = 6.55, **Supplementary Fig. 2.10**). Males in higher temperature treatments displaying advanced spawning stages may constitute a causal link to elevated *MeER2* levels. A similar effect of temperature on *MeER2* upregulation was recently observed by Koagouw and Ciocan (2018). Smolarz et al. (2018) suggested that steroids such as estrogens and androgens might be active modulators of only the final stage of the gametogenesis cycle (i.e., spawning), as they appear to be more associated with environmental cues such as water temperature. *MeER2* expression in *M. edulis* in their natural environment varied in mature gonads in different years (Ciocan et al., 2010b) suggesting that annual and seasonal environmental cues could lead to nuances in the gametogenesis status and the related estrogen-like responses. In contrast to the temperature effect, the exposure to environmentally relevant concentrations of DEHP (both 0.5 and 50 μg/L) did not elicit an estrogenic effect on males. Similarly, no effects were found in male ricefish *Oryzias latipes* exposed to concentrations up to 50 μg/L (Kim, 2003), but significantly higher concentrations of 100 and 500 μg/l caused an increase in estradiol levels and reduced number of spermatozoa in *Oryzias melastigma* males (Ye et al., 2014). In Puinean et al., (2006), the non-significance of the estrogen effect was explained by a possible homeostatic mechanism of conversion into inactive esters, alongside the duration and level of exposure. Our results suggest no reprotoxicity effect of DEHP on gametogenesis timing in male blue mussels at environmentally relevant concentrations, but other adverse effects such as germ cell toxicity cannot be excluded at this time.

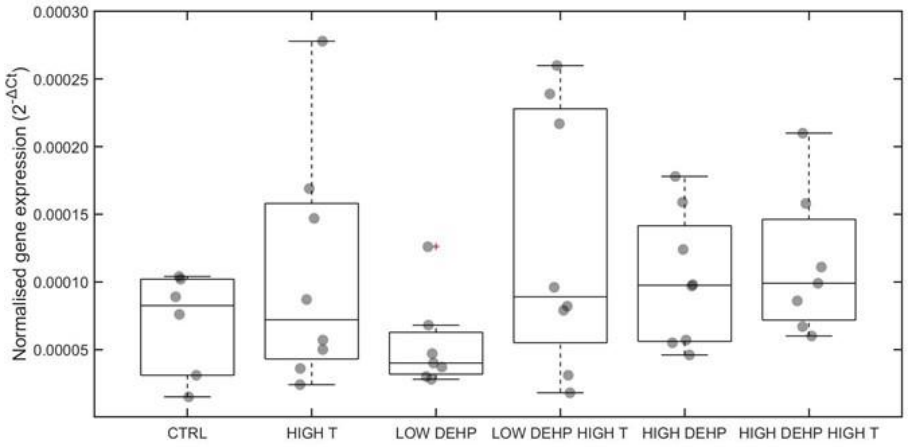

Supplementary Fig. 2.9 *MeER1* mRNA expression in males, n = 6 to 8. Abbreviations are control (CTRL), high temperature (HIGH T), low DEHP concentration (LOW DEHP), low DEHP at high temperature (LOW DEHP HIGH T), high DEHP concentration (HIGH DEHP) and high DEHP at high temperature (HIGH DEHP HIGH T). No significant differences were found

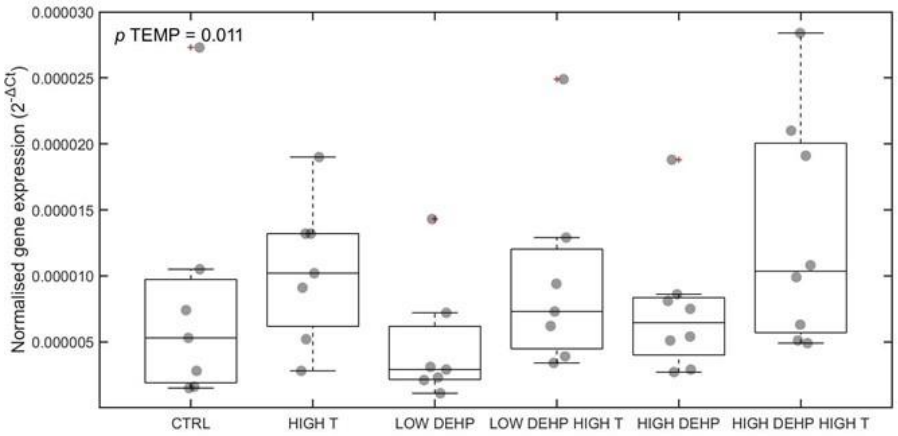

Supplementary Fig. 2.10 *MeER2* mRNA expression in males, n = 7 to 8. Abbreviations are control (CTRL), high temperature (HIGH T), low DEHP concentration (LOW DEHP), low DEHP at high temperature (LOW DEHP HIGH T), high DEHP concentration (HIGH DEHP) and high DEHP at high temperature (HIGH DEHP HIGH T). Scheirer-Ray-Hare test error probability is annotated

In female mussels, *MeER1* mRNA expression was significantly influenced by the DEHP exposure (SRH *p* DEHP = 0.041, H = 6.40, **Supplementary Fig. 2.11**), but neither temperature nor DEHP exposure had an effect on the expression of *MeER2* in females (*p* > 0.05, **Supplementary Fig. 2.12**). Similarly, exposure to chemicals such as EE2 and the surfactant sodium lauryl sulphate induced expression of *ER1* in *M. galloprovincialis* digestive tubules, while in gonads the expression was weakly downregulated, probably due to their spent stage (Lopes et al., 2022). Here, *MeER1* levels were lower in the low-

concentration groups compared to both control and high DEHP treatments, thus a linear dose response does not appear to be present. In fact, we found a lowered *MeER1* expression at 0.5 µg DEHP/L and higher expression in response to 50 µg/L DEHP at control temperature. Molluscs seem more sensitive to exposure to plasticisers in water at concentrations in the order of magnitude of micrograms per litre (Oehlmann et al., 2008), and as already described, endocrine active chemicals can follow a nonmonotonic dose-response curve (Conolly and Lutz, 2004; Do et al., 2012; Li et al., 2007; Vandenberg et al., 2012). Furthermore, it was recently described that low doses of DEHP can alter the meiotic processes in *C. elegans* nematodes, through considerable morphological defects of chromosomes in oocytes and impaired embryogenesis (Cuenca et al., 2020). Therefore, in light of the effect of DEHP on the female estrogen receptor-like responses observed in this study, we cannot exclude impairment of their reproductive cycle that could affect not only the egg maturation but also larval development.

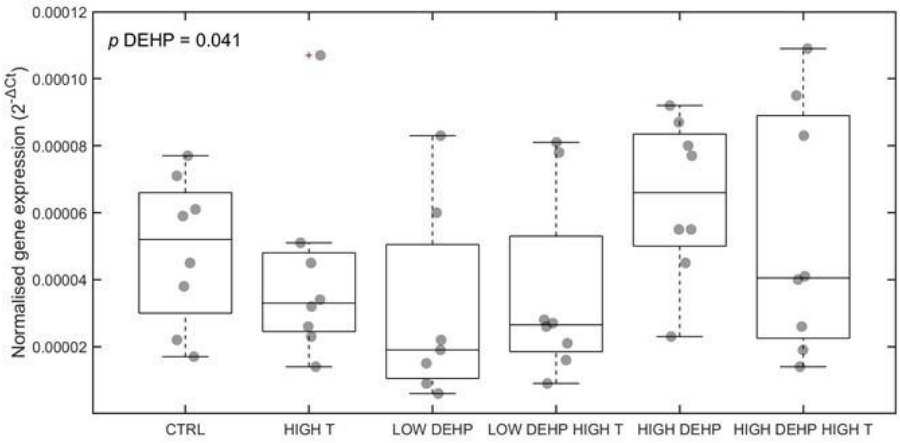

Supplementary Fig. 2.11 *MeER1* mRNA expression in females, n = 7 to 8. Abbreviations are control (CTRL), high temperature (HIGH T), low DEHP concentration (LOW DEHP), low DEHP at high temperature (LOW DEHP HIGH T), high DEHP concentration (HIGH DEHP) and high DEHP at high temperature (HIGH DEHP HIGH T). Scheirer-Ray-Hare test error probability is annotated

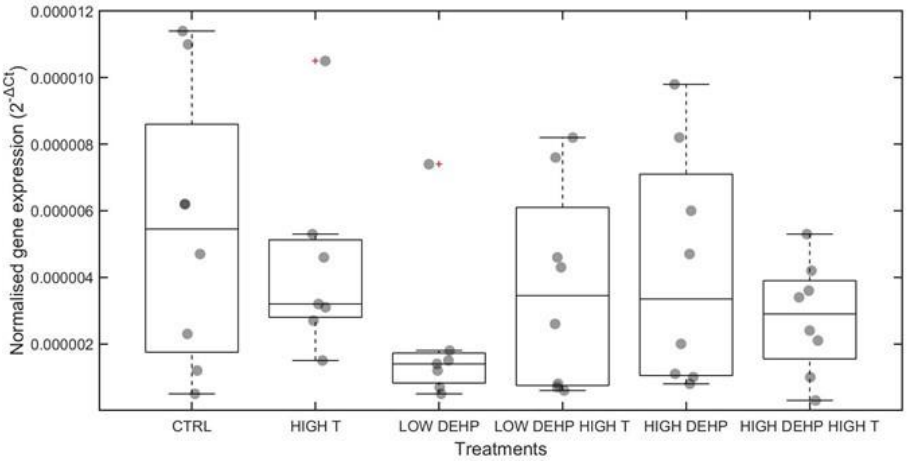

Supplementary Fig. 2.12 *MeER2* mRNA expression in females, n = 7 to 8. Abbreviations are control (CTRL), high temperature (HIGH T), low DEHP concentration (LOW DEHP), low DEHP at high temperature (LOW DEHP HIGH T), high DEHP concentration (HIGH DEHP) and high DEHP at high temperature (HIGH DEHP HIGH T). No significant differences were found

Supplementary Appendix to Chapter 3

S3.1 FastQC quality control

The quality control job was submitted to the HPC Viper as a SLURM submission batch script as follows:

```
#!/bin/bash
#SBATCH -J FASTQC.job
#SBATCH -N 1
#SBATCH -n 28
#SBATCH -o FASTQC.out
#SBATCH -e FASTQC.err
#SBATCH -p highmem
#SBATCH --exclusive
cd /home/userID/
module purge
module add fastqc/0.11.9
fastqc COMB_07_1.fq.gz | fastqc COMB_07_2.fq.gz
fastqc COMB_10_1.fq.gz | fastqc COMB_10_2.fq.gz
fastqc COMB_26_1.fq.gz | fastqc COMB_26_2.fq.gz
fastqc DEHP_12_1.fq.gz | fastqc DEHP_12_2.fq.gz
fastqc DEHP_13_1.fq.gz | fastqc DEHP_13_2.fq.gz
fastqc DEHP_17_1.fq.gz | fastqc DEHP_17_2.fq.gz
fastqc TEMP_08_1.fq.gz | fastqc TEMP_08_2.fq.gz
fastqc TEMP_13_1.fq.gz | fastqc TEMP_13_2.fq.gz
fastqc TEMP_18_1.fq.gz | fastqc TEMP_18_2.fq.gz
```

Where `-J` represents the job name, `-N` represents the number of cores, `-n` represents the number of nodes, `-o` represents the standard output, `-e` represents the standard error and `-p` represents the slurm partition. `highmem` requests more memory than the standard provision of approximately 4 GB. `--exclusive` requests exclusive access to a node.

S3.2 Read trimming with Trimmomatic

The *Trimmomatic* code command was run as follows:

```
module load java/jdk1.8.0_102
module load trimmomatic/0.38/gcc-8.2.0
java -jar /home/ViperAppsFiles/trimmomatic/0.38/gcc-8.2.0/ziyqkicrbkapjo4ugbqasxvviucog2ix/bin/trimmomatic-0.38.jar PE -phred33 -threads 16 -trimlog logfile /home/userID/sample_1.fq.gz /home/userID/sample_2.fq.gz
Paired1_sample_trim.fq Unpaired1_sample_trim.fq Paired2_sample_trim.fq Unpaired2_sample_trim.fq
ILLUMINACLIP:Nextera.fa:2:30:10:2:keepBothReads HEADCROP:11
```

S3.3 Trinity de novo assembly

The *Trinity* slurm job was launched using `-p gpu`, which requests the use of the GPU resources, not the CPU:

```
module add test-modules singularity/3.5.3/gcc-8.2.0
singularity                              exec                              -e
/home/ViperAppsFiles/singularity/containers/Trinity-v2.13.1.simg
Trinity \
            --seqType fq \
            --samples_file data/samples.txt \
          --max_memory 100G --CPU 20 \
          --output /home/userID/Trinity.output.fastafile
```

The `--samples_file data/samples.txt` consisted in a table file in the format *Treatment* (tab) *Sample_id* as follows:

```
COMB    COMB_07
COMB    COMB_10
COMB    COMB_26
DEHP    DEHP_12
DEHP    DEHP_13
DEHP    DEHP_17
TEMP    TEMP_08
TEMP    TEMP_13
TEMP    TEMP_18
```

S3.4 Assessing the read content of the transcriptome assembly

A *bowtie2* index was first built for the transcriptome:

```
singularity                              exec                              -e
/home/ViperAppsFiles/singularity/containers/Trinity-v2.13.1.simg
bowtie2-build  ./Trinity.output.fastafile
```

Then, the read alignment statistics was performed:

```
cat           COMB_07_Paired1_trim.fq           COMB_10_Paired1_trim.fq
COMB_26_Paired1_trim.fq DEHP_12_Paired1_trim.fq DEHP_13_Paired1_trim.fq
DEHP_17_Paired1_trim.fq TEMP_08_Paired1_trim.fq TEMP_13_Paired1_trim.fq
TEMP_18_Paired1_trim.fq > left.fq

cat           COMB_07_Paired2_trim.fq           COMB_10_Paired2_trim.fq
COMB_26_Paired2_trim.fq DEHP_12_Paired2_trim.fq DEHP_13_Paired2_trim.fq
DEHP_17_Paired2_trim.fq TEMP_08_Paired2_trim.fq TEMP_13_Paired2_trim.fq
TEMP_18_Paired2_trim.fq > right.fq

singularity                              exec                              -e
/home/ViperAppsFiles/singularity/containers/Trinity-v2.13.1.simg
bowtie2   -p 10 --no-unal -q -k 20 -x   ./Trinity.output -1 left.fq -2
right.fq 2>align_stats.txt

singularity                              exec                              -e
/home/ViperAppsFiles/singularity/containers/Trinity-v2.13.1.simg
samtools view -@10 -Sb -o bowtie2.bam
```

To visualise statistics:

```
cat 2>&1 align_stats.txt
```

S3.5 Explore completeness with BUSCO

In Viper, a miniconda environment (*environment1*) was first built and then the *BUSCO* command was launched as follows:

```
module load python/anaconda/4.6/miniconda/3.7
source activate /home/userID/.conda/envs/environment1
export PATH=/home/<user>/.conda/envs/bioinformatics/bin:${PATH}
python /home/user/TATT-CPU.py
busco -i /home/userID/Trinity.output.fastafile -o busco_results -m transcriptome --auto-lineage-euk
```

S3.6 Trinity transcriptome ExN50 statistics

In this case, *salmon* was used as a fast alignment-free method, which examined k-mer abundances and in the assembles:

```
$TRINITY_HOME/util/align_and_estimate_abundance.pl --transcripts Trinity.output.fastafile --seqType fq --samples_file data/samples.txt --est_method salmon --trinity_mode --prep_reference --output_dir Abundance_Estimate_Trinity

 $TRINITY_HOME/util/abundance_estimates_to_matrix.pl --est_method salmon --out_prefix Trinity --name_sample_by_basedir --quant_files quant_files.list --gene_trans_map Trinity.output.fasta.gene_trans_map
```

Additionally, the number of expressed transcripts and genes was counted:

```
$TRINITY_HOME/util/misc/count_matrix_features_given_MIN_TPM_threshold.pl Trinity.isoform.TPM.not_cross_norm | tee isoforms_matrix.TPM.not_cross_norm.counts_by_min_TPM
```

Finally, the ExN50-length statistics was run:

```
$TRINITY_HOME/util/misc/contig_ExN50_statistic.pl Trinity.isoform.TMM.EXPR.matrix Trinity.output.fastafile | tee isoforms.ExN50.stats
```

S3.7 Identification and filtering of non-target data

A standard nucleotide-type *BlastN* research was performed using *megablast* (highly similar sequences) against the *nt* database:

```
/home/userID/ncbi-blast-2.13.0+/bin/blastn \ -task megablast \ -query /home/userID/Trinity.output.fastafile \ -db /home/userID/blastdb/nt \ -outfmt '6 qseqid staxids bitscore std' \ -max_target_seqs 1 \ -max_hsps 1 \ -num_threads 28 \ -evalue 1e-25 \ -out blastn.Nt.outfmt6
```

Where `-outfmt '6 qseqid staxids bitscore std'` specifically researched for species and taxon ID of the transcripts. The .bam output file (created during the read alignment statistics in **Chapter 3.7.1:** Assessing the read content of the transcriptome assembly) was sorted and indexed increasing the RAM allowance to 16 Gb:

```
samtools sort /home/userID/bowtie.bam -o /home/userID/bowtie.sorted.bam
-m 16000000000
```

The assembly was analysed with *Blobtools* by parsing the *BlastN* output hitfile against the sorted bowtie bam file and the *Trinity* assembly output datafile. For each entry of the hit file, the taxonomy identification was generated:

```
./blobtools create \ --infile /home/userID/Trinity.output.fastafile \ -
-bam /home/userID/bowtie.sorted.bam \ --hitsfile
/home/userID/BlastN.out \ --out /home/userID/my_BlastN_blobplot && \

./blobtools view \-i /home/userID/my_BlastN_blobplot.blobDB.json \
 -o /home/userID/ && \

./blobtools plot \ -i /home/userID/my_BlastN_blobplot.blobDB.json \ -o
//home/userID/
```

S3.8 Differential expression using DESeq2

Then, the *DESeq2* analysis was launched inside the *Trinity* singularity container, using input files `Trinity.isoform.counts.matrix` and `Trinity.isoform.TMM.EXPR.matrix` (created in **Chapter 3.7.3:** *Trinity* transcriptome ExN50 statistics).

First, the *DeSeq2* analysis generated pairwise comparisons (DEHP vs TEMP, DEHP vs COMB, COMB vs TEMP):

```
$TRINITY_HOME/Analysis/DifferentialExpression/run_DE_analysis.pl --
matrix Trinity.isoform.counts.matrix --samples_file sample.txt --
method DESeq2 --output DESeq2_trans
```

Transcripts at least 4-fold differentially expressed at the significance of <= 0.001 were then extracted, including analysis of upregulation for each treatment, with the associated including log2FC and *p* adjusted value:

```
TRINITY_HOME/Analysis/DifferentialExpression/analyze_diff_expr.pl --
matrix Trinity.isoform.TMM.EXPR.matrix --samples sample.txt -P 1e-3 -C
2
```

S3.9 Assembly annotation

A blastable database was built for sequence homology research:

```
singularity exec -e
/home/ViperAppsFiles/singularity/containers/Trinity-v2.13.1.simg
makeblastdb -in uniprot_sprot.fasta -dbtype prot

singularity exec -e
/home/ViperAppsFiles/singularity/containers/Trinity-v2.13.1.simg
makeblastdb -in uniprot_sprot.pep -dbtype prot
```

The *blast* search was performed, reporting only the top alignment:

```
/home/ViperAppsFiles/singularity/containers/Trinity-v2.13.1.simg blastx
-query Trinity.output.fasta -db uniprot_sprot.fasta -out blastx.outfmt6
-evalue 1e-25 -num_threads 28 -max_target_seqs 1 -outfmt 6
```

And the percent of the aligned target by the best matching *Trinity* transcript was examined by

```
$TRINITY_HOME//util/analyze_blastPlus_topHit_coverage.pl blastx.outfmt6
Trinity.output.fastafile uniprot_sprot.fasta
```

And a scan for sequence homologies with the command *blastp* in *Transdecoder* predicted protein sequences was run to maximise the sensitivity for functionally significant ORFs.

```
/home/ViperAppsFiles/singularity/containers/Trinity-v2.13.1.simg blastp
-query /home/userID/TransDecoder-TransDecoder-
v5.5.0/Trinity.output.transdecoder.pep -db
/home/userID/uniprot_sprot.pep -num_threads 28 -max_target_seqs 1 -
outfmt 6 -evalue 1e-25 > blastp.outfmt6
```

A *HMMER* search was also run against the *Pfam* database:

```
hmmscan --cpu 20 --domtblout TrinotatePFAM.out Pfam-A.hmm
Trinity.output.fasta.transdecoder.pep
```

The SQlite database generated from

```
$TRINOTATE_HOME/admin/Build_Trinotate_Boilerplate_SQLite_db.pl
Trinotate
```

was populated by adding the followings:

- Transcript sequence (from *Trinity* de novo assembly, **Chapter 3.6**)
- Protein sequences (from *TransDecoder* definition, **Chapter 3.10**)
- Gene and Transcript Map generated by:

```
$TRINITY_HOME/util/support_scripts/get_Trinity_gene_to_trans_map.pl
Trinity.fasta > Trinity.fasta.gene_trans_map
```

The `Trinity.fasta.gene_trans_map` was then loaded into the *Trinotate* SQlite database:

```
Trinotate Trinotate.sqlite init --gene_trans_map
Trinity.fasta.gene_trans_map --transcript_fasta Trinity.fasta --
transdecoder_pep transdecoder.pep
```

Blast homologies *blastx.outfmt6* and *blastp.outfmt6* were then loaded:

`Trinotate Trinotate.sqlite LOAD_swissprot_blastp blastp.outfmt6` for protein hits

`Trinotate Trinotate.sqlite LOAD_swissprot_blastx blastx.outfmt6` for transcript hits

Followed by *Pfam* domain entries, transmembrane domains, signal peptide predictions and *Trinity* transcripts search results:

```
Trinotate Trinotate.sqlite LOAD_pfam TrinotatePFAM.out
Trinotate Trinotate.sqlite LOAD_tmhmm tmhmm.out
Trinotate Trinotate.sqlite LOAD_signalp signalp.out
Trinotate Trinotate.sqlite LOAD_rnammer
Trinity.second.output.Trinity.fasta.rnammer.gff
```

S3.10 Gene Ontology enrichment using GOseq

For all the transcripts in each treatment that resulted upregulated in **Chapter 3.9,** the GO assignments for each gene feature were extracted using:

```
${TRINOTATE_HOME}/util/extract_GO_assignments_from_Trinotate_xls.pl --
Trinotate_xls trinotate_annotation_report.xls -G --
include_ancestral_terms > go_annotations.txt
```

Then, the Bioconductor package *Goseq* was used to perform functional enrichment tests:

```
${TRINITY_HOME}/Analysis/DifferentialExpression/run_GOseq.pl --
factor_labeling factor_labeling.txt --GO_assignments
go_annotations.txt
--lengths gene.lengths.txt
```

Where `factor_labeling.txt` is a .txt file describing that subset of genes in the form `factor (tab) gene_id`

And `gene.lengths.txt` was created by:

```
${TRINITY_HOME}/util/misc/fasta_seq_length.pl Trinity.fasta >
Trinity.fasta.seq_lens
```

```
${TRINITY_HOME}/util/misc/TPM_weighted_gene_length.py  --gene_trans_map
trinity_out_dir/Trinity.fasta.gene_trans_map            --trans_lengths
Trinity.fasta.seq_lens    --TPM_matrix    isoforms.TMM.EXPR.matrix    >
Trinity.gene_lengths.txt
```

The resulting Gene Ontology matrix was visualised in *Revigo* with *Simrel* semantic similarity measure and uniprot database research (http://revigo.irb.hr/). Scatter plots and Treemaps were chosen to visualize the results for each individual treatment (**Supplementary Fig. 3.1 and 3.2** for TEMP enriched Biological Process, **Supplementary Fig. 3.3 and 3.4** for TEMP enriched Cellular Component, **Supplementary Fig. 3.5 and 3.6** for TEMP Metabolic Function; **Supplementary Fig. 3.7 and 3.8** for DEHP enriched Biological Process, **Supplementary Fig. 3.9 and 3.10** for DEHP enriched Cellular Component, **Supplementary Fig. 3.11 and 3.12** for DEHP Metabolic Function; **Supplementary Fig. 3.13 and 3.14** for COMB enriched Biological Process, **Supplementary Fig. 3.15 and 3.16** for COMB enriched Cellular Component, **Supplementary Fig. 3.17 and 3.18** for COMB Metabolic Function).

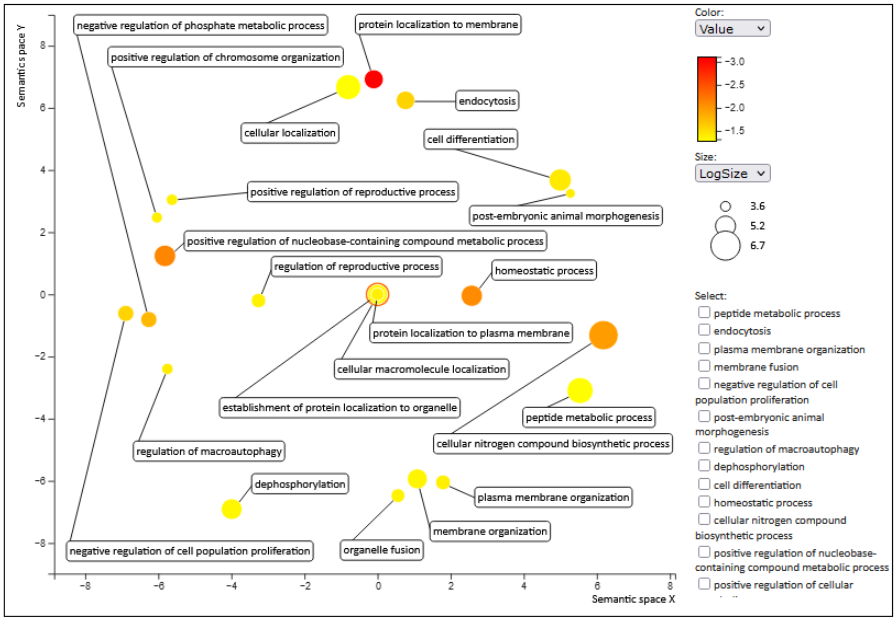

Supplementary Fig. 3.1 Biological process for TEMP (enriched) - scatter plot. REVIGO plot axes have no intrinsic meaning. Multidimensional Scaling (MDS) was used by the software to reduce the dimensionality of the GO term pairwise semantic similarity matrix, i.e., semantically similar GO terms are close together in the plot

Supplementary Fig. 3.2 Biological process for TEMP (enriched) - tree map

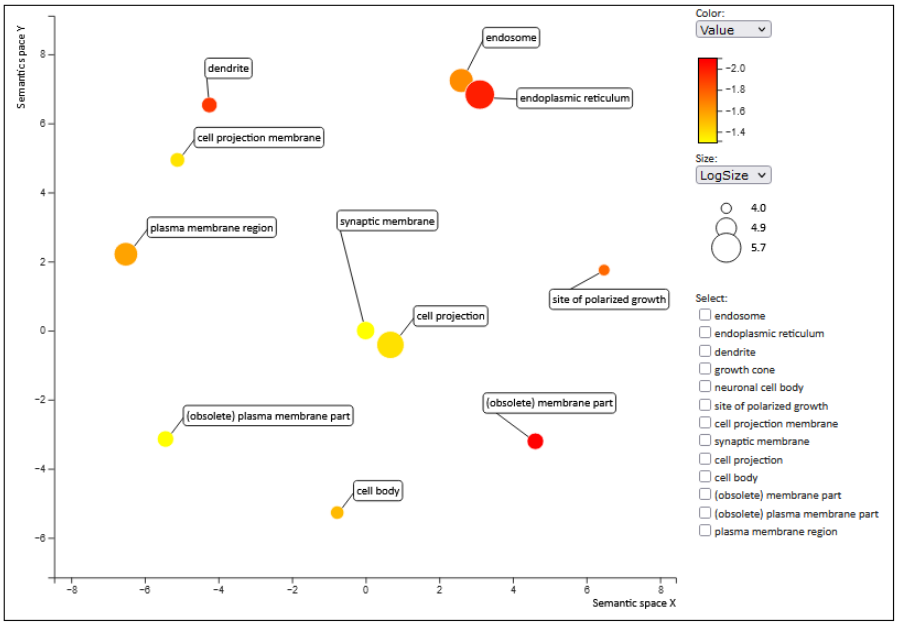

Supplementary Fig. 3.3 Cellular component for TEMP (enriched) - scatter plot. REVIGO plot axes have no intrinsic meaning. Multidimensional Scaling (MDS) was used by the software to reduce the dimensionality of the GO term pairwise semantic similarity matrix, i.e., semantically similar GO terms are close together in the plot

Supplementary Fig. 3.4 Cellular component for TEMP (enriched) - tree map

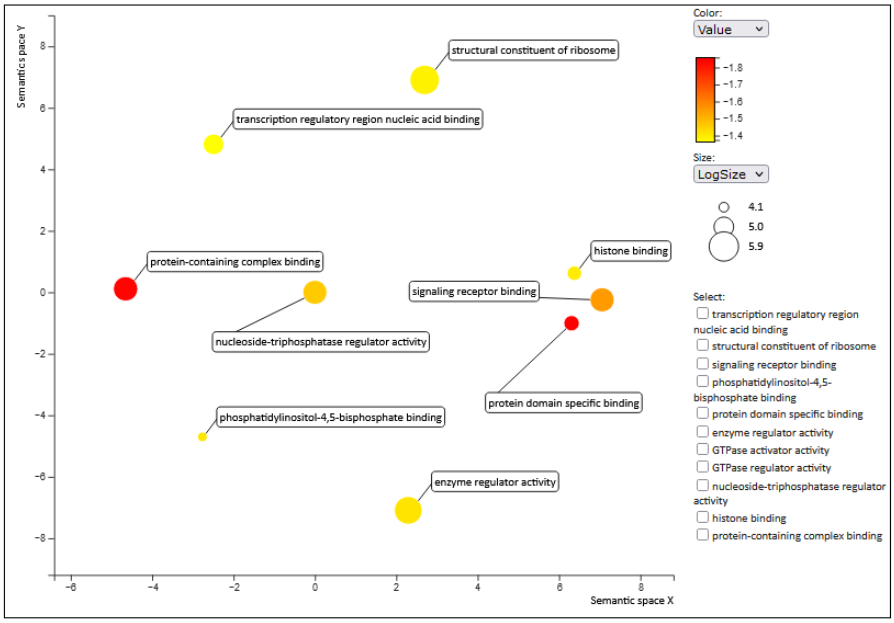

Supplementary Fig. 3.5 Molecular function for TEMP (enriched) - scatter plot. REVIGO plot axes have no intrinsic meaning. Multidimensional Scaling (MDS) was used by the software to reduce the dimensionality of the GO term pairwise semantic similarity matrix, i.e., semantically similar GO terms are close together in the plot

Supplementary Fig. 3.6 Molecular function for TEMP (enriched) - tree map

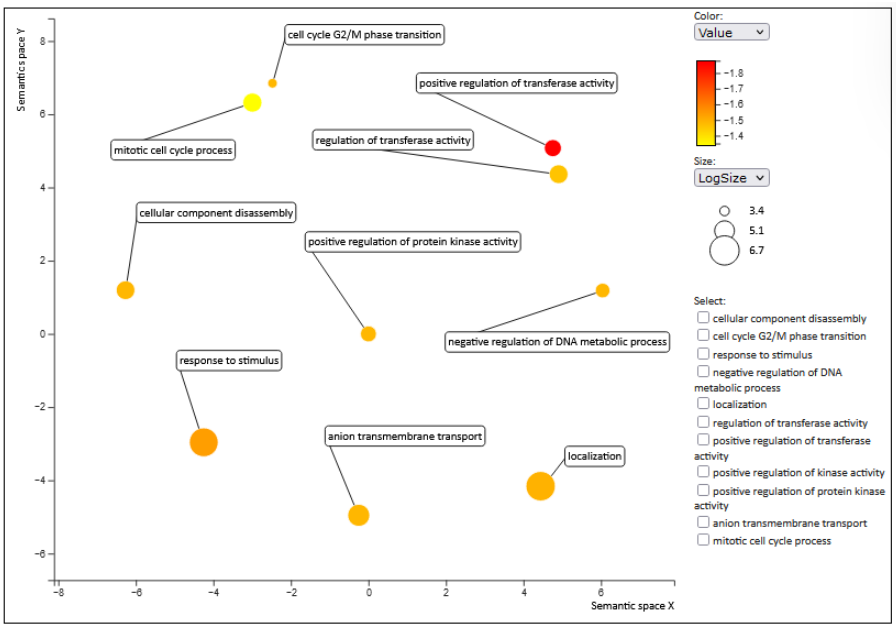

Supplementary Fig. 3.7 Biological process for DEHP (enriched) - scatter plot. REVIGO plot axes have no intrinsic meaning. Multidimensional Scaling (MDS) was used by the software to reduce the dimensionality of the GO term pairwise semantic similarity matrix, i.e., semantically similar GO terms are close together in the plot

Supplementary Fig. 3.8 Biological process for DEHP (enriched) - tree map

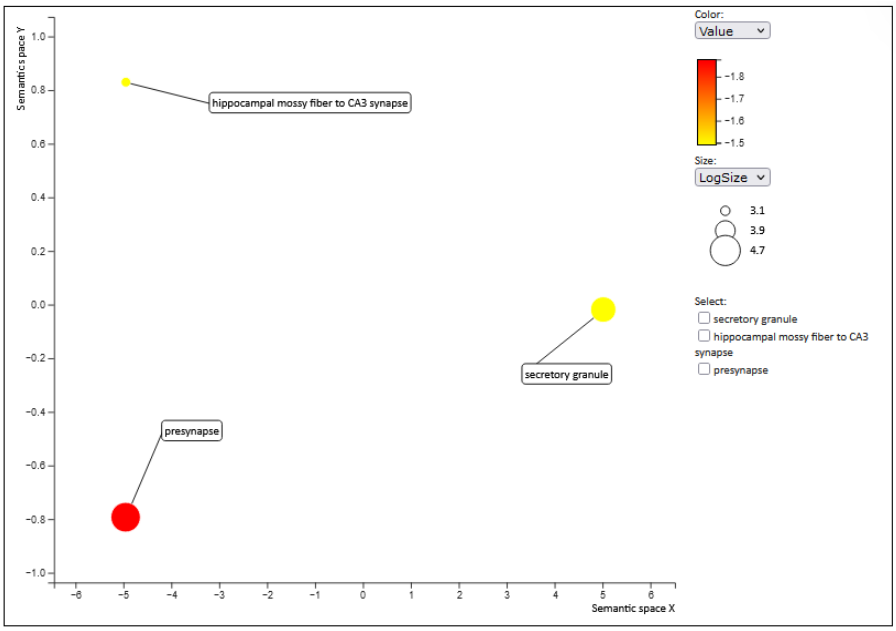

Supplementary Fig. 3.9 Cellular component for DEHP (enriched) - scatter plot. REVIGO plot axes have no intrinsic meaning. Multidimensional Scaling (MDS) was used by the software to reduce the dimensionality of the GO term pairwise semantic similarity matrix, i.e., semantically similar GO terms are close together in the plot

Supplementary Fig. 3.10 Cellular component for DEHP (enriched) - tree map

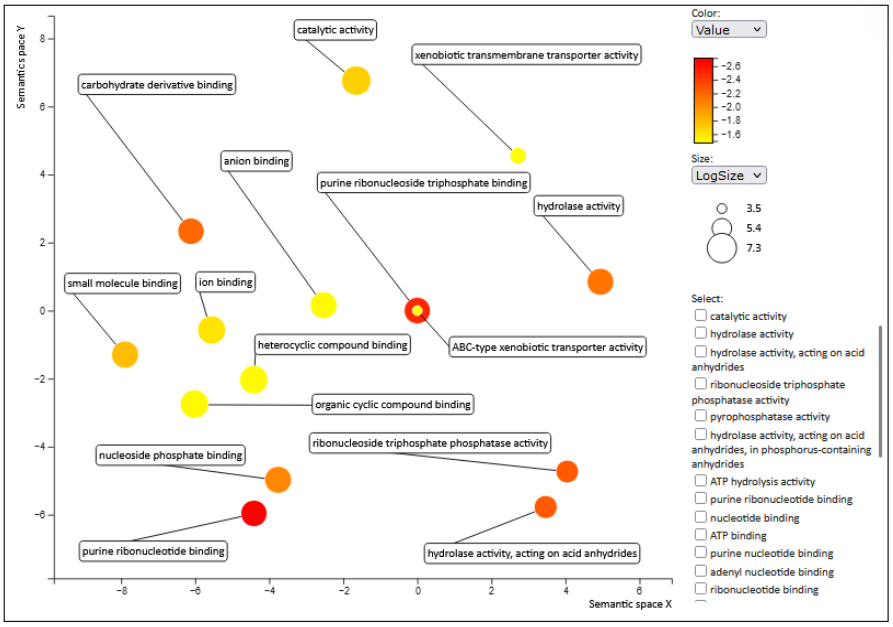

Supplementary Fig. 3.11 Molecular function for DEHP (enriched) - scatter plot. REVIGO plot axes have no intrinsic meaning. Multidimensional Scaling (MDS) was used by the software to reduce the dimensionality of the GO term pairwise semantic similarity matrix, i.e., semantically similar GO terms are close together in the plot

Supplementary Fig. 3.12 Molecular function for DEHP (enriched) - tree map

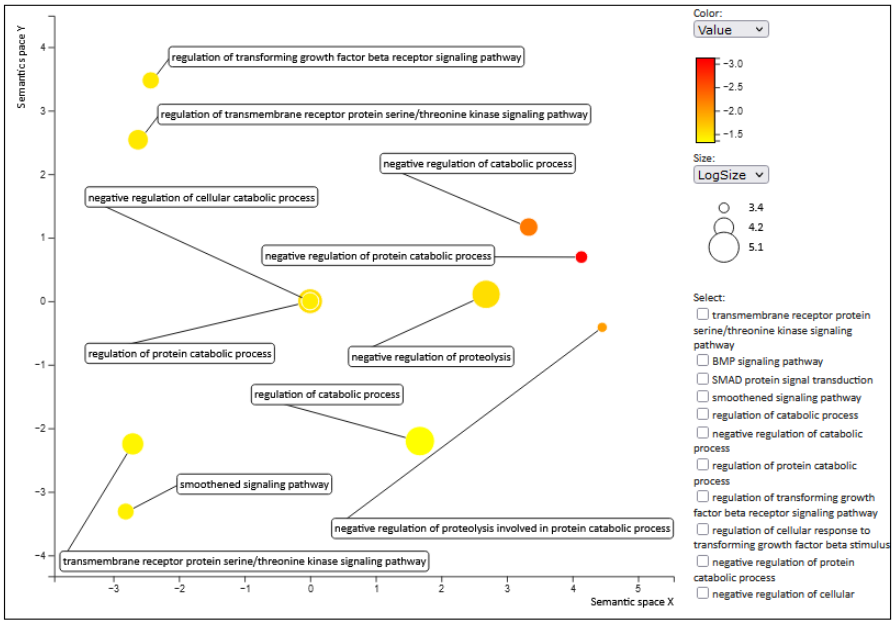

Supplementary Fig. 3.13 Biological process for COMB (enriched) - scatter plot. REVIGO plot axes have no intrinsic meaning. Multidimensional Scaling (MDS) was used by the software to reduce the dimensionality of the GO term pairwise semantic similarity matrix, i.e., semantically similar GO terms are close together in the plot

Supplementary Fig. 3.14 Biological process for COMB (enriched) - tree map

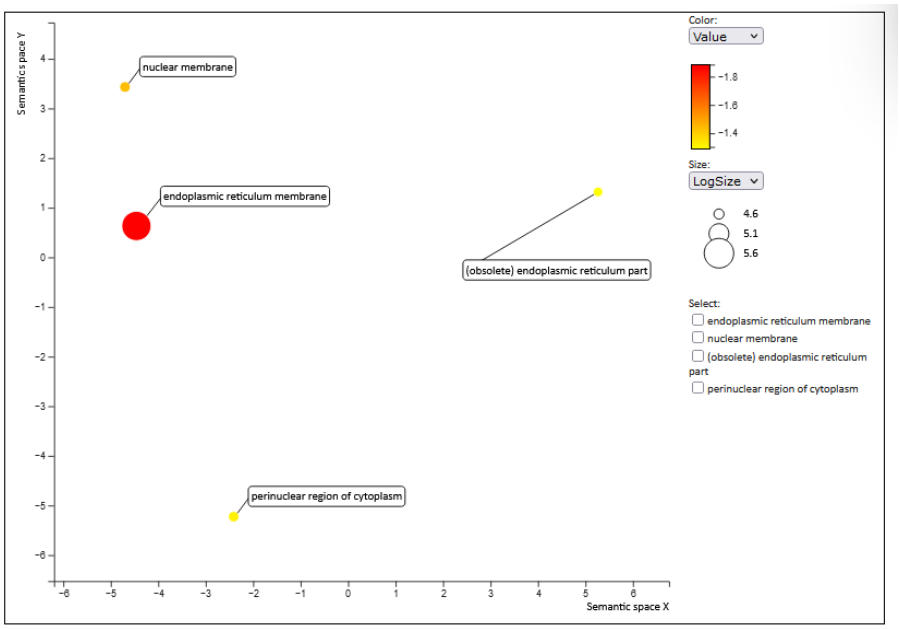

Supplementary Fig. 3.15 Cellular component for COMB (enriched) - scatter plot. REVIGO plot axes have no intrinsic meaning. Multidimensional Scaling (MDS) was used by the software to reduce the dimensionality of the GO term pairwise semantic similarity matrix, i.e., semantically similar GO terms are close together in the plot

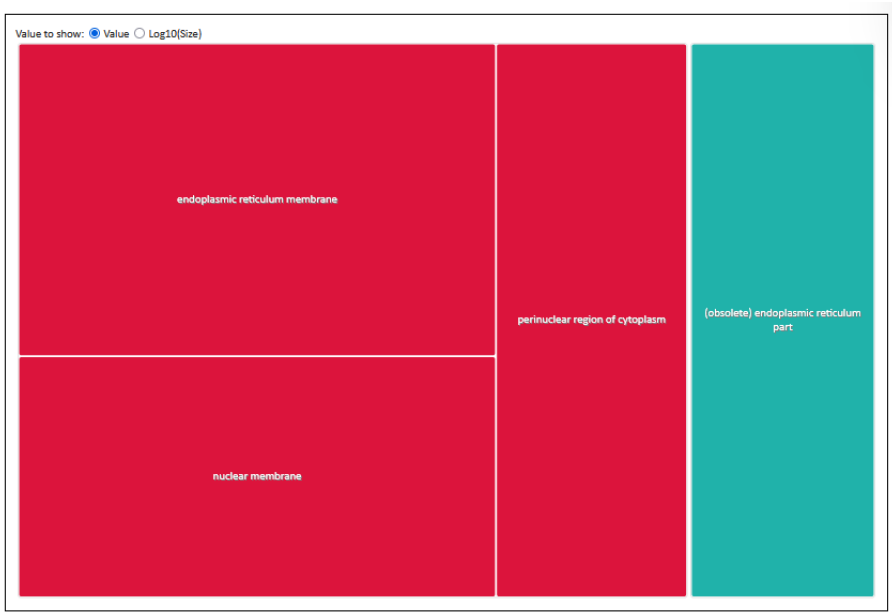

Supplementary Fig. 3.16 Cellular component for COMB (enriched) - tree map

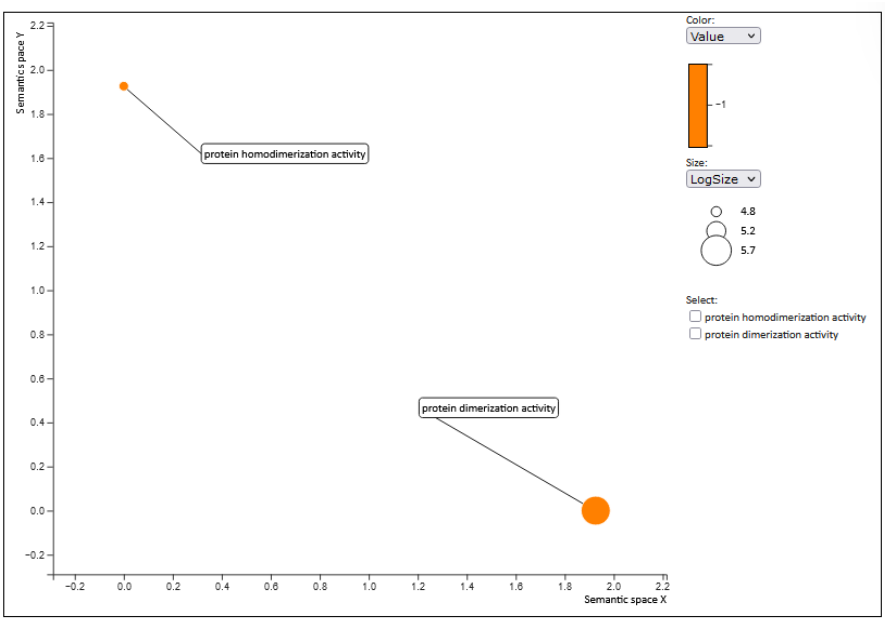

Supplementary Fig. 3.17 Molecular function for COMB (enriched) - scatter plot. REVIGO plot axes have no intrinsic meaning. Multidimensional Scaling (MDS) was used by the software to reduce the dimensionality of the GO term pairwise semantic similarity matrix, i.e., semantically similar GO terms are close together in the plot

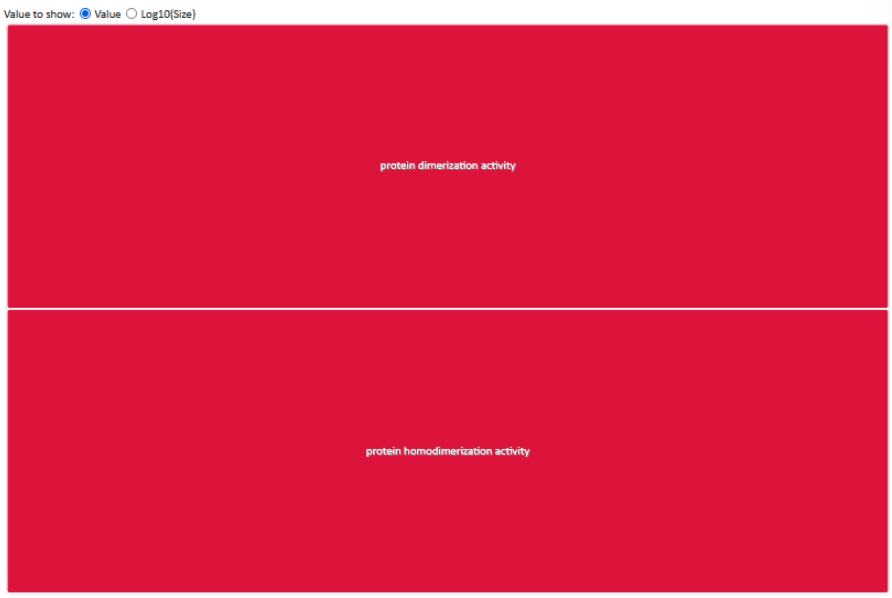

Supplementary Fig. 3.18 Molecular function for COMB (enriched) - tree map

Additionally, the GO term IDs for all the experimental treatments were listed (**Supplementary Table 3.1 - 3.3**) for depleted transcripts.

Supplementary Table 3.1 List of depleted GO terms in TEMP treatment for Biological Process (BP), Cellular Component (CC) and Molecular Function (MF)

Category	Ontology	GO_term
GO:0015630	CC	CC microtubule cytoskeleton
GO:0043410	BP	BP positive regulation of MAPK cascade
GO:0032553	MF	MF ribonucleotide binding
GO:0097367	MF	MF carbohydrate derivative binding
GO:0017076	MF	MF purine nucleotide binding
GO:0032555	MF	MF purine ribonucleotide binding
GO:0006631	BP	BP fatty acid metabolic process
GO:0006732	BP	BP coenzyme metabolic process
GO:0044272	BP	BP sulphur compound biosynthetic process

Supplementary Table 3.2 List of depleted GO terms in DEHP treatment for Biological Process (BP), Cellular Component (CC) and Molecular Function (MF)

Category	Ontology	go_term
GO:0002376	BP	BP immune system process
GO:0097159	MF	MF organic cyclic compound binding
GO:1901363	MF	MF heterocyclic compound binding
GO:0050896	BP	BP response to stimulus
GO:0010604	BP	BP positive regulation of macromolecule metabolic process
GO:0043168	MF	MF anion binding
GO:0051173	BP	BP positive regulation of nitrogen compound metabolic process
GO:0010557	BP	BP positive regulation of macromolecule biosynthetic process
GO:0009314	BP	BP response to radiation
GO:0022604	BP	BP regulation of cell morphogenesis
GO:0045893	BP	BP positive regulation of transcription, DNA-templated
GO:1902680	BP	BP positive regulation of RNA biosynthetic process

GO:1903508	BP	BP positive regulation of nucleic acid-templated transcription
GO:0033044	BP	BP regulation of chromosome organization
GO:0080134	BP	BP regulation of response to stress
GO:0016787	MF	MF hydrolase activity
GO:0051052	BP	BP regulation of DNA metabolic process
GO:0022603	BP	BP regulation of anatomical structure morphogenesis
GO:0010975	BP	BP regulation of neuron projection development
GO:0043269	BP	BP regulation of ion transport
GO:0009416	BP	BP response to light stimulus
GO:0071214	BP	BP cellular response to abiotic stimulus
GO:0071496	BP	BP cellular response to external stimulus
GO:0016462	MF	MF pyrophosphatase activity
GO:0016817	MF	MF hydrolase activity, acting on acid anhydrides
GO:0016818	MF	MF hydrolase activity, acting on acid anhydrides, in phosphorus-containing anhydrides
GO:0017111	MF	MF nucleoside-triphosphatase activity

Supplementary Table 3.3 List of depleted GO terms in COMB treatment for Biological Process (BP), Cellular Component (CC) and Molecular Function (MF)

Category	Ontology	go_term
GO:0002376	BP	BP immune system process
GO:0097159	MF	MF organic cyclic compound binding
GO:1901363	MF	MF heterocyclic compound binding
GO:0050896	BP	BP response to stimulus
GO:0010604	BP	BP positive regulation of macromolecule metabolic process
GO:0043168	MF	MF anion binding
GO:0051173	BP	BP positive regulation of nitrogen compound metabolic process
GO:0010557	BP	BP positive regulation of macromolecule biosynthetic process
GO:0009314	BP	BP response to radiation

GO:0022604	BP	BP regulation of cell morphogenesis
GO:0045893	BP	BP positive regulation of transcription, DNA-templated
GO:1902680	BP	BP positive regulation of RNA biosynthetic process
GO:1903508	BP	BP positive regulation of nucleic acid-templated transcription
GO:0033044	BP	BP regulation of chromosome organization
GO:0080134	BP	BP regulation of response to stress
GO:0016787	MF	MF hydrolase activity
GO:0051052	BP	BP regulation of DNA metabolic process
GO:0022603	BP	BP regulation of anatomical structure morphogenesis
GO:0010975	BP	BP regulation of neuron projection development
GO:0043269	BP	BP regulation of ion transport
GO:0009416	BP	BP response to light stimulus
GO:0071214	BP	BP cellular response to abiotic stimulus
GO:0071496	BP	BP cellular response to external stimulus
GO:0016462	MF	MF pyrophosphatase activity
GO:0016817	MF	MF hydrolase activity, acting on acid anhydrides
GO:0016818	MF	MF hydrolase activity, acting on acid anhydrides, in phosphorus-containing anhydrides
GO:0017111	MF	MF nucleoside-triphosphatase activity

Supplementary Appendix to Chapter 4

S4.1 Stress-related response: male and female gene expression

Considering the overall expression (i.e., *sod*, *cat*, or *hsp70* gene expression) of stress-related genes, PERMANOVA showed no significant effect of either pH or DEHP on *sod*, *cat* or *hsp70* gene expression in male or female groups ($p > 0.05$, **Supplementary Fig. 4.1**).

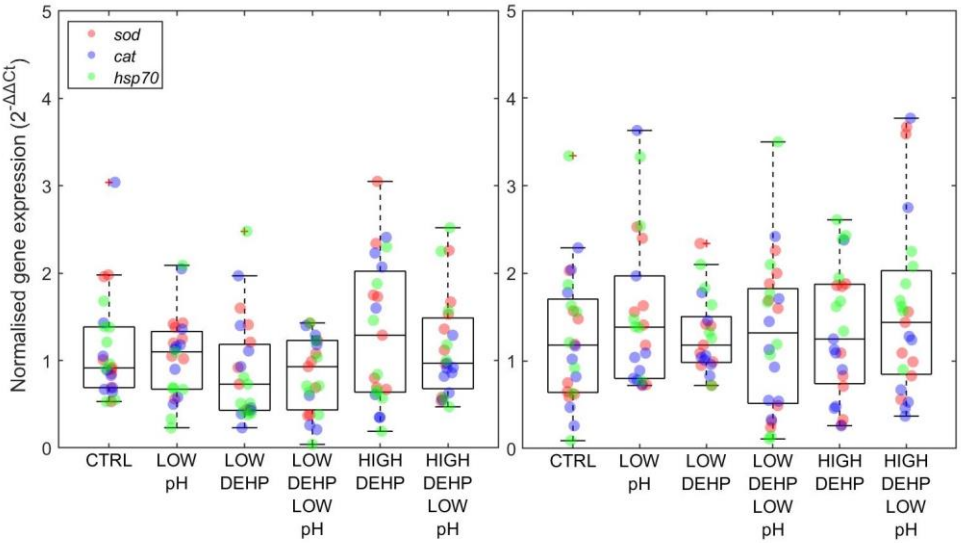

Supplementary Fig. 4.1 left) Stress-related (*sod*, *cat*, *hsp70*) gene expression in males, n = 7 to 8. **right)** Stress-related (*sod, cat*, *hsp70)* mRNA expression in females, n = 6 to 8. Abbreviations are control (CTRL), low pH (LOW pH), low DEHP concentration (LOW DEHP), low DEHP at low pH (LOW DEHP LOW pH), high DEHP concentration (HIGH DEHP) and high DEHP at low pH (HIGH DEHP LOW pH). No significant PERMANOVA differences were found

S4.2 Stress-related response: individual gene expression

No particular effect was found for the individual stress-related gene expression in males and females, respectively (**Supplementary Fig. 4.2 - 4.7**). As previously highlighted, this could be related to the adaptive strategies of intertidal organisms.

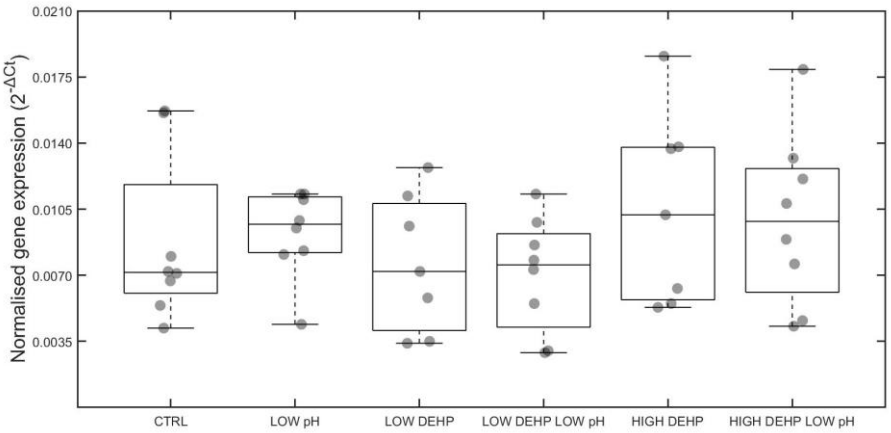

Supplementary Fig. 4.2 *sod* mRNA expression in males, n = 7 to 8. Abbreviations are control (CTRL), low pH (LOW pH), low DEHP concentration (LOW DEHP), low DEHP at low pH (LOW DEHP LOW pH), high DEHP concentration (HIGH DEHP) and high DEHP at low pH (HIGH DEHP LOW pH)

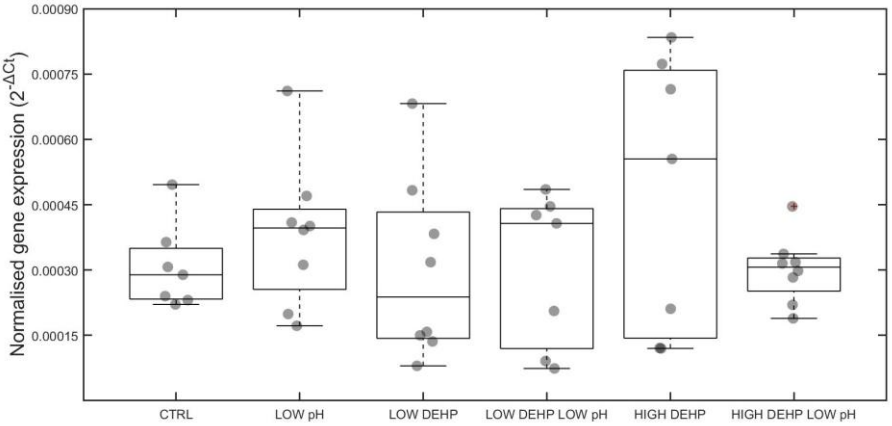

Supplementary Fig. 4.3 *cat* mRNA expression in males, n = 7 to 8. Abbreviations are control (CTRL), low pH (LOW pH), low DEHP concentration (LOW DEHP), low DEHP at low pH (LOW DEHP LOW pH), high DEHP concentration (HIGH DEHP) and high DEHP at low pH (HIGH DEHP LOW pH). No significant ANOVA *p* values were found

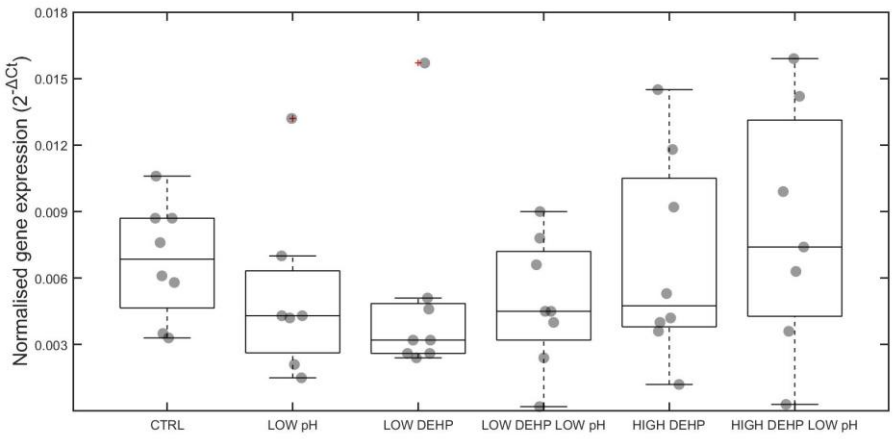

Supplementary Fig. 4.4 *hsp70* mRNA expression in males, n = 7 to 8. Abbreviations are control (CTRL), low pH (LOW pH), low DEHP concentration (LOW DEHP), low DEHP at low pH (LOW DEHP LOW pH), high DEHP concentration (HIGH DEHP) and high DEHP at low pH (HIGH DEHP LOW pH). No significant ANOVA *p* values were found

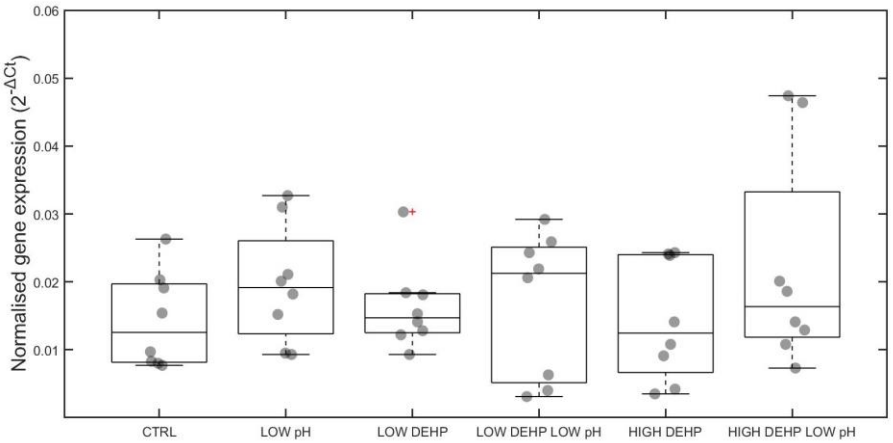

Supplementary Fig. 4.5 *sod* mRNA expression in females, n = 8. Abbreviations are control (CTRL), low pH (LOW pH), low DEHP concentration (LOW DEHP), low DEHP at low pH (LOW DEHP LOW pH), high DEHP concentration (HIGH DEHP) and high DEHP at low pH (HIGH DEHP LOW pH). No significant ANOVA *p* values were found

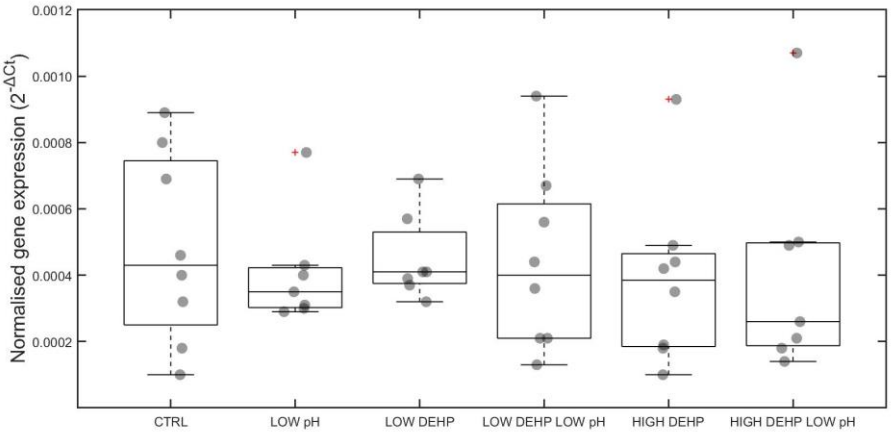

Supplementary Fig. 4.6 *cat* mRNA expression in females, n = 7 to 8. Abbreviations are control (CTRL), low pH (LOW pH), low DEHP concentration (LOW DEHP), low DEHP at low pH (LOW DEHP LOW pH), high DEHP concentration (HIGH DEHP) and high DEHP at low pH (HIGH DEHP LOW pH). No significant ANOVA *p* values were found

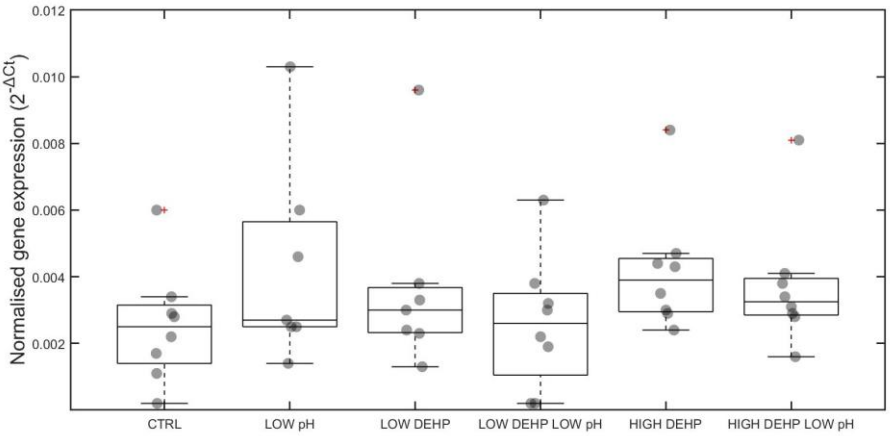

Supplementary Fig. 4.7 *hsp70* mRNA expression in males, n = 7 - 8. Abbreviations are control (CTRL), low pH (LOW pH), low DEHP concentration (LOW DEHP), low DEHP at low pH (LOW DEHP LOW pH), high DEHP concentration (HIGH DEHP) and high DEHP at low pH (HIGH DEHP LOW pH). No significant ANOVA *p* values were found

S4.3 CA2 response: individual gene expression

As with the previous outcomes, no significant differences were found observing males and females individually, apart from a mild effect of pH on females $2^{-\Delta Ct}$ values (SHR *p* value = 0.09, H = 2.72, **Supplementary Fig. 4.8 and 4.9**).

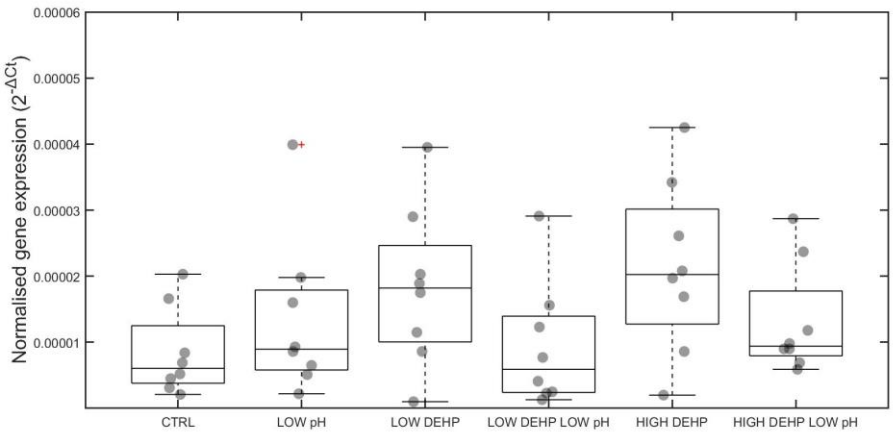

Supplementary Fig. 4.8 *CA2* mRNA expression in males, n = 8. Abbreviations are control (CTRL), low pH (LOW pH), low DEHP concentration (LOW DEHP), low DEHP at low pH (LOW DEHP LOW pH), high DEHP concentration (HIGH DEHP) and high DEHP at low pH (HIGH DEHP LOW pH). No significant ANOVA *p* values were found

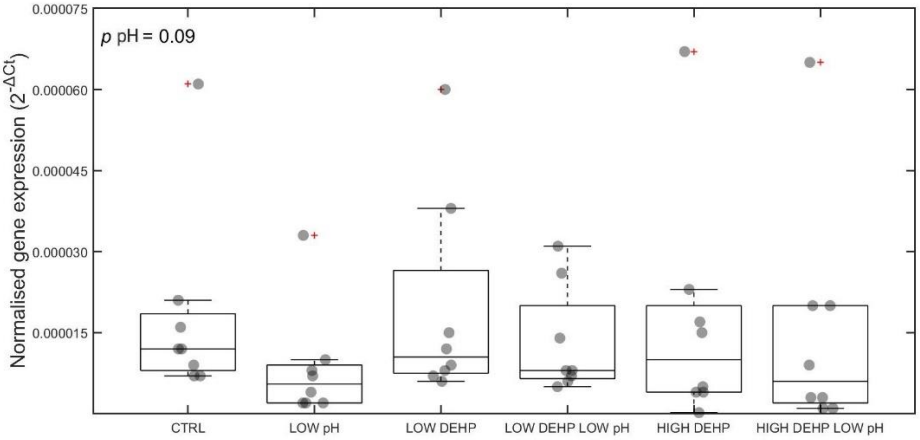

Supplementary Fig. 4.9 *CA2* mRNA expression in females, n = 8. Abbreviations are control (CTRL), low pH (LOW pH), low DEHP concentration (LOW DEHP), low DEHP at low pH (LOW DEHP LOW pH), high DEHP concentration (HIGH DEHP) and high DEHP at low pH (HIGH DEHP LOW pH). Scheirer-Rey-Hare test error probability is annotated

S4.4 Estrogen receptor-like responses

No particular effect was found on the estrogen receptor-related responses when considering individual responses or male and female levels of both *MeER1* and *MeER2* (**Supplementary Fig. 4.10 - 4.14**).

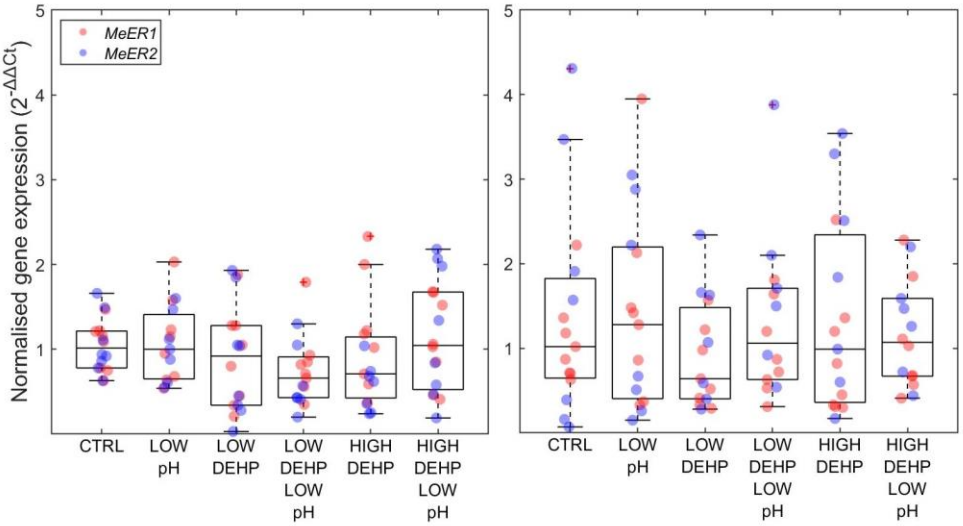

Supplementary Fig. 4.10 left) Estrogen receptor-like (*MeER1, MeER2*) gene expression in males, n = 6 to 8. **right)** Estrogen receptor-like (MeER1, MeER2) mRNA expression in females, n = 7 to 8. Abbreviations are control (CTRL), low pH (LOW pH), low DEHP concentration (LOW DEHP), low DEHP at low pH (LOW DEHP LOW pH), high DEHP concentration (HIGH DEHP) and high DEHP at low pH (HIGH DEHP LOW pH). No significant PERMANOVA differences were found

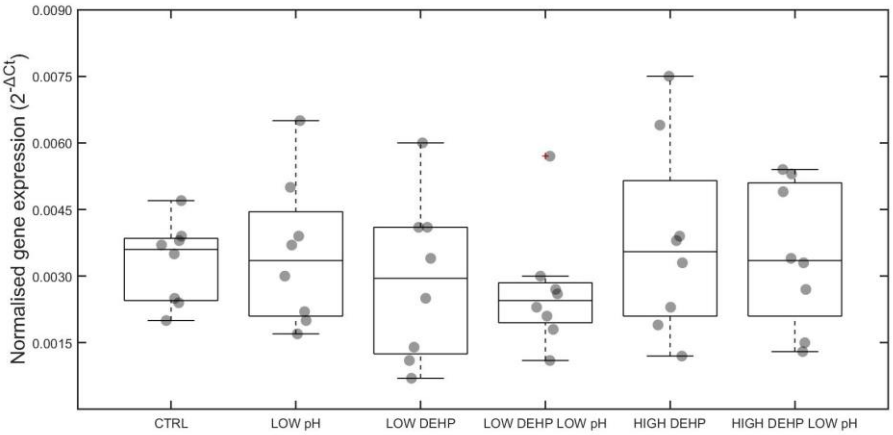

Supplementary Fig. 4.11 *MeER1* mRNA expression in males, n = 8. Abbreviations are control (CTRL), low pH (LOW pH), low DEHP concentration (LOW DEHP), low DEHP at low pH (LOW DEHP LOW pH), high DEHP concentration (HIGH DEHP) and high DEHP at low pH (HIGH DEHP LOW pH). No significant ANOVA *p* values were found

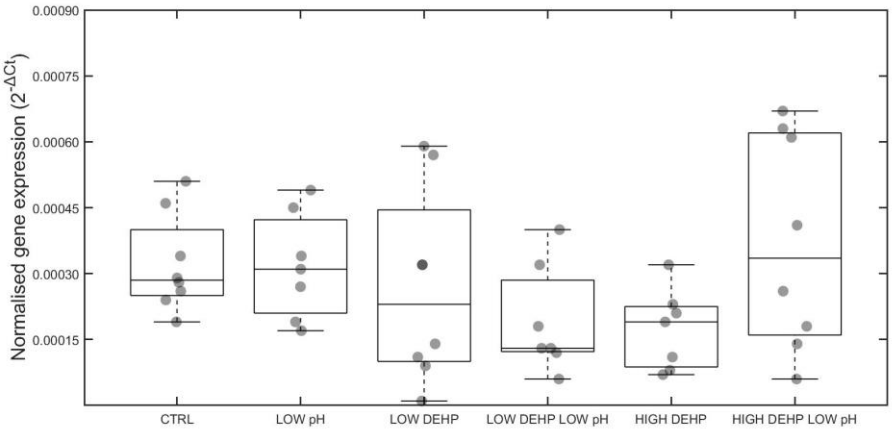

Supplementary Fig. 4.12 *MeER2* mRNA expression in males, n= 7 to 8. Abbreviations are control (CTRL), low pH (LOW pH), low DEHP concentration (LOW DEHP), low DEHP at low pH (LOW DEHP LOW pH), high DEHP concentration (HIGH DEHP) and high DEHP at low pH (HIGH DEHP LOW pH). No significant ANOVA *p* values were found

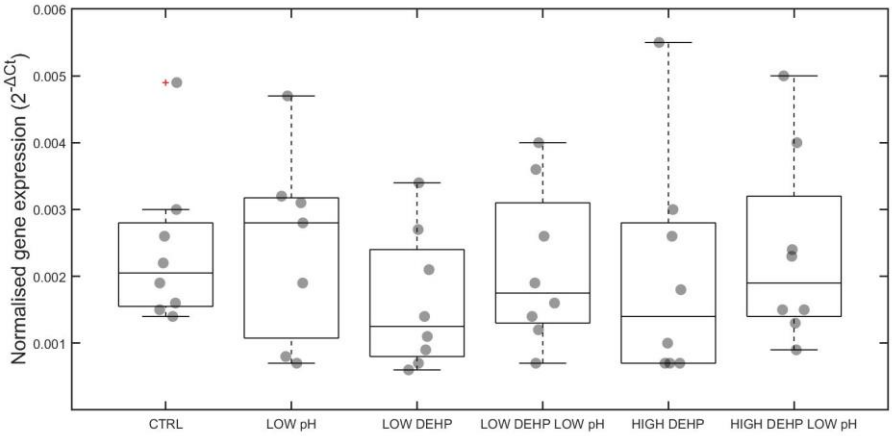

Supplementary Fig. 4.13 *MeER1* mRNA expression in females, n = 8. Abbreviations are control (CTRL), low pH (LOW pH), low DEHP concentration (LOW DEHP), low DEHP at low pH (LOW DEHP LOW pH), high DEHP concentration (HIGH DEHP) and high DEHP at low pH (HIGH DEHP LOW pH). No significant ANOVA *p* values were found

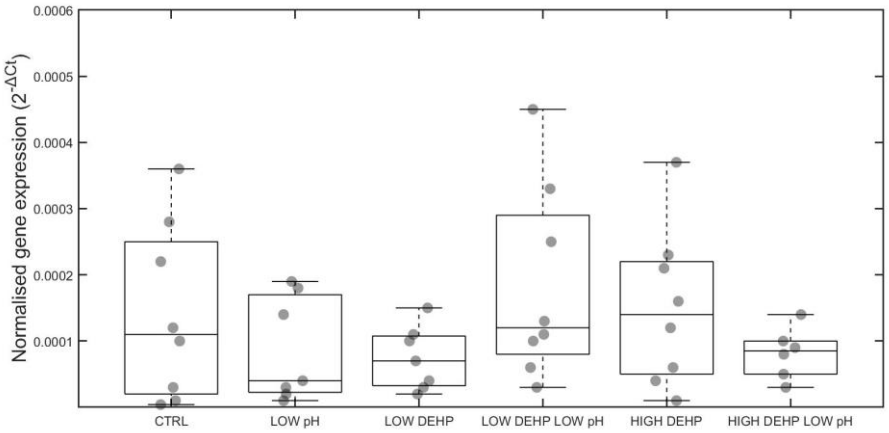

Supplementary Fig. 4.14 *MeER2* mRNA expression in females, n= 6 to 8. Abbreviations are control (CTRL), low pH (LOW pH), low DEHP concentration (LOW DEHP), low DEHP at low pH (LOW DEHP LOW pH), high DEHP concentration (HIGH DEHP) and high DEHP at low pH (HIGH DEHP LOW pH). No significant ANOVA *p* values were found

References

A

Aarab, N., Lemaire-Gony, S., Unruh, E., Hansen, P.D., Larsen, B.K., Andersen, O.K., Narbonne, J.F., 2006. Preliminary study of responses in mussel (*Mytilus edilus*) exposed to bisphenol A, diallyl phthalate and tetrabromodiphenyl ether. Aquat. Toxicol. 78, 86–92. https://doi.org/10.1016/j.aquatox.2006.02.021

Abdelmajid, H., Leclerc-David, C., Moreau, M., Guerrier, P., Ryazanov, A., 1993. Release from the metaphase I block in invertebrate oocytes: Possible involvement of Ca2+/calmodulin-dependent kinase III. Int. J. Dev. Biol. 37, 279–290.

Abele, D., 2002. The radical life-giver concepts. Nat. Concepts 420, 2002.

Abele, D., Burlando, B., Viarengo, A., Pörtner, H.O., 1998. Exposure to elevated temperatures and hydrogen peroxide elicits oxidative stress and antioxidant response in the Antarctic intertidal limpet *Nacella concinna*. Comp. Biochem. Physiol. - B Biochem. Mol. Biol. 120, 425–435. https://doi.org/10.1016/S0305-0491(98)10028-7

Adams, S.M., Greeley, M.S., 2000. Ecotoxicological indicators of water quality: Using multi-response indicators to assess the health of aquatic ecosystems. Water. Air. Soil Pollut. 123, 103–115. https://doi.org/10.1007/978-94-011-4369-1_10

Agathokleous, E., 2018. Environmental hormesis, a fundamental non-monotonic biological phenomenon with implications in ecotoxicology and environmental safety. Ecotoxicol. Environ. Saf. 148, 1042–1053. https://doi.org/10.1016/j.ecoenv.2017.12.003

Agathokleous, E., Calabrese, E.J., 2020. A global environmental health perspective and optimisation of stress. Sci. Total Environ. 704, 135263. https://doi.org/10.1016/j.scitotenv.2019.135263

Agathokleous, E., Kitao, M., Calabrese, E.J., 2018. Environmental hormesis and its fundamental biological basis: rewriting the history of toxicology. Environ. Res. 165, 274–278. https://doi.org/10.1016/j.envres.2018.04.034

Agnaou, M., Ait Alla, A., Ouassas, M., Bazzi, L., El Alami, Z., Moukrim, A., 2014. Assessment of organochlorine pesticides contamination of oued souss estuary (South of Morocco): Seasonal variability in sediment and a detritivore annelid *Neries diversicolor*. J. Mater. Environ. Sci. 5, 581–586.

Agnese, M., Rosati, L., Prisco, M., Borzacchiello, L., Abagnale, L., Andreuccetti, P., 2019. The expression of estrogen receptors during the *Mytilus galloprovincialis* ovarian cycle. J. Exp. Zool. Part A Ecol. Integr. Physiol. 331, 367–373. https://doi.org/10.1002/jez.2272

Ali, A., Salter-Cid, L., Flajnik, M.F., Heikkila, J.J., 1996. Isolation and characterization of a cDNA encoding a *Xenopus* 70-kDa heat shock cognate protein, Hsc70. Comp. Biochem. Physiol. - B Biochem. Mol. Biol. 113, 681–687. https://doi.org/10.1016/0305-0491(95)02081-0

Almeida, Â., Calisto, V., Esteves, V.I., Schneider, R.J., Soares, A.M.V.M., Freitas, R., 2022a. Salinity-dependent impacts on the effects of antiepileptic and antihistaminic drugs in *Ruditapes philippinarum*. Sci. Total Environ. 806. https://doi.org/10.1016/j.scitotenv.2021.150369

Almeida, Â., Calisto, V., Esteves, V.I., Schneider, R.J., Soares, A.M.V.M., Freitas, R., 2022b. Responses of *Ruditapes philippinarum* to contamination by pharmaceutical drugs under ocean acidification scenario. Sci. Total Environ. 824. https://doi.org/10.1016/j.scitotenv.2022.153591

Almeida, Â., Calisto, V., Esteves, V.I., Schneider, R.J., Soares, A.M.V.M., Freitas, R., 2021. Salinity-dependent impacts on the effects of antiepileptic and antihistaminic drugs in *Ruditapes philippinarum*. Sci. Total Environ. 806, 150369. https://doi.org/10.1016/j.scitotenv.2021.150369

Alonso, A., Suárez, P., Ruiz, Y., Dobal, V., San Juan, F., 2019. Gonadal histopathological disorders in *Mytilus galloprovincialis* male exposed to tars used in mussel farms. Front. Mar. Sci. 6, 1–20. https://doi.org/10.3389/fmars.2019.00577

Amaral Mendes, J.J., 2002. The endocrine disrupters: A major medical challenge. Food Chem. Toxicol. 40, 781–788. https://doi.org/10.1016/S0278-6915(02)00018-2

Anacleto, P., Maulvault, A.L., Lopes, V.M., Repolho, T., Diniz, M., Nunes, M.L., Marques, A., Rosa, R., 2014. Ecophysiology of native and alien-invasive clams in an ocean warming context. Comp. Biochem. Physiol. -Part A Mol. Integr. Physiol. 175, 28–37. https://doi.org/10.1016/j.cbpa.2014.05.003

Anantharaman, S., Craft, J.A., 2012. Annual variation in the levels of transcripts of sex- specific genes in the mantle of the common mussel, *Mytilus edulis* 7. https://doi.org/10.1371/journal.pone.0050861

Anderson, M. J., 2014. Permutational multivariate analysis of variance (PERMANOVA). Wiley statsref: statistics reference online, 1-15

Andrady, A.L., 2011. Microplastics in the marine environment. Mar. Pollut. Bull. 62, 1596–1605. https://doi.org/10.1016/j.marpolbul.2011.05.030

Anestis, A., Pörtner, H.O., Karagiannis, D., Angelidis, P., Staikou, A., Michaelidis, B., 2010. Response of *Mytilus galloprovincialis* (L.) to increasing seawater temperature and to marteliosis: Metabolic and physiological parameters. Comp. Biochem. Physiol. - A Mol. Integr. Physiol. 156, 57–66. https://doi.org/10.1016/j.cbpa.2009.12.018

Angilletta, M.J., Sears, M.W., 2000. The metabolic cost of reproduction in an oviparous lizard. Funct. Ecol. 14, 39–45. https://doi.org/10.1046/j.1365-2435.2000.00387.x

Anguis, V., Cañavate, J.P., 2005. Spawning of captive Senegal sole (*Solea senegalensis*) under a naturally fluctuating temperature regime. Aquaculture 243, 133–145. https://doi.org/10.1016/j.aquaculture.2004.09.026

Annunen, P., Helaakoski, T., Myllyharju, J., Veijola, J., Pihlajaniemi, T., Kivirikko, K.I., 1997. Cloning of the human prolyl 4-hydroxylase α subunit isoform α(II) and characterization of the type II enzyme tetramer: The α(I) and α(II) subunits do not form a mixed α(I)α(II)β2 tetramer. J. Biol. Chem. 272, 17342–17348. https://doi.org/10.1074/jbc.272.28.17342

Antizar-Ladislao, B., 2009. Polycyclic aromatic hydrocarbons, polychlorinated biphenyls, phthalates and organotins in northern Atlantic Spain's coastal marine sediments. J. Environ. Monit. 11, 85–91. https://doi.org/10.1039/b808668k

Aquino De Souza, R., Tyler, P., Hawkins, S.J., 2009. Artificial oocyte maturation in *Patella depressa* and *Patella vulgata* using NaOH-alkalinized seawater. Mar. Biol. Res. 5, 503–510. https://doi.org/10.1080/17451000802603645

Archana, G., Dhodapkar, R., Kumar, A., 2017. Ecotoxicological risk assessment and seasonal variation of some pharmaceuticals and personal care products in the sewage treatment plant and surface water bodies (lakes). Environ. Monit. Assess. 189. https://doi.org/10.1007/s10661-017-6148-3

Armengaud, J., Trapp, J., Pible, O., Geffard, O., Chaumot, A., Hartmann, E.M., 2014. Non-model organisms, a species endangered by proteogenomics. J. Proteomics 105, 5–18. https://doi.org/10.1016/j.jprot.2014.01.007

Artigaud, S., Lacroix, C., Pichereau, V., Flye-Sainte-Marie, J., 2014. Respiratory response to combined heat and hypoxia in the marine bivalves *Pecten maximus* and *Mytilus* spp. Comp. Biochem. Physiol. -Part A Mol. Integr. Physiol. 175, 135–140. https://doi.org/10.1016/j.cbpa.2014.06.005

Arukwe, A., Knudsen, F. R., Goksøyr, A. 1997. Fish zona radiata (eggshell) protein: a sensitive biomarker for environmental estrogens. Environmental Health Perspectives, 105(4), 418-422.

Avio, C.G., Gorbi, S., Milan, M., Benedetti, M., Fattorini, D., D'Errico, G., Pauletto, M., Bargelloni, L., Regoli, F., 2015. Pollutants bioavailability and toxicological risk from microplastics to marine mussels. Environ. Pollut. 198, 211–222. https://doi.org/10.1016/j.envpol.2014.12.021

Azpeitia, K., Revilla, M., Mendiola, D., 2017. Variability of the reproductive cycle in estuarine and coastal populations of the mussel *Mytilus galloprovincialis* Lmk . from the SE Bay of Biscay (Basque Country). Int. Aquat. Res. 9, 329–350. https://doi.org/10.1007/s40071-017-0180-3

B

Bælum, J., Borglin, S., Chakraborty, R., Fortney, J.L., Lamendella, R., Mason, O.U., Auer, M., Zemla, M., Bill, M., Conrad, M.E., Malfatti, S.A., Tringe, S.G., Holman, H.Y., Hazen, T.C., Jansson, J.K., 2012. Deep-sea bacteria enriched by oil and dispersant from the Deepwater Horizon spill. Environ. Microbiol. 14, 2405–2416. https://doi.org/10.1111/j.1462-2920.2012.02780.x

Baag, S., Mahapatra, S., Mandal, S., 2021. An Integrated and Multibiomarker approach to delineate oxidative stress status of *Bellamya bengalensis* under the interactions of elevated temperature and chlorpyrifos contamination. Chemosphere 264, 128512. https://doi.org/10.1016/j.chemosphere.2020.128512

Bacchetta, R., Mantecca, P., 2009. DDT polluted meltwater affects reproduction in the mussel *Dreissena polymorpha*. Chemosphere 76, 1380–1385. https://doi.org/10.1016/j.chemosphere.2009.06.020

Badger, M.R., Price, G.D., 1994. The role of carbonic anhydrase in photosynthesis. Annu. Physiol.Plant Mol.Biol. 45, 369–392. https://doi.org/10.1146/annurev.pp.45.060194.002101

Baines, S.B., Fisher, N.S., 2008. Modeling the effect of temperature on bioaccumulation of metals by a marine bioindicator organism, *Mytilus edulis*. Environ. Sci. Technol. 42, 3277–3282. https://doi.org/10.1021/es702336q

Balbi, T., Ciacci, C., Grasselli, E., Smerilli, A., Voci, A., Canesi, L., 2017. Utilization of *Mytilus* digestive gland cells for the in vitro screening of potential metabolic disruptors in aquatic invertebrates. Comp. Biochem. Physiol. Part - C Toxicol. Pharmacol. 191, 26–35. https://doi.org/10.1016/j.cbpc.2016.08.009

Balbi, T., Franzellitti, S., Fabbri, R., Montagna, M., Fabbri, E., Canesi, L., 2016. Impact of bisphenol A (BPA) on early embryo development in the marine mussel *Mytilus galloprovincialis*: Effects on gene transcription. Environ. Pollut. 218, 996–1004. https://doi.org/10.1016/j.envpol.2016.08.050

Balbi, T., Montagna, M., Fabbri, R., Carbone, C., Franzellitti, S., Fabbri, E., Canesi, L., 2018. Diclofenac affects early embryo development in the marine *bivalve Mytilus galloprovincialis*. Sci. Total Environ. 642, 601–609. https://doi.org/10.1016/j.scitotenv.2018.06.125

Bamber, S.D., Westerlund, S., 2016. Behavioral responses of *Arctica islandica* (Bivalvia: Arcticidae) to simulated leakages of carbon dioxide from sub-sea geological storage. Aquat. Toxicol. 180, 295–305. https://doi.org/10.1016/j.aquatox.2016.10.009

Banni, M., Negri, A., Mignone, F., Boussetta, H., Viarengo, A., Dondero, F., 2011. Gene expression rhythms in the mussel *Mytilus galloprovincialis* (Lam.) across an annual cycle. PLoS One 6. https://doi.org/10.1371/journal.pone.0018904

Bannister, R., Beresford, N., May, D., Routledge, E.J., Jobling, S., Rand-Weaver, M., 2007. Novel estrogen receptor-related transcripts in *Marisa cornuarietis*; a freshwater snail with reported sensitivity to estrogenic chemicals. Environ. Sci. Technol. 41, 2643–2650. https://doi.org/10.1021/es062565m

Barbariol, V., Razouls, S., 2000. Experimental studies on the respiratory metabolism of *Mytilus galloprovincialis* (Mollusca bivalvia) from the Mediterranean Sea (Gulf of Lion). Vie Milieu 50, 87–92.

Barcia, R., Lopez-Garcia, J.M., Ramos-Martinez, J.I., 1997. The 28s fraction of rRNA in molluscs displays electrophoretic behaviour different from that of mammal cells 42, 1089–1092.

Barnes, D.K.A., Galgani, F., Thompson, R.C., Barlaz, M., 2009. Accumulation and fragmentation of plastic debris in global environments. Philos. Trans. R. Soc. B Biol. Sci. 364, 1985–1998. https://doi.org/10.1098/rstb.2008.0205

Barrick, A., Mouneyrac, C., Manier, N., De Lantivy, L., Jrad, N., Châtel, A., 2018. Towards the development of a high throughput screening approach for *Mytilus edulis* hemocytes: A case study on silicon-based nanomaterials. Mar. Environ. Res. 142, 306–318. https://doi.org/10.1016/j.marenvres.2018.10.014

Baršiene, J., Šyvokiene, J., Bjornstad, A., 2006. Induction of micronuclei and other nuclear abnormalities in mussels exposed to bisphenol A, diallyl phthalate and tetrabromodiphenyl ether-47. Aquat. Toxicol. 78, 2004–2007. https://doi.org/10.1016/j.aquatox.2006.02.023

Baudrimont, A., Penkner, A., Woglar, A., Mamnun, Y.M., Hulek, M., Struck, C., Schnabel, R., Loidl, J., Jantsch, V., 2011. A new thermosensitive smc-3 allele reveals involvement of cohesin in homologous recombination in *C. elegans*. PLoS One 6. https://doi.org/10.1371/journal.pone.0024799

Baumann, H., Smith, E.M., 2018. Quantifying metabolically driven pH and oxygen fluctuations in US nearshore habitats at diel to interannual time scales. Estuaries and Coasts 41, 1102–1117. https://doi.org/10.1007/s

Bayne, B.L., 1976. Aspects of Reproduction in Bivalve Molluscs, Estuarine Processes. ACADEMIC PRESS, INC. https://doi.org/10.1016/b978-0-12-751801-5.50043-5

Bedulina, D., Meyer, M.F., Gurkov, A., Kondratjeva, E., Baduev, B., Gusdorf, R., Timofeyev, M.A., 2017. Intersexual differences of heat shock response between two amphipods (*Eulimnogammarus verrucosus* and *Eulimnogammarus cyaneus*) in Lake Baikal. PeerJ 2017. https://doi.org/10.7717/peerj.2864

Beesley, A., Lowe, D.M., Pascoe, C.K., Widdicombe, S., 2008. Effects of CO_2-induced seawater acidification on the health of *Mytilus edulis*. Clim. Res. 37, 215–225. https://doi.org/10.3354/cr00765

Béguel, J.P., Huvet, A., Quillien, V., Lambert, C., Fabioux, C., 2013. Study of the antioxidant capacity in gills of the Pacific oyster *Crassostrea gigas* in link with its reproductive investment. Comp. Biochem. Physiol. - C Toxicol. Pharmacol. 157, 63–71. https://doi.org/10.1016/j.cbpc.2012.10.004

Belivermiş, M., Besson, M., Swarzenski, P., Oberhaensli, F., Taylor, A., Metian, M., 2020. Influence of pH on Pb accumulation in the blue mussel, *Mytilus edulis*. Mar. Pollut. Bull. 156, 111203. https://doi.org/10.1016/j.marpolbul.2020.111203

Benedetto, R., Cabrita, I., Schreiber, R., Kunzelmann, K., 2019. TMEM16A is indispensable for basal mucus secretion in airways and intestine. FASEB J. 33, 4502–4512. https://doi.org/10.1096/fj.201801333RRR

Beniash, E., Ivanina, A., Lieb, N.S., Kurochkin, I., Sokolova, I.M., 2010. Elevated level of carbon dioxide affects metabolism and shell formation in oysters *Crassostrea virginica*. Mar. Ecol. Prog. Ser. 419, 95–108. https://doi.org/10.3354/meps08841

Benjamini, Y., Hochberg, Y., 1995. Controlling the false discovery rate: a practical and powerful approach to multiple testing. Journal of the Royal statistical society: series B (Methodological), 57(1), 289-300. https://doi.org/10.1111/j.2517-6161.1995.tb02031.x

Berthelin, C., Kellner, K., Mathieu, M., 2000. Storage metabolism in the Pacific oyster (*Crassostrea gigas*) in relation to summer mortalities and reproductive cycle (West Coast of France). Comparative Biochemistry & Physiology-Part B, 125, 359–369. https://doi.org/10.1016/S0305-0491(99)00187-X

Bertucci, A., Moya, A., Tambutté, S., Allemand, D., Supuran, C.T., Zoccola, D., 2013. Carbonic anhydrases in anthozoan corals - A review. Bioorganic Med. Chem. 21, 1437–1450. https://doi.org/10.1016/j.bmc.2012.10.024

Bertucci, J.I., Bellas, J., 2021. Combined effect of microplastics and global warming factors on early growth and development of the sea urchin (*Paracentrotus lividus*). Sci. Total Environ. 782, 146888. https://doi.org/10.1016/j.scitotenv.2021.146888

Beukema, J.J., Dekker, R., Jansen, J.M., 2009. Some like it cold: populations of the tellinid bivalve *Macoma balthica* (L.) suffer in various ways from a warming climate. Mar. Ecol. Prog. Ser. 384, 135–145. https://doi.org/10.3354/meps07952

Bhatia, H., Kumar, A., Du, J., Chapman, J., McLaughlin, M.J., 2013. Di-n-butyl phthalate causes antiestrogenic effects in female murray rainbowfish (*Melanotaenia fluviatilis*). Environ. Toxicol. Chem. 32, 2335–2344. https://doi.org/10.1002/etc.2304

Bianchini, A., Carvalho De Castilho, P., 1999. Effects of zinc exposure on oxygen consumption and gill Na^+, K^+- ATPase of the estuarine crab *Chasmagnathus granulata* Dana, 1851 (Decapoda - Grapsidae). Bull. Environ. Contam. Toxicol. 62, 63–69. https://doi.org/10.1007/s001289900842

Bianchini, A., Playle, R.C., Wood, C.M., Walsh, P.J., 2005. Mechanism of acute silver toxicity in marine invertebrates. Aquat. Toxicol. 72, 67–82. https://doi.org/10.1016/j.aquatox.2004.11.012

Bibby, R., Widdicombe, S., Parry, H., Spicer, J., Pipe, R., 2008. Effects of ocean acidification on the immune response of the blue mussel *Mytilus edulis*. Aquat. Biol. 2, 67–74. https://doi.org/10.3354/ab00037

Bignell, J.P., Dodge, M.J., Feist, S.W., Lyons, B., Martin, P.D., Taylor, N.G.H., Stone, D., Travalent, L., Stentiford, G.D., 2008. Mussel histopathology: Effects of season, disease and species. Aquat. Biol. 2, 1–15. https://doi.org/10.3354/ab00031

Bijma, J., Pörtner, H.O., Yesson, C., Rogers, A.D., 2013. Climate change and the oceans - What does the future hold? Mar. Pollut. Bull. 74, 495–505. https://doi.org/10.1016/j.marpolbul.2013.07.022

Bila, D., Montalvão, A.F., Azevedo, D. de A., Dezotti, M., 2007. Estrogenic activity removal of 17β-estradiol by ozonation and identification of by-products. Chemosphere 69, 736–746. https://doi.org/10.1016/j.chemosphere.2007.05.016

Bindoff, N.L., Cheung, W.W.L., Kairo, J.G., Arístegui, J., Guinder, V.A., Hallberg, R., Hilmi, N.J., Marie, J., Nianzhi, K., Saiful, M., Levin, L., O'Donoghue, S., Purca Cuicapusa, S.R., Rinkevich, B., Suga, T., Tagliabue, A., Williamson, P., 2019. Changing ocean, marine ecosystems, and dependent communities. Ocean Cryosph. a Chang. Clim. 447–588. https://doi.org/10.1017/9781009157964.013

Birnstiel, S., Soares-gomes, A., Gama, B.A.P., 2019. Depuration reduces microplastic content in wild and farmed mussels. Mar. Pollut. Bull. 140, 241–247. https://doi.org/10.1016/j.marpolbul.2019.01.044

Björnström, L., Sjöberg, M., 2005. Mechanisms of estrogen receptor signaling: Convergence of genomic and nongenomic actions on target genes. Mol. Endocrinol. 19, 833–842. https://doi.org/10.1210/me.2004-0486

Blair, J.D., Kelly, B.C., Surridge, B., Gobas, F.A.P.C., 2009. Ultra-trace determination of phthalate ester metabolites in seawater , sediments , and biota from an urbanized marine inlet by LC / ESI-MS / MS 43, 6262–6268.

Blanco-Rayón, E., Ivanina, A. V., Sokolova, I.M., Marigómez, I., Izagirre, U., 2020. Sex and sex-related differences in gamete development progression impinge on biomarker responsiveness in sentinel mussels. Sci. Total Environ. 740, 140178. https://doi.org/10.1016/j.scitotenv.2020.140178

Bloomfield, J.P., Williams, R.J., Gooddy, D.C., Cape, J.N., Guha, P., 2006. Impacts of climate change on the fate and behaviour of pesticides in surface and groundwater-a UK perspective. Sci. Total Environ. 369, 163–177. https://doi.org/10.1016/j.scitotenv.2006.05.019

Boas, M., Feldt-Rasmussen, U., Main, K.M., 2012. Thyroid effects of endocrine disrupting chemicals. Mol. Cell. Endocrinol. 355, 240–248. https://doi.org/10.1016/j.mce.2011.09.005

Bocchetti, R., Regoli, F., 2006. Seasonal variability of oxidative biomarkers, lysosomal parameters, metallothioneins and peroxisomal enzymes in the Mediterranean mussel *Mytilus galloprovincialis* from Adriatic Sea. Chemosphere 65, 913–921. https://doi.org/10.1016/j.chemosphere.2006.03.049

Bodin, N., Burgeot, T., Stanisière, J.Y., Bocquené, G., Menard, D., Minier, C., Boutet, I., Amat, A., Cherel, Y., Budzinski, H., 2004. Seasonal variations of a battery of biomarkers and physiological indices for the mussel *Mytilus galloprovincialis* transplanted into the northwest Mediterranean Sea. Comp. Biochem. Physiol. - C Toxicol. Pharmacol. 138, 411–427. https://doi.org/10.1016/j.cca.2004.04.009

Boni, R., Gallo, A., Montanino, M., Macina, A., Tosti, E., 2016. Dynamic changes in the sperm quality of *Mytilus galloprovincialis* under continuous thermal stress 173, 162–173. https://doi.org/10.1002/mrd.22604

Bonnard, M., Roméo, M., Amiard-Triquet, C., 2009. Effects of copper on the burrowing behavior of estuarine and coastal invertebrates, the polychaete *Nereis diversicolor* and the bivalve *Scrobicularia plana*. Hum. Ecol. Risk Assess. 15, 11–26. https://doi.org/10.1080/10807030802614934

Boone, A.N., Vijayan, M.M., 2002. Constitutive heat shock protein 70 (HSC70) expression in rainbow trout hepatocytes: Effect of heat shock and heavy metal exposure. Comp. Biochem. Physiol. - C Toxicol. Pharmacol. 132, 223–233. https://doi.org/10.1016/S1532-0456(02)00066-2

Borch, J., Dalgaard, M., & Ladefoged, O. (2005). Early testicular effects in rats perinatally exposed to DEHP in combination with DEHA—apoptosis assessment and immunohistochemical studies. Reproductive toxicology, 19(4), 517-525. https://doi.org/10.1016/j.reprotox.2004.11.004

Borcherding, J., 1991. The annual reproductive cycle of the freshwater mussel *Dreissena polymorpha* Pallas in lakes. Oecologia 87, 208–218. https://doi.org/10.1007/BF00325258

Boudjema, K., Kourdali, S., Bounakous, N., Meknachi, A., Badis, A., 2014. Catalase activity in brown mussels (*Perna perna*) under acute cadmium, lead, and copper exposure and depuration tests. J. Mar. Biol. 2014. https://doi.org/10.1155/2014/830657

Boutet, I., Lacroix, C., Devin, S., Tanguy, A., Moraga, D., Auffret, M., 2021. Does the environmental history of mussels have an effect on the physiological response to additional stress under experimental conditions? Sci. Total Environ. 149925. https://doi.org/10.1016/j.scitotenv.2021.149925

Braga, A.C., Camacho, C., Marques, A., Gago-Martínez, A., Pacheco, M., Costa, P.R., 2018. Combined effects of warming and acidification on accumulation and elimination dynamics of paralytic shellfish toxins in mussels *Mytilus galloprovincialis*. Environ. Res. 164, 647–654. https://doi.org/10.1016/j.envres.2018.03.045

Brandts, I., Teles, M., Gonçalves, A.P., Barreto, A., Franco-martinez, L., Tvarijonaviciute, A., 2018. Effects of nanoplastics on *Mytilus galloprovincialis* after individual and combined exposure with carbamazepine. Sci. Total Environ. 643, 775–784. https://doi.org/10.1016/j.scitotenv.2018.06.257

Bråte, I.L.N., Blázquez, M., Brooks, S.J., Thomas, K. V., 2018. Weathering impacts the uptake of polyethylene microparticles from toothpaste in Mediterranean mussels (*M. galloprovincialis*). Sci. Total Environ. 626, 1310–1318. https://doi.org/10.1016/j.scitotenv.2018.01.141

Bray, J.D., Chennathukuzhi, V.M., Hecht, N.B., 2002. Identification and characterization of cDNAs encoding four novel proteins that interact with translin associated factor-X. Genomics 79, 799–808. https://doi.org/10.1006/geno.2002.6779

Breitburg, D., Levin, L.A., Oschlies, A., Grégoire, M., Chavez, F.P., Conley, D.J., Garçon, V., Gilbert, D., Gutiérrez, D., Isensee, K., Jacinto, G.S., 2018. Declining oxygen in the global ocean and coastal waters. Science, 359(6371). https://doi.org/10.1126/science.aam7240

Breuza, L., Halbeisen, R., Jenö, P., Otte, S., Barlowe, C., Hong, W., Hauri, H.P., 2004. Proteomics of endoplasmic reticulum-golgi intermediate compartment (ERGIC) membranes from brefeldin A-treated HepG2 cells identifies ERGIC-32, a new cycling protein that interacts with human Erv46. J. Biol. Chem. 279, 47242–47253. https://doi.org/10.1074/jbc.M406644200

Bringer, A., Cachot, J., Dubillot, E., Prunier, G., Huet, V., Clérandeau, C., Evin, L., Thomas, H., 2022. Intergenerational effects of environmentally aged microplastics on the *Crassostrea gigas*. Environ. Pollut. 294. https://doi.org/10.1016/j.envpol.2021.118600

Britto, R.S., Nascimento, J.P., Serode, T., Santos, A.P., Soares, A.M.V.M., Figueira, E., Furtado, C., Lima-Ventura, J., Monserrat, J.M., Freitas, R., 2020. The effects of co-exposure of graphene oxide and copper under different pH conditions in Manila clam *Ruditapes philippinarum*. Environ. Sci. Pollut. Res. 27, 30945–30956. https://doi.org/10.1007/s11356-019-06643-4

Broeg, K., Lehtonen, K.K., 2006. Indices for the assessment of environmental pollution of the Baltic Sea coasts: Integrated assessment of a multi-biomarker approach. Mar. Pollut. Bull. 53, 508–522. https://doi.org/10.1016/j.marpolbul.2006.02.004

Brooks, S.J., Farmen, E., 2013. The distribution of the mussel *Mytilus* species along the Norwegian coast. J. Shellfish Res. 32, 265–270. https://doi.org/10.2983/035.032.0203

Brown, D., Thompson, R., 1982. Phthalates and the aquatic environment: Part II The bioconcentration and depuration of di-2-ethylhexyl phthalate (DEHP) and di-isodecyl phthalate (DIDP) in mussels (*Mytilus edulis*). Chemosphere 11, 427–435. https://doi.org/10.1016/0045-6535(82)90046-7

Browne, M.A., Dissanayake, A., Galloway, T.S., Lowe, D.M., Thompson, R.C., 2008. Ingested Microscopic PlasticTranslocates to the Circulatory System of the Mussel, *Mytilus edulis* (L.). Environ. Sci. Technol 42, 5026–5031. https://doi.org/10.1021/es800249a

Bruno, K.A., Mathews, J.E., Yang, A.L., Frisancho, J.A., Scott, A.J., Greyner, H.D., Molina, F.A., Greenaway, M.S., Cooper, G.M., Bucek, A., Morales-Lara, A.C., Hill, A.R., Mease, A.A., Di Florio, D.N., Sousou, J.M., Coronado, A.C., Stafford, A.R., Fairweather, D.L., 2019. BPA Alters Estrogen Receptor Expression in the Heart After Viral Infection Activating Cardiac Mast Cells and T Cells Leading to Perimyocarditis and Fibrosis. Front. Endocrinol. (Lausanne). 10, 1–18. https://doi.org/10.3389/fendo.2019.00598

Buckley, B.A., Owen, M.E., Hofmann, G.E., 2001. Adjusting the thermostat: The threshold induction temperature for the heat-shock response in intertidal mussels (genus *Mytilus*) changes as a function of thermal history. J. Exp. Biol. 204, 3571–3579.

Buckley, L.B., Urban, M.C., Angilletta, M.J., Crozier, L.G., Rissler, L.J., Sears, M.W., 2010. Can mechanism inform species' distribution models? Ecol. Lett. 13, 1041–1054. https://doi.org/10.1111/j.1461-0248.2010.01479.x

Burge, C.A., Closek, C.J., Friedman, C.S., Groner, M.L., Jenkins, C.M., Shore-Maggio, A., Welsh, J.E., 2016. The Use of Filter-feeders to Manage Disease in a Changing World. Integr. Comp. Biol. 56, 573–587. https://doi.org/10.1093/icb/icw048

Burger, J., 2007. A framework and methods for incorporating gender-related issues in wildlife risk assessment: Gender-related differences in metal levels and other contaminants as a case study. Environ. Res. 104, 153–162. https://doi.org/10.1016/j.envres.2006.08.001

Burger, J., 2006. Bioindicators: A review of their use in the environmental literature 1970–2005. Environ. Bioindic. 1, 136–144. https://doi.org/10.1080/15555270600701540

Burger, J., Gochfeld, M., 2001. On developing bioindicators for human and ecological health. Environ. Monit. Assess. 66, 23–46. https://doi.org/10.1023/A:1026476030728

Burgos-Aceves, M.A., Abo-Al-Ela, H.G., Faggio, C., 2021a. Impact of phthalates and bisphenols plasticizers on haemocyte immune function of aquatic invertebrates: A review on physiological, biochemical, and genomic aspects. J. Hazard. Mater. 419, 126426. https://doi.org/10.1016/j.jhazmat.2021.126426

Burgos-Aceves, M.A., Abo-Al-Ela, H.G., Faggio, C., 2021b. Physiological and metabolic approach of plastic additive effects: Immune cells responses. J. Hazard. Mater. 404, 124114. https://doi.org/10.1016/j.jhazmat.2020.124114

Burlando, B., Berti, E., Viarengo, A., 2006. Effects of seawater pollutants on protein tyrosine phosphorylation in mussel tissues. Aquat. Toxicol. 78, 79–85. https://doi.org/10.1016/j.aquatox.2006.02.020

Burmester, V., Nimptsch, J., Wiegand, C., 2012. Adaptation of freshwater mussels to cyanobacterial toxins: Response of the biotransformation and antioxidant enzymes. Ecotoxicol. Environ. Saf. 78, 296–309. https://doi.org/10.1016/j.ecoenv.2011.11.037

Burnham, K. P., Anderson, D. R., 2002. A practical information-theoretic approach. Model selection and multimodel inference, 2, 70-71.

Burns, M.J., Nixon, G.J., Foy, C.A., Harris, N., 2005. Standardisation of data from real-time quantitative PCR methods - Evaluation of outliers and comparison of calibration curves. BMC Biotechnol. 5, 1–13. https://doi.org/10.1186/1472-6750-5-31

Bustin, S.A., Benes, V., Garson, J.A., Hellemans, J., Huggett, J., Kubista, M., Mueller, R., Nolan, T., Pfaffl, M.W., Shipley, G.L., 2009. The MIQE Guidelines: M inimum I nformation for Publication of Q uantitative Real-Time PCR E xperiments SUMMARY : 622, 611–622. https://doi.org/10.1373/clinchem.2008.112797

Byrne, R.A., Dietz, T.H., 1997. Ion transport and acid-base balance in freshwater bivalves. J. Exp. Biol. 200, 457–465. https://doi.org/10.1242/jeb.200.3.457

Byrne, M., Soars, N., Selvakumaraswamy, P., Dworjanyn, S.A., Davis, A.R., 2010. Sea urchin fertilization in a warm, acidified and high pCO_2 ocean across a range of sperm densities. Mar. Environ. Res. 69, 234–239. https://doi.org/10.1016/j.marenvres.2009.10.014

C

Cajaraville, M.P., Ortiz-Zarragoitia, M., 2006. Specificity of the peroxisome proliferation response in mussels exposed to environmental pollutants. Aquat. Toxicol. 78, 117–123. https://doi.org/10.1016/j.aquatox.2006.02.016

Cai, W.J., Hu, X., Huang, W.J., Murrell, M.C., Lehrter, J.C., Lohrenz, S.E., Chou, W.C., Zhai, W., Hollibaugh, J.T., Wang, Y., Zhao, P., Guo, X., Gundersen, K., Dai, M., Gong, G.C., 2011. Acidification of subsurface coastal waters enhanced by eutrophication. Nat. Geosci. 4, 766–770. https://doi.org/10.1038/ngeo1297

Calabrese, E.J., 2001. Overcompensation stimulation: A mechanism for hormetic effects. Crit. Rev. Toxicol. 31, 425–470. https://doi.org/10.1080/20014091111749

Callaway, R., Shinn, A.P., Grenfell, S.E., Bron, J.E., Burnell, G., Cook, E.J., Crumlish, M., Culloty, S., Davidson, K., Ellis, R.P., Flynn, K.J., Fox, C., Green, D.M., Hays, G.C., Hughes, A.D., Johnston, E., Lowe, C.D., Lupatsch, I., Malham, S., Mendzil, A.F., Nickell, T., Pickerell, T., Rowley, A.F., Stanley, M.S., Tocher, D.R., Turnbull, J.F., Webb, G., Wootton, E., Shields, R.J., 2012. Review of climate change impacts on marine aquaculture in the UK and Ireland. Aquat. Conserv. Mar. Freshw. Ecosyst. 22, 389–421. https://doi.org/10.1002/aqc.2247

Cancio, I., Orbea, A., Völkl, A., Fahimi, H.D., Cajaraville, M.P., 1998. Induction of peroxisomal oxidases in mussels: Comparison of effects of lubricant oil and benzo(a)pyrene with two typical peroxisome proliferators on peroxisome structure and function in *Mytilus galloprovincialis*. Toxicol. Appl. Pharmacol. 149, 64–72. https://doi.org/10.1006/taap.1997.8358

Canesi, L., Borghi, C., Fabbri, R., Ciacci, C., Lorusso, L.C., Gallo, G., Vergani, L., 2007a. Effects of 17β-estradiol on mussel digestive gland. Gen. Comp. Endocrinol. 153, 40–46. https://doi.org/10.1016/j.ygcen.2007.02.005

Canesi, L., Ciacci, C., Lorusso, L.C., Betti, M., Gallo, G., Pojana, G., Marcomini, A., 2007b. Effects of Triclosan on *Mytilus galloprovincialis* hemocyte function and digestive gland enzyme activities: Possible modes of action on non-target organisms. Comp. Biochem. Physiol. - C Toxicol. Pharmacol. 145, 464–472. https://doi.org/10.1016/j.cbpc.2007.02.002

Canesi, L., Lorusso, L.C., Ciacci, C., Betti, M., Zampini, M., Gallo, G., 2004. Environmental estrogens can affect the function of mussel hemocytes through rapid modulation of kinase pathways. Gen. Comp. Endocrinol. 138, 58–69. https://doi.org/10.1016/j.ygcen.2004.05.004

Canesi, L., Miglioli, A., Balbi, T., Fabbri, E., 2022. Physiological roles of serotonin in bivalves: possible interference by environmental chemicals resulting in neuroendocrine disruption. Front. Endocrinol. (Lausanne). 13, 1–14. https://doi.org/10.3389/fendo.2022.792589

Cao, R., Zhang, T., Li, X., Zhao, Y., Wang, Q., Yang, D., Qu, Y., Liu, H., Dong, Z., Zhao, J., 2019. Seawater acidification increases copper toxicity: A multi-biomarker approach with a key marine invertebrate, the Pacific Oyster *Crassostrea gigas*. Aquat. Toxicol. 210, 167–178. https://doi.org/10.1016/j.aquatox.2019.03.002

Capolupo, M., Gunaalan, K., Booth, A.M., Sørensen, L., Valbonesi, P., Fabbri, E., 2021. The sub-lethal impact of plastic and tire rubber leachates on the Mediterranean mussel *Mytilus galloprovincialis*. Environ. Pollut. 283, 117081. https://doi.org/10.1016/j.envpol.2021.117081

Cappello, T., De Marco, G., Oliveri Conti, G., Giannetto, A., Ferrante, M., Mauceri, A., Maisano, M., 2021. Time-dependent metabolic disorders induced by short-term exposure to polystyrene

microplastics in the Mediterranean mussel *Mytilus galloprovincialis*. Ecotoxicol. Environ. Saf. 209, 111780. https://doi.org/10.1016/j.ecoenv.2020.111780

Cardoso, P.G., Resende-de-Oliveira, R., Rocha, E., 2019. Combined effects of increased temperature and levonorgestrel exposure on zebrafish female liver, using stereology and immunohistochemistry against catalase, CYP1A, HSP90 and vitellogenin. Environ. Pollut. 252, 1059–1067. https://doi.org/10.1016/j.envpol.2019.06.058

Carnevali, O., Tosti, L., Speciale, C., Peng, C., Zhu, Y., Maradonna, F., 2010. DEHP impairs zebrafish reproduction by affecting critical factors in oogenesis. PLoS One 5, 1–7. https://doi.org/10.1371/journal.pone.0010201

Chapman, E.C., Bonsor, B.J., Parsons, D.R., Rotchell, J.M., 2020. Influence of light and temperature cycles on the expression of circadian clock genes in the mussel *Mytilus edulis*. Mar. Environ. Res. 159, 104960. https://doi.org/10.1016/j.marenvres.2020.104960

Chapman, E.C., O'Dell, A.R., Meligi, N.M., Parsons, D.R., Rotchell, J.M., 2017. Seasonal expression patterns of clock-associated genes in the blue mussel *Mytilus edulis*. Chronobiol. Int. 34, 1300–1314. https://doi.org/10.1080/07420528.2017.1363224

Chapman, P.M., 2002. Ecological risk assessment (ERA) and hormesis. Sci. Total Environ. 288, 131–140. https://doi.org/10.1016/S0048-9697(01)01120-2

Chelomin, V.P., Mazur, A.A., Slobodskova, V.V., Kukla, S.P., Dovzhenko, N.V., 2022. Genotoxic Properties of Polystyrene (PS) Microspheres in the Filter-Feeder Mollusk *Mytilus trossulus* (Gould, 1850). J. Mar. Sci. Eng. 10, 273. https://doi.org/10.3390/jmse10020273

Chen, C.Y., 2004. Biosynthesis of di-(2-ethylhexyl) phthalate (DEHP) and di-n-butyl phthalate (DBP) from red alga - *Bangia atropurpurea*. Water Res. 38, 1014–1018. https://doi.org/10.1016/j.watres.2003.11.029

Cheng, W., Chiang, J.C.H., Zhang, D., 2013. Atlantic meridional overturning circulation (AMOC) in CMIP5 Models: RCP and historical simulations. J. Clim. 26, 7187–7197. https://doi.org/10.1175/JCLI-D-12-00496.1

Cherkasov, A.S., Grewal, S., Sokolova, I.M., 2007. Combined effects of temperature and cadmium exposure on haemocyte apoptosis and cadmium accumulation in the eastern oyster *Crassostrea virginica* (Gmelin). J. Therm. Biol. 32, 162–170. https://doi.org/10.1016/j.jtherbio.2007.01.005

Chiesa, L.M., Nobile, M., Malandra, R., Pessina, D., Panseri, S., Labella, G.F., Arioli, F., 2018. Food safety traits of mussels and clams: distribution of PCBs, PBDEs, OCPs, PAHs and PFASs in sample from different areas using HRMS-Orbitrap® and modified QuEChERS extraction followed by GC-MS/MS. Food Addit. Contam. - Part A Chem. Anal. Control. Expo. Risk Assess. 35, 959–971. https://doi.org/10.1080/19440049.2018.1434900

Chmist, J., Szoszkiewicz, K., Drożdżyński, D., 2019. Behavioural Responses of Unio tumidus Freshwater Mussels to Pesticide Contamination. Arch. Environ. Contam. Toxicol. 77, 432–442. https://doi.org/10.1007/s00244-019-00649-2

Choi, J.S., Kim, K., Hong, S.H., Park, K. Il, Park, J.W., 2021. Impact of polyethylene terephthalate microfiber length on cellular responses in the Mediterranean mussel *Mytilus galloprovincialis*. Mar. Environ. Res. 168, 105320. https://doi.org/10.1016/j.marenvres.2021.105320

Choi, J.S., Kim, K., Park, K., Park, J.-W., 2022. Long-term exposure of the Mediterranean mussels, *Mytilus galloprovincialis* to polyethylene terephthalate microfibers: Implication for reproductive and neurotoxic effects. Chemosphere 299, 134317. https://doi.org/10.1016/j.chemosphere.2022.134317

Christensen, R.H.B., 2019. "Ordinal—regression models for ordinal data." R package version 2019.12-10 https://CRAN.R-project.org/package=ordinal

Ciocan, C., Cubero-Leon, E., Puinean, M., Hill, E.M., Minier, C., Osada, M., Fenlon, K., Rotchell, J.M., 2010a. Effects of estrogen exposure in mussels, *Mytilus edulis*, at different stages of gametogenesis. Environ. Pollut. 158, 2977–2984. https://doi.org/10.1016/j.envpol.2010.05.025

Ciocan, C., Cubero-Leon, E., Minier, C., Rotchell, J.M., 2011. Identification of reproduction-specific genes associated with maturation and estrogen exposure in a marine bivalve Mytilus edulis. PLoS One 6. https://doi.org/10.1371/journal.pone.0022326

Ciocan, C., Puinean, M., Cubero-Leon, E., E. Hill, E.M., Minier, C., Osada, M., Itoh, N, Rotchell, J.M., 2010b. Endocrine Disruption, Reproductive Cycle and Pollutants in Blue Mussel *Mytilus edulis*. Environ. Chem. 121–126.

Clark, M. S. 2020. Molecular mechanisms of biomineralization in marine invertebrates. J. Exp. Biol., 223(11), jeb206961. https://doi.org/10.1242/jeb.206961

Clements, J.C., Bishop, M.M., Hunt, H.L., 2017. Elevated temperature has adverse effects on GABA-mediated avoidance behaviour to sediment acidification in a wide-ranging marine bivalve. Mar. Biol. 164, 1–11. https://doi.org/10.1007/s00227-017-3085-1

Clements, J.C., Comeau, L.A., Carver, C.E., Mayrand, É., Plante, S., Mallet, A.L., 2018. Short-term exposure to elevated pCO_2 does not affect the valve gaping response of adult eastern oysters, *Crassostrea virginica*, to acute heat shock under an ad libitum feeding regime. J. Exp. Mar. Bio. Ecol. 506, 9–17. https://doi.org/10.1016/j.jembe.2018.05.005

Clements, J.C., Poirier, L.A., Pérez, F.F., Comeau, L.A., Babarro, J.M.F., 2020. Behavioural responses to predators in Mediterranean mussels (*Mytilus galloprovincialis*) are unaffected by elevated pCO_2. Mar. Environ. Res. 161. https://doi.org/10.1016/j.marenvres.2020.105148

Cocci, P., Capriotti, M., Mosconi, G., Palermo, F.A., 2017. Transcriptional variations in biomarkers of *Mytilus galloprovincialis* sampled from Central Adriatic coastal waters (Marche region, Italy). Biomarkers 22, 537–547. https://doi.org/10.1080/1354750X.2017.1315614

Combarnous, Y., 2017. Endocrine Disruptor Compounds (EDCs) and agriculture: The case of pesticides. Comptes Rendus - Biol. 340, 406–409. https://doi.org/10.1016/j.crvi.2017.07.009

Combarnous, Y., Nguyen, D.T.M., 2019. Comparative overview of the mechanisms of action of hormones and endocrine disruptor compounds. Toxics 7, 1–11. https://doi.org/10.3390/toxics7010005

Comber, S.D.W., Gardner, M.J., Ellor, B., 2020. Seasonal variation of contaminant concentrations in wastewater treatment works effluents and river waters. Environ. Technol. (United Kingdom) 41, 2716–2730. https://doi.org/10.1080/09593330.2019.1579872

Connor, K.M., Gracey, A.Y., 2011. Circadian cycles are the dominant transcriptional rhythm in the intertidal mussel *Mytilus californianus*. Proc. Natl. Acad. Sci. U. S. A. 108, 16110–16115. https://doi.org/10.1073/pnas.1111076108

Conolly, R.B., Lutz, W.K., 2004. Nonmonotonic dose-response relationships: Mechanistic basis, kinetic modeling, and implications for risk assessment. Toxicol. Sci. 77, 151–157. https://doi.org/10.1093/toxsci/kfh007

Conway Morris, S. C., and Peel, J. S., 1995. Articulated halkieriids from the lower Cambrian of North Greenland and their role in early protostome evolution. Philosophical Transactions of the Royal Society of London. Series B: Biological Sciences, 347(1321), 305-358.

Coppola, F., Almeida, Â., Henriques, B., Soares, A.M.V.M., Figueira, E., Pereira, E., Freitas, R., 2018. Biochemical responses and accumulation patterns of *Mytilus galloprovincialis* exposed to thermal stress and Arsenic contamination. Ecotoxicol. Environ. Saf. 147, 954–962. https://doi.org/10.1016/j.ecoenv.2017.09.051

Costa, S., Coppola, F., Pretti, C., Intorre, L., Meucci, V., Soares, A.M.V.M., Solé, M., Freitas, R., 2020. Biochemical and physiological responses of two clam species to Triclosan combined with climate change scenario. Sci. Total Environ. 724. https://doi.org/10.1016/j.scitotenv.2020.138143

Costantini, D., Borremans, B., 2019. The linear no-threshold model is less realistic than threshold or hormesis-based models: An evolutionary perspective. Chemico-biological interactions, 301, 26-33. https://doi.org/10.1016/j.cbi.2018.10.007

Cotta-Ramusino, C., McDonald III, E. R., Hurov, K., Sowa, M. E., Harper, J. W., Elledge, S. J., 2011. A DNA damage response screen identifies RHINO, a 9-1-1 and TopBP1 interacting protein required for ATR signaling. Science, 332(6035), 1313-1317. https://doi.org/10.1126/science.1203430

Croll, R.P., Wang, C., 2007. Possible roles of sex steroids in the control of reproduction in bivalve molluscs. Aquaculture 272, 76–86. https://doi.org/10.1016/j.aquaculture.2007.06.031

Cruciani, V., Iovine, C., Thomé, J.-P., Joaquim-Justo, C., 2016. Impact of three phthalate esters on the sexual reproduction of the Monogonont rotifer, *Brachionus calyciflorus*. Ecotoxicology 25(1), 192–200. https://doi.org/10.1007/s10646-015-1579-5

Cubero-Leon, E., Ciocan, C.M., Hill, E.M., Osada, M., Kishida, M., Itoh, N., Kondo, R., Minier, C., Rotchell, J.M., 2010. Estrogens disrupt serotonin receptor and cyclooxygenase mRNA expression in the gonads of mussels (*Mytilus edulis*). Aquat. Toxicol. 98, 178–187. https://doi.org/10.1016/j.aquatox.2010.02.007

Cubero-Leon, E., Ciocan, C.M., Minier, C., Rotchell, J.M., 2012. Reference gene selection for qPCR in mussel, *Mytilus edulis*, during gametogenesis and exogenous estrogen exposure. Environ. Sci. Pollut. Res. 19, 2728–2733. https://doi.org/10.1007/s11356-012-0772-9

Cuenca, L., Shin, N., Lascarez-Lagunas, L. I., Martinez-Garcia, M., Nadarajan, S., Karthikraj, R., Kannan, K, Colaiácovo, M. P., 2020. Environmentally-relevant exposure to diethylhexyl phthalate (DEHP) alters regulation of double-strand break formation and crossover designation leading to germline dysfunction in *Caenorhabditis elegans*. PLoS genetics, 16(1), e1008529.Curley, E.A.M., Thomas, R., Adams, C.E., Stephen, A., 2021. Behavioural and metabolic responses of Unionida mussels to stress. Aquat. Conserv. Mar. Freshw. Ecosyst. 31, 3184–3200. https://doi.org/10.1002/aqc.3689

D

Das, M.T., Ghosh, P., Thakur, I.S., 2014. Intake estimates of phthalate esters for South Delhi population based on exposure media assessment. Environ. Pollut. 189, 118–125. https://doi.org/10.1016/j.envpol.2014.02.021

da Silva Souza, L., Bonnail, E., Maranho, L.A., Pusceddu, F.H., Cortez, F.S., Cesar, A., Ribeiro, D.A., Riba, I., de Souza Abessa, D.M., DelValls, Á., Pereira, C.D.S., 2021. Sub-lethal combined effects of illicit drug and decreased pH on marine mussels: A short-time exposure to crack cocaine in CO_2 enrichment scenarios. Mar. Pollut. Bull. 171. https://doi.org/10.1016/j.marpolbul.2021.112735

Damiens, G., His, E., Gnassia-Barelli, M., Quiniou, F., Roméo, M., 2004. Evaluation of biomarkers in oyster larvae in natural and polluted conditions. Comp. Biochem. Physiol. - C Toxicol. Pharmacol. 138, 121–128. https://doi.org/10.1016/j.cca.2004.05.010

Davis, R.A., Innocenti, A., Poulsen, S.A., Supuran, C.T., 2010. Carbonic anhydrase inhibitors. Identification of selective inhibitors of the human mitochondrial isozymes VA and VB over the cytosolic isozymes I and II from a natural product-based phenolic library. Bioorganic Med. Chem. 18, 14–18. https://doi.org/10.1016/j.bmc.2009.11.021

Deane, E.E., Woo, N.Y.S., 2004. Differential gene expression associated with euryhalinity in sea bream (*Sparus sarba*). Am. J. Physiol. - Regul. Integr. Comp. Physiol. 287, 1054–1063. https://doi.org/10.1152/ajpregu.00347.2004

Deane, E.E., Woo, N.Y.S., 2005. Cloning and characterization of the hsp70 multigene family from silver sea bream: Modulated gene expression between warm and cold temperature acclimation. Biochem. Biophys. Res. Commun. 330, 776–783. https://doi.org/10.1016/j.bbrc.2005.03.039

Deguchi, R., Osanai, K., 1995. Serotonin-induced meiosis reinitiation from the first prophase and from the first metaphase in oocytes of the marine bivalve *Hiatella flaccida*: Respective changes in intracellular Ca2+ and pH. Dev. Biol. https://doi.org/10.1006/dbio.1995.1298

Dellali, M., Gnassia Barelli, M., Romeo, M., Aissa, P., 2001. The use of acetylcholinesterase activity in Ruditapes decussatus and *Mytilus galloprovincialis* in the biomonitoring of Bizerta lagoon. Comp. Biochem. Physiol. - C Toxicol. Pharmacol. 130, 227–235. https://doi.org/10.1016/S1532-0456(01)00245-9

Del Rey, Z.R., Granek, E.F., Buckley, B.A., 2011. Expression of HSP70 in *Mytilus californianus* following exposure to caffeine. Ecotoxicology 20, 855–861. https://doi.org/10.1007/s10646-011-0649-6

De Nicola, E., Meriç, S., Gallo, M., Iaccarino, M., Della Rocca, C., Lofrano, G., Russo, T., Pagano, G., 2007. Vegetable and synthetic tannins induce hormesis/toxicity in sea urchin early

development and in algal growth. Environ. Pollut. 146, 46–54. https://doi.org/10.1016/j.envpol.2006.06.018

Denli, A.M., Tops, B.B.J., Plasterk, R.H.A., Ketting, R.F., Hannon, G.J., 2004. Processing of primary microRNAs by the Microprocessor complex. Nature 432, 231–235. https://doi.org/10.1038/nature03049

Denny, M.W., Dowd, W.W., Bilir, L., Mach, K.J., 2011. Spreading the risk: Small-scale body temperature variation among intertidal organisms and its implications for species persistence. J. Exp. Mar. Bio. Ecol. 400, 175–190. https://doi.org/10.1016/j.jembe.2011.02.006

Denoeud, F., Aury, J.M., Da Silva, C., Noel, B., Rogier, O., Delledonne, M., Morgante, M., Valle, G., Wincker, P., Scarpelli, C., Jaillon, O., Artiguenave, F., 2008. Annotating genomes with massive-scale RNA sequencing. Genome Biol. 9. https://doi.org/10.1186/gb-2008-9-12-r175

De Solla, S.R., Bishop, C.A., Van Kraak, G. Der, Brooks, R.J., 1998. Impact of organochlorine contamination on levels of sex hormones and external morphology of common snapping turtles (Chelydra serpentina serpentina) in Ontario, Canada. Environ. Health Perspect. 106, 253–260. https://doi.org/10.1289/ehp.98106253

de Souza Machado, A.A., Kloas, W., Zarfl, C., Hempel, S., Rillig, M.C., 2018. Microplastics as an emerging threat to terrestrial ecosystems. Glob. Chang. Biol. 24, 1405–1416. https://doi.org/10.1111/gcb.14020

De Stephanis, R., Giménez, J., Carpinelli, E., Gutierrez-Exposito, C., Cañadas, A., 2013. As main meal for sperm whales: Plastics debris. Mar. Pollut. Bull. 69, 206–214. https://doi.org/10.1016/j.marpolbul.2013.01.033

Détrée, C., Gallardo-Escárate, C., 2018. Single and repetitive microplastics exposures induce immune system modulation and homeostasis alteration in the edible mussel *Mytilus galloprovincialis*. Fish Shellfish Immunol. 83, 52–60. https://doi.org/10.1016/j.fsi.2018.09.018

Dias, P.J., Batista, F.M., Shanks, A.M., Beaumont, A.R., Davies, I.M., Snow, M., 2009a. Gametogenic asynchrony of mussels *Mytilus* in a mixed-species area: Implications for management. Aquaculture 295, 175–182. https://doi.org/10.1016/j.aquaculture.2009.07.007

Dias, P.J., Dordor, A., Tulett, D., Piertney, S., Davies, I.M., Snow, M., 2009b. Survey of mussel (*Mytilus*) species at Scottish shellfish farms. Aquac. Res. 40, 1715–1722. https://doi.org/10.1111/j.1365-2109.2009.02274.x

Dickey, G., Preziosi, B.M., Clark, C.T., Bowden, T.J., 2018. The impact of ocean acidification on the byssal threads of the blue mussel (*Mytilus edulis*). PLoS One 13, 1–9. https://doi.org/10.1371/journal.pone.0205908

Dickinson, G.H., Ivanina, A. V., Matoo, O.B., Pörtner, H.O., Lannig, G., Bock, C., Beniash, E., Sokolova, I.M., 2012. Interactive effects of salinity and elevated CO_2 levels on juvenile eastern oysters, *Crassostrea virginica*. J. Exp. Biol. 215, 29–43. https://doi.org/10.1242/jeb.061481

Dickson, A.G., Sabine, C.L., Christian, J.R., 2007. Guide to Best Practices for Ocean CO_2 Measurements, PICES Special Publ.

Dixon, D.R., Lowe, D.M., Miller, P.I., Villemin, G.R., Colaço, A., Serrão-Santos, R., Dixon, L.R.J., 2006. Evidence of seasonal reproduction in the Atlantic vent mussel *Bathymodiolus azoricus*, and an apparent link with the timing of photosynthetic primary production. J. Mar. Biol. Assoc. United Kingdom 86, 1363–1371. https://doi.org/10.1017/S0025315406014391

Do, R.P., Stahlhut, R.W., Ponzi, D., vom Saal, F.S., Taylor, J.A., 2012. Non-monotonic dose effects of in utero exposure to di(2-ethylhexyl) phthalate (DEHP) on testicular and serum testosterone and anogenital distance in male mouse fetuses. Reprod. Toxicol. 34, 614–621. https://doi.org/10.1016/j.reprotox.2012.09.006

Doney, S.C., Ruckelshaus, M., Emmett Duffy, J., Barry, J.P., Chan, F., English, C.A., Galindo, H.M., Grebmeier, J.M., Hollowed, A.B., Knowlton, N., Polovina, J., Rabalais, N.N., Sydeman, W.J., Talley, L.D., 2012. Climate change impacts on marine ecosystems. Ann. Rev. Mar. Sci. 4, 11–37. https://doi.org/10.1146/annurev-marine-041911-111611

Dos Reis, I.M.M., Mattos, J.J., Siebert, M.N., Zacchi, F.L., Bastolla, C.L.V., Saldana-Serrano, M., Bicego, M.C., Taniguchi, S., Gomes, C.H.A. de M., de Melo, C.M.R., Bainy, A.C.D., 2023.

Gender influences molecular and histological biomarkers in mature oysters *Crassostrea gasar* (Adanson , 1757) after pyrene exposure. Chemosphere 311. https://doi.org/10.1016/j.chemosphere.2022.136985

Dougherty, G.W., Loges, N.T., Klinkenbusch, J.A., Olbrich, H., Pennekamp, P., Menchen, T., Raidt, J., Wallmeier, J., Werner, C., Westermann, C., Ruckert, C., Mirra, V., Hjeij, R., Memari, Y., Durbin, R., Kolb-Kokocinski, A., Praveen, K., Kashef, M.A., Kashef, S., Eghtedari, F., Häffner, K., Valmari, P., Baktai, G., Aviram, M., Bentur, L., Amirav, I., Davis, E.E., Katsanis, N., Brueckner, M., Shaposhnykov, A., Pigino, G., Dworniczak, B., Omran, H., 2016. DNAH11 localization in the proximal region of respiratory cilia defines distinct outer dynein arm complexes. Am. J. Respir. Cell Mol. Biol. 55, 213–224. https://doi.org/10.1165/rcmb.2015-0353OC

Duinker, A., Haland, L., Hovgaards, P., Mortensen, S., 2021. Gonad development and spawning in one and two year old mussels (*Mytilus edulis*) from Western Norway 88, 1465–1473. https://doi.org/10.1017/S0025315408002130

Durland, E., De Wit, P., Meyer, E., Langdon, C., 2021. Larval development in the Pacific oyster and the impacts of ocean acidification: Differential genetic effects in wild and domesticated stocks. Evol. Appl. 14, 2258–2272. https://doi.org/10.1111/eva.13289

Dzierżyńska-Białończyk, A., Jermacz, Ł., Zielska, J., Kobak, J., 2019. What scares a mussel? Changes in valve movement pattern as an immediate response of a byssate bivalve to biotic factors. Hydrobiologia 841, 65–77. https://doi.org/10.1007/s10750-019-04007-0

E

Earls, A.O., Axford, I.P., Braybrook, J.H., 2003. Gas chromatography-mass spectrometry determination of the migration of phthalate plasticisers from polyvinyl chloride toys and childcare articles. J. Chromatogr. A 983, 237–246. https://doi.org/10.1016/S0021-9673(02)01736-3

Eick, G.N., Thornton, J.W., 2011. Evolution of steroid receptors from an estrogen-sensitive ancestral receptor. Mol. Cell. Endocrinol. 334, 31–38. https://doi.org/10.1016/j.mce.2010.09.003

Ekelund Ugge, G.M.O., Jonsson, A., Olsson, B., Sjöback, R., Berglund, O., 2020. Transcriptional and biochemical biomarker responses in a freshwater mussel (*Anodonta anatin*a) under environmentally relevant Cu exposure. Environ. Sci. Pollut. Res. 27, 9999–10010. https://doi.org/10.1007/s11356-020-07660-4

Elazzaoui, A., Moukrim, A., Lefrere, L., 2019. A Multibiomarker approach to assess the health state of coastal ecosystem receiving desalination plants in Agadir Bay, Morocco. Sci. World J. 2019. https://doi.org/10.1155/2019/5875027

El Jourmi, L., Amine, A., Boutaleb, N., Abouakil, N., Lazar, S., El Antri, S., 2015. The use of biomarkers (catalase and malondialdehyde) in marine pollution monitoring: Spatial variability. J. Mater. Environ. Sci. 6, 1592–1595.

Encomio, V.G., Chu, F.L.E., 2005. Seasonal variation of heat shock protein 70 in eastern oysters (*Crassostrea virginica*) infected with *Perkinsus marinus* (Dermo). J. Shellfish Res. 24, 167–175.

Engler, R.E., 2012. The complex interaction between marine debris and toxic chemicals in the ocean. Environ. Sci. Technol. 46 (22), 12302–12315.

Englund, V., Heino, M., 1994. Valve movement of *Anodonta anatina* and *Unio tumidus* (Bivalvia, Unionidae) in a eutrophic lake. Ann. Zool. Fennici 31, 257–262

Erythropel, H.C., Maric, M., Nicell, J.A., Leask, R.L., Yargeau, V., 2014. Leaching of the plasticizer di(2-ethylhexyl) phthalate (DEHP) from plastic containers and the question of human exposure. Appl. Microbiol. Biotechnol. 98, 9967–9981. https://doi.org/10.1007/s00253-014-6183-8

Esbaugh, A.J., Tufts, B.L., 2006. The structure and function of carbonic anhydrase isozymes in the respiratory system of vertebrates. Respir. Physiol. Neurobiol. 154, 185–198. https://doi.org/10.1016/j.resp.2006.03.007

Escobar, J.A., Rubio, M.A., Lissi, E.A., 1996. SOD and catalase inactivation by singlet oxygen and peroxyl radicals. Free Radic. Biol. Med. 20, 285–290. https://doi.org/10.1016/0891-58

Escudero, G., 2021. TransPi – a comprehensive TRanscriptome ANalysiS PIpeline for de novo transcriptome assembly. bioRxiv 2021.02.18.431773.

European Council for Plasticisers and Intermediates (ECPI), 2020. Plasticisers Available on https://www.plasticisers.org/factsheet/plasticisers-factsheets/ Accessed 12 Mar 2021

European Union Commission Regulation 2018/2005, 2018. Amending Annex XVII to Regulation (EC) No 1907/2006 of the European Parliament and of the Council concerning the Registration, Evaluation, Authorisation and Restriction of Chemicals (REACH) as regards bis(2-ethylhexyl) phthalate (DEHP), dibutyl phthalate (DBP), benzyl butyl phthalate (BBP) and diisobutyl phthalate (DIBP). Available on https://eur-lex.europa.eu/legal-content/EN/TXT/PDF/?uri=CELEX:32018R2005&from=E Accessed 5 Feb 2022

Evans, T.G., Chan, F., Menge, B.A., Hofmann, G.E., 2013. Transcriptomic responses to ocean acidification in larval sea urchins from a naturally variable pH environment. Mol. Ecol. 22, 1609–1625. https://doi.org/10.1111/mec.12188

F

Fabbri, R., Montagna, M., Balbi, T., Raffo, E., Palumbo, F., Canesi, L., 2014. Adaptation of the bivalve embryotoxicity assay for the high throughput screening of emerging contaminants in *Mytilus galloprovincialis*. Mar. Environ. Res. 99, 1–8. https://doi.org/10.1016/j.marenvres.2014.05.007

Fabioux, C., Huvet, A., Le Souchu, P., Le Pennec, M., Pouvreau, S., 2005. Temperature and photoperiod drive *Crassostrea gigas* reproductive internal clock. Aquaculture 250, 458–470. https://doi.org/10.1016/j.aquaculture.2005.02.038

Farrell, P., Nelson, K., 2013. Trophic level transfer of microplastic: *Mytilus edulis* (L.) to *Carcinus maenas* (L.). Environ. Pollut. 177, 1–3. https://doi.org/10.1016/j.envpol.2013.01.046

Fatoki, O.S., Vernon, F., 1990. Phthalate esters in rivers of the Greater Manchester area, UK. Sci. Total Environ. 95, 227–232.

Fearman, J.-A., Bolch, C.J.S., Moltschaniwskyj, N.A., 2009. Energy storage and reproduction in mussels, *Mytilus galloprovincialis* : the influence of diet quality . J. Shellfish Res. 28, 305–312. https://doi.org/10.2983/035.028.0212

Fearman, J., Moltschaniwskyj, N.A., 2010. Warmer temperatures reduce rates of gametogenesis in temperate mussels, *Mytilus galloprovincialis*. Aquaculture 305, 20–25. https://doi.org/10.1016/j.aquaculture.2010.04.003

Feder, M.E., Hofmann, G.E., 1999. Heat-shock proteins, molecular chaperones, and the stress response: Evolutionary and ecological physiology. Annu. Rev. Physiol. 61, 243–282. https://doi.org/10.1146/annurev.physiol.61.1.243

Feely, R.A., Doney, S.C., Cooley, S.R., 2009. Ocean acidification: present conditions and future changes in a high-CO_2 world. Oceanography 22, 36–47.

Feely, R.A., Okazaki, R.R., Cai, W.J., Bednaršek, N., Alin, S.R., Byrne, R.H., Fassbender, A., 2018. The combined effects of acidification and hypoxia on pH and aragonite saturation in the coastal waters of the California current ecosystem and the northern Gulf of Mexico. Cont. Shelf Res. 152, 50–60. https://doi.org/10.1016/j.csr.2017.11.002

Fennel, K., Testa, J.M., 2019. Biogeochemical controls on coastal hypoxia. Ann. Rev. Mar. Sci. 11, 105–130. https://doi.org/10.1146/annurev-marine-010318-095138

Fernández-Reiriz, M.J., Range, P., Álvarez-Salgado, X.A., Labarta, U., 2011. Physiological energetics of juvenile clams *Ruditapes decussatus* in a high CO_2 coastal ocean. Mar. Ecol. Prog. Ser. 433, 97–105. https://doi.org/10.3354/meps09062

Ferreira, C., Prestin, K., Hussner, J., Zimmermann, U., Meyer zu Schwabedissen, H.E., 2018. PDZ domain containing protein 1 (PDZK1), a modulator of membrane proteins, is regulated by the nuclear receptor THRβ. Mol. Cell. Endocrinol. 461, 215–225. https://doi.org/10.1016/j.mce.2017.09.017

Feugère, L., Angell, L., Fagents, J., Nightingale, R., Rowland, K., Skinner, S., Hardege, J., Bartels-Hardege, H., Wollenberg Valero, K.C., 2021. Behavioural stress propagation in benthic invertebrates caused by acute pH drop-induced metabolites. Front. Mar. Sci. 8, 1–12. https://doi.org/10.3389/fmars.2021.773870

Fink, A.L., 1999. Chaperone-Mediated Protein Folding 79, 425–449.

Fittipaldi, S., Dimauro, I., Mercatelli, N., Caporossi, D., 2014. Role of exercise-induced reactive oxygen species in the modulation of heat shock protein response. Free Radic. Res. 48, 52–70. https://doi.org/10.3109/10715762.2013.835047

Fitzer, S.C., McGill, R.A.R., Torres Gabarda, S., Hughes, B., Dove, M., O'Connor, W., Byrne, M., 2019. Selectively bred oysters can alter their biomineralization pathways, promoting resilience to environmental acidification. Glob. Chang. Biol. 25, 4105–4115. https://doi.org/10.1111/gcb.14818

Fitzer, S.C., Phoenix, V.R., Cusack, M., Kamenos, N.A., 2014. Ocean acidification impacts mussel control on biomineralisation. Sci. Rep. 4. https://doi.org/10.1038/srep06218

Fitzpatrick, J.L., Simmons, L.W., Evans, J.P., 2012. Complex patterns of multivariate selection on the ejaculate of a broadcast spawning marine invertebrate. Evolution (N. Y). 66, 2451–2460. https://doi.org/10.1111/j.1558-5646.2012.01627.x

Flory, M.R., Moser, M.J., Monnat, R.J., Davis, T.N., 2000. Identification of a human centrosomal calmodulin-binding protein that shares homology with pericentrin. Proc. Natl. Acad. Sci. U. S. A. 97, 5919–5923. https://doi.org/10.1073/pnas.97.11.5919

Fong, P.P., Huminski, P.T., D'Urso, L.M., 1998. Induction and potentiation of parturition in fingernail clams (Sphaerium striatinum) by selective serotonin re-uptake inhibitors (SSRIs). J. Exp. Zool. 280, 260–264. https://doi.org/10.1002/(SICI)1097-010X(19980215)280:3

Food and Agriculture Organization of the United Nations (FAO), 2018. Global aquaculture production online Query Available on http://www.fao.org/fishery/topic/16140/en Accessed 21 Oct 2020

Forget-Leray, J., Landriau, I., Minier, C., Leboulenger, F., 2005. Impact of endocrine toxicants on survival, development, and reproduction of the estuarine copepod *Eurytemora affinis* (Poppe). Ecotoxicol. Environ. Saf. 60, 288–294. https://doi.org/10.1016/j.ecoenv.2004.06.008

Fossi, M.C., Panti, C., Guerranti, C., Coppola, D., Giannetti, M., Marsili, L., Minutoli, R., 2012. Are baleen whales exposed to the threat of microplastics? A case study of the Mediterranean fin whale (*Balaenoptera physalus*). Mar. Pollut. Bull. 64, 2374–2379. https://doi.org/10.1016/j.marpolbul.2012.08.013

Franco, A.C., Gruber, N., Frölicher, T.L., Kropuenske Artman, L., 2018. Contrasting impact of future CO_2 emission scenarios on the extent of $CaCO_3$ mineral undersaturation in the Humboldt current system. J. Geophys. Res. Ocean. 123, 2018–2036. https://doi.org/10.1002/2018JC013857

Franzellitti, S., Balbi, T., Montagna, M., Fabbri, R., Valbonesi, P., Fabbri, E., Canesi, L., 2019a. Phenotypical and molecular changes induced by carbamazepine and propranolol on larval stages of *Mytilus galloprovincialis*. Chemosphere 234, 962–970. https://doi.org/10.1016/j.chemosphere.2019.06.045

Franzellitti, S., Canesi, L., Auguste, M., Wathsala, R.H.G.R., Fabbri, E., 2019b. Microplastic exposure and effects in aquatic organisms: A physiological perspective. Environ. Toxicol. Pharmacol. 68, 37–51. https://doi.org/10.1016/j.etap.2019.03.009

Franzellitti, S., Fabbri, E., 2005. Differential HSP70 gene expression in the Mediterranean mussel exposed to various stressors. Biochem. Biophys. Res. Commun. 336, 1157–1163. https://doi.org/10.1016/j.bbrc.2005.08.244

Freedman, A.H., Gaspar, J.M., Sackton, T.B., 2020. Short paired-end reads trump long single-end reads for expression analysis. BMC Bioinformatics 21, 1–11. https://doi.org/10.1186/s12859-020-3484-z

Freitas, R., Almeida, Â., Calisto, V., Velez, C., Moreira, A., Schneider, R.J., Esteves, V.I., Wrona, F.J., Figueira, E., Soares, A.M.V.M., 2016. The impacts of pharmaceutical drugs under ocean

acidification: new data on single and combined long-term effects of carbamazepine on Scrobicularia plana. Sci. Total Environ. 541, 977–985. https://doi.org/10.1016/j.scitotenv.2015.09.138

Freitas, R., Coppola, F., Meucci, V., Battaglia, F., Soares, A.M.V.M., Pretti, C., Faggio, C., 2021. The influence of salinity on sodium lauryl sulfate toxicity in *Mytilus galloprovincialis*. Environ. Toxicol. Pharmacol. 87, 103715. https://doi.org/10.1016/j.etap.2021.103715

Freitas, R., Leite, C., Pinto, J., Costa, M., Monteiro, R., Henriques, B., Di Martino, F., Coppola, F., Soares, A.M.V.M., Solé, M., Pereira, E., 2019. The influence of temperature and salinity on the impacts of lead in *Mytilus galloprovincialis*. Chemosphere 235, 403–412. https://doi.org/10.1016/j.chemosphere.2019.05.221

Freitas, R., Silvestro, S., Pagano, M., Coppola, F., Meucci, V., Battaglia, F., Intorre, L., Soares, A.M.V.M., Pretti, C., Faggio, C., 2020. Impacts of salicylic acid in *Mytilus galloprovincialis* exposed to warming conditions. Environ. Toxicol. Pharmacol. 80, 103448. https://doi.org/10.1016/j.etap.2020.103448

Freund, A., Zhong, F.L., Venteicher, A.S., Meng, Z., Veenstra, T.D., Frydman, J., Artandi, S.E., 2014. Proteostatic control of telomerase function through TRiC-mediated folding of TCAB1. Cell 159, 1389–1403. https://doi.org/10.1016/j.cell.2014.10.059

Friedman, L., Higgin, J.J., Moulder, G., Barstead, R., Raines, R.T., Kimble, J., 2000. Prolyl 4-hydroxylase is required for viability and morphogenesis in *Caenorhabditis elegans*. Proc. Natl. Acad. Sci. U. S. A. 97, 4736–4741. https://doi.org/10.1073/pnas.97.9.4736

Frolova, L., Le Goff, X., Rasmussen, H.H., Cheperegin, S., Drugeon, G., Kress, M., Arman, I., Haenni, A.L., Celis, J.E., Phllippe, M., Justesen, J., Kisselev, L., 1994. A highly conserved eukaryotic protein family possessing properties of polypeptide chain release factor. Nature. https://doi.org/10.1038/372701a0

Fromme, H., Küchler, T., Otto, T., Pilz, K., Müller, J., Wenzel, A., 2002. Occurrence of phthalates and bisphenol A and F in the environment. Water Res. 36, 1429–1438. https://doi.org/10.1016/S0043-1354(01)00367-0

Fuentes-Santos, I., Labarta, U., Fernández-Reiriz, M.J., Kay, S., Hjøllo, S.S., Alvarez-Salgado, X.A., 2021. Modeling the impact of climate change on mussel aquaculture in a coastal upwelling system: A critical assessment. Sci. Total Environ. 775, 145020. https://doi.org/10.1016/j.scitotenv.2021.145020

G

Gago, J., Luís, O.J., 2011. Comparison of spawning induction techniques on *Paracentrotus lividus* (Echinodermata: Echinoidea) broodstock. Aquac. Int. 19, 181–191. https://doi.org/10.1007/s10499-010-9351-6

Galgani, F., Hanke, G., Maes, T., 2015. Global distribution, composition and abundance of marine litter, Marine anthropogenic litter. https://doi.org/10.1021/acs.est.9b01360

Gandara e Silva, P.P., Nobre, C.R., Resaffe, P., Pereira, C.D.S., Gusmão, F., 2016. Leachate from microplastics impairs larval development in brown mussels. Water Res. 106, 364–370. https://doi.org/10.1016/j.watres.2016.10.016

Ganser, A.M., Newton, T.J., Haro, R.J., 2015. Effects of elevated water temperature on physiological responses in adult freshwater mussels 1705–1716. https://doi.org/10.1111/fwb.12603

Gao, P., Liao, Z., Wang, X.X., Bao, L.F., Fan, M.H., Li, X.M., Wu, C.W., Xia, S.W., 2015. Layer-by-layer proteomic analysis of *Mytilus galloprovincialis* shell. PLoS One 10, 1–19. https://doi.org/10.1371/journal.pone.0133913

García-March, J.R., Sanchís Solsona, M.Á., García-Carrascosa, A.M., 2008. Shell gaping behaviour of *Pinna nobilis* L., 1758: Circadian and circalunar rhythms revealed by in situ monitoring. Mar. Biol. 153, 689–698. https://doi.org/10.1007/s00227-007-0842-6

Gattuso, J.P., Lee, K., Rost, B., Schulz, K., 2010. Seawater carbonate chemistry. Guid. to Best Pract. Ocean Acidif. Res. Data Report. 41–52.

Gazeau, F., Alliouane, S., Bock, C., Bramanti, L., Correa, M.L., Gentile, M., Hirse, T., Pörtner, H.O., Ziveri, P., 2014. Impact of ocean acidification and warming on the Mediterranean mussel (*Mytilus galloprovincialis*). Front. Mar. Sci. 1, 1–12. https://doi.org/10.3389/fmars.2014.00062

Gazeau, F., Gattuso, J.P., Dawber, C., Pronker, A.E., Peene, F., Peene, J., Heip, C.H.R., Middelburg, J.J., 2010. Effect of ocean acidification on the early life stages of the blue mussel *Mytilus edulis*. Biogeosciences 7, 2051–2060. https://doi.org/10.5194/bg-7-2051-2010

George, M.N., Carrington, E., 2022. Mussels repair shell damage despite limitations imposed by ocean acidification. https://doi.org/10.32942/osf.io/gdc5z

Georgoulis, I., Feidantsis, K., Giantsis, I.A., Kakale, A., Bock, C., Pörtner, H.O., Sokolova, I.M., Michaelidis, B., 2021. Heat hardening enhances mitochondrial potential for respiration and oxidative defence capacity in the mantle of thermally stressed *Mytilus galloprovincialis*. Sci. Rep. 11, 1–18. https://doi.org/10.1038/s41598-021-96617-9

Geraci, F., Pinsino, A., Turturici, G., Savona, R., Giudice, G., Sconzo, G., 2004. Nickel, lead, and cadmium induce differential cellular responses in sea urchin embryos by activating the synthesis of different HSP70s. Biochem. Biophys. Res. Commun. 322, 873–877. https://doi.org/10.1016/j.bbrc.2004.08.005

Gerdol, M., De Moro, G., Manfrin, C., Milandri, A., Riccardi, E., Beran, A., Venier, P., Pallavicini, A., 2014. RNA sequencing and de novo assembly of the digestive gland transcriptome in *Mytilus galloprovincialis* fed with toxinogenic and non-toxic strains of *Alexandrium minutum*. BMC Res. Notes 7, 1–16. https://doi.org/10.1186/1756-0500-7-722

Gerdol, M., Moreira, R., Cruz, F., Gómez-Garrido, J., Vlasova, A., Rosani, U., Venier, P., Naranjo-Ortiz, M.A., Murgarella, M., Greco, S., Balseiro, P., Corvelo, A., Frias, L., Gut, M., Gabaldón, T., Pallavicini, A., Canchaya, C., Novoa, B., Alioto, T.S., Posada, D., Figueras, A., 2020. Massive gene presence-absence variation shapes an open pan-genome in the Mediterranean mussel. Genome Biol. 21, 275. https://doi.org/10.1186/s13059-020-02180-3

Gerdol, M., Venier, P., 2015. An updated molecular basis for mussel immunity. Fish Shellfish Immunol. 46, 17–38. https://doi.org/10.1016/j.fsi.2015.02.013

Gerhardt, A. 2002. Bioindicator species and their use in biomonitoring. Environmental monitoring, 1, 77-123.

Ghisari, M., Bonefeld-Jorgensen, E.C., 2009. Effects of plasticizers and their mixtures on estrogen receptor and thyroid hormone functions. Toxicol. Lett. 189, 67–77. https://doi.org/10.1016/j.toxlet.2009.05.004

Gill, S.S., Tuteja, N., 2010. Reactive oxygen species and antioxidant machinery in abiotic stress tolerance in crop plants. Plant Physiol. Biochem. 48, 909–930. https://doi.org/10.1016/j.plaphy.2010.08.016

Gismondi, E., Beisel, J.N., Cossu-Leguille, C., 2012. Influence of gender and season on reduced glutathione concentration and energy reserves of *Gammarus roeseli*. Environ. Res. 118, 47–52. https://doi.org/10.1016/j.envres.2012.06.004

Glibert, P.M., 2020. Harmful algae at the complex nexus of eutrophication and climate change. Harmful Algae 91, 101583. https://doi.org/10.1016/j.hal.2019.03.001

Gobler, C.J., 2020. Climate change and harmful algal blooms: insights and perspective. Harmful Algae 91, 101731. https://doi.org/10.1016/j.hal.2019.101731

Godoi, F.G.A., Forner-Piquer, I., Randazzo, B., Habibi, H.R., Lo Nostro, F.L., Moreira, R.G., Carnevali, O., 2021. Effects of di-isononyl phthalate (DiNP) on follicular atresia in zebrafish ovary. Front. Endocrinol. (Lausanne). 12, 1–10. https://doi.org/10.3389/fendo.2021.677853

Goksøyr, A., 2006. Endocrine disruptors in the marine environment: mechanisms of toxicity and their influence on reproductive processes in fish. Journal of Toxicology and Environmental Health, Part A, 69(1-2), 175-184. https://doi.org/10.1080/15287390500259483

Golshan, M., Hatef, A., Socha, M., Milla, S., Butts, I.A.E., Carnevali, O., Rodina, M., Sokołowska-Mikołajczyk, M., Fontaine, P., Linhart, O., Alavi, S.M.H., 2015. Di-(2-ethylhexyl)-phthalate disrupts pituitary and testicular hormonal functions to reduce sperm quality in mature goldfish. Aquat. Toxicol. 163, 16–26. https://doi.org/10.1016/j.aquatox.2015.03.017

Gonçalves, J.M., Sousa, V.S., Teixeira, M.R., Bebianno, M.J., 2022. Chronic toxicity of polystyrene nanoparticles in the marine mussel *Mytilus galloprovincialis*. Chemosphere 287. https://doi.org/10.1016/j.chemosphere.2021.132356

González-Fernández, C., Albentosa, M., Campillo, J.A., Viñas, L., Franco, A., Bellas, J., 2016. Effect of mussel reproductive status on biomarker responses to PAHs: Implications for large-scale monitoring programs. Aquat. Toxicol. 177, 380–394. https://doi.org/10.1016/j.aquatox.2016.06.012

Gorbi, S., Virno Lamberti, C., Notti, A., Benedetti, M., Fattorini, D., Moltedo, G., Regoli, F., 2008. An ecotoxicological protocol with caged mussels, *Mytilus galloprovincialis*, for monitoring the impact of an offshore platform in the Adriatic Sea. Mar. Environ. Res. 65, 34–49. https://doi.org/10.1016/j.marenvres.2007.07.006

Gosling, E., 2021. Marine Mussels: Ecology, Physiology, Genetics and Culture. John Wiley & Sons.

Gould, M.C., Stephano, J.L., De Ortz-Barrn, B.J., Prez-Quezada, I., 2001. Maturation and fertilization in *Lottia gigantea* oocytes: Intracellular pH, Ca^{2+}, and electrophysiology. J. Exp. Zool. 290, 411–420. https://doi.org/10.1002/jez.1082

Grabherr, M.G., Haas, B.J., Yassour, M., Levin, J.Z., Thompson, D.A., Amit, I., Adiconis, X., Fan, L., Raychowdhury, R., Zeng, Q. and Chen, Z., 2011a. Trinity: reconstructing a full-length transcriptome without a genome from RNA-Seq data. Nature biotechnology, 29(7), p.644. https://doi.org/10.1038/nbt.1883

Grabherr, M.G., Haas, B.J., Yassour, M., Levin, J.Z., Thompson, D.A., Amit, I., Adiconis, X., Fan, L., Raychowdhury, R., Zeng, Q., Chen, Z., Mauceli, E., Hacohen, N., Gnirke, A., Rhind, N., Di Palma, F., Birren, B.W., Nusbaum, C., Lindblad-Toh, K., Friedman, N., Regev, A., 2011b. Full-length transcriptome assembly from RNA-Seq data without a reference genome. Nat. Biotechnol. 29, 644–652. https://doi.org/10.1038/nbt.1883

Greco, L., Pellerin, J., Capri, E., Garnerot, F., Louis, S., Fournier, M., Sacchi, A., Fusi, M., Lapointe, D., Couture, P., 2011. Physiological effects of temperature and a herbicide mixture on the soft-shell clam *Mya arenaria* (Mollusca, Bivalvia). Environ. Toxicol. Chem. 30, 132–141. https://doi.org/10.1002/etc.359

Green, D.S., Colgan, T.J., Thompson, R.C., Carolan, J.C., 2019. Exposure to microplastics reduces attachment strength and alters the haemolymph proteome of blue mussels (*Mytilus edulis*). Environ. Pollut. 246, 423–434. https://doi.org/10.1016/j.envpol.2018.12.017

Greenshields, J., Schirrmacher, P., Hardege, J.D., 2021. Plastic additive oleamide elicits hyperactivity in hermit crabs. Mar. Pollut. Bull. 169. https://doi.org/10.1016/j.marpolbul.2021.112533

Gregory, S.G., 2005. Contig Assembly. eLS 1–4. https://doi.org/10.1038/npg.els.0005365

Grilo, T.F., Lopes, A.R., Sampaio, E., Rosa, R., Cardoso, P.G., 2018. Sex differences in oxidative stress responses of tropical topshells (*Trochus histrio*) to increased temperature and high pCO_2. Mar. Pollut. Bull. 131, 252–259. https://doi.org/10.1016/j.marpolbul.2018.04.031

Grove, D.E., Fan, C.Y., Ren, H.Y., Cyr, D.M., 2011. The endoplasmic reticulum-associated Hsp40 DNAJB12 and Hsc70 cooperate to facilitate RMA1 E3-dependent degradation of nascent CFTRΔF508. Mol. Biol. Cell 22, 301–314. https://doi.org/10.1091/mbc.E10-09-0760

Grubbs, F.E., 1969. Procedures for detecting outlying observations in samples. Technometrics, 11 (1) (1969), pp. 1-21

Gruber, N., Clement, D., Carter, B.R., Feely, R.A., Van Heuven, S., Hoppema, M., Ishii, M., Key, R.M., Kozyr, A., Lauvset, S.K. and Lo Monaco, C., 2019. The oceanic sink for anthropogenic CO_2 from 1994 to 2007. Science, 363(6432), pp.1193-1199. https://doi.org/10.1126/science.aau5153

Gu, H., Shang, Y., Clements, J., Dupont, S., Wang, T., Wei, S., Wang, X., Chen, J., Huang, W., Hu, M., Wang, Y., 2019. Hypoxia aggravates the effects of ocean acidification on the physiological energetics of the blue mussel *Mytilus edulis*. Mar. Pollut. Bull. 149, 110538. https://doi.org/10.1016/j.marpolbul.2019.110538

Guen, V.J., Gamble, C., Perez, D.E., Bourassa, S., Zappel, H., Gärtner, J., Lees, J.A., Colas, P., 2016. STAR syndrome associated CDK10/Cyclin M regulates actin network architecture and ciliogenesis. Cell Cycle 15, 678–688. https://doi.org/10.1080/15384101.2016.1147632

Guo, Y., Zhou, B., Sun, T., Zhang, Y., Jiang, Y., Wang, Y., 2021. An Explanation Based on Energy-Related Changes for Blue Mussel *Mytilus edulis* Coping With Seawater Acidification. Front. Physiol. 12. https://doi.org/10.3389/fphys.2021.761117

Gurr, S.J., Trigg, S.A., Vadopalas, B., Roberts, S.B., Putnam, H.M., 2022. Acclimatory gene expression of primed clams enhances robustness to elevated pCO_2 5005–5023. https://doi.org/10.1111/mec.16644

Gutowska, M.A., Pörtner, H.O., Melzner, F., 2008. Growth and calcification in the cephalopod *Sepia officinalis* under elevated seawater pCO_2. Mar. Ecol. Prog. Ser. 373, 303–309. https://doi.org/10.3354/meps07782

H

Hadjmohammadi, M.R., Fatemi, M.H., Taneh, T., 2011. Iranian chemical society coacervative extraction of phthalates from water and their determination by high performance liquid chromatography. Anal. 8, 100–106.

Haegerbaeumer, A., Mueller, M.T., Fueser, H., Traunspurger, W., 2019. Impacts of micro- and nano-sized plastic particles on benthic invertebrates: A literature review and gap analysis. Front. Environ. Sci. 7. https://doi.org/10.3389/fenvs.2019.00017

Halliwell, B., Gutteridge, J.M.C., 2015. Free radicals in biology and medicine. Oxford University Press, London.

Halldórsson, H.P., Svavarsson, J., Granmo, Å., 2005. The effect of pollution on scope for growth of the mussel (*Mytilus edulis* L.) in Iceland. Mar. Environ. Res. 59, 47–64. https://doi.org/10.1016/j.marenvres.2004.02.001

Hamer, B., Hamer, D.P., Müller, W.E.G., Batel, R., 2004. Stress-70 proteins in marine mussel *Mytilus galloprovincialis* as biomarkers of environmental pollution: A field study. Environ. Int. 30, 873–882. https://doi.org/10.1016/j.envint.2004.02.008

Han, Z.X., Wu, D.D., Wu, J., Lv, C.X., Liu, Y.R., 2014. Effects of ocean acidification on toxicity of heavy metals in the bivalve *Mytilus edulis* L. Synth. React. Inorganic, Met. Nano-Metal Chem. 44, 133–139. https://doi.org/10.1080/15533174.2013.770753

Hancock, J.R., Place, S.P., 2016. Impact of ocean acidification on the hypoxia tolerance of the woolly sculpin, *Clinocottus analis*. Conserv. Physiol. 4, 1–10. https://doi.org/10.1093/conphys/cow040

Haney, A., Abdelrahman, H., Stoeckel, J.A., 2020. Effects of thermal and hypoxic stress on respiratory patterns of three unionid species: implications for management and conservation. Hydrobiologia 847, 787–802. https://doi.org/10.1007/s10750-019-04138-4

Hannan, K.D., Jeffrey, J.D., Hasler, C.T., Suski, C.D., 2016. Physiological effects of short- and long-term exposure to elevated carbon dioxide on a freshwater mussel, *Fusconaia flava*. Can J Fish Aquat Sci 73: 1538–1546.

Hansen, J., Sato, M., 2004. Greenhouse gas growth rates. Proc. Natl. Acad. Sci. U. S. A. 101, 16109–16114. https://doi.org/10.1073/pnas.0406982101

Hariharan, G., Purvaja, R., Anandavelu, I., Robin, R.S., Ramesh, R., 2021. Accumulation and ecotoxicological risk of weathered polyethylene (wPE) microplastics on green mussel (*Perna viridis*). Ecotoxicol. Environ. Saf. 208, 111765. https://doi.org/10.1016/j.ecoenv.2020.111765

Harvey, B.P., Gwynn-Jones, D., Moore, P.J., 2013. Meta-analysis reveals complex marine biological responses to the interactive effects of ocean acidification and warming. Ecol. Evol. 3, 1016–1030. https://doi.org/10.1002/ece3.516

Hartl, F.U., 1996. Molecular chaperones in cellular protein folding. Nature 381, 571–580. https://doi.org/10.1038/381571a0

Hasler, C.T., Hannan, K.D., Jeffrey, J.D., Suski, C.D., 2017. Valve movement of three species of North American freshwater mussels exposed to elevated carbon dioxide. Environ. Sci. Pollut. Res. 24, 15567–15575. https://doi.org/10.1007/s11356-017-9160-9

Hassan, M.I., Shajee, B., Waheed, A., Ahmad, F., Sly, W.S., 2013. Structure, function and applications of carbonic anhydrase isozymes. Bioorganic Med. Chem. 21, 1570–1582. https://doi.org/10.1016/j.bmc.2012.04.044

Hauri, C., Gruber, N., Vogt, M., Doney, S.C., Feely, R.A., Lachkar, Z., Leinweber, A., McDonnell, A.M.P., Munnich, M., 2013. Spatiotemporal variability and long-term trends of ocean acidification in the California Current System. Biogeosciences 10, 193–216. https://doi.org/10.5194/bg-10-193-2013

Havenhand, J.N., Buttler, F.R., Thorndyke, M.C., Williamson, J.E., 2008. Near-future levels of ocean acidification reduce fertilization success in a sea urchin. Curr. Biol. 18, 651–652. https://doi.org/10.1016/j.cub.2008.06.015

Heindler, Alajmi, F., Huerlimann, R., Zeng, C., Newman, S.J., Vamvounis, G., van Herwerden, L., 2017. Toxic effects of polyethylene terephthalate microparticles and Di(2-ethylhexyl) phthalate on the calanoid copepod, *Parvocalanus crassirostris*. Ecotoxicol. Environ. Saf. 141, 298–305. https://doi.org/10.1016/j.ecoenv.2017.03.029

Heindler, F.M., Alajmi, F., Huerlimann, R., Zeng, C., Newman, S.J., Vamvounis, G., Herwerden, L. Van, 2017. Toxic effects of polyethylene terephthalate microparticles and Di(2-ethylhexyl) phthalate on the calanoid copepod, *Parvocalanus crassirostris*. Ecotoxicol. Environ. Saf. 141, 298–305. https://doi.org/10.1016/j.ecoenv.2017.03.029

Heise, K., Puntarulo, S., Pörtner, H.O., Abele, D., 2003. Production of reactive oxygen species by isolated mitochondria of the Antarctic bivalve *Laternula elliptica* (King and Broderip) under heat stress. Comp. Biochem. Physiol. - C Toxicol. Pharmacol. 134, 79–90. https://doi.org/10.1016/S1532-0456(02)00212-0

Helm, M.M., Bourne, N., Lovatelli, A., 2004. Hatchery culture of bivalves. A practical manual. FAO Fisheries Technical Paper No. 471. Food and Agriculture Organization (FAO) of the United Nations, Rome.

Henne, W. M., Boucrot, E., Meinecke, M., Evergren, E., Vallis, Y., Mittal, R., McMahon, H. T., 2010. FCHo proteins are nucleators of clathrin-mediated endocytosis. Science, 328(5983), 1281-1284.. https://doi.org/10.1126/science.1188462

Henry, R.P., Swenson, E.R., 2000. The distribution and physiological significance of carbonic anhydrase in vertebrate gas exchange organs. Respir. Physiol. 121, 1–12. https://doi.org/10.1016/S0034-5687(00)00110-9

Heo, H., Choi, M.J., Park, J., Nam, T., Cho, J., 2020. Anthropogenic occurrence of phthalate esters in beach seawater in the southeast coast region, South Korea. Water (Switzerland) 12. https://doi.org/10.3390/w12010122

Hermabessiere, L., Dehaut, A., Paul-Pont, I., Lacroix, C., Jezequel, R., Soudant, P., Duflos, G., 2017. Occurrence and effects of plastic additives on marine environments and organisms: A review. Chemosphere 182, 781–793. https://doi.org/10.1016/j.chemosphere.2017.05.096

Hernández-Cabanyero, C., Sanjuán, E., Fouz, B., Pajuelo, D., Vallejos-Vidal, E., Reyes-López, F.E., Amaro, C., 2020. The Effect of the Environmental Temperature on the Adaptation to Host in the Zoonotic Pathogen *Vibrio vulnificus*. Front. Microbiol. 11, 1–17. https://doi.org/10.3389/fmicb.2020.00489

Hilbish, T.J., Carson, E.W., Plante, J.R., Weaver, L.A., Gilg, M.R., 2002. Distribution of *Mytilus edulis*, *M. galloprovincialis*, and their hybrids in open-coast populations of mussels in southwestern England. Mar. Biol. 140, 137–142. https://doi.org/10.1007/s002270100631

Hilbish, T.J., Zimmerman, K.M., 1988. Genetic and nutritional control of the gametogenic cycle in *Mytilus edulis* T.J. 228, 223–228.

Hill, R.L., Janz, M., 2003. De v elopmental estrogenic exposure in zebrafish (*Danio rerio*): I . Effects on sex ratio and breeding success 63, 417–429. https://doi.org/10.1016/S0166-445X(02)00207-2

Hines, A., Yeung, W.H., Craft, J., Brown, M., Kennedy, J., Bignell, J., Stentiford, G.D., Viant, M.R., 2007. Comparison of histological, genetic, metabolomics, and lipid-based methods for sex determination in marine mussels. Anal. Biochem. 369, 175–186. https://doi.org/10.1016/j.ab.2007.06.008

Ho, K.G., Pometto, A.L., Hinz, P.N., 1999. Effects of temperature and relative humidity on polylactic acid plastic degradation. J. Environ. Polym. Degrad. 7, 83–92.

Hofmann, G.E., Barry, J.P., Edmunds, P.J., Gates, R.D., Hutchins, D.A., Klinger, T., Sewell, M.A., 2010. The effect of ocean acidification on calcifying organisms in marine ecosystems: An organism-to-ecosystem perspective. Annu. Rev. Ecol. Evol. Syst. 41, 127–147. https://doi.org/10.1146/annurev.ecolsys.110308.120227

Hölzer, M., Marz, M., 2019. De novo transcriptome assembly: A comprehensive cross-species comparison of short-read RNA-Seq assemblers. Gigascience 8, 1–16. https://doi.org/10.1093/gigascience/giz039

Hong, G.S., Lee, S.H., Lee, B., Choi, J.H., Oh, S.J., Jang, Y., Hwang, E.M., Kim, H., Jung, J., Kim, I.B., Oh, U., 2019. ANO1/TMEM16A regulates process maturation in radial glial cells in the developing brain. Proc. Natl. Acad. Sci. U. S. A. 116, 12494–12499. https://doi.org/10.1073/pnas.1901067116

Honkoop, P.J.C., Van Der Meer, J., 1998. Experimentally induced effects of water temperature and immersion time on reproductive output of bivalves in the Wadden Sea. J. Exp. Mar. Bio. Ecol. 220, 227–246. https://doi.org/10.1016/S0022-0981(97)00107-X

Horard, B., Vanacker, J.M., 2003. Estrogen receptor-related receptors: Orphan receptors desperately seeking a ligand. J. Mol. Endocrinol. 31, 349–357. https://doi.org/10.1677/jme.0.0310349

Hu, M., Li, L., Sui, Y., Li, J., Wang, Y., Lu, W., Dupont, S., 2015. Effect of pH and temperature on antioxidant responses of the thick shell mussel *Mytilus coruscu*s. Fish Shellfish Immunol. 46, 573–583. https://doi.org/10.1016/j.fsi.2015.07.025

Huang, G.L., Sun, H.W., Song, Z.H., 1999. Interactions between dibutyl phthalate and aquatic organisms. Bull. Environ. Contam. Toxicol. 63, 759–765. https://doi.org/10.1007/s001289901044

Hughes, L., 2000. Biological consequences of global warming: is the signal already apparent? Trends Ecol. Evol. 15, 56–61.

Hüning, A.K., Melzner, F., Thomsen, J., Gutowska, M.A., Krämer, L., Frickenhaus, S., Rosenstiel, P., Philipp, E.E.R., Lucassen, M., 2013. Impacts of seawater acidification on mantle gene expression patterns of the Baltic Sea blue mussel: implications for shell formation and energy metabolism 1845–1861. https://doi.org/10.1007/s00227-012-1930-9

Hurd, C.L., Lenton, A., Tilbrook, B., Boyd, P.W., 2018. Current understanding and challenges for oceans in a higher-CO_2 world. Nat. Clim. Chang. 8, 686–694. https://doi.org/10.1038/s41558-018-0211-0

Hutchison, Z.L., Hendrick, V.J., Burrows, M.T., Wilson, B., Last, K.S., 2016. Buried alive: The behavioural response of the mussels, *Modiolus modiolus* and *Mytilus edulis* to sudden burial by sediment. PLoS One 11. https://doi.org/10.1371/journal.pone.0151471

I

Ighodaro, O.M., Akinloye, O.A., 2018. First line defence antioxidants-superoxide dismutase (SOD), catalase (CAT) and glutathione peroxidase (GPX): Their fundamental role in the entire antioxidant defence grid. Alexandria J. Med. 54, 287–293. https://doi.org/10.1016/j.ajme.2017.09.001

Inoue, K., Waite, J.H., Matsuoka, M., Odo, S., Harayama, S., 1995. Interspecific variations in adhesive protein sequences of *Mytilus edulis*, *M. galloprovincialis*, and *M. trossulus*. Biol. Bull. 189, 370–375. https://doi.org/10.2307/1542155

Intergovernmental Panel on Climate Change (IPCC), 2007. Climate Change 2007: The Physical Science Basis, 2007. Contribution of working group I to the Fourth Assessment Report of the Intergovernmental Panel on Climate Change

Intergovernmental Panel on Climate Change (IPCC), 2014. Climate Change 2014: The Physical Science Basis, 2014. Contribution of working group I to the Fifth Assessment Report of the Intergovernmental Panel on Climate Change

Intergovernmental Panel on Climate Change (IPCC), 2018. An IPCC Special Report on the Impacts of Global Warming of 1.5°C.

Intergovernmental Panel on Climate Change (IPCC), 2021. Climate Change 2021: The Physical Science Basis, 2014. Contribution of working group I to the Sixth Assessment Report of the Intergovernmental Panel on Climate Change

Ivanina, A. V., Dickinson, G.H., Matoo, O.B., Bagwe, R., Dickinson, A., Beniash, E., Sokolova, I.M., 2013. Interactive effects of elevated temperature and CO_2 levels on energy metabolism and biomineralization of marine bivalves *Crassostrea virginica* and *Mercenaria mercenaria*. Comp. Biochem. Physiol. - A Mol. Integr. Physiol. 166, 101–111. https://doi.org/10.1016/j.cbpa.2013.05.016

Ivanina, A. V., Sokolova, I.M., 2015. Interactive effects of metal pollution and ocean acidification on physiology of marine organisms. Curr. Zool. 61, 653–668. https://doi.org/10.1093/czoolo/61.4.653

Iyapparaj, P., Revathi, P., Ramasubburayan, R., Prakash, S., Anantharaman, P., Immanuel, G., Palavesam, A., 2013. Antifouling activity of the methanolic extract of *Syringodium isoetifolium*, and its toxicity relative to tributyltin on the ovarian development of brown mussel *Perna indica*. Ecotoxicol. Environ. Saf. 89, 231–238. https://doi.org/10.1016/j.ecoenv.2012.12.001

Iwata, K. S., 1951. Spawning of Mytilus edulis. VIII. Comparison of abilities of salts of alkali metals and of alkali earth metals to induce spawning. *Bull. Jap. Soc. Sci. Fish*, *17*, 94-95.

Izagirre, U., Errasti, A., Bilbao, E., Múgica, M., Marigómez, I., 2014. Combined effects of thermal stress and Cd on lysosomal biomarkers and transcription of genes encoding lysosomal enzymes and HSP70 in mussels, *Mytilus galloprovincialis*. Aquat. Toxicol. 149, 145–156. https://doi.org/10.1016/j.aquatox.2014.01.013

J

Jahnsen-Guzmán, N., Lagos, N.A., Quijón, P.A., Manríquez, P.H., Lardies, M.A., Fernández, C., Reyes, M., Zapata, J., García-Huidobro, M.R., Labra, F.A., Duarte, C., 2022. Ocean acidification alters anti-predator responses in a competitive dominant intertidal mussel. Chemosphere 288. https://doi.org/10.1016/j.chemosphere.2021.132410

Jakubowska, M., Normant, M., 2015. Metabolic rate and activity of blue mussel *Mytilus edulis trossulus* under short-term exposure to carbon dioxide-induced water acidification and oxygen deficiency. Mar. Freshw. Behav. Physiol. 48, 25–39. https://doi.org/10.1080/10236244.2014.986865

Janer, G., Porte, C., 2007. Sex steroids and potential mechanisms of non-genomic endocrine disruption in invertebrates. Ecotoxicology 16, 145–160. https://doi.org/10.1007/s10646-006-0110-4

Janowicz, A., Michalak, M., Krebs, J., 2011. Stress induced subcellular distribution of ALG-2, RBM22 and hSlu7. Biochim. Biophys. Acta - Mol. Cell Res. 1813, 1045–1049. https://doi.org/10.1016/j.bbamcr.2010.11.010

Jansen, J.M., Pronker, A.E., Kube, S., Sokolowski, A., Sola, J.C., Marquiegui, M.A., Schiedek, D., Wendelaar Bonga, S., Wolowicz, M., Hummel, H., 2007. Geographic and seasonal patterns and limits on the adaptive response to temperature of European *Mytilus* spp. and *Macoma balthica* populations. Oecologia 154, 23–34. https://doi.org/10.1007/s00442-007-0808-x

Jarque, S., Prats, E., Olivares, A., Casado, M., Ramón, M., Piña, B., 2014. Seasonal variations of gene expression biomarkers in *Mytilus galloprovincialis* cultured populations: Temperature, oxidative stress and reproductive cycle as major modulators. Sci. Total Environ. 499, 363–372. https://doi.org/10.1016/j.scitotenv.2014.08.064

Jebara, A., Albergamo, A., Rando, R., Potortì, A.G., Lo Turco, V., Mansour, H. Ben, Di Bella, G., 2021. Phthalates and non-phthalate plasticizers in Tunisian marine samples: Occurrence, spatial distribution and seasonal variation. Mar. Pollut. Bull. 163, 111967. https://doi.org/10.1016/j.marpolbul.2021.111967

Jenner, L.C., Rotchell, J.M., Bennett, R.T., Cowen, M., Tentzeris, V., Sadofsky, L.R., 2022. Detection of microplastics in human lung tissue using μFTIR spectroscopy. Sci. Total Environ. 831, 154907. https://doi.org/10.1016/j.scitotenv.2022.154907

Jensen, K.M., Kahl, M.D., Makynen, E.A., Korte, J.J., Leino, R.L., Butterworth, B.C., Ankley, G.T., 2004. Characterization of responses to the antiandrogen flutamide in a short-term reproduction assay with the fathead minnow. Aquat. Toxicol. 70, 99–110. https://doi.org/10.1016/j.aquatox.2004.06.012

Ji, C., Li, F., Wang, Q., Zhao, J., Sun, Z., Wu, H., 2016. An integrated proteomic and metabolomic study on the gender-specific responses of mussels *Mytilus galloprovincialis* to tetrabromobisphenol A (TBBPA). Chemosphere 144, 527–539. https://doi.org/10.1016/j.chemosphere.2015.08.052

Ji, C., Wu, H., Wei, L., Zhao, J., Yu, J., 2013. Proteomic and metabolomic analysis reveal gender-specific responses of mussel *Mytilus galloprovincialis* to 2,2',4,4'-tetrabromodiphenyl ether (BDE 47). Aquat. Toxicol. 140–141, 449–457. https://doi.org/10.1016/j.aquatox.2013.07.009

Jiang, X., Qiu, L., Zhao, H., Song, Q., Zhou, H., Han, Q., Diao, X., 2016. Transcriptomic responses of Perna viridis embryo to Benzo(a)pyrene exposure elucidated by RNA sequencing. Chemosphere 163, 125–132. https://doi.org/10.1016/j.chemosphere.2016.07.091

Jiang, J., Zhao, Z., Gao, S., Chen, Z., Dong, Y., He, P., Wang, B., Pan, Y., Wang, X., Guan, X., Wang, C., Lin, S., Sun, H., Zhou, Z., 2021. Divergent metabolic responses to sex and reproduction in the sea cucumber *Apostichopus japonicus*. Comp. Biochem. Physiol. - Part D Genomics Proteomics 39, 100845. https://doi.org/10.1016/j.cbd.2021.100845

Jobling, S., Casey, D., Rogers-Gray, T., Oehlmann, J., Schulte-Oehlmann, U., Pawlowski, S., Baunbeck, T., Turner, A.P., Tyler, C.R., 2004. Comparative responses of molluscs and fish to environmental estrogens and an estrogenic effluent. Aquat. Toxicol. 66, 207–222. https://doi.org/10.1016/j.aquatox.2004.01.002

Jones, S.J., Mieszkowska, N., Wethey, D.S., 2009. Linking thermal tolerances and biogeography: *Mytilus edulis* (L.) at its southern limit on the east coast of the United States. Biol. Bull. 217, 73–85. https://doi.org/10.1086/BBLv217n1p73

Jonsson, H., Schiedek, D., Grøsvik, B.E., Goksøyr, A., 2006. Protein responses in blue mussels (*Mytilus edulis*) exposed to organic pollutants: A combined CYP-antibody/proteomic approach. Aquat. Toxicol. 78, 49–56. https://doi.org/10.1016/j.aquatox.2006.02.024

Jorge, R.A.D.L.V.C., Lemos, D., Moreira, G.S., 2007. Effect of zinc and benzene on respiration and excretion of mussel larvae (*Perna perna*) (Linnaeus, 1758) (Mollusca; Bivalvia). Brazilian J. Biol. 67, 111–115. https://doi.org/10.1590/S1519-69842007000100015

K

Kabani, M., Beckerich, J.-M., Brodsky, J.L., 2002. Nucleotide Exchange Factor for the Yeast Hsp70 Molecular Chaperone Ssa1p. Mol. Cell. Biol. 22, 4677–4689. https://doi.org/10.1128/mcb.22.13.4677-4689.2002

Kajiwara, M., Kuraku, S., Kurokawa, T., Kato, K., Toda, S., Hirose, H., Takahashi, S., Shibata, Y., Iguchi, T., Matsumoto, T., Miyata, T., Miura, T., Takahashi, Y., 2006. Tissue preferential expression of estrogen receptor gene in the marine snail, *Thais clavigera*. Gen. Comp. Endocrinol. 148, 315–326. https://doi.org/10.1016/j.ygcen.2006.03.016

Kallenborn, R., Halsall, C., Dellong, M., Carlsson, P., 2012. The influence of climate change on the global distribution and fate processes of anthropogenic persistent organic pollutants. J. Environ. Monit. 14, 2854–2869. https://doi.org/10.1039/c2em30519d

Kalo, D., Hadas, R., Furman, O., Ben-Ari, J., Maor, Y., Patterson, D.G., Tomey, C., Roth, Z., 2015. Carryover effects of acute DEHP exposure on ovarian function and oocyte developmental

competence in lactating cows. PLoS One 10, 1–25. https://doi.org/10.1371/journal.pone.0130896

Kaloyianni, M., Stamatiou, R., Dailianis, S., 2005. Zinc and 17β-estradiol induce modifications in Na+/H + exchanger and pyruvate kinase activity through protein kinase C in isolated mantle/gonad cells of *Mytilus galloprovincialis*. Comp. Biochem. Physiol. - C Toxicol. Pharmacol. 141, 257–266. https://doi.org/10.1016/j.cca.2005.07.001

Kamel, N., Attig, H., Dagnino, A., Boussetta, H., Banni, M., 2012. Increased temperatures affect oxidative stress markers and detoxification response to benzo[a]pyrene exposure in mussel *Mytilus galloprovincialis*. Arch. Environ. Contam. Toxicol. 63, 534–543. https://doi.org/10.1007/s00244-012-9790-3

Kang, C.K., Lee, Y.W., Eun, J.C., Shin, J.K., Seo, I.S., Hong, J.S., 2006. Microphytobenthos seasonality determines growth and reproduction in intertidal bivalves. Mar. Ecol. Prog. Ser. 315, 113–127. https://doi.org/10.3354/meps315113

Kapranov, S. V., Karavantseva, N. V., Bobko, N.I., Ryabushko, V.I., Kapranova, L.L., 2021. Sex- and sexual maturation-related aspects of the element accumulation in soft tissues of the bivalve *Mytilus galloprovincialis* Lam. collected off coasts of Sevastopol (southwestern Crimea, Black Sea). Environ. Sci. Pollut. Res. 28, 21553–21576. https://doi.org/10.1007/s11356-020-12024-z

Karuppanapandian, T., Moon, J.C., Kim, C., Manoharan, K., Kim, W., 2011. Reactive oxygen species in plants: Their generation, signal transduction, and scavenging mechanisms. Aust. J. Crop Sci. 5, 709–725.

Katsumiti, A., Losada-Carrillo, M.P., Barros, M., Cajaraville, M.P., 2021. Polystyrene nanoplastics and microplastics can act as Trojan horse carriers of benzo(a)pyrene to mussel hemocytes in vitro. Sci. Rep. 11, 1–17. https://doi.org/10.1038/s41598-021-01938-4

Kautsky, N., 1982. Quantitative studies on gonad cycle, fecundity, reproductive output and recruitment in a baltic *Mytilus edulis* population. Mar. Biol. 68, 143–160. https://doi.org/10.1007/BF00397601

Ke, A.Y., Chen, J., Zhu, J., Wang, Y.H., Hu, Y., Fan, Z.L., Chen, M., Peng, P., Jiang, S.W., Xu, X.R., Li, H.X., 2019. Impacts of leachates from single-use polyethylene plastic bags on the early development of clam *Meretrix meretrix* (Bivalvia: Veneridae). Mar. Pollut. Bull. 142, 54–57. https://doi.org/10.1016/j.marpolbul.2019.03.029

Keay, J., Thornton, J.W., 2009. Hormone-Activated Estrogen Receptors in Annelid Invertebrates : Implications for Evolution and 150, 1731–1738. https://doi.org/10.1210/en.2008-1338

Keil, R., Salemme, K., Forrest, B., Neibauer, J., Logsdon, M., 2011. Differential presence of anthropogenic compounds dissolved in the marine waters of Puget Sound, WA and Barkley Sound, BC. Mar. Pollut. Bull. 62, 2404–2411. https://doi.org/10.1016/j.marpolbul.2011.08.029

Kelly, C.D., Stoehr, A.M., Nunn, C., Smyth, K.N., Prokop, Z.M., 2018. Sexual dimorphism in immunity across animals: a meta-analysis. Ecol. Lett. 21, 1885–1894. https://doi.org/10.1111/ele.13164

Khalid, A., Zalouk-Vergnoux, A., Benali, S., Mincheva, R., Raquez, J.M., Bertrand, S., Poirier, L., 2021. Are bio-based and biodegradable microplastics impacting for blue mussel (*Mytilus edulis*)? Mar. Pollut. Bull. 167, 112295. https://doi.org/10.1016/j.marpolbul.2021.112295

Khatiwala, S., Primeau, F., Hall, T., 2009. Reconstruction of the history of anthropogenic CO_2 concentrations in the ocean. Nature 462, 346–349. https://doi.org/10.1038/nature08526

Khatiwala, S., Tanhua, T., Mikaloff Fletcher, S., Gerber, M., Doney, S.C., Graven, H.D., Gruber, N., McKinley, G.A., Murata, A., Ríos, A.F., Sabine, C.L., 2013. Global ocean storage of anthropogenic carbon. Biogeosciences 10, 2169–2191. https://doi.org/10.5194/bg-10-2169-2013

Khessiba, A., Roméo, M., Aïssa, P., 2005. Effects of some environmental parameters on catalase activity measured in the mussel (*Mytilus galloprovincialis*) exposed to lindane. Environ. Pollut. 133, 275–281. https://doi.org/10.1016/j.envpol.2004.05.035

Khlebovich, V. V., 2017. Acclimation of animal organisms: basic theory and applied aspects. Biol. Rev., 7, 279-286. https://doi.org/10.1134/S2079086417040053

Kibria, G., Nugegoda, D., Rose, G., Haroon, A.K.Y., 2021. Climate change impacts on pollutants mobilization and interactive effects of climate change and pollutants on toxicity and bioaccumulation of pollutants in estuarine and marine biota and linkage to seafood security. Mar. Pollut. Bull. 167, 112364. https://doi.org/10.1016/j.marpolbul.2021.112364

Kijewski, T., Śmietanka, B., Zbawicka, M., Gosling, E., Hummel, H., Wenne, R., 2011. Distribution of *Mytilus* taxa in European coastal areas as inferred from molecular markers. J. Sea Res. 65, 224–234. https://doi.org/10.1016/j.seares.2010.10.004

Kim, E. J., 2003. Study on anti-estrogenic activity of DEHP as an endocrine disruption chemical. Journal of Environmental Health Sciences, 29(2), 7-15.

Kim, E.J., Kim, J.W., Lee, S.K., 2002. Inhibition of oocyte development in Japanese medaka (*Oryzias latipes*) exposed to di-2-ethylhexyl phthalate. Environ. Int. 28, 359–365. https://doi.org/10.1016/S0160-4120(02)00058-2

Kim, S.A., Lee, Y.M., Choi, J.Y., Jacobs, D.R., Lee, D.H., 2018. Evolutionarily adapted hormesis-inducing stressors can be a practical solution to mitigate harmful effects of chronic exposure to low dose chemical mixtures. Environ. Pollut. 233, 725–734. https://doi.org/10.1016/j.envpol.2017.10.124

Kleypas, J.A., 2019. Impacts of ocean acidification on marine biodiversity. Biodivers. Clim. Chang. Transform. Biosph. 185–195. https://doi.org/10.2307/j.ctv8jnzw1.25

Klinge, C.M., 2001. Estrogen receptor interaction with estrogen response elements. Nucleic Acids Res. 29, 2905–2919. https://doi.org/10.1093/nar/29.14.2905

Kloukinioti, M., Politi, A., Kalamaras, G., & Dailianis, S. 2020. Feeding regimes modulate biomarkers responsiveness in mussels treated with diclofenac. Mar. Env. Res. 156, 104919. https://doi.org/10.1016/j.marenvres.2020.104919

Koagouw, W., Ciocan, C., 2018. Impact of Metformin and Increased Temperature on Blue Mussels *Mytilus edulis* - Evidence for Synergism. J. Shellfish Res. 37, 467–474. https://doi.org/10.2983/035.037.0301

Koagouw, W., Ciocan, C., 2020. Effects of short-term exposure of paracetamol in the gonads of blue mussels *Mytilus edulis*. Environ. Sci. Pollut. Res. 27, 30933–30944. https://doi.org/10.1007/s11356-019-06861-w

Koagouw, W., Hazell, R.J., Ciocan, C., 2021a. Induction of apoptosis in the gonads of *Mytilus edulis* by metformin and increased temperature, via regulation of HSP70, CASP8, BCL2 and FAS. Mar. Pollut. Bull. 173, 113011. https://doi.org/10.1016/j.marpolbul.2021.113011

Koagouw, W., Stewart, N.A., Ciocan, C., 2021b. Long-term exposure of marine mussels to paracetamol: is time a healer or a killer? Environ. Sci. Pollut. Res. 28, 48823–48836. https://doi.org/10.1007/s11356-021-14136-6

Kobak, J., Kakareko, T., 2011. The effectiveness of the induced anti-predator behaviour of zebra mussel Dreissena polymorpha in the presence of molluscivorous roach *Rutilus rutilus*. Aquat. Ecol. 45, 357–366. https://doi.org/10.1007/s10452-011-9359-7

Koehn, R.K., 1991. The genetics and taxonomy of species in the genus *Mytilus*. Aquaculture 94, 125–145. https://doi.org/10.1016/0044-8486(91)90114-M

Köhler, H.R., Kloas, W., Schirling, M., Lutz, I., Reye, A.L., Langen, J.S., Triebskorn, R., Nagel, R., Schönfelder, G., 2007. Sex steroid receptor evolution and signalling in aquatic invertebrates. Ecotoxicology 16, 131–143. https://doi.org/10.1007/s10646-006-0111-3

Kolandhasamy, P., Su, L., Li, J., Qu, X., Jabeen, K., Shi, H., 2018. Adherence of microplastics to soft tissue of mussels: A novel way to uptake microplastics beyond ingestion. Sci. Total Environ. 610–611, 635–640. https://doi.org/10.1016/j.scitotenv.2017.08.053

Kong, H., Clements, J.C., Dupont, S., Wang, T., Huang, X., Shang, Y., Huang, W., Chen, J., Hu, M., Wang, Y., 2019. Seawater acidification and temperature modulate anti-predator defenses in two co-existing *Mytilus* species. Mar. Pollut. Bull. 145, 118–125. https://doi.org/10.1016/j.marpolbul.2019.05.040

Koniecki, D., Wang, R., Moody, R.P., Zhu, J., 2011. Phthalates in cosmetic and personal care products: Concentrations and possible dermal exposure. Environ. Res. 111, 329–336. https://doi.org/10.1016/j.envres.2011.01.013

Kroeker, K.J., Kordas, R.L., Crim, R.N., Singh, G.G., 2010. Meta-analysis reveals negative yet variable effects of ocean acidification on marine organisms. Ecol. Lett. 13, 1419–1434. https://doi.org/10.1111/j.1461-0248.2010.01518.x

Kroeker, K.J., Micheli, F., Gambi, M.C., Martz, T.R., 2011. Divergent ecosystem responses within a benthic marine community to ocean acidification. Proc. Natl. Acad. Sci. U. S. A. 108, 14515–14520. https://doi.org/10.1073/pnas.1107789108

Kumar, S., Blaxter, M.L., 2012. Simultaneous genome sequencing of symbionts and their hosts 119–126. https://doi.org/10.1007/s13199-012-0154-6

Kurima, K., Peters, L.M., Yang, Y., Riazuddin, Saima, Ahmed, Z.M., Naz, S., Arnaud, D., Drury, S., Mo, J., Makishima, T., Ghosh, M., Menon, P.S.N., Deshmukh, D., Oddoux, C., Ostrer, H., Khan, S., Riazuddin, Sheikh, Deininger, P.L., Hampton, L.L., Sullivan, S.L., Battey, J.F., Keats, B.J.B., Wilcox, E.R., Friedman, T.B., Griffith, A.J., 2002. Dominant and recessive deafness caused by mutations of a novel gene, TMC1, required for cochlear hair-cell function. Nat. Genet. 30, 277–284. https://doi.org/10.1038/ng842

Kwiatkowski, L., Gaylord, B., Hill, T., Hosfelt, J., Kroeker, K.J., Nebuchina, Y., Ninokawa, A., Russell, A.D., Rivest, E.B., Sesboue, M., Caldeira, K., 2016. Nighttime dissolution in a temperate coastal ocean ecosystem increases under acidification. Sci. Rep. 6, 1–9. https://doi.org/10.1038/srep22984

Kwiatkowski, L., Torres, O., Bopp, L., Aumont, O., Chamberlain, M., R. Christian, J., P. Dunne, J., Gehlen, M., Ilyina, T., G. John, J., Lenton, A., Li, H., S. Lovenduski, N., C. Orr, J., Palmieri, J., Santana-Falcón, Y., Schwinger, J., Séférian, R., A. Stock, C., Tagliabue, A., Takano, Y., Tjiputra, J., Toyama, K., Tsujino, H., Watanabe, M., Yamamoto, A., Yool, A., Ziehn, T., 2020. Twenty-first century ocean warming, acidification, deoxygenation, and upper-ocean nutrient and primary production decline from CMIP6 model projections. Biogeosciences 17, 3439–3470. https://doi.org/10.5194/bg-17-3439-2020

L

Lacroix, C., Coquillé, V., Guyomarch, J., Auffret, M., Moraga, D., 2014. A selection of reference genes and early-warning mRNA biomarkers for environmental monitoring using *Mytilus* spp. as sentinel species. Mar. Pollut. Bull. 86, 304–313. https://doi.org/10.1016/j.marpolbul.2014.06.049

Lafont, R., Mathieu, M., 2007. Steroids in aquatic invertebrates. Ecotoxicology 16, 109–130. https://doi.org/10.1007/s10646-006-0113-1

Lamon, L., Von Waldow, H., Macleod, M., Scheringer, M., Marcomini, A., Hungerbühler, K., 2009. Modeling the global levels and distribution of polychlorinated biphenyls in air under a climate change scenario. Environ. Sci. Technol. 43, 5818–5824. https://doi.org/10.1021/es900438j

Landis, W.G., Rohr, J.R., Moe, S.J., Balbus, J.M., Clements, W., Fritz, A., Helm, R., Hickey, C., Hooper, M., Stahl, R.G., Stauber, J., 2014. Global climate change and contaminants, a call to arms not yet heard? Integr. Environ. Assess. Manag. 10, 483–484. https://doi.org/10.1002/ieam.1568

Langenbuch, M., Bock, C., Leibfritz, D., Pörtner, H.O., 2006. Effects of environmental hypercapnia on animal physiology: A 13C NMR study of protein synthesis rates in the marine invertebrate *Sipunculus nudus*. Comp. Biochem. Physiol. - A Mol. Integr. Physiol. 144, 479–484. https://doi.org/10.1016/j.cbpa.2006.04.017

Langston, W.J., Burt, G.R., Chesman, B.S., Vane, C.H., 2005. Partitioning, bioavailability and effects of oestrogens and xeno-oestrogens in the aquatic environment. J. Mar. Biol. Assoc. United Kingdom 85, 1–31. https://doi.org/10.1017/S0025315405010787h

Lannig, G., Eilers, S., Pörtner, H.O., Sokolova, I.M., Bock, C., 2010. Impact of ocean acidification on energy metabolism of oyster, *Crassostrea gigas* - Changes in metabolic pathways and thermal response. Mar. Drugs 8, 2318–2339. https://doi.org/10.3390/md8082318

Laouati, I., Rouane-Hacene, O., Derbal, F., Ouali, K., 2021. The mussel caging approach in the assessment of trace metal contamination in southern Mediterranean coastal waters: a multi-biomarker study. Environ. Sci. Pollut. Res. https://doi.org/10.1007/s11356-021-15203-8

Lardies, M.A., Arias, M.B., Poupin, M.J., Manríquez, P.H., Torres, R., Vargas, C.A., Navarro, J.M., Lagos, N.A., 2014. Differential response to ocean acidification in physiological traits of *Concholepas concholepas* populations. J. Sea Res. 90, 127–134. https://doi.org/10.1016/j.seares.2014.03.010

Lassoued, J., Babarro, J.M.F., Padín, X.A., Comeau, L.A., Bejaoui, N., Pérez, F.F., 2019. Behavioural and eco-physiological responses of the mussel *Mytilus galloprovincialis* to acidification and distinct feeding regimes. Mar. Ecol. Prog. Ser. 626, 97–108. https://doi.org/10.3354/meps13075

Lassoued, J., PadÃ-n, X.A., Comeau, L.A., Bejaoui, N., PÃrez, F.F., Babarro, J.M.F., 2021. The Mediterranean mussel *Mytilus galloprovincialis*: Responses to climate change scenarios as a function of the original habitat. Conserv. Physiol. 9, 1–16. https://doi.org/10.1093/conphys/coaa114

Lauvset, S.K., Carter, B.R., Perez, F.F., Jiang, L.Q., Feely, R.A., Velo, A., Olsen, A., 2020. Processes driving global interior ocean pH distribution. Global Biogeochem. Cycles 34, 1–17. https://doi.org/10.1029/2019GB006229

Law, R.J., Fileman, T.W., Matthiessen, P., 1991. Phthalate esters and other industrial organic chemicals in thenorth and irish seas. Water Sci. Technol. 24(10), 127–134.

Lazo, C.S., Pita, I.M., 2012. Effect of temperature on survival, growth and development of *Mytilus galloprovincialis* larvae. Aquac. Res. 43, 1127–1133. https://doi.org/10.1111/j.1365-2109.2011.02916.x

Lee, R.W., Kraus, D.W., Doeller, J.E., 1996. Sulfide-stimulation of oxygen consumption rate and cytochrome reduction in gills of the estuarine mussel *Geukensia demissa*. Biol. Bull. 191, 421–430. https://doi.org/10.2307/1543015

Lefevre, S., 2016. Are global warming and ocean acidification conspiring against marine ectotherms? A meta-analysis of the respiratory effects of elevated temperature, high CO_2 and their interaction. Conserv. Physiol. 4, 1–31. https://doi.org/10.1093/conphys/cow009

Leiniö, S., Lehtonen, K.K., 2005. Seasonal variability in biomarkers in the bivalves *Mytilus edulis* and *Macoma balthica* from the northern Baltic Sea. Comp. Biochem. Physiol. - C Toxicol. Pharmacol. 140, 408–421. https://doi.org/10.1016/j.cca.2005.04.005

Leoni, G., De Poli, A., Mardirossian, M., Gambato, S., Florian, F., Venier, P., Wilson, D.N., Tossi, A., Pallavicini, A., Gerdol, M., 2017. Myticalins: A novel multigenic family of linear, cationic antimicrobial peptides from marine mussels (*Mytilus* spp.). Mar. Drugs 15, 1–23. https://doi.org/10.3390/md15080261

Lewis, S., Handy, R.D., Cordi, B., Billinghurst, Z., Depledge, M.H., 1999. Stress proteins (HSP's): Methods of detection and their use as an environmental biomarker. Ecotoxicology 8, 351–368. https://doi.org/10.1023/A:1008982421299

Li, A., Dai, H., Guo, X., Zhang, Z., Zhang, K., Wang, C., Wang, X., Wang, W., Chen, H., Li, X., Zheng, H., Li, L., Zhang, G., 2021a. Genome of the estuarine oyster provides insights into climate impact and adaptive plasticity. Commun. Biol. 4, 1–12. https://doi.org/10.1038/s42003-021-02823-6

Li, J., Green, C., Reynolds, A., Shi, H., Rotchell, J.M., 2018. Microplastics in mussels sampled from coastal waters and supermarkets in the United Kingdom. Environ. Pollut. 241, 35–44. https://doi.org/10.1016/j.envpol.2018.05.038

Li, J., Lusher, A.L., Rotchell, J.M., Deudero, S., Turra, A., Bråte, I.L.N., Sun, C., Shahadat Hossain, M., Li, Q., Kolandhasamy, P., Shi, H., 2019a. Using mussel as a global bioindicator of coastal

microplastic pollution. Environ. Pollut. 244, 522–533. https://doi.org/10.1016/j.envpol.2018.10.032

Li, J., Qu, M., Wang, M., Yue, Y., Chen, Z., Liu, R., Bu, Y., Li, Y., 2021b. Reproductive toxicity and underlying mechanisms of di(2-ethylhexyl) phthalate in nematode *Caenorhabditis elegans*. J. Environ. Sci. (China) 105, 1–10. https://doi.org/10.1016/j.jes.2020.12.016

Li, L., Andersen, M.E., Heber, S., Zhang, Q., 2007. Non-monotonic dose-response relationship in steroid hormone receptor-mediated gene expression. J. Mol. Endocrinol. 38, 569–585. https://doi.org/10.1677/JME-07-0003

Li, Q., Osada, M., Suzuki, T., Mori, K., 1998. Changes in vitellin during oogenesis and effect of estradiol-17β on vitellogenesis in the pacific oyster *Crassostrea gigas*. Invertebr. Reprod. Dev. 33, 87–93. https://doi.org/10.1080/07924259.1998.9652345

Li, Q., Sun, C., Wang, Y., Cai, H., Li, L., Li, J., Shi, H., 2019b. Fusion of microplastics into the mussel byssus. Environ. Pollut. 252, 420–426. https://doi.org/10.1016/j.envpol.2019.05.093

Li, S., Liu, C., Huang, J., Liu, Y., Zhang, S., Zheng, G., Xie, L., Zhang, R., 2016. Transcriptome and biomineralization responses of the pearl oyster *Pinctada fucata* to elevated CO_2 and temperature. Sci. Rep. 6, 1–10. https://doi.org/10.1038/srep18943

Li, Y., Zhang, L., Li, Yajuan, Li, W., Guo, Z., Li, R., Hu, X., Bao, Z., Wang, S., 2019c. Dynamics of DNA methylation and DNMT expression during gametogenesis and early development of scallop *Patinopecten yessoensis*. Mar. Biotechnol. 21, 196–205. https://doi.org/10.1007/s10126-018-09871-w

Lian, Z., Li, F., He, X., Chen, J., Yu, R.C., 2022. Rising CO_2 will increase toxicity of marine dinoflagellate *Alexandrium minutum*. J. Hazard. Mater. 431, 128627. https://doi.org/10.1016/j.jhazmat.2022.128627

Liang, J., Slingerland, J.M., 2003. Multiple roles of the PI3K/PKB (Akt) pathway in cell cycle progression. Cell Cycle 2, 336–342. https://doi.org/10.4161/cc.2.4.433

Liao, C.M., Jau, S.F., Lin, C.M., Jou, L.J., Liu, C.W., Liao, V.H.C., Chang, F.J., 2009. Valve movement response of the freshwater clam *Corbicula fluminea* following exposure to waterborne arsenic. Ecotoxicology 18, 567–576. https://doi.org/10.1007/s10646-009-0314-5

Liebl, M.C., Moehlenbrink, J., Becker, H., Raddatz, G., Abdeen, S.K., Aqeilan, R.I., Lyko, F., Hofmann, T.G., 2021. DAZAP2 acts as specifier of the p53 response to DNA damage. Nucleic Acids Res. 49, 2759–2776. https://doi.org/10.1093/nar/gkab084

Lightfield, J., Fram, N. R., Ely, B., 2011. Across bacterial phyla, distantly related genomes with similar genomic GC content have similar patterns of amino acid usage. PloS one, 6(3), e17677. https://doi.org/10.1371/journal.pone.0017677

Lima, D., Mattos, J.J., Piazza, R.S., Righetti, B.P.H., Monteiro, J.S., Grott, S.C., Alves, T.C., Taniguchi, S., Bícego, M.C., de Almeida, E.A., Bebianno, M.J., Medeiros, I.D., Bainy, A.C.D., 2019. Stress responses in *Crassostrea gasar* exposed to combined effects of acute pH changes and phenanthrene. Sci. Total Environ. 678, 585–593. https://doi.org/10.1016/j.scitotenv.2019.04.450

Lima, F.P., Wethey, D.S., 2012. Three decades of high-resolution coastal sea surface temperatures reveal more than warming. Nat. Commun. 3. https://doi.org/10.1038/ncomms1713

Lindskog, S., 1997. Carbonic anhydrase, purification and nature of the enzyme. Pharmacol. Ther. 74, 1–20.

Lionetto, M.G., Caricato, R., Erroi, E., Giordano, M.E., Schettino, T., 2006. Potential application of carbonic anhydrase activity in bioassay and biomarker studies. Chem. Ecol. 22, 37–41. https://doi.org/10.1080/02757540600670661

Lionetto, M.G., Maffia, M., Cappello, M.S., Giordano, M.E., Storelli, C., Schettino, T., 1998. Effect of cadmium on carbonic anhydrase and Na^+-K^+-ATPase in eel, *Anguilla anguilla*, intestine and gills. Comp. Biochem. Physiol. - A Mol. Integr. Physiol. 120, 89–91. https://doi.org/10.1016/S1095-6433(98)10014-4

Lithner, D., Larsson, A., Dave, G., 2011. Environmental and health hazard ranking and assessment of plastic polymers based on chemical composition. Sci. Total Environ. 409, 3309–3324. https://doi.org/10.1016/j.scitotenv.2011.04.038

Liu, H., Cui, K., Zeng, F., Chen, L., Cheng, Y., Li, H., Li, S., Zhou, X., Zhu, F., Ouyang, G., Luan, T., Zeng, Z., 2014. Occurrence and distribution of phthalate esters in riverine sediments from the Pearl River Delta region, South China. Mar. Pollut. Bull. 83, 358–365. https://doi.org/10.1016/j.marpolbul.2014.03.038

Liu, P., Miao, J., Song, Y., Pan, L., Yin, P., 2017. Effects of 2,2',4,4'-tetrabromodipheny ether (BDE-47) on gonadogenesis of the manila clam *Ruditapes philippinarum*. Aquat. Toxicol. 193, 178–186. https://doi.org/10.1016/j.aquatox.2017.10.022

Liu, C., Tu, C., Wang, L., Wu, H., Houston, B.J., Mastrorosa, F.K., Zhang, W., Shen, Y., Wang, J., Tian, S., Meng, L., Cong, J., Yang, S., Jiang, Y., Tang, S., Zeng, Y., Lv, M., Lin, G., Li, J., Saiyin, H., He, X., Jin, L., Touré, A., Ray, P.F., Veltman, J.A., Shi, Q., O'Bryan, M.K., Cao, Y., Tan, Y.Q., Zhang, F., 2021. Deleterious variants in X-linked CFAP47 induce asthenoteratozoospermia and primary male infertility. Am. J. Hum. Genet. 108, 309–323. https://doi.org/10.1016/j.ajhg.2021.01.002

Livak, K. J., Schmittgen, T. D., 2001. Analysis of relative gene expression data using real-time quantitative PCR and the 2− ΔΔCT method. Methods, 25(4), 402-408.

Livingstone, D.R., Lips, F., Martinez, P.G., Pipe, R.K., 1992. Antioxidant enzymes in the digestive gland of the common mussel *Mytilus edulis*. Mar. Biol. 112, 265–276. https://doi.org/10.1007/BF00702471

Lopes, J., Coppola, F., Russo, T., Maselli, V., Di Cosmo, A., Meucci, V., M.V.M. Soares, A., Pretti, C., Polese, G., Freitas, R., 2022. Behavioral, physiological and biochemical responses and differential gene expression in *Mytilus galloprovincialis* exposed to 17 alpha-ethinylestradiol and sodium lauryl sulfate. J. Hazard. Mater. 426, 128058. https://doi.org/10.1016/j.jhazmat.2021.128058

López-Landavery, E.A., Carpizo-Ituarte, E.J., Pérez-Carrasco, L., Díaz, F., la Cruz, F.L. De, García-Esquivel, Z., Hernández-Ayón, J.M., Galindo-Sánchez, C.E., 2021. Acidification stress effect on umbonate veliger larval development in *Panopea globosa*. Mar. Pollut. Bull. 163. https://doi.org/10.1016/j.marpolbul.2020.111945

Lopez-Zavala, A.A., Sotelo-Mundo, R.R., Hernandez-Flores, J.M., Lugo-Sanchez, M.E., Sugich-Miranda, R., Garcia-Orozco, K.D., 2016. Arginine kinase shows nucleoside diphosphate kinase-like activity toward deoxythymidine diphosphate. J. Bioenerg. Biomembr. 48, 301–308. https://doi.org/10.1007/s10863-016-9660-1

Lotterhos, K.E., Levitan, D.R., 2010. Gamete release and spawning behaviour in broadcast spawning marine invertebrates. Evol. Prim. Sex. Characters Anim. 99–120

Louis, F., Delahaut, L., Gaillet, V., Bonnard, I., Paris-Palacios, S., David, E., 2021. Effect of reproduction cycle stage on energy metabolism responses in a sentinel species (*Dreissena polymorpha*) exposed to cadmium: What consequences for biomonitoring? Aquat. Toxicol. 230. https://doi.org/10.1016/j.aquatox.2020.105699

Louis, F., Rocher, B., Barjhoux, I., Bultelle, F., Dedourge-Geffard, O., Gaillet, V., Bonnard, I., Delahaut, L., Pain-Devin, S., Geffard, A., Paris-Palacios, S., David, E., 2020. Seasonal monitoring of cellular energy metabolism in a sentinel species, *Dreissena polymorph*a (bivalve): Effect of global change? Sci. Total Environ. 725, 138450. https://doi.org/10.1016/j.scitotenv.2020.138450

Lowe, A.T., Bos, J., Ruesink, J., 2019. Ecosystem metabolism drives pH variability and modulates long-term ocean acidification in the Northeast Pacific coastal ocean. Sci. Rep. 9, 1–11. https://doi.org/10.1038/s41598-018-37764-4

Lowe, D.M., Moore, M.N., Bayne, B.L., 1982. Aspects of gametogenesis in the marine mussel *Mytilus Edulis* L. J. Mar. Biol. Assoc. United Kingdom 62, 133–145. https://doi.org/10.1017/S0025315400020166

Lu, B.X., Zeng, Z.B., Shi, T.L., 2013a. Comparative study of de novo assembly and genome-guided assembly strategies for transcriptome reconstruction based on RNA-Seq. Sci. China Life Sci. 56, 143–155. https://doi.org/10.1007/s11427-013-4442-z

Lu, W., Zhang, Y., McDonald, D.O., Jing, H., Carroll, B., Robertson, N., Zhang, Q., Griffin, H., Sanderson, S., Lakey, J.H., Morgan, N. V., Reynard, L.N., Zheng, L., Murdock, H.M., Turvey, S.E., Hackett, S.J., Prestidge, T., Hall, J.M., Cant, A.J., Matthews, H.F., Koref, M.F.S., Simon, A.K., Korolchuk, V.I., Lenardo, M.J., Hambleton, S., Su, H.C., 2014. Dual proteolytic pathways govern glycolysis and immune competence. Cell 159, 1578–1590. https://doi.org/10.1016/j.cell.2014.12.001

Lu, Y., Zhang, P., Li, C., Su, X., Jin, C., Li, Y., Xu, Y., Li, T., 2013b. Characterisation of immune-related gene expression in clam (*Venerupis philippinarum*) under exposure to di(2-ethylhexyl) phthalate. Fish Shellfish Immunol. 34, 142–146. https://doi.org/10.1016/j.fsi.2012.10.015

Lushchak, V.I., 2011. Environmentally induced oxidative stress in aquatic animals. Aquat. Toxicol. 101, 13–30. https://doi.org/10.1016/j.aquatox.2010.10.006

Lynch, S.A., Morgan, E., Carlsson, J., Mackenzie, C., Wooton, E.C., Rowley, A.F., Malham, S., Culloty, S.C., 2014. The health status of mussels, *Mytilu*s spp., in Ireland and Wales with the molecular identification of a previously undescribed haplosporidian. J. Invertebr. Pathol. 118, 59–65. https://doi.org/10.1016/j.jip.2014.02.012

M

Ma, J., Hung, H., Tian, C., Kallenborn, R., 2011. Revolatilization of persistent organic pollutants in the Arctic induced by climate change. Nat. Clim. Chang. 1, 255–260. https://doi.org/10.1038/nclimate1167

Maas, A.E., Lawson, G.L., Bergan, A.J., Tarrant, A.M., 2018. Exposure to CO_2 influences metabolism, calcification and gene expression of the thecosome pteropod *Limacina retroversa*. J. Exp. Biol. 221. https://doi.org/10.1242/jeb.164400

Mackintosh, C.E., Maldonado, J.A., Ikonomou, M.G., Gobas, F.A.P.C., 2006. Sorption of phthalate esters and PCBs in a marine ecosystem. Environ. Sci. Technol. 40, 3481–3488. https://doi.org/10.1021/es0519637

Madeira, D., Narciso, L., Cabral, H.N., Diniz, M.S., Vinagre, C., 2012. Thermal tolerance of the crab Pachygrapsus marmoratus: Intraspecific differences at a physiological (CTMax) and molecular level (Hsp70). Cell Stress Chaperones 17, 707–716. https://doi.org/10.1007/s12192-012-0345-3

Malachowicz, M., Wenne, R., 2019. Mantle transcriptome sequencing of *Mytilus* spp. and identification of putative biomineralization genes. PeerJ 2019. https://doi.org/10.7717/peerj.6245

Manduzio, H., Monsinjon, T., Rocher, B., Leboulenger, F., Galap, C., 2003. Characterization of an inducible isoform of the Cu/Zn superoxide dismutase in the blue mussel *Mytilus edulis*. Aquat. Toxicol. 64, 73–83. https://doi.org/10.1016/S0166-445X(03)00026-2

Mangi, S.C., Lee, J., Pinnegar, J.K., Law, R.J., Tyllianakis, E., Birchenough, S.N.R., 2018. The economic impacts of ocean acidification on shellfish fisheries and aquaculture in the United Kingdom. Environ. Sci. Policy 86, 95–105. https://doi.org/10.1016/j.envsci.2018.05.008

Mangiafico, S., 2017. Package 'rcompanion'. Cran Repos, 20, 1-71.

Maradonna, F., Evangelisti, M., Gioacchini, G., Migliarini, B., Olivotto, I., Carnevali, O., 2013. Assay of vtg, ERs and PPARs as endpoint for the rapid in vitro screening of the harmful effect of Di-(2-ethylhexyl)-phthalate (DEHP) and phthalic acid (PA) in zebrafish primary hepatocyte cultures. Toxicol. Vitr. 27, 84–91. https://doi.org/10.1016/j.tiv.2012.09.018

Marchant, H.K., Calosi, P., Spicer, J.I., 2010. Short-term exposure to hypercapnia does not compromise feeding, acid-base balance or respiration of *Patella vulgata* but surprisingly is accompanied by radula damage. J. Mar. Biol. Assoc. United Kingdom 90, 1379–1384. https://doi.org/10.1017/S0025315410000457

Marguerat, S., Bähler, J., 2010. RNA-seq: From technology to biology. Cell. Mol. Life Sci. 67, 569–579. https://doi.org/10.1007/s00018-009-0180-6

Marigómez, I., Baybay-Villacorta, L., 2003. Pollutant-specific and general lysosomal responses in digestive cells of mussels exposed to model organic chemicals. Aquat. Toxicol. 64, 235–257. https://doi.org/10.1016/S0166-445X(03)00056-0

Marigómez, I., Garmendia, L., Soto, M., Orbea, A., Izagirre, U., Cajaraville, M.P., 2013a. Marine ecosystem health status assessment through integrative biomarker indices: A comparative study after the Prestige oil spill "mussel Watch." Ecotoxicology 22, 486–505. https://doi.org/10.1007/s10646-013-1042-4

Marigómez, I., Múgica, M., Izagirre, U., Sokolova, I.M., 2017. Chronic environmental stress enhances tolerance to seasonal gradual warming in marine mussels. PLoS One 12, 1–24. https://doi.org/10.1371/journal.pone.0174359

Marigómez, I., Zorita, I., Izagirre, U., Ortiz-Zarragoitia, M., Navarro, P., Etxebarria, N., Orbea, A., Soto, M., Cajaraville, M.P., 2013b. Combined use of native and caged mussels to assess biological effects of pollution through the integrative biomarker approach. Aquat. Toxicol. 136–137, 32–48. https://doi.org/10.1016/j.aquatox.2013.03.008

Markert, B.A., Breure, A.M., Zechmeister, H.G., 2003. Bioindicators and biomonitors.

Markey C.M., Rubin B.S., Soto A.M., Sonnenschein C., 2002. Endocrine disruptors: from wingspread to environmental developmental biology. Journal of Steroid Biochemistry and Molecular Biology 83 235–244 https://doi.org/10.1016/s0960-0760(02)00272-8

Marshall, D.J., McQuaid, C.D., 2020. Metabolic regulation, oxygen limitation and heat tolerance in a subtidal marine gastropod reveal the complexity of predicting climate change vulnerability. Front. Physiol. 11, 1–12. https://doi.org/10.3389/fphys.2020.01106

Marszalek, J.R., Weiner, J.A., Farlow, S.J., Chun, J., Goldstein, L.S.B., 1999. Novel dendritic kinesin sorting identified by different process targeting of two related kinesins: KIF21A and KIF21B. J. Cell Biol. 145, 469–479. https://doi.org/10.1083/jcb.145.3.469

Martin, J.A., Wang, Z., 2011. Next-generation transcriptome assembly. Nat. Rev. Genet. 12, 671–682. https://doi.org/10.1038/nrg3068

Maruyama, I.N., Brenner, S., 1991. A phorbol ester/diacylglycerol-binding protein encoded by the unc-13 gene of *Caenorhabditis elegans*. Proc. Natl. Acad. Sci. U. S. A. 88, 5729–5733. https://doi.org/10.1073/pnas.88.13.5729

Masiá, P., Ardura, A., García-Vázquez, E., 2021. Virgin polystyrene microparticles exposure leads to changes in gills DNA and physical condition in the Mediterranean mussel *Mytilus galloprovincialis*. Animals 11. https://doi.org/10.3390/ani11082317

Mathew, S., Shaabad, M., Hussain, S., Mira, L., Qadri, I., 2015. The Need behind Messenger RNA Sequencing Analysis. Int. J. Adv. Res. 3, 1260–1270.

Matoo, O.B., Lannig, G., Bock, C., Sokolova, I.M., 2021. Temperature but not ocean acidification affects energy metabolism and enzyme activities in the blue mussel, *Mytilus edulis*. Ecol. Evol. 11, 3366–3379. https://doi.org/10.1002/ece3.7289

Matozzo, V., Marin, M.G., 2010. First evidence of gender-related differences in immune parameters of the clam *Ruditapes philippinarum* (Mollusca, Bivalvia). Mar. Biol. 157, 1181–1189. https://doi.org/10.1007/s00227-010-1398-4

Matthiessen, P., 2003. Endocrine disruption in marine fish. Pure Appl. Chem. 75, 2249–2261. https://doi.org/10.1351/pac200375112249

Matthiessen, P., Waldock, R., Thain, J.E., Waite, M.E., Scropehowe, S., 1995. Changes in periwinkle (*Littorina littorea*) populations following the ban on TBT-based antifoulings on small boats in the United Kingdom. Ecotoxicol. Environ. Saf. https://doi.org/10.1006/eesa.1995.1023

Mayer, M.P., 2010. Gymnastics of molecular chaperones. Mol. Cell 39, 321–331. https://doi.org/10.1016/j.molcel.2010.07.012

Maynou, F., Costa, S., Freitas, R., Solé, M., 2021. Effects of triclosan exposure on the energy budget of *Ruditapes philippinarum* and *R. decussatus* under climate change scenarios. Sci. Total Environ. 777, 1–8. https://doi.org/10.1016/j.scitotenv.2021.146068

Mazerolle, M.J., 2020. AICcmodavg: Model selection and multimodel inference based on (Q)AIC(c). R package version 2.3-1, https://cran.r-project.org/package=AICcmodavg.

McCahon, C.P., Pascoe, D., 1988. Increased sensitivity to cadmium of the freshwater amphipod *Gammarus pulex* (L.) during the reproductive period. Aquat. Toxicol. 13, 183–193. https://doi.org/10.1016/0166-445X(88)90051-3

McClellan-Green, P., Romano, J., Oberdörster, E., 2007. Does gender really matter in contaminant exposure? A case study using invertebrate models. Environ. Res. 104, 183–191. https://doi.org/10.1016/j.envres.2006.09.008

Medaković, D., 2000. Carbonic anhydrase activity and biomineralization process in embryos, larvae and adult blue mussels *Mytilus edulis* L. Helgol. Mar. Res. 54, 1–6. https://doi.org/10.1007/s101520050030

Melzner, F., Gutowska, M.A., Langenbuch, M., Dupont, S., Lucassen, M., Thorndyke, M.C., Bleich, M., Pörtner, H.O., 2009. Physiological basis for high CO_2 tolerance in marine ectothermic animals: Pre-adaptation through lifestyle and ontogeny? Biogeosciences 6, 2313–2331. https://doi.org/10.5194/bg-6-2313-2009

Melzner, F., Stange, P., Trübenbach, K., Thomsen, J., Casties, I., Panknin, U., Gorb, S.N., Gutowska, M.A., 2011. Food supply and seawater pCO_2 impact calcification and internal shell dissolution in the blue mussel mytilus edulis. PLoS One 6. https://doi.org/10.1371/journal.pone.0024223

Metcalfe, C.D., Metcalfe, T.L., Kiparissis, Y., Koenig, B.G., Khan, C., Hughes, R.J., Croley, T.R., March, R.E., Potter, T., 2001. Estrogenic potency of chemicals detected in sewage treatment plant effluents as determined by in vivo assays with Japanese medaka (Oryzias *latipes*). Environ. Toxicol. Chem. 20, 297–308. https://doi.org/10.1002/etc.5620200210

Mezzelani, M., Nardi, A., Bernardini, I., Milan, M., Peruzza, L., d'Errico, G., Fattorini, D., Gorbi, S., Patarnello, T., Regoli, F., 2021. Environmental pharmaceuticals and climate change: the case study of carbamazepine in *M. galloprovincialis* under ocean acidification scenario. Environ. Int. 146, 106269. https://doi.org/10.1016/j.envint.2020.106269

Michaelidis, B., Haas, D., Grieshaber, M.K., 2005. Extracellular and intracellular acid-base status with regard to the energy metabolism in the oyster *Crassostrea gigas* during exposure to air. Physiol. Biochem. Zool. 78, 373–383. https://doi.org/10.1086/430223

Mikulski, A., Bernatowicz, P., Grzesiuk, M., Kloc, M., Pijanowska, J., 2011. Differential levels of stress proteins (HSPs) in male and female *Daphnia magna* in response to thermal stress: a consequence of sex-related behavioral differences? J. Chem. Ecol. 37, 670–676. https://doi.org/10.1007/s10886-011-9969-5

Miller, S.H., Breitburg, D.L., Burrell, R.B., Keppel, A.G., 2016. Acidification increases sensitivity to hypoxia in important forage fishes. Mar. Ecol. Prog. Ser. 549, 1–8. https://doi.org/10.3354/meps11695

Mincarelli, L. F., Chapman, E. C., Rotchell, J. M., Turner, A. P., Wollenberg Valero, K. C., 2022. Sex and gametogenesis stage are strong drivers of gene expression in *Mytilus edulis* exposed to environmentally relevant plasticiser levels and pH 7.7. Environmental Science and Pollution Research, 1-13. https://doi.org/10.1007/s11356-022-23801-3

Mincarelli, L.F., Rotchell, J.M., Chapman, E.C., Turner, A.P., Wollenberg Valero, K.C., 2021. Consequences of combined exposure to thermal stress and the plasticiser DEHP in *Mytilus* spp. differ by sex. Mar. Pollut. Bull. 170, 112624. https://doi.org/10.1016/j.marpolbul.2021.112624

Minier, C., Forget-Leray, J., Bjørnstad, A., Camus, L., 2008. Multixenobiotic resistance, acetyl-choline esterase activity and total oxyradical scavenging capacity of the Arctic spider crab, *Hyas araneus*, following exposure to bisphenol A, tetra bromo diphenyl ether and diallyl phthalate. Mar. Pollut. Bull. 56, 1410–1415. https://doi.org/10.1016/j.marpolbul.2008.05.005

Mitchell, J.F.B., 1989. The "Greenhouse" effect and climate change. Rev. Geophys. 27, 115. https://doi.org/10.1029/RG027i001p00115

Mladineo, I., Peharda, M., Orhanović, S., Bolotin, J., Pavela-Vrančić, M., Treursić, B., 2007. The reproductive cycle, condition index and biochemical composition of the horse-bearded mussel

Modiolus barbatus. Helgol. Mar. Res. 61 (3), 183–192. https://doi.org/10.1007/s10152-007-0065-8

Mochizuki, Y., Majerus, P.W., 2003. Characterization of myotubularin-related protein 7 and its binding partner, myotubularin-related protein 9. Proc. Natl. Acad. Sci. U. S. A. 100, 9768–9773. https://doi.org/10.1073/pnas.1333958100

Monteiro, R., Costa, S., Coppola, F., Freitas, R., Vale, C., Pereira, E., 2019. Evidences of metabolic alterations and cellular damage in mussels after short pulses of Ti contamination. Sci. Total Environ. 650, 987–995. https://doi.org/10.1016/j.scitotenv.2018.08.314

Moreira, R., Balseiro, P., Planas, J. V., Fuste, B., Beltran, S., Novoa, B., & Figueras, A., 2012. Transcriptomics of in vitro immune-stimulated hemocytes from the Manila clam *Ruditapes philippinarum* using high-throughput sequencing. PloS one, 7(4), e35009. https://doi.org/10.1371/journal.pone.0035009

Moreira, A., Figueira, E., Soares, A.M.V.M., Freitas, R., 2016. The effects of arsenic and seawater acidification on antioxidant and biomineralization responses in two closely related *Crassostrea* species. Sci. Total Environ. 545–546, 569–581. https://doi.org/10.1016/j.scitotenv.2015.12.029

Moreira, R., Pereiro, P., Canchaya, C., Posada, D., Figueras, A., Novoa, B., 2015. RNA-Seq in Mytilus galloprovincialis: Comparative transcriptomics and expression profiles among different tissues. BMC Genomics 16, 1–18. https://doi.org/10.1186/s12864-015-1817-5

Moreira, S.M., Moreira-Santos, M., Ribeiro, R., Guilhermino, L., 2004. The "Coral Bulker" fuel oil spill on the north coast of Portugal: Spatial and temporal biomarker responses in *Mytilus galloprovincialis*. Ecotoxicology 13, 619–630. https://doi.org/10.1007/s10646-003-4422-3

Morel, Y., Barouki, R., 1999. Repression of gene expression by oxidative stress. Biochem. J. 342, 481–496. https://doi.org/10.1042/0264-6021:3420481

Morse, D. E., Duncan, H., Hooker, N., Morse, A., 1977. Hydrogen peroxide induces spawning in mollusks, with activation of prostaglandin endoperoxide synthetase. Science, 196(4287), 298-300. https://doi.org/10.1126/science.403609

Moss, G.A., Illingworth, J., Tong, L.J., 1995. Comparing two simple methods to induce spawning in the New Zealand abalone (paua), *Haliotis iris*. New Zeal. J. Mar. Freshw. Res. 29, 329–333. https://doi.org/10.1080/00288330.1995.9516667

Mu, X., Liao, X., Chen, X., Li, Y., Wang, M., Shen, C., Zhang, X., Wang, Y., Liu, X., He, J., 2015. DEHP exposure impairs mouse oocyte cyst breakdown and primordial follicle assembly through estrogen receptor-dependent and independent mechanisms. J. Hazard. Mater. 298, 232–240. https://doi.org/10.1016/j.jhazmat.2015.05.052

Mubiana, V.K., Blust, R., 2007. Effects of temperature on scope for growth and accumulation of Cd, Co, Cu and Pb by the marine bivalve *Mytilus eduli*s. Mar. Environ. Res. 63, 219–235. https://doi.org/10.1016/j.marenvres.2006.08.005

Munari, M., Devigili, A., Dalle Palle, G., Asnicar, D., Pastore, P., Badocco, D., Marin, M.G., 2022. Ocean acidification, but not environmental contaminants, affects fertilization success and sperm motility in the sea urchin *Paracentrotus lividus*. J. Mar. Sci. Eng. 10. https://doi.org/10.3390/jmse10020247

Munari, M., Matozzo, V., Chemello, G., Riedl, V., Pastore, P., Badocco, D., Marin, M.G., 2019. Seawater acidification and emerging contaminants: A dangerous marriage for haemocytes of marine bivalves. Environ. Res. 175, 11–21. https://doi.org/10.1016/j.envres.2019.04.032

Munari, M., Matozzo, V., Gagné, F., Chemello, G., Riedl, V., Finos, L., Pastore, P., Badocco, D., Marin, M.G., 2018. Does exposure to reduced pH and diclofenac induce oxidative stress in marine bivalves? A comparative study with the mussel *Mytilus galloprovincialis* and the clam *Ruditapes philippinarum*. Environ. Pollut. 240, 925–937. https://doi.org/10.1016/j.envpol.2018.05.005

Munari, M., Matozzo, V., Riedl, V., Pastore, P., Badocco, D., Marin, M.G., 2020. Eat breathe excrete repeat: physiological responses of the mussel *Mytilus galloprovincialis* to diclofenac and ocean acidification. J. Mar. Sci. Eng. 8, 1–12. https://doi.org/10.3390/jmse8110907

Munday, P.L., Dixson, D.L., Donelson, J.M., Jones, G.P., Pratchett, M.S., Devitsina, G. V., Døving, K.B., 2009. Ocean acidification impairs olfactory discrimination and homing ability of a marine fish. Proc. Natl. Acad. Sci. 106, 1848–1852. https://doi.org/10.1073/pnas.0809996106

N

Naddafi, R., Eklöv, P., Pettersson, K., 2007. Non-lethal predator effects on the feeding rate and prey selection of the exotic zebra mussel *Dreissena polymorpha*. Oikos 116, 1289–1298. https://doi.org/10.1111/j.2007.0030-1299.15695.x

Naddafi, R., Rudstam, L.G., 2013. Predator-induced behavioural defences in two competitive invasive species: the zebra mussel and the quagga mussel. Anim. Behav. 86, 1275–1284. https://doi.org/10.1016/j.anbehav.2013.09.032

Nagai, K., Honjo, T., Go, J., Yamashita, H., Oh, S.J., 2006. Detecting the shellfish killer *Heterocapsa circularisquama* (Dinophyceae) by measuring bivalve valve activity with a Hall element sensor. Aquaculture 255, 395–401. https://doi.org/10.1016/j.aquaculture.2005.12.018

Nagasawa, K., Treen, N., Kondo, R., Otoki, Y., Itoh, N., Rotchell, J.M., Osada, M., 2015. Molecular characterization of an estrogen receptor and estrogen-related receptor and their autoregulatory capabilities in two *Mytilus* species. Gene 564, 153–159. https://doi.org/10.1016/j.gene.2015.03.073

Nakashima, A., Hosaka, K., Nikawa, J.I., 1997. Cloning of a human cDNA for CTP-phosphoethanolamine cytidylyltransferase by complementation in vivo of a yeast mutant. J. Biol. Chem. 272, 9567–9572. https://doi.org/10.1074/jbc.272.14.9567

Nardi, A., Benedetti, M., d'Errico, G., Fattorini, D., Regoli, F., 2018. Effects of ocean warming and acidification on accumulation and cellular responsiveness to cadmium in mussels *Mytilus galloprovincialis*: Importance of the seasonal status. Aquat. Toxicol. 204, 171–179. https://doi.org/10.1016/j.aquatox.2018.09.009

Nardi, A., Mincarelli, L.F., Benedetti, M., Fattorini, D., d'Errico, G., Regoli, F., 2017. Indirect effects of climate changes on cadmium bioavailability and biological effects in the Mediterranean mussel *Mytilus galloprovincialis*. Chemosphere 169, 493–502. https://doi.org/10.1016/j.chemosphere.2016.11.093

Nasci, C., Nesto, N., Monteduro, R.A., Da Ros, L., 2002. Field application of biochemical markers and a physiological index in the mussel, *Mytilus galloprovincialis*: Transplantation and biomonitoring studies in the lagoon of Venice (NE Italy). Mar. Environ. Res. 54, 811–816. https://doi.org/10.1016/S0141-1136(02)00122-8

Nash, S., Rahman, M.S., 2019. Short - term heat stress impairs testicular functions in the American oyster, *Crassostrea virginica*: Molecular mechanisms and induction of oxidative stress and apoptosis in spermatogenic cells 1444–1458. https://doi.org/10.1002/mrd.23268

Navarro, J.M., Torres, R., Acuña, K., Duarte, C., Manriquez, P.H., Lardies, M., Lagos, N.A., Vargas, C., Aguilera, V., 2013. Impact of medium-term exposure to elevated pCO_2 levels on the physiological energetics of the mussel *Mytilus chilensis*. Chemosphere 90, 1242–1248. https://doi.org/10.1016/j.chemosphere.2012.09.063

Negrete-García, G., Lovenduski, N.S., Hauri, C., Krumhardt, K.M., Lauvset, S.K., 2019. Sudden emergence of a shallow aragonite saturation horizon in the Southern Ocean. Nat. Clim. Chang. 9, 313–317. https://doi.org/10.1038/s41558-019-0418-8

Net, S., Sempéré, R., Delmont, A., Paluselli, A., Ouddane, B., 2015. Occurrence, fate, behavior and ecotoxicological state of phthalates in different environmental matrices. Environ. Sci. Technol. 49, 4019–4035. https://doi.org/10.1021/es505233b

Neuberger-Cywiak, L., Achituv, Y., Garcia, E.M., 2005. Sublethal effects of Zn++ and Cd++ on respiration rate, ammonia excretion, and O:N ratio of *Donax trunculus* (Bivalvia; Donacidae). Bull. Environ. Contam. Toxicol. 75, 505–514. https://doi.org/10.1007/s00128-005-0781-1

Newcomb, L.A., George, M.N., O'Donnell, M.J., Carrington, E., 2019. Only as strong as the weakest link: Structural analysis of the combined effects of elevated temperature and pCO_2 on mussel attachment. Conserv. Physiol. 7, 1–11. https://doi.org/10.1093/conphys/coz068

Newell, R.I.E., Hilbish, T.J., Koehn, R.K., Newell, C.J., 1982. Temporal variation in the reproductive cycle of *Mytilus edulis* L. (Bivalvia, Mytilidae) from localities on the east coast of the United States (Long Island, New York). Biol. Bull. 162, 299–310. https://doi.org/10.2307/1540985

Newell, R.I.E., Thompson, R.J., 1984. Reduced clearance rates associated with spawning in the mussel, *Mytilus edulis* (L.)(Bivalvia, Mytilidae).

Ni, J., Zeng, Z., Ke, C., 2013. Sex steroid levels and expression patterns of estrogen receptor gene in the oyster *Crassostrea angulata* during reproductive cycle. Aquaculture 376–379, 105–116. https://doi.org/10.1016/j.aquaculture.2012.11.023

Nicastro, K.R., Zardi, G.I., McQuaid, C.D., 2007. Behavioural response of invasive *Mytilus galloprovincialis* and indigenous *Perna perna* mussels exposed to risk of predation. Mar. Ecol. Prog. Ser. 336, 169–175. https://doi.org/10.3354/meps336169

Nikinmaa, M., 2013. Climate change and ocean acidification-Interactions with aquatic toxicology. Aquat. Toxicol. 126, 365–372. https://doi.org/10.1016/j.aquatox.2012.09.006

Nilsson, G.E., Dixson, D.L., Domenici, P., McCormick, M.I., Sørensen, C., Watson, S.A., Munday, P.L., 2012. Near-future carbon dioxide levels alter fish behaviour by interfering with neurotransmitter function. Nat. Clim. Chang. 2, 201–204. https://doi.org/10.1038/nclimate1352

Nigro, M., Falleni, A., Barga, I. Del, Scarcelli, V., Lucchesi, P., Regoli, F., Frenzilli, G., 2006. Cellular biomarkers for monitoring estuarine environments: Transplanted versus native mussels. Aquat. Toxicol. 77, 339–347. https://doi.org/10.1016/j.aquatox.2005.12.013

Nikinmaa, M., 2013. Climate change and ocean acidification-Interactions with aquatic toxicology. Aquat. Toxicol. 126, 365–372. https://doi.org/10.1016/j.aquatox.2012.09.006

Nishiya, T., Matsumoto, K., Maekawa, S., Kajita, E., Horinouchi, T., Fujimuro, M., Ogasawara, K., Uehara, T., Miwa, S., 2011. Regulation of inducible nitric-oxide synthase by the SPRY domain- and SOCS box-containing proteins. J. Biol. Chem. 286, 9009–9019. https://doi.org/10.1074/jbc.M110.190678

Norman, A., Börjeson, H., David, F., Tienpont, B., Norrgren, L., 2007. Studies of uptake, elimination, and late effects in Atlantic salmon (*Salmo salar*) dietary exposed to di-2-ethylhexyl phthalate (DEHP) during early life. Arch. Environ. Contam. Toxicol. 52, 235–242. https://doi.org/10.1007/s00244-005-5089-y

Novogene Ltd., 2020. RNA-seq Analysis without Reference Genome. Available at https://www.n-genetics.com/products/1304/1024/18000.pdf Access date 04 Mar 2020

Nowak, K., Jabłońska, E., Ratajczak-Wrona, W., 2019. Immunomodulatory effects of synthetic endocrine disrupting chemicals on the development and functions of human immune cells. Environ. Int. 125, 350–364. https://doi.org/10.1016/j.envint.2019.01.078

Nowicki, C.J., Kashian, D.R., 2018. Comparison of lipid peroxidation and catalase response in invasive dreissenid mussels exposed to single and multiple stressors. Environ. Toxicol. Chem. 37, 1643–1654. https://doi.org/10.1002/etc.4111

Noyes, P.D., McElwee, M.K., Miller, H.D., Clark, B.W., Van Tiem, L.A., Walcott, K.C., Erwin, K.N., Levin, E.D., 2009. The toxicology of climate change: environmental contaminants in a warming world. Environ. Int. 35, 971–986. https://doi.org/10.1016/j.envint.2009.02.006

Numata H, Udaka H., 2010. Photoperiodism in Mollusks. In: Nelson RJ, Denlinger DL, Somers DE, eds. Photoperiodism: the biological calendar. UK: Oxford University Press. p. 173–92.

O

O'Connor, T.P., 1998. Mussel Watch results from 1986 to 1996. Mar. Pollut. Bull. 37, 14–19. https://doi.org/10.1016/S0025-326X(98)00126-X

O'Donnell, M.J., George, M.N., Carrington, E., 2013. Mussel byssus attachment weakened by ocean acidification. Nat. Clim. Chang. 3, 587–590. https://doi.org/10.1038/nclimate1846

Oehlmann, J., Oetken, M., Schulte-Oehlmann, U., 2008. A critical evaluation of the environmental risk assessment for plasticizers in the freshwater environment in Europe, with special emphasis on bisphenol A and endocrine disruption. Environ. Res. 108, 140–149. https://doi.org/10.1016/j.envres.2008.07.016

Oksanen, J., Blanchet, F. G., Kindt, R., Legendre, P., Minchin, P. R., O'hara, R., Simpson, G. L., Solymos, P., Stevens, M. H. H., Wagner, H., 2013, "Package 'vegan'. Community ecology package, version 2.".

Orbea, A., Marigómez, I., Fernández, C., Tarazona, J. V., Cancio, I., Cajaraville, M.P., 1999. Structure of peroxisomes and activity of the marker enzyme catalase in digestive epithelial cells in relation to PAH content of mussels from two basque estuaries (Bay of Biscay): Seasonal and site-specific variations. Arch. Environ. Contam. Toxicol. 36, 158–166. https://doi.org/10.1007/s002449900456

Orbea, A., Ortiz-Zarragoitia, M., Cajaraville, M.P., 2002. Interactive effects of benzo(a)pyrene and cadmium and effects of di(2-ethylhexyl) phthalate on antioxidant and peroxisomal enzymes and peroxisomal volume density in the digestive gland of mussel *Mytilus galloprovincialis* Lmk. Biomarkers 7, 33–48. https://doi.org/10.1080/13547500110066119

Orr, J.C., Fabry, V.J., Aumont, O., Bopp, L., Doney, S.C., Feely, R.A., Gnanadesikan, A., Gruber, N., Ishida, A., Joos, F., Key, R.M., Lindsay, K., Maier-Reimer, E., Matear, R., Monfray, P., Mouchet, A., Najjar, R.G., Plattner, G.K., Rodgers, K.B., Sabine, C.L., Sarmiento, J.L., Schlitzer, R., Slater, R.D., Totterdell, I.J., Weirig, M.F., Yamanaka, Y., Yool, A., 2005. Anthropogenic ocean acidification over the twenty-first century and its impact on calcifying organisms. Nature 437, 681–686. https://doi.org/10.1038/nature04095

Ortiz-Zarragoitia, M., Cajaraville, M.P., 2006. Biomarkers of exposure and reproduction-related effects in mussels exposed to endocrine disrupters. Arch. Environ. Contam. Toxicol. 50, 361–369. https://doi.org/10.1007/s00244-005-1082-8

Ortiz-Zarragoitia, M., Garmendia, L., Barbero, M.C., Serrano, T., Marigomez, I., Cajaraville, M.P., 2011. Effects of the fuel oil spilled by the Prestige tanker on reproduction parameters of wild mussel populations. J. Environ. Monit. 13, 84–94. https://doi.org/10.1039/c0em00102c

Ortmann, C., Grieshaber, M.K., 2003. Energy metabolism and valve closure behaviour in the Asian clam *Corbicula fluminea*. J. Exp. Biol. 206, 4167–4178. https://doi.org/10.1242/jeb.00656

Osada, M., Mori, K., Nomura, T., 1992. In vitro effects of estrogen and serotonin on release of eggs from the ovary of the scallop 58, 223–227.

Osada, M., Nakata, A., Matsumoto, T., Mori, K., 1998. Pharmacological characterization of serotonin receptor in the oocyte membrane of bivalve molluscs and its formation during oogenesis. J. Exp. Zool. 281, 124–131. https://doi.org/10.1002/(SICI)1097-010X(19980601)281:2

Osorio, F.G., Soria-Valles, C., Santiago-Fernández, O., Bernal, T., Mittelbrunn, M., Colado, E., Rodríguez, F., Bonzon-Kulichenko, E., Vázquez, J., Porta-De-La-Riva, M., Cerón, J., Fueyo, A., Li, J., Green, A.R., Freije, J.M.P., López-Otín, C., 2016. Loss of the proteostasis factor AIRAPL causes myeloid transformation by deregulating IGF-1 signaling. Nat. Med. 22, 91–96. https://doi.org/10.1038/nm.4013

P

Paluselli, A., Fauvelle, V., Schmidt, N., Galgani, F., Net, S., Sempéré, R., 2018. Distribution of phthalates in Marseille Bay (NW Mediterranean Sea). Sci. Total Environ. 621, 578–587. https://doi.org/10.1016/j.scitotenv.2017.11.306

Pansch, C., Schaub, I., Havenhand, J., Wahl, M., 2014. Habitat traits and food availability determine the response of marine invertebrates to ocean acidification. Glob. Chang. Biol. 20, 765–777. https://doi.org/10.1111/gcb.12478

Parisi, M.G., Giacoletti, A., Mandaglio, C., Cammarata, M., Sarà, G., 2021. The entangled multi-level responses of *Mytilus galloprovincialis* (Lamarck, 1819) to environmental stressors as detected by an integrated approach. Mar. Environ. Res. 168. https://doi.org/10.1016/j.marenvres.2021.105292

Park, C.J., Barakat, R., Ulanov, A., Li, Z., Lin, P.C., Chiu, K., Zhou, S., Perez, P., Lee, J., Flaws, J., Ko, C.M.J., 2019. Sanitary pads and diapers contain higher phthalate contents than those in

common commercial plastic products. Reprod. Toxicol. 84, 114–121. https://doi.org/10.1016/j.reprotox.2019.01.005

Parkerton, T.F., Konkel, W.J., 2000. Application of quantitative structure--activity relationships for assessing the aquatic toxicity of phthalate esters. Ecotoxicol. Environ. Saf. 45, 61–78. https://doi.org/10.1006/eesa.1999.1841

Patra, R.W., Chapman, J.C., Lim, R.P., Gehrke, P.C., 2007. The effects of three organic chemicals on the upper thermal tolerances of four freshwater fishes. Environ. Toxicol. Chem. 26, 1454–1459. https://doi.org/10.1897/06-156R1.1

Paulino, C., Kalienkova, V., Lam, A.K.M., Neldner, Y., Dutzler, R., 2017. Activation mechanism of the calcium-activated chloride channel TMEM16A revealed by cryo-EM. Nature 552, 421–425. https://doi.org/10.1038/nature2465

Paul-Pont, I., Lacroix, C., González Fernández, C., Hégaret, H., Lambert, C., Le Goïc, N., Frère, L., Cassone, A.L., Sussarellu, R., Fabioux, C., Guyomarch, J., Albentosa, M., Huvet, A., Soudant, P., 2016. Exposure of marine mussels *Mytilus* spp. to polystyrene microplastics: Toxicity and influence on fluoranthene bioaccumulation. Environ. Pollut. 216, 724–737. https://doi.org/10.1016/j.envpol.2016.06.039

Peijnenburg, W.J.G.M., Struijs, J., 2006. Occurrence of phthalate esters in the environment of the Netherlands. Ecotoxicol. Environ. Saf. 63, 204–215. https://doi.org/10.1016/j.ecoenv.2005.07.023

Pérez, C.A., Lagos, N.A., Saldías, G.S., Waldbusser, G., Vargas, C.A., 2016. Riverine discharges impact physiological traits and carbon sources for shell carbonate in the marine intertidal mussel *Perumytilus purpuratus*. Limnol. Oceanogr. 61, 969–983. https://doi.org/10.1002/lno.10265

Pernet, F., Tremblay, R., Comeau, L., Guderley, H., 2007. Temperature adaptation in two bivalve species from different thermal habitats: Energetics and remodelling of membrane lipids. J. Exp. Biol. 210, 2999–3014. https://doi.org/10.1242/jeb.006007

Perrone, C.A., Myster, S.H., Bower, R., O'Toole, E.T., Porter, M.E., 2000. Insights into the structural organization of the I1 inner arm dynein from a domain analysis of the 1β dynein heavy chain. Mol. Biol. Cell 11, 2297–2313. https://doi.org/10.1091/mbc.11.7.2297

Peterson, D.R., Staples, C.A., 2003. Degradation of phthalate esters in the environment. Handb. Environ. Chem. 3, 85–124. https://doi.org/10.1007/b11464

Peterson, K.J., Lyons, J.B., Nowak, K.S., Takacs, C.M., Wargo, M.J., McPeek, M.A., 2004. Estimating metazoan divergence times with a molecular clock. Proc. Natl. Acad. Sci. 101, 6536–6541. https://doi.org/10.1073/pnas.0401670101

Peterson, R.A., 2021. Finding optimal normalizing transformations via bestNormalize. The R Journal, 13(1), 310–329. doi:10.32614/RJ-2021-041.

Petes, L.E., Mouchka, M.E., Milston-Clements, R.H., Momoda, T.S., Menge, B.A., 2008. Effects of environmental stress on intertidal mussels and their sea star predators. Oecologia 156, 671–680. https://doi.org/10.1007/s00442-008-1018-x

Philipp, E.E.R., Kraemer, L., Melzner, F., Poustka, A.J., Thieme, S., Findeisen, U., Schreiber, S., Rosenstiel, P., 2012. Massively parallel rna sequencing identifies a complex immune gene repertoire in the lophotrochozoan *Mytilus edulis*. PLoS One 7. https://doi.org/10.1371/journal.pone.0033091

Philippart, C.J.M., Van Aken, H.M., Beukema, J.J., Bos, O.G., Cadée, G.C., Dekker, R., 2003. Climate-related changes in recruitment of the bivalve *Macoma balthica*. Limnol. Oceanogr. 48, 2171–2185. https://doi.org/10.4319/lo.2003.48.6.2171

Picaud, S.S., Muniz, J.R.C., Kramm, A., Pilka, E.S., Kochan, G., Oppermann, U., Yue, W.W., 2009. Crystal structure of human carbonic anhydrase-related protein VIII reveals the basis for catalytic silencing. Proteins Struct. Funct. Bioinforma. 76, 507–511. https://doi.org/10.1002/prot.22411

Pipe, R.K., 1987. Ultrastructural and cytochemical study on interactions between nutrient storage cells and gametogenesis in the mussel *Mytilus edulis* 528, 519–528.

Pittura, L., Avio, C.G., Giuliani, M.E., d'Errico, G., Keiter, S.H., Cormier, B., Gorbi, S., Regoli, F., 2018. Microplastics as Vehicles of Environmental PAHs to Marine Organisms: Combined Chemical and Physical Hazards to the Mediterranean Mussels, *Mytilus galloprovincialis*. Front. Mar. Sci. 5. https://doi.org/10.3389/fmars.2018.00103

PlasticEurope, 2020. Plastic: The Facts 2020. Available at https://plasticseurope.org/knowledge-hub/plastics-the-facts-2020/ Accessed 12 Mar 2021

Porte, C., Janer, G., Lorusso, L.C., Ortiz-Zarragoitia, M., Cajaraville, M.P., Fossi, M.C., Canesi, L., 2006. Endocrine disruptors in marine organisms: Approaches and perspectives. Comp. Biochem. Physiol. - C Toxicol. Pharmacol. 143, 303–315. https://doi.org/10.1016/j.cbpc.2006.03.004

Porteus, C.S., Hubbard, P.C., Uren Webster, T.M., van Aerle, R., Canário, A.V.M., Santos, E.M., Wilson, R.W., 2018. Near-future CO_2 levels impair the olfactory system of a marine fish. Nat. Clim. Chang. 8, 737–743. https://doi.org/10.1038/s41558-018-0224-8

Pörtner, H.O., 2008. Ecosystem effects of ocean acidification in times of ocean warming: A physiologist's view. Mar. Ecol. Prog. Ser. 373, 203–217. https://doi.org/10.3354/meps07768

Pörtner, H.O., Langenbuch, M., Reipschläger, A., 2004. Biological Impact of Elevated Ocean CO_2 Concentrations: Lessons from Animal Physiology and Earth History. J. Oceanogr. 60, 705–718. https://doi.org/10.1007/s10872-004-5763-0

Power, A., Sheehan, D., 1996. Seasonal variation in the antioxidant defence systems of gill and digestive gland of the blue mussel, *Mytilus edulis*. Comp. Biochem. Physiol. - C Pharmacol. Toxicol. Endocrinol. 114, 99–103. https://doi.org/10.1016/0742-8413(96)00024-2

Pratt, N., Ciotti, B.J., Morgan, E.A., Stahl, H., Stahl, H., Hauton, C., 2015. No evidence for impacts to the molecular ecophysiology of ion or CO_2 regulation in tissues of selected surface-dwelling bivalves in the vicinity of a sub-seabed CO_2 release. Int. J. Greenh. Gas Control 38, 193–201. https://doi.org/10.1016/j.ijggc.2014.10.001

Prieto, A., Zuloaga, O., Usobiaga, A., Etxebarria, N., Fernández, L.A., 2007. Development of a stir bar sorptive extraction and thermal desorption-gas chromatography-mass spectrometry method for the simultaneous determination of several persistent organic pollutants in water samples. J. Chromatogr. A 1174, 40–49. https://doi.org/10.1016/j.chroma.2007.07.054

Pruell, R.J., Lake, J.L., Davis, W.R., Quinn, J.G., 1986. Uptake and depuration of organic contaminants by blue mussels (*Mytilus edulis*) exposed to environmentally contaminated sediment. Mar. Biol. 91, 497–507. https://doi.org/10.1007/BF00392601

Puinean, A.M., Labadie, P., Hill, E.M., Osada, M., Kishida, M., Nakao, R., Novillo, A., Callard, I.P., Rotchell, J.M., 2006. Laboratory exposure to 17β-estradiol fails to induce vitellogenin and estrogen receptor gene expression in the marine invertebrate *Mytilus edulis*. Aquat. Toxicol. 79, 376–383. https://doi.org/10.1016/j.aquatox.2006.07.006

Puinean, A.M., Rotchell, J.M., 2006. Vitellogenin gene expression as a biomarker of endocrine disruption in the invertebrate, *Mytilus edulis*. Mar. Environ. Res. 62, 211–214. https://doi.org/10.1016/j.marenvres.2006.04.035

Q

Qiu, L.L., Wang, Xuan, Zhang, X. hui, Zhang, Z., Gu, J., Liu, L., Wang, Y., Wang, Xinru, Wang, S.L., 2013. Decreased androgen receptor expression may contribute to spermatogenesis failure in rats exposed to low concentration of bisphenol A. Toxicol. Lett. 219, 116–124. https://doi.org/10.1016/j.toxlet.2013.03.011

R

Ragusa, A., Svelato, A., Santacroce, C., Catalano, P., Notarstefano, V., Carnevali, O., Papa, F., Rongioletti, M.C.A., Baiocco, F., Draghi, S., D'Amore, E., Rinaldo, D., Matta, M., Giorgini, E., 2021. Plasticenta: First evidence of microplastics in human placenta. Environ. Int. 146, 106274. https://doi.org/10.1016/j.envint.2020.106274

Rahman, M.A., Henderson, S., Miller-Ezzy, P., Li, X.X., Qin, J.G., 2019. Immune response to temperature stress in three bivalve species: Pacific oyster *Crassostrea gigas*, Mediterranean mussel *Mytilus galloprovincialis* and mud cockle *Katelysia rhytiphora*. Fish Shellfish Immunol. 86, 868–874. https://doi.org/10.1016/j.fsi.2018.12.017

Rainbow, P.S., Phillips, D.J.H., 1993. Cosmopolitan Biomonitors of Trace Metals 26, 593–601.

Raingeard, D., Bilbao, E., Cancio, I., Cajaraville, M.P., 2013. Retinoid X receptor (RXR), estrogen receptor (ER) and other nuclear receptors in tissues of the mussel *Mytilus galloprovincialis*: Cloning and transcription pattern. Comp. Biochem. Physiol. - A Mol. Integr. Physiol. 165, 178–190. https://doi.org/10.1016/j.cbpa.2013.03.001

Ram, J.L., Crawford, G.W., Walker, J.U., Mojares, J.J., Patel, N., Fong, P.P., Kyozuka, K., 1993. Spawning in the zebra mussel (*Dreissena polymorpha*): Activation by internal or external application of serotonin. J. Exp. Zool. 265, 587–598. https://doi.org/10.1002/jez.1402650515

Ramzi, A., Gireeshkumar, T.R., Habeeb Rahman, K., Balachandran, K.K., Shameem, K., Chacko, J., Chandramohanakumar, N., 2020. Phthalic acid esters – A grave ecological hazard in Cochin estuary, India. Mar. Pollut. Bull. 152, 110899. https://doi.org/10.1016/j.marpolbul.2020.110899

Rayssac, N., Pernet, F., Lacasse, O., Tremblay, R., 2010. Temperature effect on survival, growth, and triacylglycerol content during the early ontogeny of *Mytilus edulis* and *M. trossulus*. Mar. Ecol. Prog. Ser. 417, 183–191. https://doi.org/10.3354/meps08774

Rebuli, M.E., Cao, J., Sluzas, E., Barry Delclos, K., Camacho, L., Lewis, S.M., Vanlandingham, M.M., Patisaul, H.B., 2014. Investigation of the effects of subchronic low dose oral exposure to bisphenol a (BPA) and ethinyl estradiol (EE) on estrogen receptor expression in the juvenile and adult female rat hypothalamus. Toxicol. Sci. 140, 190–203. https://doi.org/10.1093/toxsci/kfu074 f

Reed, A.J., Godbold, J.A., Solan, M., Grange, L.J., 2021. Invariant gametogenic response of dominant infaunal bivalves from the Arctic under ambient and near-future climate change conditions. Front. Mar. Sci. 8, 1–10. https://doi.org/10.3389/fmars.2021.576746

Regan, T., Stevens, L., Peñaloza, C., Houston, R.D., Robledo, D., Bean, T.P., 2021. Ancestral physical stress and later immune gene family expansions shaped bivalve mollusc evolution. Genome Biol. Evol. 13, 1–9. https://doi.org/10.1093/gbe/evab177

Regoli, F., Frenzilli, G., Bocchetti, R., Annarumma, F., Scarcelli, V., Fattorini, D., Nigro, M., 2004. Time-course variations of oxyradical metabolism, DNA integrity and lysosomal stability in mussels, Mytilus galloprovincialis, during a field translocation experiment. Aquat. Toxicol. 68, 167–178. https://doi.org/10.1016/j.aquatox.2004.03.011

Regoli, F., Giuliani, M.E., 2014. Oxidative pathways of chemical toxicity and oxidative stress biomarkers in marine organisms. Mar. Environ. Res. 93, 106–117. https://doi.org/10.1016/j.marenvres.2013.07.006

Regoli, F., Principato, G., 1995. Glutathione, glutathione-dependent and antioxidant enzymes in mussel, *Mytilus galloprovincialis*, exposed to metals under field and laboratory conditions: implications for the use of biochemical biomarkers. Aquat. Toxicol. 31, 143–164. https://doi.org/10.1016/0166-445X(94)00064-W

Reis-Henriques, M.A. and Coimbra, J., 1990. Variation in the levels of progesterone in *Mytilus edulis* during the annual reproductive cycle. Comp. Physiol. 95.3, 343–348. https://doi.org/10.1016/j.comnet.2005.04.002

Reis-Henriques, M.A., Le Guellec, D., Remy-Martin, J.P., Adessi, G.L., 1990. Studies of endogenous steroids from the marine mollusc *Mytilus edulis* L. by gas chromatography and mass spectrometry. Comp. Biochem. Physiol 95, 303–309.

Ren, G., Wang, Y., Qin, J., Tang, J., Zheng, X., Li, Y., 2014. Characterization of a novel carbonic anhydrase from freshwater pearl mussel *Hyriopsis cumingii* and the expression profile of its transcript in response to environmental conditions. Gene 546, 56–62. https://doi.org/10.1016/j.gene.2014.05.039

Resgalla, C., 2016. Spawning and multiple end points of the embryo-larval bioassay of the blue mussel *Mytilus galloprovincialis* (Lmk). Ecotoxicology 25, 1609–1616. https://doi.org/10.1007/s10646-016-1716-9

Richards, R.G., Chaloupka, M., 2009. Temperature-dependent bioaccumulation of copper in an estuarine oyster. Sci. Total Environ. 407, 5901–5906. https://doi.org/10.1016/j.scitotenv.2009.07.039

Richardson, B., Martin, H., Bartels-Hardege, H., Fletcher, N., & Hardege, J. D. (2022). The role of changing pH on olfactory success of predator–prey interactions in green shore crabs, *Carcinus maenas*. Aquatic Ecology, 56(2), 409-418. https://doi.org/10.1007/s10452-021-09913-x

Richier, S., Fiorini, S., Kerros, M.E., von Dassow, P., Gattuso, J.P., 2011. Response of the calcifying coccolithophore *Emiliania huxleyi* to low pH/high pCO_2: From physiology to molecular level. Mar. Biol. 158, 551–560. https://doi.org/10.1007/s00227-010-1580-8

Riebesell, U., Aberle-Malzahn, N., Achterberg, E.P., Algueró-Muñiz, M., Alvarez-Fernandez, S., Arístegui, J., Bach, L.T., Boersma, M., Boxhammer, T., Guan, W., Haunost, M., Horn, H.G., Löscher, C.R., Ludwig, A., Spisla, C., Sswat, M., Stange, P., Taucher, J., 2018. Toxic algal bloom induced by ocean acidification disrupts the pelagic food web. Nat. Clim. Chang. 8, 1082–1086. https://doi.org/10.1038/s41558-018-0344-1

Riebesell, U., Gattuso, J.P., Thingstad, T.F., Middelburg, J.J., 2013. Preface arctic ocean acidification: Pelagic ecosystem and biogeochemical responses during a mesocosm study. Biogeosciences 10, 5619–5626. https://doi.org/10.5194/bg-10-5619-2013

Ries, J.B., Cohen, A.L., McCorkle, D.C., 2009. Marine calcifiers exhibit mixed responses to CO_2-induced ocean acidification. Geology 37, 1131–1134. https://doi.org/10.1130/G30210A.1

Riva, C., Binelli, A., Rusconi, F., Colombo, G., Pedriali, A., Zippel, R., Provini, A., 2011. A proteomic study using zebra mussels (*D. polymorpha*) exposed to benzo(α)pyrene: The role of gender and exposure concentrations. Aquat. Toxicol. 104, 14–22. https://doi.org/10.1016/j.aquatox.2011.03.008

Roberts, D.A., Hofmann, G.E., Somero, G.N., 1997. Heat-shock protein expression in *Mytilus californianus*: acclimatization (seasonal and tidal-height comparisons) and acclimation effects. Biol. Bull. 192, 309–320. https://doi.org/10.2307/1542724

Robson, A.A., Garcia De Leaniz, C., Wilson, R.P., Halsey, L.G., 2010. Behavioural adaptations of mussels to varying levels of food availability and predation risk. J. Molluscan Stud. 76, 348–353. https://doi.org/10.1093/mollus/eyq025

Rochman, C.M., Tahir, A., Williams, S.L., Baxa, D. V., Lam, R., Miller, J.T., Teh, F.C., Werorilangi, S., Teh, S.J., 2015. Anthropogenic debris in seafood: Plastic debris and fibers from textiles in fish and bivalves sold for human consumption. Sci. Rep. 5, 1–10. https://doi.org/10.1038/srep14340

Roden, C.M., Burnell, G.M., 1984. Food resource, gametogenesis and growth of *Mytilus edulis* on the shore and in suspended culture: Killary Harbour, Ireland. J. Mar. Biol. Assoc. United Kingdom 64, 513–529. https://doi.org/10.1017/S0025315400030204

Rodolfo-Metalpa, R., Houlbrèque, F., Tambutté, É., Boisson, F., Baggini, C., Patti, F.P., Jeffree, R., Fine, M., Foggo, A., Gattuso, J.P., Hall-Spencer, J.M., 2011. Coral and mollusc resistance to ocean acidification adversely affected by warming. Nat. Clim. Chang. 1, 308–312. https://doi.org/10.1038/nclimate1200

Rodrigues, A.R., Mestre, N.C.C., da Fonseca, T.G., Pedro, P.Z., Carteny, C.C., Cormier, B., Keiter, S., Bebianno, M.J., 2022. Influence of particle size on ecotoxicity of low-density polyethylene microplastics, with and without adsorbed benzo-a-pyrene, in clam *Scrobicularia plana*. Biomolecules 12. https://doi.org/10.3390/biom12010078

Roggatz, C.C., Fletcher, N., Benoit, D.M., Algar, A.C., Doroff, A., Wright, B., Wollenberg Valero, K.C., Hardege, J.D., 2019. Saxitoxin and tetrodotoxin bioavailability increases in future oceans. Nat. Clim. Chang. 9, 840–844. https://doi.org/10.1038/s41558-019-0589-3

Roggatz, C.C., Lorch, M., Hardege, J.D., Benoit, D.M., 2016. Ocean acidification affects marine chemical communication by changing structure and function of peptide signalling molecules. Glob. Chang. Biol. 22, 3914–3926. https://doi.org/10.1111/gcb.13354

Romero, A., Estévez-Calvar, N., Dios, S., Figueras, A., Novoa, B., 2011. New insights into the apoptotic process in mollusks: Characterization of caspase genes in *Mytilus galloprovincialis*. PLoS One 6. https://doi.org/10.1371/journal.pone.0017003

Romero, A., Novoa, B., Figueras, A., 2022. Genomic and transcriptomic identification of the cathepsin superfamily in the Mediterranean mussel *Mytilus galloprovincialis*. Dev. Comp. Immunol. 127, 104286. https://doi.org/10.1016/j.dci.2021.104286

Romiguier, J., Ranwez, V., Douzery, E. J., Galtier, N., 2010. Contrasting GC-content dynamics across 33 mammalian genomes: relationship with life-history traits and chromosome sizes. Genome research, 20(8), 1001-1009. https://doi.org/10.1101/gr.104372.109.20

Roper, D.S., Hickey, C.W., 1994. Population structure, shell morphology, age and condition of the freshwater mussel *Hyridella menziesi* (Unionacea: Hyriidae) from seven lake and river sites in the Waikato River system. Hydrobiologia 284, 205–217. https://doi.org/10.1007/BF00006690

Rose, R.J., Priston, M.J., Rigby-Jones, A.E., Sneyd, J.R., 2012. The effect of temperature on di(2-ethylhexyl) phthalate leaching from PVC infusion sets exposed to lipid emulsions. Anaesthesia 67, 514–520. https://doi.org/10.1111/j.1365-2044.2011.07006.x

Rosenberg, E., Ben-Haim, Y., 2002. Microbial diseases of corals and global warming. Environ. Microbiol. 4, 318–326. https://doi.org/10.1046/j.1462-2920.2002.00302.x

Rotchell, J.M., Ostrander, G.K., 2003. Molecular markers of endocrine disruption in aquatic organisms. J. Toxicol. Environ. Heal. - Part B Crit. Rev. 6, 453–495. https://doi.org/10.1080/10937400306476

Rovero, F., Hughes, R.N., Chelazzi, G., 1999. Cardiac and behavioural responses of mussels to risk of predation by dogwhelks. Anim. Behav. 58, 707–714. https://doi.org/10.1006/anbe.1999.1176

S

Saavedra, L.M., Parra, D., Martin, V.S., Lagos, N.A., Vargas, C.A., 2018. Local habitat influences on feeding and respiration of the intertidal mussels *Perumytilus purpuratus* exposed to increased pCO_2 levels. Estuaries and Coasts 41, 1118–1129. https://doi.org/10.1007/s12237-017-0333-z

Sabine, C.L., Feely, R.A., Gruber, N., Key, R.M., Lee, K., Bullister, J.L., Wanninkhof, R., Wong, C.S.L., Wallace, D.W., Tilbrook, B. and Millero, F.J., 2004. The oceanic sink for anthropogenic CO_2. Science, 305(5682), pp.367-371.

Saggese, I., Sarà, G., Dondero, F., 2016. Silver Nanoparticles Affect Functional Bioenergetic Traits in the Invasive Red Sea Mussel *Brachidontes pharaonis*. Biomed Res. Int. 2016. https://doi.org/10.1155/2016/1872351

Said, R.M., Nassar, S.E., 2022. Mortality, energy reserves, and oxidative stress responses of three native freshwater mussels to temperature as an indicator of potential impacts of climate change: A laboratory experimental approach. J. Therm. Biol. 104, 103154. https://doi.org/10.1016/j.jtherbio.2021.103154

Salánki, J., 1963. The Effect of Serotonin and Catecholamines on the Nervous Control of. Comp. Biochem. Physiol. 16, 163–171.

Salatiello, F., Gerdol, M., Pallavicini, A., Locascio, A., Sirakov, M., 2022. Comparative analysis of novel and common reference genes in adult tissues of the mussel *Mytilus galloprovincialis*. BMC Genomics 1–11. https://doi.org/10.1186/s12864-022-08553-1

Sampaio, E., Rosa, R., 2020. Climate change, multiple stressors, and responses of marine biota 264–275. https://doi.org/10.1007/978-3-319-95885-9_90

Sánchez-Avila, J., Tauler, R., Lacorte, S., 2012. Organic micropollutants in coastal waters from NW Mediterranean Sea: Sources distribution and potential risk. Environ. Int. 46, 50–62. https://doi.org/10.1016/j.envint.2012.04.013

Sanco, D., 2002. European commission, health & consumer protection directorate-general. Opinion on Medical Devices Containing DEHP Plasticised PVC.

Sanders, B.M., 1993. Stress proteins in aquatic organisms: An environmental perspective. Crit. Rev. Toxicol. 23, 49–75. https://doi.org/10.3109/10408449309104074

Santos, E.M., Paull, G.C., Look, K.J.W. Van, Workman, V.L., Holt, W. V, Aerle, R. Van, Kille, P., Tyler, C.R., 2007. Gonadal transcriptome responses and physiological consequences of exposure to oestrogen in breeding zebrafish (*Danio rerio*) 83, 134–142. https://doi.org/10.1016/j.aquatox.2007.03.019

Santos, G. A. D., Reis, S. T., Leite, K. R. M., Srougi, M., 2021. Telomere attrition and p53 response 1 (TAPR1): a new player in cancer biology?. Clinics, 76. https://doi.org/10.6061/clinics/2021/e2997

Schettler, T., Skakkebæk, N.E., De Kretser, D., Leffers, H., 2006. Human exposure to phthalates via consumer products. Int. J. Androl. 29, 134–139. https://doi.org/10.1111/j.1365-2605.2005.00567.x

Schiedek, D., Sundelin, B., Readman, J.W., Macdonald, R.W., 2007. Interactions between climate change and contaminants. Mar. Pollut. Bull. 54, 1845–1856. https://doi.org/10.1016/j.marpolbul.2007.09.020

Schirrmacher, P., Roggatz, C.C., Benoit, D.M., Hardege, J.D., 2021. Ocean acidification amplifies the olfactory response to 2-phenylethylamine: altered cue reception as a mechanistic pathway? J. Chem. Ecol. https://doi.org/10.1007/s10886-021-01276-9

Schlesinger, M.J., 1990. Heat shock proteins. J. Biol. Chem. 265, 12111–12114. https://doi.org/10.1016/s0021-9258(19)38314-0

Schmaltz, E., Melvin, E.C., Diana, Z., Gunady, E.F., Rittschof, D., Somarelli, J.A., Virdin, J., Dunphy-Daly, M.M., 2020. Plastic pollution solutions: emerging technologies to prevent and collect marine plastic pollution. Environ. Int. 144. https://doi.org/10.1016/j.envint.2020.106067

Schmittgen, T.D., Livak, K.J., 2008. Analyzing real-time PCR data by the comparative CT method. Nat. Protoc. 3, 1101–1108. https://doi.org/10.1038/nprot.2008.73

Schnatwinkel, C., Christoforidis, S., Lindsay, M.R., Uttenweiler-Joseph, S., Wilm, M., Parton, R.G., Zerial, M., 2004. The Rab5 effector Rabankyrin-5 regulates and coordinates different endocytic mechanisms. PLoS Biol. 2. https://doi.org/10.1371/journal.pbio.0020261

Schöpel, M., Shkura, O., Seidel, J., Kock, K., Zhong, X., Löffek, S., Helfrich, I., Bachmann, H.S., Scherkenbeck, J., Herrmann, C., Stoll, R., 2018. Allosteric activation of GDP-bound ras isoforms by bisphenol derivative plasticisers. Int. J. Mol. Sci. 19, 1–14. https://doi.org/10.3390/ijms19041133

Schouest, K.R., Kurasawa, Y., Furuta, T., Hisamoto, N., Matsumoto, K., Schumacher, J.M., 2009. The germinal center kinase GCK-1 is a negative regulator of MAP kinase activation and apoptosis in the C. elegans germline. PLoS One 4. https://doi.org/10.1371/journal.pone.0007450

Schulz, K.G., Bellerby, R.G.J., Brussaard, C.P.D., Büdenbender, J., Czerny, J., Engel, A., Fischer, M., Koch-Klavsen, S., Krug, S.A., Lischka, S., Ludwig, A., Meyerhöfer, M., Nondal, G., Silyakova, A., Stuhr, A., Riebesell, U., 2013. Temporal biomass dynamics of an Arctic plankton bloom in response to increasing levels of atmospheric carbon dioxide. Biogeosciences 10, 161–180. https://doi.org/10.5194/bg-10-161-2013

Schürmann, A., Koling, S., Jacobs, S., Saftig, P., Krauβ, S., Wennemuth, G., Kluge, R., Joost, H.-G., 2002. Reduced sperm count and normal fertility in male mice with targeted disruption of the ADP-Ribosylation Factor-Like 4 (Arl4) Gene . Mol. Cell. Biol. 22, 2761–2768. https://doi.org/10.1128/mcb.22.8.2761-2768.2002

Schwabl, P., Köppel, S., Königshofer, P., Bucsics, T., Trauner, M., Reiberger, T., Liebmann, B., 2019. Detection of various microplastics in human stool 453–458. https://doi.org/10.7326/M19-0618

Schwarzmann, N., Kunerth, S., Weber, K., Mayr, G.W., Guse, A.H., 2002. Knock-down of the type 3 ryanodine receptor impairs sustained Ca^{2+} signaling via the T cell receptor/CD3 complex. J. Biol. Chem. 277, 50636–50642. https://doi.org/10.1074/jbc.M209061200

Scott, A.P., 2018. Is there any value in measuring vertebrate steroids in invertebrates? Gen. Comp. Endocrinol. 265, 77–82. https://doi.org/10.1016/j.ygcen.2018.04.005

Scott, A.P., 2012. Do mollusks use vertebrate sex steroids as reproductive hormones? Part I: Critical appraisal of the evidence for the presence, biosynthesis and uptake of steroids. Steroids 77, 1450–1468. https://doi.org/10.1016/j.steroids.2012.08.009

Sechi, S., Colotti, G., Belloni, G., Mattei, V., Frappaolo, A., Raffa, G.D., Fuller, M.T., Giansanti, M.G., 2014. GOLPH3 Is Essential for Contractile Ring Formation and Rab11 Localization to the Cleavage Site during Cytokinesis in *Drosophila melanogaster*. PLoS Genet. 10. https://doi.org/10.1371/journal.pgen.1004305

Secor, C.L., Day, A.J., Hilbish, T.J., 2001. Factors influencing differential mortality within a marine mussel (*Mytilus* spp.) hybrid population in southwestern England: Reproductive effort and parasitism. Mar. Biol. 138, 731–739. https://doi.org/10.1007/s002270000418

Seed, R., 1976. Marine mussels: their ecology and physiology. Cambridge Univ. Press 10, 13–65.

Seed, R., 1969. The ecology of *Mytilus edulis* L. (Lamellibranchiata) on exposed rocky shores - I. Breeding and settlement. Oecologia 3, 277–316. https://doi.org/10.1007/BF00390380

Segner, H., Caroll, K., Fenske, M., Janssen, C.R., Maack, G., Pascoe, D., Schäfers, C., Vandenbergh, G.F., Watts, M., Wenzel, A., 2003. Identification of endocrine-disrupting effects in aquatic vertebrates and invertebrates: Report from the European IDEA project. Ecotoxicol. Environ. Saf. 54, 302–314. https://doi.org/10.1016/S0147-6513(02)00039-8

Seibel, B.A., 2013. The jumbo squid, *Dosidicus gigas* (Ommastrephidae), living in oxygen minimum zones II: blood-oxygen binding. Deep. Res. Part II Top. Stud. Oceanogr. 95, 139–144. https://doi.org/10.1016/j.dsr2.2012.10.003

Serra-Pages, C., Kedersha, N.L., Fazikas, L., Medleyl, Q., Debant, A., Streuli, M., 1995. The LAR transmembrane protein tyrosine phosphatase and a coiled-coil LAR-interacting protein co-localize at focal adhesions. EMBO J. 14, 2827–2838. https://doi.org/10.1002/j.1460-2075.1995.tb07282.x

Shang, Y., Wang, X., Shi, Y., Huang, W., Sokolova, I., Chang, X., Chen, D., Wei, S., Khan, F.U., Hu, M., Wang, Y., 2022. Ocean acidification affects the bioenergetics of marine mussels as revealed by high-coverage quantitative metabolomics. Sci. Total Environ. 858, 160090. https://doi.org/10.1016/j.scitotenv.2022.160090

Sharker, M.R., Sukhan, Z.P., Sumi, K.R., Choi, S.K., Choi, K.S., Kho, K.H., 2021. Molecular Characterization of carbonic anhydrase II (CA II) and its potential involvement in regulating shell formation in the Pacific abalone, *Haliotis discus hannai*. Front. Mol. Biosci. 8, 1–11. https://doi.org/10.3389/fmolb.2021.669235

Sheikh, I.A., Turki, R.F., Abuzenadah, A.M., Damanhouri, G.A., Beg, M.A., 2016. Endocrine disruption: Computational perspectives on human sex hormone-binding globulin and phthalate plasticizers. PLoS One 11, 1–13. https://doi.org/10.1371/journal.pone.0151444

Shen, H., Nugegoda, D., 2022. Real-time automated behavioural monitoring of mussels during contaminant exposures using an improved microcontroller-based device. Sci. Total Environ. 806, 150567. https://doi.org/10.1016/j.scitotenv.2021.150567

Shorter, J., Lindquist, S., 2008. Hsp104, Hsp70 and Hsp40 interplay regulates formation, growth and elimination of Sup35 prions. EMBO J. 27, 2712–2724. https://doi.org/10.1038/emboj.2008.194

Siah, A., Pellerin, J., Amiard, J., Pelletier, E., Viglino, L., 2003. Delayed gametogenesis and progesterone levels in soft-shell clams (Mya *arenaria*) in relation to in situ contamination to organotins and heavy metals in the St. Lawrence River (Canada). Comp. Biochem. Physiol. 135, 145–156. https://doi.org/10.1016/S1532-0456

Sif, J., Khalil, A., Abouinan, H., Rouhi, A., Mokhliss, K., 2016. Effects of phthalates on the biology of the mussel *Mytilus galloprovincialis* (from the Atlantic Coast of El Jadida, Morocco). J. Xenobiotics 6. https://doi.org/10.4081/xeno.2016.6589

Simão, F.A., Waterhouse, R.M., Ioannidis, P., Kriventseva, E. V., Zdobnov, E.M., 2015. BUSCO: Assessing genome assembly and annotation completeness with single copy orthologs. Bioinformatics 31, 3210–3212. https://doi.org/10.1093/bioinformatics/btv351

Simon, A., Arbiol, C., Nielsen, E.E., Couteau, J., Sussarellu, R., Burgeot, T., Bernard, I., Coolen, J.W.P., Lamy, J.B., Robert, S., Skazina, M., Strelkov, P., Queiroga, H., Cancio, I., Welch, J.J., Viard, F., Bierne, N., 2019. Replicated anthropogenic hybridisations reveal parallel patterns of admixture in marine mussels. Evol. Appl. 575–599. https://doi.org/10.1111/eva.12879

Sıkdokur, E., Belivermiş, M., Sezer, N., Pekmez, M., Bulan, Ö.K., Kılıç, Ö., 2020. Effects of microplastics and mercury on manila clam *Ruditapes philippinarum*: Feeding rate, immunomodulation, histopathology and oxidative stress. Environ. Pollut. 262. https://doi.org/10.1016/j.envpol.2020.114247

Skaggs, H.S., Henry, R.P., 2002. Inhibition of carbonic anhydrase in the gills of two euryhaline crabs, *Callinectes sapidus* and *Carcinus maenas*, by heavy metals. Comp. Biochem. Physiol. - C Toxicol. Pharmacol. 133, 605–612. https://doi.org/10.1016/S1532-0456(02)00175-8

Smith, J.R., Strehlow, D.R., 1983. Algal-induced spawning in the marine mussel *Mytilus californianus*. Int. J. Invertebr. Reprod. 6, 129–133. https://doi.org/10.1080/01651269.1983.10510032

Smolarz, K., Zabrzańska, S., Konieczna, L., Hallmann, A., 2018. Changes in steroid profiles of the blue mussel Mytilus trossulus as a function of season, stage of gametogenesis, sex, tissue and mussel bed depth. Gen. Comp. Endocrinol. 259, 231–239. https://doi.org/10.1016/j.ygcen.2017.12.006

Sobrino-Figueroa, A., Cáceres-Martínez, C., 2009. Alterations of valve closing behavior in juvenile Catarina scallops (*Argopecten ventricosus* Sowerby, 1842) exposed to toxic metals. Ecotoxicology 18, 983–987. https://doi.org/10.1007/s10646-009-0358-6

Sokolova, I.M., Sukhotin, A.A., Lannig, G., 2011. Marine animal stress response and biomonitoring and energy budgets in mollusks. Oxidative Stress Aquat. Ecosyst. 261–280.

Solomon, S., Plattner, G.K., Knutti, R., Friedlingstein, P., 2009. Irreversible climate change due to carbon dioxide emissions. Proc. Natl. Acad. Sci. U. S. A. 106, 1704–1709. https://doi.org/10.1073/pnas.0812721106

Sorini, R., Kordal, M., Apuzza, B., Eierman, L.E., 2021. Skewed sex ratio and gametogenesis gene expression in eastern oysters (*Crassostrea virginica*) exposed to plastic pollution. J. Exp. Mar. Bio. Ecol. 544, 151605. https://doi.org/10.1016/j.jembe.2021.151605

Soto, A.M., Calabro, J.M., Prechtl, N. V., Yau, A.Y., Orlando, E.F., Daxenberger, A., Kolok, A.S., Guillette, L.J., le Bizec, B., Lange, I.G., Sonnenschein, C., 2004. Androgenic and estrogenic activity in water bodies receiving cattle feedlot effluent in Eastern Nebraska, USA. Environ. Health Perspect. 112, 346–352. https://doi.org/10.1289/ehp.6590

Spicer, J.I., Weber, R.E., 1991. Respiratory impairment in crustaceans and molluscs due to exposure to heavy metals. Comp. Biochem. Physiol. Part C, Comp. 100, 339–342. https://doi.org/10.1016/0742-8413(91)90005-E

Spooner, D.E., Vaughn, C.C., 2008. A trait-based approach to species' roles in stream ecosystems: Climate change, community structure, and material cycling. Oecologia 158, 307–317. https://doi.org/10.1007/s00442-008-1132-9

Sprung, M., 1983. Reproduction and fecundity of the mussel mytilus edulis at helgoland (North Sea). Helgoländer Meeresuntersuchungen 36, 243–255. https://doi.org/10.1007/BF01983629

Sreedevi, P.R., Uthayakumar, V., Jayakumar, R., Ramasubramanian, V., 2014. Influence of rearing water temperature on induced gonadal development and spawning behaviour of tropical green mussel, *Perna viridis*. Asian Pacific J. Reprod. 3, 204–209. https://doi.org/10.1016/S2305-0500(14)60027-0

Sroda, S., Cossu-Leguille, C., 2011. Seasonal variability of antioxidant biomarkers and energy reserves in the freshwater gammarid *Gammarus roeseli*. Chemosphere 83, 538–544. https://doi.org/10.1016/j.chemosphere.2010.12.023

Stange, D., Sieratowicz, A., Horres, R., Oehlmann, J., 2012. Freshwater mudsnail (*Potamopyrgus antipodarum*) estrogen receptor: identification and expression analysis under exposure to (xeno-)hormones. Ecotoxicol. Environ. Saf. 75, 94–101. https://doi.org/10.1016/j.ecoenv.2011.09.003

Staples, C.A., Peterson, D.R., Parkerton, T.F., Adams, W.J., 1997. The environmental fate of phthalate esters: a literature review 35, 667–749.

Stefano, G.B., Cadet, P., Mantione, K., Cho, J.J., Jones, D., Zhu, W., 2003. Estrogen signaling at the cell surface coupled to nitric oxide release in *Mytilus edulis* nervous system. Endocrinology 144, 1234–1240. https://doi.org/10.1210/en.2002-220967

Stepanova, L., Leng, X., Parker, S.B., Wade Harper, J., 1996. Mammalian p50(Cdc37) is a protein kinase-targeting subunit of Hsp90 that binds and stabilizes Cdk4. Genes Dev. 10, 1491–1502. https://doi.org/10.1101/gad.10.12.1491

Sterling, D., Reithmeier, R.A.F., Casey, J.R., 2001. A transport metabolon: Functional interaction of carbonic anhydrase II and chloride/bicarbonate exchangers. J. Biol. Chem. 276, 47886–47894. https://doi.org/10.1074/jbc.M105959200

Sternberg, R.M., Gooding, M.P., Hotchkiss, A.K., LeBlanc, G.A., 2010. Environmental-endocrine control of reproductive maturation in gastropods: Implications for the mechanism of tributyltin-induced imposex in prosobranchs. Ecotoxicology 19, 4–23. https://doi.org/10.1007/s10646-009-0397-z

Stillman, J.H., Paganini, A.W., 2015. Biochemical adaptation to ocean acidification. J. Exp. Biol. 218, 1946–1955. https://doi.org/10.1242/jeb.115584

Suárez, M.P., Alvarez, C., Molist, P., Juan, F.S.A.N., 2005. Particular aspects of gonadal cycle and seasonal distribution of gametogenic stages of *Mytilus galloprovincialis* cultured in the estuary of Vigo 24, 531–540.

Subramaniam, T., Lee, H.J., Jeung, H. Do, Kang, H.S., Kim, C.W., Kim, H.S., Cho, Y.G., Choi, K.S., 2021. Report on the annual gametogenesis and tissue biochemical composition in the gray mussel, *Crenomytilus grayanus* (Dunker 1853) in the subtidal rocky bottom on the East coast of Korea. Ocean Sci. J. 56, 424–433. https://doi.org/10.1007/s12601-021-00042-y

Sun, C., Chen, L., Zhao, S., Guo, W., Luo, Y., Wang, L., Tang, L., Li, F., Zhang, J., 2021. Seasonal distribution and ecological risk of phthalate esters in surface water and marine organisms of the Bohai Sea. Mar. Pollut. Bull. 169, 112449. https://doi.org/10.1016/j.marpolbul.2021.112449

Sun, T., Tang, X., Zhou, B., Wang, Y., 2016. Comparative studies on the effects of seawater acidification caused by CO2 and HCl enrichment on physiological changes in *Mytilus edulis*. Chemosphere 144, 2368–2376. https://doi.org/10.1016/j.chemosphere.2015.10.117

Sundt, R.C., Pampanin, D.M., Larsen, B.K., Brede, C., Herzke, D., Bjørnstad, A., Andersen, O.K., 2006. The BEEP Stavanger Workshop: Mesocosm exposures. Aquat. Toxicol. 78. https://doi.org/10.1016/j.aquatox.2006.02.012

Sunila, I., 1981. Reproduction of *Mytilus edulis* L. (Bivalvia) in a brackish water area, the Gulf of Finland. Ann. Zool. Fenn.

Supek, F., Bošnjak, M., Škunca, N., Šmuc, T., 2011. Revigo summarizes and visualizes long lists of gene ontology terms. PLoS One 6. https://doi.org/10.1371/journal.pone.0021800

Sussarellu, R., Suquet, M., Thomas, Y., Lambert, C., Fabioux, C., Pernet, M.E.J., Goïc, N. Le, Quillien, V., Mingant, C., Epelboin, Y., Corporeau, C., Guyomarch, J., Robbens, J., Paul-Pont, I., Soudant, P., Huvet, A., 2016. Oyster reproduction is affected by exposure to polystyrene microplastics. Proc. Natl. Acad. Sci. U. S. A. 113, 2430–2435. https://doi.org/10.1073/pnas.1519019113

T

Takdastan, A., Niari, M.H., Babaei, A., Dobaradaran, S., Jorfi, S., Ahmadi, M., 2021. Occurrence and distribution of microplastic particles and the concentration of Di 2-ethyl hexyl phthalate (DEHP) in microplastics and wastewater in the wastewater treatment plant. J. Environ. Manage. 280, 111851. https://doi.org/10.1016/j.jenvman.2020.111851

Tallec, K., Huvet, A., Yeuc'h, V., Le Goïc, N., Paul-Pont, I., 2022. Chemical effects of different types of rubber-based products on early life stages of Pacific oyster, *Crassostrea gigas*. J. Hazard. Mater. 427. https://doi.org/10.1016/j.jhazmat.2021.127883

Talmage, S.C., Gobler, C.J., 2011. Effects of elevated temperature and carbon dioxide on the growth and survival of larvae and juveniles of three species of northwest Atlantic bivalves. PLoS One 6. https://doi.org/10.1371/journal.pone.0026941

Tan, G.H., 1995. Residue levels of phthalate esters in water and sediment samples from the Klang River basin. Bull. Environ. Contam. Toxicol. 54, 171–176. https://doi.org/10.1007/BF00197427

Teil, M.J., Blanchard, M., Chevreuil, M., 2006. Atmospheric fate of phthalate esters in an urban area (Paris-France). Sci. Total Environ. 354, 212–223. https://doi.org/10.1016/j.scitotenv.2004.12.083

Terhaar, J., Kwiatkowski, L., Bopp, L., 2020. Emergent constraint on Arctic Ocean acidification in the twenty-first century. Nature 582, 379–383. https://doi.org/10.1038/s41586-020-2360-3

Tessmar-Raible, K., Raible, F., Arboleda, E., 2011. Another place, another timer: marine species and the rhythms of life. BioEssays 33, 165–172. https://doi.org/10.1002/bies.201000096

Teuten, E.L., Saquing, J.M., Knappe, D.R.U., Rowland, S.J., Barlaz, M.A., Jonsson, S., Bjo, A., Thompson, R.C., Galloway, T.S., Yamashita, R., Ochi, D., Watanuki, Y., Moore, C., Viet, P.H., Tana, T.S., 2009. Transport and release of chemicals from plastics to the environment and to wildlife 2027–2045. https://doi.org/10.1098/rstb.2008.0284

Thomas, Y., Bacher, C., 2018. Assessing the sensitivity of bivalve populations to global warming using an individual-based modelling approach. Glob. Chang. Biol. 24, 4581–4597. https://doi.org/10.1111/gcb.14402

Thompson, E. L., Taylor, D. A., Nair, S. V., Birch, G., Coleman, R., & Raftos, D. A. 2012. Optimal acclimation periods for oysters in laboratory-based experiments, J. Molluscan Stud. 78 (3), 304–307, https://doi.org/10.1093/mollus/eys012

Thompson, R.C., Swan, S.H., Moore, C.J., Vom Saal, F.S., 2009. Our plastic age. Philos. Trans. R. Soc. B Biol. Sci. 364, 1973–1976. https://doi.org/10.1098/rstb.2009.0054

Thomsen, J., Casties, I., Pansch, C., Körtzinger, A., Melzner, F., 2013. Food availability outweighs ocean acidification effects in juvenile Mytilus edulis: Laboratory and field experiments. Glob. Chang. Biol. 19, 1017–1027. https://doi.org/10.1111/gcb.12109

Thomsen, J., Melzner, F., 2010. Moderate seawater acidification does not elicit long-term metabolic depression in the blue mussel *Mytilus edulis*. Mar. Biol. 157, 2667–2676. https://doi.org/10.1007/s00227-010-1527-0

Thomsen, J., Stapp, L.S., Haynert, K., Schade, H., Danelli, M., Lannig, G., Wegner, K.M., Melzner, F., 2017. Naturally acidified habitat selects for ocean acidification–tolerant mussels. Sci. Adv. 3, 1–9. https://doi.org/10.1126/sciadv.1602411

Thornton, J. W., Need, E., Crews, D., 2003. Resurrecting the ancestral steroid receptor: ancient origin of estrogen signaling. Science, 301(5640), 1714-1717. https://doi.org/10.1126/science.1086185

Thyrring, J., Blicher, M.E., Sørensen, J.G., Wegeberg, S., Sejr, M.K., 2017. Rising air temperatures will increase intertidal mussel abundance in the Arctic. Mar. Ecol. Prog. Ser. 584, 91–104. https://doi.org/10.3354/meps12369

Thyrring, J., Rysgaard, S., Blicher, M.E., Sejr, M.K., 2015. Metabolic cold adaptation and aerobic performance of blue mussels (*Mytilus edulis*) along a temperature gradient into the High Arctic region. Mar. Biol. 162, 235–243. https://doi.org/10.1007/s00227-014-2575-7

Todd, A.S., Manning, A.H., Verplanck, P.L., Crouch, C., McKnight, D.M., Dunham, R., 2012. Climate-change-driven deterioration of water quality in a mineralized watershed. Environ. Sci. Technol. 46, 9324–9332. https://doi.org/10.1021/es3020056

Tomanek, L., Somero, G.N., 1999. Evolutionary and acclimation-induced variation in the heat-shock responses of congeneric marine snails (genus *Tegula*) from different thermal habitats: Implications for limits of thermotolerance and biogeography. J. Exp. Biol. 202, 2925–2936.

Toro, E., Thompson, J., Innes, J., 2002. Reproductive isolation and reproductive output in two sympatric mussel species (*Mytilus edulis* , *M* . *trossulus*) and their hybrids from Newfoundland 897–909. https://doi.org/10.1007/s00227-002-0897-3

Tran, D., Ciret, P., Ciutat, A., Durrieu, G., Massabuau, J.C., 2003. Estimation of potential and limits of bivalve closure response to detect contaminants: application to cadmium. Environ. Toxicol. Chem. 22, 914–920. https://doi.org/10.1897/1551-5028(2003)022

Troschinski, S., Di Lellis, M.A., Sereda, S., Hauffe, T., Wilke, T., Triebskorn, R., Köhler, H.R., 2014. Intraspecific variation in cellular and biochemical heat response strategies of Mediterranean *Xeropicta derbentina* [Pulmonata, Hygromiidae]. PLoS One 9. https://doi.org/10.1371/journal.pone.0086613

Tseng, Y.C., Hu, M.Y., Stumpp, M., Lin, L.Y., Melzner, F., Hwang, P.P., 2013. CO_2-driven seawater acidification differentially affects development and molecular plasticity along life history of fish (*Oryzias latipes*). Comp. Biochem. Physiol. - A Mol. Integr. Physiol. 165, 119–1130. https://doi.org/10.1016/j.cbpa.2013.02.005

Tutar, L., Tutar, Y., 2010. Heat Shock Proteins; An Overview. Curr. Pharm. Biotechnol. 11, 216–222. https://doi.org/10.2174/138920110790909632

Tyler, P., Young, C.M., Dolan, E., Arellano, S.M., Brooke, S.D., Baker, M., 2007. Gametogenic periodicity in the chemosynthetic cold-seep mussel *Bathymodiolus childressi*. Mar. Biol. 150, 829–840. https://doi.org/10.1007/s00227-006-0362-9

U

Uren-Webster, T.M., Lewis, C., Filby, A.L., Paull, G.C., Santos, E.M., 2010. Mechanisms of toxicity of di(2-ethylhexyl) phthalate on the reproductive health of male zebrafish. Aquat. Toxicol. 99, 360–369. https://doi.org/10.1016/j.aquatox.2010.05.015

Utting, S.D., Millican, P.F., 1997. Techniques for the hatchery conditioning of bivalve broodstocks and the subsequent effect on egg quality and larval viability. Aquaculture 155, 45–54. https://doi.org/10.1016/S0044-8486(97)00108-7

V

Van Cauwenberghe, L., Claessens, M., Vandegehuchte, M.B., Janssen, C.R., 2015. Microplastics are taken up by mussels (*Mytilus edulis*) and lugworms (*Arenicola marina*) living in natural habitats. Environ. Pollut. 199, 10–17. https://doi.org/10.1016/j.envpol.2015.01.008

Van Cauwenberghe, L., Janssen, C.R., 2014. Microplastics in bivalves cultured for human consumption. Environ. Pollut. 193, 65–70. https://doi.org/10.1016/j.envpol.2014.06.010

Vandenberg, L.N., Colborn, T., Hayes, T.B., Heindel, J.J., Jacobs, D.R., Lee, D., Shioda, T., Soto, A.M., Saal, F.S., Welshons, W. V, Zoeller, R.T., Myers, J.P., 2012. Hormones and endocrine-disrupting chemicals: low-dose effects and nonmonotonic dose responses 33, 378–455. https://doi.org/10.1210/er.2011-1050

Van Wezel, A.P., Van Vlaardingen, P., Posthumus, R., Crommentuijn, G.H., Sijm, D.T.H.M., 2000. Environmental risk limits for two phthalates, with special emphasis on endocrine disruptive properties. Ecotoxicol. Environ. Saf. 46, 305–321. https://doi.org/10.1006/eesa.2000.1930

Vargas, C.A., Contreras, P.Y., Pérez, C.A., Sobarzo, M., Saldías, G.S., Salisbury, J., 2016. Influences of riverine and upwelling waters on the coastal carbonate system off Central Chile and their ocean acidification implications. J. Geophys. Res. Biogeosciences 121, 1468–1483. https://doi.org/10.1002/2015JG003213

Vargas, C.A., Lagos, N.A., Lardies, M.A., Duarte, C., Manríquez, P.H., Aguilera, V.M., Broitman, B., Widdicombe, S., Dupont, S., 2017. Species-specific responses to ocean acidification should account for local adaptation and adaptive plasticity. Nat. Ecol. Evol. 1, 1–7. https://doi.org/10.1038/s41559-017-0084

Van Weering, J.R.T., Sessions, R.B., Traer, C.J., Kloer, D.P., Bhatia, V.K., Stamou, D., Carlsson, S.R., Hurley, J.H., Cullen, P.J., 2012. Molecular basis for SNX-BAR-mediated assembly of distinct endosomal sorting tubules. EMBO J. 31, 4466–4480. https://doi.org/10.1038/emboj.2012.283

Vasanthi, R.L., Arulvasu, C., Kumar, P., Srinivasan, P., 2021. Ingestion of microplastics and its potential for causing structural alterations and oxidative stress in Indian green mussel *Perna viridis*– A multiple biomarker approach. Chemosphere 283, 130979. https://doi.org/10.1016/j.chemosphere.2021.130979

Velez, Z., Roggatz, C., Benoit, D., Hardege, J., Hubbard, P.C., 2019. Short- and medium-term exposure to ocean acidification reduces olfactory sensitivity in gilthead seabream. Front. Physiol. 10. https://doi.org/10.3389/fphys.2019.00731

Venables, W.N., Ripley, B.D., 2002. Modern applied statistics with S, Fourth edition. Springer, New York. ISBN 0-387-95457-0, https://www.stats.ox.ac.uk/pub/MASS4/.

Venier, P., De Pittà, C., Bernante, F., Varotto, L., De Nardi, B., Bovo, G., Roch, P., Novoa, B., Figueras, A., Pallavicini, A. and Lanfranchi, G., 2009. MytiBase: a knowledgebase of mussel (*M. galloprovincialis*) transcribed sequences. BMC genomics, 10(1), pp.1-16. https://doi.org/10.1186/1471-2164-10-72

Ventura, P., Jarrold, M.D., Merle, P.L., Barnay-Verdier, S., Zamoum, T., Rodolfo-Metalpa, R., Calosi, P., Furla, P., 2016. Resilience to ocean acidification: Decreased carbonic anhydrase activity in sea anemones under high pCO_2 conditions. Mar. Ecol. Prog. Ser. 559, 257–263. https://doi.org/10.3354/meps11916

Verdelhos, T., Marques, J.C., Anastácio, P., 2015. Behavioral and mortality responses of the bivalves *Scrobicularia plana* and *Cerastoderma edule* to temperature, as indicator of climate change's potential impacts. Ecol. Indic. 58, 95–103. https://doi.org/10.1016/j.ecolind.2015.05.042

Verlecar, X.N., Jena, K.B., Chainy, G.B.N., 2007. Biochemical markers of oxidative stress in Perna viridis exposed to mercury and temperature. Chem. Biol. Interact. 167, 219–226. https://doi.org/10.1016/j.cbi.2007.01.018

Vermeij, G.J., 1991. Anatomy of an invasion: the trans-Arctic interchange. Paleobiology, 17, 281–307.

Vethaak, A.D., Lahr, J., Schrap, S.M., Belfroid, A.C., Rijs, G.B.J., Gerritsen, A., De Boer, J., Bulder, A.S., Grinwis, G.C.M., Kuiper, R. V., Legler, J., Murk, T.A.J., Peijnenburg, W., Verhaar, H.J.M., De Voogt, P., 2005. An integrated assessment of estrogenic contamination and biological effects in the aquatic environment of The Netherlands. Chemosphere 59, 511–524. https://doi.org/10.1016/j.chemosphere.2004.12.053

Viarengo, A., Canesi, L., Pertica, M., Livingstone, D.R., 1991. Seasonal variations in the antioxidant defence systems and lipid peroxidation of the digestive gland of mussels. Comp. Biochem. Physiol. C. 100 (1–2), 187–190.

Viarengo, A., Lowe, D., Bolognesi, C., Fabbri, E., Koehler, A., 2007. The use of biomarkers in biomonitoring: A 2-tier approach assessing the level of pollutant-induced stress syndrome in sentinel organisms 146, 281–300. https://doi.org/10.1016/j.cbpc.2007.04.011

Virgin, S.D.S., Barbeau, M.A., 2017. Gametogenesis and Spawning of the Ribbed Mussel (*Geukensia demissa*) near the Northern Limit of its Range (Maritime Canada) 1131–1141. https://doi.org/10.1007/s12237-016-0202-1

Visser, P.M., Verspagen, J.M.H., Sandrini, G., Stal, L.J., Matthijs, H.C.P., Davis, T.W., Paerl, H.W., Huisman, J., 2016. How rising CO_2 and global warming may stimulate harmful cyanobacterial blooms. Harmful Algae 54, 145–159. https://doi.org/10.1016/j.hal.2015.12.006

Vlahogianni, T., Dassenakis, M., Scoullos, M.J., Valavanidis, A., 2007. Integrated use of biomarkers (superoxide dismutase, catalase and lipid peroxidation) in mussels *Mytilus galloprovincialis* for assessing heavy metals' pollution in coastal areas from the Saronikos Gulf of Greece. Mar. Pollut. Bull. 54, 1361–1371. https://doi.org/10.1016/j.marpolbul.2007.05.018

Voigt, O., Fradusco, B., Gut, C., Kevrekidis, C., Vargas, S., Wörheide, G., 2021. Carbonic anhydrases: an ancient tool in calcareous sponge biomineralization. Front. Genet. 12, 1–9. https://doi.org/10.3389/fgene.2021.624533

Völker, J., Ashcroft, F., Vedøy, Å., Zimmermann, L., Wagner, M., 2022. Adipogenic activity of chemicals used in plastic consumer products. Environ. Sci. Technol. https://doi.org/10.1021/acs.est.1c06316

von Hellfeld, R., Zarzuelo, M., Zaldibar, B., Cajaraville, M.P., Orbea, A., 2022. Accumulation, Depuration, and Biological Effects of Polystyrene Microplastic Spheres and Adsorbed Cadmium and Benzo(a)pyrene on the Mussel *Mytilus galloprovincialis*. Toxics 10, 18. https://doi.org/10.3390/toxics10010018

W

Wäge, J., Rohr, S., Hardege, J.D., Rotchell, J., 2016. Short-term effects of CO_2-induced low pH exposure on target gene expression in *Platynereis dumerilii*. J. Mar. Biol. Oceanogr. 5, 2. https://doi.org/10.4172/2324-8661

Wallace, R.B., Baumann, H., Grear, J.S., Aller, R.C., Gobler, C.J., 2014. Coastal ocean acidification: The other eutrophication problem. Estuar. Coast. Shelf Sci. 148, 1–13. https://doi.org/10.1016/j.ecss.2014.05.027

Wang, D.Y., Wang, Y., 2009. HLB-1 functions as a new regulator for the organization and function of neuromuscular junctions in nematode *Caenorhabditis elegans*. Neurosci. Bull. 25, 75–86. https://doi.org/10.1007/s12264-009-0119-9

Wang, J., Dong, B., Yu, Z.X., Yao, C.L., 2018. The impact of acute thermal stress on green mussel *Perna viridis*: Oxidative damage and responses. Comp. Biochem. Physiol. -Part A Mol. Integr. Physiol. 222, 7–15. https://doi.org/10.1016/j.cbpa.2018.04.001

Wang, J., Li, Y., Lu, L., Zheng, M., Zhang, X., Tian, H., Wang, W., Ru, S., 2019. Polystyrene microplastics cause tissue damages, sex-specific reproductive disruption and transgenerational effects in marine medaka (*Oryzias melastigma*). Environ. Pollut. 254, 113024. https://doi.org/10.1016/j.envpol.2019.113024

Wang, L.-S., Wang, Lin, Wang, Li, Wang, G., Li, Z.-H., Wang, J.-J., 2009a. Effect of 1-butyl-3-methylimidazolium tetrafluoroborate on the wheat (*Triticum aestivum* L.) seedlings. Environ. Toxicol. 24, 296–303. https://doi.org/10.1002/tox

Wang, W.-X., Zhang, Q., 2013. Dioxin and phthalate uptake and assimilation by the green mussel *Perna viridis*. Environ. Pollut. 178, 455–462. https://doi.org/10.1016/j.envpol.2013.03.062

Wang, X., Huang, W., Wei, S., Shang, Y., Gu, H., Wu, F., Lan, Z., Hu, M., Shi, H., Wang, Y., 2020. Microplastics impair digestive performance but show little effects on antioxidant activity in mussels under low pH conditions. Environ. Pollut. 258, 113691. https://doi.org/10.1016/j.envpol.2019.113691

Wang, X., Wang, M., Jia, Z., Qiu, L., Wang, L., Zhang, A., Song, L., 2017. A carbonic anhydrase serves as an important acid-base regulator in Pacific oyster *Crassostrea gigas* exposed to elevated CO_2: implication for physiological responses of mollusk to ocean acidification. Mar. Biotechnol. 19, 22–35. https://doi.org/10.1007/s10126-017-9734-z

Wang, X., Wang, H., Xu, B., Huang, D., Nie, C., Pu, L., Zajac, G.J.M., Yan, H., Zhao, J., Shi, F., Emmer, B.T., Lu, J., Wang, R., Dong, X., Dai, J., Zhou, W., Wang, C., Gao, G., Wang, Y., Willer, C., Lu, X., Zhu, Y., Chen, X.W., 2021. Receptor-Mediated ER Export of Lipoproteins Controls Lipid Homeostasis in Mice and Humans. Cell Metab. 33, 350-366.e7. https://doi.org/10.1016/j.cmet.2020.10.020

Wang, Y., Li, L., Hu, M., Lu, W., 2015. Physiological energetics of the thick shell mussel *Mytilus coruscus* exposed to seawater acidification and thermal stress. Sci. Total Environ. 514, 261–272. https://doi.org/10.1016/j.scitotenv.2015.01.092

Wang, Z., Gerstein, M., Snyder, M., 2009b. RNA-Seq: a revolutionary tool for transcriptomics. Nature reviews genetics, 10(1), 57-63.

Wathsala, R.H.G.R., Franzellitti, S., Scaglione, M., Fabbri, E., 2018. Styrene impairs normal embryo development in the Mediterranean mussel (*Mytilus galloprovincialis*). Aquat. Toxicol. 201, 58–65. https://doi.org/10.1016/j.aquatox.2018.05.026

Watson, G.J., Bentley, M.G., Gaudron, S.M., Hardege, J.D., 2003. The role of chemical signals in the spawning induction of polychaete worms and other marine invertebrates. J. Exp. Mar. Bio. Ecol. 294, 169–187. https://doi.org/10.1016/S0022-0981(03)00264-8

Weber, A., Jeckel, N., Wagner, M., 2020. Combined effects of polystyrene microplastics and thermal stress on the freshwater mussel *Dreissena polymorpha*. Sci. Total Environ. 718, 137253. https://doi.org/10.1016/j.scitotenv.2020.137253

Welshons, W. V., Thayer, K.A., Judy, B.M., Taylor, J.A., Curran, E.M., vom Saal, F.S., 2003. Large effects from small exposures. I. Mechanisms for endocrine-disrupting chemicals with estrogenic activity. Environ. Health Perspect. 111, 994–1006. https://doi.org/10.1289/ehp.5494

Widdows, J., 1985. Physiological responses to pollution. Mar. Pollut. Bull. 16, 129–134. https://doi.org/10.1016/0025-326X(85)90002-5

Wilhelm Filho, D., Tribess, T., Gáspari, C., Claudio, F.D., Torres, M.A., Magalhães, A.R.M., 2001. Seasonal changes in antioxidant defenses of the digestive gland of the brown mussel (*Perna perna*). Aquaculture 203, 149–158. https://doi.org/10.1016/S0044-8486(01)00599-3

Winston, G.W., Di Giulio, R.T., 1991. Prooxidant and antioxidant mechanisms in aquatic organisms. Aquat. Toxicol. 19, 137–161. https://doi.org/10.1016/0166-445X(91)90033-6

Winter, J.E., 1973. The filtration rate of *Mytilus edulis* and its dependence on algal concentration, measured by a continuous automatic recording apparatus. Mar. Biol. 22, 317–328. https://doi.org/10.1007/BF00391388

Wittassek, M., Koch, H.M., Angerer, J., Brüning, T., 2011. Assessing exposure to phthalates - The human biomonitoring approach. Mol. Nutr. Food Res. 55, 7–31. https://doi.org/10.1002/mnfr.201000121

Wofford, H.W., Wilsey, C.D., Neff, G.S., Giam, C.S., Neff, J.M., 1981. Bioaccumulation and metabolism of phthalate esters by oysters, brown shrimp, and sheepshead minnows. Ecotoxicol. Environ. Saf. 5, 202–210. https://doi.org/10.1016/0147-6513(81)90035-X

Wolfe, K., Nguyen, H.D., Davey, M., Byrne, M., 2020. Characterizing biogeochemical fluctuations in a world of extremes: A synthesis for temperate intertidal habitats in the face of global change. Glob. Chang. Biol. 26, 3858–3879. https://doi.org/10.1111/gcb.15103

Wong, R.Y., McLeod, M.M., Godwin, J., 2014. Limited sex-biased neural gene expression patterns across strains in Zebrafish (*Danio rerio*). BMC Genomics 15, 1–9. https://doi.org/10.1186/1471-2164-15-905

World Health Organization & International Programme on Chemical Safety (WHO) 2001. Biomarkers in risk assessment : validity and validation. World Health Organisation. Available at https://apps.who.int/iris/handle/10665/42363 Accessed 23 Apr 2021

Wormuth, M., Scheringer, M., Vollenweider, M., Hungerbühler, K., 2006. What are the sources of exposure to eight frequently used phthalic acid esters in Europeans? Risk Anal. 26, 803–824. https://doi.org/10.1111/j.1539-6924.2006.00770.x

Wu, C. 1995. Heat shock transcription factors: structure and regulation. Annual review of cell and developmental biology, 11(1), 441-469.

Wu, F., Sokolov, E. P., Dellwig, O., & Sokolova, I. M. (2021). Season-dependent effects of ZnO nanoparticles and elevated temperature on bioenergetics of the blue mussel *Mytilus edulis*. Chemosphere, 263, 127780. https://doi.org/10.1016/j.chemosphere.2020.127780

Wu, N.C., Rubin, A.M., Seebacher, F., 2022. Endocrine disruption from plastic pollution and warming interact to increase the energetic cost of growth in a fish. Proc. R. Soc. B Biol. Sci. 289. https://doi.org/10.1098/rspb.2021.2077

Wu, F., Sokolova, I.M., 2021. Immune responses to ZnO nanoparticles are modulated by season and environmental temperature in the blue mussels *Mytilus edulis*. Sci. Total Environ. 801, 149786. https://doi.org/10.1016/j.scitotenv.2021.149786

X

Xie, Z., Ebinghaus, R., Lohmann, R., Caba, A., Ruck, W.K.L., 2007. Occurrence and air − Sea exchange of phthalates in the Arctic. Environ. Sci. Technol. 41, 4555–4560. https://doi.org/10.1021/es0630240

Xie, Z., Ebinghaus, R., Temme, C., Caba, A., Ruck, W., 2005. Atmospheric concentrations and air-sea exchanges of phthalates in the North Sea (German Bight). Atmos. Environ. 39, 3209–3219. https://doi.org/10.1016/j.atmosenv.2005.02.021

Xu, H., Cao, W., Sun, H., Zhang, S., Li, P., Jiang, S., Zhong, C., 2021. Dose-dependent effects of di-(2-ethylhexyl) phthalate (DEHP) in mussel *Mytilus galloprovincialis*. Front. Mar. Sci. 8, 1–10. https://doi.org/10.3389/fmars.2021.658361

Xu, S., Li, C., 2020. Phthalates in house and dormitory dust: occurrence, human exposure and risk assessment. Bull. Environ. Contam. Toxicol. https://doi.org/10.1007/s00128-020-03058-7

Xu, X., Yang, F., Zhao, L., Yan, X., 2016. Seawater acidification affects the physiological energetics and spawning capacity of the Manila clam *Ruditapes philippinarum* during gonadal maturation. Comp. Biochem. Physiol. -Part A Mol. Integr. Physiol. 196, 20–29. https://doi.org/10.1016/j.cbpa.2016.02.014

Y

Yamamoto, Y. hei, Kimura, T., Momohara, S., Takeuchi, M., Tani, T., Kimata, Y., Kadokura, H., Kohno, K., 2010. A novel ER J-protein DNAJB12 accelerates ER-associated degradation of membrane proteins including CFTR. Cell Struct. Funct. 35, 107–116. https://doi.org/10.1247/csf.10023

Yamamoto-Kawai, M., McLaughlin, F. A., Carmack, E. C., Nishino, S., Shimada, K. 2009. Aragonite undersaturation in the Arctic Ocean: effects of ocean acidification and sea ice melt. Science, 326(5956), 1098-1100.

Yang, L., He, J.T., Su, S.H., Cui, Y.F., Huang, D.L., Wang, G.C., 2017. Occurrence, distribution, and attenuation of pharmaceuticals and personal care products in the riverside groundwater of the Beiyun River of Beijing, China. Environ. Sci. Pollut. Res. 24, 15838–15851. https://doi.org/10.1007/s11356-017-8999-0

Yang, J., Satuito, C.G., Bao, W., Kitamura, H., 2008. Induction of metamorphosis of pediveliger larvae of the mussel *Mytilus galloprovincialis* Lamarck, 1819 using neuroactive compounds , KCl , NH_4Cl and organic solvents 7014. https://doi.org/10.1080/08927010802340309

Ye, T., Kang, M., Huang, Q., Fang, C., Chen, Y., Shen, H., Dong, S., 2014. Exposure to DEHP and MEHP from hatching to adulthood causes reproductive dysfunction and endocrine disruption in marine medaka (*Oryzias melastigma*). Aquat. Toxicol. 146, 115–126. https://doi.org/10.1016/j.aquatox.2013.10.025

Yee T.W., 2015. Vector Generalized Linear and Additive Models: With an Implementation in R. Springer, New York, USA. https://CRAN.R-project.org/package=VGAM

Yu, P.C., Matson, P.G., Martz, T.R., Hofmann, G.E., 2011. The ocean acidification seascape and its relationship to the performance of calcifying marine invertebrates: Laboratory experiments on the development of urchin larvae framed by environmentally relevant pCO_2/pH. J. Exp. Mar. Bio. Ecol. 400, 288–295. https://doi.org/10.1016/j.jembe.2011.02.016

Yu, H., Yang, Z., Sui, M., Cui, C., Hu, Y., Hou, X., Xing, Q., Huang, X., Bao, Z., 2021. Identification and characterization of hsp90 gene family reveals involvement of hsp90, grp94, and not trap1 in heat stress response in *Chlamys farreri*. Genes (Basel). 12. https://doi.org/10.3390/genes12101592

Z

Zanette, J., Jenny, M.J., Goldstone, J. V, Parente, T., Woodin, B.R., Bainy, A.C.D., Stegeman, J.J., 2013. Identification and expression of multiple CYP1-like and CYP3-like genes in the bivalve

mollusk *Mytilus edulis*. Aquat. Toxicol. 128–129, 101–112. https://doi.org/10.1016/j.aquatox.2012.11.017

Zanotelli, V.R.T., Neuhauss, S.C.F., Ehrengrubera, M.U., 2010. Long-term exposure to bis(2-ethylhexyl) phthalate (DEHP) inhibits growth of guppy fish (*Poecilia reticulata*). J. Appl. Toxicol. 30, 29–33. https://doi.org/10.1002/jat.1468

Zapata-Restrepo, L.M., Hauton, C., Williams, I.D., Jensen, A.C., Hudson, M.D., 2019. Effects of the interaction between temperature and steroid hormones on gametogenesis and sex ratio in the European flat oyster (*Ostrea edulis*). Comp. Biochem. Physiol. -Part A Mol. Integr. Physiol. 236, 110523. https://doi.org/10.1016/j.cbpa.2019.06.023

Zardi, G.I., McQuaid, C.D., Nicastro, K.R., 2007. Balancing survival and reproduction: Seasonality of wave action, attachment strength and reproductive output in indigenous *Perna perna* and invasive *Mytilus galloprovincialis* mussels. Mar. Ecol. Prog. Ser. 334, 155–163. https://doi.org/10.3354/meps334155

Zebral, Y.D., Da Silva Fonseca, J., Marques, J.A., Bianchini, A., 2019. Carbonic anhydrase as a biomarker of global and local impacts: Insights from calcifying animals. Int. J. Mol. Sci. 20, 1–16. https://doi.org/10.3390/ijms20123092

Zeng, X., Chen, X., Zhuang, J., 2015. The positive relationship between ocean acidification and pollution. Mar. Pollut. Bull. 91, 14–21. https://doi.org/10.1016/j.marpolbul.2014.12.001

Zhang, Y., Duan, C., Yang, J., Chen, S., Liu, Q., Zhou, L., Huang, Z., Xu, Y., Xu, G., 2018. Deubiquitinating enzyme USP9X regulates cellular clock function by modulating the ubiquitination and degradation of a core circadian protein BMAL1. Biochem. J. 475, 1507–1522. https://doi.org/10.1042/BCJ20180005

Zhang, D., Lin, J., Harley, M., Hardege, J.D., 2009. Characterization of a sex pheromone in a simultaneous hermaphroditic shrimp, *Lysmata wurdemanni*. Mar. Biol. 157, 1–6. https://doi.org/10.1007/s00227-009-1290-2

Zhang, Z.M., Zhang, H.H., Zou, Y.W., Yang, G.P., 2018. Distribution and ecotoxicological state of phthalate esters in the sea-surface microlayer, seawater and sediment of the Bohai Sea and the Yellow Sea. Environ. Pollut. 240, 235–247. https://doi.org/10.1016/j.envpol.2018.04.056

Zhao, L., Liu, Baozhan, An, W., Deng, Y., Lu, Y., Liu, Bingxin, Wang, L., Cong, Y., Sun, X., 2019. Assessing the impact of elevated pCO_2 within and across generations in a highly invasive fouling mussel (*Musculista senhousia*). Sci. Total Environ. 689, 322–331. https://doi.org/10.1016/j.scitotenv.2019.06.466

Zhao, X., Guo, C., Han, Y., Che, Z., Wang, Y., Wang, X., Chai, X., Wu, H., Liu, G., 2017. Ocean acidification decreases mussel byssal attachment strength and induces molecular byssal responses. Mar. Ecol. Prog. Ser. 565, 67–77. https://doi.org/10.3354/meps11992

Zhou, J., Cai, Z.H., Li, L., Gao, Y.F., Hutchinson, T.H., 2010. A proteomics-based approach to assessing the toxicity of bisphenol A and diallyl phthalate to the abalone (*Haliotis diversicolor supertexta*). Chemosphere 79, 595–604. https://doi.org/10.1016/j.chemosphere.2010.01.052

Zhao, X., Guo, C., Han, Y., Che, Z., Wang, Y., Wang, X., Chai, X., Wu, H., Liu, G., 2017. Ocean acidification decreases mussel byssal attachment strength and induces molecular byssal responses. Mar. Ecol. Prog. Ser. 565, 67–77. https://doi.org/10.3354/meps11992

Zhu, W., Mantione, K., Jones, D., Salamon, E., Cho, J.J., Cadet, P., Stefano, G.B., 2003. tissues: Evidence for estradiol isoforms 24, 137–140.

Zhu, J., Li, J., Chapman, E.C., Shi, H., Ciocan, C.M., Chen, K., Shi, X., Zhou, J., Sun, P., Zheng, Y., Rotchell, J.M., 2022. Gonadal atresia , estrogen - responsive , and apoptosis - specific mRNA expression in marine mussels from the East China Coast : a preliminary study. Bull. Environ. Contam. Toxicol. https://doi.org/10.1007/s00128-022-03461-2

Zimmermann, L., Bartosova, Z., Braun, K., Oehlmann, J., Völker, C., Wagner, M., 2021. Plastic products leach chemicals that induce in vitro toxicity under realistic use conditions. Environ. Sci. Technol. 55, 11814–11823. https://doi.org/10.1021/acs.est.1c01103

Zoccola, D., Innocenti, A., Bertucci, A., Tambutté, E., Supuran, C.T., Tambutté, S., 2016. Coral carbonic anhydrases: Regulation by ocean acidification. Mar. Drugs 14. https://doi.org/10.3390/md14060109

Zorita, I., Ortiz-Zarragoitia, M., Soto, M., Cajaraville, M.P., 2006. Biomarkers in mussels from a copper site gradient (Visnes, Norway): An integrated biochemical, histochemical and histological study. Aquat. Toxicol. 78, 109–116. https://doi.org/10.1016/j.aquatox.2006.02.032